

SUBJ
MNG
FAIA

Frictional Attenuation: An Inherent Amplitude Dependence

GERALD M. MAVKO¹

Department of Geophysics, Stanford University, Stanford, California 94305

UNIVERSITY OF UTAH
RESEARCH INSTITUTE
EARTH SCIENCE LAB.

Frictional sliding on crack surfaces and grain boundaries is examined as a mechanism of wave attenuation. In contrast to previous work based on idealized elliptic crack models a general description of internal surfaces is considered which allows for irregularities and partially closed cracks. This leads to Q^{-1} that increases with strain amplitude. Such an amplitude dependence is often observed in large-strain laboratory measurements. This suggests that under in situ (small strain) conditions, frictional attenuation becomes secondary to linear loss mechanisms, either disappearing or becoming masked.

INTRODUCTION

Frictional sliding on crack surfaces and grain boundaries has been suggested as an important, if not the dominant, mechanism of wave attenuation in rocks at low confining pressure, particularly in the absence of a fluid phase [Walsh, 1966; Gordon and Davis, 1968; Birch, 1975; Lockner et al., 1977; Johnston and Toksöz, 1977; Orowan, 1934]. Simple friction is intuitively appealing as a mechanism because it is commonly observed on macroscopic sliding surfaces, and it is independent of frequency. In this paper we examine models for various modes of sliding that can lead to attenuation. We find that the most general description of a sliding surface exhibiting macroscopic Coulomb friction results in a Q^{-1} proportional to strain amplitude. Such an amplitude dependence is, in fact, observed, leading to the conclusions that friction may dominate in certain large-strain laboratory measurements but must be secondary to linear mechanisms at seismic wave strains.

In the next section we discuss some general considerations of frictional attenuation. Existing models for dissipation on cracks and grain contacts are reviewed, and the role of surface irregularities is discussed. In a subsequent section a new analysis is presented for dissipation on nonelliptical cracks. The remainder of the paper gives a discussion of the theoretical results in comparison with laboratory measurements of Q .

MODES OF FRICTIONAL SLIDING

Frictional attenuation requires that at least some portion of the mineral surfaces that are in contact within a rock slide under applied stress. These surfaces might be, for example, the mating faces of cracks or joints or the contacts between separate grains. When either a compressional or a shear wave passes, contact surfaces will be subjected to oscillatory stresses, resolved into shear and normal components depending on the surface orientation. If sliding takes place, work is done against friction, and mechanical energy from the passing wave is converted to heat.

To estimate frictional dissipation, three quantities must be known: (1) the magnitude of frictional stress, (2) the amount of slip, and (3) the area of surfaces in contact that slide. We will assume that frictional stress τ_f is given by Amonton's law [Bowden and Tabor, 1950]:

$$\tau_f = \gamma \cdot \sigma_n \quad (1)$$

where σ_n is the normal stress and γ is the coefficient of sliding friction. Both the amount of slip, U , and the sliding surface

area are, in general, functions of material stiffness, surface geometry, and the spatial distributions of τ_f and the applied oscillatory shear stress τ .

During a loading cycle the increment of energy dissipated on a sliding surface S as the applied shear stress varies from τ to $\tau + d\tau$ is given by the surface integral

$$dW = \iint_S \tau_f(\mathbf{r}, \tau) dU(\mathbf{r}, \tau) ds$$

where \mathbf{r} is the position on the surface.

Writing the increment of slip dU as

$$dU = \frac{\partial U}{\partial \tau} d\tau$$

the total dissipation during a full cycle is given by

$$\Delta W = \oint_{-\tau_m}^{\tau_m} \iint_S \gamma \sigma_n(\mathbf{r}, \tau) \frac{\partial U(\mathbf{r}, \tau)}{\partial \tau} ds d\tau \quad (2)$$

where τ_m is the amplitude of the oscillating stress τ .

In the next sections the behavior of (2) is discussed for two general classes of sliding surface. In the first case the frictional stress is uniform, and the area of contact surface that slides during excitation does not depend on wave amplitude. In the second, more general case, frictional stress is nonuniform, and the area does vary with wave amplitude.

Elliptic crack model. In order to describe the sliding behavior (and dissipation) of individual cracks, Walsh [1966] considered the case of a very thin two-dimensional crack with elliptic cross section, as shown in Figure 1a. As hydrostatic confining pressure P is applied, the crack becomes thinner but remains elliptic [Eshelby, 1957; Berg, 1965]. Hence at a sufficiently large confining pressure P' the crack will close simultaneously along its length. If the confining pressure is increased further, the resulting uniform normal stress on the closed crack surfaces is given by $\sigma_n = -(P - P')$ (where stress is defined as being positive in tension). This is shown in Figure 1b. It should be noted, of course, that extending the linear elastic solution to complete crack closure results in large strains at the crack tips. Hence these details of normal stress are only approximate. Nevertheless, uniform normal stress is assumed by Walsh and is essential to his result.

The sliding friction on the closed elliptic crack, given by (1), is uniform over the crack surface, because the normal stress is uniform. Hence if the shear stress due to the passing wave exceeds the frictional resistance ($\tau_m > \tau_f$), sliding and dissipation will occur over the entire crack surface. The area of sliding is determined by the crack size and is independent of τ_m . Walsh points out that in the limit of small wave amplitude, only cracks which are just barely closed ($\tau_f, \sigma_n \approx 0$) under the

¹ Now at U.S. Geological Survey, Menlo Park, California 94025.

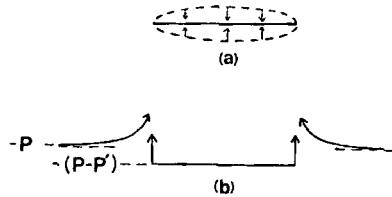


Fig. 1. Elliptic crack model. (a) Unstressed crack with elliptical cross section is shown dashed with vertical exaggeration. When applied pressure reaches P' , crack closes. (b) Normal stress in plane of closed elliptical crack. Over the closed faces, stress is uniform. Stress singularities occur outside the crack tips.

ambient confining pressure will slide and contribute to attenuation. Cracks that are not closed do not encounter friction. Those too tightly closed do not slide.

The resulting energy dissipation on each barely closed crack during one cycle of small-amplitude oscillation is proportional to τ_m^2 . The peak strain energy stored, W , is also proportional to τ_m^2 . Hence Q^{-1} , given by

$$Q^{-1} = (1/2\pi)(\Delta W/W)$$

is independent of τ_m .

The greatest weakness of the model as a mechanism of attenuation is the requirement that cracks be in the very special 'barely closed' configuration in order to slide and dissipate. To achieve a typically observed value of $Q = 100$, about one crack per grain must be contributing. (Walsh describes the density of dissipating cracks as c^3/V , where c is a typical crack dimension and V is the average volume of rock containing a single crack. One crack per grain corresponds to a value of $c^3/V \approx 1$ if the crack length is of the order of a grain diameter.) To maintain this value over a range of confining pressures would require an enormous number of cracks over a distribution of aspect ratios. *Savage* [1969] gives the following example. Consider a wave with strain amplitude 10^{-9} (10^{-4} bar). If the coefficient of friction is 0.1, the effect of increasing the confining strain by 10^{-8} (10^{-3} bar) is to immobilize all cracks that were previously just barely closed as well as to barely close some cracks that were previously open. Each successive strain increment of 10^{-9} likewise introduces a new set of barely closed cracks. Since the observed Q do not vary significantly over a range of 10 bars, i.e., over 10^4 increments of 10^{-8} strain, at least 10^4 cracks per grain must exist to produce $Q = 100$. Hence with more reasonable crack densities the model predicts a Q much higher than is observed for small-amplitude waves.

Both *Walsh* [1966] and *Savage* [1969] point out that the attenuation (Q^{-1}) predicted by the elliptic crack model will increase with finite wave amplitude. That is, the apparent amplitude independence mentioned above is a feature only of near-zero-amplitude waves. For example, with a wave of finite amplitude, cracks that are initially slightly open will close and dissipate during peak portions of the oscillation. In addition, some cracks that are initially more than just barely closed and favorably oriented will slide and dissipate. Hence the model predicts that Q^{-1} should increase with wave amplitude because more and more cracks contribute.

Contact model. A second, more general model of surface interaction is the contact model shown schematically in Figure 2. In this case, mineral surfaces are irregular and make contact where grains touch or at crack tips (Figure 2a). As confining pressure is applied, the elastic surfaces deform, and the area of contact increases. The resulting normal stress on the contact surfaces is variable, going to zero at the contact edges (Figure

2b). Consequently, the frictional stress is variable, also going to zero at the contact edges.

As a wave passes, the applied shear stress τ will almost always exceed τ_f over at least a small region near the contact edges, causing frictional sliding (Figure 2c). The area that slides depends on the wave amplitude. Because only portions of each crack surface are in frictional contact, the resulting dissipation per crack may not be as great as that for the elliptic case. However, at an arbitrary confining pressure, many more open cracks and grain contacts can be expected to contribute.

A specific example of the contact problem is that of spherical elastic surfaces, treated by *Mindlin and Deresiewicz* [1953]. This might approximate, for example, the contact of separate grains or individual asperities. When two spheres of radius R are pressed together with normal force N , the area of contact is a circle of radius

$$b = [3(1 - \nu)RN/8\mu]^{1/3}$$

Here ν is Poisson's ratio, and μ is the shear modulus. The normal stress distribution within the circle is ellipsoidal in form, given by

$$\sigma_n = \frac{-3N}{2\pi b^2} \left[1 - \left(\frac{r}{b} \right)^2 \right]^{1/2} \quad r < b \quad (3)$$

where r is the radial distance from the center of the contact circle. Any nonzero applied shear force F will cause a stress that exceeds the frictional stress around the outer edge of the contact circle. Sliding will occur over an annulus of outer radius b and inner radius

$$c = b[1 - (F/\gamma N)]^{1/3}$$

For oscillations of amplitude $F_m \ll \gamma N$ the attenuation is given by

$$Q^{-1} = (2F_m/9\gamma N)f \quad (4)$$

where f is a dimensionless function of the surface orientation relative to the principal stresses of the oscillation:

$$f = 1 - (\gamma/\beta)^2 \quad 0 < (\gamma/\beta)^2 < 1$$

Here $\beta = dF/dN$ gives the ratio of incremental shear and normal forces resolved on the contact surface. For pure shear loading, $f = 1$; for oblique loading, $f < 1$, going to zero at $\gamma dN = dF$.

The most important feature of (4) is that Q^{-1} is proportional to wave amplitude. Although the geometry is quite idealized, this result is important, because it provides an analytic solution for a three-dimensional contact problem.

Using an intuitive argument for a simple sliding block on a spring, *White* [1966] suggests that Q for contact spheres be-

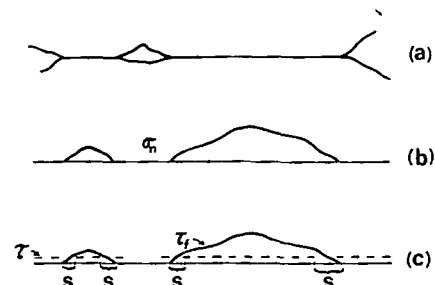


Fig. 2. (a) Two irregular elastic surfaces in contact. (b) Normal stress σ_n as a function of position on contact surfaces. (c) Frictional stress $\tau_f = \gamma\sigma_n$ and applied shear stress τ . Slip occurs over the regions S near each contact tip.

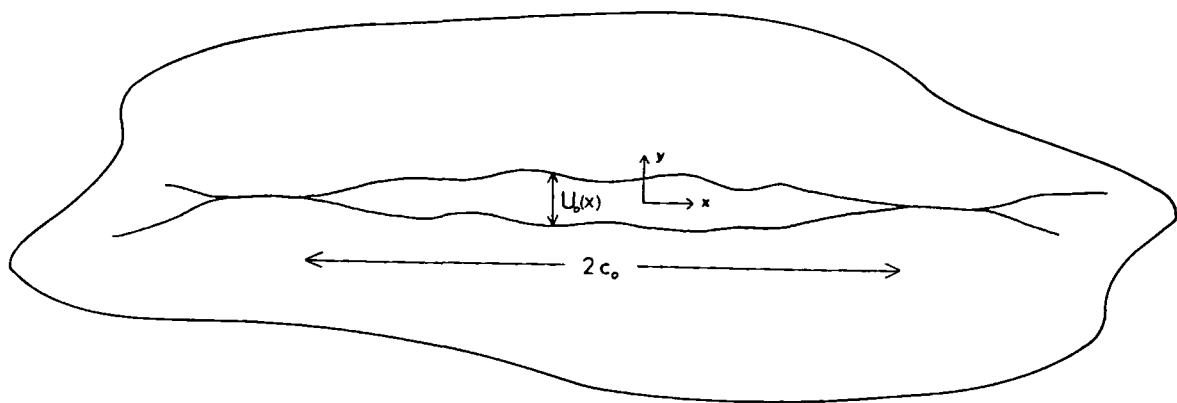


Fig. 3. A flat two-dimensional crack with tapered ends. The shape $U_0(x)$ is the width as a function of position along the crack.

comes independent of amplitude when a static coefficient of friction $\Gamma > \gamma$ exists. However, a more careful examination of the frictional stress distribution suggests that this is not so.

Consider the normal stress given by (3). The static and dynamic frictional stress distributions are similar in shape, given by σ_n multiplied by Γ and γ , respectively. Both go smoothly to zero at $r = b$. When an infinitesimal increment of shear force is applied, the static friction is exceeded, and sliding begins over an infinitesimal annulus near the contact edge. Once the static strength is exceeded, the distribution of slip is governed by the dynamic friction curve. With the next increment of stress the inner radius of the annulus grows smoothly inward, the slip always being controlled by the dynamic friction. There can be no momentary 'sticking' as the load is increased. If this occurred, even the smallest additional increment of load would cause a stress singularity at the inner edge of the annulus. This would exceed the static friction, dropping the strength to the dynamic curve and allowing the annulus to grow inward. Hence the slip and dissipation are essentially independent of the static friction, leading to the same result as was obtained in (4).

There is one subtle difference introduced by static friction. For a contact surface at arbitrary orientation, slip occurs only if $d\tau > \Gamma d\sigma$ (with static friction) or $d\tau > \gamma d\sigma$ (without static friction), where $d\tau$ and $d\sigma$ are the increments of shear and normal stress resolved on the surface during the loading cycle. Hence fewer cracks will dissipate when static friction is considered. However, this affects only the distribution function f and does not change the amplitude dependence.

Finally, as an alternative to the elliptic approximation of thin cracks, *Mavko and Nur* [1978] discuss the deformation of thin two-dimensional cracks of almost arbitrary cross-sectional shape. Of particular interest are cracks with tapered ends, as shown in Figure 3. When normal stress is applied, the cracks shorten as more and more of the crack surfaces near the tips squeeze together. In this sense the surfaces are examples of the contact problem. The dissipation on these cracks under shear stress is discussed in the next section.

ANALYSIS OF ATTENUATION WITH TAPERED CRACKS

To estimate the frictional dissipation, (2), for tapered cracks, we must once again know the normal stress and slip distributions on the contact surface throughout the stress cycle. For very thin cracks the normal stress depends only on the crack-closing deformation. Methods for computing the crack-closing deformation are given by *Mavko and Nur* [1978]. In contrast, the shear slip distribution can be more

difficult to find, particularly when the shear and normal stresses oscillate simultaneously. In this section we show, however, that for shear oscillation only, the slip is automatically obtained if the solution for closing deformation is known. We use this to estimate the attenuation for a specific crack shape.

We begin by reviewing elements of the closing problem. Consider a thin two-dimensional crack of initial shape $U_0(x)$ and length $2c_0$ (Figure 3), where $U_0(x)$ and dU_0/dx are continuous functions of x . (The shape function $U_0(x)$ is defined as the crack width as a function of position along the crack. For simplicity we will only discuss symmetric cracks, where $U_0(x)$ is an even function of x .) The crack tips are tapered such that $dU_0(\pm c_0)/dx = 0$. For mathematical simplicity it is assumed that the cracks deform in plane strain and do not interact. Furthermore, only flat planar cracks are considered with aspect ratio $\alpha \ll 1$ (where $\alpha = b/c$ and c and b are the half length and maximum half width of the crack). By limiting the discussion to flat two-dimensional cracks the deformation can be described using the theory of elastic dislocations [*Bilby and Eshelby*, 1968].

At a particular value of confining pressure P_1 the crack has shortened to some new length c_1 . The deformed shape is U_1 , and the normal stress distribution on the newly closed faces is σ_{n1} [*Mavko and Nur*, 1978]. If we now apply a small increment of tension σ_T , the crack will open by an amount $\Delta U(x, \sigma_T)$ to some new length c_2 . This increment of crack displacement can be thought of as a superimposed distribution of infinitesimal elastic edge dislocations with density function

$$\Delta B(x, \sigma_T) = -\partial \Delta U(x, \sigma_T) / \partial x$$

This increment of normal stress corresponding to this deformation is

$$\Delta \sigma_n = \frac{\mu}{2\pi(1-\nu)} \int_{-c_2}^{c_2} \frac{\Delta B(z, \sigma_T)}{x-z} dz$$

The problem of finding the change in shape reduces to finding the distribution of dislocations ΔB subject to the condition that the open crack faces are stress free, i.e.,

$$\sigma_{n1} + \sigma_T + \Delta \sigma_n = 0 \quad |x| \leq c_2$$

or

$$\int_{-c_2}^{c_2} \frac{\Delta B(z, \sigma_T)}{x-z} dz = \frac{-2\pi(1-\nu)}{\mu} (\sigma_{n1} + \sigma_T) \quad |x| \leq c_2 \quad (5)$$

The condition that the solution to (5) exists with finite stresses everywhere is given by

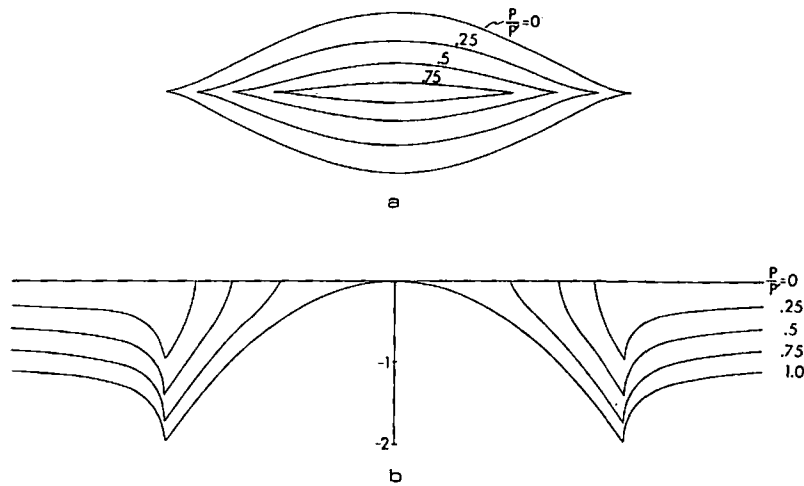


Fig. 4. (a) The deformation of a simple crack under several values of applied pressure P . (b) The normal stress in the plane of the crack for the same values of applied pressure.

$$\sigma_T = -\frac{1}{\pi} \int_{-c_1}^{c_1} \frac{\sigma_{n1}}{(c_2^2 - x^2)^{1/2}} dx \quad (6)$$

from which the length c_2 can be obtained [Muskhelishvili, 1953, p. 256; Mavko and Nur, 1978]. The solution to (5) is given by

$$\Delta B(x, \sigma_T) = \frac{2(1-\nu)}{\pi\mu} (c_2^2 - x^2)^{1/2} \int_{-c_2}^{c_2} \frac{\sigma_{n1}(z) + \sigma_T}{(x-z)(c_2^2 - z^2)^{1/2}} dz \quad |x| \leq c_2 \quad (7)$$

[Muskhelishvili, 1953, p. 257]. Finally, the shape change is found by integrating

$$\Delta U(x, \sigma_T) = \frac{-2(1-\nu)}{\pi\mu} \int_{-c_2}^x (c_2^2 - t^2)^{1/2} \int_{-c_1}^{c_1} \frac{\sigma_{n1}(z) + \sigma_T}{(1-z)(c_2^2 - z^2)^{1/2}} dz dt \quad |x| \leq c_2 \quad (8)$$

The new shape U_2 is given by

$$U_2 = U_1 + \Delta U$$

Note, in particular, in the newly opened regions where the original width U_1 was zero that

$$U_2 = \Delta U \quad c_1 \leq |x| \leq c_2 \quad (9)$$

It should be noted that this discussion refers to the incremental reopening of a crack that already exists. That is, no new fracturing is taking place. Similarly, in the following discussion we assume that sliding occurs only on preexisting surfaces.

We will now show that the plane strain sliding problem is almost identical. Consider the case where the normal stress on the crack does not change during shear loading. At the pressure P_1 the normal stress is σ_{n1} , as was already discussed. Hence the frictional stress is given by $\tau_f = \gamma\sigma_{n1}$. If a shear stress $\sigma_{xy} = \tau_s$ is applied, the crack will slide an amount ΔU_s over some width $c_s > c_1$. This sliding displacement can be thought of as a superimposed distribution of elastic edge dislocations

$$\Delta B_s = -\partial \Delta U_s / \partial x$$

with dislocation shear stress in the plane of the crack

$$\Delta \tau_s = \frac{\mu}{2\pi(1-\nu)} \int_{-c_s}^{c_s} \frac{\Delta B_s(z, \tau_s)}{x-z} dz$$

The problem reduces to finding the ΔB_s such that the total shear stress on the crack faces that slide equals the frictional resistance, i.e.,

$$-\gamma\sigma_{n1} = \tau_s + \frac{\mu}{2\pi(1-\nu)} \int_{-c_s}^{c_s} \frac{\Delta B_s(z, \tau_s)}{x-z} dz \quad |x| < c_s \quad (10)$$

where

$$\tau_s = -\frac{1}{\pi} \int_{-c_s}^{c_s} \frac{\gamma\sigma_{n1}}{(c_s^2 - x^2)^{1/2}} dx \quad (11)$$

Comparing (10) and (11) with (5) and (6), we see that the in-plane shearing problem is identical to the incremental opening problem if the following substitutions are made:

$$\begin{aligned} \sigma_{n1} &\rightarrow \gamma\sigma_{n1} \\ \sigma_T &\rightarrow \tau_s \\ \Delta U &\rightarrow \Delta U_s \\ c_2 &\rightarrow c_s \end{aligned} \quad (12)$$

It can also be shown [Bilby and Eshelby, 1968] that the antiplane shearing is identical to the opening problem if the following substitutions are made:

$$\begin{aligned} \sigma_{n1} &\rightarrow \gamma\sigma_{n1} \\ \sigma_T &\rightarrow \tau_s \\ \Delta U/(1-\nu) &\rightarrow \Delta U_s \\ c_2 &\rightarrow c_s \end{aligned} \quad (13)$$

Hence the solutions for in-plane and antiplane crack shearing at an arbitrary confining pressure are automatically obtained once the crack-closing solution is known.

To illustrate, consider the simple example given by Mavko and Nur [1978]. The original crack shape is $U_0(x) = 2b[1 - (x/c_0)^2]^{3/2}$, where c_0 is the original crack half length. As pressure P_1 is applied, the crack shortens to half length

$$c_1 = c_0[1 - (P_1/P')]^{1/2} \quad (14)$$

where $P' = 3b/2(1-\nu)c_0$ is the pressure needed to close the crack completely. The shape throughout the closing history is given by

$$U(x, P_1) = 2b\left(\frac{c_1}{c_0}\right)^3 \left[1 - \left(\frac{x}{c_1}\right)^2\right]^{3/2} \quad (15)$$

and the normal stress is

$$\sigma_{n1} = -2P' \left(\frac{c_1}{c_0} \right) \left(\frac{x}{c_0} \right) \operatorname{sgn}(x) \left[\left(\frac{x}{c_1} \right)^2 - 1 \right]^{1/2} \quad (16)$$

$c_1 < |x| < c_0$

The shape and normal stress for several values of confining pressure are shown in Figure 4.

The dissipation at a single crack tip from in-plane shearing is found by evaluating the two-dimensional form of (2):

$$\Delta W = 2d \int_{-\tau_m}^{\tau_m} \int_{c_1}^{c_s} \left\{ 2\gamma P' \left(\frac{c_1}{c_0} \right) \left(\frac{x}{c_0} \right) \left[\left(\frac{x}{c_1} \right)^2 - 1 \right]^{1/2} \right\} \cdot \frac{\partial}{\partial \tau} \left\{ 2b \left(\frac{c_s}{c_0} \right)^3 \left[1 - \left(\frac{x}{c_s} \right)^2 \right]^{3/2} \right\} dx d\tau \quad (17)$$

where d is the length into the plane, simulating the third dimension. At any given point in the loading cycle, sliding is occurring between the points c_1 and c_s , which is a function of τ . The normal stress is of the form given by (16) scaled by the open length $c = c_1$. The shear slip is of the form (15) scaled by the instantaneous value of sliding length $c = c_s(\tau)$. Integrating over x , (17) becomes

$$\Delta W = \frac{3\pi\gamma P' b d}{2} \int_{-\tau_m}^{\tau_m} \frac{c_s(c_s^2 - c_1^2)^2}{c_0^5} \frac{\partial c_s}{\partial \tau} d\tau \quad (18)$$

The open length c_1 is constant, given by (14). The sliding length $c_s(\tau)$ is of the same form as (14) but is scaled as in (12):

$$c_s(\tau) = c_0 \left[1 - \frac{P_1 - (1/2\gamma)(\tau_m + \tau)}{P'} \right]^{1/2} \quad (19)$$

Substituting (19) into (18), we obtain

$$\Delta W = \frac{\pi b d c_0}{4\gamma^2 P'^2 \tau_m^3} = \frac{\pi d c_0^2 (1 - \nu)^2}{9\gamma^2 \mu^2 \alpha_0} \tau_m^3 \quad (20)$$

where $\alpha_0 = b/c_0$ is the original crack aspect ratio.

Cracks at arbitrary orientation will generally have a larger normal stress and a smaller shear stress acting on the crack surface, resulting in a smaller dissipation. Here, as with the contact sphere, frictional sliding will go to zero in the limit $d\tau = \gamma d\sigma$, where $d\tau$ and $d\sigma$ are the increments of shear and normal stress resolved on the crack surface during the loading cycle. In this analysis we have not solved the difficult problem of general oblique loading. However, we approximate this effect by scaling (20) to give

$$\Delta W = \frac{\pi d c_0^2 (1 - \nu)^2}{9\gamma^2 \mu^2 \alpha_0} g \sigma^3$$

where σ is the peak stress amplitude of the passing wave. The coefficient g ($0 < g < 1$) gives the orientation dependence, analogous to f in (4). The total dissipation W is given by the sum over all $2N$ crack tips that slide:

$$\Delta W = \frac{2\pi(1 - \nu)^2 \bar{d} \bar{c}^2 N G}{9\gamma^2 \mu^2 \bar{\alpha}} \sigma^3$$

Here \bar{d} , \bar{c} , and $\bar{\alpha}$ are characteristic mean values of d , c_0 , and α_0 . G is defined by

$$\sum_{\alpha_0}^{2N} \frac{d c^2}{\alpha} g = \frac{\bar{d} \bar{c}^2}{\bar{\alpha}} 2NG$$

The peak strain energy in a volume of rock V is given by

$$W = \frac{1}{2} (\sigma^2 / M_e) V$$

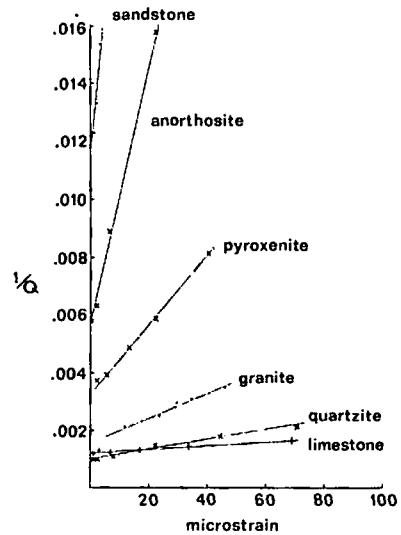


Fig. 5. Linear plot of attenuation versus strain amplitude for six different dry rocks: sandstone, *Winkler et al.* [1979]; anorthosite, pyroxenite, and quartzite, *Gordon and Davis* [1968]; granite, *Gordon and Rader* [1971]; and limestone, *Peselnick and Outerbridge* [1961].

where M_e is the effective modulus of the rock appropriate to the given wave type. For example,

P wave, infinite medium

$$M_e = K_e + \frac{1}{3}\mu_e$$

S wave, infinite medium

$$M_e = \mu_e$$

Longitudinal wave, thin rod

$$M_e = E_e$$

Here K_e , μ_e , and E_e are the effective bulk, shear, and Young's moduli. Finally, the attenuation is given by

$$Q^{-1} = \frac{2(1 - \nu)^2}{9} \left(\frac{M_e}{\mu} \right) \left(\frac{N}{V} \right) \frac{\bar{d} \bar{c}^2}{\gamma^2 \bar{\alpha}} \left(\frac{\sigma}{\mu} \right) G \quad (21)$$

Again, the most prominent feature of this mode of sliding is the amplitude dependence of Q . This dependence, also found with contact spheres, arises from the increase of sliding contact area with stress amplitude. Although the numerical coefficients may vary with different crack shapes, the amplitude dependence appears to be a fairly general result for contact surfaces exhibiting simple friction.

Recall that the elliptic crack model gives a qualitatively similar amplitude dependence but for a different reason. The attenuation from a barely closed elliptic crack is independent of amplitude. However, at larger amplitudes, more and more just barely closed cracks slide and dissipate. In contrast, with irregular surfaces in contact, each crack tip has an amplitude dependence throughout its closing history.

OBSERVATIONS OF AMPLITUDE DEPENDENCE

A number of experimental studies have shown an amplitude dependence of Q at large strains. Figure 5 shows $1/Q$ versus strain amplitude for a number of dry rocks over a wide range of frequencies. Each shows a strong amplitude dependence at strains greater than $\sim 10^{-6}$. The curve in Figure 5 labeled 'granite' is for Chester granite in quasi-static compression, measured by *Gordon and Rader* [1971]. The curve labeled

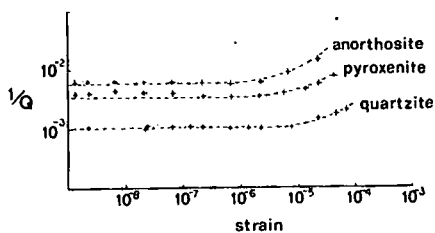


Fig. 6. Log-log plot of attenuation versus strain amplitude for three of the rocks shown in Figure 5. The dashed curves correspond to the straight-line fits obtained in Figure 5, shown here to emphasize the transition between constant Q and amplitude-dependent Q .

'limestone' is for Solenhofen limestone in a torsional pendulum of the order of 1 Hz, measured by *Peselnick and Outerbidge* [1961].

The curve labeled 'sandstone' in Figure 5 is for Massilon sandstone in extensional resonance (900 Hz), measured by *Winkler et al.* [1979]. *K. Winkler* (personal communication, 1977) observed that the amplitude effect diminished at strains less than $\sim 10^{-6}$. Furthermore, resonance peaks were symmetric at small strains but became skewed for strains greater than $\sim 10^{-6}$.

The curves in Figure 5 labeled 'anorthosite,' 'pyroxenite,' and 'quartzite' show the large-strain portions of data measured by *Gordon and Davis* [1968] for those rocks (90-kHz resonance). *Gordon and Davis* suggest that this is not a true amplitude effect but rather the result of rock damage at large strains. However, the amplitude dependence is also present on unloading curves (see Figure 5 of *Gordon and Davis* [1968]), when presumably, no new damage is occurring. At strains smaller than 10^{-6} – 10^{-8} they find Q to be essentially independent of amplitude.

In several other cases a transition from linear to nonlinear dissipation has been observed. *Brennan and Stacey* [1977] found that hysteresis loops in granite and basalt were elliptical in form for strains of the order of 10^{-6} . In contrast, *McKavanagh and Stacey* [1974] noted cusped loops in similar experiments on granite and basalt at strains of 3×10^{-5} . Similarly, *Johnson* [1955, 1961] measured Q^{-1} to be independent of amplitude for small-strain oscillation of steel and glass contacts, while *Goodman and Brown* [1962] found an amplitude dependence at larger strains, in good agreement with the *Mindlin and Deresiewicz* [1953] theory.

DISCUSSION

Two fairly general observations have been made on attenuation in dry rocks. At small strains, appropriate to seismic waves and some laboratory measurements, Q is independent of strain amplitude. However, at strains larger than 10^{-6} – 10^{-8} , Q^{-1} appears to increase with strain amplitude.

Our model results suggest a simple interpretation of these measurements. At sufficiently large strains, frictional sliding on internal surfaces should give a Q^{-1} proportional to strain amplitude. Both the contact spheres and the tapered crack analyses predict this. (For larger amplitudes, Q^{-1} for contact spheres will increase faster than the first power in strain [*Mindlin and Deresiewicz*, 1953]. For elliptical cracks, Q^{-1} may increase slower than the first power.) In contrast, at strains smaller than, say, 10^{-5} – 10^{-8} , frictional dissipation is masked by linear (amplitude independent) attenuation mechanisms which are simultaneously dissipating energy. For example, thermoelastic relaxation can lower Q to ~ 1000 or less [*Zener*, 1948; *Savage*, 1966]. The presence of a fluid phase in minute

quantities can easily lower Q to ~ 100 [*Mavko and Nur*, 1979]. The intercept of each straight line in Figure 5 is a measure of the linear losses.

Hence two simple reasons can be given why friction must be secondary at seismic wave strains. First, since frictional attenuation is inherently amplitude dependent, it must get negligibly small at sufficiently small strains. The second reason follows from a fairly model-independent argument pointed out by *Savage* [1969]: the maximum slip Δu on a crack of length l is roughly of the order of $\Delta u = \epsilon l$, where ϵ is the average rock strain. For $\epsilon = 10^{-8}$ and $l = 10^{-1}$ cm this gives $\Delta u = 10^{-9}$ cm = 100 Å. Significantly smaller strains cause displacements comparable to the atomic spacing and probably cannot be described with macroscopic sliding friction. This suggests a transition to an atomic level mechanism of grain boundary relaxation—perhaps a linear mechanism associated with the motion of lattice dislocations [*Jackson and Anderson*, 1970].

Although the detailed distribution of crack size, geometry, and density is unknown for the data in Figure 5, a rough numerical comparison with the model results can be made. Adding the effect of a constant linear attenuation Q_L^{-1} to the frictional term in (21), we obtain

$$Q^{-1} = Q_L^{-1} + \left[\frac{2(1-\nu)^2 M_e}{9 \mu} \right] \left[\frac{Nd\bar{c}^2}{V} \right] \frac{G}{\gamma^2 \bar{a}} \epsilon$$

where the strain $\epsilon \approx \sigma/\mu$. The first quantity in brackets is typically of the order of $\approx \frac{1}{2}$. If one or two crack tips per grain slide, then $Nd\bar{c}^2/\nu \approx 1$. The function G has not been determined in our analysis, but to obtain an estimate, we will use the value for a similar distribution function given by *Walsh* [1966]: $G \approx 0.1$. The coefficient of friction for single dry silicate grains is of the order of $\gamma \approx 0.1$ [*Horn and Deere*, 1962]. All of this gives

$$Q^{-1} \approx Q_L^{-1} + (\epsilon/\bar{a}) \quad (22)$$

The amplitude dependence should appear at strains large enough for the frictional term to be comparable to Q_L^{-1} . For the curves in Figure 5 a transition from constant Q to amplitude-dependent Q at strains of 10^{-8} – 10^{-6} requires aspect ratios of $\approx 10^{-1}$ – 10^{-4} . These values are reasonable but not conclusive. Straight lines were fit to the data in Figure 5, corresponding to the dependence in (22). To emphasize the transition from linear to nonlinear behavior, the straight lines fit to the curves labeled 'anorthosite,' 'pyroxenite,' and 'quartzite' in Figure 5 are replotted in Figure 6. Here the axes are logarithmic, as they were originally presented by *Gordon and Davis* [1968], and additional data are included at very low strains.

All of the models that we have examined, including the elliptical crack model, predict an amplitude dependence accompanying simple friction. We conclude that macroscopic sliding friction provides a simple and likely explanation for observed amplitude-dependent attenuation at large strains. This suggests, however, that under in situ (small strain) conditions, frictional dissipation either disappears or becomes masked by linear loss mechanisms. Hence measurement programs designed to understand the mechanisms of attenuation should cover broad ranges of both amplitude and frequency. It is also possible that part of the scatter obtained in previous attenuation measurements is due to a scatter in amplitude.

Acknowledgments. Comments by E. Kjartansson and Amos Nur were extremely helpful. I am also indebted to K. Winkler, who allowed me to use some of his unpublished data. This work was supported by grants/contracts GA 36135X and DES 75-04874 from the National Science Foundation (NSF) (Division of Earth Sciences) and

E(04-3)326-P.A. 45 from the U.S. Energy Research and Development Administration. Gerald Mavko was supported in part by an NSF postdoctoral fellowship.

REFERENCES

- Berg, C. A., Deformation of fine cracks under high pressure and shear, *J. Geophys. Res.*, **70**(14), 3447-3452, 1965.
- Bilby, B. A., and J. D. Eshelby, Dislocations and the theory of fracture, in *Fracture, an Advanced Treatise*, vol. II, edited by H. Liebowitz, p. 99, Academic, New York, 1968.
- Birch, F., Velocity and attenuation from resonant vibrations of spheres of rock, glass, and steel, *J. Geophys. Res.*, **80**, 756-764, 1975.
- Bowden, F. P., and D. Tabor, *The Friction and Lubrication of Solids*, vol. 1, Clarendon, Oxford, 1950.
- Brennan, B. J., and F. D. Stacey, Frequency dependence of elasticity of rock—Test of seismic velocity dispersion, *Nature*, **268**, 220-222, 1977.
- Eshelby, J. D., The determination of the elastic field of an ellipsoidal inclusion, and related problems, *Proc. Roy. Soc. London, Ser. A*, **241**, 376, 1957.
- Goodman, L. E., and C. B. Brown, Energy dissipation in contact friction: Constant normal and cyclic tangential loading, *J. Appl. Mech.*, **29**, 17-22, 1962.
- Gordon, R. B., and L. A. Davis, Velocity and attenuation of seismic waves in imperfectly elastic rock, *J. Geophys. Res.*, **73**, 3917-3935, 1968.
- Gordon, R. B., and D. Rader, Imperfect elasticity of rock: Its influence on the velocity of stress waves, in *The Structure and Physical Properties of the Earth's Crust*, *Geophys. Monogr. Ser.*, vol. 14, edited by J. G. Heacock, p. 235, AGU, Washington, D. C., 1971.
- Horn, H. M., and D. U. Deere, Frictional characteristics of minerals, *Geotechnique*, **12**, 319-335, 1962.
- Jackson, D. D., and D. L. Anderson, Physical mechanisms of seismic wave attenuation, *Rev. Geophys. Space Phys.*, **8**(1), 1-63, 1970.
- Johnson, K. L., Surface interaction between elastically loaded bodies under tangential forces, *Proc. Roy. Soc. London, Ser. A*, **230**, 531-549, 1955.
- Johnson, K. L., Energy dissipation at spherical surfaces in contact transmitting oscillating forces, *J. Mech. Eng. Sci.*, **3**, 362-368, 1961.
- Johnston, D. H., and M. N. Toksöz, Attenuation of seismic waves in dry and saturated rocks, *Geophysics*, **42**(7), 1511-1512, 1977.
- Lockner, D. A., J. B. Walsh, and J. D. Byerlee, Changes in seismic velocity and attenuation during deformation of granite, *J. Geophys. Res.*, **82**(33), 5374-5378, 1977.
- Mavko, G., and A. Nur, The effect of nonelliptical cracks on the compressibility of rock, *J. Geophys. Res.*, **83**(B9), 4459-4468, 1978.
- Mavko, G., and A. Nur, Wave attenuation in partially saturated rocks, *Geophysics*, **44**(2), 161-178, 1979.
- McKavanagh, B., and F. D. Stacey, Mechanical hysteresis in rocks at low strain amplitudes and seismic frequencies, *Phys. Earth Planet. Interiors*, **8**, 246-250, 1974.
- Mindlin, R. D., and H. Deresiewicz, Elastic spheres in contact under varying oblique forces, *J. Appl. Mech.*, **20**, 327-344, 1953.
- Muskhelishvili, N. I., *Singular Integral Equations*, edited by J. R. Radok, P. Noordhoff, Groningen, Netherlands, 1953.
- Orowan, E., Die Dämpfungsfähigkeit von Glimmer als empfindliche Eigenschaft, *Z. Phys.*, **87**, 749, 1934.
- Peselnick, L., and W. F. Outerbridge, Internal friction in shear and shear modulus of Solenhofen limestone over a frequency range of 10⁷ cps, *J. Geophys. Res.*, **66**(2), 581-588, 1961.
- Savage, J. C., Thermoelastic attenuation of elastic waves by cracks, *J. Geophys. Res.*, **71**(16), 3929-3938, 1966.
- Savage, J. C., Comment on 'Velocity and attenuation of seismic waves in imperfectly elastic rock' by R. B. Gordon and L. A. Davis, *J. Geophys. Res.*, **74**, 726-728, 1969.
- Walsh, J. B., Seismic wave attenuation in rock due to friction, *J. Geophys. Res.*, **71**(10), 2591-2599, 1966.
- White, J. E., Static friction as a source of attenuation, *Geophysics*, **31**(2), 333-339, 1966.
- Winkler, K., A. Nur, and M. Gladwin, Friction and seismic attenuation in rocks, *Nature*, **277**, 528-531, 1979.
- Zener, C., *Elasticity and Anelasticity of Metals*, University of Chicago Press, Chicago, Ill., 1948.

(Received April 24, 1978;
revised January 10, 1979;
accepted January 17, 1979.)

FACTORS AFFECTING LEAD JAROSITE FORMATION

J.E. DUTRIZAC, O. DINARDO and S. KAIMAN

Mineral Sciences Laboratories, Department of Energy, Mines and Resources, 555 Booth Street, Ottawa, Ontario K1A 0G1 (Canada)

(Received May 3rd, 1979; accepted October 22nd, 1979)

ABSTRACT

Dutrizac, J.E., Dinardo, O. and Kaiman, S., 1980. Factors affecting lead jarosite formation. *Hydrometallurgy*, 5: 305-324.

The importance of lead jarosite in hydrometallurgical processing and the factors affecting its formation in both the slow addition and autoclave synthesis techniques are discussed. In the slow addition method the principal factors are the amount and rate of delivery of soluble lead to the hot ferric sulphate solution; high temperatures and good agitation are also essential to avoid the formation of $PbSO_4$. The key step in the autoclave synthesis process is the selective removal of residual $PbSO_4$ from the reaction product and methods of accomplishing this are described. The major factors affecting the autoclave synthesis of lead jarosite are the ratio of $PbSO_4/Fe^{3+}$, acid concentration and the ionic strength of the solution. Time, temperature, degree of agitation and seeding all affect the reaction but to a lesser degree. The principal techniques identified to suppress lead jarosite formation were high acidity ($> 0.3 M H_2SO_4$) or the presence of substantial quantities ($> 0.3 M$) of other jarosite formers such as K_2SO_4 . Lead jarosites containing more than 16% Pb were produced and X-ray diffraction data for such material are presented.

INTRODUCTION

When sulphide concentrates containing lead are subjected to ferric sulphate or oxygen-acid pressure leaching, much of the lead reports in the residue as lead jarosite, $Pb_{0.5}Fe_3(SO_4)_2(OH)_6$ and not as $PbSO_4$ [1, 2]. If the leach solutions also contain significant concentrations of copper and zinc, these elements will be partly incorporated, and the residue can approach beaverite, $Pb(Cu, Zn)Fe_2(SO_4)_2(OH)_6$ in composition [3, 4]. Jarosite has also been found to be an efficient collector of arsenic and silver [5]; it appears that these elements are substituted in the lattice. The above observations suggest that lead jarosite plays, or is capable of playing, a much greater rôle in the leaching of sulphide concentrates than is commonly believed.

Data on the formation of lead jarosite are relatively scarce; information obtained on other jarosite-type compounds is not directly applicable be-

cause the solubility of PbSO_4 is very low relative to, say, Na_2SO_4 or K_2SO_4 . Fairchild [6] synthesized lead jarosite from 20 ml of solution containing 0.3 g PbCl_2 , 1.5 M HCl and 1.6 g $\text{Fe}_2(\text{SO}_4)_3$. Although the amount of product formed was insufficient for complete product analysis and although no test variables were studied, the experiments were interesting in that they produced a product from an acidic chloride medium. Mumme and Scott [2] prepared lead jarosite in an autoclave by reacting excess PbSO_4 with 0.125 M $\text{Fe}_2(\text{SO}_4)_3$ solution at temperatures ranging from 100 to 190°C. Unreacted PbSO_4 was dissolved with ammonium acetate or diethylenetriamine solution. Their product was always a $\text{Pb-H}_2\text{O}$ jarosite solid solution with the molar percentage of the nominal lead jarosite component ranging from 27 to 89%. Dutrizac and Kaiman [7] prepared lead jarosite by a slow addition technique whereby lead nitrate solution was slowly added to a hot ferric sulphate solution. This technique has the advantage that the product is not contaminated with PbSO_4 .

The above investigations were largely concerned with the preparation of lead jarosite and did not study thoroughly the factors influencing its formation or, conversely, those conditions where lead jarosite formation could be avoided. This paper discusses systematically the factors affecting lead jarosite formation by both the slow addition [7] and autoclave [2] techniques. Conditions where lead jarosite formation is largely suppressed have also been identified and, lastly, the various products have been characterized by chemical and X-ray diffraction techniques.

EXPERIMENTAL

Slow addition technique

In the slow addition technique a lead nitrate solution, generally 120 ml containing from 1–4 g $\text{Pb}(\text{NO}_3)_2$, was pumped at rates of 1.3 to 14 ml/h into 1 l of 95°C ferric sulphate–sulphuric acid solution which was well stirred. Iron and acid concentrations were varied. The precipitate was filtered, washed with hot water and acetone, and then dried at 110°C. The product was identified by Guinier–de Wolff X-ray diffraction analysis and was analyzed chemically.

Reaction of PbSO_4 with ferric sulphate solution

Lead jarosite was also synthesized by reacting PbSO_4 with 1 l of acidified ferric sulphate solution at temperatures ranging from 100 to 170°C in a 2-l autoclave. The charge was held in a glass liner fitted with 4 titanium baffles; agitation was by two radial impellers. Variables studied included: seeding, temperature, agitation rate, relative amount of PbSO_4 as well as the concentrations of the various solution components. The final product was filtered and then repulped with 4, 1-l portions of 10% ammonium acetate solution

at 25°C to dissolve residual lead sulphate. The repulped solids were filtered, water-washed, dried at 100°C, weighed and then analyzed by chemical and Guinier X-ray diffraction methods. The use of sensitive Guinier—de Wolff X-ray techniques permitted the detection of small amounts of residual PbSO₄ in the product. Separate experiments showed that approximately 0.3 wt. % PbSO₄ appeared as a "faint trace" on the Guinier patterns.

X-ray diffraction

Powder diffraction patterns were obtained with cobalt radiation using both a Guinier—de Wolff focussing camera and a Philips 114.6 mm diameter Debye—Scherrer powder camera [7]. Interplanar spacings were read from Philips charts [8], and relative intensities were estimated visually. It was assumed that lead jarosite possessed the same hexagonal structure (R3m) as jarosite, KFe₃(SO₄)₂(OH)₆. By comparing the patterns with those published in the Diffraction Index [9] for this structure, some lines could be indexed unequivocally and approximate cell dimensions were obtained. These were then refined by several iterations of a least-squares computer program, PARAM [10]. The final cell dimensions were used to calculate the interplanar spacings and indices were assigned to all the observed diffraction lines.

RESULTS AND DISCUSSION

Slow addition technique

In the slow addition technique, the lead solution must be added to the hot ferric sulphate solution sufficiently slowly that lead jarosite forms in preference to PbSO₄. The first experiments were done to locate the best pumping rate when 120 ml of solution containing 1.1 g Pb(NO₃)₂ was added to 1 l of stirred 0.1 M Fe³⁺ (SO₄) — 0.01 M H₂SO₄ solution at 95–100°C (Table 1).

TABLE 1

Pumping rate (ml/h)	Wt. % Pb in product	X-Ray constituents of product
1.8	8.10	Pb-jarosite
1.8	8.35	Pb-jarosite
3.0	7.20	Pb-jarosite
3.0	7.10	Pb-jarosite
6.0	7.67	Pb-jarosite
9.6	9.60	Pb-jarosite + trace PbSO ₄
13.8	9.20	Pb-jarosite + trace PbSO ₄
25.0	—	Pb-jarosite + trace PbSO ₄

Two points emerge from these data. First, there is a maximum flow rate beyond which the product becomes progressively more contaminated with PbSO_4 . Under the current conditions, this maximum flow was about 6.0 ml/h. Secondly, the lead content of the product increases as the pumping rate is decreased.

For a given rate of delivery, the lead content increased as the amount of lead pumped increased. This is illustrated in Table 2 for tests done when 120 ml of $\text{Pb}(\text{NO}_3)_2$ solution containing different amounts of Pb was pumped at 1.8 ml/h into 1 l of stirred 0.1 M Fe^{3+} — 0.01 M H_2SO_4 solution at 95–100°C.

TABLE 2

Weight $\text{Pb}(\text{NO}_3)_2$ (g)	Wt. % Pb in product	X-Ray constituents of product
0.5	5.55	Pb-jarosite
1.1	8.35	Pb-jarosite
2.2	10.30	Pb-jarosite
3.0	16.40	Pb-jarosite + PbSO_4
3.3	15.10	Pb-jarosite + PbSO_4
3.5*	11.70	Pb-jarosite
7.0*	13.60	Pb-jarosite

* NH_4 -acetate washed.

As the amount of lead pumped increases, the lead content of the product increases and eventually (~ 3 g $\text{Pb}(\text{NO}_3)_2$) PbSO_4 is detected in the product. Removal of the PbSO_4 by ammonium acetate indicated that the lead jarosite itself continued to become lead enriched, but this washing technique was not pursued since the object of the slow addition method was to avoid a subsequent purification step. A 2.0 g charge of $\text{Pb}(\text{NO}_3)_2$ was selected for the remainder of the experiments since this level consistently gave products containing $< 0.3\%$ PbSO_4 . A similar trend was also observed when the lead solution was pumped at either 3 or 6 ml/h, except that the maximum amount of lead nitrate permissible before the product became PbSO_4 contaminated decreased as the pumping rate increased.

The addition of lead jarosite seed in amounts ranging from 0 to 3.0 g was found to have no beneficial effect on the amount or lead content of the product. In fact, lead jarosite prepared in the presence of seed had slightly lower lead concentrations and was found to consist of major lead jarosite together with trace to minor hydronium jarosite. Accordingly, the bulk of the work was done relying on "natural" seeding within the vessel.

The effect of temperature on the formation of lead jarosite was investigated over the interval 70–100°C when 120 ml of solution containing 2.0 g $\text{Pb}(\text{NO}_3)_2$ was pumped at 1.8 ml/h into 1 l of well stirred 0.1 M Fe^{3+} — 0.01 M H_2SO_4 solution (Table 3).

TABLE 3

Temperature (°C)	Wt. % Pb in product	X-Ray constituents of product
100	10.11	Pb-jarosite
95	10.02–11.37	Pb-jarosite
90	12.78	Pb-jarosite + trace PbSO ₄
80	19.72	Pb-jarosite + trace PbSO ₄
70	32.20	PbSO ₄ + Pb-jarosite

As the temperature is decreased, the formation of PbSO₄ in preference to lead jarosite occurs; the higher lead contents of the products made at lower temperatures are attributable to the PbSO₄ contamination. It appears that temperatures of 95–100°C are necessary for good lead jarosite formation.

Stirring was necessary to prevent formation of both PbSO₄ and Fe₄(SO₄)(OH)₁₀. Once a minimum amount of agitation was provided, more vigorous stirring was without effect. All work was done using moderate agitation with a magnetic stirrer in a baffled 2-l reaction kettle.

Once the amount of lead and the pumping rate had been fixed, it was difficult to alter the solution composition without introducing PbSO₄ into the product. When 2.0 g of Pb(NO₃)₂ was pumped at 1.8 ml/h and 95–100°C into a 0.1 M Fe³⁺ – 0.01 M H₂SO₄ solution, only lead jarosite was formed. If the iron level decreased to 0.05 M Fe³⁺, PbSO₄ formed, presumably because there was too much lead for the available iron. Increasing the iron concentration above 0.2 M Fe²⁺ resulted in progressively more contamination. At 1.0 M Fe³⁺ only PbSO₄ was formed. The reaction was very sensitive to H₂SO₄ concentration. Increasing the H₂SO₄ concentration from 0.01 M to 0.03 M resulted in trace PbSO₄ contamination; at 0.1 M H₂SO₄ only PbSO₄ was produced.

The optimum conditions for jarosite production by the slow addition technique were identified as follows:

- (i) 120 ml of solution containing 2.0 g Pb(NO₃)₂ is pumped at 1.8 ml/h into
- (ii) 1 l of 0.1 M Fe³⁺ (SO₄) – 0.01 M H₂SO₄ solution at 95–100°C
- (iii) the reactor is baffled and well stirred
- (iv) the products are water-washed and dried at 110°C for 24 h.

TABLE 4

	Synthetic (wt.%)	Theoretical (wt.%)
Pb	10.88	18.32
Fe	31.73	29.63
SO ₄	36.49	33.98
H ₃ O ⁺ OH ⁻	20.90	18.07
(by difference)		

Under the above synthesis conditions the product consisted of lead jarosite of the composition given in Table 4. The synthesized product had the approximate formula: $\text{Pb}_{0.28} \text{H}_3\text{O}_{0.44} \text{Fe}_{2.99}(\text{SO}_4)_{2.00}(\text{OH})_6$. The slight iron deficiency and substantial substitution of H_3O for the lead ion are characteristic of natural and synthetic lead jarosites [7, 11]. The X-ray patterns obtained were essentially identical to those presented previously [7].

Reaction of PbSO_4 with ferric sulphate solution

(a) PbSO_4 leaching

This technique which was first advanced by Mumme and Scott [2] produces lead jarosite by the reaction of PbSO_4 with ferric sulphate solution at elevated temperatures; residual PbSO_4 is selectively dissolved to leave a "pure" product. This selective leach step is the key to the process since even a small amount of PbSO_4 (68% Pb) can greatly alter the composition of the lead jarosite product (theoretical 18% Pb). Accordingly, the first experiments were directed to finding the preferred conditions for leaching PbSO_4 from lead jarosite. For these tests a lead jarosite- PbSO_4 mixture was prepared by reaction of 1 l of 0.25 M $\text{Fe}^{3+}(\text{SO}_4)$ -0.025 M H_2SO_4 solution with 24.6 g PbSO_4 (2X stoichiometric) for 24 h in a well-stirred autoclave at 140°C.

Even at 25°C, washing of the product with diethylenetriamine (10% in water as suggested by Mumme and Scott [2]) caused the yellow coloured product to turn progressively orange and then brick-red. X-ray diffraction analysis of the amine-leached mixture showed only lead jarosite and this suggests an amorphous decomposition product. Amine leaching at higher temperatures hastened the change. No further work was done on the amine leaching of PbSO_4 and efforts were concentrated on 10% ammonium acetate solutions also recommended by Mumme and Scott [2].

A 10-g quantity of pure lead jarosite (11.7% Pb) was leached in 2 l of 10% NH_4Ac at various temperatures. Samples were taken at various times and analyzed for Pb; the results are presented in Fig. 1. The acetate solution does not decompose lead jarosite at 25 or 35°C in the 50 h timeframe studied. Slight decomposition occurs at 50°C and this becomes significant at 70 or 90°C; the high temperature products were brick red at the end of leaching, indicating major decomposition. Clearly, the ammonium acetate leaching must be done at low temperatures to prevent lead jarosite decomposition.

Fig. 2 shows the product composition obtained when an autoclave synthesis product consisting of PbSO_4 and lead jarosite was leached in 10% NH_4Ac solution at 25 and 50°C. The product was stirred in the acetate solution for 30 min, and then analyzed for Pb. At either temperature, the free PbSO_4 is removed after two 1 l washes. Washing at 50°C removes the PbSO_4 more quickly and achieves a slightly lower terminal lead value, likely indicative of slight lead jarosite decomposition even under these mild leaching conditions.

For all subsequent work, the autoclave product was subjected to four 1-l

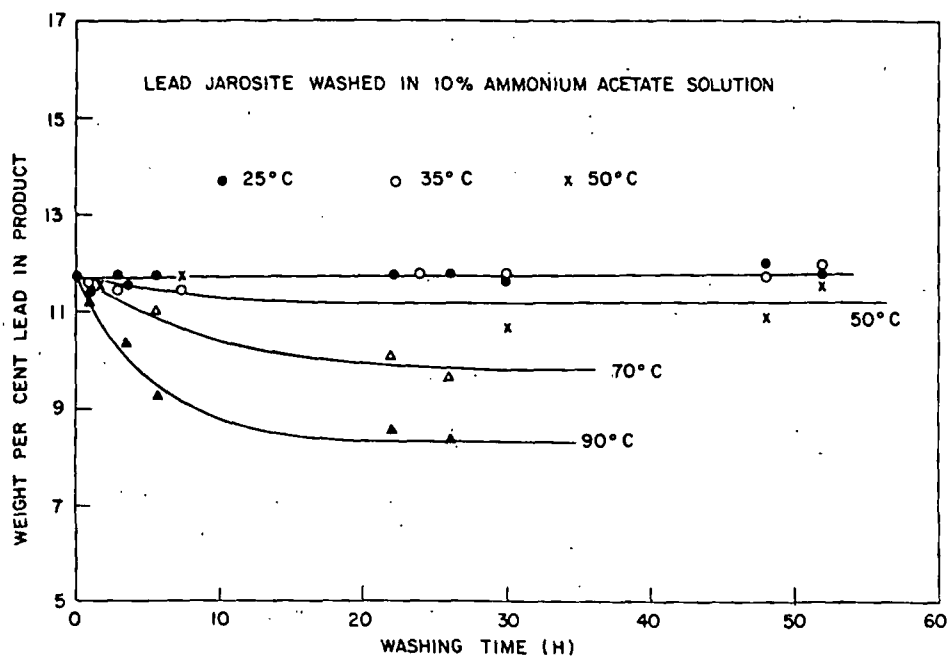


Fig. 1. Effect of temperature and reaction time on the composition of lead jarosite leached in 10% ammonium acetate solution.

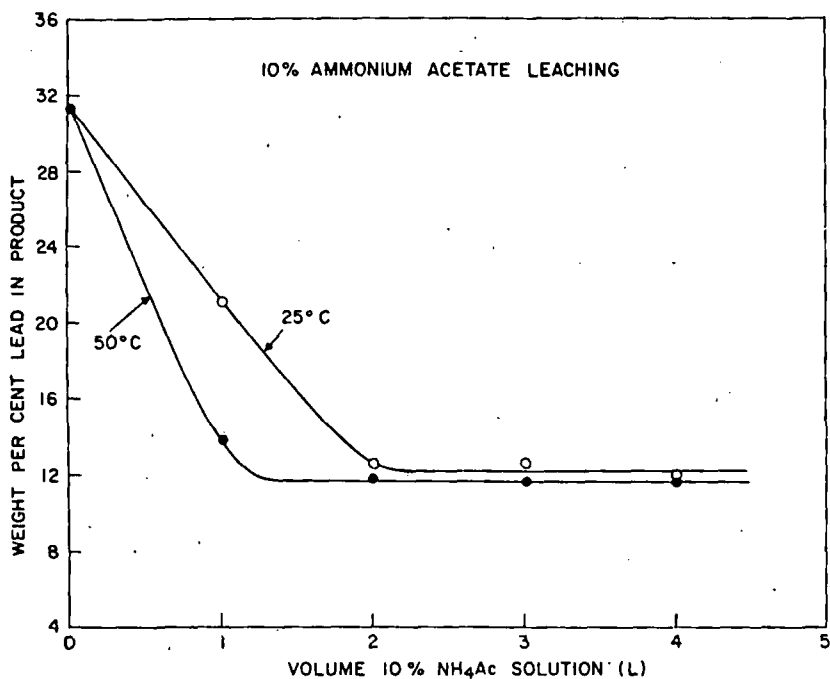


Fig. 2. The selective removal of $PbSO_4$ from $PbSO_4$ -lead jarosite mixtures by 10% ammonium acetate solution.

washes in 10% NH_4Ac solution at 25°C . The solids were slurried in the acetate solution for 30–60 min, allowed to settle, the liquid was decanted and fresh acetate solution was added. After the final wash the slurry was filtered, water-washed, and subsequently dried at 110°C . The above procedure was very effective in removing free PbSO_4 . In some instances, however, the product was contaminated with traces of PbSO_4 which could not be removed by persistent acetate treatment. In such samples the PbSO_4 appears to be encapsulated by the lead jarosite which effectively “protects” it.

(b) Effect of the $\text{PbSO}_4/\text{Fe}^{3+}$ ratio and the Fe^{3+} concentration

Figure 3 shows the effect of the ratio of $\text{PbSO}_4/\text{Fe}^{3+}$ on the lead content of the acetate-washed autoclave product. Increasing the theoretical amount of lead increases the ratio of $\text{Pb}/\text{H}_3\text{O}$ in the lead-hydronium jarosite product. When less than 0.1 theoretical fraction lead was added, the product was identified as “hydronium jarosite”; for theoretical lead fractions between 0.1 and 0.5, the product was contaminated with traces of Fe_2O_3 or persistent PbSO_4 . When greater than stoichiometric PbSO_4 was added, the final washed product consisted of lead jarosite only. It was decided to use $2.0 \times$ theoretical fraction of PbSO_4 for all syntheses since this produced maximum lead concentrations consistent with reasonable amounts of excess PbSO_4 for the acetate leaching stage.

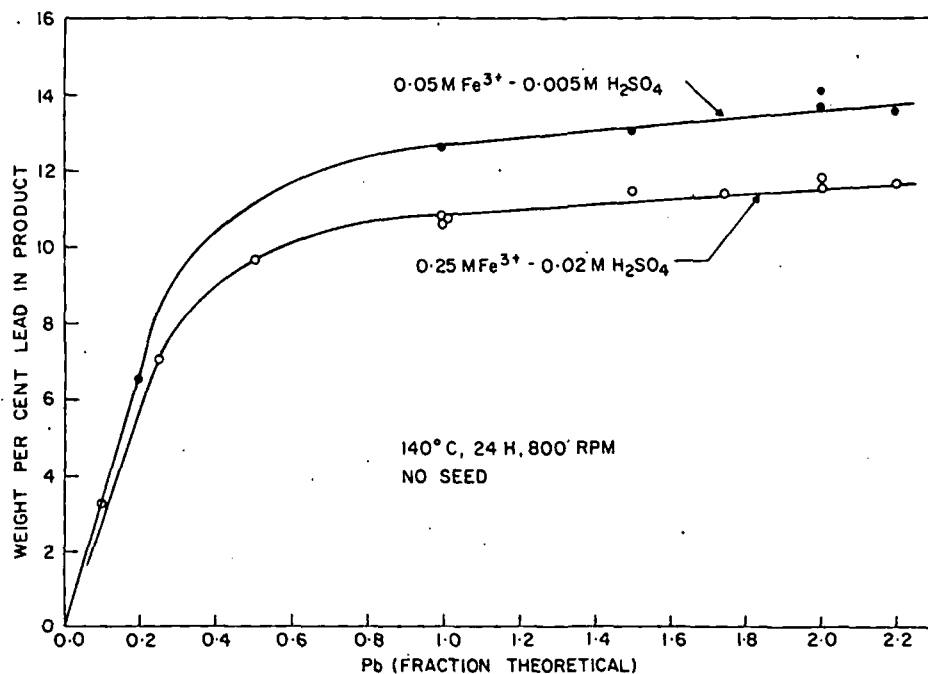
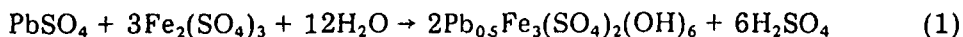


Fig. 3. Effect of initial $\text{PbSO}_4/\text{Fe}^{3+}$ ratio on the lead concentration of the jarosite product formed for two initial iron levels.

Since the solubility limit of PbSO_4 is only a few tens of ppm at 140°C , the effect produced by additional PbSO_4 cannot be associated with increased Pb activity for the reaction:



Lead jarosites prepared from low concentrations of PbSO_4 were difficult to purify by acetate leaching and this may indicate that the PbSO_4 is being encased by the product. An excess of PbSO_4 would increase the likelihood that some PbSO_4 surface would always be exposed to the solution.

Figure 4 shows the effect of the Fe^{3+} concentration on the lead content of the washed product when the ratio of $\text{PbSO}_4:\text{Fe}^{3+}$ was held at $2.0 \times$ theoretical. The percentage of Pb in the lead-hydronium jarosite increases as the ferric ion concentration decreases:

$$\text{wt.}\% \text{ Pb} = k - 2.0 \log [\text{Fe}^{3+}] \quad (2)$$

The lead content increased with increasing H_2SO_4 concentrations even though the solubility of PbSO_4 is known to decrease under these conditions.

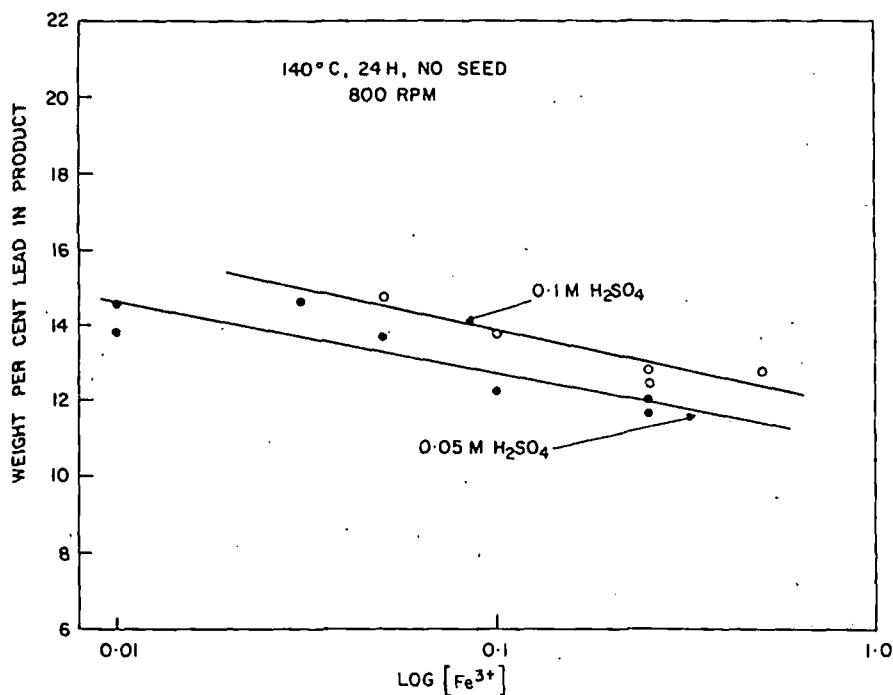


Fig. 4. Influence of initial iron concentration on the lead content of the jarosite product; the Pb/Fe^{3+} ratio was constant at $2 \times$ theoretical.

(c) *The effect of seeding and agitation*

The effect of adding small quantities of lead jarosite seed ($\sim 16\%$ Pb) in amounts from 0 to 2.0 g was studied under the preferred conditions. The seed addition had no major effect on either the amount of lead jarosite produced or its lead content. Presumably the 24-h reaction time and the presence of the stirrer, vessel walls and PbSO_4 particles gave ample time and sites for lead jarosite nucleation. In spite of the above comment, seed addition was useful, especially at the extremes of temperature, composition, stirring, etc. This is illustrated in Figure 5 which shows the effect of autoclave agitation speed in the presence and absence of lead jarosite seed on the composition of the product.

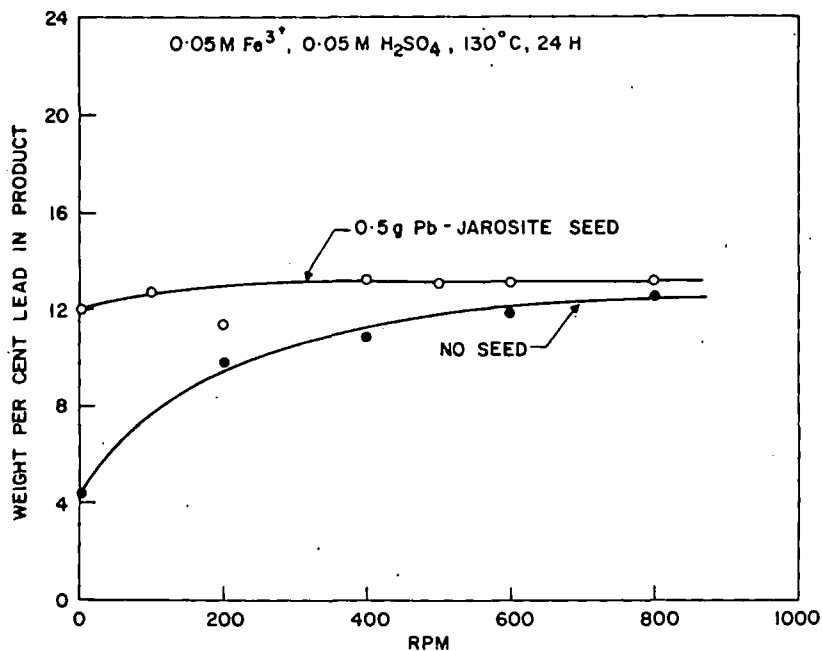


Fig. 5. Effect of agitation on the composition of the jarosite product, with and without seeding.

The addition of the seed under good mixing conditions was not overly beneficial, but the seed was most useful under poor agitation conditions. When seed was absent without good stirring, an hydronium-lead jarosite formed, but the product made in the presence of seed always contained more than 12% Pb. The seed prevents the formation of other iron compounds like hydronium jarosite, $\text{FeO}\cdot\text{OH}$, Fe_2O_3 , etc. For example, the products made in the presence of seed consisted of lead jarosite only; those made without seed were contaminated with $\text{FeO}\cdot\text{OH}$ at the low stirring speeds. The yield of product with seeding was more uniform than in its absence; with seed the yield at 200 rpm was nearly the same (6.0 g) as at 800 rpm (6.5 g).

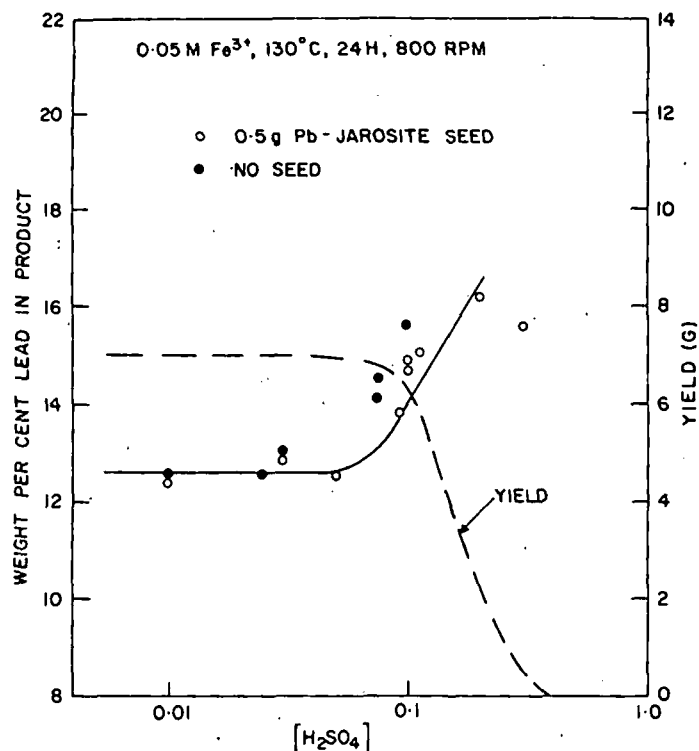


Fig. 7. Effect of sulphuric acid concentration on the yield and composition of the jarosite product made with or without seeding.

(e) *Reaction time and temperature*

The effect of time at a reaction temperature of 130°C on the lead concentration of the acetate-washed product produced at both 0.01 and 0.1 M H₂SO₄ concentrations was investigated. The composition of the product is independent of the heating times under the conditions used, although it should be noted that a 2–2½ period was required to heat the autoclave to 130°C. The yield of product increased with increasing time to about 3 h, but was independent of time thereafter. Traces of an unidentified iron compound were found in the products heated for longer than 50 h in the absence of seed. The above observations suggest that equilibrium, or at least a steady-state condition, is rapidly attained at 130°C, and that the formation of lead jarosite during leaching likely could not be avoided by manipulation of the leaching times.

The lead concentration of the lead jarosite increased as the temperature decreased as can be seen in Figure 8. Lead jarosite was produced over the temperature range 100–160°C. For the solutions containing 0.05 M H₂SO₄ and no seed, Fe₂O₃ was detected in minor quantities at 170°C; no Fe₂O₃ was noted in the test done using 0.1 M H₂SO₄ and 0.5 g lead jarosite seed, and it is not known if the difference is attributable to the different acid

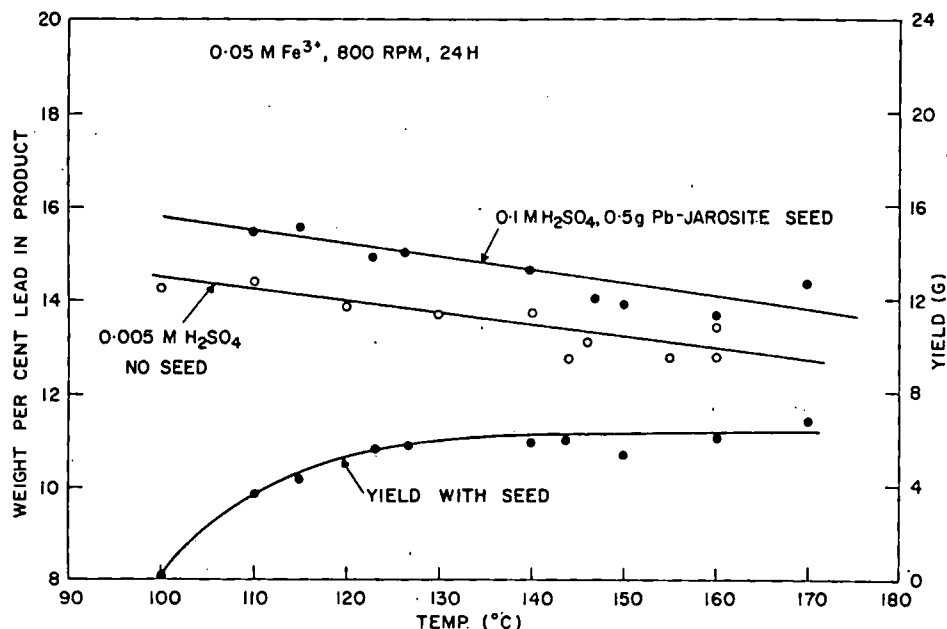
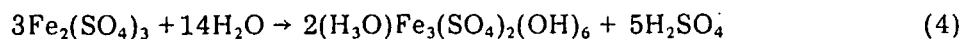


Fig. 8. Effect of synthesis temperature on the yield and composition of jarosite formed at two initial acid levels.

level or to the presence of the seed. Hydronium jarosite is favoured at elevated temperatures [7] and the declining lead concentration on increasing temperatures is probably attributable to the enhanced hydrolysis of ferric sulphate:



The yield of product increases from nearly zero at 100°C to a maximum at about 125–130°C and, thereafter, remains essentially constant. Prevention of lead jarosite formation during leaching by temperature control does not appear attractive. Leaching temperatures > 110°C and < 175°C would certainly be employed and such temperatures give a good yield of lead jarosite.

Addition of other sulphates

Although lead jarosite contains trivalent iron, it is conceivable that this compound could be produced from solutions containing significant amounts of ferrous ion. Figure 9 shows the influence of added FeSO₄ on the lead content of lead jarosite; the range of FeSO₄ compositions studied covered those likely to be encountered during leaching. The lead concentration of the product is independent of the amount of added FeSO₄ to about 1.25 M, but for larger FeSO₄ additions, the product becomes less lead rich. At the highest FeSO₄ concentrations, the product was contaminated with minor amounts of an unknown iron compound. The ferrous sulphate levels likely to be encoun-

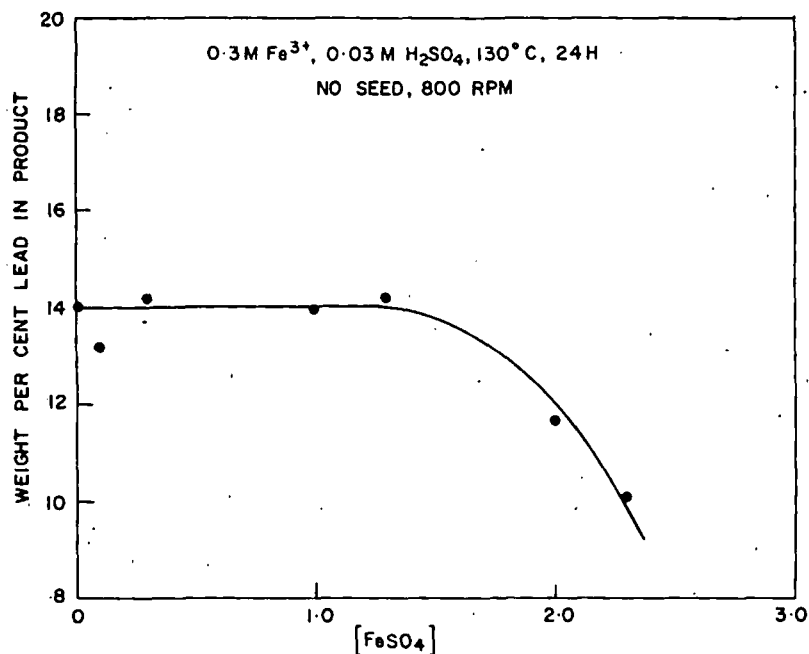


Fig. 9. Influence of ferrous sulphate on the composition of the jarosite product.

tered during a leaching operation will not prevent lead jarosite formation although high FeSO₄ levels will reduce the lead concentration of the product slightly.

Neither lithium nor magnesium form jarosite-type compounds, and the influence of ionic strength on lead jarosite formation was studied by adding various concentrations of MgSO₄, Li₂SO₄ or LiCl. An Fe(SO₄)_{1.5} concentration of 0.3 M was used since high ionic strength caused the precipitation of Fe₂O₃ or α-FeO·OH from more dilute iron solutions.

Figure 10 illustrates the influence of high concentrations of Li₂SO₄ and MgSO₄ on the lead concentration of the acetate-washed product. Increasing the ionic strength increases the percentage of lead in the lead jarosite; the yield of product was, however, essentially identical at all concentrations. The products prepared in the presence of either 2 M Li₂SO₄ or 2 M MgSO₄ contained only 0.10 wt. % Li or 0.30 wt. % Mg, respectively. The percentage of these elements in the lead jarosite was proportional to their concentration, and they could not be totally eliminated by washing. It may be that trace amounts of Li or Mg can actually be incorporated into the lead jarosite lattice, although either an entrapment or adsorption mechanism could equally apply. The high ionic strengths commonly encountered during commercial leaching will only enhance the formation of lead jarosite.

Figure 11 shows the effect of LiCl concentration on the Pb level and yield of the jarosite product. As the LiCl concentration increases, the percent-

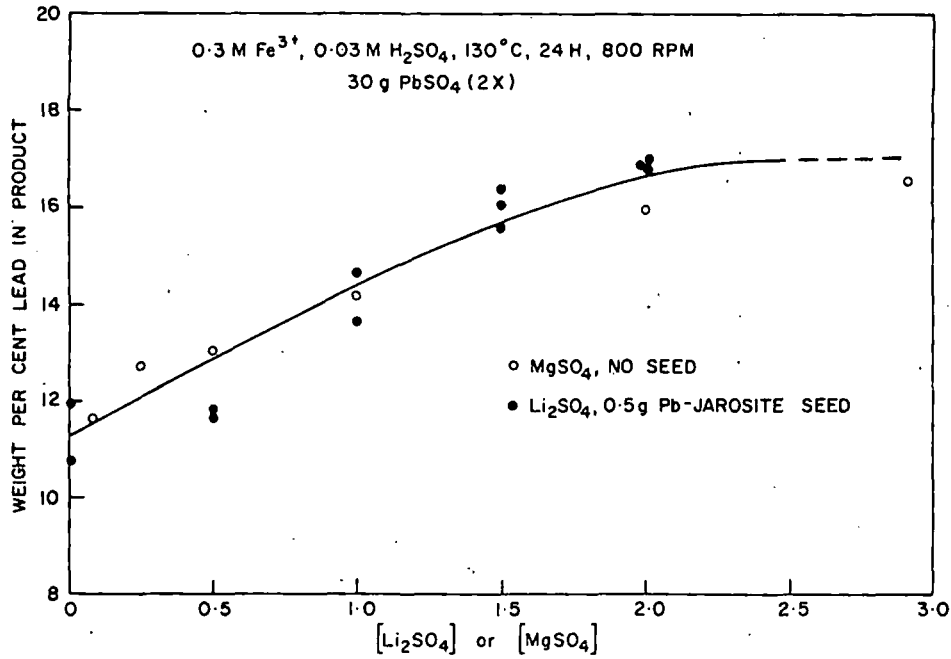


Fig. 10. Effect of dissolved Li_2SO_4 or MgSO_4 on the lead concentration of the jarosite product formed with or without seeding.

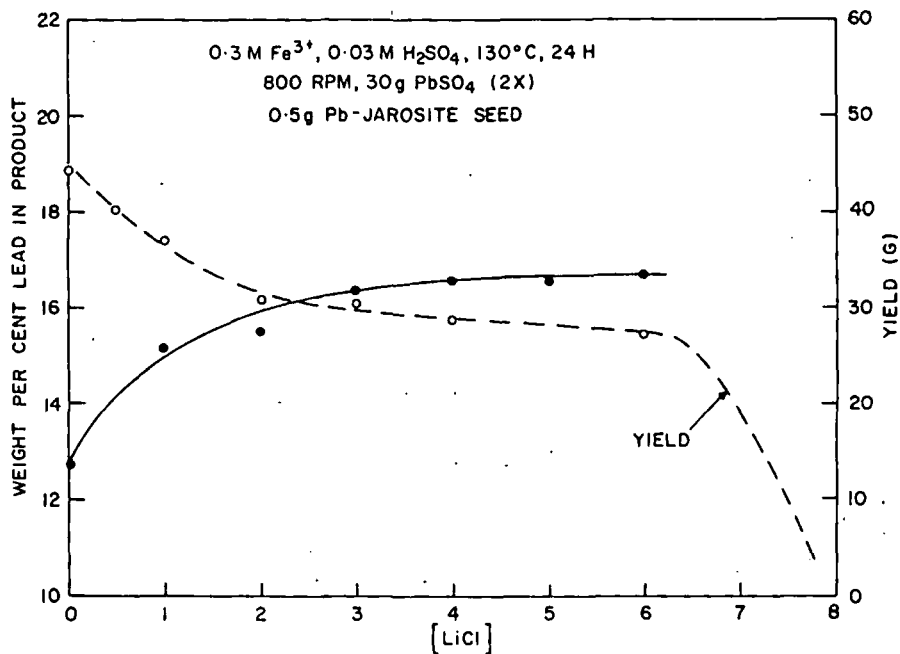


Fig. 11. Effect of LiCl concentration on the yield and composition of lead jarosite formed in an otherwise sulphate medium.

age of Pb in the product also increases. Products prepared in the presence of 4 M or less of LiCl consisted of lead jarosite with a trace of an unknown iron compound; at 4 or 6 M LiCl the unknown iron compound was present in minor amounts and at 8 M LiCl, PbSO₄ was the only reaction product. Increasing LiCl concentrations caused the yield to decrease steadily; above 6 M LiCl the yield dropped off rapidly, and no lead jarosite whatsoever was produced at 8 M LiCl. The above results show that lead jarosite can be readily prepared in concentrated chloride solutions provided a separate source of sulphate ion is available.

Sodium, potassium and ammonium sulphates all yield jarosite-type compounds with ferric sulphate solutions that also form complete solid solution series with each other and with lead jarosite [11–13]. Accordingly, attempts were made to see if the presence of alkali sulphates in solution prevented or minimized lead jarosite formation under simulated leaching conditions, and the results are presented in Figure 12. These experiments were done at 150°C [1]; lead was added as 4.5 g (2 X) of PbS which was oxidized in situ by oxygen at 0.7 MPa. Excess PbSO₄ was dissolved, and the product was subsequently analyzed. The addition of any of Na, K or NH₄ displaced lead from the jarosite solid solution; the extent increased with increasing concentration of the alkali sulphate to about 0.3 M, but thereafter remained essentially constant. Potassium and ammonium sulphates were more effective than sodium ion.

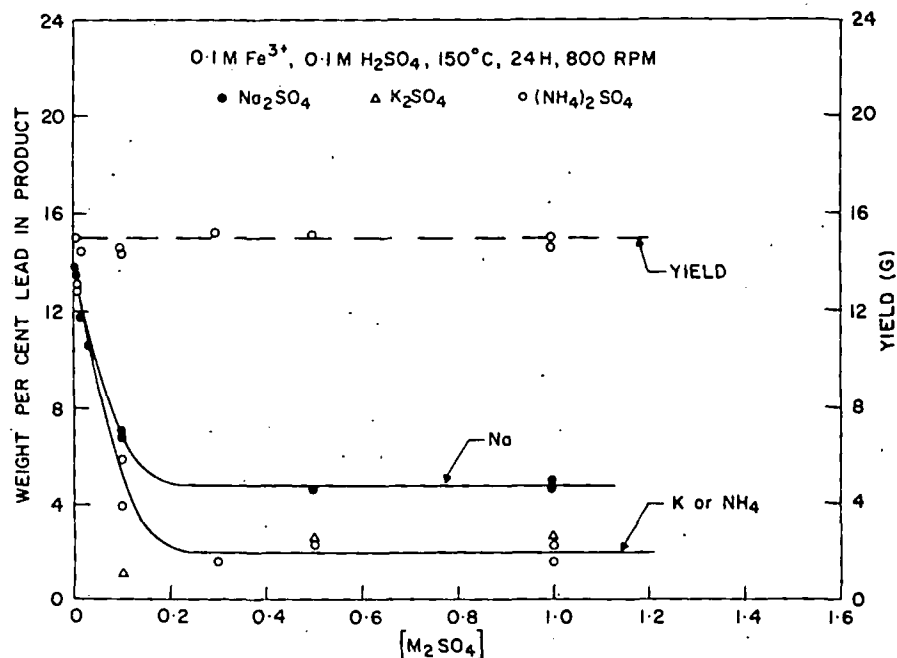
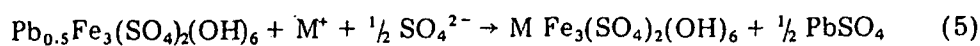


Fig. 12. Reduction of the lead concentration of the jarosite product by the addition of other jarosite forming compounds.

The free energy values for the reaction:



where M^+ is K^+ , NH_4^+ or Na^+ , are [14–16]:

K^+ : -6.4 kcal/mole

NH_4^+ : -2.91 kcal/mole

Na^+ : -1.24 kcal/mole

Reaction (5) closely approximates the synthesis conditions used since an excess of PbSO_4 was always available. These thermochemical data suggest that potassium will most effectively eliminate lead and that sodium ion will be least efficacious; the standard free energies are, however, only indicative of general trends since the single ion activities as well as the activities of the lead-alkali jarosite solid solutions are unknown. Also, the lead jarosite contains substantial hydronium substitution.

Since the yield of product remains essentially constant when alkali sulphates are added (Fig. 12), it follows that the amount of lead reporting in the jarosite phase has been substantially reduced by the presence of large quantities of M_2SO_4 in the solution. This technique might find application in leaching processes where PbSO_4 and not lead jarosite was the sought-after phase; especially in those operations where the leach solution could be recycled to conserve M_2SO_4 .

(g) The lead jarosite product

The best conditions for the synthesis of lead jarosite in the absence of possible "contaminating" ions such as Li^+ or Mg^{2+} are:

(i) 1 l of 0.05 M $\text{Fe}(\text{SO}_4)_{1.5}$ - 0.1 M H_2SO_4 solution

(ii) with 0.5 g lead jarosite seed and 5.2 g PbSO_4 (2X theoretical)

(iii) heated to 130°C for 24 h at 800 rpm in a baffled reactor

(iv) the product is given the standard ammonium acetate wash, filtered, water washed and dried at 110°C for 24 h.

Under the above conditions the product consisted of lead jarosite together with a very faint trace of PbSO_4 and had the composition given in Table 5. The product had the approximate formula: $\text{Pb}_{0.39}\text{H}_3\text{O}_{0.22}\text{Fe}_{2.99}(\text{SO}_4)_2(\text{OH})_6$. The interplanar d -values and visually estimated intensities of the X-ray diffraction patterns are presented in Table 6.

TABLE 5

	Synthetic (wt.%)	Theoretical (wt.%)
Pb	15.21	18.32
Fe	31.54	29.63
SO_4	36.31	33.98
$\text{H}_3\text{O}^+ \text{OH}^-$ (by difference)	16.94	18.07

TABLE 6

X-ray diffraction data for lead jarosite $\text{Pb}_{0.39}(\text{H}_2\text{O})_{0.12}\text{Fe}_{2.99}(\text{SO}_4)_2(\text{OH})_6$ $a = 7.314 \pm 0.001$, $c = 33.624 \pm 0.008$ Å

$d_{\text{meas.}}$	$I_{\text{est.}}$	hkl	$d_{\text{calc.}}$	$d_{\text{meas.}}$	$I_{\text{est.}}$	hkl	$d_{\text{calc.}}$
5.93	6	012	5.927	1.695	1	1.2.14	1.696
5.62	< 1/2	006	5.604	1.665	1	1.1.18	1.664
5.06	3	104	5.059	1.626	1/2	0.1.20	1.625
3.65	4	110	3.657	1.580	1/2	{ 2.1.16 042	{ 1.579
3.11	3	202	3.112				{ 1.576
3.06	10	116	3.063	1.559	4	{ 1.3.10 404	{ 1.557
2.970	3	1.0.10	2.970				{ 1.556
2.804	4	0.0.12	2.802	1.533	4	2.2.12	1.531
2.532	4	208	2.529	1.487	4B	{ 1.0.22 2.0.20	{ 1.486
2.370	1	122	2.370				{ 1.485
2.304	2	{ 0.2.10 214	{ 2.305 2.302	1.451	1	{ 321 232	{ 1.452
							{ 1.448
2.248	5	0.1.14	2.246	1.435	1/2	{ 4.0.10 324	{ 1.433
2.077	1/2B	033	2.075				{ 1.432
1.978	5	036	1.976	1.420	1	{ 235 3.1.14	{ 1.420
1.951	1/2	2.1.10	1.950				{ 1.418
1.915	1/2B	2.0.14	1.914	1.400	1	0.0.24 0.3.18	1.401
1.870	1/2B	0.0.18	1.868				1.399
1.830	5	220	1.828	1.382	1B	140	1.382
1.751	1	{ 0.2.16 312	{ 1.751 1.747	1.344	3	146	1.342

The corresponding optimum conditions for the synthesis of lead jarosite in solutions containing large quantities of added electrolyte are:

- (i) 1 l of 0.3 M $\text{Fe}(\text{SO}_4)_{1.5}$ - 0.1 M H_2SO_4 - 2 M Li_2SO_4 solution
- (ii) with 0.5 g lead jarosite seed and 30 g PbSO_4 (2X theoretical)
- (iii) heated to 130°C for 24 h at 800 rpm in a baffled reactor and washed as above.

Under these conditions the product had the composition given in Table 7. The synthesized product had the approximate formula: $\text{Pb}_{0.44}\text{H}_3\text{O}_{0.11}\text{Fe}_{2.81}(\text{SO}_4)_2(\text{OH})_6$. The interplanar d -values and estimated intensities

TABLE 7

	Synthetic (wt.%)	Theoretical (wt.%)
Pb	16.68	18.32
Li	0.08	0.00
Fe	28.36	29.63
SO_4	34.78	33.98
$\text{H}_3\text{O}^+\text{OH}^-$	20.10	18.07

of the X-ray diffraction patterns for this material are very similar to those presented in Table 6.

CONCLUSIONS

The factors affecting lead jarosite formation in both the slow addition and autoclave synthesis techniques have been investigated. In the slow addition method the principal factors are the amount and rate of delivery of soluble lead to the hot ferric sulphate solution; high temperatures (95–100°C) and good agitation are also essential to avoid the formation of PbSO_4 . When the above variables are fixed, the ferric and acid concentrations can be varied only over extremely narrow ranges if PbSO_4 is to be avoided. Under the optimum slow addition conditions, a lead jarosite containing ~11% Pb can be prepared.

The key step in the autoclave synthesis process is the selective removal of the residual PbSO_4 ; this leaching was best accomplished with cold (25°C) 10% ammonium acetate solution. The principal factors affecting the autoclave jarosite synthesis were the ratio of $\text{PbSO}_4/\text{Fe}^{3+}$, the acid concentration and the ionic strength of the solution. Time, temperature, degree of agitation and seeding all affected the synthesis but to a lesser degree. The principal methods identified for suppressing lead jarosite formation were high acidity ($> 0.3 \text{ M H}_2\text{SO}_4$) and the presence of other jarosite formers (Na_2SO_4 , $(\text{NH}_4)_2\text{SO}_4$, K_2SO_4). The autoclave synthesis technique can produce a product containing over 16% Pb; X-ray and chemical data are reported for the high-lead products.

ACKNOWLEDGEMENTS

The authors wish to thank P.E. Bélanger and E.J. Murray for helping with the X-ray determinations. The assistance of J.C. Hole and his staff with the chemical analyses is also recognized.

REFERENCES

- 1 The application of the Sherritt zinc pressure leaching process to New Brunswick zinc lead bulk concentrates, Summary Report, Sherritt Gordon Mines Ltd., Fort Saskatchewan, Alberta, Canada, April 1978.
- 2 Mumme, W.G. and Scott, T.R., The relationship between basic ferric sulphate and plumbojarosite, *Am. Mineral.*, 15 (1966) 443–453.
- 3 Palache, C., Berman, H. and Frondel, C., *The System of Mineralogy*, Vol. 2, John Wiley and Sons Inc., London, 1951, 568 pp.
- 4 Taguchi, Y., Kizawa, Y. and Okada, N., Beayerite from the Osarizawa mine, *Kobutsugaku Zasshi*, 10(5) (1972) 313–325.
- 5 Dutrizac, J.E., Characterization of Sherritt Gordon jarosite residues, CANMET Report: MSL-INT 78-22, April 1978, Dept. Energy Mines and Resources, 555 Booth Street, Ottawa, Canada.

- 6 Fairchild, J.G., Artificial jarosite — the separation of potassium from cesium, *Am. Mineral.*, 18 (1933) 543—547.
- 7 Dutrizac, J.E. and Kaiman, S., Synthesis and properties of jarosite-type compounds, *Can. Mineral.*, 14 (1976) 151—158.
- 8 Parrish, W. and Irwin, B.W., Data for X-ray analysis, Vol. 1, Charts for solution of Bragg's equation, Philips Tech. Library, 1953.
- 9 Diffraction Index, Inorganic Index to the Powder Diffraction File, Joint Committee on Powder Diffraction Standards, Swarthmore, Pa., U.S.A., 1972.
- 10 Stewart, J.M., Kruger, G., Ommann, H.L., Dickinson, C. and Hall, S.R., The X-ray System of Crystallographic Programs, Univ. Maryland Computer Sci. Centre, Tech. Rep. TR-192, 1972.
- 11 Kubisz, J., Studies on synthetic alkali-hydronium jarosites. I. Synthesis of jarosite and natrojarosite, *Mineral. Polonica*, 1 (1970) 47—59.
- 12 Brown, J.B., Chemical study of some synthetic potassium-hydronium jarosites, *Can. Mineral.*, 10(4) (1970) 696—703.
- 13 Kubisz, J., A study on minerals of the alunite-jarosite group, *Polska, Akad. Nauk, Prace Geol.*, 22 (1964) 9—93.
- 14 Kashkay, C.M., Borovskaya, Y.B. and Babazade, M.A., Determination of ΔG°_{298} of synthetic jarosite and its sulphate analogues, *Geokhim.*, 5 (1975) 778—784.
- 15 Zotov, A.V., Mironova, G.D. and Rusinov, V.L., Determination of ΔG°_{298} of jarosite synthesized from a natural solution, *Geokhim.*, 5 (1973) 739—745.
- 16 Handbook of Chemistry and Physics, 54th Edition, CRC Press, Cleveland, Ohio, 1973.

SUBJ
MINING
FCAU

Formidable Challenges Await Uranium Mining

A record 9.37 million tons (10.33 million st) of uranium ore was mined by open-pit and underground methods in 1977, according to the Department of Energy. With the demand for uranium expected to increase by about 15% annually through 1985, the challenges ahead for US miners are formidable.

While most uranium will be mined by open-pit and underground methods, contributions from nonconventional sources, such as in situ and byproduct recovery techniques, will be needed to meet the developing gap between uranium supply and demand.

In situ mining and byproduct recovery from wet process phosphoric acid could each grow to an annual capability of about 3600 ty (4000 stpy) of U_3O_8 during the next 15 years. However, as DOE's John Klemenic cautioned, "The growth of the solution mining industry is difficult to project, as the technique is still largely in the demonstration stage."

Underground Mining

DOE's Fred Facer, Jr., reported that 50% of the underground uranium mines in the US did not produce in 1977. Most of these nonproducers are small mines which in 1977 either closed or switched from production to development work. The uranium industry has compensated for this loss in production mainly by increasing ore production from operating mines.

US mines are generally larger and deeper than those of prior years. Room and pillar as well as open stoping methods are primarily used in the larger operations. The average grade of uranium ore produced from underground mines has remained at 0.17% U_3O_8 for about two years and is unlikely to change much during the next two years, according to Facer. The amount of uranium in ore produced from underground mines was slightly less than that in ore produced from open pits in 1976, and there will be little, if any, change in the proportion of uranium ore from underground mines in 1977. On a tonnage basis, 46% of the ore came from underground mines and 54% from open pit.

Open-Pit Methods

As labor costs and uranium prices increase, more firms have elected to mine ore deposits at depths greater

This article is based on information supplied by J. Fred Facer, Jr., US Department of Energy; William C. Larson, US Bureau of Mines; and William M. Leader, Uranium Recovery Corp.

than 76 m (250 ft) by the less labor-intensive open-pit methods, although there are more apparent environmental problems associated with open pits than with underground mines.

During 1977, there was extensive overburden removal in many areas to prepare deposits for mining. At the seven largest existing open-pit operations, mining plans called for the stripping of 180 million tons (200 million st) of waste, while mining 6.6 million tons (7.3 million st) of ore.

Production of uranium in ore from open pits should remain about the same as that from underground mines for the next several years. The ore grade recovered from open pits ranged from 0.025% to 0.250% U_3O_8 and averaged 0.145% for 1976 and 1977. This grade is expected to decrease slightly during the next two years, but it will be a leveling trend rather than the sharp drop of the previous four years.

In Situ Methods Accelerate

The number of new pilot-scale uranium in situ leaching operations is increasing almost monthly, according to US Bureau of Mines' William C. Larson. Operators who have completed pilot-scale or commercial operations are applying for new or expanded source material licenses. This activity is particularly true in Texas, Wyoming, and New Mexico.

Recovery of uranium by in situ methods has contributed less than 1% of US supplies. Although the 1% level will be exceeded in 1978, commercial in situ applications are expected to be few, since conditions are generally unfavorable at many ore deposits, according to Facer.

Although some firms choose the in situ method because it seems to involve fewer environmental problems than conventional mining, Facer noted that this may prove to be illusory. Restoration of an in situ leach well field to its approximate condition has not been demonstrated on a large scale.

Byproduct Uranium—Prices Spur Activity

Between 1951-1961, three firms recovered some 500 000 kg (one million lb) of U_3O_8 from wet-process phosphoric acid. Work on these processes ended in the 1960's with the discovery of the Ambrosia Lake District in New Mexico. Uranium from New Mexico sources became more economical to recover than that from phosphate byproducts.

But as William M. Leader, Uranium Recovery Corp. (URC) noted, "Although the commercial separation of uranium from phosphoric acid was stopped, considerable interest remained, owing to the fact that if the U_3O_8 is not removed from the phosphoric acid at its manufacturing point, it is essentially lost as far as its energy value is concerned." A favorable price and increasing demand have accelerated developments in recent years. According to Leader, about five thousand tons of uranium are mined along with the phosphates in central Florida every year.

Four other firms are committed to building uranium recovery facilities at phosphoric acid plants in the near future:

■ Freeport Minerals Co. has a uranium recovery plant under construction at its phosphoric acid plant at Uncle Sam, La. With an initial capital cost of \$32 million, the plant is scheduled for startup in 1979. Some 313 000 kg (690,000 lb) of yellowcake is expected to be recovered annually.

■ Gardinier Inc., in East Tampa, Fla., has contracted with Jacobs Engineering to construct a uranium recovery plant at an estimated cost of \$20 million. The Gardinier (US Phosphoric Products) plant produced considerable uranium from phosphoric acid prior to 1961 and in recent years has tested an improved process on a pilot plant scale. The plant is expected to begin operations in 1979 and is designed for 193 000 kg (425,000 lb) yellowcake capacity.

■ Wyoming Mineral Corp., a subsidiary of Westinghouse Electric, has a uranium recovery plant under construction at the phosphoric acid plant of Farmland Industries, Pierce, Fla. The 181 000-kg/y (400,000-lb-per-yr) capacity plant is expected to come onstream during 1979. Startup testing of the process was expected in 1978.

■ International Minerals Corp. (IMC) will invest about \$70 million to more than double its uranium oxide production capacity to about 910 000 kg/y (2 million lb per yr). Its plan involves an agreement with CF Industries to purchase about 540 000 kg (1.2 million lb) of uranium per year for a 12-year period.

Finally, recovering uranium as a byproduct from copper operations was initiated by Wyoming Mineral Corp. at Kennecott Copper Corp.'s Bingham Canyon copper dump leach operation in Utah. While the process is not trouble free, it has been found feasible. Potential uranium production by the various copper operations could be 500 to 1000 ty of U_3O_8 by 1983, according to Facer. □

Uranium
- Uranium
Mining Engineering
Vol. 30, No. 10
October 1978

US Uranium Mines and Mills

The following list of US companies, mines, and mills engaged in uranium production was compiled by the Health and Safety Analysis Center, Mine Safety and Health Administration, in Denver, Colo. The list includes those companies reporting to the Center in 1978.

Thanks to D. K. Walker, Chief of the Health and Safety Analysis Center, for providing the information to MINING ENGINEERING.

- Allied Shumway Minerals**
Jimbo Bob #21 Mine
Yellow Circle Mine
- Anaconda Co.**
Anaconda Jackpile P-10
Bluewater Mill
Jackpile Paguate Unit
P.W. 2/3
- Anderson Brothers Mining & Drilling Co.**
Louise Mine
- Associated Energy**
Farmers Knob Mine
- Atlas Minerals Division of Atlas Corp.**
Mine No. 2
Calliham Mine
Far West Incline
Sage Mine
Four Corners Mine 4, 5, 6, and 2
Wood Mine
Moab Mill
Snow Mine
Big Buck Group
Patti Ann Mine
Standard No. 2
Columbus UG—With Felix Mendisco
- B & L Mining Co.**
Peanut No. 2
- Bear Creek Uranium Co.**
Bear Creek Operations
- Bell Mining Co.**
Helen #1 C-SR-15
- Benson Mining and Machinery**
Uranium Girl
- Ben Urralburu Mining Co.**
Blondie
Murietta
- Blerschied Mining Co.**
Blue Bird Mine
Locust Mine
- Big Indian Uranium Corp.**
Bacardi Bobtail D & D
- Binder Mining Co.**
Peggy #2
- Birch Mining Co.**
Mine #9
- Blake Mining Co.**
Rainbow Mine
Smoky Mine
Veta Mad(C-SR-13A)—with ERDA
- Bokum Mining & Exploration**
Marquez Shaft
- Brooks Minerals Inc.**
Centennial
Horseshoe Mine
Lazy L
Parrot Railroad Tunnel
Suncup #2
- C & D Exploration Inc.**
Yellow Bird #1
Eureka
- C & H Mining Co.**
Buckhorn
Little Fawn No. 1
- Calvin Black Enterprises**
Markey-Nap-Poochie
- Centennial Development Co.**
Probe Shaft
- Chevron Resources**
Panna Maria Project
- Cimarron Mining Co.**
Spanish Trail Mine
- Cleghorn and Washburn Mining Co.**
Pandora Mine UG
Snow Mine
Rex 38
- Cobb Nuclear Corp.**
Westbranch Mine
- Coff Nuclear Corp.**
Section 12
- Cole & Co Mining**
Fox Mine
- Cott Mesa Mining Co.**
Strike No. 1
Hanni No. 1
Horse Head Mine
Smith Pit
Wild Horse Pit
- Continental Oil Co.**
Karnes County Pits
Conquista Mill
House Pit
Hurt Pit
Dybowsky Pit
- Cotter Corp.**
Bokan Mountain Dotson Claims
C-LP-21
Cotter Mill
Letty Jones
Schwartzwalder
S M 18 Mine
- C. W. Bunker Mining Co.**
Shady Lady
St. Patrick No. 7
- Dawn Mining Co.**
Dawn Mill
Midnite Dawn Mine
- D. C. Bunker Mining Co.**
C-SR-13
Early Morning—with Short and Impson
- Degerstrom N A Inc.**
Midnite-Dawn Mine
- Deloy Shumway Mining Co.**
Cottonwood #1 Mine
Strawberry Mine
- Demco Mining Co.**
Congress 46
- Doran Hunt Mining Co.**
Dexter
- Durfee Mining Co.**
Farmer Girl
- Eagle Peak Mining Co.**
Civit Cat Mine
- Earl Bell, Operator**
April Mine
- Edward E. Miller**
Alice No. 2 LC-SR-IS
- Ekker & Hunt Mining Co.**
Trackyle Pits
- Energy Fuels Nuclear Inc.**
Hanksville Uranium Buying Station
Hillside Mine
Ladwig Mine
- Eugene Shumway Mining Co.**
Cottonwood 4
- Exxon Minerals Company USA**
Buffalo Shaft
Highland Uranium Operations
Stonewall Bay
- Farris Mines Inc.**
St. Anthony Stripping
- Federal American Partners**
Table Stakes No. 2
Federal American Underground Mill
- Felix Mendisco Mining Co.**
Rim-Columbus
C-J-D-9
- Forward Drilling Inc.**
Peterson Lease
- Four Corners Mining & Mineral**
Maw
- Frank T. Wilson**
B-Chitty-U
- Gates & Fox Co. Inc.**
C-JD-5
- General Electric, Nuclear Division**
Ore Buying Station
- Getty Oil Co.**
Petrolomics Mill
- Golden Mining Corp.**
Black-Ape Mine

Graham Mining Co. Rosebud Mine	James Hamilton Construction Co. Jack Pile-Pit	Look Mining Co. Cottonwood #2 Yellow Jacket Mine V-8 Mine
Gramlich Exploration Co. San Juan	Jerry Stocks Mining Co. Bridger-Jack Mine	Lucky Mc Uranium Corp. Lucky Mc Mine Operations Big Eagle Mine Lucky Mc Mill
Graeger and Switzer Mining Showboat Mine	Jim Butt Mining Co. Yankee Girl White Canyon No. 1 Daisy Mine Yankee Girl 6 Last Hope Pit Bullseye Mine	Lyman Shumway DBA ME Mng Sad Sack Mine
Great Lakes Chemical Corp. Little Sparkler Mine	Johannsen Mining Co. Sago Lily Lou	Lysa Mining Co. Silver Dollar #1
Gulf Mineral Resources Co. Mariano Lake Mine Mt. Taylor Mine	John Beres Mining Co. Stafford #5	M & M Co. Doris-Extension
Hannert Mining Inc. Lucky Strike Mine	Johnson Brothers Co. Bill Smith Open Pit	Martin-Trost Associates Miracle Mine
Harrison-Western Industries Mt. Taylor Mine North Morton Shaft	Jones & Hopper Pond Mine Windswept Group	Michael Moore Small Fry Mine
Harry H. Harp, Jr. Midnight Mine	K-Enterprises Posey Mine Mckenzie Cliff House Mine	Mike Graeger Echo #2
Heidenfels Brothers Felder Uranium Operation	K and K Mining Co. Sinpatica No. 1	Minerals Exploration Co. Sweetwater Uranium Mine
Hlael-Miller Mining Co. Herbert C-SR-13	K M S U Mining Inc. Cougar Ventures	Minerals Recovery Corp. West Incline
Homestake Mining Co. Pitch Property	Kelley Mining Jack Knife Glade Mine	Minerals West Corp. Expectation Mine McCormick Drift
Home Town Mining Co. Radium King	Kelmine Corp. C-JD-6 C-JD-7 Mineral Joe Group Duggan Adit	Mobil Oil Co. Obern Leach Plant
Hubbard Mining Co. Hubbard Mine	Kendrick Bay Mining Co. Ross-Adams	Mosher and Nelson Mining Co. Fry 4 Mine
Hunt Key North Knob Mine	Kerr McGee Nuclear Corp. Sec 24 14N 10W Sec 30 14N 9W & 29 1 Sec 30 West Section 33 Sec 35 Mine Sec 36-UG Rio Puerco Sec 17 14N 9W Section 19 Churchrock #1 Mine Bill Smith Sullivan Mine	Murphy Mining Co. Waterfall Mine
Hydro Jet Services Inc. Lucky Strike	Koppen Mining Construction Corp. Spencer Shaft	Nelson Mining Co. Geneva Incline
I & S Trucking Radium King West Channel Mine	Krabbe Mining Happy Jack	Nicola Copper Mines Ltd. Winnfield McCormack
INCE Minerals Corp. C-LP-22 Mine C-BL-23 Peaches October Adit—with Atlas Corp.	Lammert Mining Co. State School Section ML 23598 State Lease 8058	Oral Clark Mining Co. Shinarump
Intercontinental Energy Corp. Pawnee Mine	Laura Mining Co. Laura Mine	Pacer Corp. Virginia Mine
J & J Mining & Exploration Riverview	Leland Bennett Rye 8	Palangana Dome Palangana Project—with Union Carbide
J & R Mining Co. North Wash Pit		Pathfinder Mines Corp. Shirley Basin Mine and Mill
J & S Mining Co. Alice C-SR-15		Petrofomics Petrofomics Mine
J R J Joint Ventures North Alice		Phillips Uranium Co. Noserock No. 1 Mine
Jack Thompson Mining Sears #1		Pickett Corral Andrew's Mining Co.
Jack T. Watterson Mining Co. Jack One Mine Dime Mine Drill Pit		Pierce Mining Radium #6
		Pinal Mineral and Mining Ltd. Lucky Boy

Pioneer Uranium Inc.
St. Jude Mine
Carnation
Geo #1 Mine
Mum

Plateau Mining Co.
Belmont No. 1
Arrowhead 8

Plateau Resources Ltd.
Plateau Buying Station

Quad-Honstein Joint Venture
Pine Ridge No. 1 Mine

R M E—J. V. Halliburton
Mine Mile Lake Pilot Plant

Rajah Ventures Ltd.
Rajah 49
Atlas-Bonanza
Bonanza
C G 25—with ERDA
Thornton Group
Lost Dutchman

Ralph Foster and Sons
Mesa #5 (CG-27)
Mineral Channel No. 12

Rampart Exploration Corp.
High Park Pit

Ranchers Exploration & Development
Hope Mine
Johnny M. Shaft

Ray Williams Mining
Enos Johnson

Reserve Oil & Minerals Corp.
Poison Canyon

Rio Algom Corp.
Lisbon Mine

R. L. Starks
C-SR-11 Brighton
Nota Z C-SR-16

S and M Exploration
Black Jack Mine

S & S Mining
Old Rattler Mine

Sage and Sage Mining Co.
Starlite 7

St. Jude Mining Co.
Ike C SR 11
Patrick D C-SR-16
Ann-C-SR-16
C-SR-12

Seraphin Engineering
I and L Mine

Shelco Inc.
State Lease 34281

Shumway and Shumway Mining Co.
Giveaway

Silver King Mines Inc.
Lion #2 Pit
Darrow #3 Pit
Darrow #4 Pit
Darrow Lease

Small Ray Mining Co.
Vanadium Queen

Sohio Natural Resources Co.
J J #1 Mine
L-Bar Uranium Mill

Strategic Minerals Inc.
Bujan

Taminco Inc.
Club Mines

Temple Rock Mining Co.
Vanadium King No. 6 Mine

Todillo Exploration & Development
Haystack Underground
Haystack Open-Pit

Trio Industries Inc.
C-SR-16A
TCE Mine #1

Union Carbide Corp.
East Gas Hills Mill
Coloradian
New Verde
King Solomon Mine
Grace
Maybell Pit
Rackrat Mine
Fawn Springs #9
Ura
Maybe
Nil
Wilson Spgs Pt & Pit
Lasal Mine
Snowball Mine
Sunday
September Morn
Rajah 30
Mining & Metals Div Rifle Mill
Deremo-Snyder
Blackburn Mine
Burro Mine
East Area Pit
Eula Belle
Bagger
Long Park 15
Stafford Pit School Section
Maybell Plant
Radium Hill #10
Sunbeam
Paustreak Frances Mine
Wilson Silverbell Mine
Anna May
Donald L

Union Minerals Exploration
Red Desert Project

United Nuclear Corp.
South Morton Mine
North Morton Mine
Sandstone Mine
Sec 27
Ann Lee Mine
Church Rock Mine
Church Rock Mill
St. Anthony No. 2
St. Anthony Open Pit

United Nuclear/Homestake Partners
Section 13 Mine
Section 15
Section 23
Section 25
Sections 29 & 32
Mac Uranium Mill

University of Grants
Section 24

Urango Mining Co. Inc.
Urango Mining Company

Uranium Production Co.
Cottonwood
Dim Light Mine
Almost #2
Monte Cristo

Uranium Supply Services Corp.
Jenkins Project

US Bureau of Mines, Special Studies Section
Twilight #1

US Energy Corp.
Pay Dirt North Incline
Golden Goose #2

US Steel Corp.
Clay West Uranium Plant

Utah International Inc.
Lucky Mc Mine

Utah West Mining and Development
Delta Mine

Vernon Moores and Sons
Wedge

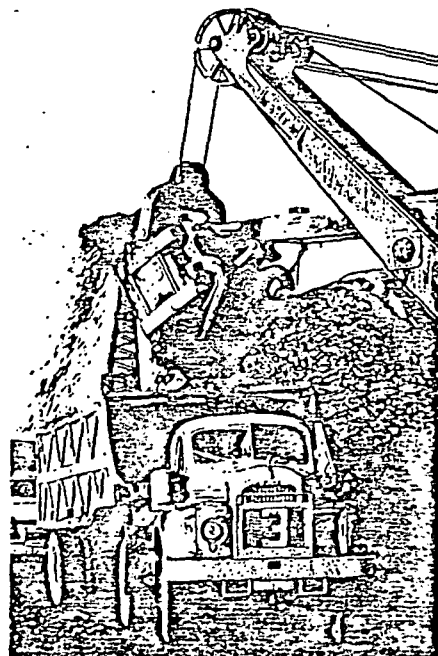
W. D. Tripp Mining Co.
Uintah

Western Nuclear Inc.
Sherwood Project
Ruby No. 1
Sheep Mountain Operations
Split Rock Mill
White King Mine

Whitelock Corp.
Thornberg Mine

Williams Inc.
Last Chance 3

Wyoming Mineral Corp.
Bruni Solution Mine
Sutter Creek Operation



In connection with the foregoing, a stagewise flotation scheme with an increased degree of additional crushing in the selective cycle is desirable.

With existing unchanged grinding conditions, before the collective and copper flotations of massive ore we must reduce the sphalerite size in the zinc cycle feed of the flotation process to 30 μm .

The weak activity of tennantite in comparison with the principal copper-containing mineral in the ore (chalcopyrite) is evidently due to the nonoptimal conditions for its flotation in a highly calcareous medium.

Thus in the organization of ore processing, the level of extraction of the metals is governed by the content of the minerals in the raw material, the crushing size of the minerals during ore preparation, and their flotation activity in the different size classes. Statistical analysis of the performance of a beneficiation plant revealed the need to shift the floatability peak of the useful minerals for most currently won sulfide ores to the $-30 + 10 \mu\text{m}$ size class; this requires an improvement in the ore preparation processes under industrial conditions and an increase in the degree of crushing of the ores.

**UNIVERSITY OF UTAH
RESEARCH INSTITUTE
EARTH SCIENCE LAB**

LITERATURE CITED

- V. I. Mitrofanov et al., Present Level and Prospects of Beneficiation of Copper and Copper-Zinc Ores of the Urals [in Russian], Tsvetmetinformatsiya, Moscow (1971).
S. I. Mitrofanov et al., Tsvet. Met., No. 9 (1975).
L. A. Barskii, Author's Abstract of Doctoral Dissertation, IGI, Moscow (1968).
V. Z. Kozin et al., Trudy SGI im. V. V. Vakhrusheva, Sverdlovsk, No. 52 (1968).
N. P. Zhukovskii and A. S. Petrov, New Methods for Technological Calculations in Beneficiation [in Russian], Nedra, Moscow (1969).
6. P. Chilstead, Eighth Int. Conf. on Mineral Beneficiation, Vol. 1, Leningrad (1968).
7. S. I. Mitrofanov, Selective Flotation [in Russian], Moscow (1958).
8. S. I. Mitrofanov, M. Ya. Ryskin, et al., in: Comprehensive Utilization of Mineral Resources [in Russian], Alastan, Erevan (1977).

SUBJ
MNG
FCES

FEASIBILITY OF COMBINING THE EXTRACTION-SORPTION TECHNOLOGY
OF TREATMENT OF SOLUTIONS WITH BACTERIAL-CHEMICAL LIXIVIATION
OF COPPER-ZINC ORES

Soov. Mining Science
v 16 N2, 1980

A. I. Golomzik, V. F. Travkin,
N. V. Dranitsyna, and T. L. Mikhailova

One of the principal trends in the development of present-day hydrometallurgy is the use of extraction-sorption processes for recovering metals from lixiviation solutions.

Undertakings have already tested and mastered the processes of extraction of copper from an electrolytic precipitate; pilot tests are being made on technological schemes for extracting copper and zinc from solutions of various compositions [1-3]. The combination of extraction and sorption processes in a single scheme may also prove promising, both from the viewpoint of complete utilization of the components of the solutions, and for the purpose of organizing water recirculation, especially in the case of a high iron content in the productive solutions.

In this article we study the theoretical possibility of using these processes to extract copper and zinc from solutions from underground or dump bacterial-chemical lixiviation. Since the spent solutions must be recirculated, we investigated the influence of extraction of copper and sorption of zinc on the activity of *Th. ferrooxidans* in the circulated solutions.

Uralsmekhanobr, Sverdlovsk. Translated from Fiziko-Tekhnicheskie Problemy Razrabotki Poleznykh Iskopaemykh, No. 2, pp. 113-116, March-April, 1980. Original article submitted May 22, 1979.

The productive solutions from lixiviation of ore from one of the sulfide deposits had low copper and zinc contents and high iron concentration.

The technological scheme shown in Fig. 1, which has been studied in scaled-up laboratory conditions, included bacterial-chemical lixiviation of the copper-zinc ore, extraction of copper from the solution, sorptive extraction of zinc from the decopperized solution, and return of the clarified solution after extraction to recirculation for lixiviation. Since the main aim of our work was to establish the feasibility of using the solutions as recirculate for lixiviation, and also owing to the difficulty of organizing counterflow in the laboratory, the extraction and sorption of the metals was carried out in nonoptimal conditions. The sample of lixiviated ore contained (per cent): Cu_{tot} , 1.79; Cu_{oxide} , 0.067; Zn, 1.12; Fe_{tot} , 34.1; $Stot$, 38.6; SiO_2 , 15.0; Al_2O_3 , 0.34; MgO , 0.1; CaO , 0.38; Co, 0.018; Ca, 0.005; As, 0.075.

One-third of the copper in the ore is in the form of secondary sulfides (mainly chalcocite); the rest is in the form of primary sulfides and oxides. The zinc, sulfur, and iron are almost entirely in the form of sulfides; the main ore component is pyrite (up to 80%). The predominant nonore components are chlorite and quartz.

The active culture of bacteria was added both to the lixiviating solution before irrigating the ore with it and to the productive solution after lixiviation. In inoculating the productive solution it is necessary to completely oxidize the ferrous iron to ferric and then to hydrolyze it; this operation avoids conversion of the iron to tar with sorption of zinc and contamination of the eluate.

After bacterial oxidation of iron, the solution (now containing 1.24 g/liter of Cu, 0.78 of Zn, 0.035 of Fe^{2+} , and 4.6 of Fe_{tot}) goes on to extraction of copper. This is effected by means of a 12% solution of ABF [4] in kerosene in the counterflow mode in the following conditions: three-stage extraction; ratio of volumes of organic and aqueous phases, 1:1.2; duration of contact between extracting agent and productive solution, 3 min; duration of layer separation of phases, 10 min. The extraction of copper into the organic phase was 84.5%.

Zinc was extracted by sorption from the decopperized solution (Cu, 0.15 g/liter; Zn, 0.76; Fe_{tot} , 4.35). The sorbent was aminocarboxyl ampholyte ANKB-10. Since its sorption capacity for zinc is greatest at pH 6.0-6.5, to the decopperized solution we added milk of lime (10% CaO). Zinc was extracted from the hydrate pulp in counterflow conditions.

In four sorption stages, 85.2% of the zinc was extracted from the solution with a 1:10 ratio of the ion-exchanger and solution currents and a contact duration of 40 min between the ion-exchanger and the solution in each stage. As a result of regeneration of the sorbent with 20% solution of sulfuric acid we obtained a zinc eluate which can be further treated by the usual techniques [5] to give zinc sulfate.

The copper eluate obtained by reextraction is suitable for the production of copper by electrolysis [6].

In connection with the necessity of recirculating the clarified solutions for lixiviation, we investigated the influence of the extraction and sorption operations on the metabolism of *Th. ferrooxidans* cells.

In the productive solution proceeding to copper extraction, the concentration of bacteria was 10^7 cells/ml. The activity of the cells, measured by means of tagged carbon dioxide ($C^{14}O_2$), was 13,600 pulses per 100 sec in 10 ml of solution. After extraction of copper the concentration of cells fell to 10^4 cells per milliliter, and the activity of the cells decreased by three orders of magnitude. In the next few days, in this solution the concentration of living bacteria remained at the level of 10^4 cells per milliliter; however, the activity of the cells fell to zero.

The number of bacteria in the pulp tailings from zinc sorption was 10^3 cells/ml. After the pulp had settled, no cells were found in the clarified solution, and the concentration of bacteria in the wet sediment was 10^3 cells per milliliter of sediment. Thus practically all the bacterial cells go into the sediment, and the clarified solution recirculated for lixiviation must be fortified with acid, iron, and active bacterial cells.

If there is a low content of bacterial cells in the original solution subjected to extraction (10^3 - 10^4 cells/ml), the cells disappear entirely from the solution after this operation.

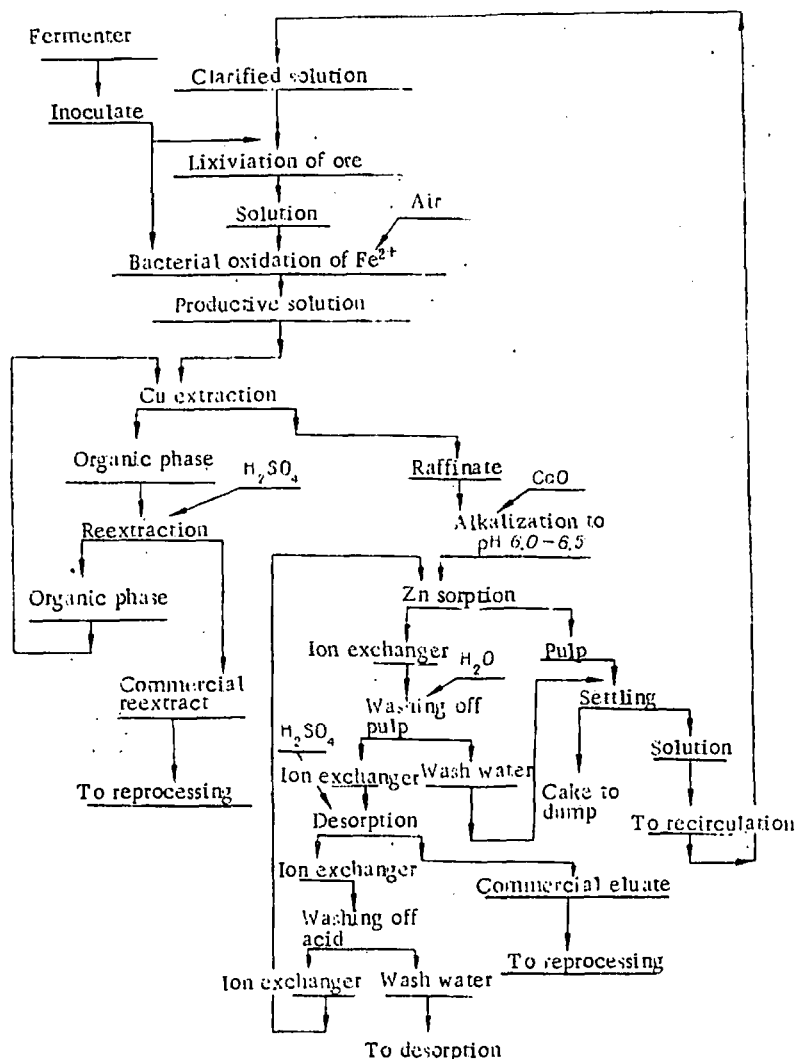


Fig. 1. Theoretical technological scheme of processing solutions from bacterial-chemical lixiviation of ore by the extraction-sorption method.

We checked up on the growth and oxidative capacity of the *Th. ferrooxidans* cells when added to the tailings from extraction of copper and sorption of zinc, to which has been added ferrous iron in a concentration of 3-5 g/liter and acid to make up to pH 1.7-1.8.

In the residual solutions after extraction of copper and sorption of zinc, the bacteria do not die and do not lose their oxidative capacity. In the solutions after extraction for 7 days their numbers increase from 10^4 to 10^6 cells/ml and the iron is completely oxidized; in the solutions after sorption of zinc when inoculating solution, ferrous iron, and acid are added this takes 3 days. Addition of elements of a nutritive bacterial medium did not influence the growth or oxidative capacity of the cells.

Thus, the tailings solutions from the metal extraction-sorption process can be used in the circulating water of bacterial-chemical lixiviation of ores. However, owing to the reduction in the absolute content of bacterial cells in these solutions, it is necessary to periodically add an inoculate from a bacterial cultivator to the circulating solutions. The amount of added inoculate must be calculated in each particular case in accordance with the bacterial content of the recirculating solution subjected to lixiviation.

LITERATURE CITED

1. V. N. Startsev et al., *Tsvet. Met.*, No. 13 (1973).
2. K. B. Lebedev (editor), *Ion-Exchangers in Nonferrous Metallurgy* [in Russian], Metallurgizdat, Moscow (1975).

3. A. V. Osina and Yu. S. Press, *Tsvet. Met.*, No. 3 (1978).
4. B. N. Laskorin et al., *Tsvet. Met.*, No. 6 (1975).
5. M. M. Lakernik and G. N. Pakhomova; *Metallurgy of Zinc and Cadmium* [in Russian], Metallurgiya, Moscow (1969).
6. V. F. Travkin, A. M. Zastavnyi, and N. P. Anikin, *Tsvet. Met.*, No. 5 (1978).

CHOICE OF PARAMETERS FOR SEPARATION IN AN ELECTROSTATIC FIELD IN DRUM-TYPE ELECTROSEPARATORS

A. I. Mesenyashin

The recommendations in the literature on the choice of optimal conditions of electroseparation are often not interrelated, owing, in particular, to the different characters of the electric fields [1]. The influence of certain electrical parameters on the separation process were discussed in [2]. In this article we will use analytical methods to investigate the influence of both electrical and mechanical parameters on the conditions of separation of weakly conducting particles in uniform and nonuniform electrostatic fields.

The efficiency of separation in an electroseparator may be regarded as depending on the distance through which the separated components of the material are removed from one another and also on the throughput of the separator. In the case of the widely used drum-type electroseparators, the optimum conditions correspond to the maximum distance between the points of breakaway of the components and the maximum peripheral velocity of the precipitation electrode (drum).

Separation in Uniform Electrostatic Field. Let us determine the angles of breakaway $\gamma_1 = \omega t_1$ and $\gamma_2 = \omega t_2$ of two components, and also the radius R_1 and rotation frequency ω of the precipitation electrode corresponding to the extremal distance between the points of breakaway of the two components, i.e.,

$$R_1(\gamma_1 - \gamma_2) = \max. \quad (1)$$

At the breakaway points M (Fig. 1) of the particles from the drum, the equations for the forces F_1 and F_2 acting, respectively, on the first and second groups of particles which are to be separated take the form

$$F_1 = m_1 g \cos \gamma_1 - m_1 \omega^2 R_1 \pm E q_1 \pm \beta_1 q_1^2 = 0, \quad (2)$$

$$F_2 = m_2 g \cos \gamma_2 - m_2 \omega^2 R_1 \pm E q_2 \pm \beta_2 q_2^2 = 0, \quad (3)$$

where mg is the force of gravity; g , acceleration due to gravity; ω , drum rotation frequency; t , time during which the particles are in contact with the drum, reckoned from the top point; $\gamma = \omega t$, angle of breakaway of the particles; R_1 , radius of the drum; q , charge on a particle; E , electric field strength; and β , coefficient depending on the geometrical shape and electrical properties of the particles.

Let us investigate the case of separation of weakly conducting particles, for which the charges on the particles, q_1 and q_2 , do not change appreciably during separation.

To determine the extremal values of expressions (2) and (3), we use Lagrange's multipliers [3].

Let us compile the function

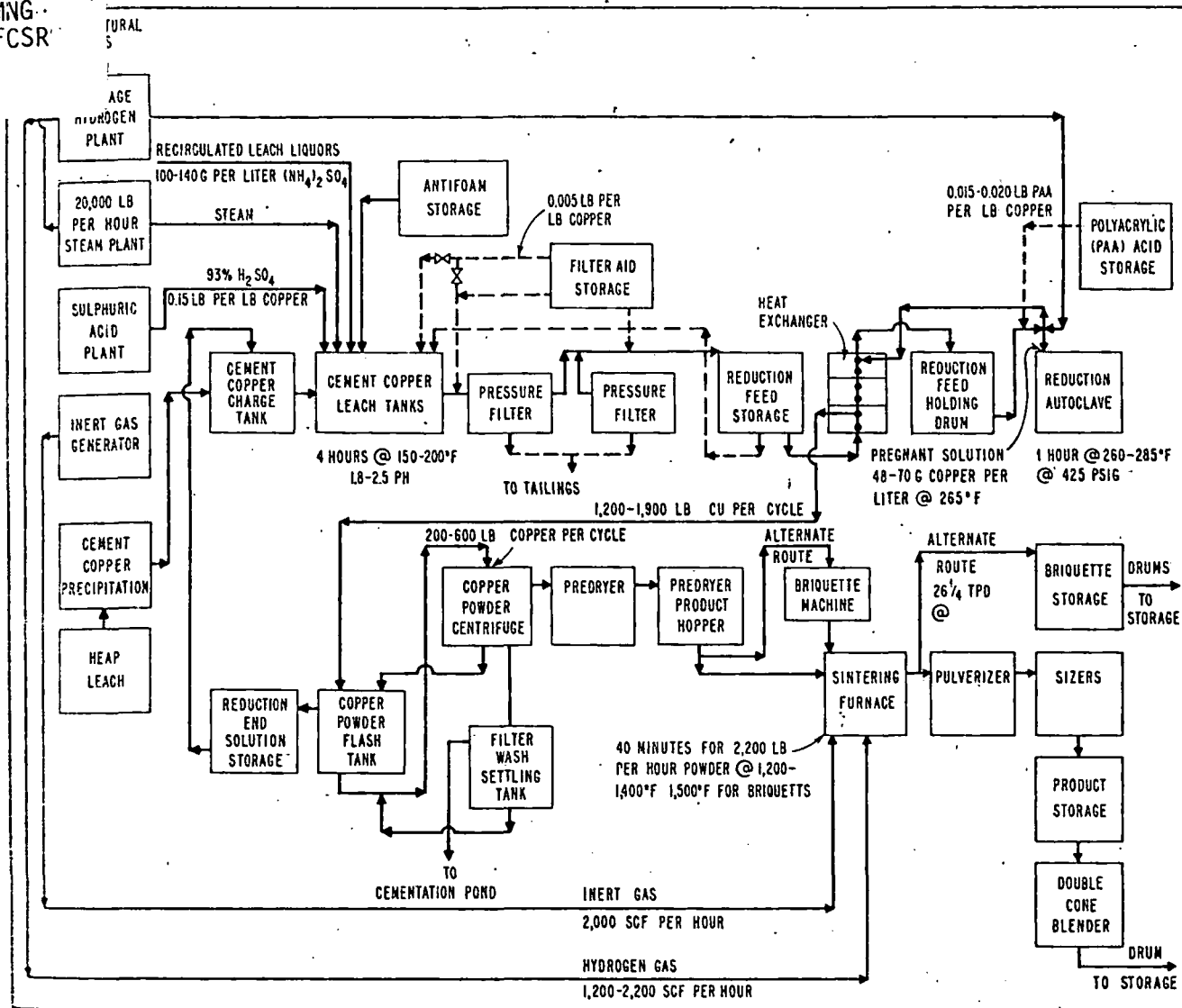
$$\Phi = R_1(\gamma_1 - \gamma_2) + \lambda_1 F_1 + \lambda_2 F_2, \quad (4)$$

where λ_1 and λ_2 are Lagrange's undetermined multipliers.

Assuming that the unknowns are $\gamma_1 = \omega t_1$, $\gamma_2 = \omega t_2$, ω , R_1 , λ_1 , λ_2 , we have the system of equations

$$F_1 = 0; \quad F_2 = 0; \quad \frac{\partial \Phi}{\partial \gamma_1} = 0; \quad \frac{\partial \Phi}{\partial \gamma_2} = 0; \quad \frac{\partial \Phi}{\partial \omega} = 0; \quad \frac{\partial \Phi}{\partial R_1} = 0. \quad (5)$$

Simferopol'. Translated from *Fiziko-Tekhnicheskie Problemy Razrabotki Poleznykh Iskopayemykh*, No. 2, pp. 116-120, March-April, 1980. Original article submitted February 14, 1977.



CHEMETALS CORP. OF NEW YORK researched gaseous reduction of copper from ammoniacal solutions over a period of years, and after a thorough economic study of these systems placed major emphasis on commercializing reduction from CuSO_4 media, as shown above.

First commercial-scale H_2 reduction plant for Cu on stream

UNIVERSITY OF UTAH
RESEARCH INSTITUTE
EARTH SCIENCE LAB.

Arizona Chemcopper's acid heap leach, hydrogen reduction of copper solution, and acid regeneration process offers a new perspective in copper metallurgy

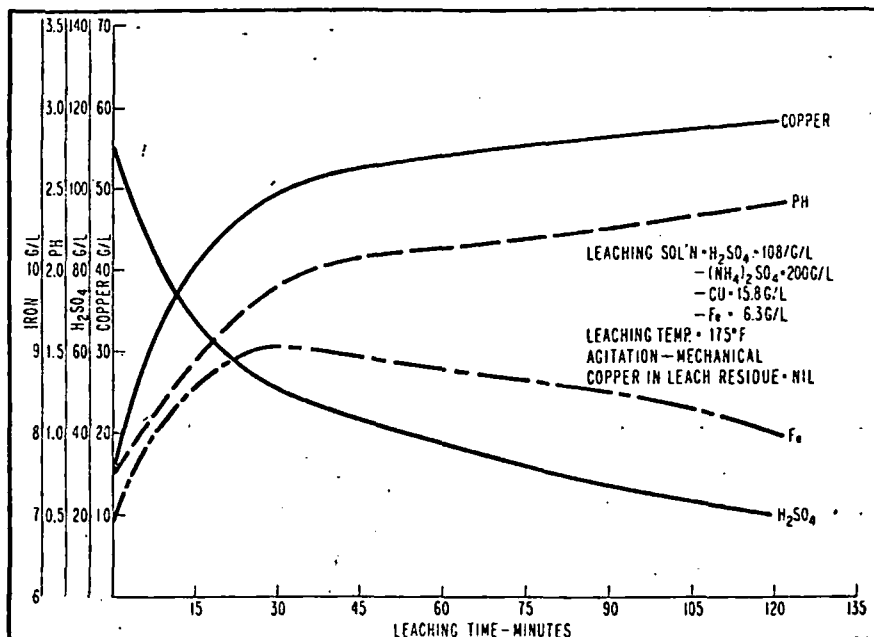
INTRODUCING a new technique to the copper industry, Arizona Chemcopper Corp.'s acid leach, hydrogen reduction route to high-purity copper products became operational in June 1966, in Bagdad, Ariz. Designed to take ore from Bagdad Copper Corp.'s open-pit, the plant will produce 8,250 tpy of either moulding grade copper powder, friction grade copper powder, copper oxide or copper briquettes. The new plant is the first commercial scale operation of its type, and is a natural development for meeting the growing demand of the powder metallurgy trade. This

market is estimated at approximately 17,000 tpy of pure copper powder and 25,000 tpy of powder for dispersion strengthened copper alloys.

Starting with cement copper precipitate, from the heap leach step at the mine, the material is fed to the copper refinery for processing into a high-conductance, essentially oxygen-free copper product. Feed material has a typical analysis of 82% Cu; 2.6% Fe; 0.4% Pb; 0.07% Sn; 0.5% acid insolubles, all on a dry-basis.

In the refinery, 15-ton batches of cement copper are

AFTER DECIDING on a major effort toward copper reduction by the acid media route, Chemetals teamed-up with Bagdad Copper Corp. of Arizona, and piloted the conversion of copper from impure precipitates into high-purity copper powder. Subsequent to this, and after the formation of Arizona Chemcopper Corp. by these two firms, Chemcopper placed its commercial-scale plant on stream, and found that ammonium-sulphate buffered solutions permitted a reduction of one-half in the leaching cycle. A buildup of Fe in solution also helped, and recovery of copper approaches 99% from the copper precipitates.



measured and slurried to 50% solids (by weight), with recycled reduction-end solution in one of two charge tanks. The slurry is then metered alternately from the charge tanks into the first of a series of five leaching cells. Here, leaching takes place in oxygen-enriched, ammonium sulphate buffered solutions.

William J. Yurko, plant manager, says that the leaching reactions are represented as:

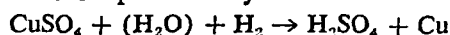
- 1) $Fe + H_2SO_4 + \frac{1}{2}O_2 \rightarrow FeSO_4 + H_2O$
- 2) $2FeSO_4 + \frac{1}{2}O_2 + H_2SO_4 \rightarrow Fe_2(SO_4)_3 + H_2O$
- 3) $Fe_2(SO_4)_3 + Cu \rightarrow CuSO_4 + 2FeSO_4$
- 4) $2FeSO_4 + 5H_2O + \frac{1}{2}O_2 \rightarrow 2Fe(OH)_3 \downarrow + 2H_2SO_4$
- 5) $3FeSO_4 + 4H_2O + \frac{1}{2}O_2 \rightarrow 2Fe(OH)_3 \cdot FeSO_4 \downarrow + H_2SO_4$

Iron is allowed to build up to 15 to 20 g per liter in the pregnant solution and, as a result, leaching rates are accelerated appreciably. During leaching, a defoamer is added to prevent excessive frothing in the cells. For this purpose, a 75% solution-strength of sodium dioctyl sulfosuccinate is metered into the leach tanks.

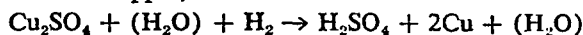
After leaching is completed at between 150° to 200°F and pH 2, the loaded solution (48 to 70 g per liter Cu) is passed through a pre-coated, leaf-type pressure filter. The clarified filter discharge is then pumped to storage in an acid brick-lined tank having a capacity of approximately 90,000 gal.

From this tank, 3,600 gal of pregnant aqueous is fed to either of the two reduction autoclaves, which are also equipped with agitators. About 1,200 to 1,900 lb of copper are reduced per cycle.

Copper concentration of the pregnant solution is thus reduced to 10 g per liter during this operation. The two autoclaves operate on a one-hour difference in cycle time over a two-hour reduction schedule. For heat conservation, one autoclave is always being discharged while the holding drum is filled. When one reactor is empty, the content of the 3,600 gal holding vessel is immediately dumped into the awaiting pressure container, thus beginning a new reduction cycle. During the cycle, sulphuric acid is regenerated and copper powder is formed. Metal is precipitated under conditions represented by:



... for raw copper, and ...



... for copper oxide.

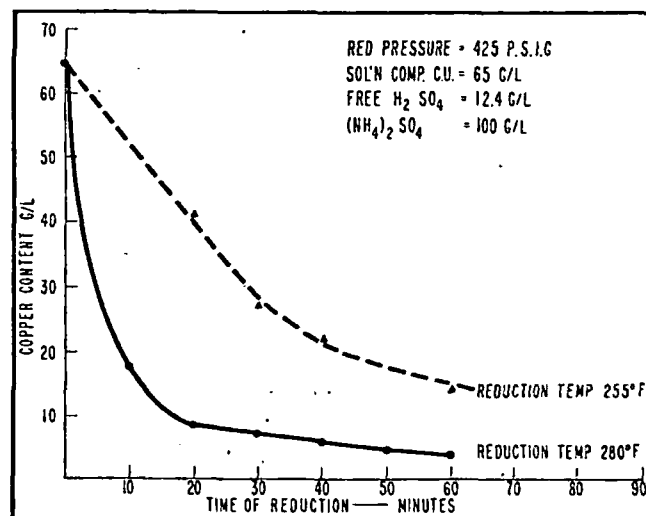
Just prior to discharging an autoclave, the agitators are shutoff to permit the copper powder to settle and to influence the next reduction charge. This operation is called powder densification, and it controls to a degree the apparent density of the copper powder produced. One operation of this nature is now being used in the production schedule.

Polyacrylic acid used as anti-plastering aid

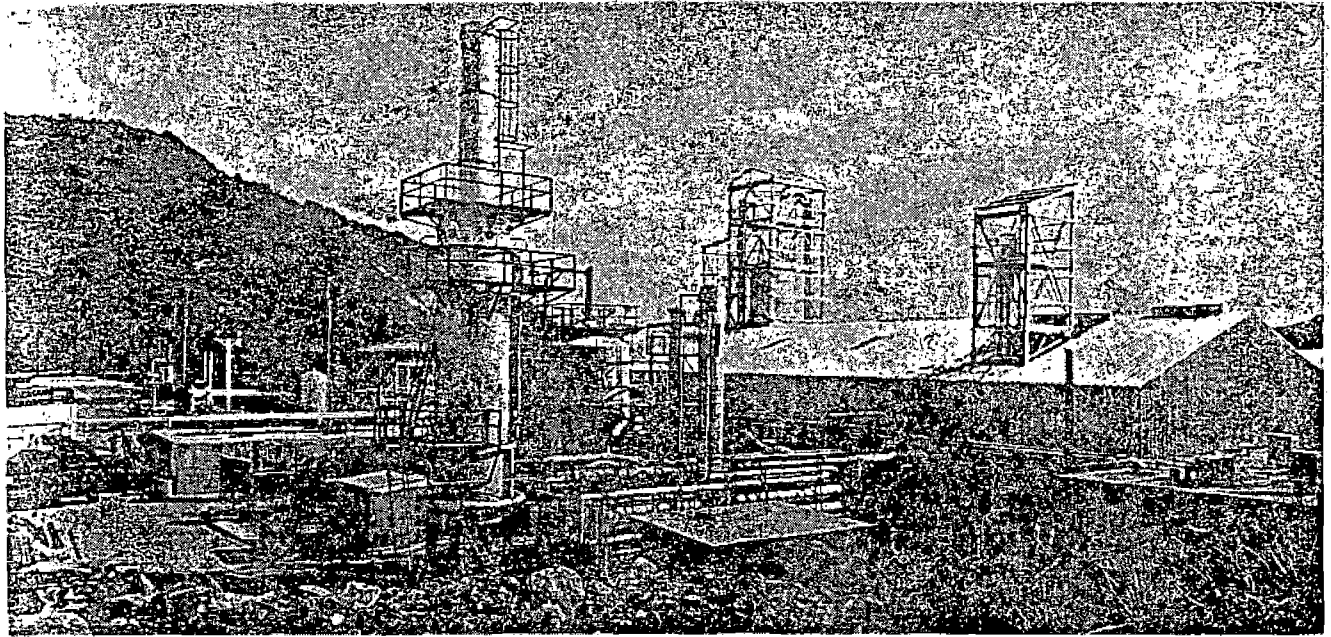
Polyacrylic acid is added during the reduction cycle at the rate of 0.01 to 0.02 lb per lb of precipitated copper powder, to minimize plating and to control particle-size distribution of the product.

Finishing (purification) of the precipitated copper powder starts with the decantation of reduction-end solution from the settled solids. The solution is then recycled to storage to be used later for dissolving more copper in the initial leach section.

After thickening, the concentrated slurry is dewatered further, and washed in a batch-type centrifuge before drying.

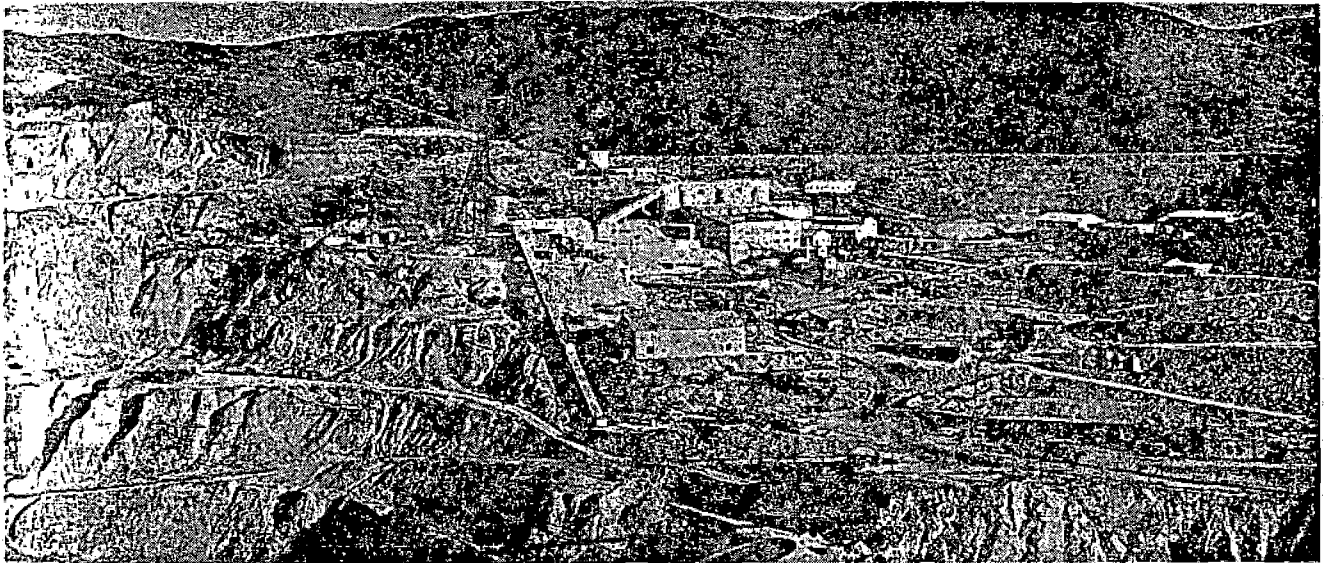


REDUCTION RATE AND DEPTH is dependent primarily on reduction temperature. Below 280°F equipment corrosion rates are acceptable.



ARIZONA CHEMCOPPER CORP.'S PLANT takes cement copper, dissolves it in H_2SO_4 , clarifies the solution, and then converts the con-

tained copper into powder of 99.9% purity. Reduction of batches in the autoclave produces from 1,200-1,900 lb of Cu powder.



BAGDAD COPPER CORP.'S open pit (shown above) supplies ore to the acid heap leach, cement copper precipitation circuit at Bagdad,

Ariz. Cement copper from this unit serves as feed material to Arizona Chemcopper's gaseous, hydrogen reduction plant that is nearby.

Drying is conducted in a rotary dryer having a controlled atmosphere which allows partial oxidation of the carbonaceous material. Besides the normal products made, it is also possible to obtain highly oxidized material from the dryer for sale as low-grade oxide.

From the dryer, the high-purity powder can be converted to copper powder directly by hydrogen reduction in a sintering furnace, or briquetted at 10,000 psi into 2 oz copper pillow blocks, prior to sintering.

Final product, boxed as briquettes, is shipped for melting stock. Copper powder is pulverized, sized, blended and packaged in steel drums for shipping. Physical and chemical characteristics of the powder are tailored to customer specifications.

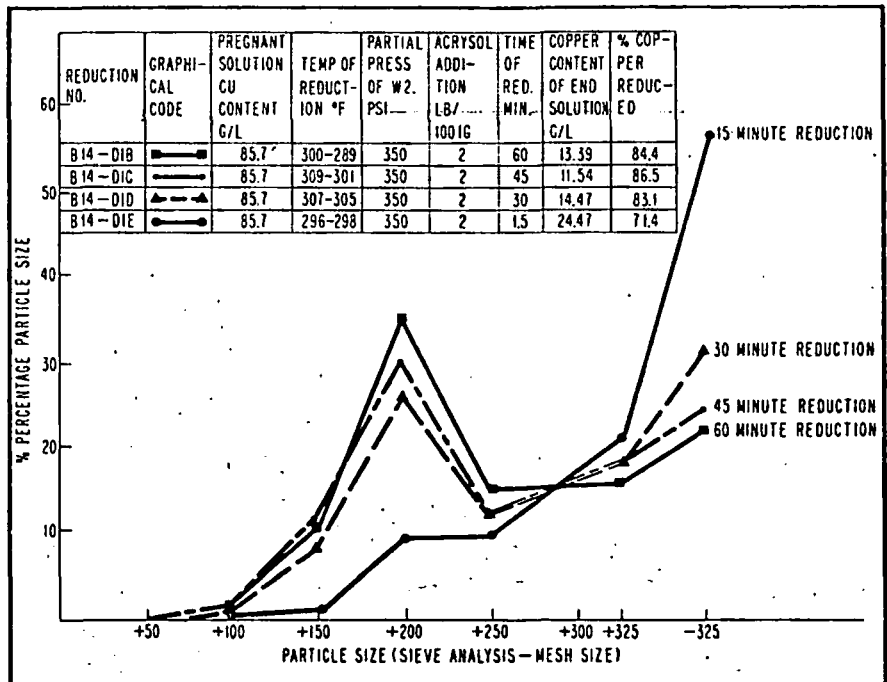
It was evident during early operation that corrosion was excessive, and something needed to be done to lower reaction temperatures so this problem could be controlled. Therefore, the present procedure differs from the pilot

plant technique in that ammonium sulphate is now used to buffer the leach solution. Even though the reduction reaction is considered to be the same as that for a straight acid-copper sulphate system, the reduction rate is more rapid, and depth of reduction is greater for any given temperature or pressure. Current changes being made to permit capacity operations in the reduction section include raising the pregnant solution concentration to 80-90 g per liter.

Operation without ammonium sulphate buffering during the initial phases of start-up resulted in severe corrosion in the reduction section. Knife-line, crevice, intergranular, and general corrosion of the Carpenter 20 Cb 3 clad reduction vessels was reduced to acceptable levels by ammonium sulphate buffering and lowering of reduction temperatures to 250° to 280°F.

The knife-line attack was attributed to carbide precipitation caused by post-heat treatment of the vessels during

PARTICLE SIZE DISTRIBUTION is dependent upon the length of the reduction cycle and the temperature at which reduction takes place. The shorter reduction cycles also produce more minus 325-mesh material making subsequent treatment more difficult. In addition, polyacrylic acid addition influenced the physical characteristics of the powder to a marked degree. It was possible to produce copper powder in the autoclave having apparent densities ranging from 0.2 to 2.9 or higher.



stress relieving, at a temperature of 1,000° to 1,050° F for 5½ hours.

It was found that copper powder was highly abrasive to plastics as well as Hypalon and Butyl rubber. Acid copper sulphate solutions were also found to chemically attack silicone rubber at temperatures above 275° F.

With experience, plant operations are being optimized, and a steadily higher grade product is being made. Today, copper of 99.95% purity is being produced. Any silicon, magnesium, and calcium impurities are believed to be partially caused by the brick lining in the pregnant solution tanks. Iron and sulphur impurities are dependent on the degree of washing in the centrifuge cycle. Carbon, resulting from polyacrylic acid decomposition, can be removed by pre-oxidation and sintering.

The present plant is staffed with a total of 37 people. Four senior officials from Bagdad Copper Corp. and Chemetals Corp. act as management.

Heat energy is one of the major cost items

Extrapolating results obtained from past operation, it is expected that at a capacity output of 25 tpd, copper powder can be produced with 0.3 kw hours electricity, 10,000 btu of heat energy, one gal make-up water, 0.15 lb H₂SO₄, 0.01 lb polyacrylic acid, 0.005 lb filter aid, and

0.05 lb ammonium sulphate per lb of copper powder produced. The self-contained plant also incorporates a packaged hydrogen plant using natural gas and steam for hydrogen production, a closed-circuit cooling water system, a 20,000 lb per hour steam boiler, a small water treatment plant capable of supplying both softened and de-alkalized water, plant and instrument air facilities, emergency power generation, an inert gas generator, and a modern, fully-equipped laboratory.

The laboratory is arranged in three sections. Part one is for routine chemical analysis, including determinations for carbon and sulphur by Leco combustion apparatus. Part two is the physical analysis laboratory for performing apparent density tests, particle size analysis, growth tests, green strength tests, sub-sieve analysis, hydrogen loss determinations, moisture content, and flow characteristics. Part three is a physical and chemical laboratory for metallographic examination and chemical analysis by atomic absorption and flame emission techniques.

Chemcopper's \$3.35-million plant is a partnership venture between Chemetals Corp. of New York, and Bagdad Copper Corp. Chemetals acquired a license—with the right to sublicense others—from Sherritt Gordon Mines Ltd., for developing and commercializing the gaseous reduction process as applied to copper and copper-bearing materials.

Semiquantitative spectrographic analysis for quality control permits optimum yield

Lot No.	Silicon	Iron	Magnesium	Manganese	Molybdenum	Calcium	Tin	All Other Elements		
								Leco Combustion Analysis Sulphur	Leco Combustion Analysis Carbon	
14	0.0035	0.024	0.0013	0.00042	0.0015	0.0021	Nil	Nil
15	0.0044	0.012	0.0015	0.00062	0.0062	0.00085	Nil	Nil
16	0.0050	0.010	0.00085	Nil	0.0041	0.00063	Nil	Nil
17	0.0050	0.014	0.00070	Nil	0.0043	0.0019	Nil	Nil
18	0.0028	0.016	0.00087	Trace	0.0037	0.0021	Nil	Nil	0.030	0.037
19	0.0039	0.014	0.0012	Trace	0.0014	0.0011	Nil	Nil	0.020	0.037
20	0.0039	0.012	0.00086	0.00059	0.0016	0.00075	Nil	Nil	0.024	0.041
21 ¹	0.0029	0.035 ¹	0.0019	Nil	Nil	0.0020	0.0025	Nil	0.047 ¹	0.034
22	0.0025	0.015	0.0016	Nil	Nil	0.0016	Nil	Nil	0.024	0.023
23	0.0026	0.015	0.00069	Nil	Nil	0.0008	Nil	Nil	0.032	0.037

¹Poor washing caused by erratic centrifuge operation.

6. Rudolfs, W. and A. Helbronner, *Soil Sci.*, 14, 459 (1922).
7. Colmer, A. R., K. L. Temple, and M. E. Hinkle, *J. Bacteriol.*, 59, 317 (1949).
8. Temple, K. L. and A. R. Colmer, *J. Bacteriol.*, 62, 605 (1951).
9. Temple, K. L. and E. W. Delchamps, *Appl. Microbiol.*, 1, 255 (1953).
10. Ashmead, D., *Colliery Guardian*, 694 (1955).
11. Fjergdingstad, *Rev. Suisse d'Hydrologie*, 18, 215 (1956).
12. Leathen, W. W. and S. A. Braley, *Bacteriol. Proc.*, 44 (1954).
13. Leathen, W. W., N. A. Kinsel, and S. A. Braley, *J. Bacteriol.*, 72, 700 (1956).
14. Silverman, M. P. and D. G. Lundgren, *J. Bacteriol.*, 78, 326 (1959).
15. Kinsel, N. A., *J. Bacteriol.*, 80, 628 (1960).
16. Davis, D. B., "Biological oxidation of copper sulfide minerals," Master's thesis, Brigham Young University (1953).
17. Zimmerley, S. R., "Cyclic leaching process employing iron oxidizing bacteria," U.S. patent 2,829,964, April, 8, 1958.
18. Bryner, L. C., J. V. Beck, D. B. Davis, and D. G. Wilson, *Ind. Eng. Chem.* 46, 2587 (1954).
19. Bryner, L. C. and R. Anderson, *Ind. Eng. Chem.*, 49, 1721 (1957).
20. Bryner, L. C. and A. K. Jameson, *Appl. Microbiol.*, 6, 281 (1958).
21. Beck, J. V., *J. Bacteriol.*, 79, 502 (1960).
22. Corrick, J. D. and J. A. Sutton, U.S. Bureau of Mines, R.I. 5718 (1961).
23. Audsley, A., G. R. Daborn, and D. Pearson, *Dept. of Scientif. and Industrial Res., Sc. Rep. N.C.L./CON.2* (1961).
24. Ivanov, V. I., F. I. Nagirnyak, and B. A. Stepanov, *Mikrobiologiya*, 30, 688 (1961).
25. Razzell, W. E., *Trans. Can. Min. Met.*, 65, 135 (1962).
26. Sutton, J. A. and J. D. Corrick, U.S. Bureau of Mines, R.I. 5839 (1961).

Factors in the Dissolution of Uranium from South African Ores and Observations on the Nature of the Undissolved Uranium

P. A. LAXEN

Head of the Chemical Processing Division,
Government Metallurgical Laboratory, Johannesburg

Abstract

The investigation described attempts to ascertain the reason for the differing extractions obtained from ores which are essentially of similar composition. A detailed mineralogical examination resulted in the identification of a number of refractory uranium-bearing minerals. These minerals are shown to be of minor importance in explaining high residual uranium contents. Using a novel standard leach technique almost complete dissolution of uranium was achieved from all ores with low acid and oxidant concentrations. The concentration in the leach solution of phosphate ions is shown to be an important factor in the leaching of ores which give low uranium extractions. This deleterious effect of phosphate ions is not attributable to their complexing action with ferric ions. Using this standard leach technique an assessment of the various chemical factors in the acid leaching of uranium ores was possible as well as a comparison of these factors on different ores.

1. INTRODUCTION

In 1959 and in 1960 South Africa produced over 6,000 tons of uranium oxide. The mines from which the ore for this production was derived are spread over a considerable distance. The map in Fig. 1 gives some idea of the extent of the deposits. Over 95% of the ores used for this production were derived from reefs of the Witwatersrand system with the remainder coming from the Dominion Reef system. The various uranium ores are basically similar, namely a gold- and uranium-bearing conglomerate in which uraninite is the principal uranium mineral. The uraninite occurs as primary grains and as secondary uraninite.^{1,2,3} Both these forms of uraninite have been shown to be readily soluble in oxidizing acid solutions containing ferric sulphate and sulphuric acid.

Despite the common origin and similar nature of the ores the uranium extractions from the different reefs on acid leaching are found to vary quite considerably, as shown in the table below.

(The extractions in Table I are rounded average figures based on laboratory scale tests on a number of samples. Extractions in the

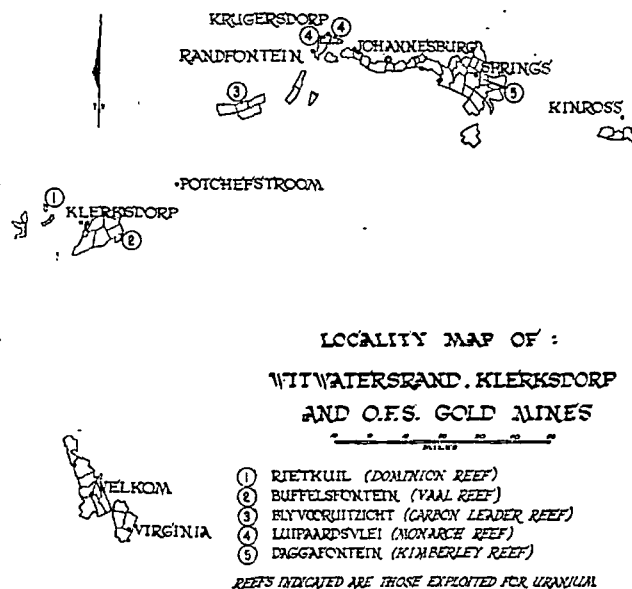


Fig. 1

plants are usually higher due mainly to operating at higher temperatures. Samples, more especially high grade hand specimens, can give extractions lying outside the range indicated.)

The nature of the undissolved uranium in the acid-leached ore and the reasons for variations in uranium extraction are thus problems of economic significance. These problems were investigated at the Government Metallurgical Laboratory in Johannesburg over a number of years and in this paper some of the observations made in the course of the investigation are presented.

The initial approach was the preparation of leach residues and of concentrates from leach residues for mineralogical examination, for it was anticipated that the nature of the residual uranium would be elucidated by the identification of one or more refractory uranium

minerals, which it was surmised would be present in varying quantities in the different reefs. Detailed mineralogical examinations by Liebenberg⁴ and Ortlepp⁵ gave much valuable information and a number of refractory uranium-bearing minerals were, in fact, identified. There was, however, little doubt that the refractory minerals found did not

TABLE I
Comparison of Uranium Extractions at 28°C from Different Reefs

Reef	Area where exploited	Uranium extraction
Kimberley Reef	East Rand (near Springs)	85-90%
Monarch "	West Rand (near Krugersdorp)	80-90%
Vaal "	Far West Rand (near Klerksdorp)	70-80%
Dominion "	West of Vaal Reef area	60-70%

by themselves account for the uranium left in the leach residues or for the variations in extraction between the different ores. A study of the behaviour of the different ores during leaching was therefore undertaken as a further approach to this problem. The procedure used in this approach,⁶ the results obtained and the conclusions drawn from the results form part of this paper. What might be termed "physico-chemical factors" are shown to be important in accounting for variations in extraction and for the presence of undissolved uranium.

A standard leach technique, termed the "dilute leach," was developed during this investigation. This technique proved useful and it is suggested that it might have application in the study of other leaching problems.

2. MINERALOGICAL BACKGROUND

Liebenberg,^{1,2} Ramdohr³ and others have described the mineralogy of the reefs of the Witwatersrand and the Dominion Reef systems in great detail. Very briefly these reefs consist of quartz pebbles cemented together by a matrix of quartz, sericitic minerals and chlorite. The gold, uraninite and accessory minerals are present in the matrix.

Uraninite is the principal uraniferous constituent. It occurs as primary grains and as stringers, veinlets and irregular masses of secondary uraninite. The primary grains are mostly minus 200 mesh in size and occur as individual grains in the matrix. The secondary uraninite, derived from the primary grains, is fine grained and occupies

any available space in, and between, the other minerals. The ratio of primary to secondary uraninite has been observed from microscopic examination of reef specimens to vary from reef to reef. For example secondary uraninite is abundant in the Monarch Reef whereas it is rare in the Dominion Reef.

Primary uraninite has a crystal structure similar to that of pure UO_2 , and chemical analysis has shown that virtually all the uranium

TABLE II
Analyses of Uraninite from Various Reefs

Mine	Reef	% U_3O_8	% ThO_2	% TiO_2	% P_2O_5
Dominion Reefs	Dominion Reef	61.9	6.25	0.65	0.15
Vaal Reefs	Vaal Reef	66.9	4.78	0.63	0.14
Blyvooruitzicht	Main Reef Carbon Leader	74.1	2.70	1.40*	
Sub Nigel	Main Reef Leader	66.6	1.63	1.04*	

* $TiO_2 + ZrO_2$.

in the primary uraninite is present in the tetravalent state. Grains of primary uraninite recovered from some of the different reefs have been found to vary only slightly in chemical composition, as shown in Table II.

Secondary uraninite is reported as being similar in crystal structure and chemical composition to the primary uraninite. No concentrates of this mineral have been recovered due to its tendency to slime on grinding.

A hydrocarbon-uraninite complex, "thucholite," is an important uraniferous constituent in some horizons, e.g. in the Carbon Leader, mined at Blyvooruitzicht, whereas it is very rare in others, e.g. in the Dominion Reef. The nature of the thucholite and its uranium content have been found to vary widely. Liebenberg¹ reports values for uranium content from 0.42% to 13.6% U_3O_8 .

3. THE LEACHING BEHAVIOUR OF THE PREDOMINANT URANIUM MINERALS

Primary Uraninite

Primary uraninite has been recovered as a gravity concentrate from a number of ores. Uraninite from the Dominion Reef has been

shown⁶ to be virtually completely soluble, viz. 99.7% dissolution, in low concentrations of sulphuric acid and ferric sulphate (4 g.p.l. of both H_2SO_4 and Fe^{+++}) in a normal leaching time of 18 hours at 28°C. In the absence of ferric sulphate the extraction dropped to about 6%.

Secondary Uraninite

By examining the behaviour of secondary and primary uraninite in polished section before and after acid leaching Liebenberg concluded that the secondary uraninite was more easily soluble than the primary uraninite.¹

Thucholite

The important factor in the dissolution of uranium from thucholite derived from the Blyvooruitzicht ore was the particle size. Uranium extractions varied from 30% for the (-28 + 35) mesh fraction to 72% for the (-150 + 200) mesh fraction.⁶ A leach solution of 4 gm $H_2SO_4/l.$ and 4 gm $Fe^{+++}/l.$ as ferric sulphate was used. Leach temperature was 28°C and leach time was 18 hours. Increased sulphuric acid concentration and leach temperature gave only slight increases in extraction. In general about 60% of the uranium contained in the thucholite in an ore dissolves under the conditions employed on the plant. There was not sufficient thucholite in any ore to account for more than a small proportion of the undissolved uranium in a leach residue.

4. ACID LEACHING OF SOUTH AFRICAN URANIUM ORES

The reagents used in the leaching process^{7,8,9} are sulphuric acid and manganese dioxide. The latter serves to oxidize ferrous ions to ferric which in turn oxidize the uraninite and render it soluble in the dilute acid.



The usual leaching procedure is to add all the acid and manganese dioxide required for leaching to the ore slurry at the commencement of the leach. The leach temperature used depends largely on the grade of the ore; temperatures from the ambient value up to 70°C are used.

In this leach procedure the acid concentration and the oxidizing potential (or ratio of Fe^{+++} to Fe^{++}) of the solution will be highest in the early part of the leach and will gradually decrease.

The acid consumption during the leaching process is accounted for by the presence of acid soluble silicates, e.g. sericite and chlorite, fine iron from grinding, lime from prior cyanidation treatment and small quantities of other acid soluble—at least in part—minerals, together with the acid required in the oxidation of ferrous ions by MnO_2 . Increases in leach temperature or of acid addition lead to an increase in acid consumption due largely to increased attack on the

TABLE III
Some Average Details* of Uranium Leaching on Various Plants

Mine	Head value % U_3O_8	Reagents added		Temp. °C	Time hours	Final leach soln.			Leach res. % U_3O_8	% Extr.
		H_2SO_4 lb/t	MnO_2 lb/t			H_2SO_4 g.p.l.	Fe^{+++} g.p.l.	Fe^{++} g.p.l.		
Luipaardsvlei	0.0692	32.0	8.1	25.9	19.6	7.5	1.4	0.21	0.00503	92.1
Daggafontein†	0.0232	51.4	11.5	30.0	15.3	4.7	3.8	2.8	0.0030	87.1
Blyvooruitzicht	0.0208	58.7	8.0	28.7	17.0	3.6	4.3	1.1	0.00325	84.4
Buffelsfontein	0.0252	52.0	19.5	49.8	26.6	3.0	1.3	1.5	0.0034	86.5
Rietkuil‡	0.137	60	18	50	18	9.5	4.4	1.4	0.0242	82.3

* Average figures from 1958.

† Daggafontein Ore contains a small proportion of flotation concentrates in addition to Kimberley Ref.

‡ Results for Rietkuil are from laboratory tests.

acid soluble silicates. Sufficient acid is added to a leach to ensure a concentration in the final pulp of about 3–5 grams H_2SO_4 per litre. This amount of acid yields a filtrate suitable for the subsequent ion-exchange treatment and is high enough to prevent any re-precipitation of uranium as phosphate and arsenate. The optimum quantity of manganese dioxide is determined empirically for each ore. Improved uranium extraction can be obtained by increasing the severity of the leach conditions, i.e. higher acid and manganese dioxide additions, higher leach temperatures and a longer leach time. The conditions used in practice are determined by economic considerations.

The variations shown by some typical ores on the plant, both as regards leaching requirements, i.e. acid and oxidant consumption, and uranium extractions, are illustrated in Table III.

5. REFRACTORY URANIUM MINERALS

Careful mineralogical examination combined with acid-leaching tests indicated the presence of four uranium-bearing minerals that might be regarded as refractory in the normal acid-leaching solutions.

These minerals were uraniferous zircon, uraniferous leucoxene, uraniferous monazite and uraniferous uranorthorite. Analysis of grains selected from unleached and leached samples resulted in the information shown in Table IV.^{4,5}

TABLE IV
Analyses on Refractory Minerals

Mineral	Grains before leaching			% of Uranium soluble in 1:1 HNO_3 *	% of Uranium dissolving during leaching	% of Uranium reporting in leach residues
	% U_3O_8	% ThO_2	% TiO_2			
Zircon	0.84	—	—	insol	nil	nil
Leucoxene	0.36	—	approx 50	70	20	50
Monazite	0.32	4.74†	—	14	9.5	4.5
Uranorthorite	9.5	34.9‡	—	100	N.D	N.D

* 1:1 HNO_3 used in digestion step during analysis of ores for uranium.

† Insoluble in hot 10% v/v H_2SO_4 .

‡ Soluble in hot 10% v/v H_2SO_4 .

Since the uranium in the zircon did not dissolve in the nitric acid digestion during chemical analysis it played no part in the uranium reported to be in leach residues. The uranium in the leucoxene and monazite was partly dissolved by digestion with nitric acid and dissolved to a lesser extent in the leaching process. Thus 50% of the uranium in leucoxene and 4.5% of the uranium in monazite did not dissolve during leaching and reported in the analysis of the leach residue. These two minerals were thus true refractory minerals. The amount of leucoxene and monazite present varies from reef to reef. By assuming that the TiO_2 content of an ore was due to leucoxene, and that the ThO_2 content which did not dissolve in 10% v/v H_2SO_4 —to distinguish it from the ThO_2 in uraninite and uranorthorite—was due to monazite, the amount of undissolved uranium attributable to these minerals could be estimated. There was not one ore in which the leucoxene and monazite could account for a significant amount of undissolved uranium after leaching.

Uranorthorite was recently found in high grade specimens from the Dominion Reef.⁵ It was shown to occur as a replacement of uraninite. Qualitatively it has been found to be soluble in a solution of approximately 4 grams H_2SO_4 /l. and 4 grams Fe^{+++} /l. but the rate of solution

was observed to be slower than that of primary uraninite. This was the only observation on the behaviour of uranothorite, and hence the proportion of this mineral remaining after leaching could not be assessed. In addition to the uranothorite, intergrowths of uraninite and uranothorite—termed uranothorite complexes—were observed, and the opinion was expressed that the presence of these complexes might

TABLE V
Distribution of Uranium in Minor Uraniferous Minerals

Uraniferous minerals	In ore before leaching	In leach residue
Leucoxene	0.0020% U ₃ O ₈	<0.0016% U ₃ O ₈
Monazite	0.00014 "	<0.00005
Uraniothorite* (based on assay of "pure" grains)	0.0057 "	unknown
Uraninite (as remainder from above)	0.12916 "	unknown
Total	0.137% U ₃ O ₈	

* (The ThO₂ soluble in 10% v/v H₂SO₄ in this ore is attributable to uraninite and uranothorite. By assuming, as a first approximation, that 75% of the uranium in the ore was present as uraninite (61.9% U₃O₈ and 6.25% ThO₂) the amount of "acid soluble" ThO₂ in the uraninite was calculated. Assuming that the remaining "acid soluble" ThO₂ was present as uranothorite (9.5% U₃O₈ and 34.9% ThO₂) the uranium in this mineral was calculated. No allowance is made for any uranothorite complexes.)

be quite widespread. This suggested that minerals or complexes, varying in composition between 61.9% U₃O₈ and 6.25% ThO₂ (uraninite) and 9.5% U₃O₈ and 34.9% ThO₂ (uranothorite), might be present and that the solubility of the uranium in these minerals or complexes might vary from the rapid solubility of uraninite to the slower solubility of the uranothorite. To date this last mentioned mineral has only been observed in the Dominion Reef.

From these mineralogical observations the importance of the uranothorite and the uranothorite complexes in explaining the presence of undissolved uranium in leach residues could not be assessed. Uranothorite was reported as dissolving so it could not be a highly refractory mineral, yet the presence of some other less soluble uraniumiferous mineral than uraninite was necessary to explain the presence of uranium in leach residues, more especially the residues high in uranium. This is illustrated in the estimations which follow. The uranothorite and the

complex with uraninite are re-introduced later in the paper to explain the results obtained in leach tests.

An ore sample from the Dominion Reef (Rietkuil Mine) with a head value of 0.137% U₃O₈ is here used to estimate the distribution of uranium in the various uraniumiferous minerals before and after leaching.

Table VI shows the uranium extractions obtained from this ore sample under a variety of conditions when leached by the normal procedure.

TABLE VI

Laboratory Extraction Tests on a Sample from the Dominion Reef (Rietkuil Mine)

Test no.	Reagent additions		Leach temp. °C	Leach time hours	Final leach solutions			% U ₃ O ₈ Extraction
	H ₂ SO ₄ lb/ton	MnO ₂ lb/ton			H ₂ SO ₄ g.p.l.	Fe ⁺⁺⁺ g.p.l.	Fe ⁺⁺ g.p.l.	
1.	50	10	28	18	7.8	4.5	0.03	73.8
2.	80	20	28	18	20.8	5.0	0.07	79.3
3.	60	18	50	18	9.5	4.4	1.4	82.3
4.	80	5	50	18	20.0	4.1	2.8	87.1
5.	150	10	28	18	70.7	6.2	0.07	88.8
6.	300	10	28	18	168.9	7.3	0.07	94.5
7.	150	10	50	18	58.0	6.4	2.03	93.9
8.	300	10	50	18	150.0	7.7	2.14	97.0

Despite the fact that 95% of the uranium was estimated to be present as uraninite, which should be readily soluble, extractions only reached 95% when using extremely high acid additions at 50°C.

These and other similar results emphasized the discrepancy between the uranium dissolutions obtained in practice and those estimated from observations on the constituents of the ore.

6. DEVELOPMENT OF A STANDARD LEACH ("DILUTE LEACH") PROCEDURE

To supplement the information obtained from mineralogical examination a systematic comparison of the leaching behaviour of various ores was undertaken. In order to study the behaviour of the various ores in the leaching process a standard leaching procedure was required. The normal laboratory leach test procedure was found to be inadequate as a means of comparison due to variations in the proportion of acid consuming constituents and reducing constituents in the different ore

samples. The normal leach procedure could result in sulphuric acid and ferric ion concentrations in comparative leach tests being very dissimilar in the initial period of the leach and becoming similar only towards the end of the leach. It could also result in wide differences in the concentration of acid soluble impurities such as iron, aluminium, phosphate, arsenate, silica etc. which were known to be present in significant quantities in leach solutions.

To overcome these difficulties a technique called the "dilute leach" was developed.⁸ This procedure provided comparable results irrespective of acid consumption or proportion of reducing constituents in the ore samples. The concentrations of the reagents in the leach solutions remained virtually constant throughout the tests, which enabled the effect of any acid or ferric ion concentration at any leach temperature to be studied.

The procedure employed a small weight of sample in contact with a large volume of leach solution made up to a definite concentration of sulphuric acid, ferric sulphate and any other substance to be tested. 10 grams of ore and 1000 mls of leach solution were usually used. The dilute mixture was agitated by rolling in a bottle in a water bath maintained at the required temperature. At the end of the leach period the solids were filtered, washed, dried, weighed and analysed. The method of uranium analysis used on these residue samples was one involving the extraction of uranium into tributyl phosphate, followed by colorimetric estimation.¹⁰ The proportion of ore dissolved during dilute leaching was similar to that dissolved during normal leaching viz. 2-4%. The extremely large volume of leach solution relative to a small weight of ore resulted in changes of reagent concentration being negligibly small and also ensured that any substance derived from acid attack on different constituents of the ore would be present in only trace concentrations. In effect the leaching characteristics of the uranium minerals in each ore were being compared under identical conditions.

7. ORE SAMPLES USED IN TESTWORK

A number of typical ore samples were selected for leach tests. From Table I the approximate uranium extraction at 28°C from each ore can be assessed, and from Table III the plant leaching conditions used in the treatment of these ores, and the extractions obtained, can be

found. The position of the mines is indicated in Fig. 1. Table VII below gives further details of the samples used.

TABLE VII
Details of Ore Samples Used

Mine	Reef exploited	% U ₃ O ₈	% Acid soluble ThO ₂	Estimated* acid soluble ThO ₂ in uraninite	Acid soluble ThO ₂ in excess of that associated with uraninite
Rietkuil	Dominion Reef	0.137	0.0310	0.0138	0.0172
Buffelsfontein	Vaal "	0.0350	0.0077	0.0025	0.0052
Blyvooruitzicht	Carbon Leader "	0.0181	0.0016	0.0005	0.0011
Luipaardsvlei	Monarch "	0.0690			
Daggafontein	Kimberley "	0.0225			

* Based on ThO₂ analyses of uraninite in Table II and assuming all uranium present as uraninite.

8. RESULTS OBTAINED BY THE DILUTE LEACH TECHNIQUE

The most unexpected results obtained from the dilute leach tests were the improved uranium extractions. This applied particularly to the samples which normally gave poor extractions. In Table VIII a comparison is given of extractions from the Rietkuil ore by the dilute leach and the normal leach.

TABLE VIII
Comparison of Normal Leach and Dilute Leach Tests on Rietkuil (Leach Time 18 hours)

Test no.	Normal leaching—60% solids						Dilute leaching 0.1% solids				
	Reagents added		Initial conc.	Final leach soln.			% Uranium dis	Leach soln.			% Uranium dis
	H ₂ SO ₄ lb/t	MnO ₃ lb/t		H ₂ SO ₄ g.p.l.	H ₂ SO ₄ g.p.l.	Fe ⁺⁺⁺ g.p.l.		Fe ⁺⁺ g.p.l.	H ₂ SO ₄ g.p.l.	Fe ⁺⁺⁺ g.p.l.	
28°C											
1	50	10	37.5	7.8	4.5	0.3	73.8	8.0	4.0	tr	83.8
2	80	20	60.0	20.8	5.0	0.07	79.3	20.0	4.0	..	90.1
50°C											
3	60	18	45.0	9.5	4.4	1.4	82.3	8.0	4.0	tr	96.4
4	80	5	60.0	20.0	4.1	2.8	87.1	20.0	4.0	..	98.5

These unusually high uranium extractions by the dilute leach on an ore which was classed as refractory were very interesting and significant. They first of all represented a breakthrough in the "chemical" investigation. They also showed that the composition of the leach solution was an important factor in the dissolution of the last portion of the uranium, i.e. the residual uranium. By merely varying the leach conditions to those used in the dilute leach near complete uranium extractions were being obtained without the use of unusually high reagent concentrations. Many tests were subsequently conducted on various ores using the dilute leach technique in order to explain

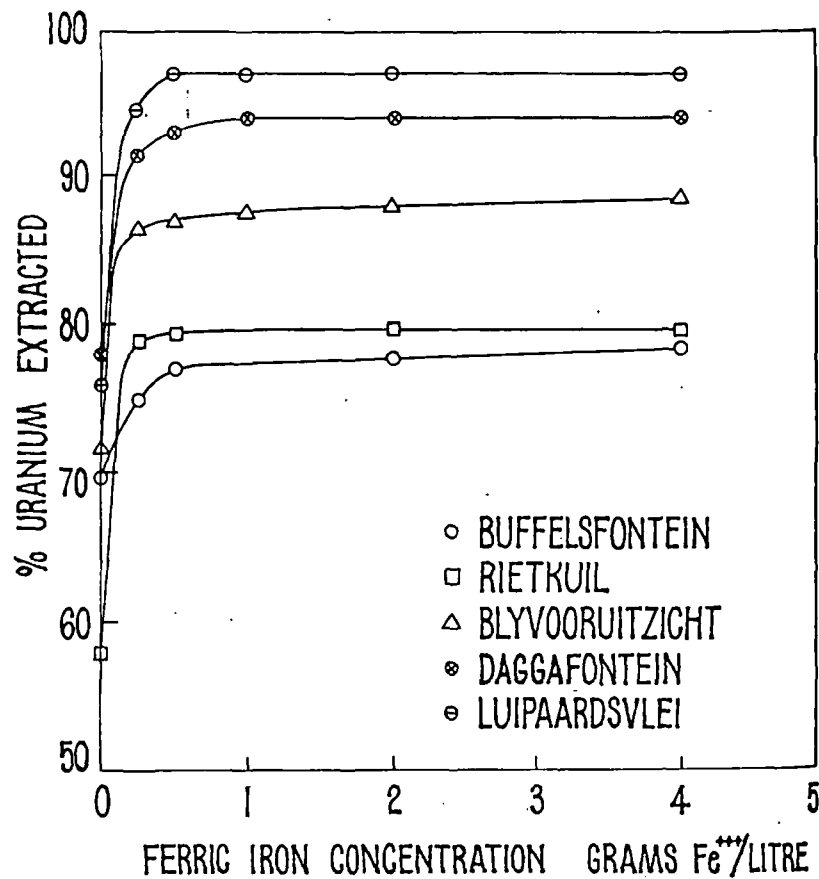


Fig. 2. Effect of Fe^{+++} concentration on uranium extractions.
Leach conditions: 4 g.p.l. H_2SO_4 , Temp. $28^\circ C$, Time 18 hrs

the improved extractions and to determine the effects of all possible factors on uranium extractions. The main results obtained from some of these tests are given in condensed form in the sections following.

8.1 Effect of Fe^{+++} and H_2SO_4 Concentrations

In Figs. 2 and 3 are shown the effect of increasing the concentration of Fe^{+++} at $28^\circ C$ and of H_2SO_4 at $50^\circ C$ respectively on uranium extractions. Increasing the Fe^{+++} concentration had a similar effect on all ore samples. Extractions increased rapidly up to a Fe^{+++} concentration of 0.25 grams/litre and remained virtually constant

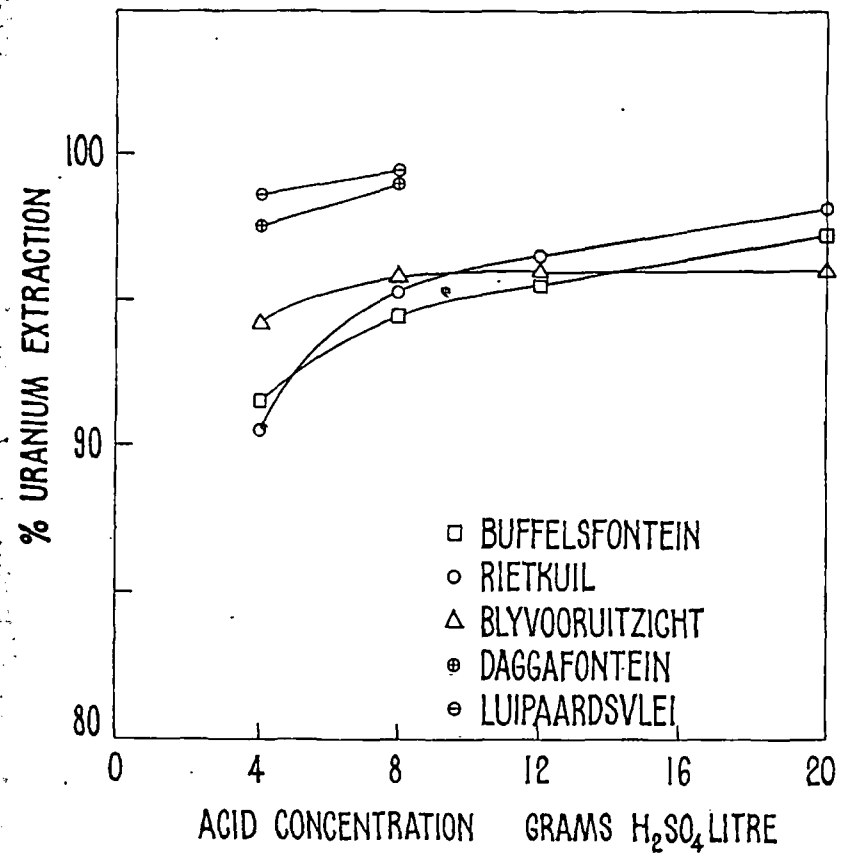


Fig. 3. Effect of acid concentration on uranium extractions.
Leach conditions: 4 g.p.l. Fe^{+++} , Temp. $50^\circ C$, Time 18 hrs

above a concentration of 0.5 grams Fe^{+++} /litre. Any effect which reduced the effective concentration of Fe^{+++} below 0.5 grams Fe^{+++} /litre, such as complexing of Fe^{+++} by phosphate and arsenate ions, would therefore result in a drop in extraction over 18 hours at 28°C . Tests at 50°C show a similar minimum Fe^{+++} concentration of approximately 0.5 grams Fe^{+++} /litre for maximum extractions. Extractions were much higher on all these ores at 50°C . The tests in Fig. 3 were of interest in that near complete uranium extractions were obtained from all ores at 50°C with reasonably low acid concentrations. The undissolved uranium from these tests could be attributed to the small amounts of the highly refractory minerals—leucoxene, monazite—present in all the ores, and the thucholite present in the Blyvooruitzicht ore and to a lesser extent in the Buffelsfontein ore.

8.2 Effect of $\text{Fe}^{+++}/\text{Fe}^{++}$ Ratio

The importance of the oxidizing potential, or $\text{Fe}^{+++}/\text{Fe}^{++}$ ratio, of the leach solutions in uranium leaching has long been realized. This factor is used as one of the controls in leaching on the uranium plants. In a dilute leach using 4 grams H_2SO_4 /litre and 4 grams Fe^{+++} /litre the concentration of Fe^{++} which would build up in the solution would be extremely small, and hence the oxidation potential of the solution would remain high. This constant and high oxidation potential of the dilute leach solution would therefore be a major difference between the dilute leach and the normal leach. The effect of this factor on uranium extraction was ascertained by varying the $\text{Fe}^{+++}/\text{Fe}^{++}$ ratio in the leach solutions on the various ores. The results from these tests are shown in Table IX.

TABLE IX

Effect of $\text{Fe}^{+++}/\text{Fe}^{++}$ Ratio on Uranium Extraction from Dilute Leach Tests
Leach Temperature 28°C . Time 18 hours

	4	3	2	1	4 g.p.l. H_2SO_4
Fe^{+++} Conc. g.p.l.	4	3	2	1	4 g.p.l. H_2SO_4
Fe^{++} „ g.p.l.	nil	1	2	3	
$\text{Fe}^{+++}/\text{Fe}^{++}$ ratio	4/0	3/1	2/2	1/3	
Luipaardsvlei	96.6	94.5	93.8	93.8	% Extraction
Daggafontein	93.9	93.1	92.0	91.6	„
Blyvooruitzicht	88.5	79.3	75.6	75.0	„
Buffelsfontein	80.3	75.2	74.3	68.0	„
Rietkuil	76.5	70.2	69.9	67.6	„

The effect of reducing the oxidation potential of the leach solution varied with the different samples. On the Luipaardsvlei and Daggafontein ores uranium extractions were only slightly lower when leaching with a solution containing 1 gram Fe^{+++} /litre and 3 grams Fe^{++} /litre as compared with the extractions when leaching with a solution containing 4 grams Fe^{+++} /litre and nil Fe^{++} . On the other three ores, however, the extractions when using the first mentioned solution were much lower than those obtained when using the second solution. In general the lower the uranium extraction the greater was the deleterious effect of reduced oxidation potentials on uranium extractions.

8.3 Effect of Phosphate Concentration

Another major point of difference between the dilute leach and the normal leach would be the dilution to an extremely low level, in the dilute leach, of any ion derived from the dissolution of the ore. Dilute leach tests were carried out in which each of the constituents that could be expected to be introduced from the ore were added in turn to the leach solutions. Of those tested only phosphate, and to a very much lesser extent arsenate, had any deleterious effect on dissolution. Figure 4 shows the effect on uranium dissolutions of increasing the phosphate concentrations in the dilute leach at a ferric ion concentration of 4 grams Fe^{+++} /litre. The phosphate was added as phosphoric acid. Additions of uranium, thorium and aluminium as sulphates were among many ions that had no effect.

Adding the phosphate at the end of the dilute leach did not result in a lower extraction, showing that the phosphate did not act by merely causing uranium to precipitate. The longer the addition of phosphate was delayed after the commencement of the leach the less was its deleterious effect. The effect of the phosphate seemed to be related to the proportion of unleached uranium.

In the presence of 4 grams Fe^{+++} /litre low phosphate additions (up to 0.5 grams P_2O_5 /litre) were without effect on extractions from Luipaardsvlei and Daggafontein ores. Even with this high concentration of Fe^{+++} these same low concentrations of phosphate had, however, quite significant effects on extractions from Blyvooruitzicht, Buffelsfontein and Rietkuil, pointing to a difference in behaviour between these ores and the Luipaardsvlei and Daggafontein ores. These low additions of phosphate could not be acting by reducing the

effective concentration of Fe^{+++} below the minimum of 0.5 grams Fe^{+++} /litre required for maximum extraction. The phosphate concentrations in plant leach solutions are usually between 0.1 and 0.2 grams P_2O_5 /litre.

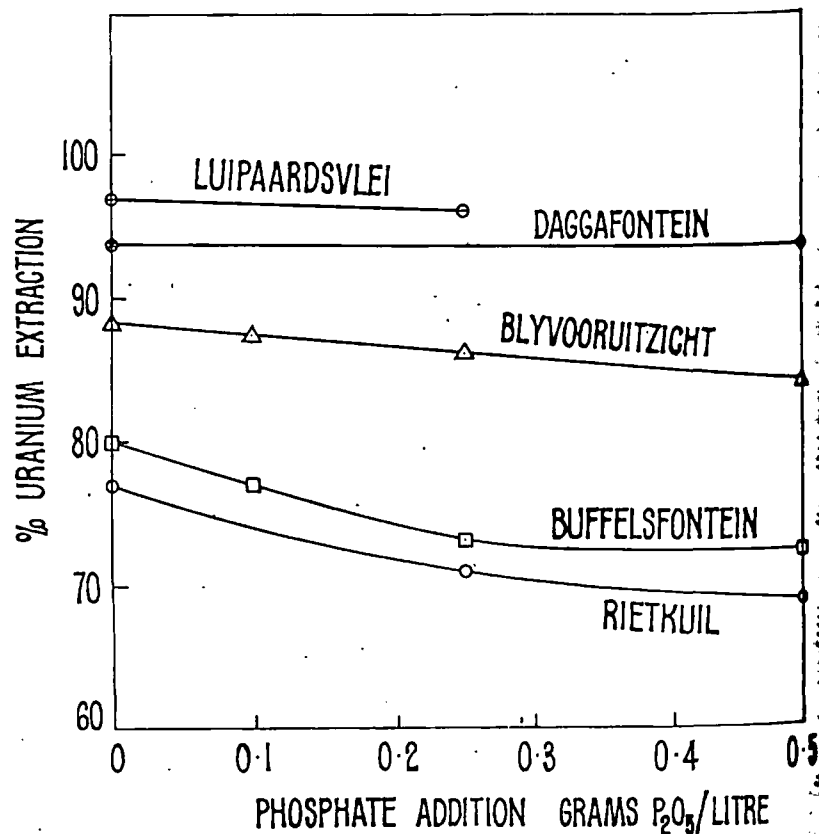


Fig. 4. Effect of phosphate concentration on uranium extraction.
Leach conditions: 4 g.p.l. H_2SO_4 , 4 g.p.l. Fe^{+++} Temp. 28°C Time 18 hrs

8.4 Effect of Temperature

At 50°C uranium extractions were more rapid and more complete. Phosphate additions and variation of oxidation potential had similar effects to those shown for 28°C , although the uranium extractions were much higher.

8.5 Effect of Prolonging the Leach Time

A further unusual effect of the dilute leach was the improvement in extraction obtained on greatly prolonging the time of leaching. Figure 5 shows the extractions obtained from the Buffelsfontein and Rietkuil

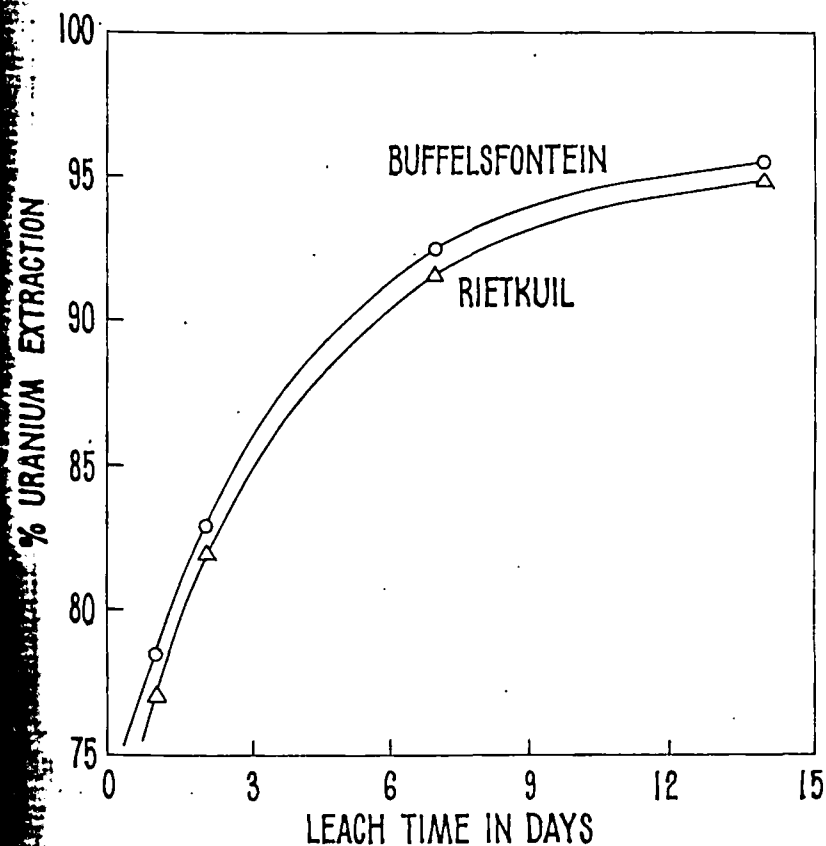


Fig. 5. Effect of prolonged contact by dilute leach on uranium extractions.
Leach conditions: 4 g.p.l. H_2SO_4 , 4 g.p.l. Fe^{+++} Temp. 28°C

samples on extending the contact time to 14 days. Despite the moderate conditions of these tests—viz. 4 grams H_2SO_4 and 4 grams Fe^{+++} /litre at 28°C —extractions of over 95% were obtained.

8.6 Comparison of Uranium and Thorium Extractions

The dilute leach was used to compare uranium and "acid soluble" thorium extractions from a large number of high grade reef samples from different areas of the Dominion Reef. The leach conditions

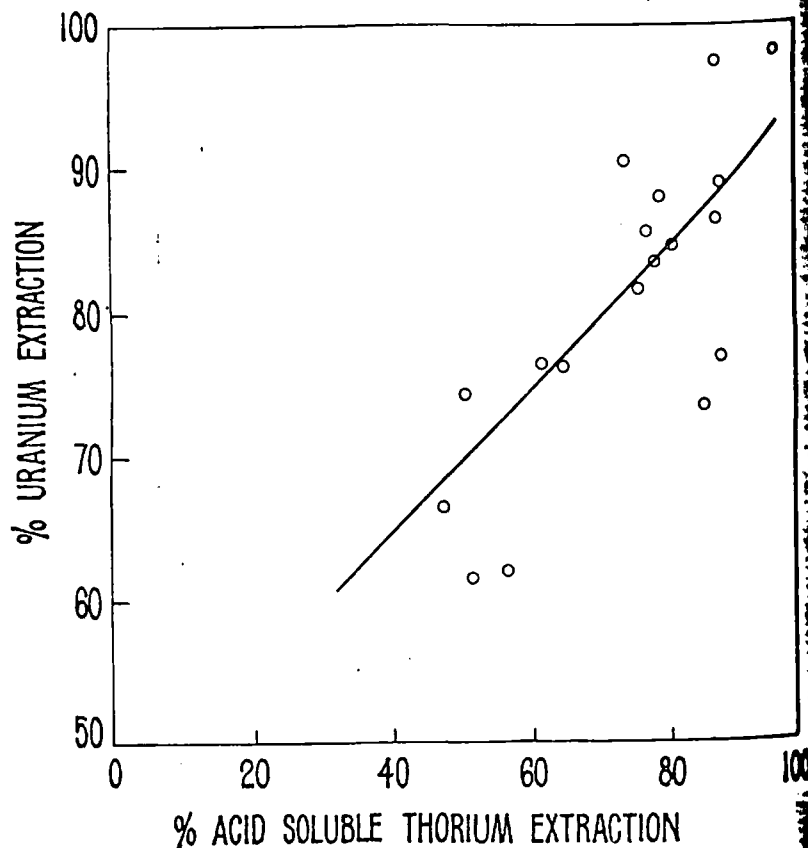


Fig. 6. Uranium and thorium extractions from various samples from the Dominion Reef.

Leach conditions: 4 g.p.l. H_2SO_4 , 4 g.p.l. Fe^{+++} Time 18 hours Temp. $28^\circ C$

for all these tests were 18 hours at $28^\circ C$ and a solution of 4 grams H_2SO_4 /litre and 4 grams Fe^{+++} /litre. Figure 6 shows the results obtained. High extractions of "acid soluble" ThO_2 are accompanied by high extractions of uranium, and samples in which the extractions

of "acid soluble" ThO_2 are low yield low uranium extractions. All these samples showed an excess of "acid soluble" ThO_2 over that associated with uraninite.

9. DISCUSSION OF RESULTS

The following observations are made from the results of the dilute leach tests:

- (1) In the absence of any complexing action on Fe^{+++} by impurities derived from the ores, e.g. phosphate, 0.5 grams Fe^{+++} /litre is shown to be adequate for maximum uranium extraction from all ores at $28^\circ C$. Similarly at $50^\circ C$ a low concentration of Fe^{+++} is sufficient for maximum extraction.
- (2) Despite the incomplete extractions in plant scale leaching none of the ores tested contained a uranium mineral present in any significant amount that could not be dissolved by relatively mild leach conditions. This is shown by the near complete uranium extractions possible by the dilute leach procedure from all ores using low acid concentrations at $50^\circ C$ (Fig. 3) and low acid concentrations for 14 days at $28^\circ C$ (Fig. 5), both with 4 grams Fe^{+++} /litre.
- (3) The improved extractions obtained by the dilute leach procedure compared with extractions from comparable normal leach tests showed the nature of the leach solution, i.e. physico-chemical factors, to be important in preventing near complete extractions in a plant scale leach. These effects varied from one ore to another indicating variation in the minerals present.

The high extractions with the dilute leach are shown to be attributable both to the consistently high oxidizing potential possible with the dilute leach solutions, and to the fact that interfering ions, such as phosphate, are diluted to the point where they no longer interfere. The deleterious effects of reduced oxidation potential and of the presence of phosphate in solution vary from ore to ore. In general, the lower the extraction with high oxidation potential and with no phosphate present the greater is the deleterious effect of the two factors mentioned above. This observation is supported by tests on further samples. This would seem to indicate that these two factors are influencing the undissolved or "difficult to dissolve" portions of the uranium in the ores.

The position of the curves in Fig. 2 establishes a definite order for ease of leaching of the different ores. The curves show a similar behaviour for the uranium dissolving from each ore under the conditions tested. Above a concentration of 0.5 grams Fe^{+++} /litre the concentration of Fe^{+++} is no longer the rate controlling factor in the dissolution of uranium from any of these ores. Any effect which reduces the concentration of uncomplexed Fe^{+++} below 0.5 g.p.l. will adversely affect uranium extractions from all ores.

A tentative theory is here offered to account for the results obtained by the dilute leach procedure and to correlate them with the mineralogical observations.

Mineralogical observation reports that Daggafontein ore from the Kimberley reef contains primary uraninite as its principal uraniferous mineral. The results from the dilute leach tests reported for the Daggafontein sample can be taken as typical of an ore containing mainly primary uraninite. The high extractions normally obtained from Daggafontein samples are consistent with this observation. Primary uraninite, based on the results of the dilute leach tests on Daggafontein, is only slightly affected by lowering the oxidation potential and is practically unaffected by the presence of low concentrations of phosphate ions in the presence of 4 grams Fe^{+++} /litre. The higher extractions over 18 hours in Fig. 2 from the Luipaardsvlei sample compared with the Daggafontein sample can be attributed to the secondary uraninite in the Luipaardsvlei ore, which form of uraninite has been qualitatively observed to dissolve more rapidly than primary uraninite. The uraninite in the Luipaardsvlei ore is also only slightly affected by lowered oxidation potentials and by low concentrations of phosphate ions in the presence of "excess" Fe^{+++} .

Based on the results in Fig. 2 uranium extractions possible after leaching for 18 hours at 28°C from the Luipaardsvlei and Daggafontein ores are >97% and >94% respectively. Figure 3 shows that at 50°C these extractions rise to >98.5% and >97.5% respectively. Lower extractions than these in plant leaching must be attributed to the nature of the leach solution—less than 0.5 grams Fe^{+++} /litre, uncomplexed Fe^{+++} and low oxidation potentials.

Testwork on a concentrate of primary uraninite from the Dominion Reef had shown that this mineral was virtually completely soluble in dilute leach tests at 28°C. Dissolution of the uraninite was unaffected by low concentrations of phosphate in the presence of 4 grams Fe^{+++} /litre. This supports the contention that uraninite in all the ores tested

would dissolve to a similar extent under similar conditions. The percentage uranium dissolution shown in Fig. 2 for Rietkuil, viz. 77.5%, would therefore be due largely to the uraninite in this ore. It would also include some portion of the uranium from any other more slowly soluble minerals. Uranium in uranothorite and any uraninite-uranothorite complex would presumably dissolve to some extent in these tests and would be included in the 77.5% dissolution. Assuming that uraninite in the Rietkuil ore would behave as uraninite in the Daggafontein ore then the large drop in uranium dissolution from the Rietkuil ore both on decreasing the oxidation potential of the leach solution and on adding phosphate in the presence of 4 grams Fe^{+++} /litre must be attributable to an effect on some other uranium mineral than uraninite. This is presumed to be an effect on the portion of the uranothorite which is dissolving at high oxidation potentials and no addition of phosphate. It has been shown that uranothorite alone can only account for about 4% of the uranium in this ore, so the presence of uranothorite complexes is presumed to occur and, along with uranothorite, to account for most of the uranium not dissolving from the Rietkuil ore under the conditions used for the tests in Fig. 2.

The tests reported in Fig. 6 support the contention that the uranium not dissolving under the test conditions is associated as a complex containing uranium and thorium. On this group of samples, when the uranium extraction is high from a sample then the "acid soluble" thorium extraction is also high, while low uranium extraction corresponds with low thorium extraction.

The uranium undissolved from the Rietkuil sample after the tests reported in Fig. 2 is soluble in dilute leach tests both at 50°C, with reasonably low acid concentrations, and at 28°C, with prolonged contact time. This uranium, however, requires extremely high acid concentrations in plant scale leaching for complete dissolution due to the effects of phosphate in solution and of the generally lower oxidation potential of the plant leach solutions.

The tests on the Rietkuil ore reported in Fig. 2 show that 0.5 grams Fe^{+++} /litre is sufficient for maximum uranium extraction at 28°C. In the tests to which phosphate was added 4 grams Fe^{+++} /litre was used. In view of this large excess of Fe^{+++} present in the leach solution the effect on uranium dissolution of the added phosphate does not seem to be due to the complexing of sufficient Fe^{+++} to affect the dissolution, but would appear to be rather an effect of the phosphate ions in hindering the dissolution of the uranium in a mineral—the uranothorite complexes.

The dissolution of the least soluble portion of the uranium mineral in the Rietkuil ore, as shown over 14 days in Fig. 5, appears to depend on diffusion of some species to or from the mineral surface. It is suggested that phosphate in solution markedly affects this diffusion process.

The Buffelsfontein ore sample behaves in a very similar fashion to the Rietkuil ore in all tests. The Buffelsfontein ore also contains more "acid soluble" ThO_2 than can be accounted for by the presence of thorium in uraninite alone. The dissolution of the uranium in the Buffelsfontein sample over 14 days at 28°C was very similar to that of Rietkuil. Based on all considerations it is suggested that the Buffelsfontein ore (i.e. the Vaal Reef) also contains uranothorite complexes to explain the lower extractions from this ore on normal leaching without the use of fairly severe leach conditions.

Similarly it is suggested that the behaviour of the Blyvooruitzicht ore in the dilute leach tests, together with the presence of more "acid soluble" ThO_2 than is attributable to the uraninite in this ore, indicates the presence of uranothorite complexes.

Figure 2 shows that the uranium extractions possible from Blyvooruitzicht, Buffelsfontein and Rietkuil ores after leaching for 18 hours at 28° are $>87.5\%$, $>79.5\%$ and $>77.5\%$. At 50°C , as shown in Fig. 3, these extractions are $>94.5\%$, $>91.5\%$ and $>90.5\%$ respectively. Lower extractions in plant leaching are attributable to the leach solutions—the adverse effect of low concentrations of phosphate in the leach solutions even with high Fe^{+++} concentrations, low oxidation potentials and an uncomplexed Fe^{+++} concentration of less than 0.5 grams Fe^{+++} /litre.

10. SUMMARY AND CONCLUSIONS

Despite the essentially similar nature of the various reefs of the Witwatersrand and Dominion Reef system uranium extractions on these ores (after normal acid leach tests at 28°C) varied from reef to reef over quite a wide range viz. 70%–90%. The uranium in some ores, notably those ores from the Dominion Reef and Vaal Reef, required very high acid additions and high leach temperatures for near complete extractions in plant scale tests. The varying extractions and the refractory behaviour of these ores could not be accounted for on the basis of mineralogical information alone.

A leach technique called the "dilute leach" was used to compare the

behaviour of ore samples from the various reefs. The results from these tests have thrown further light on the complex problem of the nature of the uranium which does not dissolve in plant scale leaching.

The dilute leach tests gave higher uranium extractions than obtained from comparable normal leach tests. The improvement in extraction was greatest with the ores which gave the lowest extractions. Near complete uranium extractions were obtained from all the ores tested under reasonable reagent concentrations and leach temperatures by the dilute leach. These results altered the previously held concept of a highly refractory mineral.

The nature of the leach solution was shown to be an important contributing factor to the presence of undissolved uranium in plant leach residues. The lower extractions in normal leach tests compared with dilute leach tests were shown to be attributable to two factors concerning the nature of the leach solution:

- (1) Lower $\text{Fe}^{+++}/\text{Fe}^{++}$ ratios, i.e. lower oxidation potentials, during normal leaching,
- (2) the presence of impurities, mainly phosphate, in normal leach solutions. These impurities are derived from acid attack on constituents in the ore.

The deleterious effects of these two factors vary from ore to ore and, in general, are highest on the ores which leach the worst. The effect of lowered oxidation potentials is shown to be very slight on uraninite in the ores tested, while the effect of low concentrations of phosphate—up to 0.5 grams P_2O_5 /litre—in the presence of 4 grams Fe^{+++} /litre is shown to be without effect on uraninite.

Uraniothorite and uranothorite-uraninite complexes have been observed in the Dominion Reef. It is suggested that it is uranium dissolution from this complex which is largely affected by lowered oxidation potentials and by the presence of phosphate—under the conditions tested. At temperatures of 50°C this mineral dissolves readily in dilute leach tests. It is further suggested that the uranothorite complex is present in the Buffelsfontein and Blyvooruitzicht ores in which it has not as yet been observed. The presence of varying proportions of the uranothorite complex, together with the effects attributable to the leach solution, is held to account for much of the variations in extractions between the different reefs tested and for much of the undissolved uranium in plant leach residues from these ores.

Acknowledgements

The Author wishes to acknowledge the encouragement received from Dr. R. E. Robinson, Director of the Government Metallurgical Laboratory, in the preparation of this paper and his permission to publish the results. The valuable advice from Dr. W. R. Liebenberg, and Messrs. J. Levin and R. J. Ortlepp on many occasions is gratefully acknowledged.

References

1. Liebenberg, W. R., *Trans. Geol. Soc. S. Afr.* LVIII p. 101 (1955).
2. Liebenberg, W. R., *N. Jb. Miner., Abh.* 94, Festband Ramdohr, Stuttgart, p. 831, Juli, 1960.
3. Ramdohr, P., *Abh. Dt. Akad. Wiss.*, Berlin, Jg. 1954, No. 5 (1955).
4. Liebenberg, W. R., *J. S. Afr. Inst. Min. Metall.* 57, No. 4 (1956).
5. Ortlepp, R. J., *Trans. Geol. Soc. S. Afr.* (in print) (1962).
6. Laxen, P. A., Progress Report (Leaching) No. 259 and 261, Government Metallurgical Laboratory, 1960.
7. Gaudin, A. M., Schuhmann, R., and Dasher, J. J. *Metals*, 8, p. 1065 (1956).
8. Pinkney, E. T., *J. S. Afr. Inst. Min. Metall.*, 57, No. 6 (1957).
9. Laxen, P. A. and Atmore, M. G., *J. S. Afr. Inst. Min. Metall.*, 57, No. 6 (1957).
10. Steele, T. W. and Taylor, J. D., Progress Report (Analytical) No. 26, Government Metallurgical Laboratory, February, 1959.

PART II PRESSURE LEACHING AND REDUCTION

SUBJ
MNG
FDWN

RI

bureau of mines
report of investigations 6996

UNIVERSITY OF UTAH
RESEARCH INSTITUTE
EARTH SCIENCE LAB.

FRACTURING A DEPOSIT WITH NUCLEAR
EXPLOSIVES AND RECOVERING COPPER
BY THE IN-SITU LEACHING METHOD

By William R. Hardwick



UNITED STATES DEPARTMENT OF THE INTERIOR

BUREAU OF MINES

November 1967

This document is released by the Bureau of Mines in recognition of the necessity for prompt and timely reporting. It is understood that the information contained herein may be superseded by subsequent publications. Some concessions in form and style are made in the interest of timeliness.

Walter R. Howard
Director

FRACTURING A DEPOSIT WITH NUCLEAR EXPLOSIVES AND RECOVERING COPPER BY THE IN-SITU LEACHING METHOD

By William R. Hardwick

* * * * * report of investigations 6996



UNITED STATES DEPARTMENT OF THE INTERIOR
Stewart L. Udall, Secretary

BUREAU OF MINES
Walter R. Hibbard, Jr., Director

The work on which this report is based was done under an agreement between the Bureau of Mines, U.S. Department of the Interior, and the San Francisco Operations Office, U.S. Atomic Energy Commission.

This publication has been cataloged as follows:

Hardwick, William R

Fracturing a deposit with nuclear explosives and recovering copper by the in-situ leaching method. [Washington] U.S. Dept. of the Interior, Bureau of Mines [1967]

48 p. illus., tables. (U. S. Bureau of Mines. Report of investigations 6996)

Based on work done in cooperation with the San Francisco Operations Office, U. S. Atomic Energy Commission.

1. Copper. 2. Explosives. I. Title. (Series)

TN23.U7 no. 6996 622.06173

U. S. Dept. of the Int. Library

Ab
In
Ac
Hi
Co
Ch
The
r
Med
Nuc
Pub
Saf

APP
Eco
Con

Fig

1.
2.
3.
4.
5.
6.
7.
8.
9.
10.
11.
12.
13.
14.
15.

CONTENTS

	<u>Page</u>
Abstract.....	1
Introduction.....	1
Acknowledgments.....	3
History and commercial examples of in-situ copper leaching methods.....	3
Copper deposits.....	10
Chemistry of leaching copper.....	13
The effect of bacteria on the solubility of copper minerals and the reaction of bacteria to radioactivity.....	17
Mechanics of leaching.....	19
Nuclear explosives.....	21
Public liability.....	30
Safety problems.....	33
Air blast.....	33
Ground shock.....	34
Radioactivity.....	35
Radiation hazards to off-site environment.....	36
Radiation hazards to on-site personnel.....	36
Contamination of copper.....	36
Application of in-situ leaching to nuclear fractured deposit.....	37
Economics of nuclear fracturing and in-situ copper leaching.....	42
Conclusions.....	47

ILLUSTRATIONS

Fig. 1. Mine plant showing dump leaching as an integral part of copper recovery systems.....	5
2. Stope leaching.....	6
3. Open-drainage leaching system.....	7
4. Flood-leaching system.....	9
5. Typical dump copper leaching circuit.....	21
6. Projected charges for thermonuclear explosives.....	23
7. Five-kiloton nuclear explosive being lowered into 2,700-foot emplacement hole.....	24
8. Crater radius vs. depth of burst on alluvium.....	25
9. Tonnage curves of rock broken by intermediate underground nuclear explosions.....	26
10. Cavity radii for contained underground nuclear explosions in granitic rock.....	27
11. Chimney heights for contained underground nuclear explosions in granitic rock.....	27
12. Tonnages of granitic rock broken by underground nuclear explosions	28
13. Schematic section of explosion at maximum rock breaking depth.....	29
14. View across Danny Boy crater showing hard basalt rock fractured by a nuclear explosive.....	29
15. Schematic cross section of Blanca.....	30

ILLUSTRATIONS--Continued

Fig.

	Page
16. Schematic cross section of granitic rock broken by contained nuclear explosion.....	31
17. Broken granitic rock in the chimney of a contained underground nuclear explosion.....	32
18. Damage to mine workings from nuclear explosions in granite rock...	35
19. Surface mound of broken rock after nuclear explosion.....	38
20. System for leaching copper from deposit broken by intermediate-depth nuclear explosion.....	39
21. Recovering copper by flood leaching in situ after the deposit is broken by a contained nuclear explosion.....	41
22. Recovering copper by open-drainage leaching in situ after the deposit is broken by a contained nuclear explosion.....	41
23. Use of multiple contained underground nuclear explosives to fracture deposit.....	42
24. Hypothetical section of small copper deposit after nuclear explosion.....	45

TABLES

1. Comparative rate of dissolution of various copper minerals sized to minus 100, plus 200 mesh at a temperature of 35° C.....	11
2. Sulfuric acid added per pound of recovered copper.....	15
3. Iron required to recover copper from solution.....	16
4. Comparison of explosive energy costs.....	22
5. Cost of breaking rock with nuclear explosives.....	22
6. Diameters of nuclear explosives.....	23
7. Typical fragment-size distribution from underground explosions in hardrock.....	30
8. Cost of fracturing a deposit in cents per pound of recoverable copper.....	33
9. Estimated cost of a copper precipitating plant.....	34
10. Estimated operating costs.....	44
11. Estimated cost of producing copper per pound.....	44
12. Estimated copper in deposit.....	44
13. Estimated cost of producing copper from hypothetical deposit.....	44
14. Comparison of the estimated cost per pound for recovering copper by nuclear fracturing and in-situ leaching with cost of conventional methods.....	47

Pr
red w
-situ
resent
is a
a fu
ethod

Pr
posit
me ca
cover
: reco
: less

Nu
metho
dicat
e cop
th
s cos
be

Th
over
ucle
copp

ing
of M

on

31
32
35
38
39
41
41

FRACTURING A DEPOSIT WITH NUCLEAR EXPLOSIVES AND RECOVERING
COPPER BY THE IN-SITU LEACHING METHOD

by

William R. Hardwick¹

42
45
41

ABSTRACT

Present information indicates that a copper deposit can be safely fractured with a nuclear explosive and the copper successfully recovered by the in-situ leaching method. The process is not yet at the stage where it can be presented to the mining industry as a technique proven in all its aspects, but it is a method with high success potential. Unknown factors must be evaluated in a full-scale test before the economics or the extent of the use of the method by the mining industry can be predicted.

13
15
16
22
22
23

Preliminary calculations indicate that the cost of fracturing a copper deposit with nuclear explosives may range from 1.8 to 55.2 cents per ton or in some cases less than a cent per pound of recoverable copper. Copper may be recovered at less cost than by conventional methods. Deposits with 4 pounds of recoverable copper may be economic and production from a deposit may begin in less than half the time required for conventional methods.

30

INTRODUCTION

43
43
44
44
45
46

Nuclear explosive fracturing followed by in-situ leaching is proposed as a method for the recovery of copper; it is assumed, and present information indicates, that control of radiation hazards, including any contamination of copper produced, will be feasible. Tests are currently in progress to confirm that these hazards will be controllable, both from the operational and cost viewpoints. Complete evaluation of the method, including economics, will be made only after a full scale test has been completed.

47

This Bureau of Mines report describes copper deposits, current methods of recovering copper by percolation leaching, and methods of fracturing rock with a nuclear explosive. It considers the application of current leaching methods to copper deposits that have been broken and fractured with a nuclear

¹Mining engineer, Area V Mineral Resource Office, Tucson Field Office, Bureau of Mines, Tucson, Ariz.

explosive. A brief resume of the extent of the copper industry and the recognized copper reserve of the United States is included. The mineralization of copper deposits, available information on the solubility of copper minerals, chemistry of leaching copper, and mechanics of leaching copper are described in sufficient detail to serve as a guide for the laboratory study of potential safety problems that may be induced when the deposit is subjected to the radioactive activity of a nuclear explosion.

Research by the U.S. Atomic Energy Commission (AEC) and various contractor agencies under the Plowshare Program has indicated that large masses of rock can be fractured safely by the use of nuclear explosives. Cooperative research by the AEC and the Bureau of Mines has indicated that fracturing a deposit containing leachable copper minerals with nuclear explosives will permit recovery of the copper by in-situ leaching methods.

The term "in situ" is used in this report in preference to the more ambiguous term "in place" to designate ore that may have been broken or fractured, but otherwise has not been removed from its original geologic location by the process of recovering the copper. Ore in dumps as well as in situ is said to be leached in place by the copper industry in contrast to ore that is crushed, ground, pulped, and said to be leached in process.

Recovering copper by leaching rock in situ is not new. However, it can be done only when rock is broken and fractured so that solvent solutions can be percolated through to contact the copper minerals. The method has been successfully used after mining was discontinued at block-caving mines where large masses of rock containing copper minerals were broken and left in the mine. Before the advent of nuclear explosives, there was no method of breaking and fracturing large masses of rock except by large-scale mining methods. These would not be economical if used solely to prepare a low-grade copper deposit for in-situ leaching, but a deposit could be fractured economically and safely with nuclear explosives.

Cost reduction in the United States has resulted from mining and metallurgical research leading to more efficient extraction and beneficiation of copper ores. Research on any method that gives promise of reducing the cost of producing copper and making available low-grade reserves not presently economic is well justified by the increasing demand for this vital metal. The successful application of nuclear fracturing and in-situ leaching may substantially increase the copper reserve and lower the cost of copper to American industry. The method eliminates the time consuming and costly construction of concentrating and smelting plants to process large tonnages of rock and may provide a method of expanding copper production rapidly in times of emergency.

Details on the formation, description, and phenomenology of nuclear explosives are described and a bibliography has been compiled and published by the U.S.

Atomic Energy Commission.² Information has been used freely from these publications.

Information has been used from numerous reports by the Bureau of Mines on various phases of copper leaching and processing. Some have been listed as footnotes. The reader is referred to the general list of publications by the Bureau of Mines, U.S. Department of the Interior, for a complete listing.³

ACKNOWLEDGMENTS

Thanks are due for information obtained from interviews with members of the University of California, Lawrence Radiation Laboratory; Sandia Corp.; Oak Ridge National Laboratory; San Francisco and Nevada Operations offices of the Atomic Energy Commission; and many mining companies.

HISTORY AND COMMERCIAL EXAMPLES OF IN-SITU COPPER LEACHING METHODS

A rapid growth in the use of copper has occurred in the last 150 years as a result of the development of electric power and the expansion of the brass and bronze industry. During this period world demand for copper has expanded from 10,000 tons to more than 5 million tons per year. The copper mining, smelting, refining, and fabricating industries throughout the world have expanded rapidly in the past half century.

About 1940, the United States shifted from its position as the world's largest exporting country to that of the world's largest importing country, at the same time continuing to be the world's largest producer as well as consumer of copper. The copper position of the United States, on the basis of current mine output and apparent low cost of production, ranks first. However, on the basis of grade and extent, the United States copper reserve may be third. Huge African reserves are reported to contain 3 to 6 percent, Chilean reserves are reported to exceed 2 percent, while the reserves of the United States average less than 1 percent copper. Known domestic copper ore reserves that might be mined at present copper prices probably will be exhausted in 30 years or less. However, copper ores of progressively lower grades probably will continue to be mined, and more emphasis may be placed on in-situ leaching as a method of recovery.

The method of recovering copper from ore by acid leaching first was used in ancient times, probably in Cyprus, Armenia, Egypt, and other places. Agricola described methods used to recover vitrol and copper from ore in the

²Voress, Hugh E., William F. King, and Carl R. Gerber. Peaceful Uses for Nuclear Explosives. A Selected Annotated Bibliography. TID 3522, 7th Rev., Division of Technical Information, U.S. Atomic Energy Commission, Oak Ridge, Tenn., 1964, 55 pp. (For sale from Office of Technical Services, Department of Commerce, Washington, D. C.)
³For sale by the Superintendent of Documents, U.S. Government Printing Office, Washington, D. C.

15th Century.⁴ Dump or heap leaching in Europe began in Germany in the 16th Century and reached great efficiency in the Rio Tinto mine in Spain where it is still used.

In the United States, the precipitation of copper from mine waters began about 1890 at Butte, Mont., and has been used at various localities. The first serious attempt to apply heap (dump) leaching to copper ores in the United States was made by Phelps Dodge Corp. about 1900, after James S. Douglas visited Rio Tinto in Spain and was impressed with the possibilities of the process for Bisbee ore.⁵ Subsequently the method was used on many of the dumps from large open-pit copper mines. Many mining plants now incorporate dump leaching as an integral part of the copper recovery system (fig. 1).

The first significant application of the leaching method to rock in situ was at the Ohio copper mine, Utah, in 1922. Previous to this time, inoperative mines in the Butte district had been flooded and the dissolved copper recovered from solutions. After mining by the block-caving method was terminated at the Ohio copper mine, an inverted cone of broken rock containing about 38 million tons remained. Water was applied to the top of the broken rock, percolated down through the copper-bearing rock and collected in an adit below. The copper was recovered in a successful leaching operation. After the success at the Ohio copper mine, in-situ leaching was generally attempted and often succeeded on large masses of broken copper-bearing rock that remained after large-scale mining operations were terminated.

After considerable areas of copper-bearing ore had been developed in the Butte district of Montana and many stopes filled with waste containing some copper sulfide, copper sulfate began to appear in the mine water. After years of underground work, extensive areas of stope, drift, and other underground workings were opened, and these became filled with waste containing some copper minerals. The copper minerals were oxidized by exposure to the air, which made them more soluble in the mine water and increased the copper content.

In November 1889, water was channeled into the St. Lawrence mine in an effort to extinguish a fire. When this water was pumped from the mine it was rich in copper sulfate and the first production of copper from mine water resulted. Some time after 1890, the Anaconda Company began operating a precipitating plant and has produced copper from the mine water ever since.

Special effort is made to bring the acid mine water in contact with old filled stopes. Where possible, parts of the mine are flooded then the water is pumped to the surface and passed through a copper precipitating plant. Water is introduced into old filled stopes by drilling long holes with a percussion drill to intersect the stopes from lateral drifts on the footwall of parallel to the stopes (fig. 2). During some months, production of copper by leaching has yielded 1,500,000 pounds.

⁴Agricola, Georgius. De Re Metallica. Trans. by Herbert C. Hoover and L. E. Hoover. Dover Publications, Inc., New York, 1950.

⁵Hudson, A. W., and G. D. Van Arsdale. Heap Leaching at Bisbee, Ariz. Trans. AIME, Vol. 65, 1923, pp. 137-154.



FIGURE 1. - Mine Plant Showing Dump Leaching as an Integral Part of Copper Recovery Systems.

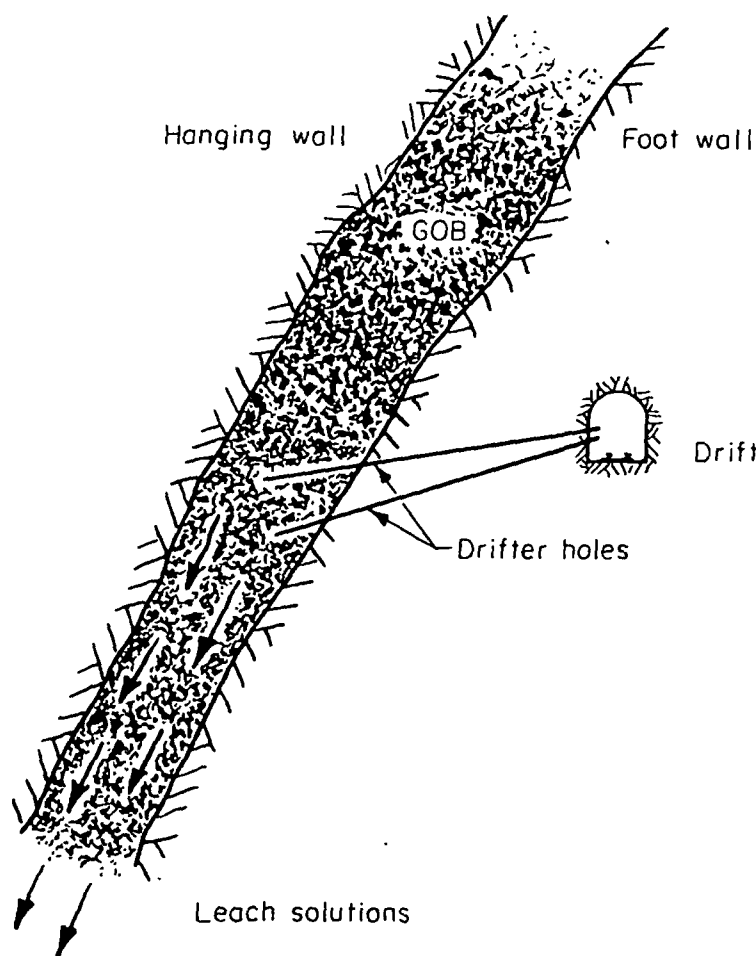


FIGURE 2. - Stope Leaching.

occur in seams, veinlets, and as disseminated particles in Precambrian Pinal schist and Tertiary Schultz granite. There is practically no pyrite in the capping and very little in the ore.

Solution of tail water from the copper precipitating plant and fresh water are pumped to a storage tank through Transite⁷ pipe (fig. 3). The solution discharged from the precipitating plant contains only a trace of acid; about 0.5 pound of sulfuric acid per ton of water is added. This amount is sufficient to prevent iron salts from precipitating, but does not attack the Transite pipe and storage tanks. From the storage tank, the solution is pumped to distribution centers above the caved surface where it is measured in weir boxes, and additional sulfuric acid is added to bring the strength to

The open drainage in-situ leach method is successfully used for the recovery of copper at the Miami mine of Tennessee Corp., a subdivision of Cities Service Corp., in Gila County, Ariz.⁶ During the active life of the Miami mine, about 153 million tons of ore was mined from a deposit that ranged from 200 to 1,000 feet in depth. The ore was mined by the block-caving method, and the subsidence resulted in a crater of about 1,500 feet in diameter and 300 feet deep. From this crater, broken rock extends downward to the mine level.

The broken rock contains portions of capping, oxide ore, crushed stope pillars, and stope ore diluted with waste rock, all of which contain some copper. Overall, the chief copper mineral is chalcocite, with chalcopyrite, bornite, covellite, malachite, azurite, chrysocolla, cuprite, and native copper as minor minerals. The copper minerals

⁶Fletcher, J. B. In-Place Leaching at Miami Mine. Milling Division, Arizona Section, AIME, Apr. 6, 1962, 7 pp.

Hardwick, W. R. Block-Caving Copper Mining Methods and Costs at the Miami Mine, Miami Copper Company, Gila County, Ariz. BuMines Inf. Circ. 8271, 1965, p. 81.

⁷References to specific brands is made for identification only and does not imply endorsement by the Bureau of Mines.

about 10 pounds per ton of water. After the acid is added, the solution flows by gravity in polyethylene plastic pipe to points of application. Ponds, drill holes, and sprays are used to introduce the solution into the ground.

The depth of the broken material averages about 600 feet. Most of the copper is believed to be in the bottom 150 feet. It requires 3 to 4 weeks after a spray is turned on the surface before solution percolates through the broken rock and comes through on the 1,000 level. The flow stops about 2 weeks after the spray is turned off. The first solution emerging is high in copper content. The spray is left in one place until the grade drops below 3 pounds of copper per ton of solution. The spray is then turned off and the area is allowed to dry. Drying and wetting periods are alternated; each new wetting brings high-grade solution but the period for which the copper content remains high decreases with repeated wettings. Many sprays are operated, some in high-grade areas and some in low-grade or partly depleted areas, and the number in each area is adjusted so that the average copper content of the recovered solution is at the desired level.

The solution is collected on the 1,000 level and pumped to a precipitation plant on the surface where it passes through cells containing detinned shredded cans. The copper precipitates as dendrites of metallic copper on the iron and is washed by high-pressure water through wooden screens. The precipitates discharge on a concrete decant slab and are drained, washed, and moved with a front-end loader to a concrete drying pad. Dried precipitates, which contain about 79 percent copper, are loaded with a front-end loader into a railroad car and shipped.

Major factors affecting the cost are the iron and sulfuric acid consumption. If the acid content of the pregnant solution becomes too high, the iron consumption in the precipitating cells is high. If the acid content of the solution pass through the broken ore is high, the consumption of acid by gangue minerals is increased. Iron salts precipitate as the solution passes through the caved material at the rate of about 4.2 pounds of iron per ton of solution. At Miami the acid strength is kept below 15 pounds per ton of solution and the consumption is .24 pounds of acid per pound of copper. About 1.5 pounds of scrap iron is required per pound of copper produced.

The Miami mine is operated every day of the year circulating 2,000 gpm. The pumps are operated three shifts. Underground repair crews and maintenance crews operate 5 days per week. The operation requires about 123 manshifts per week. About 9,000 tons of refined copper per year is produced from the "cement copper" precipitate.

The flood-leaching method is successfully used in a combined dump and in-situ leaching operation for the recovery of copper at the Ray Mines Division of Kennecott Copper Corp. in Arizona. During the active life of the underground mine, many millions of tons of copper ore was mined from a deposit that ranged from 200 to 600 feet in depth. The ore was mined by the block caving method, and the subsidence resulted in an elongated crater 1,000 feet wide, 2,000 feet long, and 150 feet deep. When a nearby open pit was strip material containing some leachable copper was used to fill this crater.

pil
cop
Mal
the
tic
Pyr
cha

rou
is
pit
wer
Min
per
the
sul

by
worl
cip
the
ret
tion
tion
flow
dmi
cit

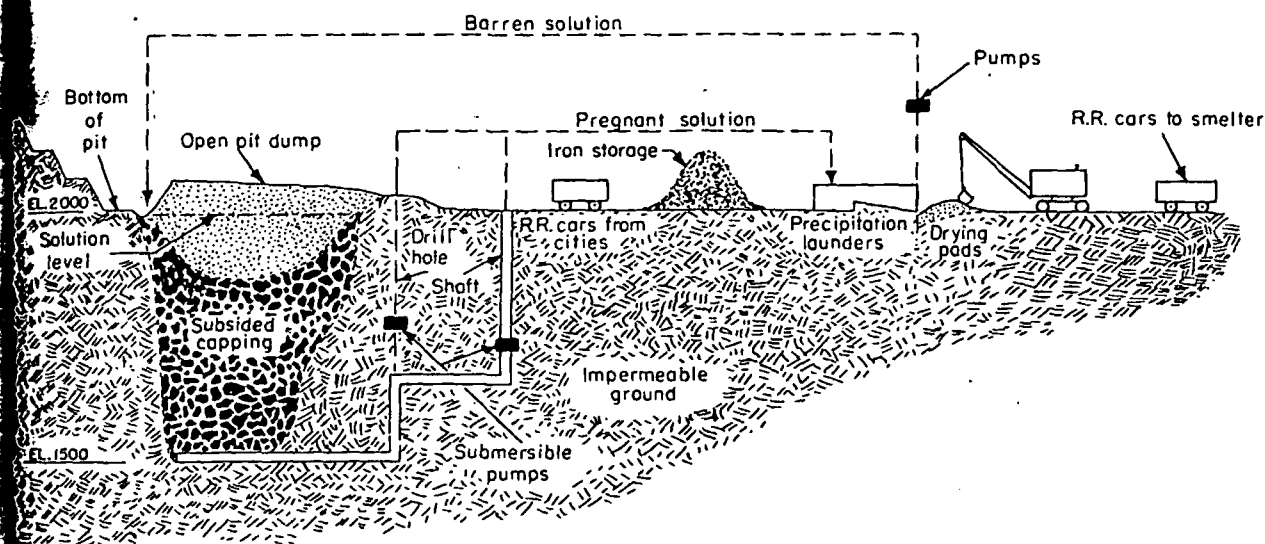


FIGURE 4. - Flood-Leaching System.

The broken rock consists of portions of capping, oxide ore, crushed stope pillars, diluted stope fill, and stripping from the nearby open pit. Most copper occurs in the minerals chalcocite, chalcopyrite, and cupiferous pyrite. Malachite, azurite, chrysocolla, diopside, cuprite, and native copper occur in the capping. The ore minerals are in seams, veinlets, and disseminated particles; the rock is Precambrian schist, diabase, and monzonite porphyry. Pyrite is plentiful in the primary ore, and some is intermingled with the chalcocite.

The bottom of the ore is well below ground-water level, and the rock surrounding the broken ore in workings is tight and impermeable. The bottom level is at 1,500 feet above sea level and the bottom level of the adjoining open pit is at 2,000 feet above sea level. After the mine was closed, the workings were flooded to the 2,000-foot level. Water, obtained from the gravels of Mineral Creek, is in short supply during part of the year. During this dry period, the water level may be lower than the 2,000-foot level, thus exposing the material to oxygen. Dissolved sulfates and oxidizing pyrite and other sulfides provide abundant acid.

Copper-bearing solution is pumped from the flooded mine at three points by submersible pumps in shafts and drill holes connected with the underground workings. About 2,000 gallons per minute is pumped and passed through a precipitation plant where the copper is removed. Spent solution is returned to the flooded mine. No attempt is made to distribute the return water; it is returned to a sump on the surface distant from points at which pregnant solution is withdrawn. It again becomes charged with dissolved copper by diffusion as it percolates through the broken rock (fig. 4). In addition to the flood-leaching operation in the abandoned underground mines, open-drainage dump leaching is used to recover copper from low-grade material in the open-pit waste dumps.

COPPER DEPOSITS

Most copper has been deposited in the earth's crust as a sulfide mineral by solutions in channels through which the mineral-bearing solutions escaped from the interior of the earth. Sometimes the path of the solution was a definite, confined, and comparatively narrow fracture or pipe, and the minerals were deposited in this channel or in connected cavities to form a high-grade deposit. At other times the channel was a wide zone containing many small fractures, and the copper minerals were deposited in small seams, fractures, cavities and as disseminated particles in the rock over a wide area to form a low-grade but extensive deposit.

Weathering processes, either in the present or former geologic periods, have altered the near-surface sulfide minerals to oxide, carbonate, silicate, or sulfate minerals. Sometimes, after the oxide minerals are formed, geological processes have covered the deposit with sedimentary or volcanic rock. Thus, although generally formed near the surface, deposits of oxide copper minerals may occur at great depths.

The weathering process continues in deposits where sulfide copper minerals are exposed to air and moisture. Soluble copper minerals are dissolved from the upper oxidized part of the deposit by rain water, and the solutions migrate downward. Copper is removed from the rock near the surface, and a blanket of leached capping is formed. The copper content of the underlying sulfide zone, when compared to the copper content of this leached capping, may be a measure of the amount of copper that is recoverable from a sulfide deposit by in-situ leaching.

When the solutions reach permanent water level, the hydrogen-ion concentration increases because of the inaccessibility to oxygen and slight ionizing of sulfide material. The copper is precipitated from the downward migrating solution as the minerals chalcocite, covellite, or bornite, thus forming a zone where secondary sulfide copper minerals intermingle with and enrich the primary sulfide minerals. This enriched zone often consists of copper ore that ranges from 200 to 600 feet or more in thickness and forms deposits that sometimes exceed a billion tons. Deposits of this type are the source of most of the copper ore that is now mined.

Copper minerals are widely distributed in the surface of the earth. Rock that contains copper minerals is classed as ore when copper is in a recoverable form and its recovery is profitable. The cost of mining and processing the ore including finding the deposit and recovering, refining, and marketing the copper must be less than the sale value of the copper recovered.

Large deposits of copper-bearing rock become ore when the selling price increases more rapidly than the cost of recovering the copper or when a new extraction method is developed that will reduce the cost of production, as proposed use of nuclear fracturing and in-situ leaching may do.

In copper mining the term "oxide ore" indicates rock containing combinations of oxide, carbonate, silicate, sulfate, and sulfide copper minerals.

are dissolved from a laboratory sample in a short period of time by a dilute acid, generally 5 to 10 percent sulfuric acid by volume.⁸ Copper in this form generally is not readily concentrated by the flotation method although most sulfide minerals are recovered.

The term "sulfide ore" is used by the industry to indicate rock containing those copper minerals that are not readily soluble in dilute sulfuric acid and generally can be successfully recovered by the flotation process. Native copper, recoverable by the flotation method, is usually included with the sulfide minerals. Although sulfide minerals generally are not quickly soluble in an acidic solution, most may be dissolved slowly by an oxidizing agent such as ferric sulfate, and all are soluble in long periods of time.

In 1963, 1.2 million tons of copper valued at \$747 million was produced by the copper mining industry in the United States. About 81 percent of the ore and 74 percent of the 1963 copper was from open-pit mines.⁹ The average copper content of the ore was 0.75 percent. About 10 percent of the copper was recovered by leaching. The total material mined was 426 million tons of which 146.5 million tons was copper ore and the remainder was waste. Much of the waste contained a small amount of copper that eventually will be recovered by dump-leaching methods.

The Geological Survey and the Bureau of Mines published a figure of 32.5 billion tons for United States copper reserves in 1959.¹⁰ Since that time more than 6.75 million tons of metal has been produced. How much of this production has been offset, or how much of the reserve has been increased by new discoveries and extensions of known ore bodies is not known.

Some industry spokesmen have quoted a reserve tonnage at least 50 percent larger than that mentioned in the 1959 release. The 32.5 million-ton copper reserve of 1959 was contained in ore estimated to average 0.9 percent or 18 pounds of copper per ton. At this average figure, the copper reserve would be contained in more than 3.6 billion tons of ore.

The 1959 reserve figures did not include metal in subeconomic deposits and mine dumps that can be leached. Large tonnages known to contain from 0.25 to 0.5 percent copper were not economic in the past nor at present, and the metal contained is not included as reserve. Reserve forecast over the past decades show an upward trend in quantity of copper available in spite of large tonnage of ore mined. This increase in reserve has resulted partly from lowering the cutoff grade as a result of improved techniques in mining and processing the ore.

⁸ Dean, R. S., F. S. Wartman, A. J. Thompson, E. K. Pryor, J. D. Sullivan, G. L. Oldright, A. F. Hallet, S. L. Brown, W. A. Sloan, and C. W. Davis. Progress Reports--Metallurgical Division. 3. Studies in the Metallurgy of Copper. BuMines Rept. of Inv. 3228, 1934, pp. 57-63.

⁹ Wideman, F. L. Copper. BuMines Minerals Yearbooks, 1963, v. I, 1964, p. 444.

¹⁰ Bureau of Mines. Copper Reserves of the United States Estimated by Interior. Press Release, June 5, 1959.

Not included in the reserves are many small tonnage deposits containing as much as 2 percent copper. Such deposits contain a tonnage too small to amortize the construction of a concentrating plant and are too low grade to justify direct shipment to a smelter. Many of these deposits are contained in pipe-like form that would be ideal for nuclear fracturing and subsequent in-situ leaching.

Copper deposits containing leachable copper minerals might be successfully fractured with the use of nuclear explosives, and the copper leached from the rock in situ. Such a method of production might substantially lower the cost of producing copper from deposits of this type, thus adding them to increase copper reserves. Statistics are not available to separate leachable from nonleachable reserve and resource deposits. Until this information is available, it is difficult to predict the extent to which the proposed method may be applicable.

Leaching is the term applied to the process of recovering valuable minerals or metals from an ore by dissolution leaving the gangue or waste material virtually unaffected. Subsequent recovery of the metal or metals from solution is effected through either chemical or electrolytic precipitation.

An important factor in determining the leachability of a copper deposit is the type of host rock in which the minerals are deposited. Copper is found in rock types ranging from carbonate to silicate in sedimentary, metamorphic, or igneous formations. Some deposits are in carbonate rocks and cannot be leached economically with acid because the gangue consumes excess amounts of acid. Some crystalline rocks that are hosts for disseminated copper deposits are diabase, monzonite, granite, tactite, argillite, hornfel, and schist. Many deposits have few or no acid-consuming minerals in the associated gangue; these may be suitable for nuclear fracturing and in-situ leaching. Next to percentage of copper extraction, the solvent consumption of the gangue rock is the most important item investigated in the examination of a deposit for possible in-situ leaching. The copper extraction and acid consumption of the rock can be approximated from a metallurgical test.

Copper minerals are oxidized and may be dissolved eventually in geologic periods of time. Before the perfection of the flotation method, research was directed toward the determination of solvent and mechanics for the rapid dissolution of sulfide copper minerals. Efforts were pointed toward determining the solubility of copper minerals in terms of hours and days. More research is needed to determine the rate of dissolution of the more difficult soluble copper sulfide minerals in periods of months and years.

Oxide minerals are readily soluble; simple sulfide minerals chalcocite and covellite are easily dissolved by combinations of sulfuric acid and ferric sulfate; the complex mineral bornite is dissolved with some difficulty; and chalcopyrite (CuFeS_2) is dissolved in a short time, with extreme difficulty; it is often considered nonleachable when ore is treated in leaching tanks. The time required for dissolution of the copper minerals in a tank-leaching operation is extremely important and must be short, but time may not be so critical in an in-situ leaching project. The dissolution of a copper mineral

such
vid
rate
test

Azur
Mala
Teno
Chry
Do

Cupri

Chalc

Bornit

Covel

Chalc

Chalc

Enarg

Tenna

Tetra

Adap

th

Grou

throu

ing t

is o)

such as a chalcopyrite at a slow rate may not preclude in-situ leaching providing the rate of acid consumption by gangue minerals is low. The amount and rate at which copper was dissolved from various minerals by Bureau of Mines tests is indicated in table 1.

TABLE 1. - Comparative rate of dissolution of various copper minerals sized to minus 100, plus 200 mesh at a temperature of 35° C¹

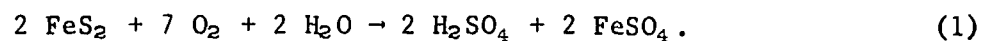
Mineral	Time	Solvent	Copper, percent
Azurite.....	1 hour	1 pct of H ₂ SO ₄	100
Malachite.....	1 hour	1 pct of H ₂ SO ₄	100
Tenorite.....	2 hours	1 pct of H ₂ SO ₄	98
Chrysocolla.....	24 hours	5 pct of H ₂ SO ₄	100
Do.....	1 hour	2 pct of iron as Fe ₂ (SO ₄) ₃ + 2 pct of H ₂ SO ₄	100
Cuprite.....	1 hour	2 pct of iron as Fe ₂ (SO ₄) ₃ + 2 pct of H ₂ SO ₄	100
Chalcocite.....	20 days	1 pct of iron as Fe ₂ (SO ₄) ₃ + 0.5 pct of H ₂ SO ₄	97
Bornite.....	21 days	1 pct of iron as Fe ₂ (SO ₄) ₃ + 0.5 pct of H ₂ SO ₄	99
Covellite.....	47 days	1 pct of iron as Fe ₂ (SO ₄) ₃ + 0.5 pct of H ₂ SO ₄	57
Chalcopyrite.....	43 days	1 pct of iron as Fe ₂ (SO ₄) ₃ + 1 pct of H ₂ SO ₄	2
Chalcopyrite ²	42 days	5 pct of iron as Fe ₂ (SO ₄) ₃ + 0.5 pct of H ₂ SO ₄	30
Ernargite.....	60 days	1 pct of iron as Fe ₂ (SO ₄) ₃ + 0.5 pct of H ₂ SO ₄	2
Tennantite.....	30 days	2 pct of iron as Fe ₂ (SO ₄) ₃ + 0.5 pct of H ₂ SO ₄	7
Tetrahedrite.....	23 days	1 pct of iron as Fe ₂ (SO ₄) ₃ + 0.5 pct of H ₂ SO ₄	95

¹Adapted from pages 47-50 of reference cited in footnote 9 in the main body of this report.

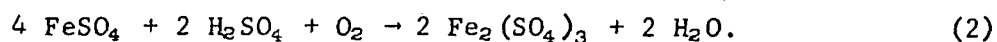
²Ground to 350 mesh.

CHEMISTRY OF LEACHING COPPER

When water and air or water containing dissolved air is percolated through broken rock containing pyrite, sulfuric acid is formed slowly according to equation 1:

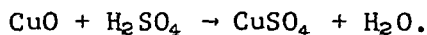


In the presence of abundant oxygen and sulfuric acid the ferrous sulfate is oxidized slowly to ferric sulfate according to equation 2:



Ferric sulfate in the presence of sulfuric acid forms a solution that will dissolve most copper minerals. Most copper deposits contain varying amounts of pyrite associated with the copper minerals. When a deposit does not contain sufficient pyrite to form sulfuric acid the acid must be added to the leach solution. Some basic equations for the dissolution of various copper minerals are:

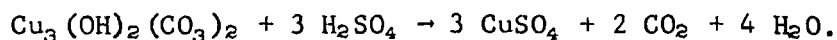
Tenorite, CuO:



Malachite, $\text{Cu}_2(\text{OH})_2\text{CO}_3$:



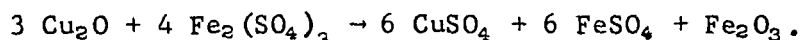
Azurite, $\text{Cu}_3(\text{OH})_2(\text{CO}_3)_2$:



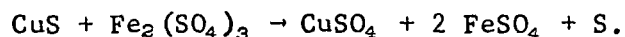
Chrysocolla, $\text{CuSiO}_3 \cdot 2 \text{H}_2\text{O}$:



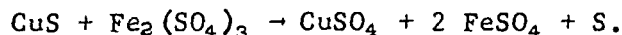
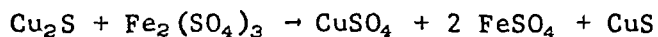
Cuprite, Cu_2O :



Covellite, CuS:



Chalcocite, Cu_2S (in two stages):



The dissolution of the double sulfides of copper and iron, bornite, Cu_5FeS_4 , cubonite, CuFe_2S_4 , chalmersite, CuFe_2S_3 , and chalcopyrite, CuFeS_2 , is normally difficult. Bureau of Mines tests indicate that when bornite is leached with sulfuric acid and ferric sulfate, the iron is attacked preferentially and the mineral is dissolved.¹¹ Tests show that with chalcopyrite the ratio of combined Cu:Fe:S in the residue remains the same as the original mineral at any stage in the dissolution and the mineral generally is dissolved very slowly.

Chalcopyrite is not soluble in an aqueous solution of sulfuric acid and is not oxidized at normal temperatures over long periods of time. It is

¹¹Sullivan, John D. Chemistry of Leaching Bornite. BuMines Tech. Paper 486, 1931, 20 pp.

oxidized
ferric
sulfate
paste

abundant
sulfuric
solution
acid
sulfuric
leach

methanol

the copper

causing

the copper

equation

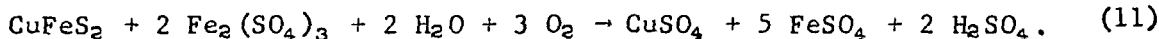
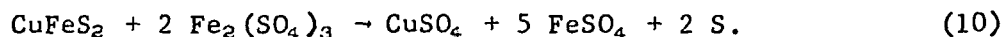
replace

circulation

Page

20 A m

oxidized and dissolved slowly by solutions that contain ferric sulfate or ferric chloride. Rate of dissolution may be about 1 percent per month (table 1). Sullivan and Brown studied the dissolution of chalcopyrite in 1934¹² and suggested equations:



Some leachable copper deposits have no sulfide minerals; others have abundant pyrite and sulfide copper minerals. Generally deposits containing sulfide minerals do not require the addition of sulfuric acid to the leach solution. Acid is generated when water is percolated through the broken ore. Acid must be added to the solution for those deposits that are deficient in sulfide or sulfate minerals. The amount of sulfuric acid that is added to the leach solution is shown for several operating plants on table 2.

TABLE 2. - Sulfuric acid added per pound of recovered copper

Plant	Method of application	Acid-pounds
Inspiration.....	in situ	2.25
Miami Copper.....do.....	2.4
Bagdad.....	dump	4.8
Ray.....	in situ	.0
Silver Bell.....	dump	.0
Chino.....do.....	.0
Esperanza.....do.....	.0

Copper has been recovered commercially from acid solution by three methods:¹³

1. Copper in solution as a sulfate is replaced by metallic iron causing the copper to precipitate.
2. The copper ion in a sulfate solution is reduced by an electric current causing the copper to precipitate at the cathode.
3. The acidity of the solution is reduced by addition of lime causing the copper to precipitate as a basic carbonate.

Copper in an acid solution is replaced by metallic iron according to equation 12:

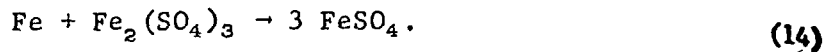
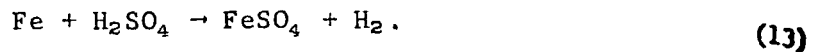


Theoretically 0.88 pounds of iron will replace 1 pound of copper. The replaced copper immediately precipitates as dendrites on the iron; however, circulating solutions contain free sulfuric acid and ferric salts in solution

¹² Page 47 of work cited in footnote 9.

¹³ A method using the liquid ion exchange process is under development.

that also consume iron according to equations 13 and 14:



In actual operations the metallic iron consumed per pound of copper recovered ranges from 1.3 to 3 pounds. Good clean, compact iron or mild steel will precipitate more copper than detinned cans and light iron, but presents handling and mechanical problems. Sponge iron, a porous product resulting from the chemical reduction of solid iron-bearing material at a temperature short of its melting point, is sometimes used. The iron consumed at several plants is shown on table 3.

TABLE 3. - Iron required to recover copper from solution

Plant:	<u>Pounds of iron per lb of copper</u>
Rio Tinto, Spain.....	1.4
Silver Bell, Ariz.....	1.5
Ray, Ariz.....	1.8
Esperanza, Ariz.....	1.35
Bagdad, Ariz.....	1.7
Miami, Ariz.....	1.3
Chino, N. Mex.....	1.4
Cananea, Mexico.....	2.9

The precipitation of copper by electric current from leach solution, called electrowinning, is accomplished by several large producers. Advantages of the method are that a refined product is produced and ferric sulfate and/or sulfuric acid is regenerated. The reaction is endothermic; electrical energy sufficient for the decomposition of CuSO_4 is consumed. A solution containing copper sulfate (CuSO_4) is passed through a cell containing alternate insoluble anodes and thin copper starting sheets.

If the CuSO_4 is considered to ionize as Cu^{++} and SO_4^{-} ions, the reaction at the cathode is:

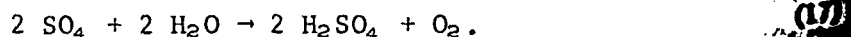


The copper, soluble as an ion but very insoluble when neutralized, immediately precipitates as a deposit on the cathode.

At the anode the reaction is:



The SO_4 immediately combines with water to release oxygen and form sulfuric acid according to equation 17:



A choice between the use of iron and electricity for copper recovery is generally made on the basis of size and duration of the operation; small and short time operations use metallic iron and large operations use the electrolytic method. Economic factors such as the cost of power and transportation are also important.

Depending on company preference, several methods are used to report the assay values of solutions: percent, grams per liter, pounds per ton, or pounds per 1,000 gallons. The flow of solutions is measured in gallons per minute. One gallon of solution weighs about 8-1/3 pounds. A flow of one gallon per minute for 24 hours is equal to 8-1/3 x 1,400/2,000 or 6 tons per day.

Copper recovery plants are designed to treat a specified amount of solution, and the copper content of the solution is adjusted to produce the desired amount of copper. The solution is circulated through high-grade (new) and low-grade (partly leached) areas of the deposit or dump. The area is controlled by the placement of the spray or solution pond. The flow is adjusted by area so that the blended flow from all areas contains the desired amount of copper. One in-situ leaching operation was designed to circulate 2,000 gpm and produce 50,000 pounds of copper per day. The calculations for grade of solution are as follows:

$$2,000 \times 6 = 12,000 \text{ tons of solution per day.}$$

$$\frac{50,000}{12,000} = 4.17 \text{ pounds of copper per ton of solution.}$$

To the 4.17 pounds must be added that in the tail water (0.04) and the loss in smelting (0.07). The required copper content for feed water to the plant must then be 4.28 pounds of copper per ton of water. To assure a uniform copper content at the desired level, the outflow from the deposit is sampled. When the copper content drops below the desired amount, less solution is distributed over low-grade or partially leached areas and more over high-grade areas of the broken ore. The copper content of the solution recovered by a flood-leaching operation may be controlled by the rate of flow through the deposit.

THE EFFECT OF BACTERIA ON THE SOLUBILITY OF COPPER MINERALS AND THE REACTION OF BACTERIA TO RADIOACTIVITY

The activities of bacteria influence the oxidation of some sulfide minerals.¹⁴ Water samples were collected from five Arizona copper mines and three species of oxidizing bacteria were isolated from the samples.¹⁵ The results of extended tests indicate that the sulfur oxidizing bacterium, *Thiobacillus thiooxidans*, can readily convert sulfur to acid but is not able to

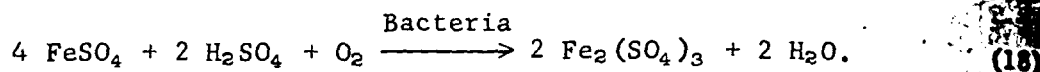
¹⁴ Sutton, Joseph A., and John D. Corrick. Possible Uses for Bacteria in Metallurgical Operations. BuMines Inf. Circ. 8003, 1961, 8 pp.

¹⁵ Corrick, John D., and Joseph A. Sutton. Three Chemosynthetic Autotrophic Bacteria Important to Leaching Operations at Arizona Copper Mines. BuMines Rept. of Inv. 5718, 1961, 8 pp.

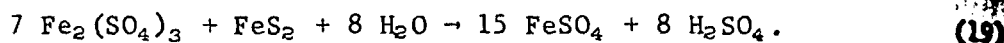
assimilate and oxidize the sulfur as it occurred in sulfide minerals of copper.¹⁶ *Ferrobacillus ferrooxidans* is capable of producing quantities of acid ferric sulfate from ferrous iron that dissolve significant quantities of copper from the minerals chalcocite, covellite, and bornite. The iron oxidizing bacteria *Ferrobacillus ferrooxidans* and *Thiobacillus ferrooxidans* are able to accelerate the dissolution of the iron in the minerals pyrite and chalcopyrite.

The chemistry involved in microbial dissolution of iron and copper from sulfide minerals has been described by Sutton by reference to a series of chemical equations.¹⁷ Pyrite in the presence of oxygen and water is slowly oxidized according to equation 1.

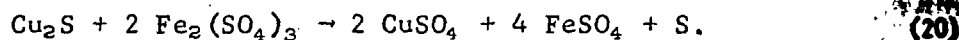
The iron oxidizing bacteria in the presence of oxygen and sulfuric acid then oxidize the available ferrous sulfate and, acting as a catalytic agent, accelerate the formation of ferric sulfate as shown in equation 18:



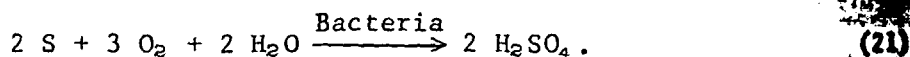
The ferric sulfate reacts with pyrite to form sulfuric acid and ferrous sulfate according to equation 19:



Ferric sulfate also reacts with a copper sulfide mineral, such as chalcocite, to form copper sulfate, ferrous sulfate, and elemental sulfur as shown in equation 20:



The ferrous sulfate is then reoxidized by the iron oxidizing bacteria to form more ferric sulfate, and the cycle is repeated. The elemental sulfur free in the dissolution of the copper mineral is oxidized by the sulfur oxidizing bacteria *Thiobacillus concretivovus*, in the presence of oxygen and water, to form sulfuric acid as shown in equation 21:



Apparently the sulfur and iron oxidizing bacteria, by expediting the production of sulfuric acid and ferric sulfate, increase the dissolution of the copper minerals but do not attack the copper minerals directly. Basically, these bacteria do not change the nature of the chemical reaction but increase the rate of the reaction.

¹⁶Sutton, Joseph A., and John D. Corrick. *Bacteria in Mining and Metallurgy: Leaching Selected Ores and Minerals; Experiments With Thiobacillus Thiobacillus ferrooxidans*. BuMines Rept. of Inv. 5839, 1961, 16 pp.

¹⁷Sutton, Joseph A., and John D. Corrick. *Leaching Copper-Sulfide Minerals With Selected Autotrophic Bacteria*. BuMines Rept. of Inv. 6423, 1964, 23 pp.

Investigations of bacterial leaching under conditions similar to those expected to exist in the environment of a nuclear chimney have indicated that the bacteria most important in accelerating leaching of sulfide ores can be expected to grow under these conditions. The small quantities of radioactive explosion byproducts present do not inhibit bacterial leaching. The residual heat left in the rock surrounding the nuclear explosion in most cases will tend to stimulate rather than inhibit the growth of the bacteria.¹⁸

MECHANICS OF LEACHING

Four factors are necessary for the successful leaching of copper ores; they are:

1. A solution that will attack the copper minerals must be brought into contact with the particles of ore.
2. The copper minerals must be dissolved by chemical action of the solution.
3. The solution must find its way out of the voids of the rock and be recovered in a collecting system.
4. The copper in the solution must be recovered.

Leach solutions are applied to copper-bearing rock under three circumstances in conventional practices:

1. Ore is mined, crushed, and processed in a tank.
2. Unsorted ore is mined, placed in a heap or dump and leached in place.
3. Ore is broken or fractured and the copper is leached from the rock in situ.

There are two methods of applying solutions for percolation leaching; flood leaching (the ore is immersed in solution that percolates either up or down through the ore) and open-drainage leaching (the solution is distributed on top of the ore and collected below after percolating down through the ore).

Not classed as a leaching method is the leach-precipitate-float (LPF) system for ore containing mixed soluble and floatable copper minerals. The LPF system is actually an adaption of vat leaching to continuous processing. Acid is added to the pulp in or after the grinding section followed by finely ground metallic iron which precipitates the copper. The pulp is treated by conventional flotation to recover both sulfide copper minerals and precipitated metallic copper.

¹⁸Hansen, Spent M. Nuclear Blasting for Mining and Leaching. World Min., September 1965, p. 61.

In the process of flood leaching, a solvent solution surrounds the rock and then penetrates into the body of the rock where by chemical action it dissolves the copper minerals and holds them in a soluble state. The solution around the rock has a lower concentration of dissolved copper salts than has the solution inside the rock after chemical action starts. A diffusion pressure is created and the salts diffuse from the area of higher to the area of lower concentration. After a period of time, the solution surrounding the rock is drawn and the copper removed; the rock and solution must be contained either in a vat or in a tight ground formation in order to flood the rock with solution and dissolve the copper by this method.¹⁹

The ore is immersed in the solution in a tank as at Inspiration or in situ as at Ray where broken rock in the caved area surrounded by a tight impervious rock is flooded with solution. The solution occupies the interstices between the ore fragments and will obey the laws of liquid flow; it tends to follow the path of least resistance among the coarse particles. The extraction of the copper from within the particles of ore is dependent on the rate of diffusion.

In the process of open-drainage leaching, the solution is applied at the top, trickles down through the ore, and, if conditions are properly controlled, is present as a film over the particles of the ore. The interstices between particles of ore are filled with air. Soluble copper salts on the surface of the rock are dissolved and carried downward and some solution enters the rock. Gravity, assisted by the cohesion of water causes the solution to pass over and through the particles of ore. The penetration of the rock is a function of time and varies with the size and type of rock. When the copper content of the recovered solution drops below an acceptable limit, the surface sprays are stopped, the solution supply is cut off, and the rock begins to dry. Capillary forces bring the contained solution and dissolved copper to the surface of the rock where the water evaporates and the soluble salts crystallize; they are easily dissolved and collected by the next application of solution. Success of the open-drainage method depends on alternate wetting and drying of the ore. Complete recovery is dependent on proper distribution of the solution over the surface and through the ore.

In contrast to the flood-leaching method, the open-drainage method does not require lateral confinement of the solution. This method is most popular in dump-leaching operations and a typical dump-leaching flowsheet is illustrated in figure 5. An impervious surface on which the solutions can be collected must underlie the ore. Increased recovery results because the film condition of the solution compels it to make contact with the particles of ore rather than to pass through void spaces, as it does when the ore is flooded. The amount of water removed from the rock during each drying period and retained during each wetting period determines the rate of extraction of the soluble copper minerals. As with the flood-leaching method, a long period of contact is necessary when large size ore lumps are being leached.

¹⁹Sullivan, J. D., and Alvin J. Sweet. Factors Governing Removal of Soluble Copper From Leached Ores. BuMines Tech. Paper 453, 1929, 26 pp.

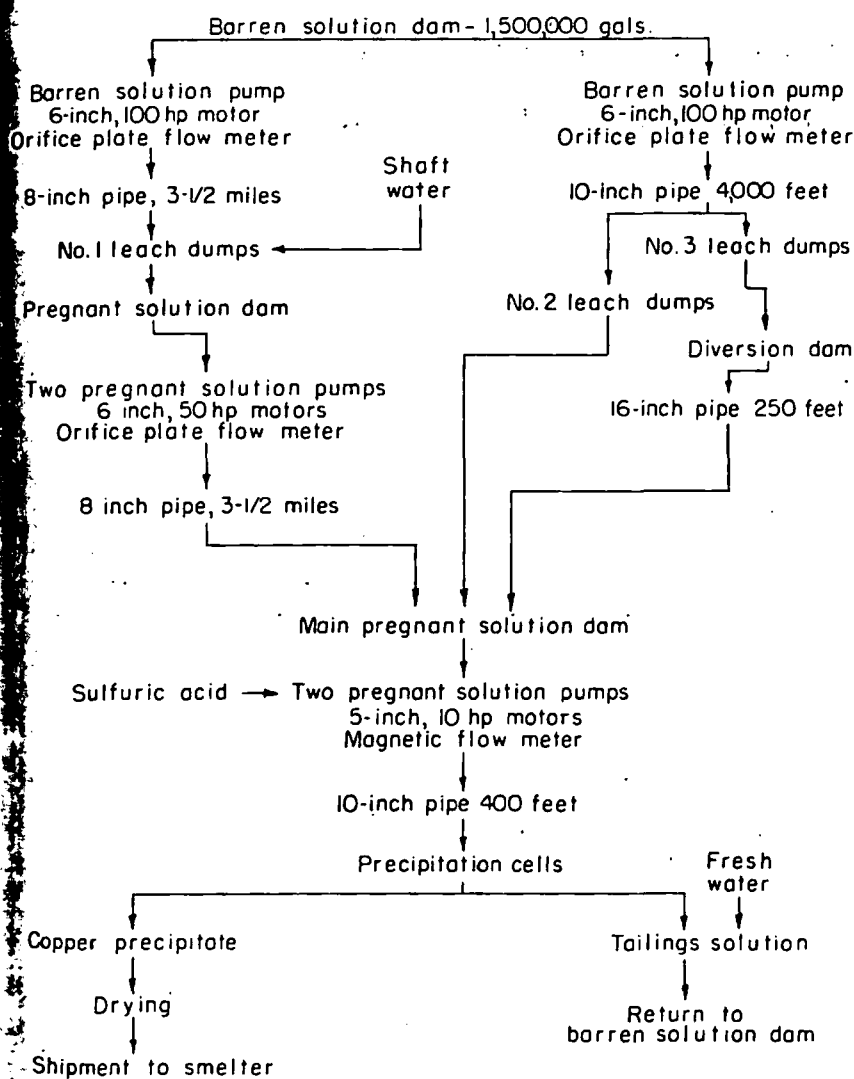


FIGURE 5. - Typical Dump Copper Leaching Circuit.

A study of the mechanism of percolation leaching comparing extractions by flood and open-drainage methods showed that alternate wetting and drying brings the copper to the surface much more rapidly than chemical diffusion. Under comparable conditions, higher and more rapid extraction was obtained by the open-drainage method in laboratory tests by the Bureau of Mines.²⁰ In practice the choice between flood leaching and open-drainage leaching is based on the characteristics of the ore body and surrounding conditions. The characteristics of the ore are determined by laboratory tests, surrounding conditions by a field examination.

NUCLEAR EXPLOSIVES

Basically, a nuclear explosive is a source of energy. Nuclear explosions are measured

according to their yield. Because the amount of energy release is so great, this yield is measured in terms of kiloton units. A kiloton is defined as a prompt release of 4×10^9 Btu or about the same amount of energy as 1,000 tons of TNT. The nuclear device is the most compact and most powerful source of energy known to man. Because of the large amount of energy released, the cost per energy unit is low. Based on costs published by the AEC during May 1964, the cost of energy on a per unit basis is compared with conventional explosives in table 4.

Cost estimates for breaking rock with nuclear explosives have been tabulated for a scaled depth of 210 feet per kton^{1/3}.⁴ and are shown in table 5.

²⁰Guggenheim, Morris, and John D. Sullivan. Acceleration of Extraction of Soluble Copper From Leached Ores. BuMines Tech. Paper 472, 1930, p. 27.

In mining applications the optimum scaled depth of burst might range from 190 to 220 feet per kton^{1/3}.⁴ depending on rock characteristics.

TABLE 4. - Comparison of explosive energy costs

Explosive:	<u>Cost per million Btu</u>
TNT.....	\$115.00
Dynamite.....	100.00
Ammonium nitrate-fuel oil.....	30.00
10 kiloton nuclear explosive.....	8.75
100 kiloton nuclear explosive....	1.12
1 megaton nuclear explosive.....	0.145
2 megaton nuclear explosive.....	0.075

TABLE 5. - Cost of breaking rock with nuclear explosives¹

Explosive yield, kiloton	Rock broken, million tons	Cost			
		Explosive	Other	Total	Per ton-cent
10.....	6	\$350,000	\$200,000	\$550,000	9.2
20.....	11	390,000	225,000	615,000	5.6
50.....	25	425,000	250,000	675,000	2.7
70.....	33	450,000	275,000	725,000	2.2
100.....	43	475,000	300,000	775,000	1.8

¹Adapted from Hansen, Spenst M., and John Toman. Aggregate Production With Nuclear Explosives. University of California, Lawrence Radiation Laboratory, UCRL 12180, Rev. II, 1965, p. 20.

Included in these costs are: AEC charges for nuclear explosives and their arming and firing; emplacement and related engineering costs for site development; and support and other miscellaneous costs. Not included are direct costs of safety studies, which vary greatly, and are highly dependent on the region in which the project is located, and on whether a single explosion or a series is used. Projected charges for thermonuclear explosives published by the AEC are shown in figure 6.²¹

Nuclear explosives can be designed to optimize particular characteristics such as explosive package size, cost, radioactive byproducts, and others. Of particular interest to mining is the size of the explosive. The AEC has declassified a range of yields and associated diameters of explosives that could be made available using current designs (table 6). A 5-kton nuclear explosive being lowered into a 2,700-foot hole is shown in figure 7.

²¹Atomic Energy Commission. Policy Statement on Projected Charges for Peaceful Nuclear Explosives, Press Release G-106, May 6, 1964.

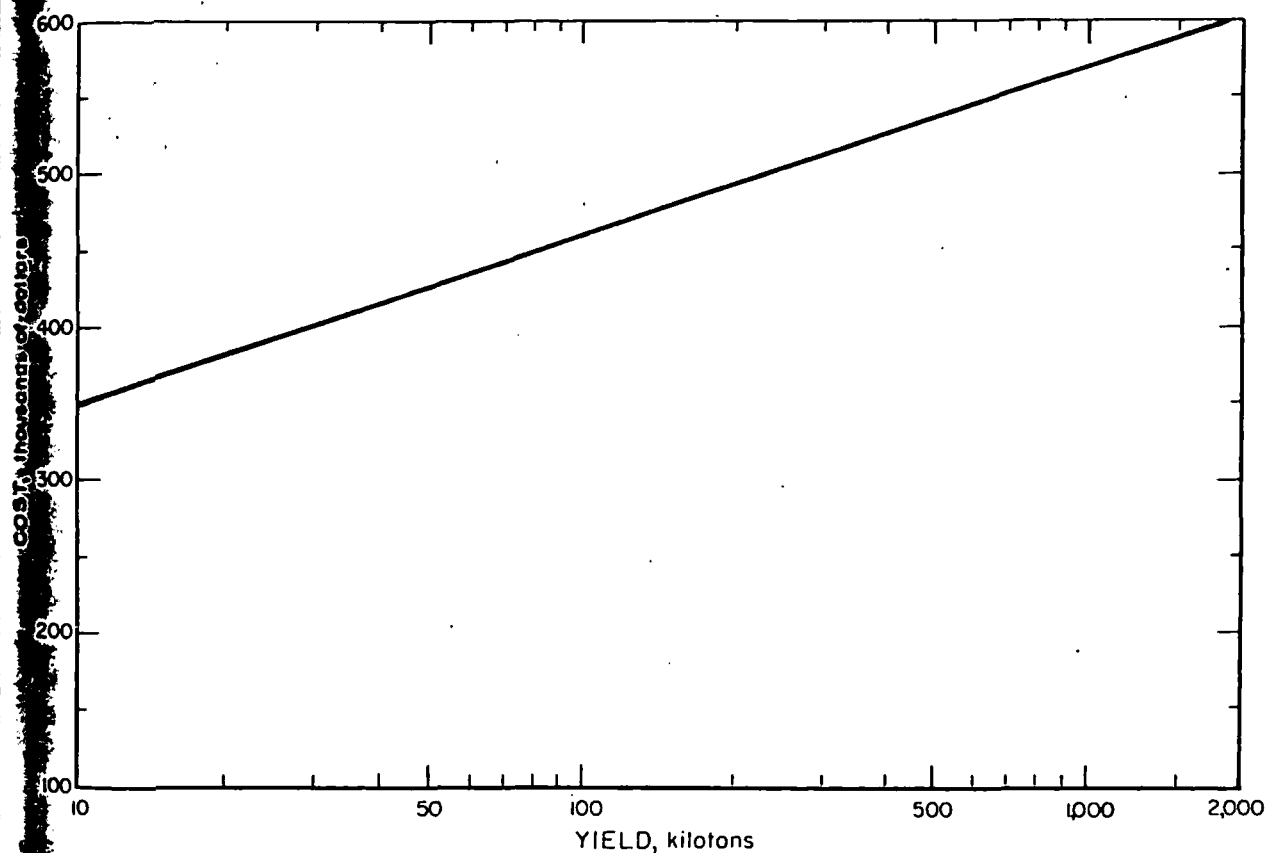


FIGURE 6. - Projected Charges for Thermonuclear Explosives.

TABLE 6. - Diameters of nuclear explosives

Yield:	Diameter of Cannister
Up to 10 KT....	12 inches
Up to 100 KT....	18 inches
Up to 1,000 KT....	24 inches
Up to 10,000 KT....	36 inches

The internal diameter of the emplacement hole would have to be slightly larger, of course, to accommodate the cannister. The length of the cannister is roughly two to four times the diameter.^{2a}

Underground experiments in hard rock have established the capability of nuclear explosives to break and fracture rock. More than 150 nuclear explosions have been detonated underground. The effects of a nuclear explosive

^{2a}Lekas, M. A., and H. C. Carpenter. Fracturing Oil Shale With Nuclear Explosives for In-Situ Retorting. Hearing on Peaceful Applications of Nuclear Explosives - Plowshare, before the Joint Committee on Atomic Energy. 89th U.S. Cong., 1st sess., Jan. 5, 1965, p. 570.

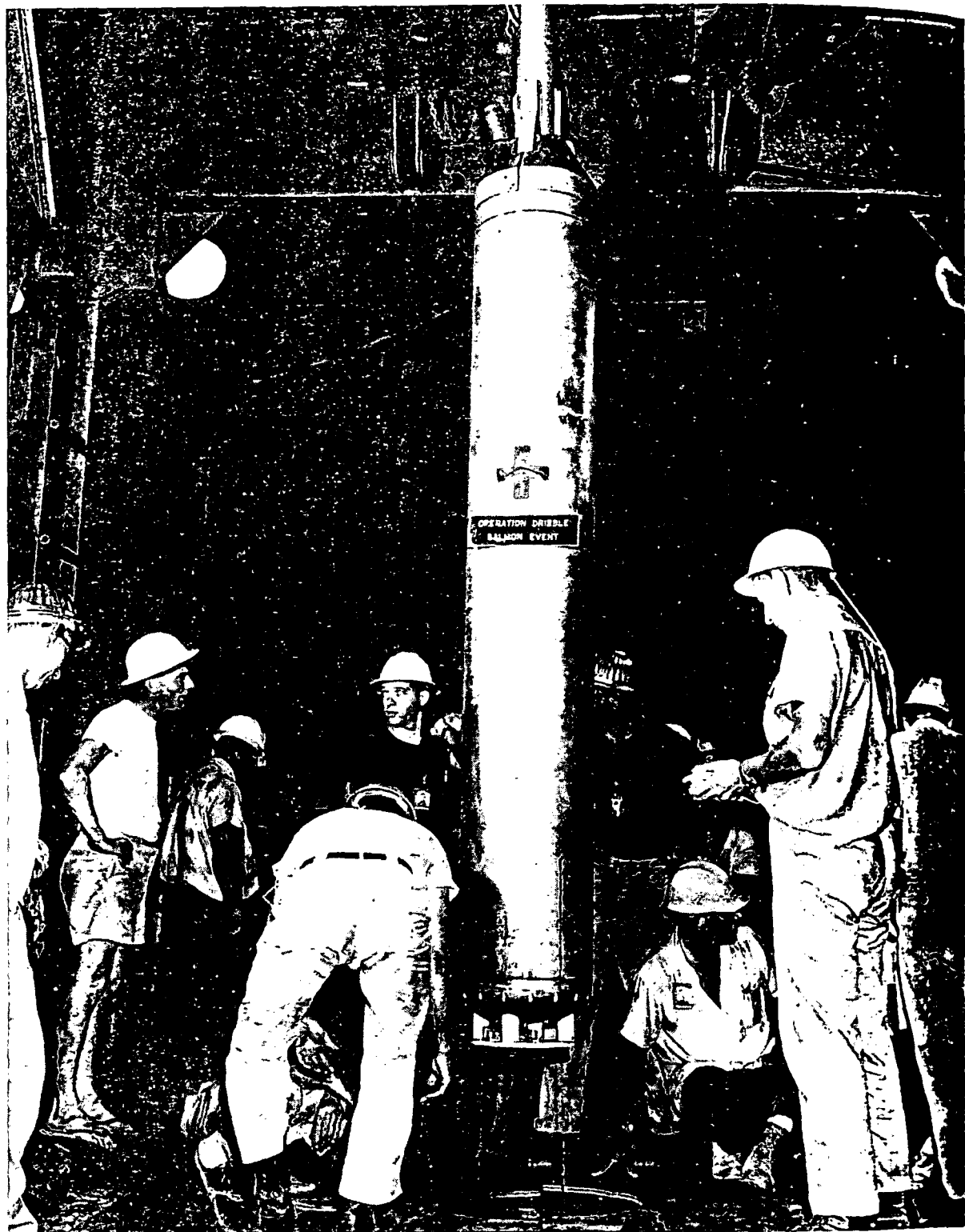


FIGURE 7. - Five-Kiloton Nuclear Explosive Being Lowered Into 2,700-Foot Emplacement Hole. (Photograph supplied through the courtesy of the Lawrence Radiation Laboratory, Livermore, Calif., and the Atomic Energy Commission.)

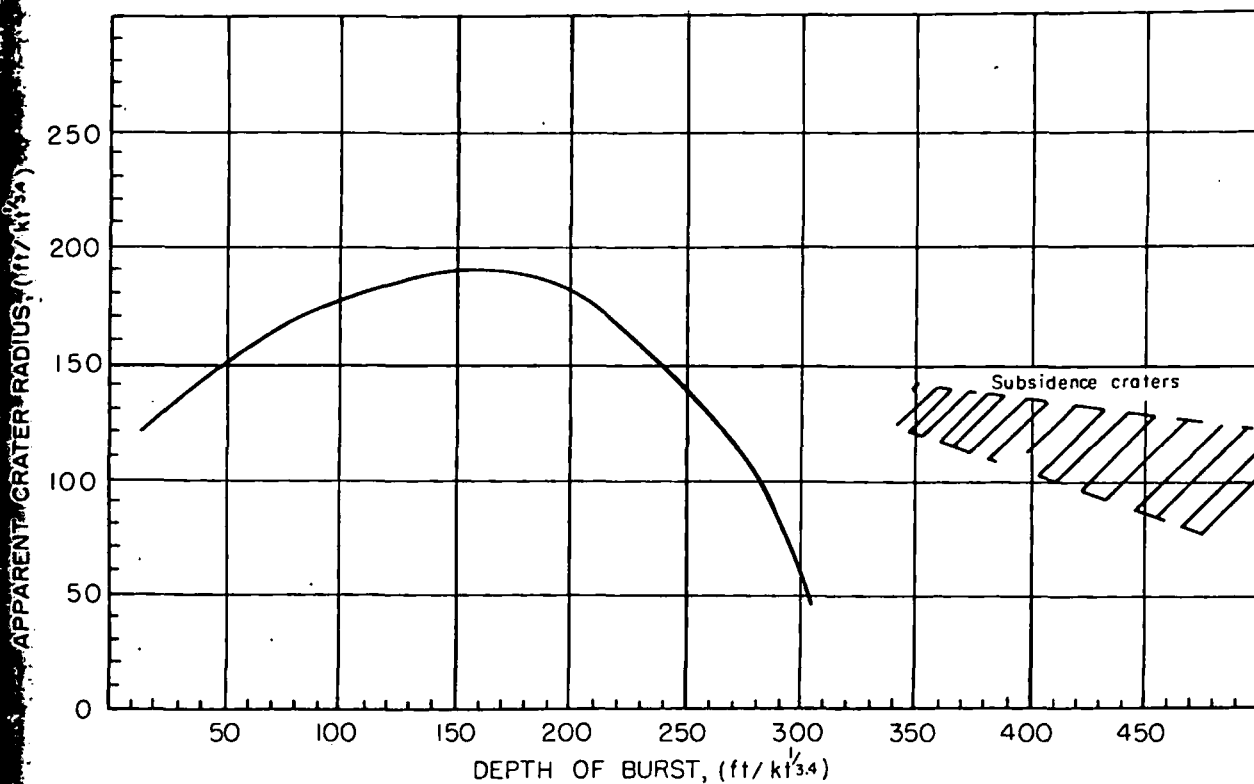


FIGURE 8. - Crater Radius vs. Depth of Burst in Alluvium.

differ on the depth of burial. A factor, the scaled depth of burial, is determined by dividing the actual depth of burial in feet by the 3.4 root of the yield of the explosive in kilotons. The effects differ for different types of rock. The curve (fig. 8) shows crater radius versus scaled depth of burst for alluvium. From this type of curve, the depth of burial that will break the largest volume of rock for a yield is determined. For hard rock, this optimum rock-breaking point is slightly greater than 200 feet/kton^{1/3.4}. With this basis, the family of curves shown in figure 9 can be drawn to show tonnage data as a function of yield and depth of burst. These curves apply to cratering or intermediate nuclear explosions.

Scaling for a completely contained nuclear explosion is related to the cube root of the yield in contrast to the 3.4 root that is used for cratering and intermediate-depth explosions. Containment, as used here, means that the gross explosion effects, such as surface subsidence, the ejection of rock fragments, rubble moved, and crater formation, are prevented from developing at the surface by rock overlying the explosion; some cracks may reach the surface.

A chimney of broken rock is formed above and around the explosion center. This chimney is formed by gravity collapse of the fractured and weakened rock overlying the nuclear-explosive cavity void. Available experimental data for

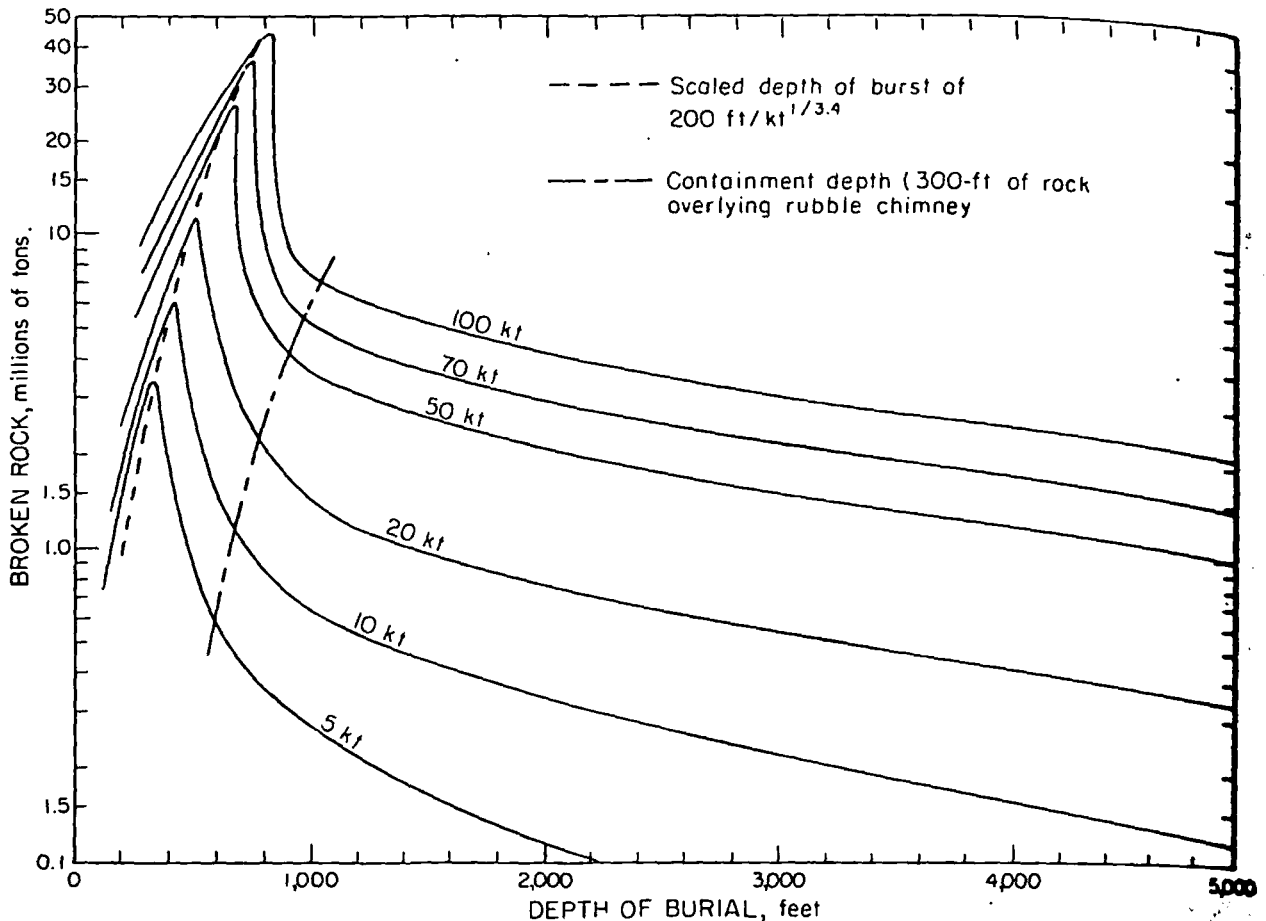


FIGURE 9. - Tonnage Curves of Rock Broken by Intermediate Underground Nuclear Explosions.
(Courtesy, Lawrence Radiation Laboratory, UCRL 12180.)

contained underground nuclear explosions permits the prediction of cavity size, chimney height, and tonnage of rock broken with considerable confidence.²³

Curves have been developed to show the cavity radius as a function of the depth of burial (fig. 10), the chimney height as a function of the depth of burial (fig. 11), and the tonnages of rock broken as a function of the depth of burial (fig. 12) for different yields.

An example of an emplacement for maximum rock breakage was the Sulky nuclear explosion in hard, dry basalt. The explosion, which had a yield of approximately 87 tons of TNT, took place on December 8, 1964. Fired at a depth of 90 feet the explosion formed a mound of rubble with a maximum height of 25 feet above preshot ground surface and a diameter of over 160 feet. Scaled depth of burst was 184 feet/kton^{1/3.4}. Radiation levels were

²³Hansen, S. M., and D. B. Lombard. Completely Contained Nuclear Explosives for Mining by Caving. Proceedings of the Third Flowshare Symposium, Lawrence Radiation Laboratory, TID 7695, 1964, pp. 371-384.

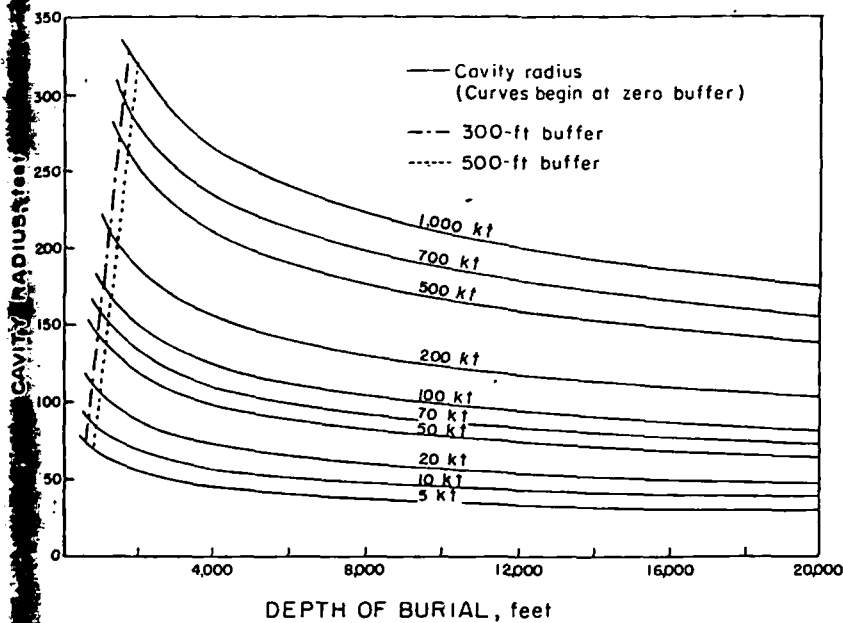


FIGURE 10. - Cavity Radii for Contained Underground Nuclear Explosions in Granitic Rock. (Courtesy, Lawrence Radiation Laboratory, TID 7695.)

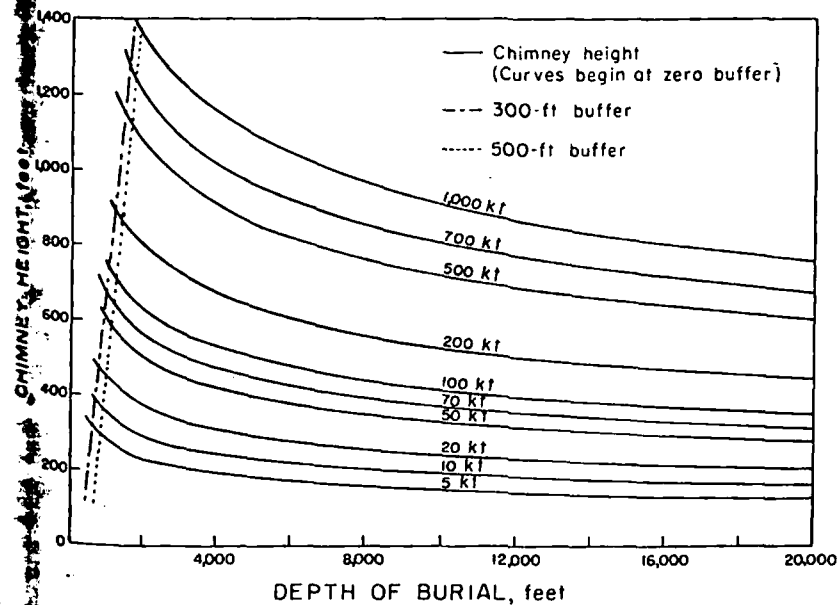


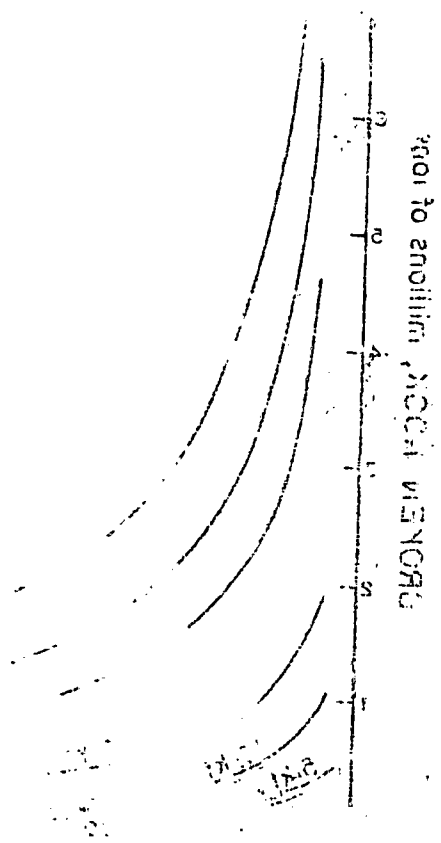
FIGURE 11. - Chimney Heights for Contained Underground Nuclear Explosions in Granitic Rock. (Courtesy, Lawrence Radiation Laboratory, TID 7695.)

sufficiently low that personnel were able to move freely about the rubble mound within a few days and excavation of trenches and broken rock began within a month. A schematic cross section of a shot designed for maximum rock breakage is shown in figure 13. Fractured rock from a cratering nuclear explosion in hard basalt is shown in figure 14.

The Blanca explosion was a 19-kton explosion fired in a tunnel in bedded tuff on the edge of a mesa. The bulk density of the bedded tuff in situ was about 1.9 g/cm^3 . The explosion was at a vertical depth of 988 feet, and the nearest point on the surface was 835 feet. A dome section of the mesa 1,600 feet in diameter was moved upward about 25 feet at the center then settled back. About 15 seconds after the explosion the cavity collapsed to the surface (fig. 15). The rubble zone, an inverted cone with a radius of 500 feet and a height of 1,100 feet, was estimated to contain 15 million cubic yards or 22 million tons of rock. About 0.05 percent of the total radioactivity was released to the surface.



FIGURE 3



The curves in Figure 3 show the percentage of ionization as a function of wavelength in microns. The curves are very similar to those in Figure 2, indicating a consistent relationship between the variables. The ionization percentage increases rapidly with wavelength, particularly in the region between 1 and 5 microns.

The curves in Figure 3 show the percentage of ionization as a function of wavelength in microns. The curves are very similar to those in Figure 2, indicating a consistent relationship between the variables. The ionization percentage increases rapidly with wavelength, particularly in the region between 1 and 5 microns.

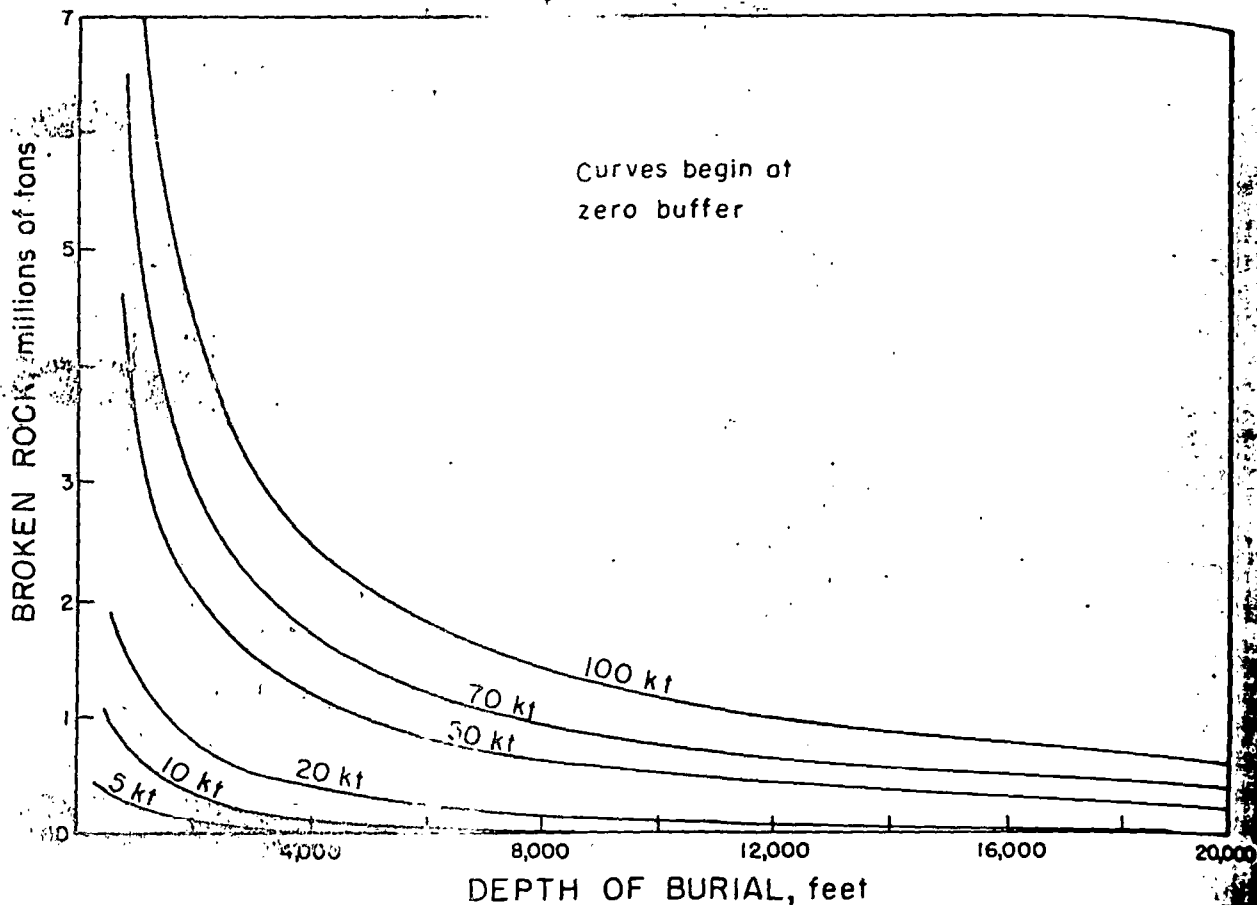


FIGURE 12. - Tonnages of Granitic Rock Broken by Underground Nuclear Explosions.
(Courtesy, Lawrence Radiation Laboratory, TID 7695.)

The Hardhat test, a contained explosion, was a 5.4-kton shot fired from a 36-inch diameter drill hole in granite (specific gravity 2.67) at a depth of 939 feet on February 15, 1962 (fig. 16). The surface raised 4 feet and sank back; permanent displacement was about 2 feet. A cavity 126 feet in diameter was formed. Eleven hours after the explosion the roof began to cave, eventually forming a chimney that reached a height of about 300 feet and contained an estimated 20,000 tons of broken rock. A drift was driven through the caved chimney 90 feet above the point of detonation, and 3,000 tons of broken rock was drawn from the 4-foot finger raises. Material mined appeared well broken; the size distribution appeared to be suitable for extraction by methods similar to caving or in-situ leaching (fig. 17). After the cavity collapsed, small amounts of radioactive gases were detected on the surface.

Porosity of the broken material after a nuclear explosion ranged from 18 to 25 percent in tuff. The porosity of the Hardhat chimney in grandodiorite was about 28 percent. Factors that influence the overall rubble size distribution and maximum rock fragment size and shape included the following: (1) characteristics and frequency of natural fractures; (2) physical properties of the parent rock; (3) explosion yield; and (4) depth of burial. Typical fragment sizes are summarized in table 7.

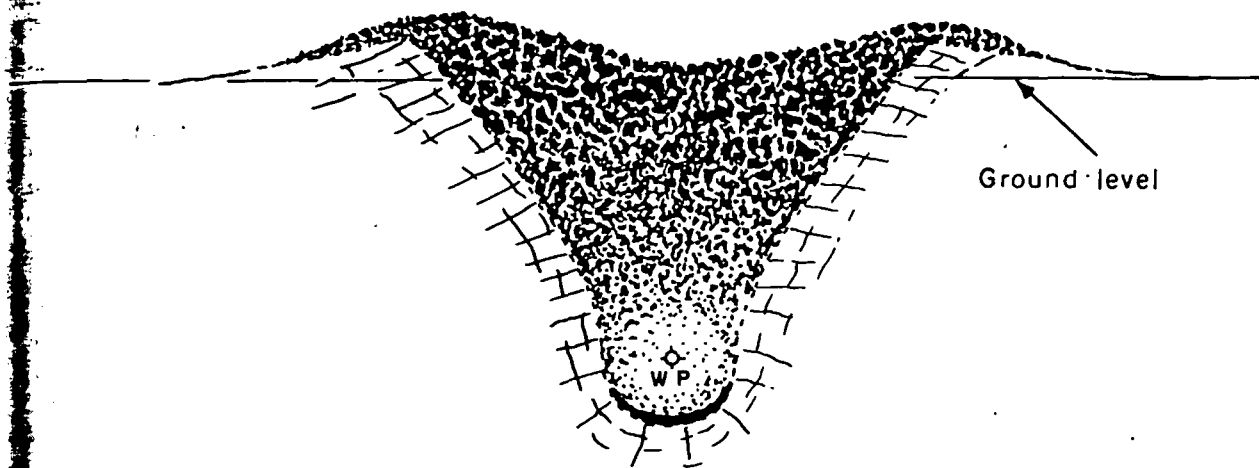


FIGURE 13. - Schematic Section of Explosion at Maximum Rock-Breaking Depth.



FIGURE 14. - View Across Danny Boy Crater Showing Hard Basalt Rock Fractured by a Nuclear Explosive. (Photograph supplied through the courtesy of the Lawrence Radiation Laboratory, Livermore, Calif., and the Atomic Energy Commission.)

20,000
rom a
of
ank
eter
ntur-
ned
oken
ll
eth-
l-
n 18
ite
tri-
er-

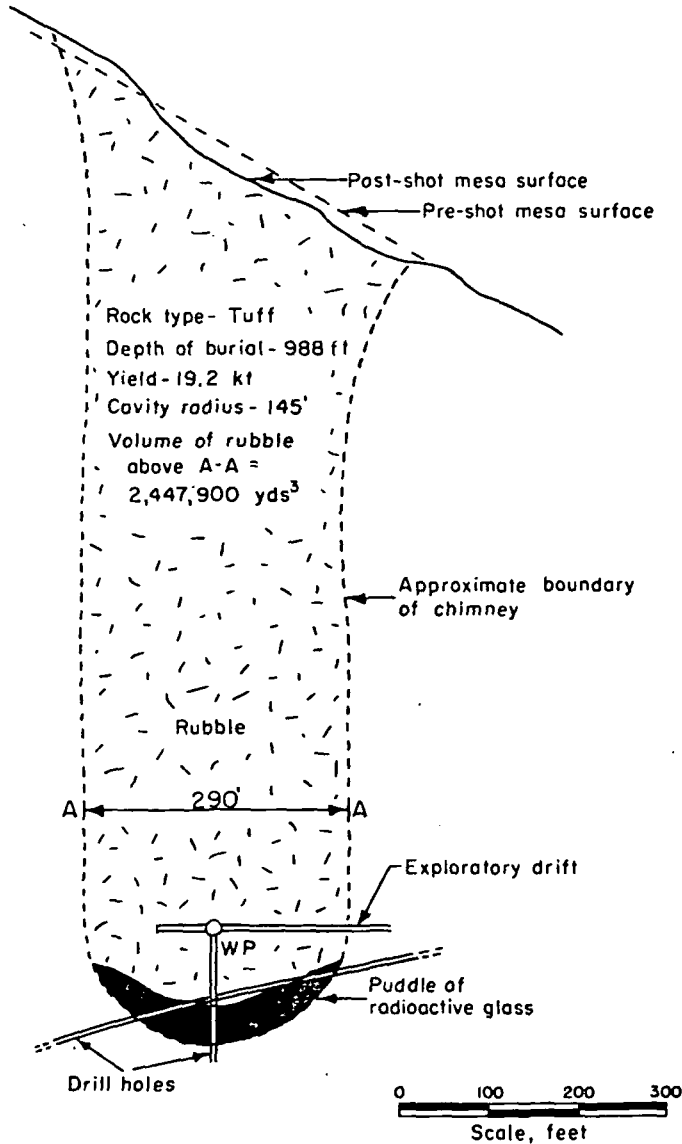


FIGURE 15. - Schematic Cross Section of Blanca.
(Courtesy, Lawrence Radiation Laboratory, UCRL 7350.)

TABLE 7. - Typical fragment-size distribution from underground explosion in hardrock¹

Sieve size: ²	Percent passing
6 ft.....	100
5 ft.....	95
4 ft.....	88
3 ft.....	75
2 ft.....	60
1 ft.....	40
6 in.....	30
4 in.....	25
2 in.....	20
1-1/2 in.....	16
1 in.....	14
3/4 in.....	12
1/2 in.....	10
3/8 in.....	9
#4.....	7

¹Adapted from Hansen, Spent M., and John Toman. Aggregate Production With Nuclear Explosives. University of California, Lawrence Radiation Laboratory, UCRL 12180, Rev. II, p. 11.

²Based on size distribution data obtained by the U.S. Army Corps of Engineers from the Danny Boy and Pre-Schooner experiments in basalt on Buckboard Mesa, and on Lawrence Radiation Laboratory data from the Hardhat experiment in granite.

PUBLIC LIABILITY

In any undertaking by industry to apply nuclear explosives, industry is taking the assets of a going business and investing them in a new idea. Accordingly, it must assure its stockholders that those assets will not be in danger. In order to provide assurance to industry and to the public, the Atomic Energy Act of 1954, as amended, authorizes the Atomic Energy Commission to execute indemnification agreements with its contractors who are engaged in activities for the benefit of the United States involving a risk of public liability for a substantial nuclear incident. These agreements indemnify against claims for public liability for nuclear incidents arising out of or in

Medium: granite
Yield: 5 kt
Depth of burial: 939 ft

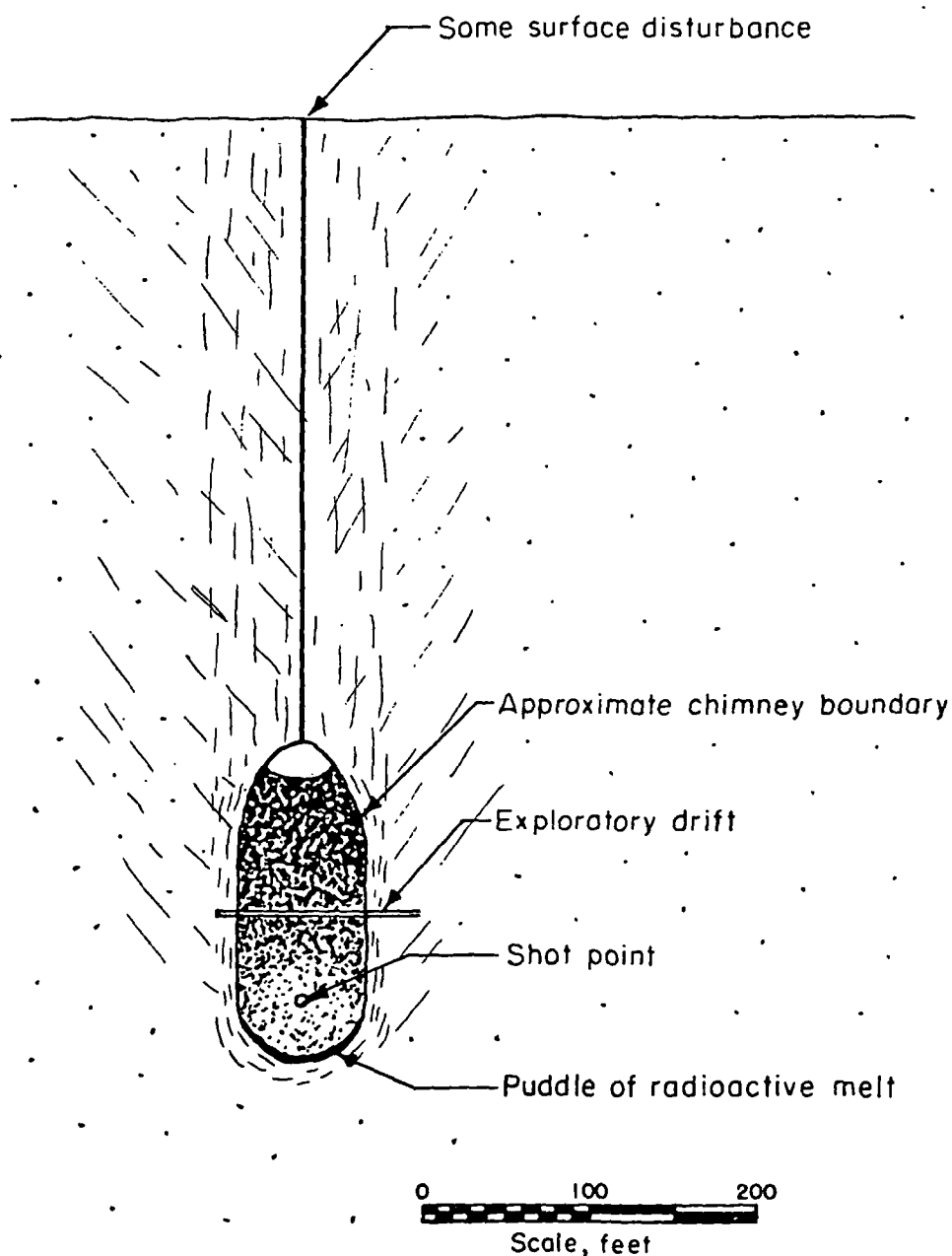


FIGURE 16. - Schematic Cross Section of Granitic Rock Broken by Contained Nuclear Explosion.



FIGURE 17. - Broken Granitic Rock in the Chimney of a Contained Underground Nuclear Explosion. (Photograph supplied through the courtesy of the Lawrence Radiation Laboratory, Livermore, Calif., and the Atomic Energy Commission.)

con
and
rec
agg
exc
to

rio
thr
AEC
ind
lia
men
have
for

hanc
pate
rior
from
Nucl
the
new

prob
the
Test
asse

the
outw
or m

that
gase
by v
her
vent
cone

Th

connection with the contractual activity in the amount of \$500 million over and above any financial protection (insurance etc.) that the Commission may require of its contractors. The act also provides that in no event shall the aggregate liability for a single nuclear incident for persons indemnified exceed this amount. Thus far, the Commission has not required its contractors to procure such financial protection.

Under existing statutory authority, fabrication, emplacement and detonation of the nuclear explosive in any such application by industry must be done through the AEC. Those of its contractors who provide this service for the AEC have been extended indemnification agreements. Such agreements not only indemnify the contractor but any other person who may be liable for public liability. Accordingly, anyone who participates with the AEC in an experimental application of nuclear energy, such as fracturing copper deposits, will have assurance because of the existence of such an agreement that all risks for public liability will be covered.

SAFETY PROBLEMS

The use of explosives is an important part of all mining operations. The handling of the explosives must be accomplished safely and the effects anticipated and controlled. The problem of what effects the air and ground vibrations resulting from blasting have on structures of various types has existed from the time explosives were discovered and developed for mining purposes. Nuclear explosives, because of the large amount of energy involved, amplify the safety problems connected with air blast and ground shock and introduce a new problem, radioactivity.

Because the general public is directly involved in the blasting vibration problem, many investigations have been conducted. The behavior pattern for the effects of vibration from quarry and mine blasting can be predicted.²⁴ Tests and follow-up investigations have provided a basis for reliable preshot assessments of potential hazards from the effects of nuclear explosives.

Air Blast

Air blast from a surface explosion results from the rapid expansion of the hot gases. The explosion causes a shock wave to form in the air and move outward at high velocity. Waves move radially along the surface of the ground or may rise and be ducted and refracted by atmospheric conditions.

The air-blast wave from a buried explosion may consist of two pulses, one that results when ground shock reaches the surface and one that results when gases are vented. Both pulses decrease with charge burial. The pulse caused by venting gases becomes zero when the explosion is completely contained. Where nuclear charges have been fired in basalt and rhyolite rock, peaks from venting gases have been less than those that were ground-shock induced. The zone of air-blast damage for nuclear explosions at depths contemplated for

²⁴Thoenen, J. R., and S. L. Windes. Seismic Effects of Quarry Blasting. BuMines Bull. 442, 1942, 83 pp.

fracturing copper deposits can be expected to be well inside the region of ground-shock damage.

Ground Shock

Ground shock or seismic effects of a nuclear explosion are similar to those of conventional explosives. Ground shock results when the shock wave caused by an explosion is transmitted outward through the rock. Criteria for estimating damage to residences and engineering structures has been established. Particle velocity or acceleration in terms of gravity are used to measure particle motion.

Damage appears as cracks and as structural deformation. A recent statistical analysis by the Bureau of Mines suggested that a particle velocity of 2 inches per second is a reasonable point of demarcation between shock levels in the safe zone and the damage zone.²⁵

Ground motion resulting from nuclear explosions and the effects on buildings and structures has been studied.²⁶ A surface velocity of 10 cm/sec was determined as a damage threshold. Damage to engineering structures begins at a much higher velocity, depending on the type of structure. For many structures it may be about 100 cm/sec. A formula was presented by Hansen and Lombard to calculate the peak velocity at a distance from the explosion.²⁷

The peak vertical component can be approximated at any distance from the explosion by the formula:

$$V = \frac{K W^{2/3}}{R^{3/2}} \text{ cm/sec.}$$

Where $K = 1.4 \times 10^{-2}$ for explosions in alluvium,

$= 3.5 \times 10^{-2}$ for explosions in tuff,

$= 8.6 \times 10^{-2}$ for explosion in granite,

R is the range in kilometers,

and W is the energy yield in tons.

²⁵Duvall, Wilbur I., and David E. Fogelson. Review of Criteria for Estimating Damage to Residences From Blasting Vibrations. BuMines Rept. of Inv. 596, 1962, 19 pp.

²⁶Cauthen, Lewis S., Capt., U.S. Army Corps of Engineers. Survey of Shock Damage to Surface Facilities and Drilled Holes Resulting From Nuclear Detonations. Lawrence Radiation Laboratory, UCRL 7964, 1964, 32 pp.

²⁷Hansen, S. M., and David B. Lombard. Mining by Caving With Nuclear Explosions. Lawrence Radiation Laboratory, UCRL 14201, 1965, p. 32.

YIELD OF EXPLOSION, kilotons

DIS
FIGURE

A special consideration is the shock damage to mine workings.

Shock damage to unsupported mine workings in granitic rock has been plotted as a function of explosive yield and range by Hansen and Lombard (fig. 18).²⁸

Minor damage includes limited spalling, minor offsets of shaft guides and track and slight damage to mounted equipment. Complete closure is defined as complete collapse of the mine opening from top, sides, and bottom. Although probably not important in a mining operation involving a single nuclear explosion, this phenomena may introduce a serious problem at operations where several nuclear explosions separated by periods of ore extraction are involved.

Radioactivity

Radioactivity that is vented to the atmosphere at explosion returns as fallout. For purposes of fracturing and leaching a copper deposit in situ, the nuclear explosive would be placed at a depth such that the radioactive products are completely contained or, at most, only an insignificant fraction escapes. When the explosion is completely contained radiological safety problems encountered from activity will be introduced in the ore from the following sources:

1. Radionuclides that result from fission or fusion products of the explosion.
2. Radionuclides that result from the activation by bombardment of the ore and materials in the nuclear explosive with neutrons released in the explosion (neutron activation products).

Eliminating the possibility of hazards from fallout, potential radiation hazards associated with fracturing a copper deposit with a nuclear explosive and subsequent in-situ leaching to recover the copper are: (1) Radiation hazards to off-site environment, (2) radiation hazards to on-site personnel, and (3) contamination of the copper product.

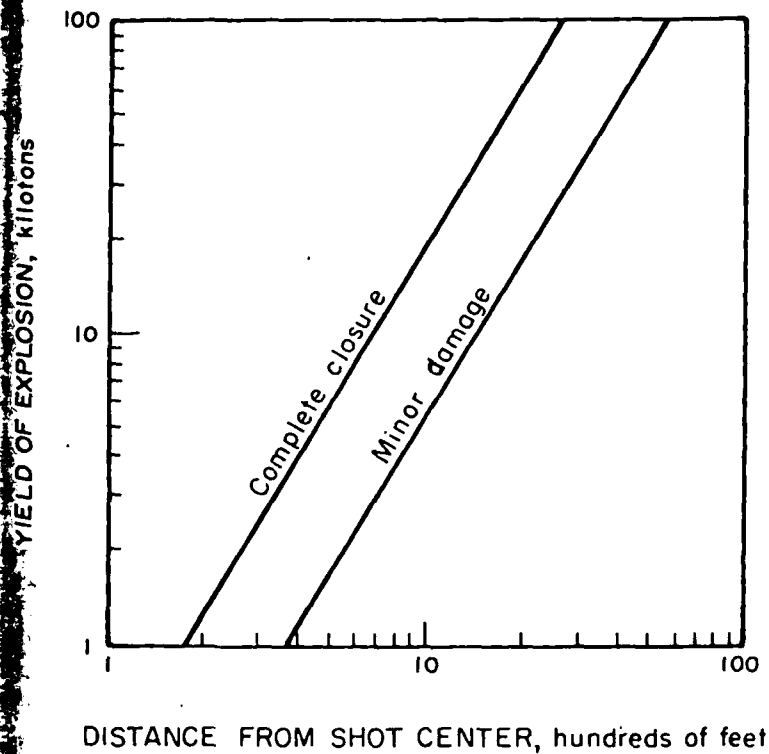


FIGURE 18. - Damage to Mine Workings From Nuclear Explosions in Granite Rock.

(Courtesy, Lawrence Radiation Laboratory UCRL 14201.)

²⁸Work cited in footnote 25.

Radiation Hazards to Off-Site Environment

Assuming that the nuclear explosion was contained and there was no significant venting of the radioactivity to the air, the off-site environment may still be subjected to radionuclides from waste products or from contamination of ground water. Some activity, particularly tritium, may be carried into the ground water flow. Ordinarily, ground water moves slowly, requiring years to travel a distance of one mile. Underground disposal of radioactive wastes has been practiced for many years. The distribution in ground water of radionuclides has been studied²⁹ with the conclusion that the ground water transport of radionuclides, following the initial explosion-produced distribution may not create any unmanageable problems. The radiation hazards to off-site environment should be controllable, but a study of ground water movement and waste-solution disposal will be advisable.

Radiation Hazards to On-Site Personnel

Radiation hazards to on-site personnel can come from two sources: radionuclides may build up in circulating solutions from an in-situ leaching operation; they may be present in shattered ground through which development openings are necessary.

The Oak Ridge National Laboratory is studying potential safety problems that may result from radioactive contaminants in the processing cycle and the copper product. Copper ore samples from New Mexico and Arizona have been mixed with radioactive debris from nuclear explosions on the Nevada Test Site and bombarded with neutrons by equipment at Oak Ridge National Laboratory. Preliminary studies indicate that expected concentrations of radioactivity in process solutions and product will be manageable. Planning may be required in designing the operation particularly with respect to disposal of waste solutions.

During a mining experiment on the Nevada Test Site one year after the explosion, the average exposure was 11 millirem per working shift corresponding to 2.2 rem per year. The National Council on Radiation Protection (NCRP) recommended maximum permissible whole body dose for workers is 3 rem per quarter year or 5 rem average per year beyond age 18.³⁰

Contamination of Copper

In tests by Oak Ridge National Laboratory ruthenium was the only fission product which significantly followed the cement copper. The chemistry of ruthenium is very complex and the results obtained with ruthenium traces may

²⁹Stead, Frank W. Distribution in Ground Water of Radionuclides From Underground Nuclear Explosions. Proceedings, Third Plowshare Symposium, TID 7695, Lawrence Radiation Laboratory, 1964, pp. 127-137.

³⁰U.S. Atomic Energy Commission. Standards for Protection Against Radiation, Title 10--Atomic Energy. Federal Register, ch. 1, pt. 20, Nov. 17, 1960.

or may
rice.
copper
sive ev
actual
from a
electro

Co
deposits
leaching
following

1.
2.
clock sc
3.
minerals

4.
5.
6.
sulfate.

7.
8.
at exce
9.

In a
ctors a
ant. Sc

1.
2.
structure
3.
4.

or may not be representative of those that would be obtained in actual practice. The indicated amount of damaging radioactivity that will follow the copper is not great and does not appear to present serious problems. Conclusive evaluation of potential separation methods cannot be determined until actual process products are available. Ruthenium would probably be eliminated from a copper product when it was removed from solution or refined by the electrolytic method. Methods of removing ruthenium from solution are known.

APPLICATION OF IN-SITU LEACHING TO NUCLEAR FRACTURED DEPOSIT

Copper deposits differ greatly, and no single method is applicable to all deposits. Regardless of method or preparation, successful application of a leaching method to recover copper from ore in situ requires existence of the following favorable factors in high degree:

1. Non-acid-consuming host rock.
2. Host rock that will not decrepitate to seal intrarock cavities and block solution flow.
3. Rock sufficiently fractured to permit access of solution to copper minerals.
4. Copper minerals that dissolve within required time limit.
5. Copper minerals concentrated largely along fracture planes of rock.
6. Sufficient pyrite in the deposit to form sulfuric acid and ferric sulfate.
7. A solid impervious surface under or surrounding the deposit.
8. Ability to recirculate the solution through the ore many times without excessive loss or contamination.
9. Availability of adequate water at low cost.

In addition to the limitations inherent to in-situ leaching, some further factors arising from the characteristics of nuclear explosions become important. Some important factors requiring investigation are:

1. Hydrology pattern including ground and surface water movement.
2. Safety considerations in connection with proximity to engineering structures that may be affected.
3. The effect of radionuclides on plant design.
4. The effect of radiation on bacteria.



FIGURE 19 Surface Mound of Broken Rock After Nuclear Explosion. (Photograph supplied through the courtesy of the Lawrence Radiation Laboratory, Livermore, Calif., and the Atomic Energy Commission.)

lea
a s

sel
con
bro
ait
roc

L
A
F
F

Pur

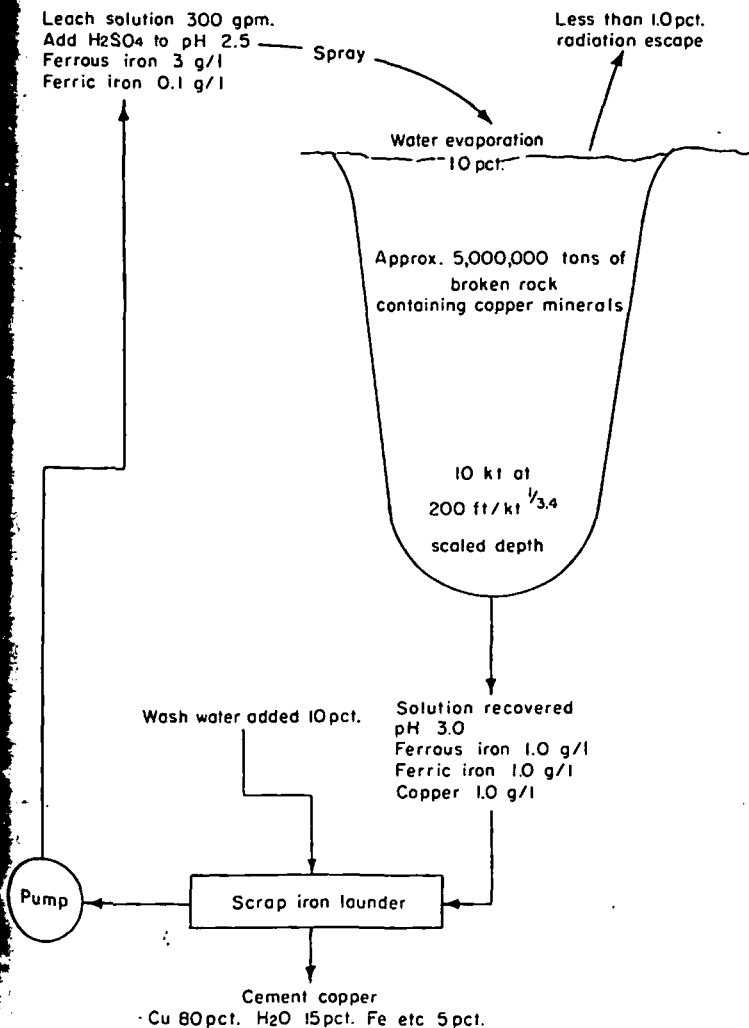
FIG

5. Area available for waste solution disposal.

6. Population density and public attitude.

Copper deposits that may be fractured with a nuclear explosive and leached in situ are divided into two types: Those that can be fractured with a single explosion, and those that require more than one explosion.

Either intermediate or contained placement of a nuclear explosive may be selected to fracture a copper deposit for in-situ leaching; the choice will be controlled by the position of the deposit and adjacent development. Once broken, the optimum method of percolating the solution through the ore may be either flood or open drainage depending on the condition of the surrounding rock, the texture of the broken material, and the method of solution recovery.



An intermediate explosion to fracture the surface but not close enough to crater or release a significant amount of radioactivity to the atmosphere may be the most efficient, if there is not too much overburden, for two reasons. First, more rock is broken per energy unit by the explosive. Second, solutions can be more easily and economically distributed on the exposed surface and recovered from the near surface sump (fig. 19). A diagrammatic system for leaching copper from ground broken in this manner is illustrated in figure 20.

Solution would be distributed by plastic pipe on the surface. Where the rock was impervious and solution was contained, it could be recovered by pump from the bottom of the crater. A characteristic of the nuclear explosive is that the rock immediately below the bottom half of the cavity is compacted. In some formations, this compaction may form a depression sufficiently

FIGURE 20. - System for Leaching Copper From Deposit Broken by Intermediate-Depth Nuclear Explosion.

impervious to contain the solutions from open-drainage application; they could be recovered by pumps in drill holes. However, in some cases where the rock is not impervious, it may be necessary to develop drifts and crosscuts to collect the solution either from an adit or a shaft.

Many deposits containing copper in leachable minerals are formed near an erosional surface. However, the deposit may have been formed in a past geological period and may now be covered deeply by more recent rock. These deposits can be economically broken only by a contained nuclear explosion. After the deposit is fractured, the solution could be percolated through the rock either by the flood method as illustrated in figure 21, or by the open-drainage method as illustrated in figure 22.

The development for applying solutions by the flood method may be most economical as two drill holes, one to the top and one to the bottom of the broken ore would be sufficient to apply and withdraw the leaching solution. Obviously, this method could be used only where the surrounding rock was impervious to the extent that the solution was contained and no significant loss occurred.

Contained nuclear explosions may be limited in size by safety considerations to less than 100 kton in most locations and to less than 10 kton in many locations. This restriction may not be serious because the conformation of many deposits is such that they can be more efficiently fractured by multiple explosions. This may not be the most economical method of breaking rock but, overall, may be the most economical method of fracturing and preparing ore for in-situ leaching (fig. 23).

Wash water added 10pci

Leach solution 300 gpm.
Add H₂SO₄ to pH 2.5

Wash water added 10

Leach solution 300 gpm.
Add H₂SO₄ to pH 2.5

Screen line installed

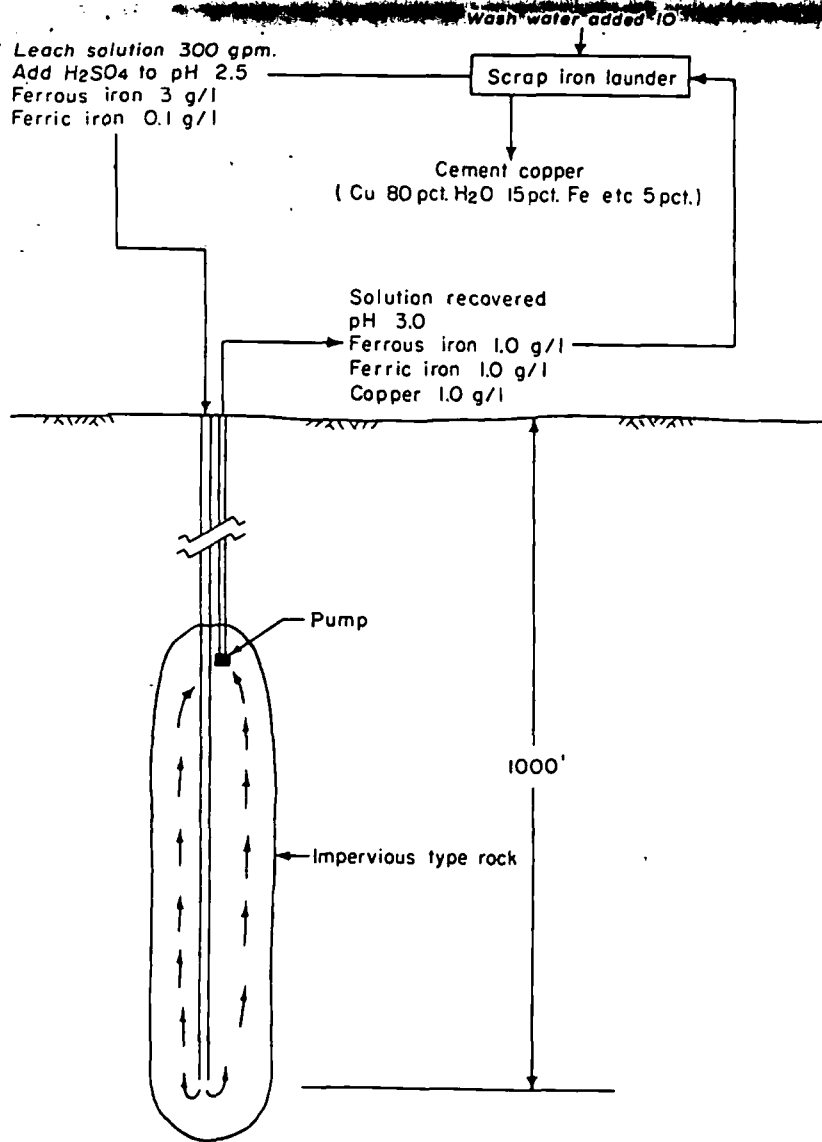


FIGURE 21. - Recovering Copper by Flood Leaching In Situ After the Deposit Is Broken by a Contained Nuclear Explosion.

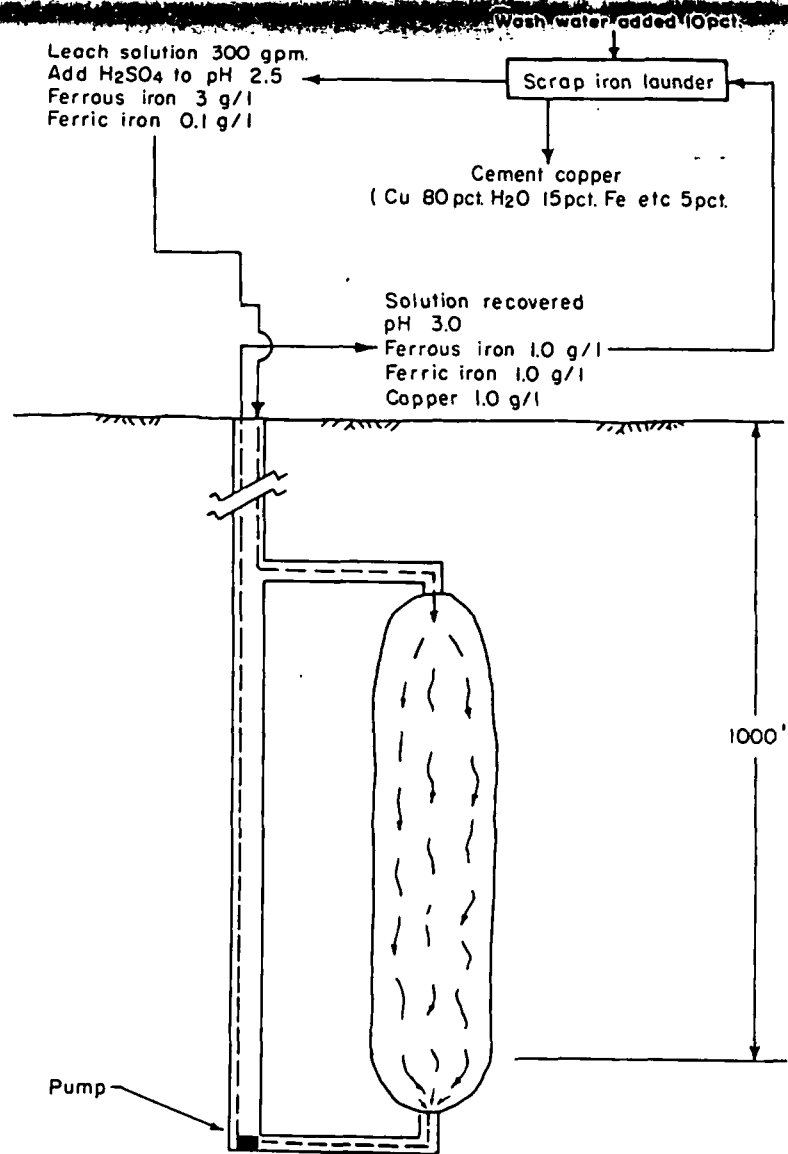


FIGURE 22. - Recovering Copper by Open-Drainage Leaching In Situ After the Deposit Is Broken by a Contained Nuclear Explosion.

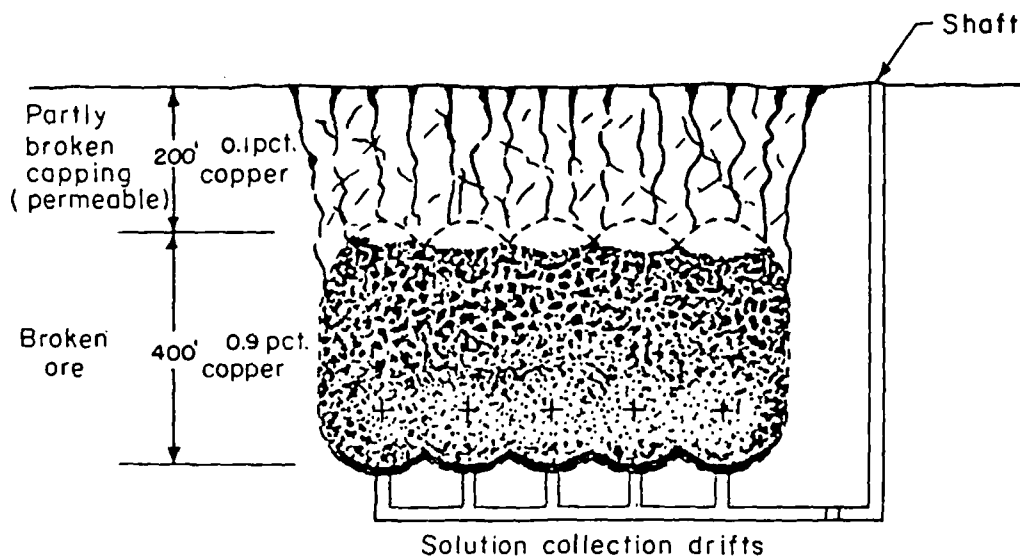
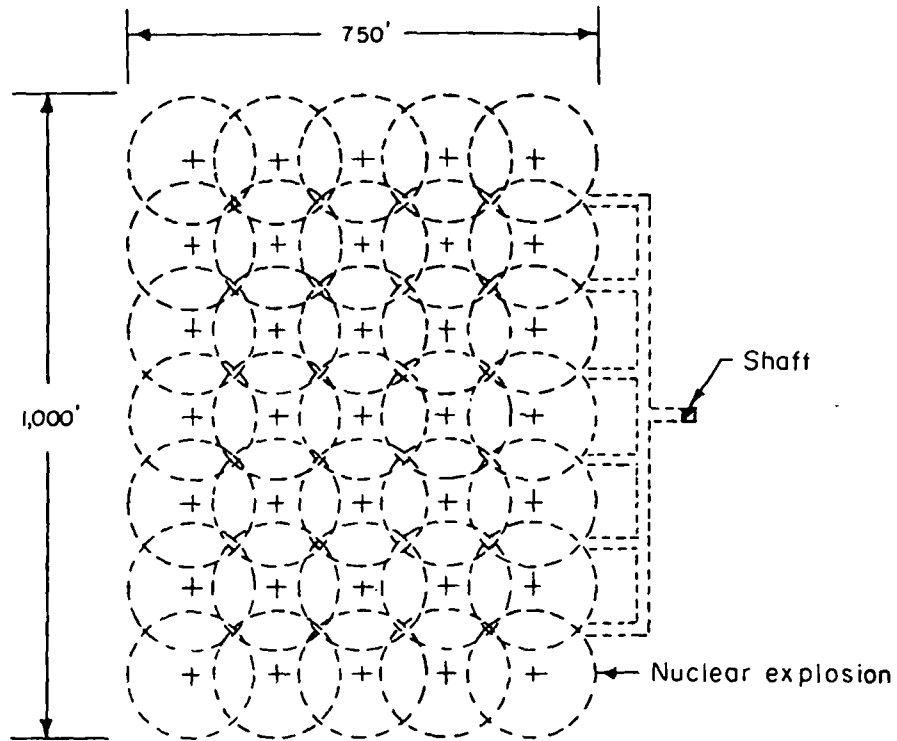


FIGURE 23. - Use of Multiple Contained Underground Nuclear Explosives to Fracture Deposit

ECONOMICS OF NUCLEAR FRACTURING AND IN-SITU COPPER LEACHING

In-situ leaching operations have not been charged with the cost of breaking and fracturing the deposit in the past. This cost has been carried by

pri
in

tab
the
a c
Thi
dep
ment
cate
cost
esti

by me
pipe
resis
Estim

Precip
Solut
Solut
Water
Shop a
Miscel
Ret
Ne
sc
fi
li

primary mining operation that required the development. This cost is included in the following estimate.

The cost per ton of breaking rock with nuclear explosives is shown in table 5. These costs are for explosives placed for maximum rock breakage in the form of a retarc.³¹ The ratio of rock broken in a retarc exceeds that of a contained explosion by a factor of 6 to 1 at the minimum contained depth. This ratio increases with the depth of placement beyond the minimum contained depth. Fracturing a mineral deposit may be expected to require deeper placement than this optimum depth and is estimated to break about a sixth the indicated tonnage of table 5 or to break rock at six times the cost per ton. The cost per pound of recoverable copper for breaking and fracturing a deposit is estimated in table 8.

TABLE 8. - Cost of fracturing a deposit in cents per pound of recoverable copper

Explosive		Estimated recoverable copper				
Yield, kilotons	Cost, cents per ton of ore broken	per ton				
		20 lb	16 lb	12 lb	8 lb	4 lb
10	55.2	2.8	3.5	4.6	6.9	13.8
20	33.6	1.7	2.1	2.8	4.2	7.4
50	16.2	.8	1.0	1.4	2.0	4.1
70	13.2	.7	.8	1.1	1.7	3.3
100	12.8	.6	.8	1.1	1.6	3.2

The plant and equipment necessary to recover copper from leach solution by metallic iron is simple and inexpensive with the exception of pumps and pipe required to circulate the solution; these require costly corrosion-resistant materials. The cost of plant construction varies with many factors. Estimated cost for typical plants is shown in table 9.

TABLE 9. - Estimated cost of a copper precipitating plant

Cost factors	Plant capacity, lbs per year	
	10,000,000	1,000,000
Precipitating launder and drying pads.....	\$ 195,000	\$ 65,000
Solution recovery, including pumps.....	270,000	50,000
Solution distribution system.....	195,000	45,000
Material handling equipment.....	140,000	60,000
Shop and maintenance facilities.....	100,000	20,000
Miscellaneous.....	100,000	10,000
Total.....	\$1,000,000	\$250,000

³¹ Retarc is the term coined by Lawrence Radiation Laboratory geologist at the Nevada Test Site for rubble mounds formed by explosions at intermediate scaled depths of burst. A retarc is defined as the mound of broken rock filling the true crater when the lowest inside part of the apparent crater lies at an elevation above preshot ground surface.

Assuming a 10-year operation, the capital investment per pound of copper produced is 1 cent for the larger plant and 2.5 cents for the smaller plant.

A plant producing 10 million pounds of copper per year is estimated to require about 25 employees, while one producing 1 million pounds of copper per year might require 6 employees. It is estimated each employee will cost \$6,511 per year.³²

Operating supplies include sulfuric acid, scrap iron, power, and miscellaneous items. Estimated operating costs for the two plants are shown in table 10.

TABLE 10. - Estimated operating costs

Cost factors	Plant capacity, lbs per year	
	10,000,000	1,000,000
Employees required.....	25	6
Labor.....	\$163,000	\$39,000
Supervision.....	15,000	10,000
Supplies.....	400,000	40,000
Miscellaneous.....	25,000	5,000
Total.....	\$603,000	\$94,000
Cost per lb of copper.....	\$.060	\$.094

Assuming repair and replacement are equal to capital cost, and allowing for general expenses, fringe benefits, insurance, safety, and refining and marketing, the total cost of producing copper by in-situ leaching (not including the cost of breaking and fracturing the ground) is estimated as shown in table 11.

TABLE 11. - Estimated cost of producing copper per pound

Cost factors	Plant capacity, lbs per year	
	10,000,000	1,000,000
Capital.....	\$0.01	\$0.025
Repair and replacement.....	.01	.025
Operating.....	.06	.094
Refining and marketing.....	.04	.04
General company expense.....	.01	.02
Fringe benefits, insurance, safety, etc.....	.04	.04
Total.....	\$.17	\$.244

General company expense is estimated to be somewhat lower for the larger plant. To these totals must be added the cost of breaking and fracturing the deposit which, as indicated in table 8 may range from 0.8 to 13.8 cents per pound of copper.

³²Average annual earnings for years 1962-64 as reported by Frank J. Tuck, *Copper Industry*. Statistics for 1964 as compared with other years, Arizona Department of Mineral Resources, August 1965, p. 22.

FIG

A
assumed
erals cl
body is
bonate r
capping
200 feet
12.

—
Sur
100
200

—
The
the sulf
tally c
and remc
ing oper

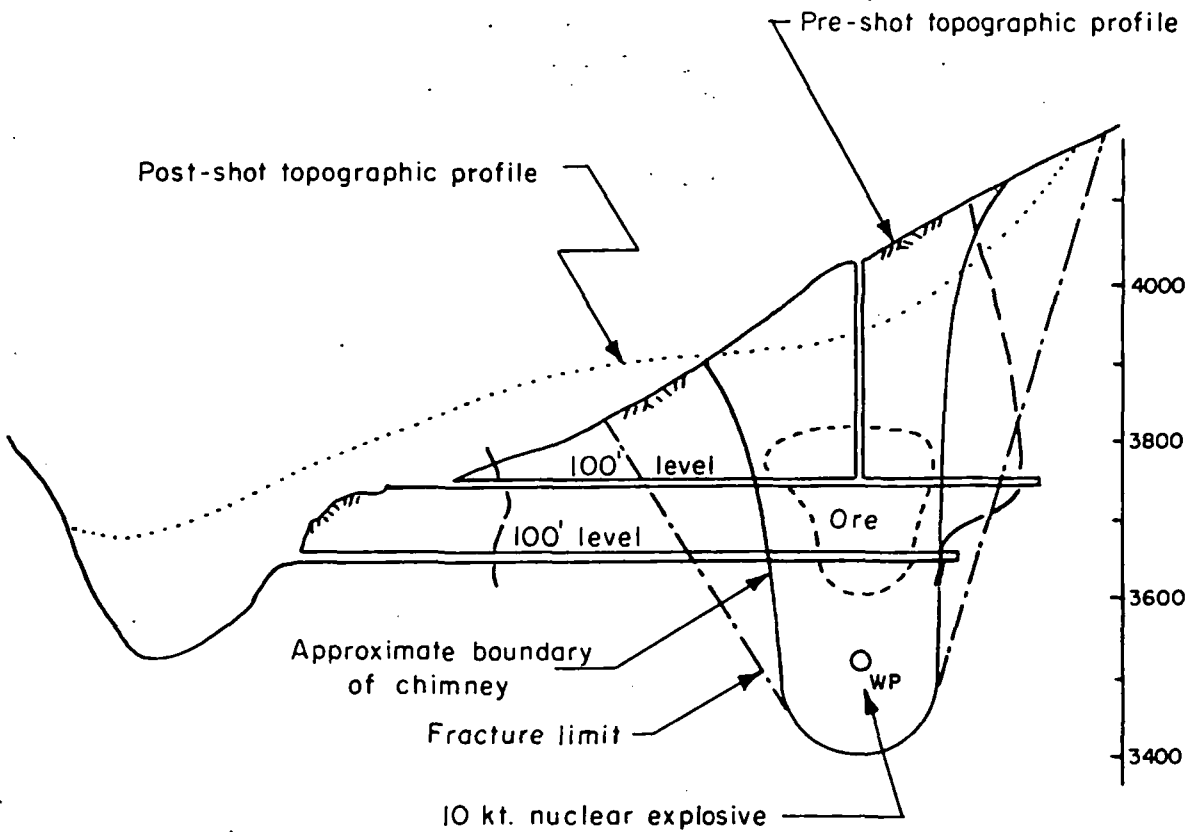


FIGURE 24. - Hypothetical Section of Small Copper Deposit After Nuclear Explosion.

A typical small deposit is shown on figure 24. The outlined ore body is assumed to contain 500,000 tons with a grade of 2.5 percent copper in the minerals chalcocite, bornite, chalcopyrite. The rock immediately above the ore body is assumed to contain 1.5 percent copper mostly in the silicate and carbonate minerals, and the 100 feet near the surface is assumed to be leached capping with a copper content of 0.15 percent. The copper content of a column 200 feet in diameter and 400 feet high through the deposit is shown in table 12.

TABLE 12. - Estimated copper in deposit

Vertical interval, ft	Tons	Copper lbs/ton	Total copper
Surface to 100.....	250,000	3	750,000
100 to 200.....	250,000	30	7,500,000
200 to 400.....	500,000	50	25,000,000
Total.....	1,000,000	-	33,250,000

The leached capping of this deposit contains 3 pounds of copper per ton; the sulfide ore contains 50 pounds. Assuming that the leached capping initially contained 50 pounds of copper 47 pounds or 96 percent has been leached and removed. Not all of this copper will be leached during the life of leaching operations but the assumption that 70 percent can be leached is reasonable.

The deposit is contained in a column of rock 400 feet high and 200 feet in diameter. A nuclear fracturing explosion with the broken rock reaching the surface (fig. 13) is indicated for efficient leaching.

Referring to figure 9, a 10-kton explosive at a depth of 500 feet is indicated for a cavity radius of 100 feet. The estimated chimney height (fig. 10) for a shot of this size is about 400 feet and the chimney might be expected to reach the surface from a depth of 500 feet. The indicated tonnage broken (fig. 11) is 1.0 million tons.

The cost of a 10-kton explosive from table 5 is \$550,000 to which must be added the cost of the safety study, which can be determined only after site has been selected. For this study, the safety investigation is estimated to equal the cost of the explosive making a total of \$1,100,000 for breaking ground. Assuming 70 percent of 33,250,000 pounds of copper or 23,275,000 pounds will be recovered, the cost per pound of copper for breaking the deposit is 4.8 cents.

An annual production of 2.3 million pounds of copper is indicated. Referring to table 5 the costs of an operation are estimated to be somewhat less but approach those for the smaller plant and the total cost of producing copper not including royalty, taxes and profit are estimated in table 13.

TABLE 13. - Estimated cost of producing copper from a hypothetical deposit

Cost factor:	Cost, cents per pound <u>produced</u>
Breaking and fracturing.....	4.8
Capital investment.....	2.5
Repair and replacement.....	2.5
Operating.....	9.4
Refining and marketing.....	4.0
General company expense.....	2.0
Fringe benefits, insurance, safety, etc...	<u>4.0</u>
Total.....	29.7

To illustrate the possible use of multiple explosives, a deposit of copper ore 750 feet wide, 1,000 feet long, and 400 feet thick is assumed. A leached capping 200 feet thick and containing 0.1 percent copper is assumed to cover the ore which contains 1.0 percent copper in the leachable mineral chalcocite.

The copper content of the leached capping is 10 percent of that in the ore and indicates that 90 percent of the copper in the original material has been leached. Eighty percent of the copper is assumed to be recoverable in a period of 10 years. Eighty percent of the copper is also assumed to be recoverable by flotation.

The deposit is estimated to contain 24 million tons of copper ore that contains 384 million pounds of recoverable copper by either method. Multiple explosions are required to fracture the deposit.

Production costs by the nuclear fracturing in-situ leaching method includes those for fracturing the ore with 35 nuclear explosives in drill holes, preparing a 700-foot shaft and 17,000 feet of drifts and raises to collect the solution, constructing a copper precipitating plant, and operating for 10 years.

Production costs by conventional methods include those for development of a caving mine, development of a 6,700-ton per day concentrating plant, and operation for 10 years. The estimated costs of recovering copper by the two methods are compared in table 14.

TABLE 14. - Comparison of the estimated cost per pound for recovering copper by nuclear fracturing and in-situ leaching with cost of conventional methods

Method	Cost, cents per lb	
	Nuclear	Conventional
Nuclear fracturing.....	4.6	-
Mine development.....	.2	0.5
Mining ore.....	-	6.0
Plant development.....	.8	2.7
Operating cost.....	17.0	25.8
Fringe benefits, insurance, safety, etc.....	4.0	4.0
Total.....	26.6	39.0

CONCLUSIONS

The copper in many large low-grade and small high-grade deposits³³ cannot be economically recovered by conventional methods because the value of the copper content of the large low-grade deposits is less than the cost of recovery, and the tonnage in the small deposits is not enough to amortize a recovery plant. These deposits are suitable targets for nuclear fracturing. Fracturing of such deposits with a nuclear explosive will permit circulation of solutions through the rock, and recovery of the copper at a cost estimated to be lower than by conventional methods which require mining, concentrating, smelting, and refining.

It should not be inferred that the use of nuclear explosives would be necessarily confined to low-grade or small ore bodies. Some of the ore bodies presently minable by conventional methods and containing copper in leachable minerals such as chalcocite, bornite, covellite, the oxide minerals, and even chalcopyrite may be more economically mined by fracturing with nuclear explosives and subsequent leaching than by conventional methods. Some deposits may

³³A small deposit is defined as one that contains from 250,000 to 10,000,000 tons; a large deposit as one containing more than 10,000,000 tons of ore.

be mined by conventional methods to a point beyond which the operation is economic then converted to nuclear fracturing and in-situ leaching methods.

The development of any new method or process progresses systematically from an idea through laboratory tests, bench tests, and pilot plant tests, to a full-scale operating test. Nuclear explosives are not adapted to small-scale test work. Much laboratory and analytical work has been completed, and nuclear explosive fracturing followed by in-situ leaching appears to be a practical method for recovering copper. However, many combinations of factors are involved, and the method can be proved effective and economical only by a full-scale test in a copper deposit.

Some points that can be determined only by a full-scale test are the percolation rate of solutions through the fractured rock, the copper recovery rate, the extent to which radiation safety measures will influence costs, and the time required, if any, for the decay of radioactivity to reach a level that will permit safe leaching.

Indicated advantages over conventional methods of recovering copper are the lower cost and the shorter time interval from inception to production. The method may be applicable and may prove economic when used on very low-grade deposits and thus greatly increase copper reserve.

SUBJ
MNG
FEFI

PRESENTED BEFORE AIME UPPER PENINSULA MEETING, HOUGHTON, MICH., MAY 1-2, 1974

A FRAGMENTATION EXPERIMENT FOR IN SITU EXTRACTION

UNIVERSITY OF UTAH
RESEARCH INSTITUTE
EARTH SCIENCE LAB.

by

Dennis V. D'Andrea¹, Richard A. Dick²
Robert C. Steckley³, and William C. Larson³

UNIVERSITY OF UTAH
RESEARCH INSTITUTE
EARTH SCIENCE LAB.

ABSTRACT

A fragmentation experiment was performed in cooperation with Duval Corporation in a porphyry copper molybdenum deposit near the Sierrita pit south of Tucson, Ariz. A 10-hole test blast was detonated to establish relationships between blasthole spacing and the resulting fragmentation. Blastholes were 9 in. in diameter and 110 ft deep. The 10 blastholes contained a total of 17,400 lb. of aluminized slurry blasting agent in 50-ft columns with 60 ft of stemming. Blasthole spacings of 25, 20, and 15 ft were tested. Diamond drill core examination was the primary method used to determine the condition of the rock before and after blasting. Topographic surveys were used to measure the rock swell produced by the blast and a fragment size distribution was obtained for the rubblized material on the surface. The rubble zone at the surface was ideal for in situ leaching. Fragmentation to depths of 110 ft was excellent from the 15- to 20-ft blasthole spacing patterns. Good breakage was also produced by the 25-ft pattern although the effects of the blast were not as obvious. In situ leaching tests were not conducted. However, based on size consideration only, all three blasting patterns produced adequate breakage for successful leaching.

INTRODUCTION

The Federal Bureau of Mines is developing fragmentation technology for in situ extraction systems. The in situ extraction system is attractive because it can be applied to deposits that are presently too low grade to be mined by conventional methods, thereby increasing domestic reserves. Other advantages of in situ extraction are a reduction of exposure of workers to health and safety hazards, minimized detrimental environmental effects, and lower energy consumption during mining and beneficiation (1-2). The objective of the Bureau research is to develop fragmentation processes to effectively fragment rock in place and economically prepare low-grade deposits for in situ extraction. The initial research is directed primarily at mining porphyry copper deposits. However, much of the information developed will be applicable to in situ extraction of other mineral deposits.

In situ leaching has been practiced at Ray and Miami (3) to take advantage of fragmented zones of rock created by block caving operations. The Old Reliable mine near Mammoth, Ariz., was the site of a 4,000,000 lb AN-FO coyote blast to prepare the ore body for in situ leaching (4). The blast,

¹Geophysicist.

²Mining engineer.

³Geologist.

All authors are with the Twin Cities Mining Research Center, Bureau of Mines, U.S. Department of the Interior, Minneapolis, Minn.

a joint effort of Ranchers Exploration and Development Corp. and Du Pont, was detonated in March 1972. Ranchers also detonated a borehole blast with 400,000 lb of explosive to break and move ore into the pit for in situ leaching at the Big Mike mine near Winnemucca, Nev., in July 1973 (5). McAlester Fuel Co. detonated a 4,000,000-lb AN-FO blast in vertical boreholes at its Zonia mine near Kirkland Junction, Ariz., in April 1973. Initial results at the Old Reliable, the Big Mike, and the Zonia mines have been encouraging. The concept of using nuclear explosives for in situ leaching has received considerable attention (6). Public opposition to the commercial use of nuclear explosives and difficulties in leaching deep-lying primary sulfide ores have delayed its application. However, Kennecott and AEC continue efforts to solve the environmental and technical problems associated with this method (7).

Although industry activities in in situ extraction are increasing, many problems remain to be solved. Improved techniques for determining in situ rock properties and in place characteristics of ore bodies are needed to properly evaluate a potential deposit for in situ extraction. Blasting methods are required that produce ideal fragmentation so that maximum recoveries can be obtained. More sophisticated solution injection and recovery systems are needed. Environmental controls must be improved. Research in these areas will undoubtedly contribute to continued industry expansion of in situ mining operations.

TEST SITE

Duval Corporation's Sierrita open pit copper molybdenum mine is located in Pima County, Ariz., approximately 24 miles south of Tucson. The test site is located on the northeast side of the Sierrita pit, about 1,500 ft from the pit boundary. This area was chosen for study because it contained low-grade copper oxide mineralization, was readily accessible to drilling and blasthole loading equipment, and was remote enough not to interfere with mining activities.

The dominant rock type at the test site is a quartz monzonite porphyry. This rock is well-weathered with considerable jointing and faulting (8). Assays of samples taken during blasthole drilling average 0.14 pct total copper, 0.13 pct acid soluble copper, and 0.005 pct molybdenum.

EXPERIMENTAL PROCEDURE

Preshot Study

Preshot studies at the test area included a detailed topographic survey, drilling of three 120-ft-deep NX core holes and down-the-hole geophysical logging. The detailed topographic survey was run so that an accurate measure of elevation changes produced by the blast could be made. Wooden stakes were used to establish 68 permanent survey points so that preshot and postshot elevations could be measured at the same point, and elevation changes could be determined to within ± 0.2 ft.

The three preshot diamond drill holes were located to obtain samples in the middle of the 15-, 20-, and 25-ft blasthole spacing areas as shown in figure 1. These drill holes were NX diameter and produced drill core about 2 in. in diameter. Four types of geophysical logs were recorded on each preshot hole. These logs included (1) gamma, (2) selfpotential, (3) resistivity, and (4) induced polarization.

Laboratory tests on the drill core were conducted to measure core recovery based on both length and weight, rock-quality designation (RQD), size distribution, and standard physical properties.

Test Blast

Figure 1 shows the blasthole locations and the blast delay sequence. This pattern was selected so that blasthole spacings based on equilateral triangles of 25, 20, and 15 ft could be tested. The ten 9-in-diam blastholes were each 110 ft deep with 60 ft of stemming and a 50-ft powder column. The blastholes were connected with 50-gr/ft core load detonating cord and bottom initiated with 1-lb cast primers. Although it was felt that instantaneous initiation would improve the fragmentation, ground vibration considerations dictated that the blast be delayed with 9-ms detonating cord delay connectors.

The blast contained a total of 17,440 lb of 10 pct aluminized slurry blasting agent. This blasting agent had specific gravity of 1.20 and a heat of detonation of 1.00 Kcal/g. The slurry was site mixed. Each hole contained about 1,700 lb of slurry and the maximum charge weight per delay interval was 5,300 lb. A portable three-component particle-velocity-recording seismograph was used to measure ground vibrations at a distance of 800 ft from the blast.

Powder factors, assuming infinite patterns, were 0.79, 1.24, and 2.20 lb/cu yd for the 25-, 20-, and 15-ft patterns, respectively.

Postshot Study

Postshot studies at the test site included a topographic survey, detailed mapping of surface fractures, fragment-size distribution measurements of broken rock on the surface; and drilling of six NX diameter core holes into the broken zone. Geophysical logs were not run on the postshot holes because the logging tools required water-filled boreholes, and the postshot holes would not hold water. Laboratory measurements on the rock core were used to determine core recovery by length, core recovery by weight, RQD index, fragment size distribution, and physical properties.

Two methods were used to obtain estimates of the fragment size distribution of the broken surface material. With the first method, two 50-gal drums of broken rock were returned to the laboratory for screening. The second method included selecting two sampling areas, each 1 yd², in the muck pile. At each sampling area, the two longest dimensions of 150 rock samples were measured. Although the two sampling methods are subject to statistical sampling errors, they do give a measure of the size distribution of surface material.

Figure 2 shows the test area during blasthole drilling. Blasthole loading is shown in figure 3. Figure 4 shows the results of the blast. After the blast and before postshot diamond drilling, a bulldozer was used to push aside 4 to 5 ft of surface rubble above the test area. Figure 5 shows the test site during postshot diamond drilling.

The location of the six postshot diamond drill holes are shown in figure 1. These holes were drilled in the center of equilateral triangles formed by the 25-, 20-, and 15-ft blasthole spacings. Minimum breakage would be expected in the center of these equilateral triangles with fragmentation improving near the blastholes. In an attempt to establish how the fragmentation changed away from the center of the 25-ft pattern, hole 9 was drilled in the 25-ft pattern, but only 7 ft from a blasthole.

Diamond drilling into the broken zone did present problems. The postshot holes were all drilled without return circulation of drill muds, and bit life averaged only 67 ft/bit. However, six postshot holes were successfully drilled to depths of 100 to 120 ft and no holes were lost due to caving.

RESULTS

The maximum peak particle velocity recorded on the three component portable seismograph was 0.95 in/sec at a distance of 800 ft. This value was lower than expected and indicated that the rock was weathered and fractured.

The rubblized surface material was well fragmented. The size distribution studies of the surface material showed that the greatest number of fragments were in the 2- to 3-in size range, and the vast majority of pieces were less than 11 in long. These size characteristics are similar to those of core from preshot holes 1, 2, and 3, suggesting that few new fractures were developed, and that the surface rubble zone was created by opening up old fractures. Blast-induced fractures on the surface and outside of the rubble zone were found to have three preferred orientations, one of which was controlled by the geologic structure, and the other two were interpreted to be caused by blast-induced doming of the rock mass.

Figure 6 shows the elevation changes produced by the blast. The greatest elevation changes were caused by rubble material being piled up about 50 ft to the northeast of the center of the blast. It is felt that three factors contributed to this irregular muck pile distribution: (1) The pattern changed from 25- to 15-ft blasthole spacing toward the northeast; (2) the blast was initiated in the southwest, and the delay sequence proceeded to the northeast; (3) the surface fell off in the northeast direction. The surface rise over the blast averaged about 5 ft, and the total-volume increase produced by the blast was 5,100 cu yd. A swell factor, defined as the final volume divided by the original volume, was difficult to determine because of uncertainty over what areas to use for these volumes. Assuming an overbreak region of 12.5 ft around each blasthole, an

original volume of 16,800 cu yd was calculated, and the resulting swell factor was 1.30.

Geophysical logs run on preshot diamond drill holes included gamma, self-potential, resistivity, and induced polarization. The resistivity log was the most diagnostic at delineating fracturing, although the correlation with fractures was not strong. Geophysical logs that would be of value for this kind of work are a dry hole acoustic log and an oriented caliper log.

Figure 7 shows rock core from preshot diamond drill hole 2, and figure 8 shows postshot core from hole 5. Both hole 2 and hole 5 were in the 20-ft blasthole spacing pattern. The preshot core shows that the rock was originally well fractured. The effect of the blast on the rock can be seen by comparing figure 7 with figure 8.

Table 1 lists the location, length core recovery, weight core recovery, RQD, largest piece, and the average size of pieces greater than 1 in for nine diamond drill core holes. Length core recovery and weight core recovery were measured after the core was returned to the laboratory. The length core recoveries measured in the core boxes were higher (101 pct for hole 1) than would have been obtained from measurements taken before the core was removed from the core barrel. Although there is a good correlation between length and weight recovery, the weight core recovery was considered the most accurate method.

TABLE 1. - Drill core data

Hole number	Location	Length recovery, pct	Weight recovery, lb/ft	RQD, pct	Largest piece, in	Average size of pieces > 1 in, in
1	Preshot	101	2.63	37	13	3.1
2	do.	98	2.58	35	17	3.2
3	do.	96	2.58	37	12	3.2
4	25-ft pattern	81	2.08	28	10	2.8
7	do.	76	1.90	19	11	2.8
9	25-ft pattern (off center)	62	1.61	19	12	2.7
5	20-ft pattern	53	1.20	9	8	2.2
6	do.	51	1.20	12	9	2.5
8	15-ft pattern	37	.99	10	9	2.3

The RQD is the total length of all pieces greater than 4 in divided by the core run, and this value is expressed as a percent (9). Rock quality is considered very poor for $0 \leq RQD \leq 25$ and poor for $25 \leq RQD \leq 50$ so that rock in the test area was originally classified as poor, and the blast changed the quality of the rock to very poor.

The largest piece of drill core averaged 14 in for preshot holes, 11 in for core from the 25-ft pattern, 8.5 in for core from the 20-ft pattern,

and 9 in for core from the 15-ft pattern. The average size of core pieces 1 in or greater was determined by dividing the total length of all pieces greater than 1 in by the number of pieces greater than 1 in. This average size was about 3.2 in for preshot core and between 2.2 and 2.8 in for the postshot core.

When compared with the successful fragmentation results obtained by Ranchers in their recent blasts at the Old Reliable and Big Mike mines (2, 5), the drill core data listed in table 1 support the conclusions that all three blasthole spacing patterns produced adequate fragmentation for leaching. For this test the average fragment size was less than the average 9-in-diam fragments obtained at the Big Mike mine and within the 9 in or less range at the Old Reliable mine. However, factors other than fragmentation, such as permeability and copper mineralization, affect the leaching process and the final copper recovery. A complete evaluation of this experiment would require in situ leaching tests.

The drill core data listed in table 1 also show that the 20-ft pattern produced better breakage than the 25-ft pattern, the 15-ft pattern produced better breakage than the 20-ft pattern, and fragmentation improves away from the center of the equilateral triangle patterns (see hole 9).

Logs of length recovery, weight recovery, RQD, and the average size of pieces larger than 1 in were prepared for approximate 10-ft intervals of drill hole depth. Figure 9 shows weight recovery versus hole depth for hole 6 and illustrates the main conclusions drawn from a careful examination of all logs of this type. Figure 9 and these logs show that the fragmentation is not as good in the stemming region, 0 to 60 ft, as it is in the blasting zone, 60 to 110 ft, and breakage does not extend deeper than the 100-ft blasthole depth. The logs also show a doming effect with best breakage in the stemming region in the center of the blast.

CONCLUSIONS

In this fragmentation study, 10 blastholes 9 in. in diameter and 110 ft deep were arranged in a pattern so that blasthole spacings of 25, 20, and 15 ft could be tested. Blastholes had 60 ft of stemming and a 50-ft column of 10 pct aluminized slurry blasting agent. Preshot and postshot diamond drill core was studied to determine the effects of the blast. Length core recovery, weight core recovery, RQD, largest piece of core, and average size of core pieces larger than 1 in were examined. Factors other than fragmentation affect copper recovery, and actual in situ leaching tests would have been desirable. However, the fragmentation analysis indicates that all three blasthole spacing patterns produced adequate breakage for in situ leaching.

REFERENCES

1. Dick, R. A. "In Situ Fragmentation for Solution Mining - A Research Need," presented before the Second International Symposium on Drilling and Blasting, Phoenix, Ariz., Feb. 12-16, 1973. Available for consultation at the Twin Cities Mining Research Center, Minneapolis, Minn.

2. Ward, M. H., "Engineering for In Situ Leaching," Mining Congress Journal, v. 59, No. 1, January 1973, pp. 21-27.
3. Fletcher, J. B., "In-Place Leaching at Miami Mine, Miami, Ariz.," Trans. SME/AIME, v. 250, No. 4, December 1971, pp. 310-316.
4. Engineering and Mining Journal, "Ranchers' Big Blast Shatters Copper Ore Body for In Situ Leaching," v. 174, No. 4, April 1973, pp. 98-100.
5. Mining Engineering, "Ranchers Development Sets Off Blast: Will Leach at Big Mike," v. 25, No. 8, August 1973, p. 10.
6. Hardwick, W. R., "Fracturing a Deposit With Nuclear Explosives and Recovering Copper by the In Situ Method," BuMines RI 6996, November 1967, 48 pp.
7. Engineering and Mining Journal, "AEC and KCC Will Jointly Study Potential of Nuclear Blasting to Mine Copper," v. 174, No. 4, April 1973, p. 26.
8. Savely, J. P., "Orientation and Engineering Properties of Jointing in the Sierrita Pit, Ariz.," Dept. of Min. and Geol. Eng., M.Sc. Thesis, University of Arizona, 1972, 134 pp.
9. Deere, D. U., A. H. Merritt, and R. F. Coon, "Engineering Classification of In Situ Rock," Technical Report No. AFWL-TR-67-144, Air Force Weapons Lab., Air Force Systems Command, Kirkland Air Force Base, New Mex., 1968, 271 pp.

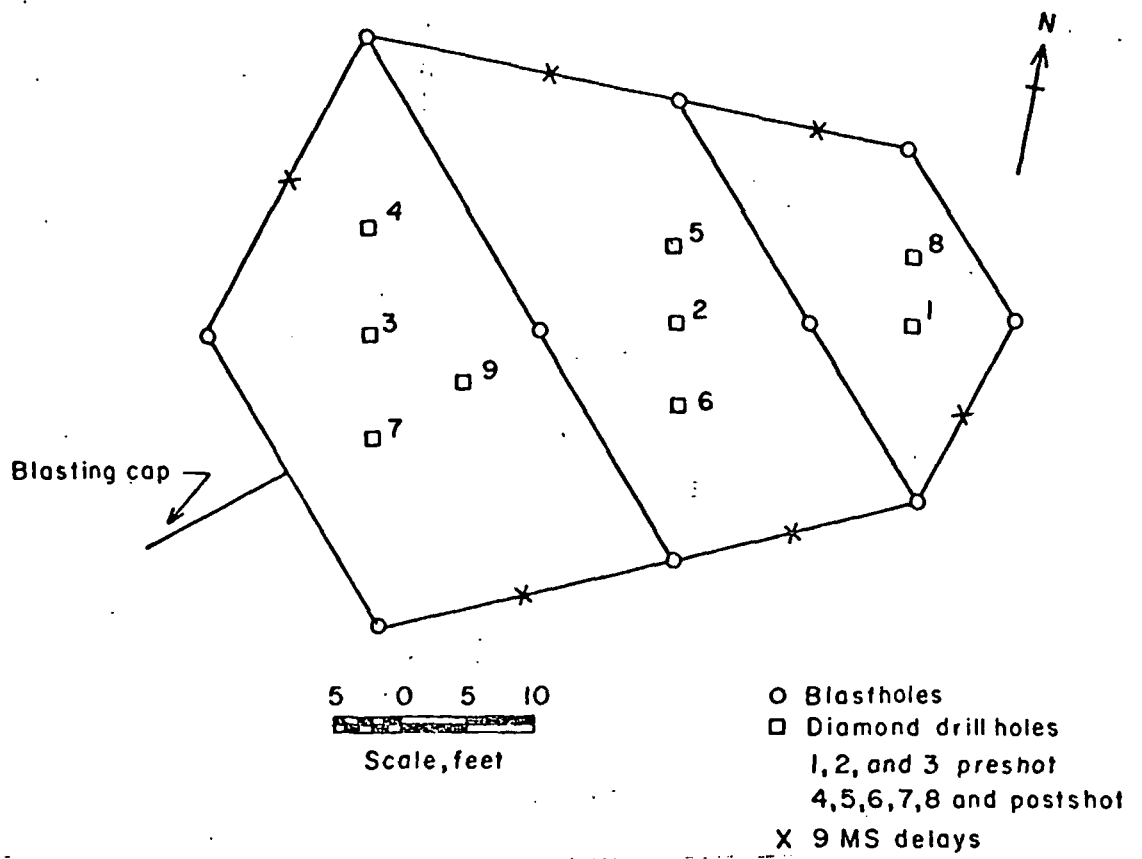


FIGURE 1. - Test Blast Design.

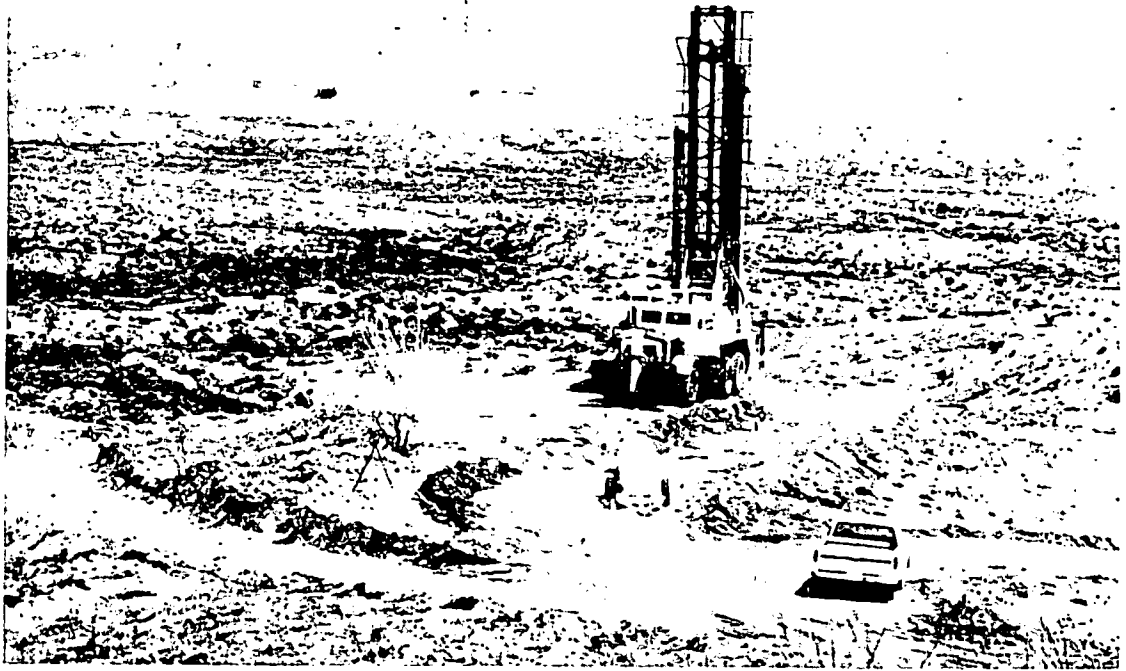


FIGURE 2. - Blasthole drilling.



FIGURE 3.- Blasthole loading.



FIGURE 4. - Blast results.

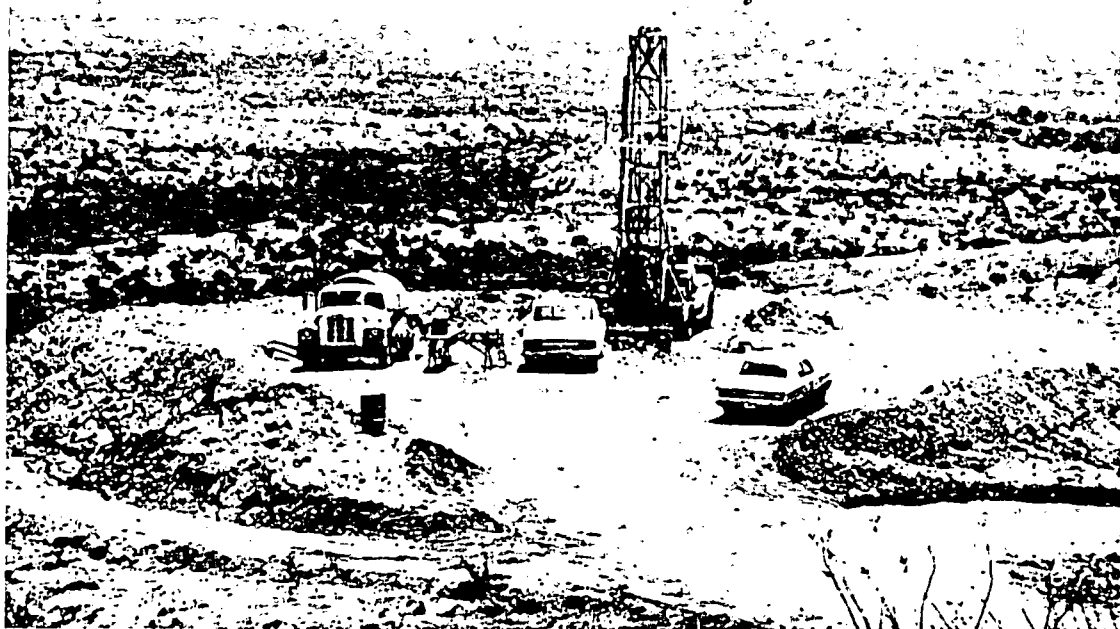


FIGURE 5. - Diamond drilling.



FIGURE 6. - Elevation Changes Produced by the Blast.



FIGURE 7. - Preshot diamond drill core, hole 2, 20-ft blasthole spacing.



FIGURE 8. - Postshot diamond drill core, hole 5, 20-ft blasthole spacing.

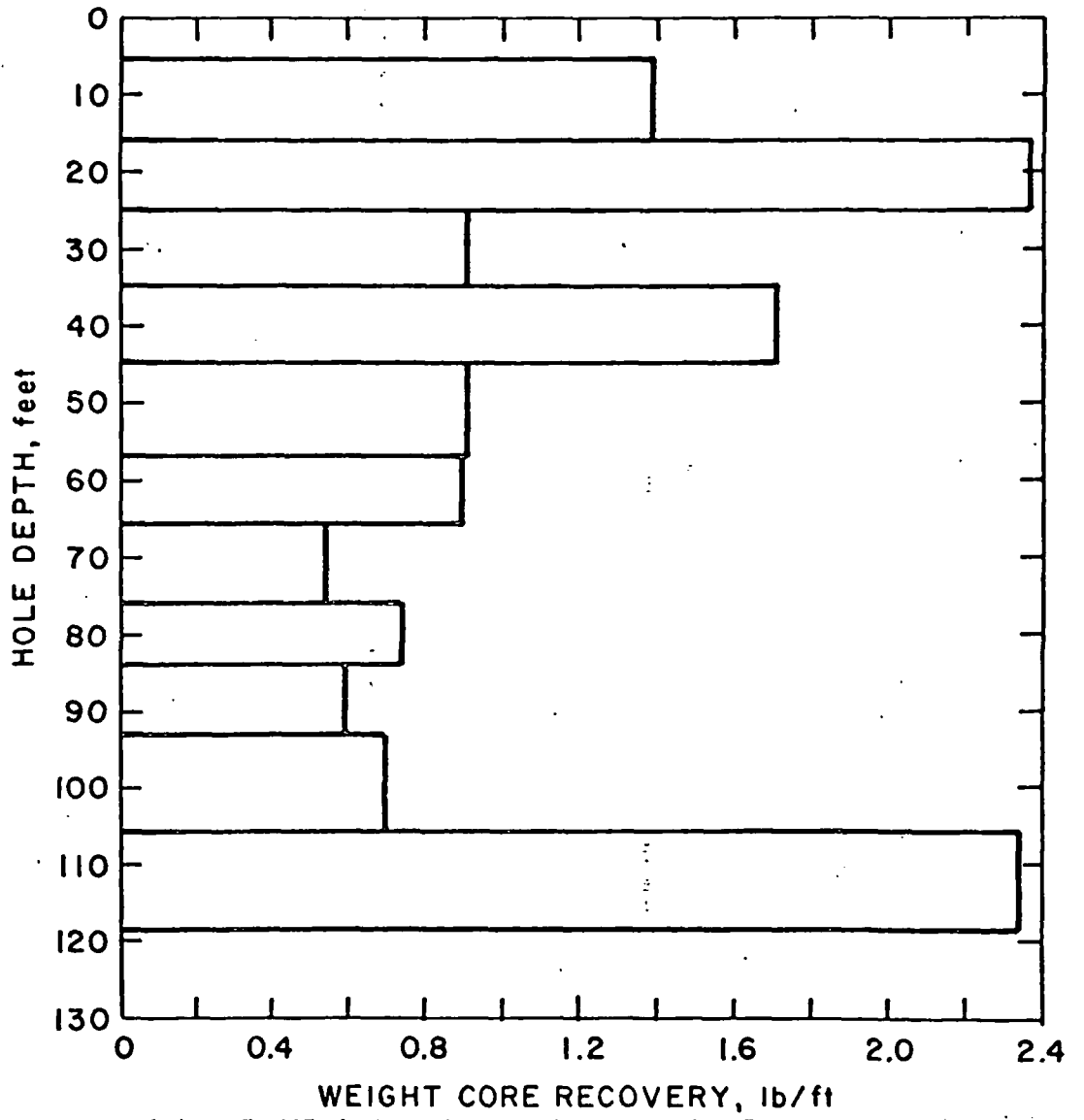


FIGURE 9. - Weight Core Recovery Versus Drill Hole Depth, Hole 6, 20-ft Spacing.

Soviet Mining Science Jour.
Sov. Mining Sci,
№ 2 1971
vol 7 no 2 1971

GEOTECHNOLOGICAL METHODS

FORECASTING THE EFFECT OF GEOLOGICAL FACTORS

UNDERGROUND LEACHING OF COPPER - NICKEL SULFIDE ORES

A. A. Antonov

UDC 622.272 + (553.43 + 553.48) + 622.277

SUBJ
MING
FEG

As in the case of many other commercial types of sulfide ores, the feasibility of extracting the valuable components of copper-nickel sulfide ores by the geotechnological method results from the relative ease with which sulfides are decomposed in an air-water medium and the high solubility and stable migration in acid waters of sulfates of nickel, copper, cobalt, and many other metals, formed during decomposition of sulfides.* Therefore, underground leaching of copper-nickel sulfide ores by reagents which decompose sulfides under natural conditions may be an essentially feasible (and probably the most suitable) method of geotechnological exploitation of copper-nickel sulfide ores, just as copper is extracted by underground leaching of copper pyrites [1, 2]. In general form, geotechnological extraction of nonferrous metals from copper-nickel ores is represented as a process of ore leaching effected by feeding chemical reagents via boreholes or mine workings into the precrushed ore body and removing the solutions enriched with the valuable components to the surface via boreholes or mine workings; i.e., extraction is in principle similar to natural leaching of ores in the supergenesis zone.†

Whereas nobody has any doubts about the feasibility of leaching nonferrous metals from copper-nickel sulfide ores, the economic advantages of the method, and the actual extraction process in its commercial form, must be theoretically and experimentally substantiated. A preliminary (albeit approximate and qualitative) assessment of the effect of natural factors on copper-nickel sulfide ores enables us to demarcate the most important trends in efforts to develop an extraction method, to determine the criteria for selecting objects for experimental and semicommercial extraction, to perform investigations which take account of the geological characteristics of the selected bodies, and to make a preliminary assessment of different types of sulfide deposits with regard to the applicability of the geotechnological method for their exploitation.

If the geotechnological system and the technological parameters of extraction are constant, the intensity and efficiency of leaching will depend on various different natural factors. The labor required for extraction work, the degree of complexity of the geotechnical system, and the degree of complexity of extraction control will also depend largely on the characteristics of the ore deposit.

Let us examine the possible effect of the most important geological factors on geotechnological extraction of nonferrous metals from copper-nickel sulfide ores, taking as our geological basis deposits in the Kola Peninsula (3, 4), which are typical commercial deposits of these ores.

Material Composition of the Ores and Rocks. The sulfide component of the ores is virtually the same for all these deposits in the Kola Peninsula. The principal sulfides composing the ores are pyrrhotite, pentlandite, and chalcopyrite; pyrrhotite is usually predominant, chalcopyrite being present in the smallest amounts. The quantitative ratios of the sulfides vary within these constraints. Certain types of the ores exhibit a higher content of pyrite and magnetite. Small amounts of other sulfides and oxides are found.

The silicate minerals contained in the ores and forming the wall rocks are represented principally by serpentine, chlorite, and talc in deposits associated with metamorphosed intrusions of ultrabasic composition (Pechenga

*However, certain metals (for example, the platinum group) do not go into solution under these conditions.

†If the mining process includes a stage of extraction of the metals from solutions, it may be represented as similar to natural precipitation of metals from solutions.

Mining-Metallurgical Institute, Kola Branch, Academy of Sciences of the USSR, Apatity. Translated from *Fiziko-Tekhnicheskie Problemy Razrabotki Poleznykh Iskopaemykh*, No. 2, pp. 58-65, March-April, 1971.

Original article submitted March 3, 1970.

© 1972 Consultants Bureau, a division of Plenum Publishing Corporation, 227 West 17th Street, New York, N. Y. 10011. All rights reserved. This article cannot be reproduced for any purpose whatsoever without permission of the publisher. A copy of this article is available from the publisher for \$15.00.

UNIVERSITY OF UTAH
RESEARCH INSTITUTE
EARTH SCIENCE LAB.

region), or pyroxenes, plagioclases, hornblende, and biotite in deposits associated with intrusions of basic composition (gabbro-norites, gabbro (Lovnoozersk, Fedorovo-Tundrovsk, and to some extent the Monchegorsk, Nyud, and other deposits), or pyroxenes, plagioclases, and olivine in deposits developed in intrusive formations of ultrabasic composition (the Monchegorsk deposits). Carbonate veinlets are found in the ores and rocks of certain deposits.

Under natural conditions removal of metals from ores is effected mainly by oxidation of sulfides by atmospheric oxygen and by oxygen dissolved in subsurface waters, and by decomposition of sulfides by the resultant intermediate products: sulfuric acid, ferric sulfate, and copper sulfate, and also partly by electrochemical solution [5, 6]. Oxidation of such sulfates as pyrrhotite, pyrite, and marcasite by air and water leads to formation of sulfuric acid and sulfates; oxidation of chalcopyrite leads to formation only of sulfates. Oxidation (and solution) is accelerated by the effect of the oxidation products of pyrrhotite and pyrite - sulfuric acid, ferric sulfate (formed when ferrous sulfate reacts with oxygen), and copper sulfate.

With respect to the degree of decomposability (oxidation, solution in sulfuric acid solutions), these sulfide minerals decompose in the following sequence: pyrrhotite and pentlandite, chalcopyrite, and pyrite. Pyrrhotite more stable than pentlandite is also found. Pyrrhotite and pentlandite are far more readily decomposed than chalcopyrite and pyrite; therefore in oxidized ores pyrrhotite and pentlandite are often completely leached, whereas chalcopyrite and pyrite are only partly leached. These minerals may be placed in the following sequence with respect to the weight of the reagents formed from a unit mass of sulfides, and with respect to the chemical activity of these reagents when they attack sulfides: pyrite, pyrrhotite, chalcopyrite, pentlandite. The capacity of sulfides to accelerate leaching of sulfide ores is based on these characteristics. The sulfides may be placed in the following sequence with respect to this capacity: pyrrhotite, pyrite, pentlandite, chalcopyrite.

The predominance of pyrrhotite in the ores is of dual significance. Decomposition of pyrrhotite intensifies leaching of the ores (additional oxidizing agents and solvents - ferric sulfate and sulfuric acid - are formed and heat is evolved by the exothermic reactions). However, owing to decomposition of pyrrhotite a considerable amount of iron goes into solution; if the conditions are appropriate (presence of oxygen, an increase in the solution pH) this iron is precipitated as hydroxides and thus retards subsequent leaching of the sulfide ores. Furthermore, the bulk of the reagents reacting with the sulfides is consumed in the reaction with pyrrhotite. On the whole, however, the presence of pyrrhotite in ores intensifies their leaching and increases the acidity of the medium, which is necessary for migration of metals as sulfates. The higher the pyrrhotite content of ores, other conditions being equal, the more rapidly and more markedly will the ores be leached.

At a sufficiently high pyrrhotite (particularly the monoclinic form) content of the ores, and in the presence of other favorable natural or artificially induced conditions, it is apparently only the beneficial effect of pyrrhotite on the overall process of leaching of the ores that enables one to employ geotechnological extraction (underground processing), albeit temporarily, by means of natural reagents - water and air (and, of course, by circulating solutions enriched with oxidizers and solvents of sulfides).

The reagents which attack sulfides, as well as minerals which are unstable in an oxidizing medium, also decompose the silicate minerals present in the ores and form the rocks, and are therefore consumed unproductively (they are neutralized). This negative role of silicate minerals must be particularly pronounced in the leaching of lean impregnation ores, in which the silicate mineral content reaches 99 vol. %. A much greater amount of reagents will be consumed on leaching the silicates in lean ores than on leaching sulfides. This is confirmed by the pattern exhibited by natural leaching of lean impregnation ores, the particular characteristics of which are as follows: as well as sulfides, leaching of silicates is observed; during the oxidation of lean impregnation copper-nickel sulfides ores, relatively uniform leaching of the whole ore mass occurs without formation of cavities from the sulfide impregnation (pyrite, chalcopyrite); in fissure water, the chemical composition of which is formed by leaching of lean impregnation ores, the content of ions removed from silicate minerals is usually hundreds or thousands of times greater than that of nonferrous metals removed from the sulfides, and the pH of the ore water is about 7 (between 6 and 8), never reaching 4-5 [7, 8].

The principal silicate minerals of the ores and rocks of nickel sulfide deposits in the Kola Peninsula may be placed in the following sequence with respect to the degree of chemical stability: talc, hypersthene, enstatite, forsterite, augite, hornblende, medium and basic plagioclases, biotite, fayalite, chrysotile, antigorite, chlorites.* Their deleterious effect on ore leaching (mainly manifested in neutralization of the reagents and the resultant reduced

* More data are required on the relative solubilities of these minerals.

rate of leaching of the ores) depends markedly not only on the chemical stability of these minerals, but also on their content of magnesium, calcium, ferrous iron, and sodium, and on the amount of these minerals in the ores and rocks. Therefore, other conditions being equal, a higher consumption of reagents and a lower rate of ore leaching will be observed during processing of ores associated with ultrabasic intrusions, olivinites, olivine pyroxenites, and serpentinites, whose average overall content of magnesium, calcium, ferrous iron, and sodium (in terms of oxides) is 43%. Minimal consumption of reagents and a high leaching rate may be expected when processing ores associated with basic intrusions, gabbro, and gabbro-norites and their varieties, whose total content of magnesium, calcium, ferrous iron, and sodium (in terms of oxides) is about 30%.

Other conditions being equal, to effect extraction by underground leaching, sulfide ores which occur among basic rocks are preferable to those associated with ultrabasic rocks, with the exception of pyroxenites, composed of such chemically stable minerals as hypersthene and enstatite; the most favorable ores are those which occur among acid or intermediate rocks, but the latter types of ore are very rare. A particularly deleterious effect on the leaching of ores may be exerted if carbonates are present in them and the wall rocks. Note that leaching will be accompanied by adsorption of nonferrous metals by silicates and their alteration products (argillaceous minerals, iron hydroxides).

Whereas the sulfide component of the ores has, on the whole, a beneficial effect on leaching, the silicate component has a markedly deleterious effect. It is therefore of interest to determine the effectiveness of attack of the air-water mixture on the ores and to investigate the applicability of reagents which selectively decompose sulfides.

Thus, the material composition of the ores and the wall rocks is one of the principal factors which have a decisive effect on extraction of nonferrous metals by underground leaching of nickel sulfide ores.

Texture and Structure of the Ores, Fracturing of Ores and Rocks. The textures of ores differ and depend to a certain extent on their sulfide content. Lean ores are predominantly of the impregnation type, occasionally of the veinlet-impregnation type. Rich ores, which are usually found in relatively small amounts in deposits, are represented by the aggregate-veinlet-impregnation, brecciated, and massive types.

The size of the sulfide impregnations is also usually linked with the sulfide content of the ores and the character of the texture: the higher the sulfide content, the larger the impregnations. The size of sulfide impregnations in lean ores is usually very small, being less than 0.5 mm in diameter and on the average about 0.1 mm; the sulfide impregnations are usually isolated from one another by silicate minerals. In certain types of ore (the Pechenga deposits), the sulfide impregnations exhibit close intergrowths with silicate minerals (talc, serpentine, and chlorite). Rich ores usually have structures of the sulfide contact type.

The effective porosity of unfissured specimens of ores and rocks is usually low, and their permeability almost nil. The porosity of the ore bodies and the adjoining rock mass; expressed as open-joint fissures (fissure porosity), is low, being on the average only tenths of a percent. Under natural conditions, filtration of water takes place only via fissures. Leaching occurs at the walls of fissures, gradually progressing into the body of massive and brecciated ore owing to diffusion of the reagents deep into the crystals via the porous formations (iron hydroxides, etc.) produced by leaching, but hardly penetrates into the body of lean impregnation ores, even after many years, owing to marked retardation of diffusion of the reagents into the depths of the ore by silicates. In lean impregnation ores natural leaching takes place only over geological epochs.

The fissuration of ores and the adjoining rocks has a dual effect on extraction. A high degree of development of microfissures (hairline cracks) in ores ensures better crushing of the ore body and a high reaction surface of the crushed ore, thus providing better conditions for leaching. However, the presence of large open-joint fissures in the ore body and adjoining rocks promotes formation of large ore fragments when the ore body is crushed and creates conditions for leakage of solutions and an intense influx of subsurface waters into the crushed ore body; this makes the leaching performance much poorer and complicates extraction control.

The following conditions favor geotechnological extraction: a massive, brecciated (to a lesser extent, veinlet or densely impregnated) texture and structure of the ores in the form of sulfide contact (sideronitic structure, etc.), and a high degree of microfissuration of the ores; unfavorable conditions are: a rare impregnation texture of the ores, small sulfide impregnations, their intergrowth with silicate and other nonsulfide minerals, and the presence of large open tectonic fissures.

In all the deposits of the Kola Peninsula, the temperature of the ores and the adjoining rocks at depths of up to 300 m is on the average 3°C, fluctuating between 0 and 5°C. Such a low temperature of the medium will have a marked retarding effect on leaching, and speeding up of the latter requires preheated reagents.

These physical characteristics of the ores (ore bodies) are of essential importance for geotechnological extraction and require the development of measures to prepare the ore body (or a sector of this body) for geotechnological processing, i.e., thorough crushing of the ore (ore body). Crushing of the ore body is necessary in all cases; the higher the degree of crushing (up to the optimal limit),* the more effective will be the geotechnological process, and the greater the amount of metals extracted from the ores. The required size of the ore fragments will differ for different ores. It may be much greater for massive brecciated ores than for impregnation ores. It is important to determine the required fragment size for lean impregnation ores because the basis of geotechnological extraction of nonferrous metals in the Kola Peninsula and in other regions of the Soviet Union is constituted largely by these ores, extraction and beneficiation of which by the methods used at present leave much to be desired. On the basis of the sulfide content of lean impregnation ores (a few percent) and the mean size of the sulfide impregnations (about 0.1mm), we can approximately determine the required fragment size of these ores for effective geotechnological extraction of metals. The diameter of these fragments should generally be less than 10 mm. The optimal fragment size of lean ores is apparently a diameter of a few millimeters, but the exact size may be determined experimentally, and it will differ for different lean ores. Crushing of lean impregnation ores of this fragment size is a very complex and laborious operation, requiring considerable expenditure of resources.

Thickness of the Ore Body. Increasing thickness of the ore body is accompanied by an increase in the ore reserves prepared for exploitation (calculated per unit volume of drilling work) and by improved conditions for use of the various facilities for preparatory drilling; the working systems are also the most effective. When the ore body is very thick, we have improved conditions for various efficient charge location patterns for effective crushing of the ore body.

Leaching of large ore masses will be accompanied by evolution of a relatively large quantity of heat (oxidation is exothermic) and by a rise in temperature of the medium (when the ore mass is large, the heat losses in the middle of the ore body will be relatively small); therefore, the velocity of the chemical reactions will increase and leaching will be intensified. Furthermore, regardless of the heat evolved, in the middle of a large leached ore mass leaching is accelerated by formation of a relatively high reagent concentration in this part, provided that the reagents (solutions) are not greatly diluted by waters from the adjoining rocks. These effects will be considerable in thick bodies of rich ores, where spontaneous intensification of leaching may be so marked that it is possible to use for extraction (albeit temporarily) the most accessible reagents — air and water (and, of course, circulating solutions).

When the volume of crushed ore is great, one may use relatively simple working systems (something like the natural system of leaching), and it is possible to effect continuous extraction of relatively large ore bodies as wholly in one stage, eliminating measures to remove the harmful effect of the worked-out area on extraction and thus simplifying control of the latter. However, leaching of thick ore bodies is accompanied by formation of unusual geotechnological zones in the ore bodies; these zones are displaced in time and space, and extraction control must be adapted to meet the resultant difficulties, thus possibly complicating the process as a whole.

Structure of the Ore Body. Other conditions being equal, a single monosomatic ore body is more suitable for geotechnological extraction than an ore body which consists of alternating ore and nonmetallic zones or which contains large barren xenoliths, because crushing of such a body is not accompanied by impoverishment of the ores and, furthermore, exploitation is relatively simplified. The degree of crushing of the ore body into blocks at faults (tectonic) may have dual significance: if the tectonic zones (faults) are open and carry much water, exploitation of the ore body by sectors (blocks) may be complicated owing to the highly probable dilution of the solutions by influx water, leakage of solutions, and the deleterious effect of the worked-out (leached) area on geotechnological extraction; but if the tectonic zones (faults) are closed and impermeable (or only slightly permeable) to water, such an ore body is apparently suitable for exploitation by sectors.

Mode of Occurrence of the Ore Body. Other conditions being equal, ore bodies with steep dips are more suitable for geotechnological extraction. This is largely due to the fact that in such bodies relatively large reserves of ore are concentrated per unit area of the deposit (or worked sector of the deposit); furthermore, crushing may be effected in a large volume of the ore body, although the steep dip may sometimes complicate geotechnological extraction (if the depth of occurrence of the ore body varies markedly, or if it is waterlogged).

*With increasing degree of crushing of impregnation ores, the specific surface of the nonmetallic minerals increases far more markedly than that of the ore minerals, and in consequence there is a marked increase in neutralization of the reagents and adsorption of nonferrous metals. Furthermore, very intense crushing of the ores may be accompanied by a marked reduction of their permeability.

Position of the Ore Body in the Relief and Its Depth. Ore bodies lying in an elevated area or at relatively shallow points are evidently more suitable for geotechnological exploitation and enable one to use simpler and less laborious working systems than those which occur in depressions or at great depths.

Hydrogeological Conditions. Copper-nickel sulfide deposits and their individual parts differ markedly with respect to hydrogeological conditions. The most marked differences in the latter are exhibited by ore bodies which lie in elevated or depressed sectors of the relief. In the first case (elevated sectors) the occurrence of the ore body in a zone of aeration, the moderate amount of flooding, the generally descensional movement of the subsurface waters, their saturation with oxygen, and their low mineralization will assist geotechnological leaching of the ores and the organization of extraction from the hydrodynamic aspect and will also simplify extraction. However, leakage of solutions may occur, and in many cases it may be difficult to organize the water supply for the geotechnological facilities.

In deposits associated with depressions of the relief, the hydrogeological conditions are complicated (the ore bodies lie in a permanently water-saturated area; the fissure waters have a high-pressure head and an ascensional character; there is frequently a porous horizon with a high water content in the cover deposits; surface water basins are present; and the hydrodynamic conditions are reducing) and do not favor the geotechnological process or its control. If the rocks (ores) are markedly saturated with water, the subsurface waters may greatly dilute the reagents and productive solutions, thereby complicating leaching and making it more difficult; dilution of the solutions by subsurface waters increases the solution pH, which may lead to undesirable precipitation of certain compounds; the high pressure heads of the fissured rocks at depth and the frequently ascensional character of the fissure waters often make it necessary to force the reagents into the lower parts of the ore body, using high pressures for this purpose. In the zone of constant water saturation, leaching must generally be performed in a drained ore body (or a part of it) so as to enable the operatives to perform the necessary work involved in "drying" and wetting the ores in order to make leaching possible. Prereduction of the fissure-water levels to the required depths, and control of the levels of these waters and solutions, are complex processes.

Thus the sulfide content of the ores, the material composition of the latter and the adjoining rocks, the physical properties of the ores and the rocks (principally their texture and fissuration), the thickness and structure of the ore body, and the hydrogeological conditions are the main factors which have a decisive effect on geotechnological extraction of nonferrous metals and which must be taken into account when planning scientific investigations, developing the scientific bases of the extraction method, selecting suitable bodies for experimental and semicommercial extraction work, and planning and effecting such operations.

The information in this paper and the method employed may be used for predicting the effects of natural factors on geotechnological extraction of nonferrous metals from other commercial types of sulfide ores, which are relatively readily oxidized and leached in the supergenesis zone; the sulfates of many metals thus obtained readily dissolve in water and migrate relatively stably in the dissolved state.

LITERATURE CITED

1. I. N. Plaksin and D. M. Yukhtanov, Hydrometallurgy [in Russian], Metallurgizdat, Moscow (1949).
2. P. A. Pozdnikov, Summaries of the Conference on Geotechnological Methods of Extracting Minerals [in Russian], Izd. MIREM, Moscow (1965).
3. N. A. Eliseev, G. I. Gorbunov, É. N. Eliseev, V. A. Maslennikov, and K. N. Utkin, Ultrabasic and Basic Intrusions at Pechenga [in Russian], Izd-vo AN SSSR, Moscow-Leningrad (1961).
4. N. A. Eliseev, É. N. Eliseev, E. K. Kozlov, P. V. Lyalin, and V. A. Maslennikov, Geology and Ore Deposits of the Mohegorsk Pluton [in Russian], Izd-vo AN SSSR, Moscow (1956).
5. S. S. Smirnov, The Oxidation Zone of Sulfide Deposits [in Russian], Izd-vo AN SSSR, Moscow (1955).
6. G. B. Svěshnikov, Electrochemical Processes in Sulfide Deposits [in Russian], Izd. Leningrad. Un-ta, Leningrad (1967).
7. A. A. Antonov, Razvedka i Okhrana Nedra, No. 3 (1962).
8. A. A. Antonov, Removal of Elements by Subsurface Waters from Intrusive Massifs of the Central Part of the Kola Peninsula and Hydrogeochemical Indices of the Rocks. Relief and Geological Structure of the Sedimentary Cover of the Kola Peninsula [in Russian], Nauka, Moscow-Leningrad (1964).

Feasibility of "Enhanced" Solution Mining at Searles Lake, California

James L. Giulianelli, Sam Carpenter,
Warren L. Dowler, and Roger V. Carlson

Researchers at the Jet Propulsion Laboratory have done a preliminary investigation of a new in situ method of extracting trona from brines at Searles Lake, CA—an area that has received commercial interest since the late 1800s. This "enhanced" solution mining method is defined as the injection of some fluid to either cause production of a fluid with a mineral value or to improve the value of an existing fluid. In contrast, ordinary solution mining is defined as any mining operation that removes mineral values in a fluid state. The present Searles Lake operations, where interstitial salt brines are pumped, is an example.

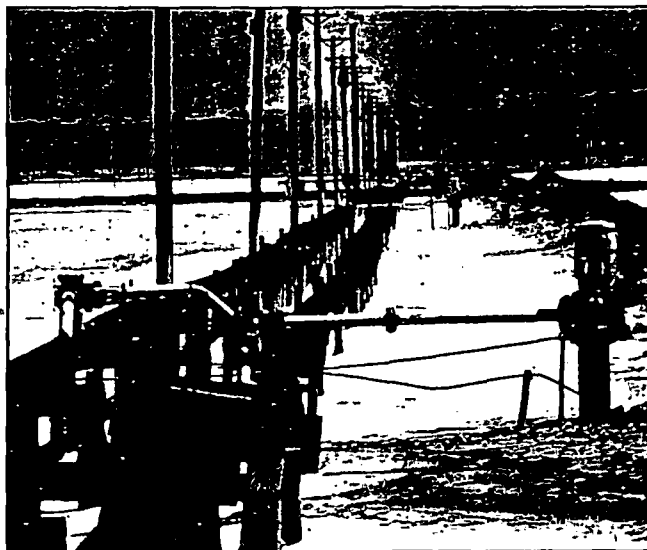
When compared with conventional mining, solution mining has numerous advantages:

- Less environmental impact;
- Lower costs;
- Recovery of low concentrations of mineral values otherwise unattainable;
- Ability to operate in otherwise inaccessible locations (deep strata, rugged terrain, beneath water tables, beneath the ocean floor, etc.); and
- Cost effectiveness for small mining operations.

There are, however, problems and limitations to ordinary solution mining at Searles Lake, including:

- Limited brine concentration (the concentration of mineral values in the brine is limited by the solution phase relationships). The various salts tend to be in equilibrium, with the chloride ion being dominant. By weight, only 4-10% of the sodium carbonate and sodium bicarbonate can be in the brine even if it originates from a strata consisting almost entirely of these two salts.
- Collapse and mixing of separated strata. Removing solids without

A portion of Kerr-McGee Corp.'s collection and distribution system for its conventional solution mining operation at Searles Lake.



at least partial replacement of their volumes would inevitably lead to local collapse and layer intermixing. Also, for the mixed layer, shown on the accompanying diagram, replacement of extracted brine may be a problem. Attempts to inject unsaturated water rather than a saturated brine result in the lighter water being forced upward by brine, again causing a possible connection with above layers.

- Vertical mixing of layers via abandoned cores and wells.
- Complexity and, in turn, cost of processing brines to separate multiple salts.

The enhanced method of solution mining offers three unique innovations:

- In situ processing that would be used to exchange one brine for another to obtain a simpler brine than those presently available;
- A method that would maintain the existing volume of solids in the mined strata to prevent strata collapse and mixing with other layers; and
- Salinity gradient solar ponds to provide inexpensive, low-temperature process heat to improve economics and displace fossil fuels.

The Resource

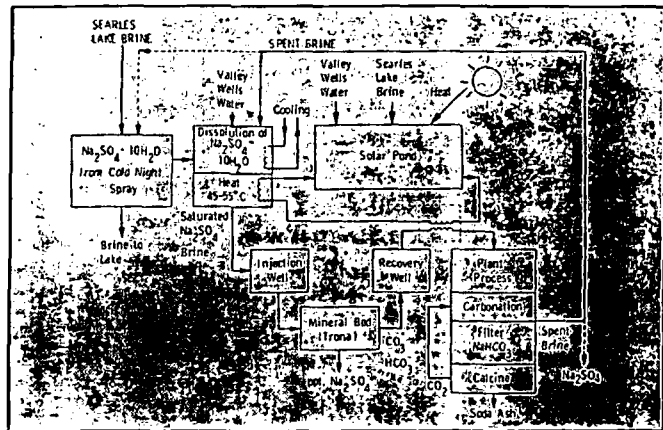
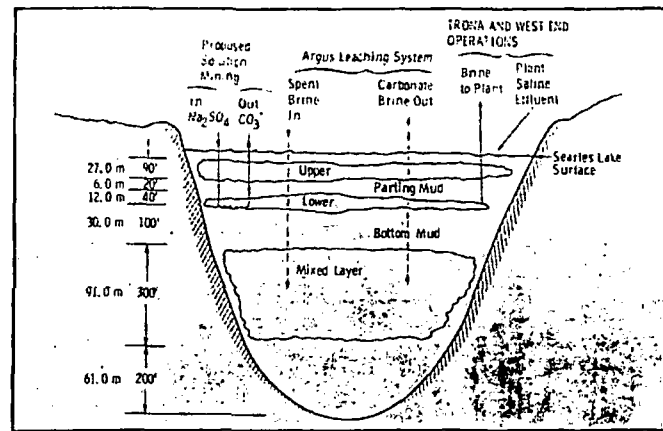
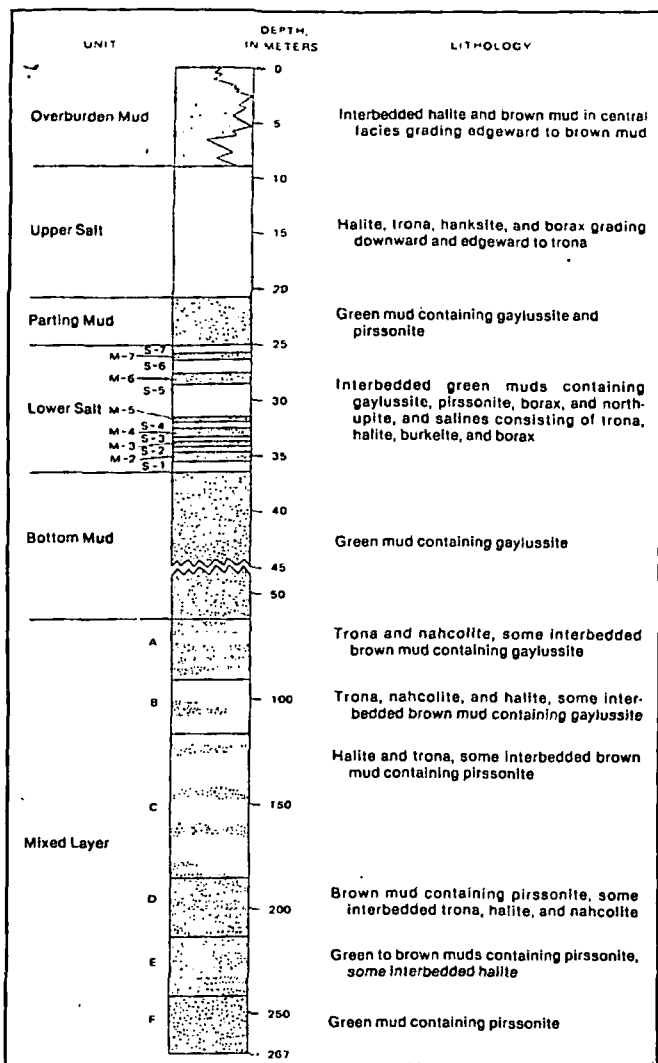
Searles Lake is a dry lake in east-central California containing evapo-

rites available in the form of solids at the surface and saturated interstitial brines from saline layers beneath the surface. During glacial times, a chain of lakes began at Mono Lake, including the Searles Lake area, and ended at what is now Death Valley. The alternating pluvial and interpluvial periods resulted in deposition of a complex mixture of muds and salts with an area of more than 110 km² and a depth exceeding 250 m in some locations.

The brines and their enclosing salines are composed chiefly of sodium carbonate, sodium bicarbonate, sodium sulfate, and sodium chloride. Sodium carbonate (soda ash) is one of the most important products, and its most important source is trona. There are also commercially useful amounts of potassium salts and borate. The three main saline stratigraphic units lying from near the surface to deep strata are:

- Upper Salt—typical thickness of about 15 m; less than 10 m below the surface. Most abundant minerals include halite, trona, and hanksite.
- Lower Salt—consists of interbedded layers of salines (S-1 to S-7) and muds (M-2 to M-7); only about 12 m thick but commercially important. The most abundant saline minerals in order of decreasing abundance are: trona, halite, burkeite,

This article is largely derived from experimental work by James Giulianelli and Sam Carpenter at the Jet Propulsion Laboratory, California Institute of Technology, Pasadena, CA.



The diagram at left illustrates the stratigraphic units in the Searles Lake evaporite sequence. At right, the top diagram shows a simplified cross section of present and proposed brine extraction. A schematic of the proposed enhanced solution mining method using solar pond process heat is shown above.

northupite, borax, and thenardite. The lower three layers (S-1 to S-3) are almost entirely trona.

- **Mixed Layer**—composed mostly of salines with mud at the top and mostly muds with some salines at the bottom. Saline layers are composed predominately of minerals made up of sodium carbonate and chloride ions, and minerals containing magnesium and sulfate ions are rare. This layer has been divided into six stratigraphic units with the top (A) layer being predominantly trona and nahcolite and the second (B) layer being mostly trona and halite with some nahcolite.

Currently, solid minerals are extracted from the three main saline stratigraphic units by pumping brines from these layers and using complex chemical processing techniques to separate constituents. Spent brine, saline water, and natural runoff flow onto the surface to slowly replenish the brines in the upper salt and lower salt regions. Replenishment water or brine must be pumped directly into the mixed layer because it has little if any communication with above strata.

Searles Lake produced nearly 1.8 Mt of product in 1979, including soda ash, potash, salt cake, and borax.

Kerr-McGee Corp. now operates three main plants to process brine extracted from each salt layer.

Enhanced Solution Mining Concept

The enhanced solution mining method studied consists of injecting a saturated sulfate brine at warmer than ambient temperature to extract trona from the lower salt layer, specifically from levels S-1, S-2, and S-3 which are almost entirely trona. The sulfate would partially precipitate out while the carbonate and bicarbonate would be dissolved and removed from solid trona. Additionally, salinity gradient solar ponds could be used for heating the injection brine.

For a successful operation, the following criteria must be satisfied:

- Solvent must be brought into contact with the ore;
- Target minerals must be dissolved;
- Generated fluid must be able to flow to the collection system; and
- Valuable components must be processed out of the liquid.

A currently conceived operation, shown in the accompanying diagram,

would have the following characteristics (calculated for 20% solar collecting efficiency in the solar pond, 2100 kWh/m² per year insolation, and a brine specific heat equivalent to water):

- Flow rate of 0.19 m³/s from a multitude of injection wells in an array around exit wells.
- Injection brine saturated with sodium sulfate, which is about 32 weight percent (47 parts per 100 parts water) and a density of about 1.3 t/m³.
- Injection brine heated from ambient (22°C) to 55°C causing heat demand of 33 MW_{th}, which would require roughly 70 hm² of salinity gradient ponds. (An injection brine of 45°C would require only 49 hm² for a 23 MW_{th} demand).
- Injection into the S-1 and S-2 layers of the lower salt region.
- Generation of an exit brine yielding about 14 weight percent sodium carbonate at 60°C and 12.6 weight percent at 45°C. (For comparison, the highest concentration of sodium carbonate in brine reported was 9.75%).

A sulfate solution was chosen for the makeup brine for two reasons: (1) a less dense fluid, such as hot water,

would simply either return to the surface at the injection well or rise through many old core or bore holes, thus connecting and further contaminating adjacent layers; and (2) using a sulfate solution would allow at least partial replacement of extracted volumes, through precipitation, and would help avoid local collapse, subsidence, and layer intermixing that may upset today's mining operation. Also, using a sodium sulfate solution may plug unwanted connections between strata, such as old bore holes, by forming Glauber's salt ($\text{Na}_2\text{SO}_4 \cdot 10\text{H}_2\text{O}$) upon cooling in place.

A second innovation for the proposed Searles Lake operation is the use of solar ponds to heat injection brine. A solar pond is a body of still water that captures solar radiation and stores it as usable heat. The most promising and proven concept is the salt gradient solar pond.

In a gradient pond, a dense (nearly saturated) layer of brine is covered by a less dense gradient layer in which salinity decreases toward the top. The upper layer is nonconvecting because the salinity density differences are greater than those caused by temperature; therefore, heat is trapped in the lower or storage layer. Working temperatures of 80-90°C can be maintained in the storage layer, and useful amounts of heat can be obtained even during winter months.

Salinity gradient solar ponds would provide cost advantages for an enhanced solution mining operation at Searles Lake because of the following circumstances:

- Low land costs;
- High insolation levels (equivalent to those of functioning salinity gradient solar ponds); and
- Successful use of ponds for both brine conditioning and solar evaporation since 1968 in the area. Currently, more than 400 hm^2 of ponds are in service.

Other site characteristics also permit economical operation of salinity gradient solar ponds at Searles Lake. For example, the cost of purchasing salt is eliminated because salt is available in the area. Also, to avoid saline contamination of local ground water and to prevent loss of pond water, a liner is usually necessary. However, a liner is probably not required at Searles Lake since readily available impermeable clays will be sufficient to prevent most leakage.

Phase Relationships and Carbonate Yield

The struggle to profitably mine Searles Lake depends on knowledge of phase relationships among various salts. Searles Lake brines can be rep-

Point	Na_2CO_3	NaHCO_3	NaCl	Na_2SO_4	Solids
66	74.1	25.9	—	—	B + T
67	97.3	2.7	—	—	C ₁ + T
68	45.6	0.9	53.5	—	C ₁ + X + T
69	11.1	4.8	84.3	—	B + X + T
70	81.1	1.1	—	17.8	C ₁ + X + T
71	36.1	4.4	—	59.5	S ₀ + X + T
72	26.5	8.35	—	65.15	S ₀ + B + T
73	43.5	1.0	50.1	5.4	C ₁ + X + T
74	9.8	5.1	69.8	15.3	S ₀ + X + T

B = NaHCO_3 T = $\text{Na}_2\text{CO}_3 \cdot \text{NaHCO}_3 \cdot 2\text{H}_2\text{O}$ (trona)
 C₁ = $\text{Na}_2\text{CO}_3 \cdot \text{H}_2\text{O}$ X = NaCl
 S₀ = Na_2SO_4 (thenardite) Y = $\text{Na}_2\text{CO}_3 \cdot 2\text{Na}_2\text{SO}_4$ (burkeite)

resented by a five-component system consisting of sodium carbonate, sodium bicarbonate, sodium sulfate, sodium chloride, and water. By representing only relative salt compositions within saturated solutions (water as an understood member), a simpler four-component system is created. The accompanying table lists weight percentages of this system at 45°C, a reasonable candidate temperature for the enhanced mining operation. The weight percentages given are at the so-called "invariant points," a position at which the solution will tend to stay as long as these solids are present around the solution.

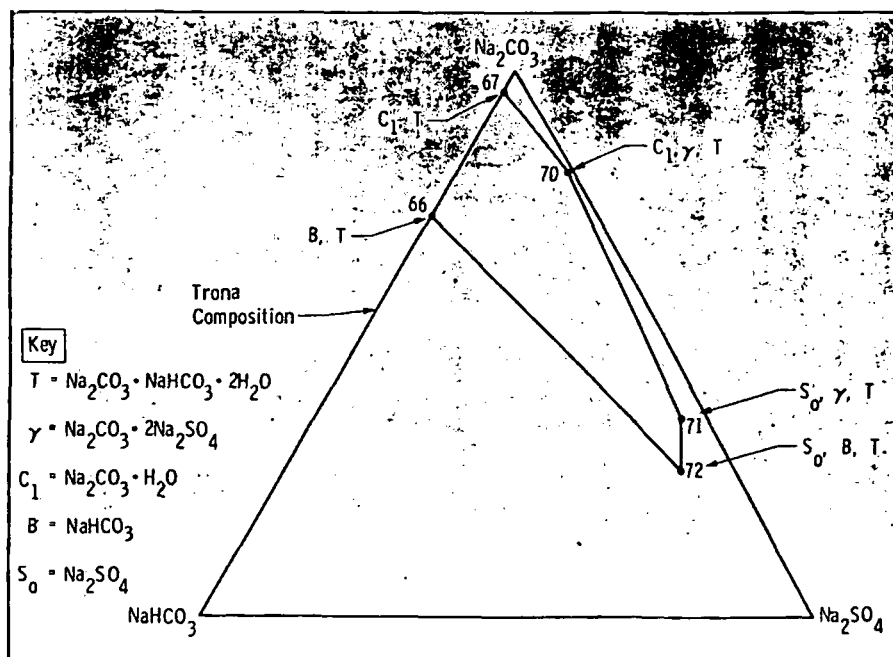
Note in the accompanying table that whenever chloride occurs, it depressed carbonate solubility. Effects of the chloride ion are still significant in the S-1 and S-2 of the lower salt layer, even though sodium chloride is only a small fraction of the solid phase present. However, when the dense sodium sulfate leach solution is injected and displaces the original brine, chloride will no longer be present. This initial flushing away of chloride ions is a crucial function of the sulfate solution.

In the absence of chloride and with

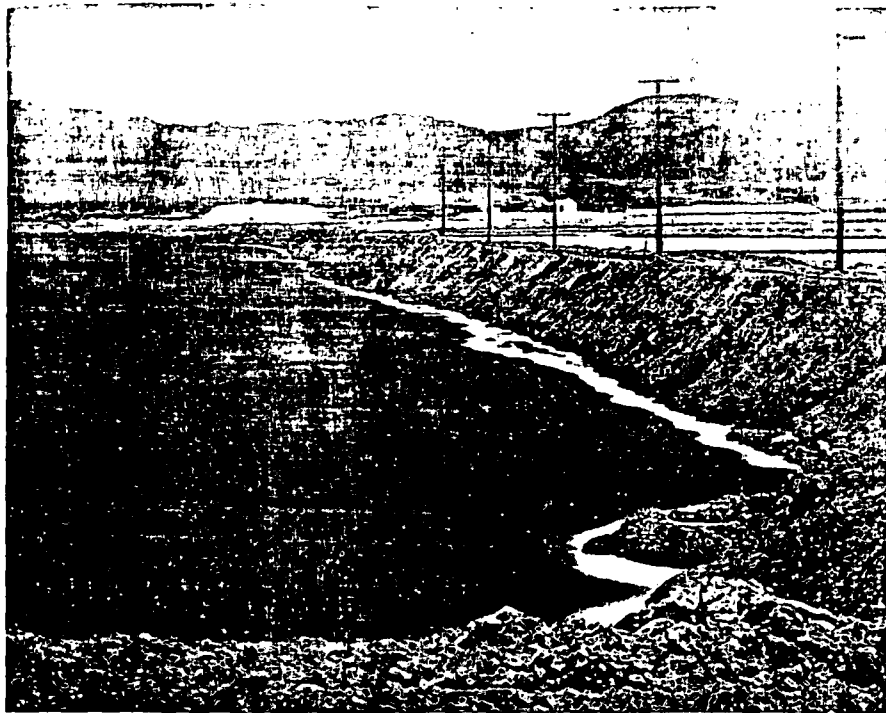
water as an understood member, data can be represented by the three-component system shown in the accompanying figure.

If trona (whose composition is shown by the arrow on the diagram) is placed in distilled water, the incongruent decomposition into bicarbonate and carbonate yields the solution shown at point 66. This point has a much higher carbonate value, and the concept of injecting hot water or carbonate brine was patented (Pike, 1945; Bays, 1961; Caldwell and Frint, 1962); but these methods are not applicable for the unconsolidated sediments at Searles Lake. Because water is less dense than the existing Searles Lake brines, its use would simply cause a convection current disrupting and dispersing desired salines. Carbonate brine would be an expensive injection fluid that may be partially lost underground, and neither water nor carbonate brine leaves any material to prevent strata collapse.

Dissolving trona in the presence of sulfate ion causes the composition to approach point 72 along the line connecting points 66 and 72. If enough burkeite precipitates, however, point 71 is approached, which is undesirable.



The above illustration depicts the solution composition (excluding water) when in equilibrium with the indicated solids at 45°C.



ble because carbonate is precipitated as part of the burkeite and may not be recoverable.

Calculations based on available phase data show that increasing the temperature causes the phase equilibrium and thus carbonate yield to shift in favor of a greater percentage of carbonate and bicarbonate in solution. Selecting the optimum operating temperature will depend on the trade-off between cost of additional heat to the injection brine versus cost decreases of processing a richer carbonate brine.

Another uncertainty concerns yields at 60°C and above. The question is whether burkeite or sodium sulfate precipitates at point 71. This is important because burkeite precipitation would decrease the amount of carbonate available for eventual solution. (Conversely, the loss of total recoverable carbonate could be traded for the richer output brine represented by point 71. Also, burkeite precipitation would contribute to volume maintenance.)

Volume Maintenance

Preliminary calculations indicate that strata volume can be kept close

enough to the original level to maintain strata integrity. This would occur from sodium bicarbonate and sulfate precipitation. Also, below about 33°C, sodium sulfate undergoes a phase change to the decahydrate, Glauber's salt. This salt would occupy more space than replaced trona.

Case II, shown in the accompanying table, is expected to be enough to maintain integrity, and some partial occurrence of Case III would give added assurance.

Conclusions

The phase relationship analyses and experiments performed at the Jet Propulsion Laboratory support the feasibility of an enhanced solution mining operation. Results show that by using a sulfate input brine at 45°C, the output brine would consist of about 13% total soda ash (14% at 60°C), and precipitates left in the cavity could be enough to support the structure.

However, additional information is needed before any attempts are made to use the method. For example, phase relationships for salts at Searles Lake must be more clearly delineated for temperatures above 45°C in order

Solar evaporation ponds have been used for concentrating brine at Searles Lake since 1968. The ponds have been highly successful because of the large land area available and the easily accessible impervious muds in the area. Solar evaporation ponds now occupy about 4.2 km².

to answer questions concerning dissolution levels of carbonate, precipitation levels of Glauber's salt, and possible precipitation of burkeite (which would decrease the amount of sodium carbonate available for solution).

Work is needed on rapid identification of various minerals and their phases, which are important in delineating these phase relationships. In addition, dynamic flow experiments are needed to model brine flow and carbonate exit yields prior to field tests. These flow experiments could also be expected to help predict answers to strata-collapse problems. Researchers say that these efforts, if confirming earlier work, could lead to a pilot-scale production unit at Searles Lake. □

References

- Bays, C. A., 1961. Solution Mining of Trona, US Patent 2 979 317.
- Caldwell, N. A. and Frint, W. R., 1962. Method of Recovering Sodium Values by Solution Mining of Trona, US Patent 3 050 290.
- Giulianelli, J. L., Carpenter, S., Dowler, W. L., and Carlson, R. V., 1980. Solution Mining of Searles Lake Evaporites Using Solar Ponds, Jet Propulsion Laboratory, Internal Document 5105-58, (in press).
- Jayadev, T. S. and Edesess, M., 1980. Solar Ponds, SERI/TR-731-587, Solar Energy Research Institute, Golden, Colorado, April.
- Makarov, S. Z. and Sedelnikov, G. S., 1940. Izv. Akad. Nauk. SSR, Ser. Khim, pp. 835-863.
- Ormat Turbines, Ltd., 1980. A Study of the Feasibility of a Solar Salt Pond Generating Facility in the State of California, USA, prepared for the Southern California Edison Co., April.
- Pike, R. D., 1945. Solution Mining of Trona. US Patent 2 388 009.
- Sedelnikov, G. S., 1945. Zh. Prikl. Khim., Vol. 18, pp. 430-438.
- Smith, G. I., 1962. Subsurface Stratigraphy and Geochemistry of Late Quaternary Deposits, Searles Lake, California—A Summary, in Geol. Surv. Res., 1952, US Geol. Surv. Prof. Paper 450, pp. C-65—C-69.
- Smith, G. I., 1979. Subsurface Stratigraphy and Geochemistry of Late Quaternary Evaporites, Searles Lake, California, US Geol. Surv. prof. paper 1043.
- Teeple, J. E., 1929. The Industrial Development of Searles Lake Brines with Equilibrium Data, Amer. Chem. Soc., Mon. Ser., No. 49.

Case Examples

Case	Temperature (°C)	Solids	Net Percent of Original Volume
I. Water leach only	40	NaHCO ₃	22
II. Na ₂ SO ₄ brine leach	40	NaHCO ₃ + Na ₂ SO ₄	63
III. Na ₂ SO ₄ phase change*	22	NaHCO ₃ + Na ₂ SO ₄ + Na ₂ SO ₄ · 10H ₂ O	>175

*As the temperature is lowered, some amount of sulfate decahydrate phase change occurs plus possible additional precipitation of sodium bicarbonate and carbonate.

Conversions

Convert From	To	Divide By
m	ft	0.3048
km ²	sq mi	2.590
m ³	gallons	0.003 78
°C	°F	°C = (°F - 32)/1.8*

Prefixes: h(hecto) 10²; k(kilo) 10³; M(mega) 10⁶; G(giga) 10⁹

* Formula only

J. E. Dutrizac, Ph.D. and R. J. C. MacDonald, B.Sc.

Extraction Metallurgy Division, Department of Energy, Mines and Resources, Ottawa, Canada

SUBJ
MNG
FILM

FERRIC ION AS A LEACHING MEDIUM

UNIVERSITY OF UTAH
RESEARCH INSTITUTE
EARTH SCIENCE LAB.

SYNOPSIS

The purpose of this paper is to review the leaching of base metal sulphides and of uranium oxides by acidic ferric ion media. A description is also given of the preparation, regeneration, and properties of such leaching media. From the discussion of the kinetics of reaction of various minerals with ferric ion, it emerges that, for many minerals, the reaction rates are sufficiently rapid to be of commercial interest for recovering the sought-after metal. A brief discussion of actual and proposed commercial processes using ferric ion leaching is also given.

INTRODUCTION

Hydrometallurgical processes are playing an increasingly important role in the extractive metallurgy of both the common and the rare metals. There are several reasons for this upsurge of interest in process hydrometallurgy, of which the most commonly cited is, perhaps, the comparative absence of pollution, especially air pollution. Other stated reasons include: the necessity to process low-grade ores that cannot be economically upgraded by conventional milling, concentrating, and smelting; the desire of relatively small mines to be independent of large smelters with their associated smelter charges; the possibility of lower capital costs of plants based on aqueous metallurgy; the rising costs of certain types of fuel; and the ease with which hydrometallurgical operations can be instrumented and controlled. In certain areas, hydrometallurgical processes appear to offer the best approach from both the technical and the economic points of view. In other operations, hydro- and pyrometallurgical processes have been wisely and efficiently combined to utilize the best aspects of each technique.

Hydrometallurgy can be conveniently divided into three broad areas: namely, the dissolution of the desired element into solution, the purification of the resulting solution, and, finally, the recovery of the desired metal, often in elemental form, from the purified leach liquor. In leaching, the sought-after element is usually extracted into solution, although in some instances the impurities are dissolved thereby leaving the valuable element in

the leach residue. Leachable materials include elements, oxides, silicates, and, especially, sulphides. The dissolution can be effected under oxidizing, neutral, or reducing conditions. The apparatus used to impose different temperature and pressure regimes is highly developed and also highly diversified. The present review will be largely confined to the leaching aspect, although brief mention of the purification and regeneration of the ferric ion leaching solutions will also be made. The review will be limited to leaching under the oxidizing conditions that are imposed by the presence of ferric ion in the leaching solutions at ambient pressure. In general, this area is limited to the leaching of the sulphide minerals although the dissolution of uranium oxide-type ores is very similar and will also be included.

Forward and Warren¹ reviewed the extraction of metals from sulphide ores by hydrometallurgical processes and discussed the feasibility of a large number of possible lixiviants, including ferric ion. These workers felt that ferric ion leaching had limited applicability in the hydrometallurgical processing of sulphide ores. Woodcock² also reviewed the leaching of sulphide minerals by a variety of leaching media and observed that ferric ion was a more effective oxidizing agent than oxygen gas, but that the ferric ion leaching medium had to be maintained strongly acidic to keep the iron in solution. He noted that the same mineral from different locations dissolved at different rates: these differences were attributed to defects in the sulphide lattice or to the electrochemical effects produced by relatively minor amounts of second sulphide phases co-existing with the principal mineral. Wadsworth³ recently summarized the experimental work that illustrated the importance of electrochemical processes operative during leaching operations. He also reviewed, in general terms, the leaching of sulphide minerals, especially the copper sulphides. Recently Burkin⁴ and Monhemius⁵ have discussed some advances in the leaching of sulphides; these works both provide excellent summaries of progress in ferric ion leaching.

J. E. Dutrizac obtained his B.A.Sc. at the University of Toronto in 1963 and his Ph.D. from the same institution in 1967. He spent one year at the Noranda Research Centre before joining the Mines Branch where he has since been employed as a research scientist. He is presently engaged in investigating the dissolution of sulphide minerals and in studying the reactions between metals and sulphur and selenium vapours.

R. J. C. MacDonald obtained his B.Sc. at St. Francis Xavier University, Nova Scotia, Canada, in 1956. He worked with Union Carbide Corporation in the United States for three years before returning to Canada to work for Atlas Steels. During his six years with Atlas Steels his interests centred on the development of zirconium alloys for nuclear reactors. Since 1967 he has been employed at the Mines Branch doing research on automated chemical analysis and chemical metallurgy.

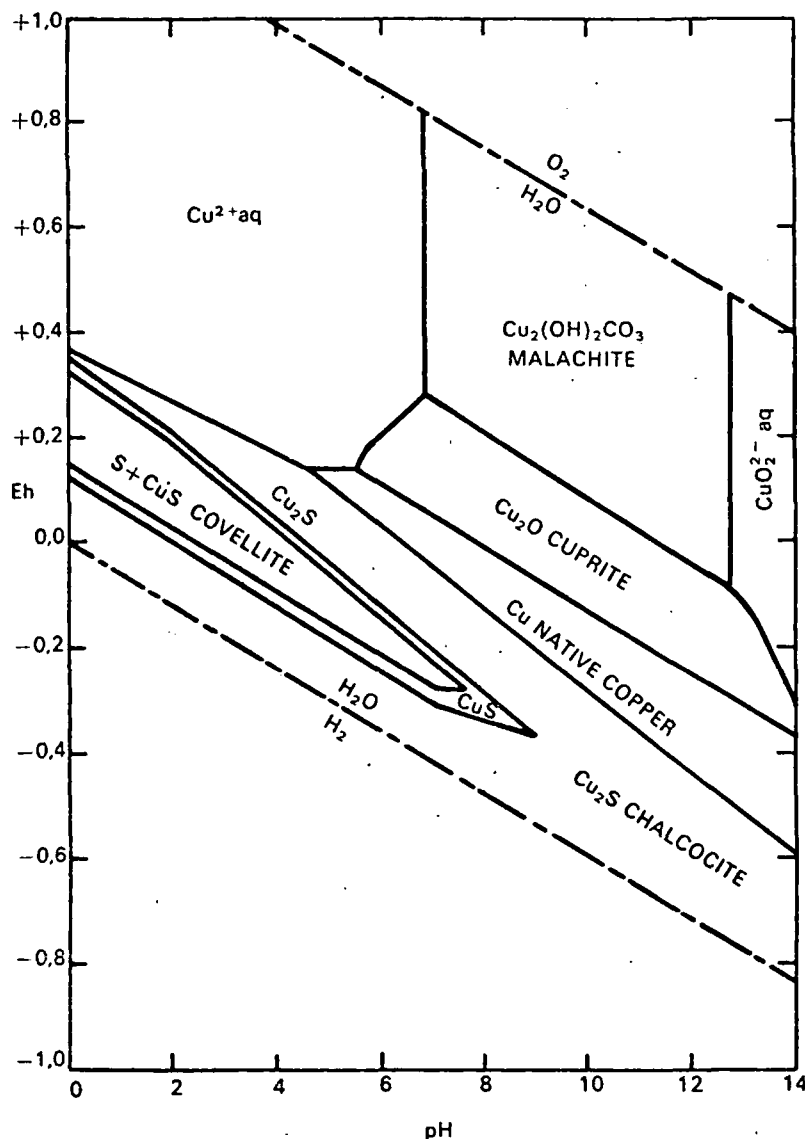


FIGURE 1 Eh-pH diagram for the Cu-H₂O-O₂-S-CO₂ system at 25°C and 1 atm total pressure. Concentration of dissolved species is 10⁻⁶; Pco₂ is 10⁻³, 5 - atm and total dissolved sulphur species is 10⁻¹ M. (From Ref. 6)

GENERAL ASPECTS OF FERRIC ION LEACHING

Although most base metal oxides are readily soluble in mineral acids, the corresponding sulphides require the presence of an oxidizing agent to effect their dissolution. A similar situation exists for the relatively abundant tetravalent uranium oxides that must be oxidized to the hexavalent state before they become acid soluble. Figure 1 shows an Eh-pH diagram at 25°C, which illustrates the need for oxidizing conditions to dissolve the simple copper sulphides covellite (CuS) and chalcocite (Cu₂S); this diagram is taken from the text by Garrels and Christ⁶. In acid media, both CuS and Cu₂S are stable under neutral or slightly oxidizing conditions. At low pH values, oxidizing potentials between 0,2 and 0,4 volts are required to convert the copper sulphides into a sulphur species and soluble copper. In neutral or basic solutions, insoluble oxide-type products are formed. Although the Eh-pH diagram of each sulphide assemblage is unique, it can be generally stated that most base

metal sulphides require a fairly strong oxidizing potential to effect their dissolution in acidic media.

Figure 2 shows the Eh-pH diagram for sulphur at 25°C. In acid solutions, elemental sulphur is stable under neutral or very slightly oxidizing conditions. For Eh values greater than about +0,3 V, elemental sulphur becomes unstable with respect to bisulphate or sulphate formation, depending on the pH of the solution. It might be expected from purely thermodynamic considerations that when a base metal sulphide is oxidized in acidic media, only soluble metal ions and bisulphate or sulphate ions would be obtained.

Figure 3 shows the Eh-pH diagram for the Fe-H₂O-CO₂ system at 25°C illustrating the existence fields of the metastable iron hydroxides. For this diagram, the total dissolved carbonate species is 10⁻² M. This diagram illustrates the well-known fact that the pH stability range of Fe²⁺ ion is much greater than that of the trivalent species;

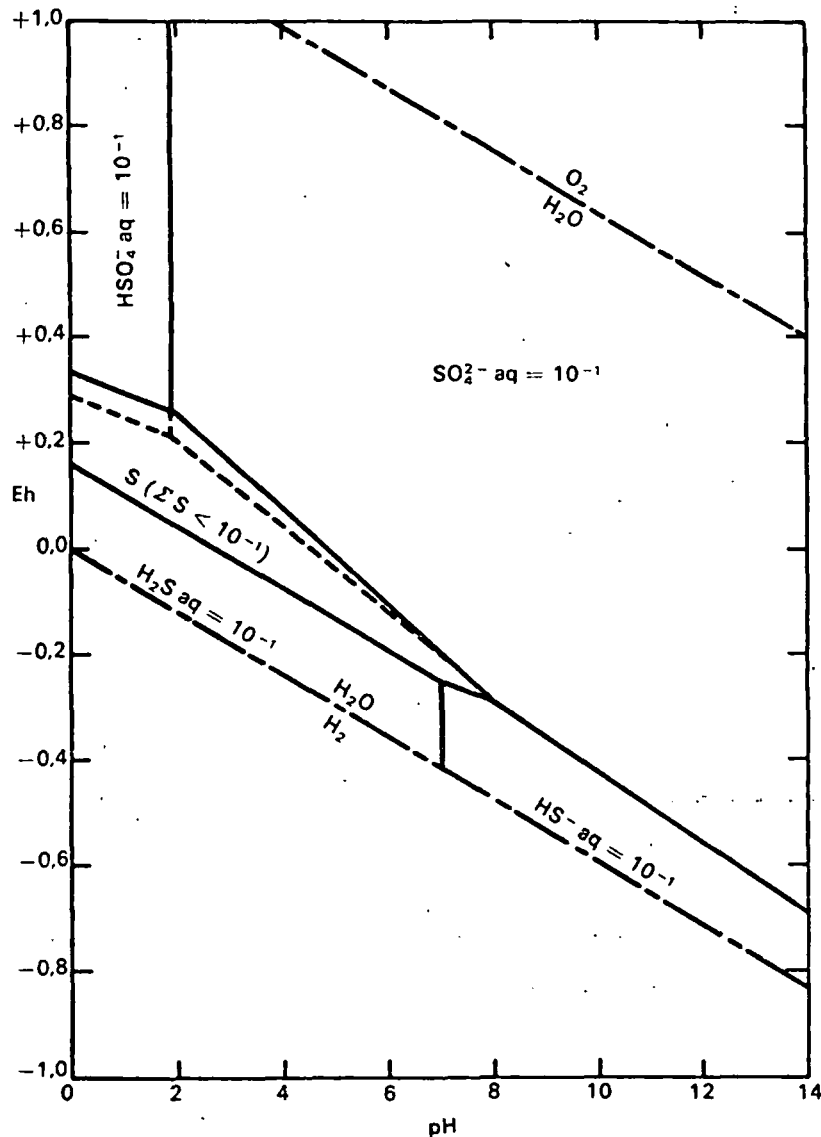


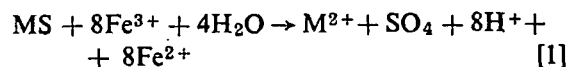
FIGURE 2 Eh-pH diagram for the S-H₂O system at 25°C and 1 atm total pressure. Concentration of dissolved sulphur is 10⁻¹ M. (From Ref. 6)

ferric hydroxide precipitation is a serious problem once the pH value rises above about 3. It is also evident that acid solutions of trivalent iron possess high oxidation potentials.

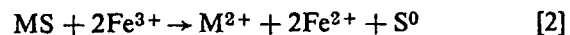
Figure 4 shows the equilibrium iron species existing in a solution containing 0,1 M Fe³⁺ and 0,5 M total sulphate. This diagram was taken from the work of Bhappu *et al*⁷. The rapid decline in the total iron content of the solution at pH > 3 is especially evident in this diagram. Under acidic leaching conditions, the most common ionic species are (FeSO₄)⁺ and (Fe(SO₄)₂)⁻. The simple hydrated ferric ion occurs only at the lowest pH values; the iron hydroxide species become prevalent in the more basic solutions. The ferric species present has been shown to be of great importance in the leaching of uranium oxides; little attempt has been made to correlate the leaching behaviour of sulphides with the ferric species actually present in the solution.

Solutions containing trivalent iron are strong oxidizing agents with associated oxidation poten-

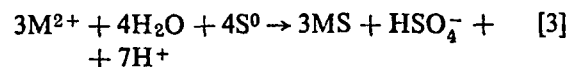
tials of about + 0,8 V. Accordingly, when a metal sulphide (MS) is immersed in an acidified ferric ion solution the following reaction is predicted according to the thermodynamic data:



In acidic ferric media, it is known, however, that the dissolution reaction often produces elemental sulphur and very little sulphate; that is, the actual leaching reaction is better typified by:



Etienne⁸ showed that the sulphur formed according to reaction [2] is not thermodynamically stable, but should be oxidized according to the equation:



Kinetically, however, this reaction does not appear

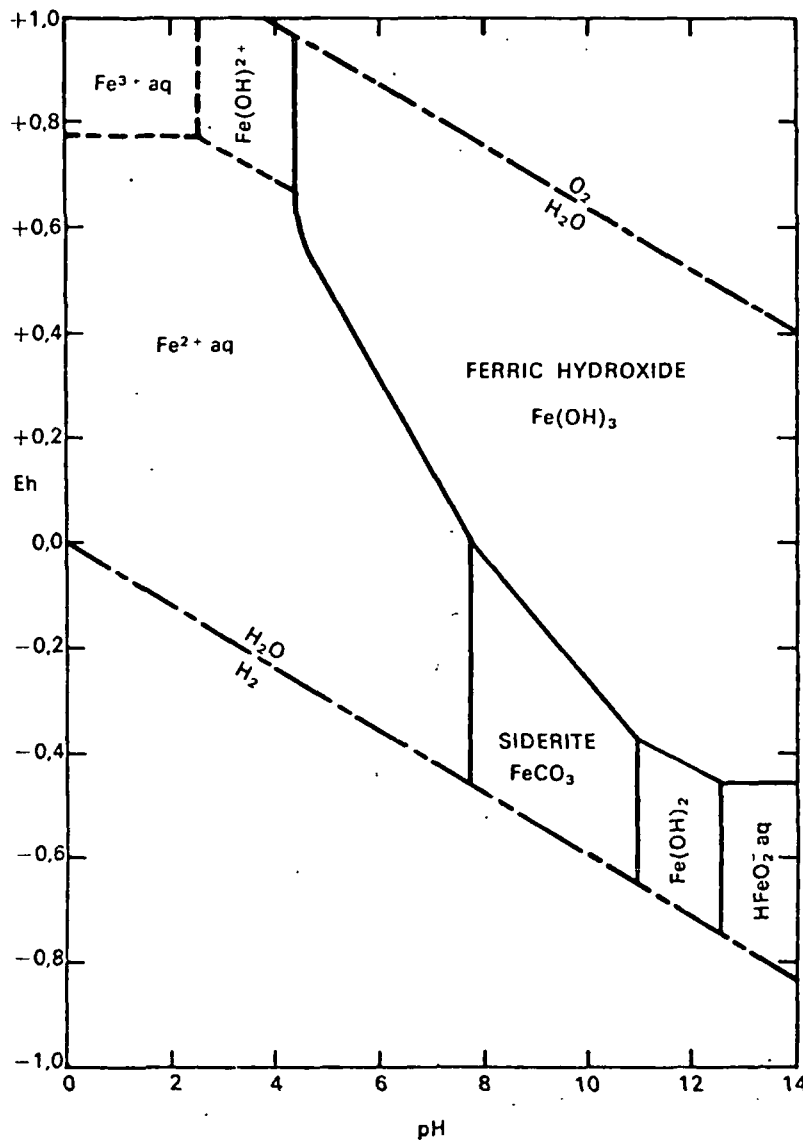


FIGURE 3 Eh-pH diagram showing the relationship among metastable iron hydroxide species and siderite at 25°C and 1 atm total pressure. Concentration of dissolved species 10^{-6} M. (From Ref. 6)

to occur, possibly because of the hydrophobic character of the elemental sulphur. Once elemental sulphur forms, it enjoys an extraordinary stability under a wide range of conditions and at temperatures at least as high as its melting point. According to Etienne, the elemental sulphur is not simply an intermediate product formed on the way to sulphate ion, but it represents a metastable end-product of one separate corrosion reaction. That is, both sulphur and sulphate are produced simultaneously by separate oxidation processes, each with its own temperature dependence and set of important variables. Peters⁹ has summarized many of the important reactions occurring during the dissolution of sulphides in various media, including ferric ion. He gave the following equation for the oxidizing potential of the ferrous/ferric couple at 25°C:

$$E = 0,771 + 0,0591 \log \frac{a_{\text{Fe}^{3+}}}{a_{\text{Fe}^{2+}}} \quad [4]$$

This equation indicates that solutions containing even one part Fe^{3+} per million parts Fe^{2+} have an

oxidizing potential higher than +0,4 V and could, consequently, attack most base metal sulphides.

Both ferric sulphate and ferric chloride are readily soluble in cold water; ferric chloride dissolves to the extent of about 1000 g FeCl_3 per 1000 g H_2O and ferric sulphate dissolves to the extent of about 60 to 70 g/l H_2O . Since the solubilities of the corresponding ferrous salts (which are formed by the reduction of ferric ion during leaching) are also high, concentrated ferric solutions can be utilized for leaching with little danger of salt crystallization occurring. Ferric ion leaching solutions are very sensitive to pH changes and this is a practical difficulty, especially if appreciable temperature changes are encountered during the leaching operations¹. The production of ferrous ion during leaching has also proved troublesome during the metal recovery stage because it is difficult to remove from the leach liquor. Recent advances in liquid-liquid extraction have tended to minimize this problem, especially as concerns copper leach solutions⁵.

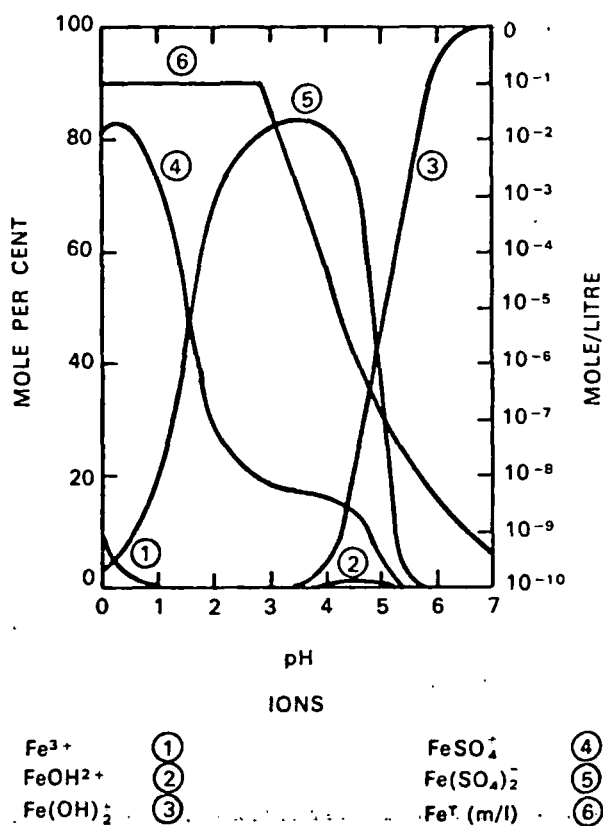


FIGURE 4 Equilibrium iron species existing in a solution containing 0.1 M Fe^{3+} and 0.5 M total sulphate at 25°C. (From Ref. 7)

APPLICATIONS OF FERRIC ION LEACHING

Ferric ion leaching media are currently used, or have been suggested for use, in the following metallurgical processes:

- leaching in stirred or agitated reactors
- *in situ* leaching of low-grade ores
- dump or heap leaching
- in conjunction with bacterial leaching in any of the above processes.

At present, most examples of ferric ion leaching of base metals are in dump or heap leaching, although considerable interest is shown in using ferric ion media for either *in situ* or conventional stirred reactor leaching. The leaching of uranium by acidic ferric ion is currently effected using all four of the processes indicated above.

In certain instances ferric ion leaching has been used effectively in conventional agitated reactors to dissolve the metal values. The range of apparatus available is considerable. Early workers such as Traill^{10,11,12} used concentrated ferric chloride solutions in stirred reactors to dissolve pyrrhotite. The dissolved iron was electrolysed to give iron powders and to regenerate the leaching medium. Zapevalov and Vygoda¹³ dissolved complex Pb-Zn-Fe sulphide mattes in stirred reactors using solutions containing 100 g/l $FeCl_3$ and 100 g/l HCl at 100°C. A 20 to 30 per cent excess of solution completely extracted the metal values in 1 to 2

hours. Tseft *et al*¹⁴ proposed a somewhat similar operation. They advocated two-stage leaching of a complex Pb-Zn-Fe ore by chloride solutions containing 100 g/l Fe^{3+} and 50 g/l Fe^{2+} at 106°C. The ratio of solid to liquid used was 1 to 2.7; over 95 per cent recovery was obtained for each element. A similar technique was recently proposed by Haver and Wong¹⁵ as a pollution-free method of treating chalcopyrite concentrates with ferric chloride solutions in reactor vessels. The recently proposed Cymet Process¹⁵ combines ferric chloride leaching of chalcopyrite concentrates and anodic dissolution of the sulphides. This type of process usually regenerates ferric ion either electrolytically or by chlorine gas and recovers much of the sulphur in the elemental form. Uranium ores are generally digested in hot sulphuric acid containing ferric ion in order to oxidize the uranium to the soluble hexavalent state. Other oxidizing agents are frequently used, but it has been stated¹⁷ that the active oxidizing agent for uranium ores is the ferric ion, the other oxidizers serving only to keep the iron fully oxidized. Although 'ferric ion' leaching of uranium ores in reactor vessels is a commercial reality, there appears to be no instance where rich concentrates or mattes of other metals are leached in stirred reactors by ferric ion. It should be noted, however, that the Cymet Process has generated a great deal of interest and that a 20-t.p.d. demonstration unit will be started in 1973 on leaching chalcopyrite concentrates.

In situ leaching techniques are currently being used to extract both copper and uranium using ferric ion leaching media. In this technique, an orebody is fractured and then leached in place by flooding with leach solution or by percolating the solution through the fractured ore. The great advantage of this method is its simplicity and its very low operating cost; its obvious disadvantage is the long time required to recover the sought-after metals. Fletcher¹⁸ described the development and current practice of *in situ* leaching of copper at the Miami Mine, Arizona, from a block caved mine mineralized with chalcocite, chalcopyrite, and bornite. Excess sulphuric acid must be added to the leach solutions to compensate for that used to dissolve gangue minerals. The solution is sprayed on the rock surfaces and rest periods are employed to induce the removal of dissolved copper from fine cracks and pores. The dissolution of the sulphide minerals was attributed to the direct action of ferric sulphate. MacGregor¹⁹ described the *in situ* leaching of uranium at the Stanrock Mine, Ontario, Canada. A combination of fast high-pressure washing of stopes and the sprinkling of low-grade heaps has enabled this company to produce over 10 000 lb of U_3O_8 per month from worked-out mine areas.

The above examples demonstrate that *in situ* leaching can be, under certain circumstances, an economical alternative to conventional processing. This technique has also been investigated in the Soviet Union²⁰ as an alternative to conventional processing. In America, it has been suggested that nuclear explosions could be used to fracture an

orebody to open it for leaching by acidified ferric sulphate solutions²¹. It was felt that a chalcocite deposit could be leached over the course of a few years, but that chalcopyrite orebodies would require decades for complete dissolution. One of the great problems of *in situ* leaching is to obtain a good air flow into the fractured orebody. This problem would be acute for nuclear-fractured orebodies because it is usually envisioned that only a few drilled holes into the active area be utilized. It has been pointed out²² that two tons of oxygen are needed to oxidize one ton of copper, as chalcopyrite, to soluble sulphates. This weight of oxygen is contained in 230 000 ft³ of air. It would obviously be very difficult to pass such large quantities of air, even assuming complete oxygen utilization, down a relatively small opening and through a fractured ore body. The solubility of oxygen in typical leach liquors is just a few p.p.m. with the result that little oxygen would be delivered into the ore by the leaching medium. It is necessary, then, to find an oxidizing agent that can be pumped to the fractured ore body in a concentrated form, and ferric sulphate-sulphuric acid solutions are generally viewed as the most acceptable leaching medium for this type of operation^{23,24}. Ferric ion concentrations in the range 0,2 to 2 M are usually suggested, together with sufficient sulphuric acid to keep the medium acidic even in the presence of acid-consuming gangue. It is usually anticipated that the ferric ion leaching medium would be regenerated after the desired metal has been recovered.

The most popular example of ferric ion leaching is that of dump or heap leaching. Heap or dump leaching has been used for many years to recover copper from massive chalcopyrite-bearing pyrites at Rio Tinto, Spain. A review of this operation by Taylor and Whelan²⁵ presents an excellent account of the development of this type of operation and also gives some idea of the temperatures encountered during leaching. Temperatures varied between 20 and 70°C; under some conditions actual ignition of the heaps occurred. The elevated temperatures are important since the rate of leaching of chalcopyrite increases markedly with temperature. In modern practice, heap or dump leaching is usually confined to low-grade copper sulphide ores contained in silicate gangue or to mixed oxide-sulphide ores that are not amenable to conventional flotation. Dump leaching is applied to the recovery of metals from the large tonnages of waste rock generated during open-pit mining. For this type of operation, the rock is usually dumped in an unprepared convenient site, although prepared impervious pads have been used as at Butte, Montana, U.S.A. The grade of waste rock encountered during the dump leaching of copper ores assays between 0 and 0,5 per cent Cu depending on the particular operation. An iron sulphate-sulphuric acid solution is sprayed or flooded on the upper surface of the dump and allowed to percolate through it. A variety of reactions occurs in the upper layers of the rock pile including the oxidation of the dissolved iron to the ferric state. The solutions pass through the ore pile and are

collected at the bottom of the dump for processing to recover the valuable metals. Heap leaching is an essentially similar operation except that the ore grades tend to be higher; frequently oxide-sulphide ores are treated and sometimes, as at Rio Tinto, Spain, more care is exercised in the construction of the heaps. Both heap and dump leaching are inherently simple as can be seen from the block diagram presented in Figure 5 for copper heap

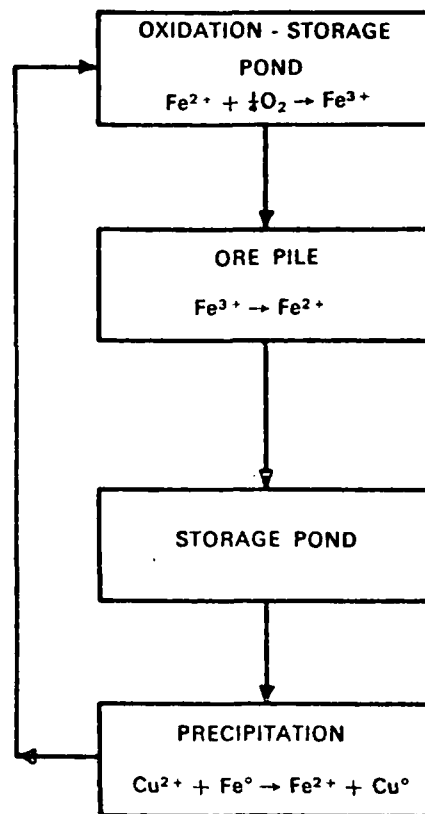


FIGURE 5 Schematic diagram illustrating the dump leaching of copper ores by ferric ion, followed by the cementation of copper on iron.

leaching followed by copper recovery by cementation on scrap iron. In some operations the iron oxidation occurs in the upper reaches of the dump and not in a separate operation. The reactions occurring in the interior of the rock pile itself are complex; the result, however, is the reduction of some or all of the trivalent iron contained in the leaching medium.

Dump leaching is becoming steadily more important and now accounts for about 15 per cent of the total production of primary copper in the U.S.A.⁴. Malouf and Prater²⁶ have described the dump leaching operations at Bingham Canyon, Utah, U.S.A. This is currently the largest single example of dump leaching, processing 250 000 tons per day of waste rock. A survey of copper dump leaching was presented by Woodcock²⁷. Dump and heap leaching as practised in the United States has been the subject of two recent reviews^{28,29} by

the U.S. Bureau of Mines. As might be expected, the reactions occurring during leaching are complex and probably change with geometric position within the dump and with elapsed leaching time at any particular site. Woodcock²⁷ discussed the direct oxygen attack of sulphide minerals, the bacterial attack of these sulphides, and the dissolution by acidified ferric sulphate solutions. It is probable that all three processes are involved in the leaching of actual dumps. Although oxygen supply is not as serious a problem in an exposed dump as it is for the *in situ* leaching of an underground ore body, it is, nonetheless, a major factor in dump leaching. Harris³⁰ has discussed the importance of oxygen supply during dump leaching and has developed a mathematical model to predict oxygen requirements for this process. Ferric sulphate solutions are a convenient method of oxidizing sulphides in the interior of dumps where aeration is difficult.

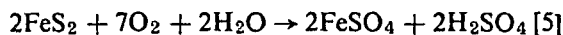
It is now widely recognized that bacteria play an important role in some types of leaching although the exact function of bacteria still remains uncertain, especially under commercial leaching conditions. Some confusion exists concerning the number of bacterial species involved during leaching. Torma³¹ concluded that only two species were active during leaching operations, viz., *Thiobacillus ferrooxidans* and *Thiobacillus thiooxidans*. It was concluded that the reported species *Thiobacillus ferrooxidans*, *Ferrobacillus ferrooxidans*, and *Ferrobacillus sulphooxidans* were identical and should be called *Thiobacillus ferrooxidans*. More recently, Bounds and Colmer³² observed that these three bacteria behaved differently, and these workers concluded that these represented different types of bacteria. Whatever the final number of species may be, these bacteria can assist in the dissolution of various ores. Two general bacterial leaching mechanisms have been postulated: first, the direct bacterial attack of the mineral in the presence of dissolved oxygen, which has been demonstrated for some sulphides such as ZnS and CuS, and, second, the indirect leaching action of ferric ion brought about by bacterial oxidation of dissolved iron in the presence of oxygen. It is probable that both mechanisms are operative during actual leaching operations involving commercial ores.

This review is primarily interested in the role of bacteria in generating ferric sulphate leaching media that can be used for leaching sulphide minerals. Some mention is made of the bacterial leaching of each mineral, however, since this is often an approximate indication of the mineral's reactivity in ferric media. For a description of the bacteria and their role in leaching the reader is referred to the following reviews. Pings³³ described the work up to 1968 on the bacteria, their tolerance to dissolved metals and the metals that have been solubilized by bacterial leaching. Moss and Andersen³⁴ also discussed the bacteria and where they are being used for leaching. These authors described some of the research methods used for investigating bacterial leaching. Fletcher³⁵ discussed the role played by bacteria in percolation

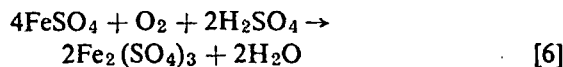
leaching and the possible growth of this technique in view of the continual depletion of high-grade ores. Several commercial operations were described. Ito³⁶ discussed the mechanisms involved during bacterial leaching and the scope of this technique as it is used in Japan. Lastly, Trudinger³⁷ described the role of bacteria in the metallurgical industry in general, and also dealt with the particular problem of bacterial leaching of sulphides. This recent review stated that many bacterial species were active during leaching.

GENERATION OF THE FERRIC ION LEACHING MEDIUM

One great advantage of ferric ion leaching is the ease and variety of methods available for the generation of the lixiviant. Acidic iron sulphate and iron chloride solutions are frequently produced as unwanted by-products of many commercial processes such as during the pickling of iron and steel. The leaching medium could also be prepared by the reaction of waste sulphuric or hydrochloric acids with scrap iron or with iron ores. In certain operations where large tonnages of acid are produced in regions remote from conventional sources of consumption, this method could be used to dispose of the acid and, at the same time, prepare a leaching medium suitable for the recovery of valuable metals. Johnson³⁸ has described a process whereby acidified ferric sulphate solutions suitable for chemical mining could be prepared by the oxidation of pyrite at high temperatures and pressures. At 140°C, pyrite reacts quickly with air to give ferrous sulphate and sulphuric acid:



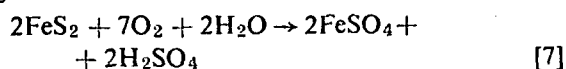
Ferric sulphate is subsequently produced by further air oxidation:



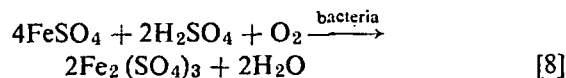
The ferric sulphate could be hydrolysed to iron oxide if insufficient acid were present. It was possible to prepare solutions containing 12% H₂SO₄ and/or 6 per cent ferric ion using this technique. Such solutions would be suitable for many types of leaching operation.

An iron sulphate-sulphuric acid leaching medium can also be prepared by the bacterial oxidation of pyrite, either *in situ* or in separate aerated batch reactors. Solutions prepared *in situ* tend to be of fairly low strength (pH ~2, Fe_{tot} < 10 g/l), but those produced in batch reactors can be very concentrated. Early work by Sutton and Corrick^{39,40,41} on the bacterial oxidation of pyrite showed that solutions containing about 20 g/l iron at a pH value of ~1.6 could be produced by the bacterial leaching of pyrite. About 70 days of aeration were required to produce such solutions. Acid-consuming gangue in the pyrite retarded the bacterial oxidation. Sutton and Corrick believed that the pyrite was attacked only by an indirect ferric ion leaching of the mineral. According to their theory,

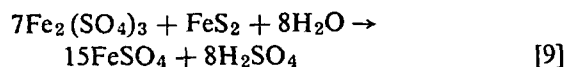
the oxidation was initiated by the air oxidation of pyrite:



The bacteria then oxidized the ferrous ion:

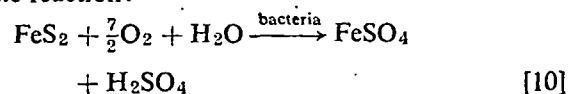


The ferric sulphate subsequently attacked the pyrite to form sulphuric acid and more ferrous sulphate, which was then oxidized by reaction [8].



These workers noted that the acidic ferric sulphate medium produced by bacterial action on pyrite could leach other base metal sulphides.

Pyrite is known to dissolve in ferric sulphate media⁴² and the indirect mechanism postulated by Corrick and Sutton must always occur to some extent. Several workers, including Malouf and Prater⁴³ and Ivanov^{44,45}, have emphasized the importance of the indirect leaching mechanism. The latter worker felt the bacteria removed a protective sulphur layer from the pyrite and thereby facilitated the ferric sulphate dissolution of this mineral. It now appears fairly well established, however, that bacteria can directly attack pyrite to form an acidic ferric sulphate solution that is suitable for leaching. Early work by Bryner *et al*^{46,47} showed that bacteria oxidized pyrite at least 20 times faster than control experiments lacking bacteria. The activity of the bacteria in oxidizing pyrite increased with increasing temperatures and also increased in the absence of light. The pH of the leaching solutions decreased as free sulphuric acid was produced by the chemical reaction. It was believed that the bacteria derived their energy for growth from the oxidation of sulphide ion to sulphate. It was stated that the organisms could attack pyrite in the absence of iron although it should be remarked that soluble iron is produced during the attack of the pyrite, which dissolves according to the reaction:



Lorenz and Tarpley⁴⁸ and Duncan, Landesman, and Walden⁴⁹ compared the rates of dissolution of pyrite in ferric sulphate solutions to those obtained by bacterial leaching and concluded that bacterial leaching was the more important factor in the production of acidified ferric sulphate solutions from pyrite. Bryner, Walker, and Palmer⁵⁰ showed that over 80 per cent pyrite dissolution could occur after 76 days of leaching at 35°C. The leaching rate increased with increasing temperatures to a rate maximum at 35°C and thereafter declined. The presence of bacteria accelerated the dissolution of pyrite even at temperatures as high as 55°C.

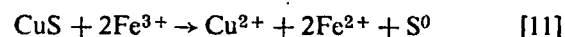
Napier, Wood, and Chambers⁵¹ described the

production of acidified ferric sulphate solutions by the bacterial leaching of pyrite. Such solutions were suitable for the leaching of uranium from uraninite or brannerite ores. Over 30 per cent of the pyrite could be dissolved in 30 weeks giving solutions containing about 1 g Fe³⁺/l at a pH value of 1 to 2; these solutions were suitable for uranium leaching. These workers found that aeration and temperature were important variables in the rate of solution generation. It was also observed that a large pyrite area enhanced the rate of leaching. Rather than generating the lixiviant in a separate step, it was proposed to mix pyrite with the uranium ores and to generate the leaching medium *in situ*.

THE DISSOLUTION OF COPPER MINERALS

Covellite

The first systematic study of the dissolution of covellite in acidic-ferric sulphate media was done by Sullivan⁵². He found this sulphide to dissolve according to the equation:



The rate increased rapidly with increasing temperature but was insensitive to the ferric concentration for concentrations above 1 g/l Fe³⁺. The rate of covellite dissolution was independent of the acid concentration and, furthermore, sulphuric acid, in combination with excess dissolved atmospheric oxygen, dissolved copper at about half the rate of the acidic ferric sulphate solutions. Sullivan found that, at 35°C, the acidic ferric sulphate medium was more effective than acidic ferric chloride solutions. At 98°C, however, the two rates were virtually the same. This latter observation was confirmed by Brown⁵³ and by Brown and Sullivan⁵⁴. Sullivan⁵⁵ also observed widely differing dissolution rates for covellites from different sources or for synthetic CuS. This variation was attributed to widely varying amounts of impurities that are commonly associated with natural covellite.

Thomas and Ingraham⁵⁶ leached discs of synthetic sintered CuS in acidified ferric sulphate solutions over the temperature range 25 to 80°C. Although their reaction rates appear to be much faster than those reported by Sullivan⁵², these workers found that synthetic CuS dissolved according to the same equation that Sullivan reported for covellite dissolution (Equation [11]). They found that only 4 per cent of the leached sulphur reported as sulphate; the remainder was in the elemental form. Their dissolution curves showed that the rate increased steadily during the initial parts of the reaction, but then became linear. Over the temperature range investigated two rate-controlling steps were identified. Below 60°C the rate was controlled by a chemical reaction on the surface of the sulphide; the associated apparent activation energy was 22 kcal/mol. At higher temperatures, the rate was solution-transport controlled with an apparent activation energy of 8 kcal/mol. The dual



FIGURE 6 Cross-section of a partly leached specimen of natural covellite (Colorado, U.S.A.) illustrating the uneven nature of the dissolution. Sample leached for 44 hours at 95°C by 0,1 M Fe³⁺ and 0,1 M H₂SO₄ solution.

(From Ref. 60)

mechanism of covellite dissolution has not been confirmed by other workers. Thomas and Ingraham found that the leaching rate was directly dependent on the ferric concentration below about 0,005 M Fe³⁺ but was insensitive to higher concentrations of ferric sulphate.

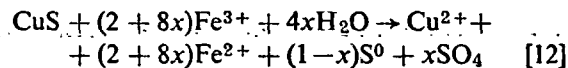
King⁵⁷ investigated the dissolution of the CuS formed as an intermediate product during chalcocite leaching in acidified ferric chloride media. There was evidence that the CuS was non-stoichiometric, and was, therefore, different from the materials used by most other workers. The CuS dissolution rate increased with increasing ferric ion concentrations in the range 0,25 to 1,0 M Fe³⁺. The apparent activation energy for the rate-controlling step was 25 kcal/mol. The rate-controlling process was felt to be a chemical reaction occurring on the surface of the CuS.

Lowe⁵⁸ studied the dissolution of mounted specimens of covellite in acidified ferric sulphate solutions over the temperature interval 40 to 70°C. He reported linear kinetics together with an apparent activation energy of 14 kcal/mol. The dissolution rate was found to be independent of the H₂SO₄ concentration, but increased slightly with increasing ferric sulphate concentrations between 0,006 M and 0,212 M Fe₂(SO₄)₃. The rate-controlling process was thought to be a chemisorption process occurring on the surface of the covellite. The overall dissolution reaction proposed by Lowe was similar to that advanced by previous workers^{52,56}.

Mulak⁵⁹ investigated the dissolution of dispersed synthetic CuS in acidified ferric sulphate solutions over the temperature range 30 to 90°C. Linear kinetics were observed and the rate was independent of the solution agitation speed. An apparent activation energy of 20 kcal/mol was obtained and this, together with the linear kinetics, led Mulak to conclude that the rate was controlled by a slow chemical reaction step at the surface of the CuS.

The rate was independent of the solution pH for values less than 3,0 and was also independent of the ferric ion concentration for concentrations greater than 0,005 M Fe³⁺. The rate depended directly on the ferric concentration for concentrations less than 0,005 M Fe³⁺.

Recently Dutrizac and MacDonald⁶⁰ studied the dissolution of pure synthetic CuS discs and high-grade natural covellite in acidified ferric sulphate solutions in the temperature range 15 to 95°C. For both natural and synthetic materials, the rates were relatively slow and increased during the initial parts of the dissolution, but eventually became linear. The activation energy, as determined from the initial dissolution rates, was 18 kcal/mol. Microscopic examination of partly leached CuS revealed that the attack occurred preferentially in certain areas. Figure 6 shows a cross-section of a partially leached piece of massive natural covellite from Colorado, U.S.A. The grey phase at the bottom is mounting resin, the top grey areas are large covellite crystals, and the black is the sulphur reaction product. This product always contains some retained but finely-divided CuS. The sulphur layer formed a thin coating across the leached surface, although most of this element appeared to be concentrated in a few patches. It was felt that the progressive development of these pits was responsible for the gradual rate increase observed during the initial stage of leaching. The dissolution reaction was described by the equation:



The values of x were such that from 0 to 10 per cent of the leached sulphur reported in the sulphate form. The rate of copper dissolution from the synthetic CuS decreased sharply with increasing ferrous sulphate concentrations in the initial

leaching medium. The rate depended directly on the ferric concentration for initial concentrations below 0,005 M Fe^{3+} , but was insensitive to increases in the ferric strength beyond this level. The natural covellite was found to dissolve at the same rate and with approximately the same temperature dependence as the synthetic CuS . The rate-controlling step for the dissolution of both synthetic and natural CuS was believed to be a chemical reaction on the surface of the CuS . Although the sample pitting suggests galvanic corrosion, it is not evident that the actual rate of electron transfer is rate controlling for the dissolution of this material.

Table 1 summarizes the work obtained for the ferric sulphate attack of both synthetic and natural CuS . As far as is known, these researches were done on material in the absence of active bacteria. There appears to be general agreement that the rate is chemically controlled with a high associated activation energy. Ferric ion concentration exerts a pronounced effect on the rate only for concentrations less than about 0,005 M Fe^{3+} .

Several workers have investigated the oxidation of CuS by bacterial action. Bryner *et al*⁴⁶ studied the dissolution of museum-grade natural covellite by bacteria; these workers did not add iron deliberately to their leaching solution. Their

bacteria were, however, grown on an iron medium and their covellite probably contained ~1 per cent iron, although no analysis of this material was given. In any event there was probably some iron in their leach solutions. It appears that very low iron contents are able to dissolve covellite^{56,60} and some of the reported dissolution may well have been due to direct ferric attack of this mineral. Bryner *et al* observed that 29 per cent of the copper in the covellite had been dissolved after 73 days. The covellite was found to dissolve more rapidly than chalcocite. This is the opposite to that observed for the indirect ferric attack and may indicate that direct bacterial dissolution of the CuS was the predominant reaction operating during these experiments. Bryner *et al* believed that the bacteria were directly attacking the CuS by oxidizing the sulphide sulphur to sulphate. Razzell and Trussell⁶¹ and Razzell⁶² were able to dissolve 80 per cent of the copper from a covellite ore after six months leaching by bacteria. Since their final solutions assayed only 12 p.p.m. iron, it must be concluded that their work indicated direct bacterial attack of this sulphide.

Sutton and Corrick^{39,40,41} concluded that direct bacteria attack of CuS was not possible⁴⁰ and, in fact, the presence of the bacteria actually suppressed the normal air oxidation of this mineral. They

TABLE 1

LEACHING KINETICS OBSERVED FOR CuS DISSOLUTION IN ACIDIFIED FERRIC SULPHATE SOLUTIONS

Material	Fe^{3+} dependence	Activation energy (kcal/mol)	Temperature (°C)	Rate-controlling process	Ref.
Natural ores of different purities	No effect for $Fe^{3+} > 1$ g/l	high	35 - 95	—	52
Synthetic	No effect for $Fe^{3+} > 0,005$ M Fe^{3+} ; directly proportional to Fe^{3+} conc. at lower levels	22	T < 60	Essentially linear kinetics (surface reaction)	56
		8	60 - 80	Solution transport with linear kinetics	56
Intermediate product from the leaching of pure synthetic Cu_2S	Increased with increasing Fe^{3+} conc. in the range 0,25 - 1,0 M Fe^{3+}	25	20 - 80	Chemically controlled	57
Mounted natural crystals	Increased gradually between 0,0064 M and 0,212 M $Fe_2(SO_4)_3$	14	40 - 70	Chemisorption process with linear kinetics	58
Synthetic powders	$Fe^{3+} > 0,005$ M, no effect $Fe^{3+} < 0,005$ M, rate proportional to ferric strength	20	30 - 90	Slow chemical step with linear kinetics	59
Pure synthetic, natural crystals	No effect for $Fe^{3+} > 0,005$ M Fe^{3+} ; directly proportional to Fe^{3+} conc. at lower levels	18	15 - 95	Rates increased slightly with time; kinetics essentially linear; chemically controlled	60

further concluded⁴¹ that dissolved copper suppressed the bacterial oxidation of pyrite, which produced the acidic ferric sulphate environment. These workers believed the bacteria attacked iron sulphide minerals to produce an acidic ferric sulphate leaching medium that then attacked the covellite (CuS). They observed that the bacterially generated acidic ferric sulphate leaching medium dissolved 56 per cent of the copper from a covellite ore in 56 days. De Cuyper⁶³ dissolved 80 per cent of the copper in CuS in 30 weeks using a bacterial solution containing 113 mg/l Fe; only 40 per cent of the copper was dissolved by a solution containing 9 mg/l Fe. He believed that dissolved iron, even in low concentrations, was necessary for the bacteria to dissolve CuS. Ivanov⁴⁴ studied the dissolution of synthetic covellite by bacterial solutions. The dissolution reaction was attributed to the ferric sulphate, which was maintained at a high oxygen potential by the iron oxidizing bacteria. The bacteria also removed the partly-protective sulphur layer from the CuS, thereby permitting the ferric ion easy access to the sulphide.

Duncan and Trussell⁶⁴ observed that 50 per cent of the copper in a covellite ore (97,6% CuS) could be leached by *Thiobacillus ferrooxidans* in 76 days. They found that CuS was attacked slowly relative to either chalcocite or bornite. This observation is contrary to that noted by Bryner *et al*⁴⁶ but is consistent with the results obtained for straight ferric sulphate attack. Duncan assumed that the addition of ferric sulphate was not necessary for the bacterial oxidation but that its presence would be useful as a pH buffer. Bryner, Walker, and Palmer⁵⁰ studied the dissolution of CuS in bacterial solutions with and without added ferric sulphate. Although bacteria were able to attack the CuS

directly, the presence of dissolved iron accelerated this dissolution by 3 to 4 times. They reported an optimum Fe³⁺ content of 0,5 g/l for bacterial dissolution; this concentration of iron would provide an adequate concentration for direct ferric sulphate leaching (Table 1). These workers observed that about 40 per cent of the copper was dissolved after 90 days in the bacterial solution containing 0,5 g/l Fe³⁺. Recently Corrans, Harris, and Ralph⁶⁵ investigated the dissolution of synthetic CuS in acidified ferric sulphate solutions and concluded that direct bacterial attack was the more important dissolution mechanism for this particular sulphide. They attributed this to the continuous removal of the sulphur layer on the covellite, which, they felt, was protective in this medium. The inhibiting effect of the sulphur layer on partially leached covellite has also been reported by Bauer, Gibbs, and Wadsworth⁶⁶ for leaching with oxygenated sulphuric acid solutions. Fox⁶⁷ investigated the dissolution of synthetic CuS in solutions containing bacteria and concluded that the dissolution reaction was controlled by direct bacterial attack of the sulphide ion in the CuS lattice. It was also noted that 68 mg/l Fe in the leaching solution accelerated the covellite dissolution at a pH value of 3,5; this was attributed to a pH effect on the surface of the sulphide.

Chalcocite

Chalcocite (Cu₂S) is, after chalcopyrite, the most common copper sulphide and, understandably, its leaching behaviour has been thoroughly studied. Sullivan^{55,68} investigated the dissolution of chalcocite ores containing 5 to 10 per cent Fe over the temperature range 23 to 95°C. He showed that

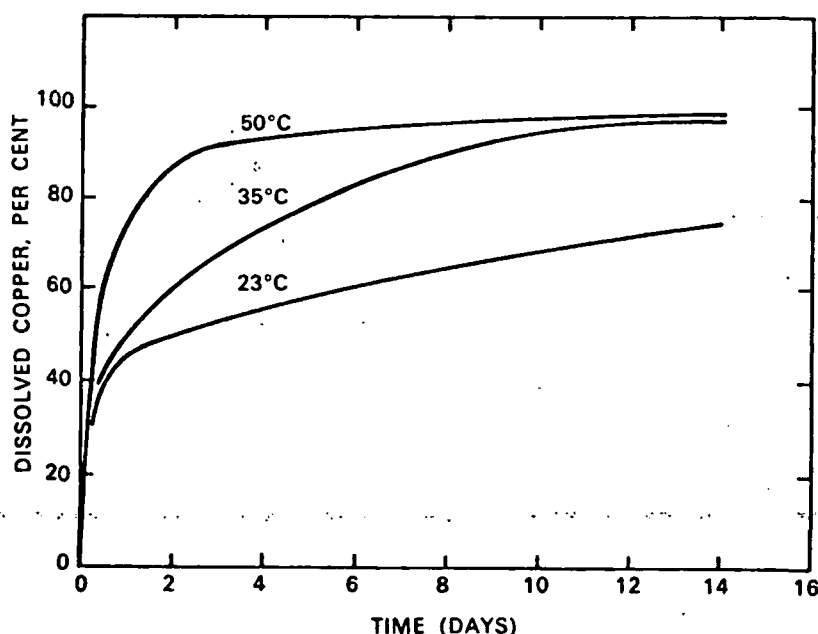
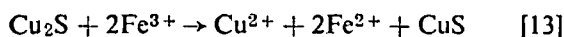


FIGURE 7 The leaching of chalcocite (Cu₂S) ore by ferric ion. (From Ref. 55)

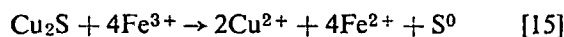
Cu₂S dissolves in two steps according to the following reactions:



The CuS formed in equation [13] was noted to be different from the mineral covellite:



The total reaction is the sum of the two:



Sullivan noted that no free sulphur was formed until about 50 per cent of the copper had been dissolved; this indicates that reaction [13] is rapid when compared to the rate of CuS dissolution. About half of the copper in Cu₂S is leached quickly, but the complete dissolution requires much longer times as can be seen in Figure 7. The initial dissolution rate is weakly affected by temperature and this suggests mass-transport control. The later stages are more strongly temperature dependent. That the initial stage of dissolution is mass-transfer controlled was strengthened by the observation that the rate was almost independent of particle size. That is, the hydrodynamic area and not the true surface area controlled the reaction. Sullivan also noted the rate to be independent of pH and of the concentration of Cu²⁺ or Fe²⁺ in the leaching solution, provided these concentrations were small. The rate was independent of the ferric concentration. At room temperature, ferric chloride and ferric sulphate solutions were equally effective in dissolving this mineral but at 95°C, the chloride media were more corrosive towards Cu₂S.

Colombo and Frommer⁶⁹ leached chalcocite contained in mine tailings with acidified ferric sulphate solutions using techniques essentially similar to those of Sullivan. These workers largely confirmed Sullivan's results in that the rate was reported to occur in two stages: an initial stage to form synthetic CuS followed by the subsequent slow dissolution of this sulphide. The rate was independent of the pH and of the ferric ion concentration for solutions containing 2 to 10 per cent of ferric sulphate.

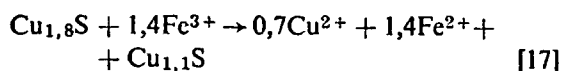
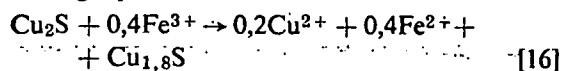
Tkachenko and Tseft⁷⁰ showed that high-purity natural chalcocite dissolves in acidic ferric chloride solutions in a manner similar to that reported for the dissolution in acidified ferric sulphate media. Rapid dissolution was obtained in the temperature interval 60 to 105°C and these rapid rates were interpreted as indicating rate control by mass transfer in the aqueous solution. As was observed for ferric sulphate dissolution, the attack by ferric chloride proceeded through the formation of a CuS intermediary. The dissolution of the CuS intermediate product produced elemental sulphur that was reported to interfere with additional dissolution.

Mulak⁷¹ investigated the kinetics of dissolution of synthetic Cu₂S in acidic ferric sulphate solutions using a rotating-disc technique in the temperature interval 30 to 90°C. He also observed that the dissolution of Cu₂S proceeded through the forma-

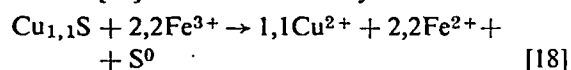
tion of a CuS intermediate product. At temperatures below 60°C the rate was controlled by mass transfer to the rotating disc; the associated activation energy for this process was 1,5 kcal/mol. It was reported that the build-up of the CuS reaction product impeded the mass transport of reagents and, consequently, caused the rate to fall. At temperatures above 60°C, the rate of dissolution of the CuS becomes significant and mixed kinetics with an apparent energy of activation of 5,3 kcal/mol were observed. The initial dissolution rate was insensitive to the acid concentration but was directly proportional to the ferric concentration of the leaching solution in the range 0,005 to 0,05 M Fe³⁺. Kopylov and Orlov⁷² observed that the dissolution of natural chalcocite in acidified ferric sulphate solutions proceeded through a CuS intermediate product. They observed rapid rates that increased with increasing Fe³⁺ concentration for ferric sulphate strengths between 5 and 27 per cent.

King⁵⁷ studied the kinetics of reaction between high-purity synthetic Cu₂S and acidified ferric chloride solutions. Using solutions containing 0,5 M Fe³⁺ and 0,2 M HCl he confirmed that the initial reaction gave CuS, followed by the much slower dissolution of this intermediate product. The rate of the initial stage was independent of the ferric ion concentration but the rate of the second (CuS) dissolution step increased with increasing ferric ion concentrations over the range 0,25 to 1,0 M. The activation energy for the initial dissolution of Cu₂S was found to be 0,8 kcal/mol. Microprobe analysis of partially leached pieces of Cu₂S indicated that copper was selectively leached from the Cu₂S to create a continuous solid solution phase between Cu₂S and CuS. This solid solution is, of course, thermodynamically unstable. The width of the diffusion zone, which includes the compositions of both digenite and blue-remaining covellite, was about 3 mm. At 40°C, there was some evidence that copper could be leached continuously from this compound to give a terminal product of composition Cu_{0,8}S. This work showed that the extraction of copper at one surface of the mineral created diffusion gradients that penetrated deeply into the solid. The transition boundary of CuS to copper and sulphur was considerably sharper than for Cu₂S/CuS. The rate-controlling step in Cu₂S dissolution was felt to be the solid state diffusion of copper through the Cu_{2-x}S phase.

Thomas, Ingraham, and MacDonald⁷³ leached discs of synthetic Cu₂S (chalcocite) and Cu_{1,8}S (digenite) in acidified ferric sulphate solutions in the temperature range 5 to 80°C. The two sulphides dissolved by the same mechanism and at nearly the same rate. It was stated that Cu₂S was converted to Cu_{1,8}S in the initial leaching step. The overall reaction occurred in two stages as indicated in the following equations:



Reaction [17] is then followed by:



These equations are similar to those found by Sullivan⁶⁸ except for the formation of blue-remaining covellite, $\text{Cu}_{1,1}\text{S}$, in place of normal covellite. Thomas *et al* detected no normal covellite during their leaching experiments. The blue remaining or *blaubleibender* covellite has recently been described by Moh⁷⁴. At temperatures below 60°C the dissolution of Cu_2S or $\text{Cu}_{1,8}\text{S}$ determined the amount of soluble copper; at higher temperatures the blue-remaining covellite also dissolved at an appreciable rate and mixed kinetics were observed. In the initial leaching stage linear kinetics, with an apparent activation energy of 5 to 6 kcal/mol, were observed. The dissolution rate was directly dependent on the ferric ion concentration of the solution and on the square root of the disc rotation speed. These observations led the authors to conclude that the initial leaching step was mass-transfer controlled in the aqueous solution. The second leaching stage had a higher activation

energy suggestive of chemical control.

Lowe⁵⁸ studied the dissolution of mounted pieces of high-grade natural chalcocite in acidified ferric sulphate solutions in the temperature range 40 to 70°C. The reaction proceeded through a CuS intermediate product. It was found that the initial rate was first-order with respect to Fe^{3+} concentration for ferric strengths between 0,007 and 0,299 M. The copper dissolution rate was also proportional to the 0,25 power of the acid concentration. These two factors, when taken together with the observed apparent activation energy of 6.7 kcal/mol, led the author to conclude that the rate of the initial dissolution reaction was controlled by ferric sulphate diffusion in the aqueous phase to reaction sites on the surface of the Cu_2S mineral. The activation energy theoretically deduced according to this model agreed closely with the measured value.

Table 2 summarizes the leaching behaviour of Cu_2S in acidified ferric sulphate and ferric chloride solutions in the absence of bacteria. Certain parts of the reaction mechanism would appear to be well established. First, the reaction proceeds through a CuS intermediate product; this CuS is not normal

TABLE 2

LEACHING KINETICS OBSERVED FOR Cu_2S DISSOLUTION IN ACIDIFIED FERRIC SULPHATE AND FERRIC CHLORIDE MEDIA

Material	Medium	Fe^{3+} dependence	Activation energy (kcal/mol)	Temperature (°C)	Rate-controlling process	Ref.
Natural Cu_2S	Ferric sulphate	Independent of Fe^{3+} conc.	Low	23 - 95	Solution controlled	68
Cu_2S in tailings	Ferric sulphate	None for ferric conc. between 2-10% ferric sulphate	—	25	—	69
Pure natural Cu_2S	Ferric chloride	—	Low	60 - 105	Solution controlled	70
Synthetic Cu_2S	Ferric sulphate	Directly proportional to Fe^{3+} conc.	1,5	30 - 90	<60°C, solution controlled	71
Natural Cu_2S	Ferric sulphate	Rate increased slightly with increasing Fe^{3+} for conc. of $\text{Fe}_2(\text{SO}_4)_3$ between 5-27%	Low	20 - 70	Solution controlled	72
Pure synthetic Cu_2S	Ferric chloride	Independent of Fe^{3+} conc.	0,8	20 - 80	Solid state diffusion of Cu in Cu_{2-x}S	57
Synthetic Cu_2S Synthetic $\text{Cu}_{1,8}\text{S}$	Ferric sulphate	Directly proportional to conc. of Fe^{3+}	5 - 6	5 - 80	Solution control, Fe^{3+} diffusion to Cu_2S surface	73
Pure natural Cu_2S	Ferric sulphate	Directly proportional to conc. of Fe^{3+}	6,7	28 - 70	Solution control, Fe^{3+} diffusion to Cu_2S surface	58

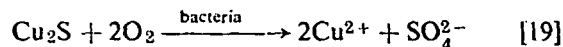
covellite and, in fact, appears to be rich in copper. The initial dissolution is rapid with a low activation energy; this suggests rate control by mass transport in the aqueous phase. Acid appears to have only a slight effect on the rate. The effect of Fe^{3+} concentration is not wholly clear, although most recent studies indicate that the initial rate is directly proportional to the ferric concentration.

It has been demonstrated that chalcocite is rapidly attacked by ferric solutions even at very low iron concentrations. This fact has complicated the interpretation of the bacterial leaching of chalcocite (Cu_2S) and digenite ($\text{Cu}_{1,8}\text{S}$). Most specimens of these minerals, even so-called museum specimens, often contain large amounts of iron, often more than 1 per cent Fe. Furthermore, many workers have grown their bacterial cultures on iron substrates. As a consequence, most of the bacterial leach solutions used to study chalcocite dissolution have contained small but significant amounts of iron. As an example, Nielsen and Beck⁷⁵ recently concluded that the bacteria directly attacked chalcocite containing only 0.17 per cent Fe. Even for this low amount of iron, however, these workers could not exclude the possibility that the cyclic oxidation of the iron could provide some or, indeed, all of the energy required by the bacteria. These workers also observed that digenite and covellite were formed as intermediate products during the dissolution of Cu_2S . The digenite reaction product has been previously detected by Thomas *et al*⁷³.

Sutton and Corrick^{39,40} dissolved chalcocite containing 1.4 per cent Fe in the presence of bacteria. Twenty-four per cent copper extraction was obtained after 56 days and the dissolution was attributed to the small amount of ferric sulphate in solution. It was stated that bacteria did not attack the mineral directly. Sutton and Corrick studied briefly the dissolution of digenite in the presence of bacteria, and obtained about 5 per cent copper extraction after 10 days. The attack was again attributed to the ferric leaching medium and not the bacteria. Bryner *et al*⁴⁶ obtained 21 per cent copper recovery after 42 days by bacterially leaching chalcocite. Duncan and Trussell⁶⁴ dissolved 93 per cent of the copper in 30 days from the same mineral. Both groups of workers felt that the bacteria directly attacked the mineral. De Cuyper⁶³ used bacterial leaching to extract 92 per cent of the copper from chalcocite after 125 days. He emphasized the role of ferric sulphate as the active leaching agent. Razzell and Trussell⁷⁶ obtained solutions containing over 3 g/l Cu by bacterially leaching Cu_2S . A direct bacterial attack of the Cu_2S was postulated, although it was noted that dissolved iron accelerated the dissolution rate.

Several of the more recent publications have emphasized the role of ferric sulphate during the bacterial leaching of chalcocite. Fox⁶⁷ studied this dissolution reaction in detail and concluded that the bacteria directly attacked the Cu_2S . It was noted, however, that the addition of iron (only 9 mg/l) to synthetic iron-free Cu_2S accelerated the rate of copper dissolution from this compound.

Fox noted that an intermediate sulphur compound, possibly elemental sulphur, accumulated during leaching and was not oxidized bacterially until three to four days after its appearance. This observation might be indicative of ferric sulphate attack (equation [15]) since it is generally assumed that the bacterial oxidation reaction produces no elemental sulphur:



Ivanov⁷⁷ believed that the bacteria oxidized ferrous ion to the ferric state, which then attacked the chalcocite. He found that ferrous ion retarded the sulphide dissolution rate and suggested that the ferrous ion be oxidized in a separate step to increase the effectiveness of the overall leaching process. Stanchev *et al*⁷⁸ investigated the dissolution of Cu_2S (?) in slags. They stated that the bacteria oxidized Fe^{2+} to Fe^{3+} , which then dissolved the copper sulphide. Corrans, Harris, and Ralph⁶⁵ investigated the dissolution of synthetic Cu_2S specimens by *Thiobacillus ferrooxidans*. They postulated that copper was dissolved by ferric ion, which was subsequently re-oxidized bacterially.

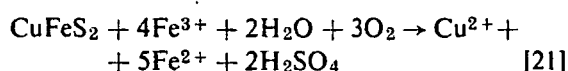
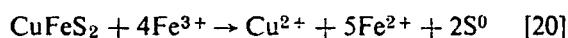
Chalcopyrite

Chalcopyrite (CuFeS_2) is probably the most common copper ore mineral. When put in this perspective, it is not too surprising that considerable effort has been expended to study the kinetics of dissolution of this mineral in acidified ferric chloride and ferric sulphate solutions. In spite of this effort, however, several aspects of the dissolution of chalcopyrite are not fully resolved and certainly warrant additional detailed study.

Early work by Traill and McClelland^{79,80,81} related experiments aimed at dissolving chalcopyrite concentrates in hot concentrated (70 g/l) ferric chloride solutions at 95°C. Using ground ore, about 90 per cent copper extraction could be obtained after five hours of leaching. The recovery of iron from the concentrate was only 60 to 70 per cent; this was probably indicative of iron hydrolysis and precipitation during the experiments. The recovery of elemental sulphur was only about 5 per cent. It was noted that if the concentrate were given a non-oxidizing roast at about 725°C prior to leaching the recoveries were slightly improved. Over 95 per cent copper recovery was obtained after five hours dissolution of the roasted concentrate. It was concluded, however, that the additional copper recovery was probably not worth the cost of the pre-roasting operation. Pike *et al*⁸² studied the dissolution of chalcopyrite concentrates on both bench and pilot-plant scales. Ferric chloride was selected as the lixiviant, first, because it was felt to be more effective than ferric sulphate, and, second, because of the possibility of sulphur contamination from sulphates in the electrolytic iron that was to be produced from the leach solutions. These workers were able to dissolve 85 to 90 per cent of the copper from various concentrates using solutions containing 4 to 10 per cent

Fe³⁺ as the chloride at the boiling point of the solution. At 160 to 170°C it was found that the copper was cemented on the residual sulphides and lower extraction rates were thereby obtained. Under the intensive leaching conditions employed by these authors, the ferric chloride lixiviant was about 50 per cent more effective than an equivalent ferric sulphate solution. A 326 lb/day pilot plant was run for about four months and gave recoveries similar to those noted for the bench-scale tests. Elemental sulphur recoveries ran to about 60 to 70 per cent of the feed sulphur.

Sullivan⁵⁵ and Brown and Sullivan⁵⁴ studied the dissolution of chalcopyrite concentrates in both ferric chloride and ferric sulphate media. Fine grinding was considered necessary because of the refractory nature of this mineral. These workers were able to dissolve 33 per cent of the copper from a minus-350-mesh concentrate after 57 days using a 1% Fe³⁺ solution, as ferric sulphate, at 35°C. The rate increased sharply as the temperature was raised; the above concentrate yielded 44 per cent of its copper after 14 days of leaching at 50°C. At the solution boiling temperature, 38 per cent copper extraction occurred in just five hours. Variations in the ferric sulphate concentration in the range 0,25 to 5 per cent Fe₂(SO₄)₃ had little real effect on the dissolution rate; in some experiments the rate increased slightly with increasing ferric strengths, but in other tests it decreased. The dissolution reactions by which chalcopyrite dissolved in ferric sulphate solutions were stated to be:

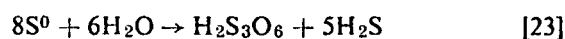


About 75 per cent of the chalcopyrite dissolved according to reaction [20], and the remainder according to reaction [21]. The minor sulphate production was attributed to dissolved oxygen and not to the action of the ferric ion. These workers also noted that ferric chloride was a better leaching agent for chalcopyrite than ferric sulphate. At the boiling point, 18 per cent of the copper was extracted in 3 h by a 5 per cent ferric chloride solution but only 4 per cent copper extraction was achieved by an equivalent ferric sulphate solution under the same conditions. At 35°C, the advantage of the chloride medium appears to be less. A 1 per cent ferric chloride solution dissolved 45 per cent of the copper from the concentrate after 57 days, and the sulphate medium leached out 33 per cent of the copper. The rate of dissolution in ferric chloride media was also reported to increase rapidly with increasing temperatures.

Klets and Liopo⁶³ investigated the reaction of sized chalcopyrite ore in acidic ferric chloride media. They stated that the chalcopyrite dissolved according to the reaction:



The sulphur was subsequently dissolved:



If high yields of elemental sulphur were desired, these workers believed that some device would have to be used to remove the sulphur as it formed. Ermilov, Tkachenko, and Tseft⁶⁴ investigated the kinetics of chalcopyrite dissolution in ferric chloride solutions in the temperature interval 60 to 106°C. The reaction increased moderately rapidly with increasing temperature; the apparent activation energy was about 12 kcal/mol. The rate depended directly on the ferric ion concentration for initial ferric chloride concentrations between 50 and 100 g/l. The sulphur formed during dissolution did not interfere with the dissolution kinetics. Ozolins and Rusikhina⁶⁵ observed that the application of a d.c. field or of ultrasonic energy accelerated the dissolution of chalcopyrite in a 5% Fe₂(SO₄)₃ and 2% H₂SO₄ solution at 50°C. The d.c. field was reported to be more effective than the use of ultrasonic energy.

Ichikuni⁶⁶ observed that ferric sulphate attacked chalcopyrite according to the reaction shown in equation [20]. Later, the same investigator⁶⁷ suggested that slight variations in the ratio of dissolved copper to dissolved ferrous ion, which were observed during the initial stages of leaching by ferric chloride solutions, were caused by the preferential leaching of iron from the chalcopyrite lattice. He also concluded that ferric ions react on pyrite-chalcopyrite mixtures with little selectivity. That is, no galvanic effect was observed on the chalcopyrite dissolution rate when pyrite was present.

Dutrizac, MacDonald, and Ingraham⁶⁸ studied the dissolution of sintered discs of synthetic chalcopyrite in acidic ferric sulphate solutions. The stoichiometry of chalcopyrite dissolution was described by equation [20]. Over the investigated temperature range of 50 to 94°C, the reaction displayed parabolic kinetics with an associated apparent activation energy of 17 kcal/mol. Below about 0,01 M Fe³⁺ concentration, the rate-controlling process was attributed to ferric sulphate diffusion through a constantly thickening sulphur layer formed on the surface of the chalcopyrite. At higher ferric sulphate concentrations the rate was independent of the ferric strength. The rate was also independent of the acid concentration between 0,001 and 1,0 M H₂SO₄. For ferric ion concentrations above 0,01 M the rate decreased sharply with the addition of ferrous sulphate to the leaching medium. Natural chalcopyrites dissolved more slowly than did the discs of the synthetic material, and this was probably caused by the larger true surface area of the porous sintered discs as compared to the massive natural chalcopyrite. Dutrizac and MacDonald⁶⁹ also showed that the addition of chloride ion to the acidic ferric sulphate leaching medium accelerated the dissolution of chalcopyrite at temperatures above 50°C. At lower temperatures it was noted that chloride ion additions were not beneficial.

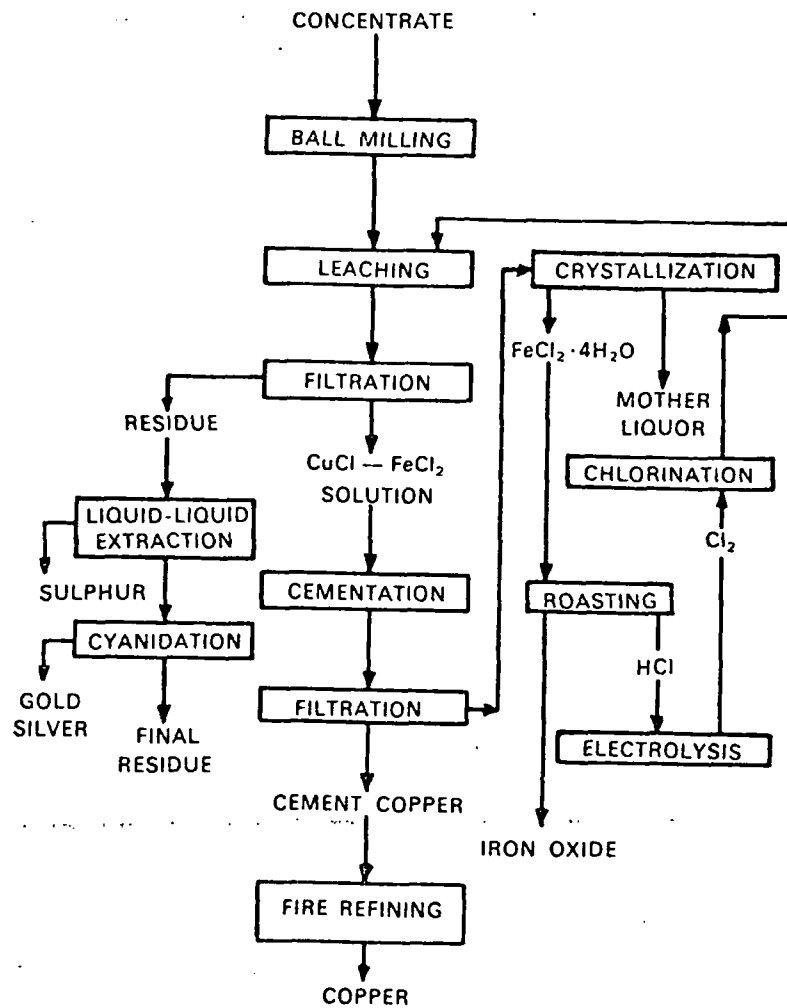


FIGURE 8 Schematic flowsheet proposed by Haver and Wong for the treatment of chalcopyrite concentrates. (From Ref. 15 and 90)

Lowe⁵⁸ studied the dissolution of ground and sized natural chalcopyrite in acidified ferric sulphate solutions over the temperature range 32 to 50°C. Linear kinetics were observed and the apparent activation energy associated with the reaction was 18 kcal/mol. Variations in the sulphuric acid concentration over the range 0.05 to 0.78 M H₂SO₄ had no effect on the rate of copper dissolution. The rate was also insensitive to changes in the ferric ion concentration for ferric sulphate concentrations greater than 0.02 M. Lowe interpreted these results as indicating rate control by surface-controlled chemisorption.

Haver and Wong¹⁵ recently proposed an integrated hydrometallurgical process for the treatment of chalcopyrite concentrates, using concentrated acidified ferric chloride solutions. Experiments to determine the important leaching variables were done in the temperature interval 30 to 106°C. At the higher temperatures copper extractions in excess of 99 per cent were achieved. Parabolic kinetics were reported and this effect was attributed to mass transfer through the constantly thickening

sulphur layer formed on the surface of the chalcopyrite during leaching. These authors found that at a ratio of FeCl₃ to CuFeS₂ of 1 to 2.7 virtually all the dissolved copper was in the monovalent form. Thus the following equation must describe the overall reaction:



About 70 per cent of the sulphur reported in the elemental form; the remainder was presumably oxidized to sulphate. The process described by Haver and Wong is interesting because it is a complete hydrometallurgical process; in this respect it is similar to the older works of Traill^{79,80,81} and Pike *et al*⁸². Figure 8 shows a simplified form of the process flowsheet proposed by Haver and Wong; this form of the flowsheet is taken from a recent review on chalcopyrite hydrometallurgy by Subramanian and Jennings⁹⁰. The copper was recovered by cementation on sponge iron and this operation required only 0.625 parts of iron to one part copper because the copper was in the monovalent state. It was proposed that the elemental sulphur

be recovered by extracting it from the leach residue with perchloroethylene. The precious metals were recovered from the residue by cyanidation after sulphur removal. It was proposed to re-oxidize the spent ferrous chloride solution by electrolytically generated chlorine gas.

The Cymet Process¹⁶ combines multiple-stage acid ferric chloride leaching of chalcopyrite concentrates, direct anodic dissolution of the undissolved sulphides, and electrolytic regeneration of the iron chloride leaching medium. The leaching step is done at about 80°C using 70 per cent minus-200-mesh concentrates. The direct ferric chloride leach is more important than the electrochemical dissolution step and accounts for about 70 per cent of the dissolved metal values. The dissolution reaction produces cuprous chloride and elemental sulphur according to reaction [24]. This process recovers about 85 per cent of the elemental sulphur, and it should be noted that the leach residue still contains significant amounts of elemental sulphur even after the sulphur recovery step.

Uchida *et al*⁹¹ investigated the low temperature dissolution of chalcopyrite in acidified ferric sulphate solutions. The rate increased with increasing ferric sulphate concentrations for ferric strengths below 0,2 g/l but was insensitive to further increases in the iron concentration. A solution containing 0,4% Fe³⁺ and 0,01 N H₂SO₄ leached 4 to 5 per cent of the copper from the CuFeS₂ after two weeks.

Bauer, Gibbs, and Wadsworth⁶⁶ studied the dissolution of natural chalcopyrite powders in acidified ferric sulphate solutions; corrections were applied for the changes in surface area that occurred during leaching. The experiments were done in the temperature interval 27 to 85°C using solutions containing from 0 to 0,69 M Fe³⁺ at a pH value of 1,25. These workers observed that the chalcopyrite dissolved according to a parabolic law. This was attributed to the diffusion of the oxidizing agent through the constantly thickening layer of elemental sulphur plus basic sulphates that formed during the dissolution of the chalcopyrite. The relatively low leaching rate of chalcopyrite was attributed to the formation of this impervious layer. The calculated activation energy of 20 ± 5 kcal/mol is consistent with the postulated solid-state diffusion-controlled reaction. These workers noted that the oxidation rate was insensitive to the ferric content of the lixiviant for ferric strengths above about 0,01 M Fe³⁺. At lower ferric concentrations the rate was directly proportional to the ferric strength. Figure 9 shows the type of dissolution curve that Bauer *et al* obtained for leaching chalcopyrite at 85°C. The ordinate 'F' is the weight squared of dissolved copper, corrected for the ferric ion depletion of the solution. Except at the lowest ferric strength, the dissolution curves closely follow the parabolic law over the entire leaching interval. Such parabolic kinetics are required by the postulated mechanism of diffusion through the constantly thickening layer of sulphur (plus basic sulphates?) formed during leaching. Such parabolic kinetics are consistent with the results obtained by Dutrizac, MacDonald, and Ingraham⁸⁸ for sulphate systems,

and by Haver and Wong¹⁵ for ferric chloride media.

Table 3 compares the results obtained by various workers for chalcopyrite dissolution in both chloride and sulphate media. It is noteworthy that, despite the economic importance of chalcopyrite, there is little unanimity among the various authors concerning the dissolution kinetics in Fe³⁺ solutions. About half the papers report parabolic kinetics; the authors note linear dissolution rates in the other investigations. Different kinetics have been observed under different conditions⁸⁹. When ferric sulphate is used, the rate is directly proportional to the ferric strength at low concentrations, but is independent of ferric concentrations greater than about 0,01 M. When ferric chloride is used, the rate appears to depend directly on the concentration of ferric ion. The apparent activation energies for chalcopyrite dissolution are high and it may be that the values are slightly higher when sulphate media are used. All authors agree that chalcopyrite is relatively refractory towards dissolution.

A number of authors have reported studies on the leaching of relatively pure chalcopyrite or high-grade chalcopyrite concentrates by bacterial solutions. In addition, there exists a large number of papers dealing with the dissolution of 'ores' that contain chalcopyrite as one of the constituents. This latter type of work normally shows only that a certain percentage of copper can be extracted in a certain period from all the copper minerals in the ore, but does not elucidate the mechanism by which the chalcopyrite dissolves. When CuFeS₂ is dissolved in aerated acidic solutions in the presence of *Thiobacillus ferrooxidans*, the leach solution eventually contains some Fe³⁺ ions. Thus the bacterial dissolution of this mineral probably

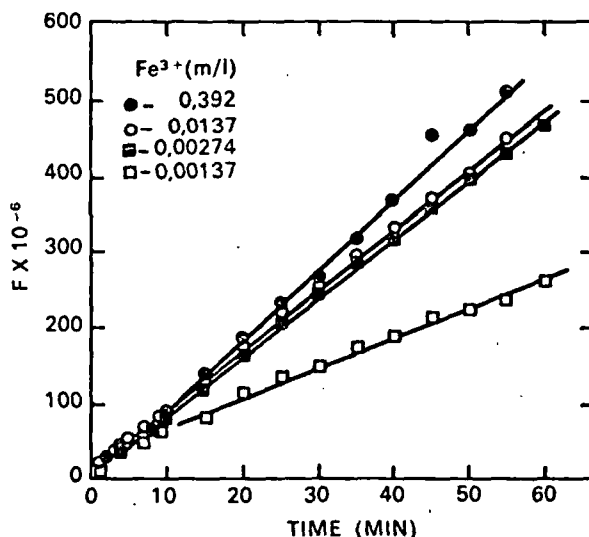


FIGURE 9 Chalcopyrite dissolution curve at 85°C illustrating parabolic kinetics; ordinate represents the square of the dissolved copper corrected for surface area and ferric ion concentration changes.

(From Ref. 66)

TABLE 3

LEACHING KINETICS OBSERVED FOR CuFeS_2 DISSOLUTION IN ACIDIFIED FERRIC SULPHATE AND FERRIC CHLORIDE MEDIA

Material	Medium	Fe^{3+} dependence	Activation energy (kcal/mol)	Temperature ($^{\circ}\text{C}$)	Rate-controlling process	Ref.
CuFeS_2 concentrate	Ferric chloride	—	High	35 - 100	Not given	54
	Ferric sulphate	No effect between 0,25 and 5% $\text{Fe}_2(\text{SO}_4)_3$	High	35 - 100	Not given	55
CuFeS_2	Ferric chloride	Direct dependence between 50-100 g/l FeCl_3	12	60 - 106	Not given	84
Synthetic CuFeS_2	Ferric sulphate	$\text{Fe}^{3+} < 0,01$ M, direct dependence $\text{Fe}^{3+} > 0,01$ M, no effect	17	50 - 94	Parabolic kinetics, transport control	88 89
Natural CuFeS_2	Ferric sulphate	$\text{Fe}^{3+} > 0,02$ M, no effect	18	32 - 50	Linear kinetics, surface controlled chemisorption	58
CuFeS_2 concentrates	Ferric chloride	—	High	30 - 106	Parabolic kinetics, transport control	15
Natural CuFeS_2	Ferric sulphate	$\text{Fe}^{3+} < 0,01$ M, direct dependence $\text{Fe}^{3+} > 0,01$ M, little effect	20	27 - 85	Parabolic kinetics, transport control	66

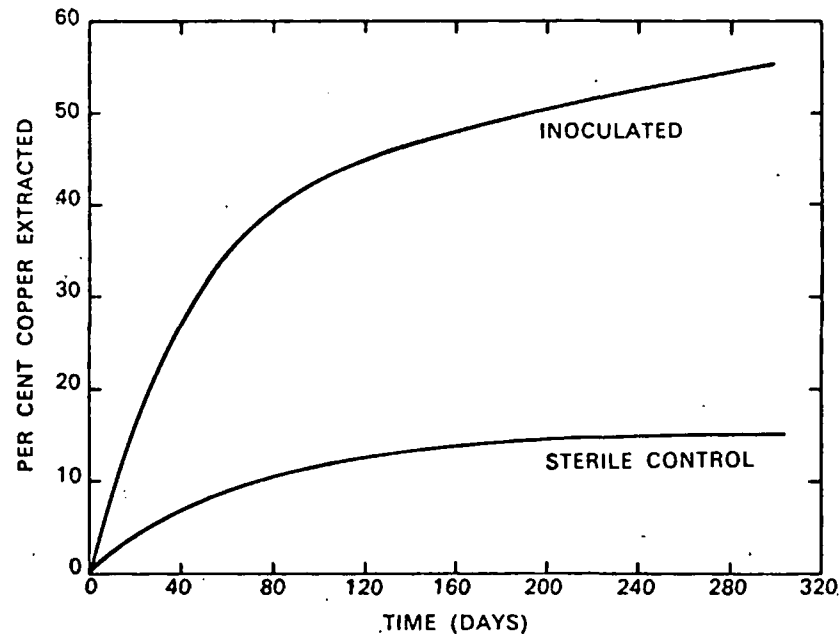
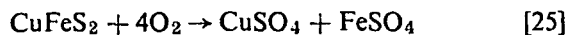
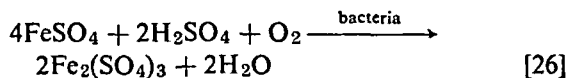


FIGURE 10 Dissolution curves for chalcopyrite ore obtained in the presence and absence of active bacteria. (From Ref. 93)

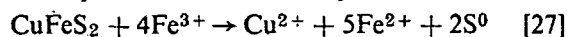
always consists of two parts: a direct bacterial attack of the sulphide in the chalcopyrite crystal lattice and an indirect ferric ion leaching of the CuFeS_2 . It is not always easy to deduce the relative importance of the respective mechanisms. Sutton and Corrick^{39,40,92} concluded that chalcopyrite was attacked only by the indirect leaching mechanism. They stated that their particular bacterial strain could not oxidize sulphide ions in the crystal lattice. Their proposed leaching mechanism involved the initial air oxidation of the chalcopyrite:



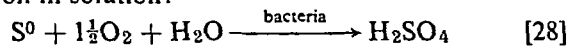
The ferrous sulphate produced was quickly oxidized by oxygen in the presence of bacteria:



The ferric sulphate produced then attacked the chalcopyrite forming still more ferrous sulphate, which repeated the oxidation cycle:



The sulphur formed by the indirect dissolution of chalcopyrite was oxidized to acid, which kept the iron in solution:

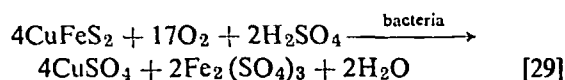


Reaction [25] proceeds slowly and for this reason the initial leaching rate is relatively slow, but accelerates with time to some limiting value.

A similar mechanism was postulated by Malouf and Prater⁹³ to explain the dissolution of chalcopyrite during dump leaching. Figure 10 shows some of their data for the dissolution of chalcopyrite with and without bacteria being present. Relatively high rates of extraction were obtained, but only after long times. It should also be noted that the dissolution curves level off more rapidly than would be expected for a simple reduction in the surface area of the particles. This suggests that, perhaps, the dissolution kinetics are not linear. The mechanism advanced by Malouf and Prater was used by Ivanov^{77,45}, who also believed that the chief role of bacteria during sulphide leaching was to provide an active ferric sulphate lixiviant.

Under certain conditions it appears that chalcopyrite can also be oxidized directly by certain bacteria with the production of soluble iron and copper. The exact mechanism of attack does not appear to be known. It has been shown that flotation reagents do not interfere with the bacterial activity⁹⁴. Watanabe, Uchida, and Furuya⁹⁵ reported that sucrose additions accelerated both the bacterial activity and the rate of copper extraction. Duncan and Trussell⁶⁴ and Duncan, Trussell, and Walden⁹⁶ showed that surface-active agents could accelerate the leaching of some chalcopyrite minerals and ores. Several workers have stated that the direct bacterial attack mechanism predominates during chalcopyrite dissolution^{61,62,46,49}. Razzell and Trussell⁷⁶ believed that bacteria were more effective than ferric ion for leaching chal-

copyrite and that dissolved ferric ion actually suppressed the normal bacterial leaching. The direct bacterial leaching is thought to be:



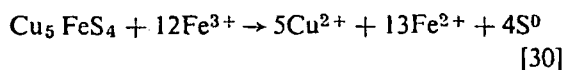
There is also some evidence of galvanic corrosion effects during bacterial leaching. Bryner and Anderson⁹⁷ noted that the presence of pyrite accelerated the rate of copper extraction from chalcopyrite, but that molybdenite suppressed the dissolution. These effects are consistent with the known order of rest potentials for these minerals. It is not clear how a galvanic effect is related to the direct biological attack of the chalcopyrite. Wyckoff⁹⁸ observed that chalcopyrites from different sources responded differently to bacterial leaching. He attributed the differences to different valence states of iron in the various chalcopyrites. This explanation has not been substantiated by Mossbauer studies of chalcopyrites and it may be that Wyckoff was also observing galvanic corrosion effects during bacterial attack.

Bruynesteyn and Duncan⁹⁹ have proposed a process for the bacterial leaching of chalcopyrite concentrates. This consists of leaching in aerated tanks at 35°C and at a pH value of 2.5 followed by liquid-solids separation. The copper is recovered by electrowinning and the unreacted chalcopyrite is recycled to the leaching step after acid neutralization. It was shown that copper could be extracted at rates of 300 to 350 mg/l h. Such high rates were possible by supplying nutrients and CO_2 for the bacteria; the ultimate rate was controlled by the oxygen supply. To obtain rapid rates, the concentrate must be ground to 100 per cent minus-400 mesh and this must be considered a practical problem because it would be difficult to separate and recycle such fine concentrates from the iron-bearing sludge formed during the acid neutralization step. An additional supply of nutrients for the bacteria appears essential for high chalcopyrite leaching rates; the lack of such nutrients may be one reason why early investigators interpreted the overall bacterial leaching of chalcopyrite as occurring by an indirect ferric ion leaching mechanism.

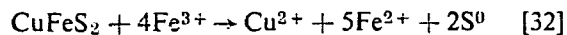
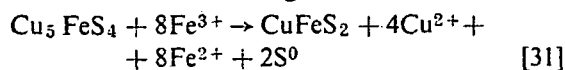
Bornite

The mineral bornite (Cu_5FeS_4) is frequently associated with chalcopyrite or chalcocite ore deposits, and it can also be an important copper mineral in its own right. Sullivan^{55,100} studied the dissolution of ground bornite ore containing some chalcocite in both ferric sulphate and ferric chloride solutions. The dissolution curves showed two distinct parts: a very rapid initial step followed by a slower secondary stage. Over the temperature range 23 to 98°C the initial step increased only moderately with increasing temperature for either the sulphate or chloride media. The bornite dissolution rate was independent of the ferric sulphate concentration over the range 0.25 to 10% Fe^{3+} ; the rate also appeared to be independent of the con-

centration of ferric chloride. The pH of the solution did not alter the dissolution rate at constant temperature. Bornite was dissolved more rapidly by ferric chloride than by ferric sulphate; however, ferric chloride acidified with hydrochloric acid dissolved copper from bornite more slowly than solutions containing ferric chloride alone. Sullivan also noted that during the initial stages of leaching, copper was dissolved from the bornite without the production of soluble iron or elemental sulphur. He presented the following equation to describe the overall leaching of bornite:



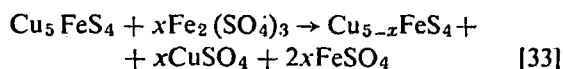
Kopylov and Orlov^{72,101} investigated the dissolution of lumps of pure natural bornite by a rotating-disc method over the temperature interval 30 to 70°C. The bornite dissolved rapidly in the acidified ferric sulphate medium; the dissolution rates were about one-half those observed for chalcocite dissolution under similar conditions. Linear kinetics were observed with an associated apparent activation energy of 4 to 6 kcal/mol. The dissolution increased slightly with increasing ferric ion concentrations in the range 9 to 36 g/l Fe³⁺. Kopylov and Orlov also noted that the reaction produced a layer of chalcopyrite on the surface of the bornite. Since the chalcopyrite dissolved relatively slowly, this phase accumulated during leaching and eventually blocked the surface of the bornite. That is, bornite dissolved according to the reactions:



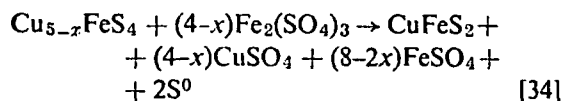
The initial stage of leaching (reaction [31]) was controlled by diffusion across the solution boundary layer. This sequence of reactions is only partly consistent with Sullivan's observation¹⁰⁰ that copper, but no iron or sulphur, is produced during the initial leaching of bornite. Uchida *et al*⁹¹ also studied the dissolution of bornite in acidified ferric sulphate solutions. They noted that 40 per cent of the copper could be leached from bornite in two weeks leaching at room temperature. The dissolution rate increased with increasing acid concentration in the pH interval 1 to 2. The rate was independent of ferric ion concentration for ferric strengths above about 0.5 g/l; the rate was a direct function of the ferric strength at lower concentrations.

Dutrizac, MacDonald, and Ingraham¹⁰² measured the rate of dissolution of synthetic bornite in acidified ferric sulphate solutions using a rotating-disc technique. In the temperature interval 40 to 94°C, essentially linear kinetics were obtained with an associated activation energy of 5 kcal/mol. The rate-controlling step at the high temperatures was felt to be solution diffusion through the liquid boundary layer adjacent to the mineral. The rate was virtually insensitive to the acid concentration. Below about 0.1 M Fe³⁺ the rate increased directly with the ferric ion concentration but was insensitive

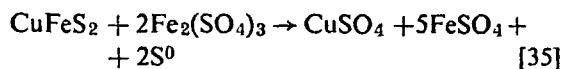
to increases above this ferric sulphate concentration. At 0.1 M Fe³⁺ concentration, the bornite dissolution rate decreased sharply with increasing additions of ferrous sulphate in the solution. As the leaching temperature was lowered below 40°C, the kinetics became progressively more parabolic. The activation energy for the parabolically controlled step was 6 kcal/mol. The rate-controlling process was thought to be solution diffusion, but through solution paths in a constantly thickening layer of non-stoichiometric bornite that formed during the reaction. Natural bornite dissolved at the same rate as the synthetic material and by the same mechanism. Dutrizac *et al* noted that the dissolution proceeded through a series of intermediate products. A non-stoichiometric bornite was formed in the first stage:



At temperatures below 25°C this was the only reaction observed and it is consistent with Sullivan's observation¹⁰⁰ that, initially, copper dissolved without the formation of elemental sulphur or the removal of iron from the bornite. The non-stoichiometric bornite is next dissolved to give chalcopyrite:



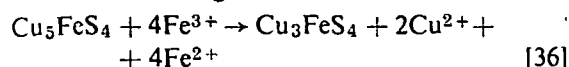
There was evidence that copper was removed continuously from the bornite to yield the non-stoichiometric bornite. The limiting non-stoichiometric bornite composition reported was Cu_{3.8}FeS₄. The other transformations observed appeared to occur at relatively precise compositions. The gradual removal of copper from the bornite to give a non-stoichiometric product was similar to the effect reported by King⁵⁷ for the continuous removal of copper from chalcocite to yield CuS. The chalcopyrite formed according to equation [34] was only slowly decomposed:



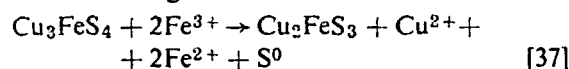
Dutrizac, MacDonald, and Ingraham¹⁰³ also noted the effect of certain impurities on the rate of bornite dissolution in acidified ferric sulphate solutions. These workers pressed pellets of synthetic bornite to which had been added pyrite, chalcopyrite, or digenite and the pellets were then sintered. The presence of pyrite, chalcopyrite, or digenite had little effect on the kinetics of dissolution at 70°C. At 15°C, however, the presence of pyrite increased the rate of dissolution of the bornite. It was believed that the dissolution of the discs of the mixed sulphides was still solution controlled. These results indicated that although electrochemical reactions are important, the actual charge-transfer step is not necessarily rate controlling.

Lowe⁵⁸ investigated the dissolution of mounted pieces of natural bornite in acidified ferric sulphate

solutions in the temperature interval 28 to 70°C. His bornite contained from 4 to 10 per cent chalcocite. The reported dissolution rates fell rapidly with time and then levelled off. This led Lowe to postulate that the reaction occurred in three stages. The initial stage was felt to be controlled by ferric sulphate diffusion to the bornite. The apparent activation energy reported for this process was 6 kcal/mol. The rate varied directly with the ferric ion concentration over the interval 0,006 to 0,28 M Fe₂(SO₄)₃. Acid had no effect for this stage or for any of the other postulated steps. The initial reaction thought to occur was:



Regrettably, Lowe did not characterize thoroughly his reaction intermediates and it is impossible to state if the Cu₃FeS₄ formed during leaching was really synthetic idaite (Cu₃FeS₄) or the limiting composition of the non-stoichiometric bornite reported by Dutrizac *et al*¹⁰². The second stage of bornite leaching was considered to be cuprous ion diffusion through the Cu₃FeS₄ layer formed. The activation energy for this stage of leaching was 10 kcal/mol and the rate was only slightly dependent on the ferric strength. The second stage proceeded according to the reaction:



According to Cabri¹⁰⁴ Cu₂FeS₃ is not a stable phase in the Cu-Fe-S system. It is not certain if this composition really represents a new metastable phase or whether it is simply an impure form of the chalcopyrite intermediate reaction product produced during bornite dissolution and noted by Dutrizac *et al*¹⁰² and Kopylov and Orlov¹⁰¹. The final stage in the dissolution of bornite was felt to be a chemisorption reaction with an apparent activation energy of 12 kcal/mol.

Sullivan¹⁰⁰ did a few experiments on the percolation leaching of bornite ores at 25°C. The solution was dripped constantly onto the ore at a rate of 1 litre every 24 hours. Although the percolation leaching rates were slower than those obtained when the ore was leached in rotating bottles, between 73 and 87 per cent of the available copper could be leached from the ore in 15 days using solutions containing either 0,5 or 1% Fe³⁺ as the sulphate. Dutrizac and MacDonald¹⁰⁵ also studied the percolation leaching of bornite ores. They noted that up to 80 per cent of the copper in a bornite ore could be leached in about 1000 h with acidified ferric sulphate solutions percolating at a rate of 0,1 l/h. The upper limit for rapid copper extraction was set by the conversion of bornite to slowly dissolving chalcopyrite. The dissolution occurred in two stages: a rapid linear initial stage followed by a slower non-linear stage. The initial step was controlled by the rate of supply of the ferric ion oxidizing agent; temperature was not an important variable during the initial reaction in the temperature interval 25 to 60°C. The second leaching stage was controlled by chemical and physical factors

and was temperature dependent. The initial copper leaching rates were insensitive to both the concentration of the ferrous sulphate reaction product and the sulphuric acid concentration; these rates depended directly on the ferric concentration of the solution and the apparent solution percolation rate.

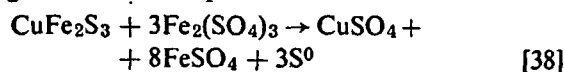
Because iron is a constituent of the bornite lattice and because ferric sulphate solutions attack bornite readily even at low temperatures, virtually all bacterial leaching work has included some indirect mineral attack. Sutton and Corrick⁴⁰ dissolved 30 per cent of the copper from a bornite ore in five to six days; they attributed all the dissolution to the action of bacterially generated ferric sulphate. Bryner *et al*⁴⁶ showed that 7 per cent copper dissolution from a bornite ore could be obtained in 42 days. The dissolution was attributed only to direct bacterial action on the sulphide ions in the lattice. Razzell and Trussell⁷⁶ extracted 50 to 85 per cent of the copper from a bornite ore after 19 days of leaching at a pH value of 2,5. Virtually no dissolution was noted at a pH value of 4,0. Duncan and Trussell⁶⁴ extracted 100 per cent of the copper from bornite in 20 days using bacterial leaching; a control experiment yielded 34 per cent copper extraction in 57 days of leaching. Duncan and Trussell believed that direct bacterial attack was the predominant factor in bornite dissolution but they also recognized the importance of the indirect ferric sulphate leach.

Table 4 summarizes the kinetic information available for the dissolution of bornite in acidified ferric chloride or ferric sulphate solutions. There is general agreement that the initial stage of dissolution is solution controlled with a low activation energy. The initial rate varies directly with the ferric strength at low concentrations but is independent of higher ferric concentrations. There is little agreement on either the reaction products or on the rate-controlling processes operative during the later stages of the dissolution.

OTHER COPPER MINERALS

Cubanite

Cubanite (CuFe₂S₃) occurs associated with chalcopyrite and the platinum-group minerals in several ore deposits. Dutrizac, MacDonald, and Ingraham¹⁰⁶ investigated the dissolution of sintered synthetic CuFe₂S₃ discs in acidified ferric sulphate solutions in the temperature interval 45 to 90°C. It was not possible to prepare stable orthorhombic cubanite directly from the elements and the material used was a metastable, high-temperature form of CuFe₂S₃ that dissolved slowly according to the overall equation:



The dissolution kinetics were linear with an associated activation energy of 12 kcal/mol. The dissolution rate, at constant temperature, increased according to the 0,6 power of the ferric ion concentration and also increased slightly with de-

TABLE 4

SUMMARY OF THE KINETICS OF DISSOLUTION OF BORNITE IN ACIDIFIED SOLUTIONS OF FERRIC SULPHATE OR FERRIC CHLORIDE

Material	Medium	Fe ³⁺ dependence	Activation energy (kcal/mol)	Temperature (°C)	Rate-controlling process	Ref.
Natural bornite	Ferric sulphate	No effect 0,25-10% Fe ³⁺	Low	23 - 98	Not given	35, 100
	Ferric chloride	No effect 0,25-10% Fe ³⁺	Low	23 - 98	Not given	
Natural bornite	Ferric sulphate	Rate increased slightly with increasing Fe ³⁺ conc. in the range 9-36 g/l	4 - 6	30 - 70	Initially diffusion controlled	72, 101
Synthetic bornite	Ferric sulphate	—	6	5 - 40	Parabolic kinetics (transport control in aqueous phase) Linear kinetics, solution diffusion	102, 103
	Ferric sulphate	Fe ³⁺ < 0,1 M, directly dependent on ferric conc. Fe ³⁺ > 0,1 M, no effect	5	40 - 94		
Natural bornite	Ferric sulphate	Initially rate varied directly with Fe ³⁺ conc.	6	28 - 70	Solution diffusion	58
			10			
			12			
Natural bornite ore	Ferric sulphate	Directly dependent on Fe ³⁺ conc.	0 (initial leaching stage)	25 - 60	Mass transport control	105

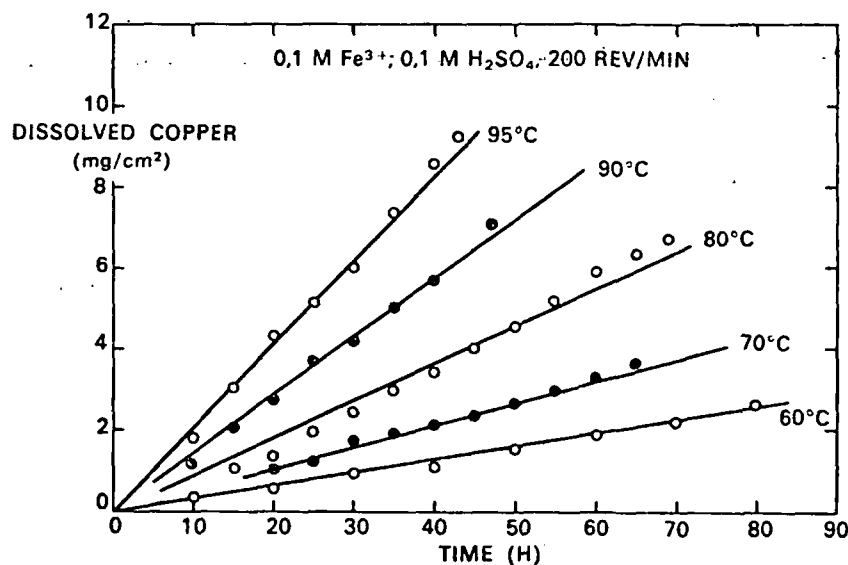


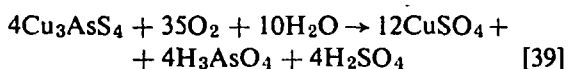
FIGURE 11 Dissolution curves obtained for synthetic enargite (Cu₃AsS₄) at various temperatures. (From Ref. 110)

creasing acid concentration. The rate of dissolution decreased sharply with the addition of ferrous sulphate to the solution. From these observations it was concluded that the rate of dissolution of synthetic CuFe_2S_3 was controlled by a surface reaction on the sulphide; there was some evidence that a hydrolysed form of the ferric ion participated directly in the rate-controlling reaction. The addition of small amounts of chloride ion, either as NaCl or HCl , accelerated the dissolution of the CuFe_2S_3 in the acid ferric sulphate solutions.

The same authors also studied the dissolution of cubanite ores in the acid ferric sulphate leaching medium. The ore contained about 70 per cent cubanite with the major impurity being chalcopyrite. The cubanite dissolved according to a linear law, but about one-seventh as rapidly as the synthetic CuFe_2S_3 . This difference was attributed to the larger true surface area of the sintered synthetic material. The cubanite dissolved to give the same reaction products as the synthetic CuFe_2S_3 and the apparent activation energies for dissolution of the two materials were essentially identical.

Enargite

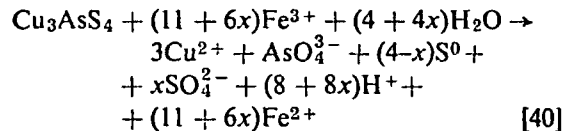
Brown⁵³, Sullivan⁵⁵, and Brown and Sullivan⁵⁴ reported on the dissolution of pure natural enargite (Cu_3AsS_4) in acidified ferric sulphate solutions. These workers found enargite to be resistant to chemical attack; only 3 per cent of the copper in minus-100-mesh, plus-200-mesh enargite was extracted after 146 days of leaching at 25°C by a 5 per cent ferric sulphate solution. The copper, arsenic, and sulphur were all attacked at approximately the same rates. Sulphuric acid, in the absence of the ferric sulphate oxidizing agent, dissolved negligible amounts of copper from this mineral. Koch and Grasselly¹⁰⁷ investigated the dissolution of enargite and enargite-pyrite mixtures in acidic ferric sulphate solutions containing 0.23 g/l Fe^{3+} . They observed slow reactions that were slightly accelerated by the presence of pyrite in the ore mixture. This observation would appear to indicate that the dissolution of enargite occurs by a galvanic mechanism. Since the test vessels were open to the air, these workers postulated that the overall reaction was:



The beneficial presence of ferric ion was attributed to the higher oxidizing potential of the leaching medium when ferric ion was present. Ehrlich¹⁰⁸ studied the action of acidic ferric sulphate solutions on enargite ores in the presence of the Thiobacillus-Ferrobacillus group of bacteria. He concluded that these bacteria could oxidize enargite to produce either soluble or insoluble arsenates. Unfortunately, the enargite used by Ehrlich had a Cu/As weight-per-cent ratio of 5.31 to 1 (theory Cu/As = 2.54/1); this indicates that the ore was very impure. Because enargite dissolves slowly and because only the initial dissolution stage was examined in this work, it may well be that his observations apply

more to the impurities than to the enargite. One important observation arising from this work is that active bacteria can exist in the presence of dissolved arsenic or antimony. This particular observation has been confirmed by other workers¹⁰⁹.

Dutrizac and MacDonald¹¹⁰ investigated the kinetics of dissolution of enargite in acidified ferric sulphate solutions over the temperature range 60 to 95°C. These workers found that sintered discs of synthetic enargite dissolved slowly in acidified ferric sulphate solutions yielding both elemental and sulphate sulphur together with soluble copper and arsenic. The overall reaction was:



The value of x fluctuated widely, but had an average value of 1.25. The dissolution kinetics were linear and this was interpreted as indicating rate control by a reaction occurring on the surface of the mineral. Figure 11 shows the type of reaction curves obtained by these authors when synthetic enargite was leached at temperatures between 60 and 95°C. This figure clearly shows that the total dissolution kinetics are linear and that the rates of dissolution, even at 95°C, are comparatively slow. The apparent activation energy calculated from these curves for the rate-controlling process was 13 kcal/mol. The rate of copper extraction increased according to the 0.6 power of the ferric sulphate concentration and the 0.2 power of the sulphuric acid strength. The rate decreased in a complex manner with increasing strengths of the ferrous sulphate reaction product. Natural enargite dissolved like the synthetic sulphosalt and at approximately the same rate.

Tetrahedrite-tennantite

The tetrahedrite ($\text{Cu}_{12}\text{Sb}_4\text{S}_{13}$)-tennantite ($\text{Cu}_{12}\text{As}_4\text{S}_{13}$) series is commercially important not only because of its copper content but also because of its substitutionally dissolved silver values¹¹¹. Nishihara¹¹² performed qualitative experiments on the relative leachability of tetrahedrite ores and observed that this mineral dissolved rapidly in acidified ferric sulphate solutions. Sullivan⁵⁵ and Brown and Sullivan⁵⁴ studied the dissolution of relatively pure tennantite containing only a small percentage of impurities. When a leaching medium containing 2% Fe, as ferric sulphate, plus ½% H_2SO_4 was used at 35°C, 10 per cent of the copper was extracted in the first day, but only an additional 1.6 per cent copper was dissolved in the next 55 days. The authors attributed the initial reactivity to impurity dissolution, and they concluded that tennantite dissolved very slowly in ferric ion solutions. The same authors⁵⁴ also studied the dissolution of tetrahedrite in the acid ferric sulphate medium. Their tetrahedrites were very impure. When leach solutions containing 1 to 5% Fe^{3+} as ferric sulphate and ½% H_2SO_4 were employed at 35°C, the copper recoveries

ranged from 52 to 95 per cent after 30 days of leaching. Tetrahedrite was only slightly attacked by sulphuric acid solutions containing no ferric ion. Koch and Grasselly¹¹³ slickered acidic iron sulphate solutions over tetrahedrite as well as over tetrahedrite-pyrite and tetrahedrite-chalcopyrite-pyrrhotite ore mixtures. The purity of the ores was not described. From the initial rates of dissolution, these authors noted qualitatively that tetrahedrite ore dissolved more rapidly than pyrite, sphalerite, galena, or chalcopyrite. In view of the rather low purity of most tetrahedrite ores investigated, even the qualitative dissolution rates of the tetrahedrite-tennantite minerals remain somewhat in doubt and nothing whatsoever is known of the kinetics of dissolution of these minerals in acidified ferric ion media.

Bryner *et al*⁴⁶ reported briefly on the bacterial dissolution of museum-grade tetrahedrite. They observed that only 3 mg of copper dissolved from a 1 g sample after 42 days of leaching. Since their bacterial cultures were grown on a ferrous sulphate substrate, their leach media must have contained some iron at a low concentration, although none was deliberately added. Regardless of the leaching mechanism actually operating, their tetrahedrite was relatively inert.

Copper selenides and tellurides

Kholmanskikh, Ilyashevich, and Kosnareva¹¹⁴ investigated the dissolution of synthetic Cu_2Se and Cu_2Te in acidified ferric chloride solutions using a rotating-disc technique. Both compounds behaved similarly during dissolution in this medium. The

dissolution proceeded according to the reactions:



The dissolution rate was dependent on the stirring speed for speeds below 800 rev/min and was directly proportional to the concentration of ferric ion in the solution. Activation energies in the range 4 to 6 kcal/mol were reported for both reactions. These observations led the authors to postulate rate control by diffusion of ferric ion across the liquid boundary layer adjacent to the rotating disc. At disc-rotation speeds in excess of 800 rev/min, the rate was controlled by a chemical reaction on the surface of the reacting solid. It was suggested that this reaction involved the formation of a layer of slightly soluble cuprous chloride on the reaction surface and the subsequent oxidation of this material to the cupric state.

Table 5 summarizes the data obtained for the dissolution of the less frequently studied copper compounds in acidified ferric chloride or sulphate solutions.

THE DISSOLUTION OF NICKEL AND COBALT MINERALS

Nickel

Nickel minerals are broadly divided into oxides and sulphides. Nickel oxide ores are normally processed either by straight acid leaching or by selective reduction followed by ammonia-ammonium carbonate leaches. The metallurgy of nickel

TABLE 5
SUMMARY OF THE KINETICS OF DISSOLUTION OF SOME COPPER COMPOUNDS IN ACIDIFIED FERRIC SULPHATE OR FERRIC CHLORIDE MEDIA

Material	Medium	Fe^{3+} dependence	Activation energy (kcal/mol)	Temperature ($^{\circ}\text{C}$)	Rate-controlling process	Ref.
Synthetic CuFe_2S_3	Ferric sulphate	Rate increased with 0.6 power of Fe^{3+} conc.	12	45 - 90	Linear kinetics and surface controlled reaction	106
Synthetic $\text{Cu}_3\text{As}_4\text{S}_4$	Ferric sulphate	Rate increased with 0.6 power of Fe^{3+} conc.	13	60 - 95	Linear kinetics and surface controlled reaction	110
Natural tetrahedrite ($\text{Cu}_{12}\text{Sb}_4\text{S}_{13}$)	Ferric sulphate	Rate appeared independent of Fe^{3+} conc.	—	35	Slow reaction	54
Synthetic Cu_2Se	Ferric chloride	Directly dependent on Fe^{3+} conc.	4 - 5	—	Linear kinetics, solution diffusion control	114
Synthetic Cu_2Te	Ferric chloride	Directly dependent on Fe^{3+} conc.	4 - 6	—	Linear kinetics, solution diffusion control	114

sulphide ores is dominated by pyrometallurgical processes that produce a nickel-copper matte. The exception to this generalization is the Sherritt-Gordon ammoniacal pressure leach process for sulphidic nickel ores and concentrates. Within this general framework, very little work on the dissolution of nickel sulphides or nickel matte in acidified ferric sulphate or ferric chloride solutions has taken place. This general lack of published information about ferric ion leaching of nickel sulphides can also be attributed to the fact that the common nickel sulphides are readily soluble in hydrochloric acid solutions without an oxidizing agent. Thornhill, Wigstol, and Van Weert¹¹⁵ have pointed out that the presence of oxidizing agents in such chloride leaching media is undesirable because they fix the sulphur in the elemental form. It was considered to be preferable to recover the sulphur as H₂S gas rather than as elemental sulphur from the leach residues. The presence of ferric ion also tends to solubilize copper minerals; this is generally undesirable because an effort is usually made to effect a preferential nickel dissolution. There have been, nonetheless, some published studies on the dissolution of nickel sulphides by ferric ion and these are discussed below.

Urazov and Bogatskii¹¹⁶ studied the dissolution of nickel silicate minerals in acidic ferric sulphate and acidic ferric chloride solutions. They were able to extract up to 96 per cent of the nickel from garnierite (Ni₆Si₄O₁₀(OH)₈) by leaching for six hours with a 25 g/l ferric sulphate solution. The rate appeared to be directly proportional to the ferric concentration at 100°C. Other nickel silicate minerals were more refractory and required longer retention times even at high ferric ion concentrations. Almost no reaction occurred at room temperature for any of the silicate minerals. Acidified ferric sulphate solutions were stated to be more effective than either hydrochloric acid or nitric acid leaches; the ferric sulphate medium was more reactive than acidic ferric chloride solutions.

Tseft and Kryukova¹¹⁷ studied the leaching of 20 per cent nickel mattes (Ni₃S₂) in 65 g/l HCl and 100 g/l FeCl₃ solutions. Over 98 per cent of the contained nickel and cobalt were recovered in one hour by leaching at the boiling point of the solution. The nickel extraction tripled when the leaching temperature was raised from 22 to 109°C. The highest extractions were obtained with a 15 to 25 per cent stoichiometric excess of ferric chloride. These workers believed that a major advantage of the ferric chloride leach was that most of the sulphur reported in the elemental form; only 2 per cent of the sulphur was solubilized as sulphate. The ferric chloride leach was more rapid than straight hydrochloric acid dissolution and yielded a convenient sulphur product. Clearly, the advantages of obtaining either elemental sulphur or H₂S gas will depend on the particular operation under consideration¹¹⁵.

Klets and Serikov¹¹⁸ studied the dissolution of nickel concentrates in acidified ferric chloride solutions over the temperature range 20 to 80°C. The rate increased sharply with increasing tempera-

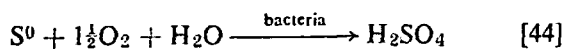
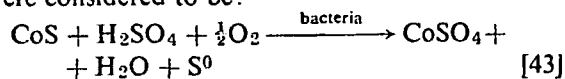
tures but was insensitive to concentrations of the ferric chloride oxidizing agent greater than stoichiometric. Over 90 per cent of the nickel was solubilized after eight hours of leaching; elemental sulphur and the platinum metals concentrated in the leach residue. Kryukova and Tseft¹¹⁹ investigated the dissolution of nickel matte (Ni₃S₂) containing 78 per cent Ni in acidified 1,0 N ferric chloride media. Over the temperature interval 22 to 78°C, the temperature coefficient of the rate was 1,2 to 1,3/10°C. The nickel matte dissolved at a rate of about 1,0 mg/cm² · min at 78°C.

Dutrizac and MacDonald²⁰⁹ studied the percolation leaching of pentlandite contained in a pyrrhotite-pentlandite ore by trickling ferric sulphate solutions through columns of the ore. Linear dissolution rates were observed up to about 75 per cent theoretical nickel extraction; slower rates were noted thereafter. At 60°C, 50 per cent nickel dissolution occurred in about 600 hours, but 2 200 hours were necessary to obtain the same extraction at room temperature. The calculated activation energy was 9 kcal/mol, which was interpreted as indicating rate control by the actual chemical dissolution of the pentlandite and not by mass transport within the leaching column. Most of the sulphur reported in the elemental form. The nickel dissolution rate increased according to the 0,20 power of the ferric ion concentration over the concentration range 0,004 to 0,2 M Fe³⁺. Increasing acid concentrations in the range 0,01 M to 1,0 M H₂SO₄ caused the rate of nickel extraction to decrease slightly. High acid concentrations not only decreased the nickel extraction rate but also increased the undesirable dissolution of the silicate gangue minerals. The nickel extraction rate increased rapidly with increasing apparent percolation flowrates to about 25 ml/h, but thereafter the flowrate had only a slight effect on the amount of nickel dissolved. Although higher flowrates produced a slight increase in the nickel dissolution rate such flows would appear to be undesirable because of the larger solution volumes thereby produced.

The bacterial leaching of nickel sulphides has also been studied. Early work by Razzell and Trussell⁷⁶ and Duncan and Trussell⁶⁴ showed that over 70 per cent of the nickel could be leached from NiS (millerite) in 14 days. The dissolution of nickel from pentlandite ((Fe, Ni)₉S₈) ores was very rapid; 87 per cent of the nickel was solubilized in five days. The authors considered the dissolution to be effected by direct bacterial action. This mechanism was confirmed by Torma¹²⁰ who obtained dissolution rates as high as 555 mg Ni/l · h from pure NiS using iron-free bacterial cultures. It appears that bacteria can solubilize nickel sulphides directly; from the previous discussion, however, it would also appear that ferric ion attack would be an important factor if iron-bearing solutions were used for bacterial leaching.

Very little work has been reported on the dissolution of cobalt sulphides, arsenides, or sulphur-arsenides in ferric media. Sutton and Corrick⁹² studied the dissolution of a low-grade cobaltite (CoAsS) ore using bacterial solutions. About 18

per cent of the cobalt was dissolved after 70 days of leaching. It was felt that the dissolution was caused by the indirect ferric sulphate attack. De Cuyper⁶³ investigated the dissolution of cobalt from carrollite (Co_2CuS_4) mineral specimens in both ferric sulphate solutions and bacterial leaching media. It was noted that no cobalt was dissolved from this mineral after 32 weeks of attack by the bacterial medium. The absence of dissolution was explained by the fact that carrollite was only slowly attacked by acidified ferric sulphate solutions. It was possible, for example, to dissolve only 2,6 mg of cobalt from 1 gram of minus-200-mesh carrollite after nine hours of leaching by a solution containing 60 g/l ferric sulphate at a pH value of 1,5. De Cuyper felt the indirect ferric sulphate leaching mechanism was of paramount importance and the absence of ferric sulphate attack on the mineral precluded any bacterial dissolution of this compound. Torma^{120,121} showed that bacterial leaching extracted up to 86 per cent of the Co from synthetic CoS after 10 days of leaching. At a 12 per cent pulp density, the cobalt extraction rate was 490 mg/l · h for the finely divided sulphide. The reactions occurring were considered to be:

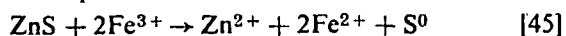


Since the sulphides were iron-free and since the bacteria were maintained in an iron-free environment, it was concluded that CoS was attacked directly by the bacteria.

THE DISSOLUTION OF ZINC AND LEAD MINERALS

Zinc

Sphalerite (ZnS) is the only zinc sulphide of any commercial significance. Its dissolution behaviour in acidic ferric solutions and in acidic bacterial solutions containing iron has been widely studied. Kuzminkh and Yakhontova¹²² investigated the dissolution of commercial sphalerite concentrates in acidified ferric sulphate solutions in the temperature interval 80 to 100°C. Rapid dissolution rates with a temperature coefficient of 1,25/10°C rise in temperature were obtained. This was interpreted as indicating rate control by solution diffusion; the rate did not appear to be impeded by the elemental sulphur reaction product, which formed according to the equation:



The initial dissolution rate was directly proportional to the concentration of Fe^{3+} in the leaching medium and this presumably indicated that the rate-controlling diffusing species was trivalent iron. The dissolution rate was independent of the initial zinc sulphate concentration of the solution (0 to 80 g/l ZnSO_4) and of the initial content of ferrous sulphate (0 to 60 g/l Fe^{2+}). It was also noted that, at constant concentration of ferric sulphate, the dissolution rate decreased with increasing acid

strengths. As the acid concentration was increased from 2 to 20 g/l, the amount of zinc dissolved decreased from 75 to 50 per cent. Later, Kuzminkh and Yakhontova¹²³ discussed the dissolution of sphalerite in the presence of other sulphides and gangue minerals. The overall kinetics and rate-controlling process appeared to be the same as for the sphalerite concentrate, although some significant differences were noted. The zinc extraction rate increased with increasing ferric concentrations to a maximum at two to three times the stoichiometric requirement; thereafter, additional ferric ion increases did not affect the rate. The rate of extraction did not depend on the concentration of ferrous sulphate nor on the acidity of the medium. In this latter regard, the results differed from those obtained for the high-grade concentrates. The rate was also shown to decrease sharply with the accumulation of the ZnSO_4 reaction product; this effect was most pronounced for ZnSO_4 concentrations below 20 g/l.

Ablanov *et al*¹²⁴ showed that a 150 per cent theoretical excess of an acid chloride solution containing 100 g/l Fe^{3+} and 50 g/l Fe^{2+} could extract over 85 per cent of the zinc from a sphalerite-bearing pyrite ore. Six hours of leaching at the solution boiling point were required. This solution could also extract 100 per cent of the zinc contained as sphalerite in a smelter matte by leaching for four to six hours at 100°C. The addition of xylene to the ferric chloride leaching medium permitted the simultaneous extraction of the elemental sulphur formed during leaching. Ermilov¹²⁵ studied the dissolution of zinc from polymetallic ores containing sphalerite. The chloride lixiviant contained 94 g/l Fe^{3+} , 60 g/l Fe^{2+} , and 5 g/l HCl together with xylene, which was added to extract the elemental sulphur liberated by the reaction. Almost 100 per cent Zn extraction was obtained by leaching for six hours at 95 to 106°C and at a 10 per cent pulp density. Total acid consumption was only 6.6 kg/tonne of ore leached. Agracheva, Volskiy, and Egorov¹²⁶ showed that sphalerite was readily soluble in acidic ferric chloride solutions. Zapevalov and Vygoda¹²⁷ found that zinc sulphide could be readily leached from mattes in one to two hours at 100°C using solutions containing 50 to 100 g/l FeCl_3 . A 20 to 30 per cent excess of oxidant was desirable.

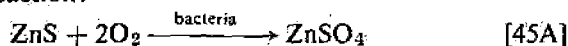
Tseft *et al*¹²⁸ used two-stage counter-current flow reactors to extract over 98 per cent of the zinc from a sphalerite ore at 106°C. The leaching solution contained 100 g/l Fe^{3+} and 50 g/l Fe^{2+} ; the ratio of liquids to solids was 2,7 to 1. Schikuni and Kamiya¹²⁹ observed that ferric ion was especially suitable for dissolving zinc from sphalerite. In oxygenated media, the dissolution of sphalerite was accelerated by the presence of dissolved Fe^{2+} and Cu^{2+} but was retarded when only Fe^{2+} or Cu^{2+} or oxygen was present. No explanation of this phenomenon was given. Many of the above works were intended to show that sphalerite could be readily dissolved under certain circumstances; accordingly, the kinetics of sphalerite dissolution were not extensively studied. An

examination of the conditions used by these authors does, however, suggest that the important parameters involved in the leaching of sphalerite by ferric ion are temperature and ferric ion concentration. The dissolution rates appear to be rapid, at least near the solution boiling temperatures.

Rudolfs and Helbronner¹³⁰, in 1922, were the first to observe that bacteria could attack zinc sulphide forming soluble zinc sulphate. Since that time, several workers have studied the bacterial dissolution of zinc sulphide or of sphalerite ores. Since ferric sulphate solutions appear to attack sphalerite rapidly, it is possible that some of the early studies on bacterial leaching included an indirect ferric ion leaching component. Indeed, Ivanov^{77,44} stated that the chief role played by bacteria in the dissolution of zinc sulphide ores was the oxidation of ferrous sulphate to the trivalent state. The ferric ion thus produced was responsible for the dissolution of the ZnS.

Although dissolved iron doubtless plays an important role in the dissolution of ZnS, especially under commercial conditions, several workers have shown that bacteria can extract zinc from more or less iron-free systems. In this connexion it should be noted that the dissolution of natural sphalerite inevitably produces some Fe³⁺ ions because iron is an integral part of the lattice of naturally occurring sphalerite. Only synthetic sphalerite is free of the several per cent iron that is characteristic of this mineral. For this reason the results reported by Golbraikhy and Ilyaletdinov¹³¹ for the dissolution of sphalerite from complex Fe-Zn-S ores must have included some indirect leaching by the ferric ion, although these workers noted that the dissolution rates in the presence of bacteria were 2 to 10 times more rapid than in the absence of the bacteria.

It is now well established that bacteria can attack zinc sulphide directly according to the reaction:



Duncan and co-workers^{94,132,133,134} achieved high rates of zinc extraction from zinc sulphide by optimizing the conditions for bacterial growth. This was done by adding nutrients to the solutions and by enriching the aerating gas with carbon dioxide. The enhanced dissolution rates under conditions of rapid bacterial growth presumably indicated direct bacterial attack of the ZnS. Torma^{120,121} dissolved pure synthetic zinc sulphide in iron-free solutions and obtained very high dissolution rates. Zinc extraction rates as high as 1150 mg/l · h were realized, using very small particle sizes. Since iron-free media were used in these studies, it is clear that rapid direct bacterial attack of ZnS is feasible under suitable conditions.

It has been possible to achieve very concentrated zinc sulphate solutions by bacterial leaching or by bacterial-ferric sulphate leaching of sphalerite concentrates. An estimate of the solution concentrations that can be obtained by these leaching techniques can be determined from Table 6. A steady increase in the maximum dissolved zinc

concentration has been achieved over the years. The concentrations reported by Torma³¹ appear to be suitable for zinc recovery by commercial electrolytic processing. Such high zinc concentrations have been made possible by finely grinding the zinc concentrate and by optimizing the conditions for bacterial activity. The high concentrations also reflect a high immunity by the micro-organisms towards soluble zinc; such immunity can be gradually acquired by the bacteria. There appears to be no fundamental reason why similarly high solution concentrations could not be produced by bacterial leaching of copper, nickel, or other elements.

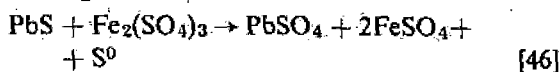
TABLE 6
MAXIMUM DISSOLVED ZINC
CONCENTRATIONS ACHIEVED BY VARIOUS
WORKERS

Workers	Date	Maximum zinc concentration g/l
Zimmerley, Wilson, and Prater ¹²³	1958	17
Marchlewitz and Schwartz ¹²⁶	1961	25
Silverman and Ehrlich ¹²⁷	1964	40
Moss and Andersen ²⁴	1968	30-50
Torma ³¹	1970	120

Lead

Galena (PbS) is readily attacked by ferric ion over a wide range of conditions. If the leaching is done in a chloride media, soluble lead chloride complexes are formed; if the attack is done by sulphate solutions, an insoluble lead sulphate is produced that is, however, soluble in an excess of chloride ion. Both types of leaching medium have been advocated for various ores. If the ore mineralogy is simple, the direct dissolution of lead as the soluble chloride would appear to be advantageous. If the galena is associated with other sulphides, it might be possible to use a ferric sulphate leach to extract much of the impurity content while leaving the lead as an insoluble precipitate for subsequent processing.

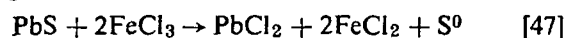
Kuzminkh and Yakhontova¹²³ studied the dissolution of galena-sphalerite concentrates in acidified ferric sulphate solutions in the temperature interval 80 to 110°C. The galena was attacked according to the reaction:



Linear kinetics were observed and the rate increased about 1.5 times as the temperature was raised from 80 to 100°C. The rate of dissolution was propor-

tional to the pulp density. Approximately half of the lead was oxidized during five hours of leaching at 100°C. Haver, Uchida, and Wong¹³⁸ described a process that embodied acid-ferric sulphate leaching of galena followed by the production of electrolytic lead and elemental sulphur. These workers noted a rapid increase in the rate of reaction as the temperature was raised from 25 to 100°C. An initially rapid reaction was observed, followed by a slower second stage of leaching. The reaction between ferric sulphate and galena displayed parabolic kinetics, probably because of the progressive thickening of the sulphur film formed on the particles during leaching. The rate of reaction increased with increasing ferric sulphate concentrations to a limit of 400 g/l Fe₂(SO₄)₃; the rate was independent of higher ferric ion concentrations. The galena oxidation rate was independent of the pH of the leach solution. The authors concluded that the rate was controlled by ferrous sulphate diffusion through the constantly thickening sulphur layer formed on the galena surface.

Vasilev and Muratova¹³⁹ investigated the reaction between galena and acidified ferric chloride solutions. The galena was found to dissolve according to the reaction:



It was observed that the elemental sulphur coated the galena and made complete dissolution of this mineral very difficult. Volskii, Agracheva, and Egorov^{140,126,141} described a process based on the leaching of galena by ferric chloride solutions followed by the electrolytic deposition of lead and the electrolytic reoxidation of the iron chloride leaching medium. The galena concentrates were leached at 80°C by an acidified solution containing 100 to 200 g/l Fe³⁺. Recoveries of 98 to 99 per cent were claimed for lead processed by this technique. Tseft, Livinskii, and Vygoda¹⁴² also demonstrated the effectiveness of acidified ferric chloride solutions in dissolving galena concentrates. At 100°C, 100 per cent lead extraction was achieved by leaching for two hours in solutions containing 28 to 147 g/l Fe³⁺. The ferric chloride leaching medium was more effective than ferric sulphate solutions under similar conditions. Pande¹⁴³ has shown that a similar process is possible using ferric nitrate solutions that were selected because of the high solubility of lead nitrate.

The bacterial leaching of lead-bearing sulphides has not been widely investigated, probably because of the low solubility of the lead sulphate reaction product. Corrick and Sutton¹⁴⁴ studied the bacterial leaching of Pb-Cu-Fe mattes under a wide range of experimental variables. Leaching minus-325-mesh matte at a liquid-to-solids ratio of 30 to 1, they were able to extract 70 per cent of the contained lead after 11 days. The extraction rate decreased as the pH increased. Lyalikova *et al*¹⁴⁵ have shown that bacterial leaching can oxidize the minerals boulangerite (Pb₅Sb₄S₁₁), zinkenite (Pb₅Sb₄S₂₇), jamesonite (Pb₅FeSb₆S₁₁), and geocronite (Pb₅Sb₂S₈) with the formation of insoluble lead sulphate.

THE DISSOLUTION OF PYRRHOTITE AND PYRITE

The reaction of pyrrhotite (Fe_{1-x}S) and pyrite (FeS₂) with acidified ferric solutions is an important part of ferric ion leaching. These iron minerals are ubiquitous and their reaction with oxygen in either the presence of or the absence of bacteria can lead to a substantial increase in the ferric ion concentration of the solution. By contrast, their reaction with dissolved ferric ion in the absence of free oxygen can lead to the eventual depletion of the ferric ion content of the leaching solution. In some deposits pyrite and pyrrhotite contain significant quantities of cobalt and/or nickel, and the dissolution of these minerals can also lead to the eventual liberation of the more valuable elements.

Relatively little recent work has been published on the ferric ion leaching of pyrrhotite. Pyrrhotite reacts rapidly with hydrochloric acid under rather mild conditions; consequently, the addition of an oxidizing agent has not proved necessary to dissolve this mineral. Parsons and Ingraham¹⁴⁶ recently reviewed the kinetics of reaction of pyrrhotite with hydrochloric acid. Ingraham, Parsons, and Cabri¹⁴⁷ studied the dissolution of pyrrhotite in hydrochloric acid. They observed very rapid reactions leading to complete dissolution of the mineral. The degree of reaction was dependent on a combination of temperature and acid concentration; with 35 per cent HCl in the leaching medium, the reaction went to completion at all temperatures above 40°C. The reaction with stoichiometric FeS produced only H₂S:



When iron-deficient pyrrhotites were used, some elemental sulphur was produced:



Pilgrim and Ingraham¹⁴⁸ summarized the processes used to recover elemental sulphur from H₂S-containing gases. Presently available processes can economically recover sulphur from a variety of gas streams under a wide range of conditions. Within this framework, much of the recent work on pyrrhotite dissolution has concentrated on direct hydrochloric acid leaching, and little work has been done on the ferric ion leaching of this mineral.

Ferric ion leaching has, however, several advantages over direct acid attack. First, the sulphur is produced in the elemental form; this removes the need for a Claus-type sulphur recovery plant. Second, acid is not consumed during the reaction; also, relatively low acid concentrations can be employed. Third, the iron leaching media can be conveniently regenerated, either by electrolysis or by bacterial action. Several early workers attempted to use ferric ion leaching of pyrrhotite as a means of producing high purity electrolytic iron. This early work has been summarized by Traill^{10,11,12} whose own experiments showed that boiling concentrated ferric chloride solutions could completely oxidize ground pyrrhotite ores during two hours of leaching. The dissolution kinetics were initially

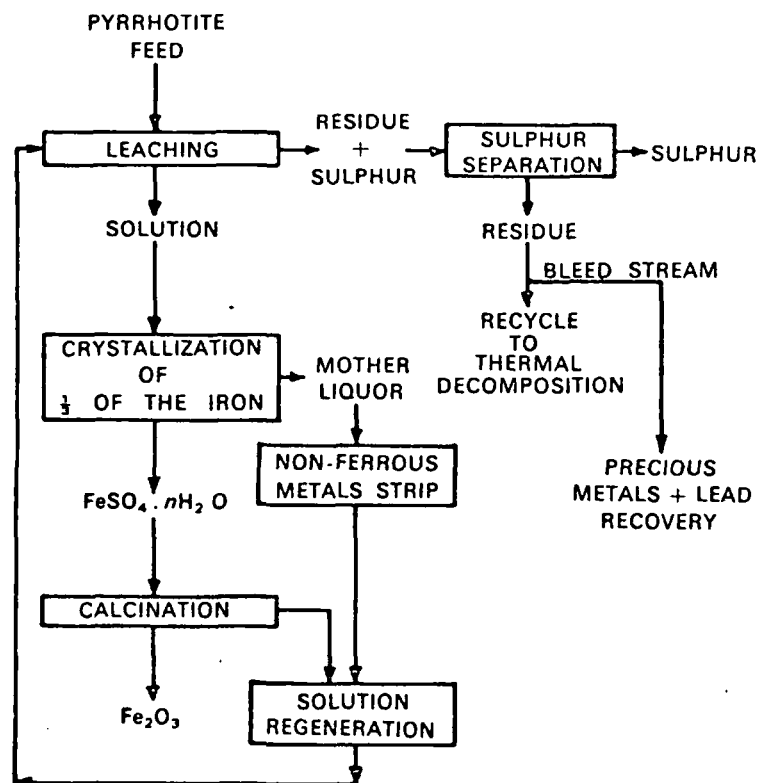
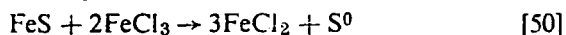


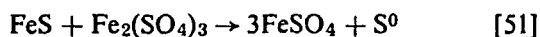
FIGURE 12 Proposed flowsheet for the leaching of pyrrhotite concentrates by acidified ferric sulphate solutions. (From Ref. 149)

linear and the pyrrhotite was found to dissolve according to the reaction:



The reaction was not retarded by the accumulation of the ferrous chloride reaction product. The ferric leaching solution was regenerated during electrolysis, which was primarily designed to produce pure iron powders.

Lowe⁵⁸ studied the dissolution of mounted specimens of pyrrhotite in acidified ferric sulphate solutions in the temperature interval 32 to 68°C. At temperatures below 50°C, linear kinetics were observed together with an apparent activation energy of 9 kcal/mol. The rate was independent of the ferric ion concentration for ferric strengths between 0,025 and 0,208 M. The rate varied in a complex manner with changing pH. Lowe interpreted these results to indicate rate control by chemisorption on the surface of the pyrrhotite. At temperatures above 50°C, the rate decreased sharply because of the formation of H₂S by direct acid attack of the sulphide. At the lower temperatures, the pyrrhotite was found to dissolve according to the reaction:



Subramanian, Stratigakos, and Jennings¹⁴⁹ recently described a process by which both iron oxide suitable for iron making and elemental sulphur, could be recovered by leaching pyrrhotite in acidi-

fied ferric sulphate solutions according to the reaction:

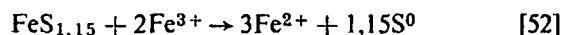
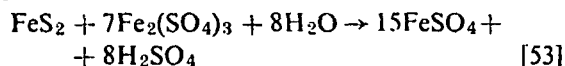


Figure 12 shows the proposed flowsheet for this process. About 50 per cent of the pyrrhotite was dissolved in the first 2 h of leaching (11 g/l Fe³⁺) but five hours of attack were needed for complete iron extraction. The accumulation of the ferrous sulphate reaction product did not retard the dissolution reaction. Subramanian *et al*¹⁴⁹ also proposed a similar process for leaching pyrrhotite in acidified ferric chloride media, which attacked this mineral more rapidly than ferric sulphate solutions. Most of the iron was extracted in less than 1 h at 95°C by an excess of 40% FeCl₃ solution. The evolution of H₂S occurred under all conditions and accounted for 6 to 25 per cent of the oxidized sulphur. The addition of Cu²⁺ ions catalysed the oxidation of H₂S, and reduced the amount of sulphur reporting in this form to less than 3 per cent of the feed total. These authors believed that the rapid and efficient re-oxidation of the iron leaching medium was a vital part in any leaching process using either ferric chloride or ferric sulphate media.

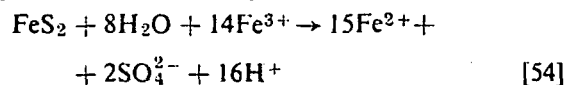
Pyrite (FeS₂) does not respond favourably to leaching by ferric ion. Tseft and Tatarinova¹⁵⁰ studied the dissolution of pyrite in both ferric chloride and ferric sulphate media and postulated that the slow rate of attack was caused by the formation of a protective sulphur layer on the

sulphide surface during leaching. Ferric chloride was found to be a more effective lixiviant than ferric sulphate solutions. Thomas and Whalley¹⁵¹ observed that minus-200-mesh pyrite reduced 25 per cent of the Fe³⁺ ion from a ferric sulphate solution after 3½ h of leaching at 90°C. The reaction was thought to occur according to the equation:



The rate of ferric ion attack was more rapid than either the direct air oxidation of pyrite to ferric sulphate or the air oxidation of ferrous ion to the ferric state.

Garrels and Thompson⁴² studied the dissolution of pyrite specimens from different sources in acidified ferric sulphate solutions. The various pyrites dissolved at widely differing rates, although the mechanism of dissolution appeared to be the same for all the specimens. The rate was independent of the acid concentration over the pH interval 0 to 2.0. The rate was also independent of the initial Fe³⁺ concentration of the solution over the range 10⁻⁵ to 10⁻³ M Fe³⁺. The rate depended, however, on the ratio of Fe³⁺ to Fe²⁺ in the leaching medium. These authors interpreted the results as indicating rate control by differential adsorption of ferric and ferrous ions on the surface of the pyrite. The rate of the postulated reaction:



was felt to be directly proportional to the fraction of the pyrite surface occupied by ferric ions.

THE DISSOLUTION OF OTHER SULPHIDE-TYPE MINERALS

Molybdenum

Usataya¹⁵² studied the dissolution of molybdenite (MoS₂) under a variety of experimental conditions. He found that dissolved ferric ion promoted the dissolution of this mineral but that ferrous ion prevented its oxidation. The dissolution of molybdenum was greatly complicated by the formation of insoluble reaction products under certain conditions. Increasing the temperature of the ferric leaching medium produced poor results, since the formation of insoluble molybdates increased rapidly with increasing temperatures in acidic media. Elemental sulphur was observed as a reaction product during the leaching. Bhappu *et al*^{153,154,155} investigated the dissolution of molybdenite in various media, but these workers observed no molybdenum dissolution after 25 hours of leaching at room temperature by acidified ferric chloride solutions.

The leaching of molybdenite in the presence of bacteria was studied by Bryner and Anderson⁹⁷ who noted that molybdenite was readily solubilized. After nine months of leaching, 35 to 55 per cent of the molybdenum in various sulphide ores could be extracted by the bacterial leaching solu-

tions. Molybdenum concentrations in excess of 25 p.p.m. were obtained by acclimatizing the bacteria to this dissolved metal. The bacterial leaching rate increased rapidly in the presence of dissolved iron as can be seen in Figure 13, which

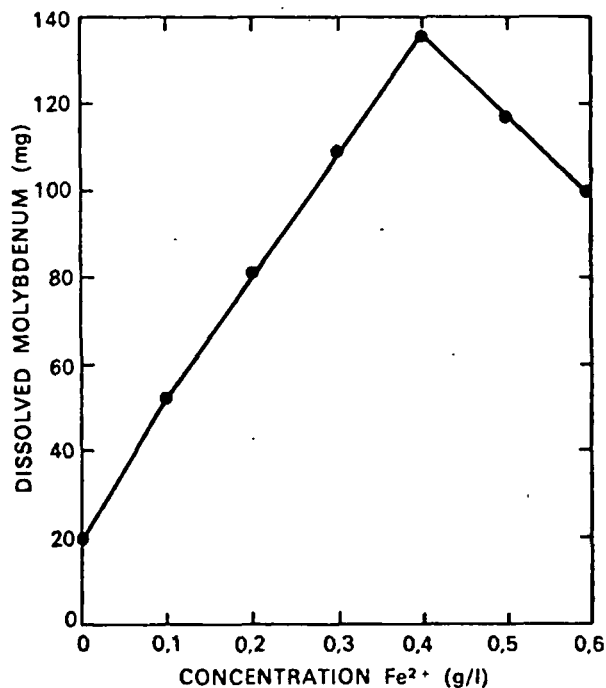


FIGURE 13 The effect of the initial dissolved iron concentration on the bacterial leaching of molybdenum from molybdenite ores.

(From Ref. 97).

shows the effect of the initial dissolved iron content on the final quantity of dissolved molybdenum. Since dissolved iron would be quickly oxidized to the ferric state by the bacteria, the results shown in this figure may indicate a substantial indirect ferric ion leaching component during the bacterial oxidation of MoS₂. Bryner and Jameson⁴⁷ and Kramarenko¹⁵⁶ also observed that molybdenite could be dissolved during bacterial leaching. Bhappu *et al*^{153,154,155} showed that molybdenite was dissolved about five times more rapidly in the presence of bacteria than in their absence. They were able to obtain solutions containing 15 to 25 p.p.m. molybdenum by progressively adapting their bacteria to this element. Under certain conditions insoluble molybdenum compounds formed and this rendered further dissolution of the molybdenite impossible. Duncan *et al*¹³² were able to obtain molybdenum concentrations as high as 90 p.p.m. by repeatedly transferring the bacterial culture in the presence of molybdenum. Thus it appears that bacteria can acclimatize to molybdenum but only at relatively low concentrations. The solution concentrations achieved to date are not overly promising and it appears that ferric ion attack, with or without bacteria, is not an attractive method of leaching molybdenite.

Arsenic and antimony

Ehrlich¹⁵⁷ studied the dissolution of orpiment (As_2S_3) by *Ferrobacillus ferrooxidans*. Both arsenate and arsenite were produced during the reaction and the sulphur was oxidized to sulphate, a fact that caused the solution to become more acidic during the tests. The biological leaching appeared to be about three times more effective than the straight chemical attack caused by air or by ferric ion leaching. It should be noted, however, that the iron content of the bacterial leaching media increased during the tests and that the presence of this soluble ferric sulphate could be a factor in the overall dissolution process. Ehrlich¹⁰⁸ also studied the dissolution of arsenopyrite ($FeAsS$) under similar conditions. For this mineral, it was found that the biological leaching rates were about twice as fast as the sterile control experiments. The concentrations of dissolved iron increased during the experiments and, thus, there may have been a substantial ferric ion leaching component in these results. It was noted that the dissolved arsenic was present as both arsenate and arsenite. Some of the iron liberated during leaching formed insoluble iron arsenates. The sulphur was oxidized to sulphuric acid, which lowered the pH of the leaching medium as the experiments progressed; during 21 days of leaching the pH value fell steadily from 3,5 to about 2,5. Polkin *et al*¹⁵⁸ used bacterial leaching to remove arsenic from sulphide-oxide tin

ores prior to tin recovery; the mineralogical state of the arsenic was not given. Solutions containing *Thiobacillus ferrooxidans* at 30°C and a pH value between 2,2 and 2,5 were found to effect complete removal of the arsenic. It was noted, however, that some of the dissolved arsenic was re-precipitated as iron arsenate or iron arsenite. Dissolved ferric sulphate assisted the dissolution of the arsenic from the sulphide ores.

Tugov and Tsyganov¹⁵⁹ leached stibnite (Sb_2S_3) ores with acidified ferric chloride solutions in order to extract the antimony; this was subsequently precipitated by metallic iron. Elemental sulphur was produced during the dissolution and the leaching medium was regenerated by chlorine gas.

Cadmium and mercury

Brissette, Champagne, and Jutras¹⁶⁰ leached pure CdS plus elemental sulphur using acidified ferric sulphate media containing *Thiobacillus thiooxidans*. This leaching medium extracted about 70 per cent of the cadmium after six weeks of leaching. Optimum leaching conditions were found to occur at 32°C using solutions at a pH value of 0,7; this pH is low for bacterial activity. An indirect leaching mechanism is suggested since the bacteria were unable to oxidize the sulphide sulphur in the absence of added elemental sulphur. Pande^{161,162} has shown that mercury sulphide ores can be selectively leached by acidified solutions of ferric

TABLE 7

SUMMARY OF THE KINETICS OF DISSOLUTION OF NON-COPPER SULPHIDES IN ACIDIFIED FERRIC SULPHATE AND FERRIC CHLORIDE MEDIA

Material	Medium	Fe ³⁺ dependence on rate	Activation energy (kcal/mol)	Temperature (°C)	Rate-controlling process	Ref.
Ni ₃ S ₂ in matte	1,0 N Ferric chloride	—	~6	22 - 78	—	119
Pentlandite ore (Ni, Fe) ₉ S ₈	Ferric sulphate	Rate increased with 0,20 power of Fe ³⁺ concentration	9	25 - 60	Chemically controlled	209
ZnS concentrate	Ferric sulphate	Directly proportional to Fe ³⁺ concentration	~6	80 - 100	Fe ³⁺ diffusion in solution	122, 123
PbS	Ferric sulphate	Rate increased with increasing Fe ³⁺ concentrations to 400 g/l Fe ₂ (SO ₄) ₃ ; thereafter independent	High	25 - 100	Parabolic kinetics indicative of diffusion through protective sulphur layer	138
Pyrrhotite 'FeS'	Ferric sulphate	Independent of Fe ³⁺ conc. between 0,025-0,21 M Fe ³⁺	9	32 - 50	Chemisorption on surface of pyrrhotite	58
Pyrite FeS ₂	Ferric sulphate	Independent of Fe ³⁺ conc. between 10 ⁻⁵ and 10 ⁻³ M Fe ³⁺	—	33	Differential chemisorption on surface of pyrite	42

nitrate or ferric acetate. The mercury enters the solution and the sulphur remains in the residue in the elemental form.

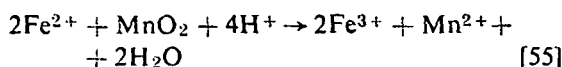
Table 7 summarizes some of the kinetic data available for the ferric ion leaching of sulphide minerals that do not contain copper. It is clear that none of these sulphides has been studied in great detail, and much work remains to be done in this area. The limited data available suggest that ferric ion rapidly attacks the indicated minerals and that possible commercial applications might be found for a ferric ion leaching process.

THE DISSOLUTION OF URANIUM MINERALS

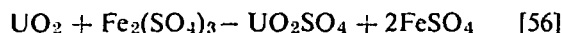
Uranium minerals can be conveniently divided into three general groups:

- primary oxides such as uraninite or pitchblende (UO_2+x),
- primary minerals such as brannerite (UTi_2O_6) in which the uranium is compounded with other metal oxides,
- secondary minerals containing hexavalent uranium such as carnotite ($\text{K}_2(\text{UO}_2)_2(\text{VO}_4)_2 \cdot 3\text{H}_2\text{O}$) or autunite ($\text{Ca}(\text{UO}_2)_2(\text{PO}_4)_2 \cdot 10\text{H}_2\text{O}$).

Although the third group of minerals is readily soluble in dilute mineral acids, minerals of the first two types require the presence of an oxidizing agent to effect the uranium dissolution. From this point of view, the uranium oxide minerals are similar to the base metal sulphides. Many oxidizing agents have been used during the dissolution of uranium from its ores; the choice is usually made on economic grounds. Some of the leaching agents used include: ferric ion, manganese dioxide, hydrogen peroxide, sodium and potassium chlorates, and nitric acid. It has been suggested that the addition of an oxidant such as sodium chlorate or manganese dioxide is sufficient, by itself, to effect the dissolution of uranium. This does not appear to be the case, however, and it has been noted¹⁷ that dissolved iron must also be present. The iron can be added deliberately to the leaching medium, it can be generated by bacterial activity, or it can simply be present as an acid soluble iron mineral in the uranium ore. The purpose of the other oxidizing agents is then to assure that all the iron is oxidized to the trivalent state; for example:



The ferric ion then attacks tetravalent uranium oxidizing it to the acid-soluble hexavalent state:



Several general reviews of the overall processing of uranium ores are available, and the reader is referred to those of Pinkney, Lurie, and Van Zyl¹⁶³, Thunæs and Colborne¹⁶⁴, Merritt¹⁶⁵ and Wilkinson¹⁶⁶.

In practice the leaching of South African ores is conducted at 60 per cent solids using solutions containing 50 to 80 lb/t sulphuric acid and 5 to 10 lb/t MnO_2 at temperatures up to about 60°C.

Laxen¹⁶⁷ studied the dissolution of South African uranium ores in acidified ferric sulphate solutions. He showed that a concentration of 0,5 g/l Fe^{3+} was adequate to achieve maximum uranium extraction from all the ores studied when using a laboratory-scale leaching technique at 1 per cent solids. It was also shown that nearly complete uranium extractions were possible with this technique by leaching for 14 days at 28°C with solutions containing 4 g/l each of ferric ion and of sulphuric acid. It was noted that the presence of phosphate was deleterious to the dissolution reaction. This was postulated to be an effect on some uranium minerals in the ores and not due to the complexing action of phosphate on ferric ions. The work indicated that the important reagent during uranium dissolution was ferric sulphate. This last observation has been emphasized by several workers. For example, Miller, Napier, and Wells,¹⁶⁸ observed that uraninite dissolution was easily affected by acidified ferric sulphate solutions containing as little as 0,2 g/l Fe^{3+} . Ehrlich, Roach, and Hester¹⁶⁹ observed that the uranium leaching solutions must contain at least 2 g/l Fe^{3+} , even when sodium chlorate or nitric acid were added to the ore. Arden¹⁷⁰ reviewed the early leaching of uranium ores and noted that the uranium dissolution reaction was catalysed by the presence of soluble compounds of trivalent iron. He also observed that the use of small amounts of a soluble iron intermediary made it apparently possible to use insoluble oxidizing agents, such as MnO_2 , to dissolve uranium.

Several workers^{171,172,173} have patented the use of ferric ion as a catalyst to dissolve uranium oxide ores. Ferric ion was added to the leach solutions in amounts ranging from 0,3 g/l to 10 g/l Fe^{3+} ; additional oxidizing agents were also added to keep all the iron in the trivalent state. In every instance, sulphuric acid solutions were the leaching medium. Acid consumption during leaching was always much greater than that required to dissolve the contained uranium because the major acid consumption is determined by the gangue minerals present. The generation¹⁷⁴ of acidified ferric sulphate solutions suitable for uranium leaching and the re-generation¹⁷⁵ of reduced uranium leach liquors have also been investigated and patented.

Kanevskii, Filippov, and Nesmeyanova¹⁷⁶ studied the kinetics of dissolution of UO_2 in acidified ferric media in the presence of various oxidizing agents. When the leaching was done in the presence of manganese dioxide, the ferric ion functioned as the active oxidizing agent. Certain hydrolysed forms of the ferric ion, such as $\text{Fe}(\text{OH})^{2+}$ or $\text{Fe}(\text{OH})_2^+$ were highly effective in oxidizing the uranium contained in uraninite ores. It should be remarked, however, that such hydrolysed species are not abundant under the acidic conditions used for uranium leaching (see Figure 4). It was stated that ferric ion was not an efficient oxidizing agent at low temperatures, but this observation does not appear to be in accord with general uranium leaching practice. It was also stated that iron did not

play an important catalytic role during the oxidation of UO_2 by nitric acid.

Celeda and Lara¹⁷⁷ investigated the mechanism of acid dissolution of pure synthetic U_3O_8 powders in the presence of ferric ion. Essentially linear dissolution curves were obtained up to 30 per cent total dissolution; thereafter, the rates decreased, probably because of the reduction of the active surface area of the powders used in these experiments. The pH of the solution was found to have relatively little effect on the dissolution rate at constant iron concentration. Increasing the acid concentration from a pH value of 2,0 to 0,7 increased the uranium extraction rate only by a factor of 2. It was felt that increasing acid concentrations liberated more ferric ions from sulphato- or hydroxo-complexes, and that the liberated ions were responsible for the observed rate acceleration. Increasing sulphate ion concentrations, at constant ferric strength, caused the rate to decrease sharply. This effect was attributed to the preferential adsorption of sulphate ions on the surface of the U_3O_8 . The rate of uranium extraction was found to increase according to the square root of the ferric ion concentration. Figure 14 shows the effect

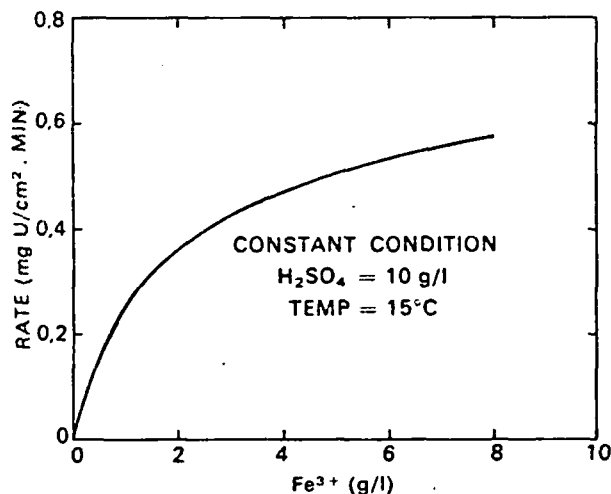


FIGURE 14 The effect of the ferric ion concentration on the rate of leaching of uraninite.

(From Ref. 178)

of ferric ion concentration on the rate of uranium dissolution from uraninite ores. This particular diagram is taken from the work of Laxen¹⁷⁹. This figure shows that the uranium leaching rate is strongly dependent on the ferric concentration at low ferric strengths, but is relatively independent of the ferric concentration at the higher ferric strengths. The activation energy calculated by Celeda and Lara¹⁷⁷ for the rate-limiting step was 15 to 19 kcal/mol. The rate was controlled by the transformation of activated surface centres in the oxidized products prior to their dissolution. It was felt that these centres were created as the result of the establishment of a redox-equilibrium between

the solution containing ferric ions and the surface of the solid U_3O_8 . The presence of other dissolved ions reduced the uranium reaction rate by a process of competitive adsorption on the active sites.

Arden and Beaumont¹⁷⁸ showed that only hydrogen peroxide of all the common oxidizing agents could rapidly oxidize uraninite in the absence of ferric ions; other common oxidizing agents required the presence of dissolved Fe^{3+} ion. The ratio of uraninite oxidation depended on the oxidation potential, and hence upon the $\text{Fe}^{3+}/\text{Fe}^{2+}$ ratio. If this rate were less than about 4 g/l, the rate of oxidation was very slow. It was felt that solutions of ferric sulphate only were unsatisfactory as a lixiviant, since the ferrous sulphate, formed as a result of the reaction, slowed and eventually stopped the reaction. If large amounts of Fe^{2+} were in solution, then a great excess of ferric ion had to be added to obtain satisfactory dissolution rates. According to these authors, it is better to use about 0,5 g/l Fe^{3+} in solution to effect the actual dissolution and to add other oxidizing agents to guarantee that the ferrous ion reaction product is immediately re-oxidized to the ferric state. Most commercial operations have used this approach. The reaction of ferric ion with UO_2 is strongly temperature dependent. As an example, after 24 h of leaching at 8°C only 16 per cent of the uranium was extracted from a UO_2 sample. Under the same conditions, but at 26°C, about 90 per cent uranium dissolution was achieved; at 40°C, 100 per cent dissolution occurred in this time interval.

Laxen¹⁷⁹ has discussed the dissolution of UO_2 by ferric ion in terms of electron transfer mechanisms. The rate of dissolution of UO_2 in acidified perchlorate solutions depended to a great extent on the anions present and on the pH of the medium. The rate of dissolution in a perchlorate medium — in which the uncomplexed ferric ion would be present — was virtually zero, while small additions of sulphate catalysed the reaction due to the formation of the active ferric complexes — thought to be mainly FeSO_4^+ . Sulphate solutions were found to be ideally suited for rapid uranium dissolution. At constant ferric ion concentration, the rate of dissolution of uranium from UO_2 passed through a rate maximum at about pH = 2; it was felt that this acidity produced the maximum concentration of the active ferric complexes in the solution. Apparent activation energies of about 16 kcal/mol were obtained from the rate-controlling dissolution reaction over the temperature interval 15 to 35°C. The uranium dissolution rate was found to increase as the Fe^{3+} concentration, while the presence of the ferrous ion reaction product in the leaching solution reduced the dissolution rate of UO_2 .

The Butler-Volmer equation is a mathematical expression connecting the chemical reaction rate of an electron transfer reaction occurring under the influence of an electrical field. Needes and Nicol¹⁸⁰ showed that the dependence of the dissolution rate of UO_2 on the Fe^{3+} was in accordance with the Butler-Volmer relationship. Needes and Nicol further showed that the Butler-Volmer equation predicted that at constant Fe^{3+} concentration the $\text{Fe}^{3+}/\text{Fe}^{2+}$

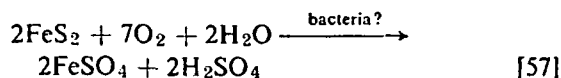
ratio should vary as the inverse square of the rate of dissolution of UO_2 . Laboratory results were in agreement with this prediction.

Sklibova-Klbalova and Neumann¹⁸¹ found the uranium leaching rate in acidified ferric sulphate solutions to be controlled by the transfer of an intermediate reaction product from the surface of the UO_2 into the bulk leaching medium. In an earlier publication, Laxen¹⁸² studied the dissolution of pure natural uraninites in acidified ferric sulphate solutions. Linear dissolution curves were obtained under all conditions and the activation energies associated with the dissolution of the natural uraninites were in the range 11 to 15 kcal/mol. The dissolution rate increased with increasing Fe^{3+} concentrations and appeared to approach a constant value at ferric concentrations greater than about 8 g/l. These observations are consistent with those reported earlier by Sobkowski, Stuglik, and Minc¹⁸³ for the dissolution of U_3O_8 in acidified ferric sulphate solutions. These latter workers found the dissolution reaction to vary with the 1/3 power of the ferric ion concentration and to have an activation energy of 14.5 kcal/mol. Both laboratories concluded that the rate was controlled by a chemical reaction occurring at the surface of the uranium mineral; this reaction directly involved adsorbed ferric ion.

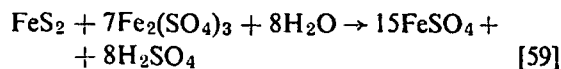
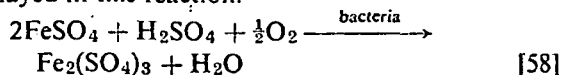
Laxen¹⁸² also noted that increasing hydrogen ion concentrations, at constant Fe^{3+} and SO_4^{2-} concentrations, first decreased, and then increased the uranium dissolution rate. Increasing sulphate ion concentrations sharply decreased the extraction rate. The decrease was attributed to the complexing of the ferric ion to form relatively unreactive iron-sulphate complexes. The presence of some sulphate ion is, however, essential to form the active leaching complex for U^{4+} dissolution. Control of the total sulphate concentration is an important part of uraninite leaching. The addition of Fe^{2+} or Mn^{2+} ions decreased the uranium dissolution rate.

Uranium oxide minerals are readily soluble in acidified dilute ferric sulphate solutions; such solutions are conveniently generated by bacterial action on pyrite or dissolved iron sulphates. Such bacterial leaching media have been proposed as one means of recovering uranium from low-grade ores. This method was used commercially at Stanrock Uranium Mines¹⁹ to recover over 10 000 lb U_3O_8 /month. Water was applied to the stopes and the combination of moisture, air, and bacteria generated an acidic ferric ion lixiviant, which extracted the uranium. Fisher¹⁸⁴ described the bacterial leaching of worked-out stopes at the Milliken Mine, Elliot Lake District, Canada. The bacterium *Thiobacillus ferrooxidans* was identified as being the active species in these waters. During a one-year leaching programme, 127 000 lb of uranium were recovered from bacterial leach solutions containing 0.13 g/l U. Nutrients to support bacterial growth were added in dry form to the ore and this practice greatly accelerated the overall uranium leaching rate. The cost of the nutrients (added at 3 g of 9K nutrient per ft^2 of floor area) was relatively small

compared to the value of the additional uranium recovered. The rate of bacterial leaching was strongly temperature dependent. When the normal mine temperature of 18°C was lowered to 14°C during the winter months, the bacterial activity dropped 30 to 40 per cent. It was felt that the major role played by the bacteria was to keep all the iron in the trivalent state, thereby providing a solution with a high oxidizing potential. Harrison, Gow, and Ivarson¹⁸⁵ have described the isolation and identification of the *Ferrobacillus-Thiobacillus* group of bacteria from Elliot Lake mine waters. It was shown that the presence of these microorganisms resulted in a substantial increase in the rate of uranium leaching from the ores. These workers believed that the accelerated leaching rate was brought about as a result of the following reactions:



The authors were not sure what role bacteria played in this reaction.



The ferric sulphate produced according to reaction [58] then oxidized the uranium oxides:



Duncan *et al*¹³² showed that uranium inhibited *Thiobacillus ferrooxidans*, but that the bacteria could adapt rapidly to increasing uranium concentrations. A single bacteria transfer enabled the microorganisms to function in the presence of 500 p.p.m. uranium. It was felt that uranium inhibition of bacterial activity would not be an important factor in the leaching of low-grade ores. Duncan and Bruynesteyn¹⁸⁶ also discussed the role of bacteria in uranium leaching. They believed the chief role played by the bacteria was to generate, from pyrite, the acidified ferric sulphate leaching medium that ultimately extracted the uranium. In experiments conducted on actual stopes, it was found that the addition of minor amounts of ammonium sulphate and other nutrients resulted in improved rates of uranium recovery. It was also observed that maximum uranium production was obtained from stopes that were never permitted to become fully dry. Aslam and Aslam¹⁸⁷ pointed out the process advantages to be gained by deliberately adding nutrients to accelerate the bacterial activity. Gow *et al*¹⁸⁸ stated that the bacterial production of acid from pyrite is the slow step in the bacterial leaching of uranium ores. The rate of uranium leaching can be accelerated by enhancing the bacterial oxidation of pyrite; the addition of nutrients is one convenient method of accelerating this activity. Mroost and Lloyd¹⁸⁹ investigated the leaching of uranium from gold slimes by bacterial activity. Again it was felt that the role of the bacteria was to generate a suitable

TABLE 8

SUMMARY OF THE KINETICS OF DISSOLUTION OF URANIUM OXIDES IN ACIDIFIED FERRIC SULPHATE MEDIA

Material	Medium	Fe ³⁺ dependence on rate	Activation energy (kcal/mol)	Temperature (°C)	Rate-controlling process	Ref.
Synthetic U ₃ O ₈	Ferric sulphate	Rate increased according to conc. of (Fe ³⁺) [‡]	15 - 19	25 - 55	Surface reaction controlled by transformation of active centres	177
Synthetic UO ₂	Ferric sulphate	Rate increased according to conc. of (Fe ³⁺) [‡] as predicted by Butler-Volmer	16	15 - 35	Surface adsorption controlled	179 180
Uraninite	Ferric sulphate	Directly dependent at low Fe ³⁺ conc.; independent of Fe ³⁺ conc. > 8 g/l	11 - 15	5 - 30	Surface adsorption controlled	182
Synthetic U ₃ O ₈	Ferric sulphate	Rate increased according to conc. of (Fe ³⁺) [‡]	14,5	25 - 50	Surface adsorption controlled	183

acid-ferric sulphate leaching medium. It was noted that the gold slimes contained adequate nutrients for bacterial growth, but that the oxygen supply was rate controlling. These authors showed that improved uranium extractions could be effected by injecting air into the slimes piles.

Now that the role of bacteria has been recognized, it should be possible to design systems to promote bacterial activity and, hence, the uranium leaching rates. In large dumps or compacted tailings ponds, oxygen deficiency is a serious problem that can be overcome by aeration¹⁸⁹ of the pile or by prior oxidation of the recycled leach solution in especially designed vessels¹⁹⁰. A solution of known oxidizing potential can be prepared by oxidation outside the dump or tailings pond. The addition of finely divided pyrite to the oxidizing reactor can result in considerable acid production. Various techniques of utilizing bacterial activity for the leaching of uranium have been described^{188,191}.

Table 8 summarizes the kinetic information available for the dissolution of uranium oxides in acidic ferric sulphate media. Kinetic information appears to be available only for the simple uranium oxides; the dissolution behaviour of the complex uranium oxides has, in general, received little attention. Laxen¹⁷⁹ refers to low dissolution rates for uranothorianite and for UO₂-ThO₂ crystals. There is general accord concerning the uranium dissolution kinetics. The kinetics are linear with an associated activation energy of about 15 kcal/mol; the actual rates are fairly rapid. Ferric ion concentrations strongly affect the dissolution rate with a relationship of dissolution rate being proportional to the Fe³⁺. The rate is apparently controlled by

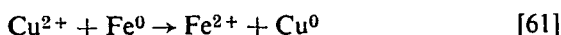
some surface reaction, probably an adsorption reaction involving the ferric ion species. The importance of the ferric complexes on dissolution rates has been demonstrated.

REGENERATION OF FERRIC ION LEACHING MEDIA

Spent ferric ion leaching solutions will contain, in addition to the sought-after metal, excess acid, some unreacted ferric ion and a ferrous sulphate or ferrous chloride reaction product. The sought-after element can be recovered from such solutions by a variety of techniques. Direct electrodeposition of the desired element from the leach solution is one possible way to recover metal values from suitably concentrated liquors and, simultaneously, to re-oxidize the ferric ion leaching medium. This method has been used to deposit iron powders^{10,11,12} from pyrrhotite leach liquors and has been advocated to recover copper in the Cymet Process¹⁶. The major disadvantage of the direct electrodeposition process is the need for a membrane to separate the anode and cathode compartments of the cell. Liquid-liquid extraction and ion exchange have been used to recover both uranium and copper from such leaching media. Merritt¹⁶⁵ has summarized recent work on the recovery of uranium from acidic iron sulphate solutions by both IX and SX techniques. Ion-exchange resins used in the uranium industry are of the strong and intermediate base anionic type; anionic liquid ion-exchange systems are used to extract uranium from sulphuric acid leach solutions. Liquid ion-exchange media are currently being used to extract copper from acidified ferric sulphate leach solutions

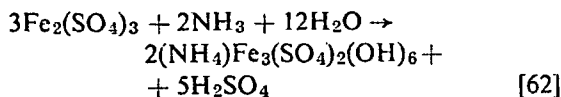
obtained during heap or *in situ* leaching¹⁹². The combination of liquid-liquid extraction of copper from leach liquors followed by electrowinning from the stripped solution is gaining in popularity. The economics of this latter type of process appear favourable¹⁹³ when compared to conventional cementation.

Copper can be conveniently recovered from ferric ion leach solutions by cementation on scrap iron. High ferric ion or acid concentrations lead to increased consumption of scrap metal, but in spite of this deficiency, cementation on scrap iron is widely used in the copper industry. Cementation practice, as employed by the copper industry, has been summarized by Woodcock²⁷ and by Sheffer and Evans²⁹. The kinetics of reaction of dissolved copper with iron have been recently studied by Biswas and Reid¹⁹⁴ and by Nadkarni *et al*¹⁹⁵. The rate of the reaction:



increases with increasing stirring speed to some maximum value and, thereafter, is insensitive to further changes in the relative speed between metal and solution. The rate decreases with increasing copper concentrations and with increasing pH of the solution. Activation energies in the range 6 to 9 kcal/mol were obtained for this reaction. Cementation on iron increases the total iron content of the solution by the amount of scrap metal consumed.

After metal recovery, it is often necessary to remove some of the dissolved iron from the solution. This excess iron might have originated from the oxidation of iron-bearing minerals such as pyrite or chalcopyrite or from the dissolution of iron during a cementation process. Excess acid, say, from pyrite oxidation, might also be present in certain operations. Both iron and excess acid can be removed by neutralizing the solution with lime; the precipitates are often difficult to filter. A better approach has recently been developed whereby the iron is precipitated as a jarosite compound: $\text{MFe}_3^{3+}(\text{SO}_4)_2(\text{OH})_6$ where M can be NH_4^+ , Na^+ , K^+ or H_3O^+ . The iron must be in the trivalent state for the reaction to occur:



Since acid is generated during the jarosite reaction, neutralization during precipitation is required. Although this process was originally developed to remove iron from zinc leach solutions, it could also be used to modify the iron content of nickel or copper leach solutions with minimum loss of the base metal in the precipitate¹⁹⁶. The actual jarosite compound is readily filterable. A form of jarosite precipitation is currently used to precipitate excess iron in oxidation ponds before the solutions are used to leach copper-bearing waste rock. If solutions too rich in iron are used for dump leaching, there exists the danger that jarosite will precipitate locally and plug the dump, thereby greatly lowering the leaching efficiency¹⁹⁷.

In a leaching operation where the medium is recycled, it is necessary to re-oxidize the dissolved iron after the metal recovery stage. This need arises because the ferrous ion concentration has increased at the expense of the active ferric ion during leaching. Large amounts of ferrous ion can also be introduced into solution by the reaction of acid with gangue minerals, such as silicates or siderite, or by the cementation reaction. If the leaching medium is to be of maximum effectiveness, then all the iron must be in the trivalent state. Several methods exist to effect this iron oxidation:

- electrolytic oxidation,
- use of chlorine gas,
- use of strong oxidizers,
- use of oxygen under pressure,
- use of oxygen at ambient pressure,
- use of bacteria in the presence of oxygen.

Electrolytic regeneration of the iron leaching medium is usually contemplated only when the sought-after metal is recovered by electrolysis. As an example, when iron is electrolytically deposited on the cathode, ferrous ion is oxidized to the ferric state at the anode. The Cymet Process regenerates its ferric chloride leaching medium by this technique¹⁶. The cathode reaction is:

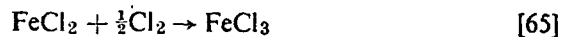


The corresponding anodic reaction is:



The anode and cathode cell compartments must be separated by some type of diaphragm.

The regeneration of iron chloride leaching solutions by chlorine gas is a convenient method of obtaining a solution rich in ferric chloride. Haver and Wong¹⁵ proposed this technique to regenerate their leaching media; they believed that this method was better than either electrolytic or air oxidation. Chlorine gas at 2 psig could oxidize 100 per cent of the iron in the solution in 1½ h; the temperature rose from 20 to 70°C during the chlorination step. The chlorination reaction is given by:



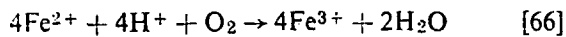
The kinetics of this reaction have been investigated recently by Sysoeva *et al*^{198,199}. It was found that the rate of chlorination of Fe^{2+} ions was first-order with respect to both ferrous ion and the chlorine gas pressure. The rate was slowed by increasing amounts of dissolved ferric ion.

The use of strong oxidizing agents such as chlorates, MnO_2 , or permanganate to oxidize iron is clearly limited by the high costs of such reagents. Their use is limited to the leaching of metals, with a high unit value, such as uranium. Merritt¹⁶⁵ has summarized the use of such reagents in the uranium-processing industry where relatively small amounts of dissolved iron are kept in the trivalent state by the presence of the strong oxidant.

The oxidation of iron solutions with oxygen under high pressure can overcome the inherently low rate of oxidation of the ferrous ion. A major disadvantage associated with this technique is the capital cost of the autoclaves. Johnson²⁰⁰ proposed

to re-oxidize spent iron sulphate leach liquors at 175°C and 300 psig of air; good oxidation conversions were obtained in one to two hours under these conditions. It was proposed to use a vertical autoclave of unique design to effect the oxidation. The kinetics of oxidation of Fe²⁺ to Fe³⁺ by oxygen in an autoclave were investigated by Riecke²⁰¹ at temperatures between 100 and 180°C and oxygen pressures up to 40 atm. It was found that the solutions were stable at pH values below 1.5; solid iron phases precipitated from more basic solutions. The rate of Fe²⁺ oxidation varied directly with the pressure of oxygen and the square of the ferrous ion concentration. The reported activation energy was 14 kcal/mol. The relatively high activation energy, coupled with the direct oxygen pressure dependence, clearly show the technical advantage to be gained by effecting this oxidation at high temperatures and pressures. It was also noted that the addition of 0.05 M Cu²⁺ to the solution increased the oxidation rate eight times and lowered the activation energy to 9 kcal/mol.

The oxidation of ferrous ion by oxygen under ambient conditions is widely used to prepare ferric lixiviants. The kinetics of this reaction have been investigated many times and a summary of these studies was presented by Woodcock²⁷. A description of the rate equations found by various authors has been given by Mathews and Robins²⁰². For the oxidation of ferrous ion in acidic media, the reaction:



is generally believed to depend directly on the oxygen pressure and on the square of the ferrous ion concentration^{202,203,204}. The rate depends inversely on the hydrogen ion concentration to the 0.25 power; the activation energy is 13 to 19 kcal/mol²⁰². It is known²⁰² that the presence of Cu²⁺ causes an increase in the oxidation rate, the greatest effect being noted for Cu²⁺ concentrations in the range 0.001 to 0.01 M. Although this catalytic effect is probably of considerable importance during the dump leaching of copper ores, it appears that other common metallic ions have little effect on the rate of iron oxidation. It is also recognized²⁰⁵ that the presence of activated carbon catalyses the oxidation of ferrous ion in the presence of air; the rate increases with the increasing fineness of the carbon²⁰⁶. The activation energy for ferrous oxidation falls to a low value in the presence of activated carbon, and the rate appears to depend on the ferrous ion concentration in a manner different from that observed in the absence of the carbon. The carbon can be used repeatedly with little loss in efficiency and can be recovered from pulps or slurries by flotation or by mechanical means. Although activated carbon is too expensive to be incorporated into dumps or heaps, it could be added during separate batch processes to regenerate the spent leaching medium. It is doubtful if naturally occurring graphite functions in a manner similar to that of activated carbon. The oxidation of ferrous ion in neutral or slightly acid media has

also been studied²⁰⁷, but is of little interest for leaching since such an oxidation would lead to the precipitation of the ferric ion. This technique is, however, one means of removing iron from leaching solutions.

It is now recognized that bacteria can catalyse the air oxidation of ferrous to ferric ion. The presence of bacteria causes the oxidation to proceed orders of magnitude faster than for the same solution without bacteria. The microorganisms require certain nutrients and, especially, oxygen to effect the oxidation. During dump or *in situ* leaching the lack of oxygen probably limits the bacterial activity. In aerated reactors, the lack of certain nutrients or carbon dioxide can control the reaction. Since it is difficult to aerate solutions within stopes, dumps, or thick slurries, it may be advisable to oxidize the leach solutions in a separate reactor where optimum conditions for bacterial growth, including a temperature of 35°C, could be maintained. The oxidized solution could be continuously or intermittently pumped to the leaching system and spent leach liquor recycled to the aeration tanks. Although most work on bacterial oxidation has been done on sulphate systems, it is known²⁰⁸ that bacterial strains can function in chloride media. Leaching solutions containing 5 g/l each of FeCl₃ and NaCl were kept in an oxidized state by bacterial oxidation.

SUMMARY

This review has shown that acidified ferric ion leaching solutions are capable, either alone or in the presence of bacteria, of leaching many metal sulphides or uranium oxide compounds. In some instances commercially favourable rates can be obtained but in other instances the rates of reaction are painfully slow. Ferric ion leaching can be used in a variety of circumstances depending on the type or grade of ore. The leaching medium can be easily generated and maintained at a high oxidation potential. The recovery of elemental sulphur, the major sulphur product in ferric ion leaching, is a major advantage of this process. The recovery of precious metals from ores treated by ferric ion leaching has received little attention. It is possible to separate and to recover elements from ferric ion leaching solutions, but some metals are difficult to extract from the iron-bearing solutions and this area requires additional research.

REFERENCES

1. FORWARD, F. A., and WARREN, I. H. Extraction of metals from sulphide ores by wet methods. *Metall. Revs.*, vol. 5, 1960. pp. 137-164.
2. WOODCOCK, J. T. Some aspects of the oxidation of sulphide minerals in aqueous suspension. *Proc. Australas. Inst. Min. Metall.*, no. 198, 1961. pp. 47-84.
3. WADSWORTH, M. E. Advances in the leaching of sulphide minerals. *Miner. Sci. Engng.*, vol. 4, no. 4, 1972. pp. 36-47.
4. BURKIN, A. R. Progress report on recent advances in extraction metallurgy: (A) Hydrometallurgy. *Metall. Revs.*, vol. 16, 1971. pp. 47-56.

5. MONHEMIUS, A. J. Trends in copper hydrometallurgy. *Chem. Process Engng*, vol. 51, no. 1, 1970. pp. 65-68.
6. GARRELS, R. M., and CHRIST, C. L. *Solutions, minerals and equilibria*. New York, Harper and Row, 1965. p. 241.
7. BHAPPU, R. B., et al. Theoretical and practical studies on dump leaching. *Trans. Soc. Mnr. Engrs, AIME*, vol. 244, 1969. pp. 307-320.
8. ETIENNE, A. Electrochemical aspects of the aqueous oxidation of copper sulphides. *Ph.D. Thesis*, University of British Columbia, Vancouver, 1971.
9. PETERS, E. Thermodynamic and kinetic factors in the leaching of sulphide minerals from ore deposits and dumps. *AIME Short Course on Bio Extractive Mining*, Denver, Colorado, February 1970.
10. TRAILL, R. J. Investigations in ore dressing and metallurgy, 1922. Ottawa, Dept. of Mines, Mines Branch, *Rep. 608*, 1924. pp. 185-190.
11. *Ibid*, Investigations in ore dressing and metallurgy, 1923. Ottawa, Dept. of Mines, Mines Branch, *Rep. 617*, 1925. pp. 101-114.
12. TRAILL, R. J., and McCLELLAND, W. R. Investigations in ore dressing and Metallurgy, 1924. Ottawa, Dept. of Mines, Mines Branch. *Rep. 643*, 1926. pp. 92-102.
13. ZAPEVALOV, G. G., and VYGODA, R. M. Leaching complex mattes with acid and ferric chloride solutions. *Trudy Irkutsk. Politekhn. Inst.*, vol. 18, 1963. pp. 92-99.
14. TSEFT, A. L., et al. *Trudy Inst. Metall., Obogashch. Alma Ata*, vol. 14, 1965. pp. 41-47.
15. HAVER, F. P., and WONG, M. M. Recovery of copper, iron and sulphur from chalcopyrite concentrate using a ferric chloride leach. *J. Metals, N. Y.*, vol. 23, no. 2, 1971. pp. 25-29.
16. KRUESI, P. R., ALLEN, E. S., and LAKE, J. L. Cymet process, hydrometallurgical conversion of base metal sulphides to pure metals. *Conference of metallurgists*, Halifax, Nova Scotia, 1972.
17. GITTUS, J. H. *Uranium*. London, Butterworths, 1963. p. 34.
18. FLETCHER, J. B. In-place leaching at Miami Mine, Miami, Arizona. *Trans. Soc. Mnr. Engrs, AIME*, vol. 250, 1971. pp. 310-314.
19. MACGREGOR, R. A. Recovery of U_3O_8 by underground leaching. *CIM Bull.*, vol. 59, 1966. pp. 583-587.
20. VELICHKIN, A. N. Possibility of processing ore blocks by a subsurface leaching method. *Trudy Inst. gorn. Dela, Alma Ata*, vol. 12, 1963. pp. 159-163.
21. ROSENBAUM, J. B., and MCKINNEY, W. A. *In situ* recovery of copper from sulphide ore bodies following nuclear fracturing. *Symposium on engineering with nuclear explosives*, Las Vegas, 1970. Oak Ridge, Tenn. AEC, 1970. vol. 2. pp. 877-887.
22. DONALD, M. B. Percolation leaching in theory and practice. *Trans. Inst. Chem. Engrs*, vol. 15, 1937. pp. 77-109.
23. JOHNSON, P. H. Leaching ores with acid in a deep vertical underground tube. *U.S. Patent 3 264 099*. 1964.
24. ORTLOFF, G. D., COOKE, C. E., and ATWOOD, D. K. *In situ* recovery of copper values from copper ores. *U.S. Patent 3,574,599*. 1971.
25. TAYLOR, J. H., and WHELAN, P. F. Leaching and precipitation of copper at Rio Tinto, Spain. *Trans. Instn Min. Metall.*, vol. 52, 1942-1943. pp. 35-96.
26. MALOUF, E. E., and PRATER, J. D. New technology of leaching waste dumps. *Min. Congr. J.*, vol. 48, no. 11, 1962. pp. 82-85.
27. WOODCOCK, J. T. Copper waste dump leaching. *Proc. Australas. Instn Min. metall.*, no. 224, 1967. pp. 47-66.
28. COOPER, F. D. *Copper hydrometallurgy*. Washington D.C., U.S. Bureau of Mines, *IC-8394*, 1968.
29. SHEFFER, H. W., and EVANS, L. G. *Copper leaching practices in the western United States*, Washington, D.C., U.S. Bureau of Mines, *IC-8341*, 1968.
30. HARRIS, J. A. Development of a theoretical approach to the heap leaching of copper sulphide ores. *Proc. Australas. Inst. Min. Metall.*, vol. 230, 1969. pp. 81-92.
31. TORMA, A. E. Microbiological leaching of a zinc sulphide concentrate. *Ph.D. Thesis*, University of British Columbia, 1970.
32. BOUNDS, H. C., and COLMER, A. R. Comparison of the kinetics of thiosulphate oxidation by three iron-sulphur oxidizers. *Can. J. Microbiol.*, vol. 18, 1972. pp. 735-740.
33. PINGS, W. B. Bacterial leaching, Colorado School of Mines. *Miner. Ind. Bull.*, vol. 11, no. 3, 1968. pp. 1-19.
34. MOSS, F. J., and ANDERSEN, J. E. The effects of environment on bacterial leaching rates. *Proc. Australas. Inst. Min. Metall.*, no. 225, 1968. pp. 15-25.
35. FLETCHER, A. W. Metal winning from low-grade ore by bacterial leaching. *Trans. Instn Min. Metall.*, vol. 79, 1970. pp. C247-252.
36. ITO, I. Bacterial leaching, *Kwangsan Hakhoe Chi*, vol. 8, no. 3, 1971. pp. 120-135.
37. TRUDINGER, P. A. Microbes, metals, and minerals. *Miner. Sci. Engng*, vol. 3, no. 4, 1971. pp. 13-25.
38. JOHNSON, P. H. Acid-ferric sulphate solutions for chemical mining. *Min. Engng*, vol. 17, no. 8, 1965. pp. 64-68.
39. SUTTON, J. A., and CORRICK, J. D. Microbial leaching of copper minerals. *Min. Engng*, vol. 13, no. 6, 1963. pp. 37-40.
40. *Ibid*, Leaching copper sulphide minerals with selected autotrophic bacteria, Washington, D.C., U.S. Bureau of Mines, *RI-6423*, 1964.
41. CORRICK, J. D., and SUTTON, J. A. Copper extraction from a low-grade ore by *Ferrobacillus ferrooxidans*. Washington, U.S. Bureau of Mines, *RI-6714*, 1965.
42. GARRELS, R. M., and THOMPSON, M. E. Oxidation of pyrite by iron sulphate solutions. *Am. J. Sci.*, vol. 258A, 1960. pp. 57-67.
43. MALOUF, E. E., and PRATER, J. D. Role of bacteria in the alteration of sulphide minerals. *J. Metals N. Y.*, vol. 13, 1961. pp. 353-356.
44. IVANOV, V. I. Role of sulphur bacteria in the leaching of sulphide ores, *Dokl. Akad. Nauk, SSR*, vol. 146, 1962. pp. 447-449.
45. IVANOV, V. I., NAGIRNYAK, F. I., and STEPANOV, B. A. Bacterial oxidation of sulphide ores. I. The role of *Thiobacillus ferrooxidans* in the oxidation of chalcopyrite, *Mikrobiologiya*, vol. 30, 1961. pp. 688-692.
46. BRYNER, L. C., et al. Microorganisms in leaching sulphide minerals. *Ind. Engng Chem.*, vol. 36, 1954. pp. 2587-2592.
47. BRYNER, L. C., and JAMESON, A. K. Microorganisms in leaching sulphide minerals. *Appl. Microbiol.*, vol. 6, 1958. pp. 281-287.
48. LORENZ, W. C., and TARPLEY, E. G. Oxidation of coal mine pyrites, Washington, D.C., U.S. Bureau of Mines, *RI-6247*, 1963.
49. DUNCAN, D. W., LANDESMAN, J., and WALDEN, C. C. Role of *Thiobacillus ferrooxidans* in the oxidation of sulphide minerals. *Can. J. Microbiol.*, vol. 13, 1967. pp. 397-403.
50. BRYNER, L. C., WALKER, R. B., and PALMER, R. Some factors influencing the biological and non-biological oxidation of sulphide minerals. *Trans. Soc. Min. Engrs, AIME*, vol. 238, 1967. pp. 56-61.

51. NAPIER, E., WOOD, R. G., and CHAMBERS, L. A. Bacterial oxidation of pyrite and production of solutions for ore leaching. *Symposium on advances in extractive metallurgy*, London, 1967. London, Institution of Mining and Metallurgy, 1968. pp. 942-957.
52. SULLIVAN, J. D. Chemistry of leaching covellite. Washington, D.C., U.S. Bureau of Mines, *TP 487*, 1930.
53. BROWN, S. L. Dissolution of some common copper minerals. *M.Sc. Thesis*, University of Arizona, 1931.
54. BROWN, S. L., and SULLIVAN, J. D. Dissolution of various copper minerals. Washington, D.C., U.S. Bureau of Mines, *RI-3228*, 1934.
55. SULLIVAN, J. D. Chemical and physical features of copper leaching. *Trans. Am. Inst. Min. Metall.*, vol. 106, 1933. pp. 515-546.
56. THOMAS, G., and INGRAHAM, T. R. Kinetics of dissolution of synthetic covellite in aqueous acidic ferric sulphate solutions. *Can. Metall. Q.*, vol. 6, 1967. pp. 153-165.
57. KING, J. A. Solid state changes in the leaching of copper sulphides. *Ph.D. Thesis*, University of London, 1966.
58. LOWE, D. F. The kinetics of the dissolution reaction of copper and copper-iron sulphide minerals using ferric sulphate solutions. *Ph.D. Thesis*, University of Arizona, 1970.
59. MULAK, W. Kinetics of dissolving polydispersed covellite in acidic solutions of ferric sulphate. *Roczn. Chem.*, vol. 45, 1971. pp. 1417-1424.
60. DUTRIZAC, J. E., and MACDONALD, R. J. C. Kinetics of dissolution of covellite in acidified ferric sulphate solution. *Can. Metall. Q.*, (In press, 1974.)
61. RAZZELL, W. E., and TRUSSELL, P. C. Isolation and properties of an iron-oxidizing thiobacillus. *J. Bact.*, vol. 85, 1963, pp. 595-603.
62. RAZZELL, W. E. Bacterial leaching of metallic sulphides. *CIM Bull.*, vol. 65, 1962. pp. 135-136.
63. DE CUYPER, J. A. Bacterial leaching of low grade copper and cobalt ores. *International symposium on unit-procedures in hydrometallurgy*, Dallas, Texas, 1963. M. E. Wadsworth, and F. T. Davis, eds. New York, Gordon and Breach, 1964. pp. 126-142.
64. DUNCAN, D. W., and TRUSSELL, P. C. Advances in microbiological leaching of sulphide ores. *Can. Metall. Q.*, vol. 3, 1964. pp. 43-55.
65. CORRANS, I. J., HARRIS, B., and RALPH, B. J. Bacterial leaching. Introduction to its application and theory, and a study on its mechanism of operation, *J. S. Afr. Inst. Min. Metall.*, vol. 72, 1972. pp. 221-230.
66. BAUER, J. P., GIBBS, H. L., and WADSWORTH, M. E. Initial stage sulphuric acid leaching kinetics of chalcopyrite using radiochemical techniques. Metallurgical Society, *AIME, offprint 72-B-96*, 1972.
67. FOX, S. I. Bacterial oxidation of simple copper sulphides. *Ph.D. Thesis*, Rensselaer Polytechnic Institute, 1968.
68. SULLIVAN, J. D. Chemistry of leaching chalcocite, Washington, D.C., U.S. Bureau of Mines; *TP-473*, 1930.
69. COLOMBO, A. F., and FROMMER, D. W. Leaching Michigan copper ore and mill tailings with acidified ferric sulphate. Washington, D.C., U.S. Bureau of Mines, *RI-5924*, 1962.
70. TKACHENKO, O. B., and TSEFT, A. L. Kinetics of the dissolution of chalcocite in ferric chloride. *Trudy Inst. Metall. Obogashch., Alma Ata*, vol. 30, 1969. pp. 15-23.
71. MULAK, W. Kinetics of cuprous sulphide dissolution in acidic solutions of ferric sulphate. *Roczn. Chem.*, vol. 43, 1969. pp. 1387-1394.
72. KOPYLOV, G. A., and ORLOV, A. I. Rates of bornite and chalcocite dissolution in ferric sulphate. *Jr Irkutsk. Politekh. Inst.*, vol. 46, 1969. pp. 127-132.
73. THOMAS, G., INGRAHAM, T. R., and MACDONALD, R. J. C. Kinetics of dissolution of synthetic digenite and chalcocite in aqueous acidic ferric sulphate solutions. *Can. Metall. Q.*, vol. 6, 1967. pp. 281-291.
74. MOH, G. H. Blue remaining covellite and its relation to phases in the sulphur rich portion of the copper-sulphur system at low temperatures. *7th general meeting international mineralogical association*, Tokyo, 1970. Papers and proceedings. Tokyo, Mineralogical Society of Japan, 1971. Spec. Pap. 1. pp. 226-232.
75. NIELSEN, A. M., and BECK, J. V. Chalcocite oxidation and coupled carbon dioxide fixation by *Thiobacillus ferrooxidans*, *Science*, vol. 175, 1972. pp. 1124-1126.
76. RAZZELL, W. E., and TRUSSELL, P. C. Microbiological leaching of metallic sulphides. *Appl. Microbiol.*, vol. 11, 1963. pp. 105-110.
77. IVANOV, V. I. Iron oxidation by *Thiobacillus ferrooxidans*. *Mikrobiologiya*, vol. 31, 1962. pp. 795-799.
78. STANCHEV, L., et al. *Thiobacillus ferrooxidans*, its use in copper extraction from copper slag. *Pochvozn. Agrokhim.*, vol. 7, no. 3, 1972. pp. 19-23.
79. TRAILL, R. J., and McCLELLAND, W. R. Investigations in ore dressing and metallurgy, 1926. Ottawa, Department of Mines, Mines Branch, *Rep. 688*, 1928. pp. 101-109.
80. TRAILL, R. J., McCLELLAND, W. R., and JOHNSON, J. D. Investigations in ore dressing and metallurgy, 1927. Ottawa, Department of Mines, Mines Branch, *Rep. 695*, 1928. pp. 138-153.
81. TRAILL, R. J., McCLELLAND, W. R., and JOHNSON, J. D. Investigations in ore dressing and metallurgy, 1928. Ottawa, Department of Mines, Mines Branch, *Rep. 711*. pp. 132-141.
82. PIKE, R. D., et al. Electrolytic iron from sulphide ores. *Trans. Am. Inst. Min. Metall.*, vol. 90, 1930. pp. 311-345.
83. KLETS, V. E., and LIPO. Behaviour of chalcopyrite in salt leaching. *Trudy-Irkutsk. Politekh. Inst.*, vol. 27, 1966. pp. 123-130.
84. ERMILOV, V. V., TKACHENKO, O. B., and TSEFT, A. L. Kinetics of the dissolution of chalcopyrite in ferric chloride. *Trudy Inst. Metall., Obogashch., Alma Ata*, vol. 30, 1969. pp. 3-14.
85. OZOLINS, L., and RUSIKHINA, L. P. Leaching of copper from copper-containing ores under the effect of external fields. *Soversh. Tekh. Tekhnol. Razrab. Mestorozhd. Polez. Iskop.*, 1968. pp. 103-110.
86. ICHIKUNI, M. The dissolution of sulphide minerals in various media. III. Factors intervening in the dissolution of chalcopyrite. *Bull. Chem. Soc. Japan*, vol. 33, 1960. pp. 1159-1162.
87. *Ibid.* The action of ferric ions on chalcopyrite. *Bull. Chem. Soc. Japan*, vol. 35, 1962. pp. 1765-1768.
88. DUTRIZAC, J. E., MACDONALD, R. J. C., and INGRAHAM, T. R. The kinetics of dissolution of synthetic chalcopyrite in aqueous acidic ferric sulphate solutions. *Trans. Metall. Soc. AIME*, vol. 245, 1969. pp. 955-959.
89. DUTRIZAC, J. E., and MACDONALD, R. J. C. The effect of sodium chloride on the dissolution of chalcopyrite under simulated dump leaching conditions. *Metall. Trans.*, vol. 2, 1971. pp. 2310-2312.
90. SUBRAMANIAN, K. N., and JENNINGS, P. H. Review of the hydrometallurgy of chalcopyrite concentrates. *Can. Metall. Q.*, vol. 11, 1972. pp. 387-400.
91. UCHIDA, T., et al. Leaching of copper from copper-bearing ores with a dilute solution of sulphuric acid

- and ferric sulphate. *Hakko Kyokaiishi*, vol. 25, 1967. pp. 168-172.
92. SUTTON, J. A., and CORRICK, J. D. Bacteria in mining and metallurgy: Leaching selected ores and minerals, experiments with thiobacillus thiooxidans, Washington, D.C., U.S. Bureau of Mines, RI-5839, 1961.
 93. MALOUF, E. E., and PRATER, J. D. Role of bacteria in the alteration of sulphide minerals. *J. Metals. N. Y.*, vol. 13, 1961. pp. 353-356.
 94. DUNCAN, D. W., WALDEN, C. C., and TRUSSELL, P. C. Biological leaching of mill products. *CIM Bull.*, vol. 69, 1966. pp. 1075-1079.
 95. WATANABE, A., UCHIDA, T., and FURUYA, S. Identification of sulphur oxidizing bacteria and iron bacteria and properties of iron-oxidizing bacteria in metal mine water. II — Leaching of chalcopyrite by iron bacteria and sulphur oxidizing bacteria: *Ferrobacillus ferrooxidans* and *Thiobacillus ferrooxidans*. *Hakko Kyokaiishi*, vol. 25, 1967. pp. 431-440.
 96. DUNCAN, D. W., TRUSSEL, P. C., and WALDEN, C. C. Leaching of chalcopyrite with *Thiobacillus ferrooxidans*: effect of surfactants and shaking. *Appl. Microbiol.*, vol. 12, no. 2, 1964. pp. 122-126.
 97. BRYNER, L. C., and ANDERSON, R. Microorganisms in leaching sulphide minerals. *Ind. Engng Chem.*, vol. 49, 1957. pp. 1721-1724.
 98. WYCKOFF, R. W. G. Two kinds of chalcopyrites demonstrated by bacterial oxidation. *Bull. Soc. fr. Minér. Cristallogr.*, vol. 93, 1970. pp. 120-122.
 99. BRUYNESTEYN, A., and DUNCAN, D. W. Microbiological leaching of sulphide concentrates. *Can. Metall. Q.*, vol. 10, 1971. pp. 57-63.
 100. SULLIVAN, J. D. Chemistry of leaching bornite. Washington, D.C., U.S. Bureau of Mines. TP-486. 1931.
 101. KOPYLOV, G. A., and ORLOV, A. I. Kinetics of dissolving of bornite. *Izv. vyssh. ucheb. Zaved., Tsvet. Metall.*, vol. 6, 1963. pp. 68-74.
 102. DUTRIZAC, J. E., MACDONALD, R. J. C., and INGRAHAM, T. R. The kinetics of dissolution of bornite in acidified ferric sulphate solutions. *Metall. Trans.*, vol. 1, 1970. pp. 225-231.
 103. *Ibid.* Effect of pyrite, chalcopyrite and digenite on rate of bornite dissolution in acidic ferric sulphate solutions. *Can. Metall. Q.*, vol. 10, 1971. pp. 3-7.
 104. CABRI, L. J. New data on phase relations in the Cu-Fe-S system. *Econ. Geol.*, vol. 68, no. 4, 1973. pp. 443-454.
 105. DUTRIZAC, J. E., and MACDONALD, R. J. C. Percolation leaching of bornite ore. *Proc. Australas. Inst. Min. Metall.*, no. 245, 1973. pp. 25-31.
 106. DUTRIZAC, J. E., MACDONALD, R. J. C., and INGRAHAM, T. R. The kinetics of dissolution of cubanite in aqueous acidic ferric sulphate solutions. *Metall. Trans.*, vol. 1, 1970. pp. 3083-3088.
 107. KOCH, S., and GRASSELLY, G. Data on the oxidation of sulphide ore deposits. *Acta. Miner. Petrogv. Szeged.*, vol. 6, 1952. pp. 23-29.
 108. EHRLICH, H. L. Bacterial oxidation of arsenopyrite and enargite. *Econ. Geol.*, vol. 59, 1964. pp. 1306-1312.
 109. POLKIN, S. I. *et al.* Bacterial-selective leaching of arsenic and copper from sulphide-oxide tin concentrates; mechanism of leaching. *Proc., 9th International Mineral Processing Congress*, Prague, 1970. pp. 346-353.
 110. DUTRIZAC, J. E., and MACDONALD, R. J. C. The kinetics of dissolution of enargite in acidified ferric sulphate solutions. *Can. Metall. Q.*, vol. 11, 1972. p. 469.
 111. SPRINGER, G. Electron-probe analyses of tetrahedrite. *Neues Jb. Mineral., Mh.* vol. 1, 1969. pp. 24-32.
 112. NISHIHARA, G. S. The rate of reduction of acidity of descending waters by certain ore and gangue minerals and its bearing upon secondary sulphide enrichment. *Econ. Geol.*, vol. 9, 1914. pp. 743-757.
 113. KOCH, S., and GRASSELLY, G. Processes occurring during the decomposition of sulphide ores. *Acta Mineral. Petrogy. Szeged.*, vol. 5, 1951. pp. 15-37.
 114. KHOLMANSKIKH, Y. B., ILYASHEVICH, I. I., and KOSNAREVA, I. A. Kinetics of dissolution of copper and its compounds in aqueous solutions. *Trudy ural, nauch-issled. Proekt. Inst. Mednoi Prom.*, vol. 9, 1966. pp. 289-293.
 115. THORNHILL, P. G., WIGSTOL, E., and VAN WEERT, G. The Falconbridge matte leach process. *J. Metals N.Y.*, vol. 23, 1971. pp. 13-18.
 116. URAZOV, G. G., and BOGATSKII, D. P. Basis for new methods of chemical treatment of complex iron and nickel ores. *Bull. Acad. Sci. USSR, Div. Chem. Sci.*, 1956. pp. 1047-1054.
 117. TSEFT, A. L., and KRYUKOVA, V. N. Investigation of the process of leaching nickel matte with HCl and with salts. *Khim. Metall.*, vol. 25, 1960. pp. 69-75.
 118. KLETS, V. E., and SERIKOV, A. P. Solution conditions for copper-nickel bulk concentrate in a ferric chloride solution. *Trudy Irkutsk. Politekh. Inst.*, vol. 18, 1963. pp. 31-39.
 119. KRYUKOVA, V. N., and TSEFT, A. L. Complex hydrometallurgical processing of nickel matte. *Trudy Inst. Metall., Obogashch., Alma Ata*, vol. 11, 1964. pp. 3-9.
 120. TORMA, A. E. Microbiological oxidation of synthetic cobalt, nickel and zinc sulphides by *Thiobacillus ferrooxidans*. *Rev. Can. Biol.*, vol. 30, 1971. pp. 209-216.
 121. TORMA, A. E. Effect of the surface on the dissolution of metals from sulphide minerals by *Thiobacillus ferrooxidans*. *Proc. 55th Canadian Chemical Conference*, Quebec City, 1972. Ottawa, Chemical Institute of Canada. Paper.
 122. KUZMINKH, I. N., and YAKHONTOVA, E. L. Action of ferric sulphate solutions on zinc sulphide. *Zh. Priklad. Khim.*, vol. 23, 1950. pp. 1121-1126.
 123. KUZMINKH, I. N., and YAKHONTOVA, E. L. Wet extraction of zinc from mixtures of sulphides. *Op. cit.* (122). pp. 1142-1148.
 124. ABLANOV, A. D., *et al.* Treatment of ores of Nikolaevsk deposit. *Trudy Inst. Metall. Obogashch., Alma Ata*, vol. 3, 1960. pp. 90-104.
 125. ERMILOV, V. V. Leaching sulphide concentrates with simultaneous dissolution of liberated sulphur. *Op. cit.* (124). pp. 168-183.
 126. AGRACHEVA, R. A., VOLSKIY, A. N., and EGOROV, A. M. Treatment of lead sulphide concentrates by the application of ferric chloride solutions. *Iz. Akad. Nauk USSR, Otel. Tekh. Nauk Met. Toplivo*, vol. 3, 1959. pp. 37-46.
 127. ZAPEVALOV, G. G., and VYGODA, R. M. Leaching of complex mattes with acid and ferric chloride solutions. *Trudy Irkutsk. Politek. Inst.*, vol. 18, 1963. pp. 92-99.
 128. TSEFT, A. L., *et al.* Processing complex sulphide ores with ferric chloride. *Trudy Inst. Metall. Obogashch., Alma Ata*, vol. 14, 1965. pp. 41-47.
 129. SCHIKUNI, M., and KAMIYA, H. Dissolution of sulphur-containing ores in various media. V-dissolution of sphalerite. *Bull. Chem. Soc. Japan*, vol. 34, 1961. pp. 1780-1786.
 130. RUDOLFS, W., and HELBRONNER, A. Oxidation of zinc sulphide by microorganisms. *Soil Sci.*, vol. 14, 1922. pp. 459-464.
 131. GOLBRAIKHY, A. I., and ILYALEDTINOV, A. N. Bacterial leaching of copper and zinc from some Kazakhstan complex ores. *Izv. Akad. Nauk, Kaz. SSR, Seri. Biol.*, vol. 8, 1970. pp. 40-48.

132. DUNCAN, D. W., *et al.* Recent advances in the microbiological leaching of sulphides. *Trans. Soc. Min. Engrs. AIME*, vol. 238, 1967, pp. 122-128.
133. DUNCAN, D. W., WALDEN, C. C., and TRUSSELL, P. C. Accelerated microbiological ore extraction. *U.S. Patent 3 305 353*, 1967.
134. DUNCAN, D. W., and MCGORAN, C. J. M. Rapid bacteriological extraction of metals from materials containing metallic sulphides. *U.S. Patent 3 607 235*, 1971.
135. ZIMMERLEY, S. R., WILSON, D. G., and PRATER, J. D. Cyclic leaching process employing iron-oxidizing bacteria. *U.S. Patent 2 892 964*, 1958.
136. MARCHLEWITZ, B., and SCHWARTZ, W. Microbe association of acid mine waters. *Z. allg. Microbiol.*, vol. 1, 1961, pp. 100-144.
137. SILVERMAN, M. P., and EHRLICH, H. L. Microbial formation and degradation of minerals. *Adv. appl. Microbiol.*, vol. 6, 1964, pp. 153-206.
138. HAVER, F. P., UCHIDA, K., and WONG, M. M. Recovery of lead and sulphur from galena concentrate, using a ferric sulphate leach. Washington, D.C. Bureau of Mines, *RI-7360*, 1970.
139. VASILEV, V. V., and MURATOVA, N. E. Phase analysis of lead ores. *Uchen. Zap. lenigr. gos. Univ., A.A. Zhdanova, no. 211, Ser. Khim. Nauk*, vol. 15, 1957, pp. 129-134.
140. VOLSKII, A. N., AGRACHEVA, R. A., and EGOROV, A. M. Hydrometallurgical procedure for treating materials containing lead sulphide. *U.S.S.R. Patent 112 502*, 1958.
141. AGRACHEVA, R. A., and VOLSKII, A. N. Processing of lead sulphide concentrates by treatment with ferric chloride. *Sb. Nauch. Trud. Inst. Tsvetn. Metall.*, vol. 33, 1960, pp. 26-33.
142. TSEFT, A. L., LIVINSKII, D. Y., and VYGODA, R. M. Kinetics of solution of galena and sphalerite. *Vest. Akad. Nauk Kazakh. SSR*, vol. 15, no. 2, 1959, pp. 38-49.
143. PANDE, J. Leaching sulphidic ores. *German Patent 680 518*, 1939.
144. CORRICK, J. D., and SUTTON, J. A. Oxidation of lead blast furnace matte by *Ferrobacillus ferrooxidans* or a dilute acid solution. Washington, D.C., U.S. Bureau of Mines, *RI-7126*, 1968.
145. LYALIKOVA, N. N., *et al.* Transformation product of complex antimony and lead sulphides under the action of bacteria. *Izv. Akad. Nauk SSSR, Ser. Biol.*, vol. 4, 1972, pp. 564-567.
146. PARSONS, H. W., and INGRAHAM, T. R. The hydrogen sulphide route to sulphur recovery from base metal sulphides. Part 1: The generation of H₂S from base metal sulphides. Ottawa, Dept. of Mineral Resources, Mines Branch, *IC 242*, 1970.
147. INGRAHAM, T. R., PARSONS, H. W., and CABRI, L. J. Leaching of pyrrhotite with hydrochloric acid. *Can. Metall. Q.*, vol. 11, 1972, pp. 407-411.
148. PILGRIM, R. F., and INGRAHAM, T. R. The hydrogen sulphide route to sulphur recovery from base metal sulphides. Part 2: The recovery of sulphur from gases containing H₂S. Ottawa, Department of Mineral Resources, Mines Branch, *IC 243*, 1970.
149. SUBRAMANIAN, K. N., STRATIGAKOS, E. S., and JENNINGS, P. H. Hydrometallurgical processing of pyrrhotite. *Can. Metall. Q.*, vol. 11, 1972, pp. 425-434.
150. TSEFT, A. L., and TATARINOVA, A. A. Methods of selective extraction of iron, copper and sulphur from copper concentrates of Central Kazakhstan. *Vest. Akad. Nauk kazakh. SSR*, vol. 14, no. 8, 1958, pp. 32-42.
151. THOMAS, G., and WHALLEY, B. J. P. The leaching of manganese from pyrolusite ore by pyrite. *Can. J. Chem. Engng*, vol. 36, 1958, pp. 37-43.
152. USATAYA, E. S. Oxidation of molybdenite by water solutions. *Zap. Vses. Miner. Obschch.*, vol. 8, 1952, pp. 298-303.
153. BHAPPU, R. B. *et al.* Hydrometallurgical recovery of molybdenum from the Questra Mine, New Mexico Bureau of Mines, *Mineral Resources, Circ. 81*, 1965.
154. BHAPPU, R. B., REYNOLDS, D. H., and ROMAN, R. J. Molybdenum recovery from sulphide and oxide ores. *J. Metals N.Y.*, vol. 17, 1965, pp. 1199-1205.
155. BHAPPU, R. B. *et al.* Studies on the hydrometallurgical recovery of molybdenum from the Questra Mine. Melbourne, Australian Institute of Mining and Metallurgy, *Mongr. Ser. No. 2*, 1967.
156. KRAMARENKO, L. E. Bacterial biocenoses in underground waters of beds of some useful fossils and their geological significance. *Mikrobiologiya*, vol. 31, 1962, pp. 694-701.
157. EHRLICH, H. L. Bacterial action on orpiment. *Econ. Geol.*, vol. 58, 1963, pp. 991-994.
158. POLKIN, S. I. *et al.* Bacterial selective leaching of arsenic and copper from sulphide-oxide tin concentrates; mechanism of leaching. *Op. cit.* (109), pp. 346-353.
159. TUGOV, N. O., and TSYGANOV, G. A. Hydrometallurgical method of obtaining metallic antimony from concentrates. *Uzbek. khim. Zh.*, vol. 7, no. 2, 1963, pp. 17-21.
160. BRISSETTE, C., CHAMPAGNE, J., and JUTRAS, J. R. Bacterial leaching of cadmium sulphide. *CIM Bull.*, vol. 64, 1971, pp. 85-88.
161. Treating sulphide ores. *British patent 492 621*, 1938.
162. PANDE, J. Leaching sulphidic ores, *German patent 680 518*, 1939.
163. PINKNEY, E. T., LURIE, W., and VAN ZYL, P. C. N. Chemical processing of uranium ores. Vienna, International Atomic Energy Agency. *Rev. Ser. 23/24*, 1962, pp. 9-77.
164. THUNAES, A., and COLBORNE, G. F. Uranium milling technology - Trends in flowsheet design. *CIM Bull.*, vol. 61, 1968, pp. 1211-1216.
165. MERRITT, R. C. *The extractive metallurgy of uranium*. Golden, Colorado School of Mines Research Institute, 1971.
166. WILKINSON, W. D. *Uranium metallurgy*. New York, Interscience; Wiley; 1962.
167. LAXEN, P. A. Factors in the dissolution of uranium from South African ores and observations on the nature of the undissolved uranium. *Op. cit.* (63), pp. 143-166.
168. MILLER, R. P., NAPIER, E., and WELLS, R. A. Natural leaching of uranium ores, Part 1 - Preliminary tests on Portuguese ores. *Bull. Instn. Min. Metall.*, no. 674, 1963, pp. 217-234.
169. EHRLICH, R. P., ROACH, A. G., and HESTER, K. D. Treating Blind River uranium ores by leaching, ion exchange, precipitation. *J. Metals N.Y.*, vol. 11, 1959, pp. 628-633.
170. ARDEN, T. V. The concentration of uranium from low grade ores. *Ind. Chem.*, vol. 32, 1956, pp. 202-209.
171. GAUDIN, A. M., and SCHUHMAN, R. Extracting uranium from its ores. *U.S. Patent 2 736 634*, 1956.
172. MICHAL, E. J., and PORTER, R. R. Recovery of uranium from ores and concentrates. *U.S. Patent 2 890 933*, 1959.
173. Recovery of uranium from ores. *Brit. Patent 851 991*, 1960.
174. NEYTZELL-de WILDE, F. G., and TAVERNER, L. Experiments relating to the possible production of an oxidizing acid leach liquor by autooxidation for the extraction of uranium. *Proc. 2nd International Con-*

- ference on the peaceful uses of atomic energy, Geneva, 1958. New York, United Nations, 1958. Geneva, vol. 3, pp. 303-307.
175. LEGGE, D. I., and LIPWORTH, M. Extraction of uranium from its ores with acid solutions. *U.S. Patent 3 092 447*, 1959.
 176. KANEVSKII, E. A., FILIPPOV, A. P., and NESMEYANOVA, G. M. Heterogeneous oxidation of UO_2 and uranium leaching processes in acid solutions. *Proc. 3rd International conference on the peaceful uses of atomic energy, Geneva*, 1964. New York, United Nations, vol. 12, 1965. pp. 242-249.
 177. CELEDA, J., and LARA, J. G. The kinetics and mechanism of the dissolution of uranous-uranic oxide in sulphuric acid in the presence of ferric ion. *J. Inorg. Nucl. Chem.*, vol. 27, 1965. pp. 2561-2572.
 178. ARDÉN, T. V., and BEAUMONT, J. H. Factors influencing the extraction of uranium from minerals and ores. Part I. A study of the solution of uranium dioxide in sulphuric acid in the presence of oxidizing agents, *CRL/AE-55*, April 1950.
 179. LAXEN, P. A. A fundamental study of the dissolution in acid solutions of uranium minerals from South African ores. *Ph.D. thesis*. University of the Witwatersrand, 1972.
 180. NEEDES, C. R. S., and NICOL, M. J. An electrochemical model for the leaching of uranium dioxide. *Nat. Inst. Metall. Report no. 1380*. Jan. 1972.
 181. SKLIBOVA-KLABALOVA, J., and NEUMANN, L. Mechanism and kinetics of solution of uranium dioxide in sulphuric acid solutions in the presence of ferric ions, *Coll. Czech. Chem. Commun.*, vol. 33, 1968. pp. 1678-86.
 182. LAXEN, P. A., A kinetic study of the dissolution of uraninites in sulphuric acid, *Research in Chemical and Extraction Metallurgy, Aust. Inst. Min. Met.*, 1967.
 183. SOBKOWSKI, J., STUGLIK, Z., and MINC, S., Kinetics of the reaction between uranium oxide (U_3O_8) and iron(II) ions in sulphuric acid, *Nukleonika*, vol. 11, 1966. pp. 799-806.
 184. FISHER, J. R., Bacterial leaching of Elliot Lake uranium ore, *CIM Bull.*, vol. 59, 1966. pp. 588-92.
 185. HARRISON, V. F., GOW, W. A., and IVARSON, K. C. Leaching of uranium from Elliot Lake ore in the presence of bacteria, *Can. Mining J.*, vol. 87, 1966. pp. 64-67.
 186. DUNCAN, D. W., and BRUYNESTEYN, A. Enhancing bacterial activity in a uranium mine. *CIM Bull.*, vol. 64, 1971. pp. 32-36.
 187. ASLAM, K. M., and ASLAM, M. Bacteria aided water leaching of uranium ores. *Nucleus, Karachi*, vol. 7, 1970. pp. 28-36.
 188. GOW, W. A., *et al.* Bacteria-based processes for the treatment of low-grade uranium ores. Recovery of uranium. *Proc. Symp.* 1971. pp. 195-211. *Op. cit.* (180). pp. 195-211.
 189. MROST, M., and LLOYD, P. J. Bacterial oxidation of Witwatersrand slimes. *Op. cit.* (180), pp. 223-239.
 190. GOREN, M. B. Regenerative oxidation with bacteria of acid leach solutions for uranium ores. *U.S. Patent 3 268 288*, 1966.
 191. MCCREEDY, H. H., HARRISON, V. F., and GOW, W. A. A proposed method, using bacteria, for the continuous leaching of a uranium ore. *CIM Bull.*, vol. 62, 1969. pp. 135-140.
 192. SPINK, D. R., and OKUHARA, D. N. Comparative equilibrium and kinetics of Kelex 100/120 and LIX 63/65N/64N Systems for the extraction of copper. *International symposium on hydrometallurgy, Chicago*. 1973. D. J. I. Evans, ed. New York, AIME, 1973. pp. 497-534.
 193. PALLEY, J. N., and PAIGE, P. M. Can electro-winning replace cement copper? *Engng Min. J.*, vol. 173, no. 7, 1972. pp. 94-96.
 194. BISWAS, A. K., REID, J. G. Investigation of the cementation of copper on iron. *Proc. Australas. Inst. Min. Metall.*, no. 242, 1972. pp. 37-45.
 195. NADKARNI, R. M., *et al.* A kinetic study of copper precipitation on iron - Part I. *Trans. Metall. Soc., AIME*, vol. 239, 1967. pp. 581-585.
 196. WOOD, J. T. Treatment of electrolytic zinc plant residues by the jarosite process. *Aust. Min.*, vol. 65, 1973. pp. 23-27.
 197. BECK, J. V. The role of bacteria in copper mining operations. *Biotechnol. Bioengng*, vol. 9, 1967. pp. 487-497.
 198. SYSOEVA, V. V. Mechanism of the oxidation of iron ions by chlorine. *Zh. prikl. Khim. Lening.*, vol. 44, 1971. pp. 2558-2560.
 199. SYSOEVA, V. V., *et al.* Kinetics of the oxidation of iron(II) ions by atmospheric oxygen and by chlorine. *Zh. prikl. Khim., Lening.*, vol. 41, 1968. pp. 1946-1950.
 200. JOHNSON, P. H. The production of acid-ferric sulphate solutions for chemical mining. Nevada Bureau of Mines, *Rept. 13(B)*, 1966. pp. 75-86.
 201. RIECKE, H. G. Oxidation of Fe^{2+} to Fe^{3+} with oxygen in an autoclave. *Ph.D. Thesis*. Berlin Technical University, 1960.
 202. MATHEWS, C. T., and ROBINS, R. G. The oxidation of aqueous ferrous sulphate solutions by molecular oxygen. *Proc. Australas. Inst. Min. Metall.*, no. 242: 1972. pp. 47-58.
 203. MACEJEVSKIS, B., and LIEPINA, L. Kinetics of oxidation of iron salts in aqueous solutions by oxygen under dynamic conditions. I. Kinetics of isothermal oxidation of iron sulphate. *Latv. PSR Zinat. Akad. Vest.*, vol. 9, 1960. pp. 109-116.
 204. LIEPINA, L., and MACEJEVSKIS, B. Mechanism of the oxidation of lower valence cations by oxygen in aqueous solutions. *Dokl. Akad. Nauk SSSR.*, vol. 173, 1967. pp. 1336-1338.
 205. MIHOK, E. A. Use of activated carbon for mine water treatment. *Amer. Chem. Soc., Div. Fuel Chem., Prepr.*, vol. 14, no. 1, 1970. pp. 51-57.
 206. THOMAS, G., and INGRAHAM, T. R. Kinetics of the carbon catalyzed air oxidation of ferrous ion in sulphuric acid solutions. *Op. cit.* (63). pp. 67-79.
 207. STAUFFER, T. E., and LOVELL, H. L. The oxygenation of iron(II) solutions. Relationships to coal mine drainage treatment. *Amer. Chem. Soc., Div. Fuel Chem., Prepr.*, vol. 13, no. 2, 1969. pp. 88-94.
 208. MAYLING, A. A. Using bacteria to keep ferric chloride solutions oxidized for leaching, *Can. Patent 744 701*.
 209. DUTRIZAC, J. E., and MacDONALD, R. J. C. The percolation leaching of pentlandite ore. *C.I.M. Bull.*, 1974. (In press.)

[54] FOAM INJECTION LEACHING PROCESS FOR FRAGMENTED ORE

3,841,705 10/1974 Girard et al. 299/4
3,894,770 7/1975 Huff et al. 299/5
4,017,120 4/1977 Carlson et al. 299/5

[75] Inventor: William H. Engelmann, Minneapolis, Minn.

FOREIGN PATENT DOCUMENTS

219,785 of 1928 Australia 75/101 R

[73] Assignee: The United States of America as represented by the Secretary of the Interior, Washington, D.C.

Primary Examiner—G. Ozaki
Attorney, Agent, or Firm—William S. Brown; Donald A. Gardiner

[21] Appl. No.: 749,586

[22] Filed: Dec. 10, 1976

[57] ABSTRACT

[51] Int. Cl.² C22B 15/10

[52] U.S. Cl. 423/32; 75/101 R; 75/103; 75/117; 299/5; 423/41

[58] Field of Search 75/101 R, 117, 103; 299/5; 423/32, 41

This invention relates to a process for leaching broken or fragmented ore or metal-value containing bodies with a reagent-carrying foam. The foam is generated by adding a surfactant to a leaching solution and passing air or other gas through the solution to generate relatively stable foam bubbles which are propelled through the fragmented mass by gas pressure. The foam can be injected in cycles, allowing drain time, or can be injected continuously with the leachant drainage taking place at the periphery of the ore mass and removed continuously.

[56] References Cited

U.S. PATENT DOCUMENTS

2,161,800 6/1939 Cross 299/5
2,822,158 2/1958 Brinton 299/5 X
3,498,674 3/1970 Matthews 299/5 X
3,647,423 3/1972 Acoveno 75/117 X
3,708,206 1/1973 Hard et al. 299/5
3,799,764 3/1974 Opic et al. 75/117 X

7 Claims, No Drawings

SUBJ
MNG
FILP

UNIVERSITY OF UTAH
RESEARCH INSTITUTE
EARTH SCIENCE LAB.

FOAM INJECTION LEACHING PROCESS FOR FRAGMENTED ORE

FIELD OF THE INVENTION

This invention relates to a method for leaching a fragmented ore body or broken ore, mill tailings, or dumps or other fragmented metal-value containing bodies with a reagent-carrying foam. More particularly the invention is directed to the formation of a relatively stable reagent-carrying foam propelling the foam through the fragmented material, permitting the foamed leachant to drain, and recovering the drained leachant containing metal values. The term fragmented ore or ore-body as employed herein is to be understood to include mill tailings, dumps or other fragmented metal-value containing bodies unless otherwise indicated.

DESCRIPTION OF THE PRIOR ART

In situ leaching has been developed over the past several decades as a method for the recovery of mineral values which could not economically be recovered by other means. Usually this involves the flooding of leaching agents into the ore body, or trickle leaching of fragmented ore-bodies or tailings.

Illustrative of the numerous patents that have been issued in the field and perhaps closest to the present invention are U.S. Pat. Nos. to Hard et al 3,708,206 and to Huff et al 3,894,770. Hard et al shows injecting a leach solution containing a pressurized oxygen-containing gas into an underground ore body. On releasing the pressure an oxygen-containing foam is created. The patentees suggest that the multitude of small bubbles penetrate further into the crevices of the ore formation. Huff et al show the removal of leaching liquor from a deep wellbore in an in-situ mining operation by a gas lift. After treatment the column of lixivant is frothed by injection of air which may contain additional oxygen and/or SO₂. A chemical reaction is affected simultaneously with the gas lift operation in the leachant. Neither of these patents however, are directed to contacting a broken ore body or other fragmented metal-value containing bodies with a relatively stable reagent-containing foam. The relatively large volumes of leach solution required by the prior art methods present a potential environmental hazard should the leach solution find its way into ground water or surface waterways. In addition channelization of flow of the leach solution through the ore body can be a serious problem.

It is the primary object of the present invention to provide a method for leaching a broken or fragmented ore or metal value-containing mass using a leaching reagent-containing relatively stable foam which is passed through the mass and leaches out metal values, whereby the amount of leaching solution required is significantly reduced, the danger of environmental pollution is lessened and the overall efficiency is enhanced.

It is a further object of the invention to drive the foam through the mass by gas pressure.

It is a further object of the invention to leach the mass by driving the foam in a generally upward direction and then permitting the leaching reagent to drain down.

Still another object of the invention is to leach a mass by applying the foam to the top portion of the mass and passing the foam downward by employing gases heavier than air as foaming and driving means.

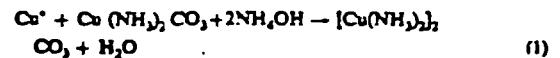
Yet a further object of the invention is to backfill a mine stope with fragmented ore, mill tailings or other

fragmented metal-value-containing mass and then leaching with reagent-containing foam, injecting the foam at the bottom of the mass either in a periodic cycle with drain down periods, or continuously, with drain-down occurring at the periphery of the mass.

Further objects will become apparent from the rest of the specification and from the appended claims.

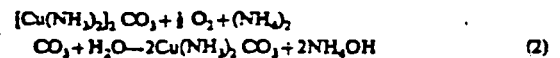
BRIEF DESCRIPTION OF THE INVENTION

Although in situ leach mining is applicable to the recovery of many minerals, to date it has been largely applied to the recovery of copper from underground ore bodies, or heap or dump leaching. Where copper exists in native metal form, leaching may be accomplished by use of cupric ammonium carbonate solutions containing 200 percent equivalent of ammonia. The reaction, forming the reduced compound, cuprous ammonium carbonate, takes place according to the following equation:



To regenerate more leaching agent the cuprous form is reoxidized by contact with air to the cupric form in the presence of ammonium carbonate (formed by reacting CO₂ with NH₄OH) and water.

The overall reaction is:



This process has been used for many decades to recover metal values from low-grade copper ore and also for reprocessing copper mill tailings.

Where copper exists in a combined form, dilute sulfuric acid solution of a pH 1-2 has been used to extract copper as copper sulfate.

Both of these methods use flood leaching or downward percolation of leachant to contact the ore in situ. A number of disadvantages are inherent in the system. Because of the large volume of leachant required, the cost of flood leaching is significant. In the event of an unexpected fissure below the ore body, a considerable loss of reagent may take place with concomitant financial loss. In addition, such loss of reagents poses a serious environmental threat to ground water systems.

In employing downward percolation of leach solutions which are applied by sprays or trickle tubes to fragmented ore heaps or to underground mineral deposits, the volume of reagents is considerably less than in flood leachings. As a result, the cost is less and the environmental impact is lessened. However, the percolation technique is limited to a downward advancement of leach solution.

In many cases contacting a fragmented ore or metal value containing body in a generally upward or horizontal advancement would be highly beneficial. However, the prior art flooding or downward percolation techniques do not readily permit this.

I have devised a method for passing reagent-carrying foam through the fragmented material employing air or other gas pressure.

A surface active agent or surfactant is incorporated in the leaching solution. Surfactants usually lower surface tension of water or other liquids by 50 to 70 pct with as low a concentration as 0.1 pct. Their presence in the solution also effect temporary entrapment of air or

carrier gas used for bubble generation. The concentration of surfactant determines the foam standup time, with higher concentration effecting easier foaming action and longer foam duration. Foam stabilizers may be added to extend standup time.

In the case of leaching native copper with cupric ammonium carbonate, the oxygen required to regenerate the leaching agent as shown in equation 2 is supplied by air or oxygen-containing gas under pressure. It serves the three-fold function of being an oxidant for the reaction, a foam producer and as the driving means to propel the foam through the mass.

In other leaching systems, such as acid leaching of sulfide types of copper ores, air or oxygen is not required for the leaching reaction and serves only as the foam carrier and driving medium. However, other gases may be substituted for air with advantages where it is desired to move the foam in directions other than the vertical (such as laterally) or with greater speed.

Gases lighter than air, such as helium or helium/air mixtures as foam carriers increases the traverse speed upward through a fractured or rubbled ore body. Carbon dioxide, or vapors of halogenated hydrocarbons, either in pure form or as mixtures with air, will effect a more rapid downward migration of foam through the fractured ore since they are heavier than air. Sloping veins of fragmented ore deposits are particularly amenable to treatment according to this modification.

Use of this foaming technique serves to reduce channelization of reagent flow patterns within a fragmented ore body. This results from the lower density of the foamed reagent (as compared with reagent liquid) flowing through the interstitial spaces of the rubbled ore. The foam can be injected in cycles, allowing drain down, or continuously.

EXAMPLE I

The following example illustrates the process. To simulate a sloping, fragmented ore vein, a plastic tube (6 in. diam. X 6 ft length), was closed at the bottom end and was supported in a stand at an angle of 30° from the horizontal. It was three quarters filled with native copper ore fragments (ranging in mesh size of minus 2 in, plus 1 in). The volume of voids within the ore fragments was determined to be about 10 liters.

An ammoniacal ammonium carbonate 0.2 molar leachant solution was mixed with 1 percent by weight of a foaming-type surfactant, Tergitol NPX⁽¹⁾

⁽¹⁾ A nonyl-phenol-polyethyleneoxide surfactant containing an average of 10 1/2 C₂H₄O units per molecules and distributed by Union Carbide Corporation

A measured quantity of the leachant was added to the tube and allowed to flow down to the bottom. Air was admitted into the bottom end of the tube via a 1/4 inch fitting and bubbled through the solution to cause foaming. The minimum amount of leachant solution which produced a foam which emerged at the top of the ore mass was about 200 ml, with a preferred volume found to be about 400 ml. Thus, the volume of leaching solution required with the foaming technique of this invention is only about 2 to 4 percent of that required in full-flooding leaching.

The diffusion of leachant into the pore spaces or cracks of each ore fragment is generally considered to be the limiting factor in the total leaching process. Superficial contact of the leaching solution and the ore, therefore, need only be intermittent as in trickle leach-

ing, as in the process of this invention in which foam carries the leaching agents.

The foaming agent or surfactant employed was a nonionic material. However, almost any surfactant type can be used, care only being needed where possible incompatibility might be encountered, as with strong acids or basic type leaching agents which could decompose the surfactant.

EXAMPLE II

The effect of concentration of foaming agent on the stability of the foam is shown in the following example.

A plastic tube, 6 inches in diameter and 77 inches long, inclined 55% from the vertical, was filled with broken copper ore having a mesh size of minus two inches, plus one inch. About 400 ml of a 0.2 normal ammonium carbonate leach solution to which Tergitol NPX was added was employed as the leaching solution. The solution was poured into the tube and collected at the bottom. It was then aerated with a flow of air adjusted to produce foaming and the resulting foam ascended in the tube. So long as the air flow was sufficient to produce foaming, the rate of air flow appeared to have only a slight effect on foam height.

The following table gives the height of the foam in the tube and the foam stability and shows the stability of the foam to be a function of the concentration level.

TABLE I

Foam stability and rise height as a function of surfactant concentration in a 0.2 normal ammonium carbonate solution		
Surfactant, pct	Foam height, inches	Maximum foam stability, minutes
0.05	17	12
0.10	32	35
0.20	45	40
0.40	60	50
0.80	75	70
1.60	77	75
3.20	77	85

EXAMPLE III

The experiment of Example 2 was repeated using a 0.2 normal sulfuric acid solution. Table 2 sets forth the results obtained.

TABLE 2

Foam stability as a function of surfactant concentration in a 0.2 normal sulfuric acid solution		
Surfactant, pct	Foam height, inches	Maximum foam stability, minutes
0.05	19	23
0.10	30	50
0.20	41	55
0.40	48	60
0.80	70	70
1.60	77	75
3.20	77	90

As shown in Tables 1 and 2 nonionic surfactants function well in either acid or basic solutions. The foam stability times were adequate with Tergitol NPX, slightly greater time periods being observed in the acidic leaching medium.

Under comparable experimental conditions, the 0.2 N ammonium carbonate solution yielded 1,080 parts per million (ppm) copper after seven successive foam injection-foam drain down cycles. The 0.2 N sulfuric acid solution yielded 150 ppm after seven foaming cycles. The test ore was a native copper ore.

These tests simulated a fragmented ore body with no fracture or fissure to allow leaks. With this closed system, recoveries of drained-down foam approximated 90 to 95 pct. Most losses or retention of foam or fluid occur within capillary-sized pore spaces and hairline fissures. In a further typical experiment, surfactant solutions were aerated to convert about 150 ml to foam, to fill a void volume of about 10 liters. After the foam collapsed, the liquid recovered from the foam fraction was about 135 to 143 ml (90 to 95 pct recovery).

Examples 1-3 relate to leaching fragmented sloping ore bodies. The process may be employed to leach mine stopes, backfilled with low-grade ore or mill tailing. The surfactant-containing leachant can be introduced at the bottom of the ore mass and caused to foam-up and rise through the mass using air or lighter than air gas mixture, such as a helium-air mixture. The leaching process can be carried out cyclically, with foam-up and drain-down cycles or continuously, with the drain-down occurring at the periphery of the mass.

Another modification of the process is to foam the leachant with a heavy gas, such as CO₂ or vapors of halogenated hydrocarbons to produce a foam with a relatively high density. Said foam is then applied to the top surface of mill tailings, piles or dumps where because of the greater density more rapid downward movement of the foam is achieved.

What is claimed is:

1. A process for the recovery of copper values from fragmented copper-containing bodies which comprises:
 - a. introducing a leaching solution comprising a leaching agent consisting of ammonium carbonate or sulfuric acid and a surfactant into a mass of said fragmented bodies,
 - b. foaming said solution by introducing a gas thereinto,
 - c. passing the foamed leaching solution through the said mass whereby said foamed leaching solution forms pregnant leachant containing copper values, and
 - d. recovering the pregnant leachant.
2. The method of claim 1 wherein the fragmented body is a sloping ore body, the surfactant is non-ionic and the foam is passed generally in an upward direction through said body.
3. The method of claim 2 wherein the ore body comprises a sulfide type copper ore, and the leaching agent comprises dilute sulfuric acid.
4. The method of claim 3 wherein the gas introduced to foam the leaching solution is lighter than air.
5. The method of claim 1 wherein the fragmented body comprises mill tailings, dumps or heaps and the foamed leaching solution is applied at the top of said fragmented body.
6. The method of claim 5 wherein the gas introduced to foam the leaching agent is heavier than air.
7. The method of claim 1 wherein the foamed solution is passed upwardly through the mass, periodically alternating with drain down cycles.

35

40

45

50

55

60

65

North America has been conducted by *Sbar and Sykes* [1973]. They compiled all the available data from fault plane solutions of earthquakes, in situ stress measurements by overcoring and hydrofracturing, and geologic observations and discovered that they all yield nearly identical directions for the principal stresses. From west of the Appalachian Mountain system to the Rocky Mountains and from Illinois to Ontario the maximum compressive stress trends east to northeast. The authors relate unhealed fault zones and high stresses and suggest their use as a means to assess earthquake risk within plates. They conclude that stress measurements may provide one of the best clues to the driving mechanism of plate tectonics. In a second paper, *Sykes and Sbar* [1973] use stress measurement results and analyses of focal mechanism of earthquakes to infer the state of stress within lithospheric plates on a worldwide scale. Another attempt to explain global tectonics in terms of crustal stress has been made by *Raleigh* [1974]. He used available stress measurement results, geological observations, and focal mechanism solutions to conclude that the stresses in the far western United States are related to the differential motion of the Pacific and North American plates. The San Andreas type faulting gradually changes into normal faulting as the western Basin and Range is approached. The pattern of deformation then becomes more complex as the Rocky Mountains are approached but is dominated by an east-west extension.

Efforts are being made to discover the sources of present-day stresses. *Friedman* [1972] identifies two types of stresses: one due to existing external loads and the other due to residual strain. The latter can be

defined as a stress or strain acting within a body of rock and satisfying internal equilibrium with no external loads across the boundaries. Such stresses can be related to paleotectonics and thermal history. Present loads can be attributed to present topography, present tectonics, and man-induced conditions. *Friedman* has found large differential residual stresses (up to 400 bars). He also discovered that residual stresses completely relax only when grains are freed from constraints of nearest neighbors. These stresses help produce strength anisotropy and sometimes control the orientation of fractures. Field measurements of residual strain in rock masses have been conducted by *Swolfs et al.* [1974].

In summary, it is apparent that although the perfect method for measuring in situ stresses is yet to be devised, the existing techniques do provide results that are often consistent enough to be credible. Removing the depth limitation and reducing the number of assumptions made in calculating stresses should be the goal of those striving to improve measuring techniques. As to actual stress measurements, regardless of the method, a two-prong program is recommended. First, the existing data from all over the world should be collected, it being kept in mind that almost any mining area and large dam site has had some stress measurements carried out. The scientific compiling and mapping of these measurements on a global basis could have an immediate effect on our understanding of plate tectonics. In addition, regional stress measurements in crucial areas are urged, either to determine the state of stress for the first time (e.g., San Andreas fault) or to confirm and extend previous results (e.g., Iceland).

the processes which involve cohesion, ability to fracture into two or more pieces, energy [Griggs and others] are two basic types. One is normal to the least principal stress and are termed tensile fractures. The other type of fracture motion is parallel to the least principal stress and inclined from 45° to the maximum principal stress. Surfaces contain the same amount of energy. Reviews by *Priddy* [1971] and *Obert* [1968-1972]. This volume emphasizes the progress in the last 4 years. Apologies are extended for omissions and criteria by a review of rock mass.

FRACTURE

It is necessary to understand the physical processes, i.e., the physical mechanisms, and fracture relations between material properties and criteria here referred to as macroscopic. The forces between the grains they undergo relative to fracture studied at grain boundaries as a function of position, texture, produced by pores, principal stress. Multiple to the unaided eye, outcrop, and treated in relation to and primarily by the macroscopic or microscopic. Submicroscopic this scale has dealt with energy, study of the recognition of the chemical bonds up and that this energy. Because of its importance in the criteria in the Griggs from knowledge of stable fractures of silicate and carbon 10² and 10³

UNIVERSITY OF UTAH
RESEARCH INSTITUTE
EARTH SCIENCE LAB,

SUBJ
MNG
FIR

Fracture in Rock

Melvin Friedman

Center for Tectonophysics, Texas A&M University, College Station, Texas 77843

INTRODUCTION

Fracture is perhaps the most important topic in rock mechanics today, primarily because it is the dominant mechanism of rock failure at the relatively low pressures and temperatures at shallow depths in the earth's crust and because existing fractures strongly influence the physical and mechanical behavior of the rock mass. Fracture considerations therefore pervade all of man's interests dealing with exploration and production of natural resources, engineering projects under or on the earth's surface, and the prediction, modification, and control of earthquakes. For example, (1) estimates indicate that about 5% of the energy generated in the United States is consumed in fracturing rocks [Lewis, 1966]; (2) in the petroleum industry an understanding of fracture is essential in relation to 'fracture porosity' reservoirs, hydraulic fracturing, secondary recovery programs, structural in-

ferences from existing fractures, underground storage of gas, and drilling technology; (3) in certain geothermal projects, fractures serve both as subsurface permeability channels and as surfaces to heat circulating water; (4) the in situ 'mining' of oil shale or of the gasification of coal is primarily a matter of man's ability to fracture the rock mass under controlled conditions; (5) in mining and tunneling operations, fractures influence the stability of the openings as well as the extraction of rock or ore; and (6) recent developments in earthquake research have focused attention on fracture (dilatancy) as the source of a host of premonitory events from which it may someday be possible to predict earthquakes [Nur, 1972; Whitcomb et al., 1973; Scholz et al., 1973]. Accordingly, there is ample motivation to gain a better understanding of fracture processes in rock and of the mechanical behavior of rock masses containing fractures.

Regardless of scale, fracture (fracturing) is defined as

the processes which involve at least momentary loss of cohesion, ability to resist differential stress, separation into two or more parts, and release of stored elastic strain energy [Griggs and Handin, 1960, p. 348]. In general there are two basic types of fracture. Extension fractures occur normal to the least principal compressive stress σ_3 ; these are termed tensile fractures if σ_3 is tensile, i.e., negative in sign. The other type is the shear fracture for which particle motion is parallel to the fracture surface that may be inclined from 45° to a few degrees in the direction of the maximum principal compressive stress σ_1 . Both fracture surfaces contain the intermediate principal stress σ_2 .

Reviews by Price [1966], Jaeger [1967], Brace [1964, 1971] and Obert [1972] are recommended for additional general reading. Further, fracture is covered in detail in the seven volume advanced treatise edited by Liebowitz [1968-1972]. This work is particularly valuable because it emphasizes the thinking of fracture mechanicians working with metals and ceramics. In the present review, advances in the last 4 years are emphasized, but earlier work is included to provide the necessary background. Apologies are extended in advance to all whose work I have overlooked. Advances in study of fracture mechanisms and criteria will be discussed first and then followed by a review of recent work dealing with fractures in the rock mass.

FRACTURE MECHANISMS AND CRITERIA

It is necessary to distinguish between fracture mechanisms, i.e., the physical and chemical processes involved in fracture, and fracture criteria which express functional relations between stress, strain, fracture strength, and material properties [Bieniawski, 1967a]. Fracture mechanisms and criteria have been studied at different scales, here referred to as submicroscopic, microscopic, and macroscopic. The first involves rupture of the cohesive forces between the ultimate structural units of a body as they undergo relative displacement. Microscopic refers to fracture studied at the level of the constituent grains and grain boundaries and takes into account rock type (composition), texture, fabric, and stress inhomogeneities produced by pores, preexisting cracks, grain contacts, and residual stress. Macroscopic aspects involve fracture visible to the unaided eye in the test specimen, hand specimen, outcrop, and greater rock mass. Here fracture is treated in relation to 'macroscopic' or average stresses and primarily by the Coulomb-Mohr criterion, which does not deal with phenomena that occur at the submicroscopic or microscopic levels [Handin, 1969].

Submicroscopic aspects. Recent work on fracture at this scale has dealt with measurements of fracture surface energy, study of chemisorption phenomena, and consideration of the role of dislocations. Griffith [1921, 1924] recognized that energy is absorbed in the breaking of chemical bonds upon the creation of new fracture surface and that this energy γ is a fundamental material property. Because of its importance in the development of fracture criteria in the Griffith tradition, γ has been measured from knowledge of the input energy and the surface area of stable fractures created in stiff testing devices. For common silicate and carbonate single crystals, γ ranges between 10^2 and 10^3 ergs/cm² [Gilman, 1960; Brace and

Walsh, 1962; Santhanam and Gupta, 1968]. Measurements of γ for rocks at room temperature and pressure and for nominal or partially corrected surface areas are $>10^4$ ergs/cm², significantly higher than that for the intact grains [Perkins and Bartlett, 1963; Perkins and Krech, 1966; Moavenzadeh et al., 1966; Forootan-Rad and Moavenzadeh, 1968; Summers et al., 1971; Friedman et al., 1972b; Hoagland et al., 1973]. Energy γ increases further with increasing effective confining pressure (P_e) to 200 bars [Perkins and Krech, 1966] and decreases with heat treatment (due to thermal cracking) and surface active agents [Moavenzadeh et al., 1966; Forootan-Rad and Moavenzadeh, 1968]. The apparently higher values for rock led to speculations that energy-dissipating processes, especially plastic work, occur at propagating crack tips. Friedman et al. [1972b] and Hoagland et al. [1973] show, however, that if all the fracture surface area created during fracturing is considered, γ is reduced to the level of that for the constituent grains or crystals and there is no necessity to call upon inelastic processes, particularly at low P and T . This point is supported by measurements of γ for single crystals of calcite [Santhanam and Gupta, 1968]. The importance of energy considerations in rock fracture is emphasized in recent work [e.g., Hardy et al., 1973; Hudson et al., 1973; Krech, 1974; Cain et al., 1974].

Included in the submicroscopic view are the chemical effects termed chemisorption, stress corrosion, or the 'Rebinder effect,' i.e., the sum total of all surface strength interactions. That water and solutions of several cations tend to reduce fracture strength has long been known to quarrymen, miners, and drillers. In recent years, however, the chemical effects have been separated from mechanical ones, and the exact nature of the changes in the type and strength of the chemical bonds has been studied [Griggs and Blacic, 1965; Griggs, 1967, 1974; Colback and Wüid, 1965; Moavenzadeh et al., 1966; Wiederhorn, 1967; Westwood et al., 1967, 1968; Westbrook and Jorgensen, 1968; Blacic, 1971, 1972; Swolfs, 1972; Martin, 1972; Cornet, 1972; McCarter and Willson, 1973; Balderman, 1974; Jackson et al., 1974; Vutukuri, 1974]. The work of Griggs, Blacic, and Balderman is included, even though it deals with the ductile flow of quartz at high P_e and T , since it provides insight into hydrolytic effects that may influence fracture at lower P_e and T . The substitution of OH bonds for some of the very strong Si-O bonds drastically weakens quartz and probably most other silicates. At low P_e and T , however, the fracture strength of quartzose sandstone is reduced only 8-15% [Swolfs, 1972], and the tensile strength of limestone only about 20% [Vutukuri, 1974] in the presence of surface active solutions. On the other hand, Jackson et al. [1974] report up to a 20-fold increase in drilling rate due to matching environmental chemistry, bit design, and the chemomechanical properties of the rock. Most probably the chemical effects serve to lower the fracture surface energy γ and hence the fracture strength. This further indicates the importance of γ in the fracture process.

The third submicroscopic topic involves the idea that cracks can be represented by continuous arrays of dislocations. Consequently, dislocations enter the theory of fracture in two ways, as crystal dislocations which play a part in the physics of fractures and also as a convenient mathematical or conceptual element in the macroscopic

treatment of cracks [e.g., *Bilby and Eshelby*, 1968]. The basic problem in the theory of cracks is the determination of the way in which a crack modifies an applied stress field [*Griffith*, 1921, 1924; *Orowan*, 1959; *Irwin*, 1960; *Barenblatt*, 1962; *McClintock and Walsh*, 1963, among others]. Using dislocations, *Bilby and Eshelby* [1968, p. 159] show that *Barenblatt's* theory completely corresponds to the theories of *Griffith*, *Orowan*, and *Irwin*. Most of the descriptive work relating dislocations and cracks has been done on metal foils [*Patterson and Wilsdorf*, 1968] and on ceramics [*Stokes*, 1972]. Although dislocation arrays have been studied in relation to gliding and recrystallization flow in geological materials [e.g., *Christie et al.*, 1964; *McLaren et al.*, 1967, 1970; *McLaren and Hobbs*, 1972; *Hobbs et al.*, 1972; *Phakey et al.*, 1972; *Green and Radcliffe*, 1972; *Heard*, 1972; *White*, 1973a, b; *Christie and Ardell*, 1974], little if any systematic study of the genetic relations between dislocations and cracks has been made for rocks.

Microscopic aspects. Perhaps the greatest advances in recent years in our understanding of fracture in rock have come from direct and indirect study of when microfractures form in relation to loading history, where and in what orientations they occur, how they propagate, and how microfractures develop into macrofractures. A microfracture here is any intergranular or intragranular fracture that cannot be seen with the unaided eye; for a detailed classification of different types, see *Simmons and Richter* [1975]. Current understanding has come from determination of dilatancy or fracturing precursory to macroscopic tensile or shear fracture (1) by measurement of volumetric strain versus differential stress [*Brace et al.*, 1966; *Bieniawski*, 1967b, c; *Crouch*, 1970; *Wawersik and Fairhurst*, 1970; *Zoback and Byerlee*, 1974b]; (2) through study of microseismicity, electrical resistivity, and acoustic properties [*Mogi*, 1962; *Brown*, 1965; *Brace et al.*, 1965; *Brace and Orange*, 1968a, b; *Brace*, 1971, 1974; *Scholz*, 1968a, b, c, d, e; *Hoshino and Koide*, 1970; *Nur and Simmons*, 1969; *Hardy et al.*, 1970; *Chugh et al.*, 1972; *Thill*, 1973; *Rao and Ramana*, 1974; *Thomsen and Wu*, 1974; *Hadley and Brace*, 1974; *Byerlee*, 1974; *Gramberg*, 1974; *Rummel*, 1974; *Simmons et al.*, 1975]; (3) through study of permeability changes up to the macroscopic fracture strength [*Mordecai and Morris*, 1971; *Zoback and Byerlee*, 1974a; *Farran and Perami*, 1974]; (4) through cyclic loading tests which further demonstrate the importance of fracture initiation at stress levels below those for macroscopic fracture upon monotonic loading [*Hardy and Clugh*, 1970; *Haimson and Kim*, 1972; *Haimson et al.*, 1973; *Haimson*, 1974; *Attewell and Farmer*, 1973; *Peng et al.*, 1973; *Bombolakis*, 1973; *Douglas and McDougall*, 1973; *Cruden*, 1974; *Zoback and Byerlee*, 1974b; *Kranz and Scholz*, 1974; *Cain et al.*, 1974; *Montoto*, 1974]; and (5) by means of direct microscopic observation [*Hoek*, 1965; *Paulding*, 1965; *Wawersik*, 1968; *Wawersik and Brace*, 1971; *Bombolakis*, 1968, 1973; *Willard and McWilliams*, 1969; *Hoshino and Koide*, 1970; *Friedman and Logan*, 1970a, b; *Friedman et al.*, 1970, 1972a, 1973, also manuscript in preparation, 1975; *Baldrige and Simmons*, 1971; *Peng and Johnson*, 1972; *Savanick and Johnson*, 1972, 1974; *Koons and Ulmer*, 1972; *Gay*, 1973; *Dunn et al.*, 1973; *Sriruang and Hamil*, 1973; *Boland and Hobbs*, 1973; *Hallbauer et al.*, 1973; *Sangha et al.*, 1974; *Sprunt and*

Brace, 1974a, b; *Conrad*, 1974; *Olsson*, 1974a, b; *Simmons et al.*, 1973, 1975; *Simmons and Richter*, 1975; *Engelder*, 1974; *Gallagher*, 1974; *Gallagher and York*, 1974; *Gallagher et al.*, 1974; *Gramberg*, 1974; *Tapponnier and Brace*, 1974]. In addition, photoelastic model work and experiments with glass give insights on how fractures modify the far field stresses and propagate [*Brace and Bombolakis*, 1963; *Bieniawski*, 1967b; *Bombolakis*, 1968]. The recent photoelastic study of a granular aggregate by *Gallagher et al.* [1974] provides, at least for porous sandstones, a heuristic model to help explain precursive microfracturing, the extension fracture nature of these microfractures, the growth of macroscopic shear fracture from extension microfractures, the widening of fault zones with increasing effective confining pressure, and why residual strains can control fracture orientations and strength and anisotropies [*Friedman and Logan*, 1970a; *Friedman*, 1972a, b; *Friedman and Bur*, 1974].

The deformational history of an experimentally deformed brittle or semibrittle rock can be characterized by seven regions [*Brace*, 1964, 1971] (Figure 1a). This scheme is modified by *Wawersik and Brace* [1971] to describe more accurately the postfailure history as detected in stiff testing apparatus (Figure 1b). Although the details of this history vary with rock type (composition), texture, fabric, and P_e , certain generalizations are possible as follows: In region 1 (Figure 1a), preexisting cracks and pores not previously closed by application of confining pressure are closed further until they are stabilized. The load-bearing framework of the rock deforms essentially elastically in region 2. The boundary between regions 2 and 3 marks the onset of stable crack initiation and growth as internal stress concentrations exceed the local fracture strength of favorably oriented elements. The initiation of microfractures at this point is reasonably well predicted by *Griffith* or modified *Griffith* theory [*Bieniawski*, 1967a, b, c]. Throughout regions 3 and 4 in crystalline textured rocks, most of the intragranular microfractures are nearly parallel or are inclined at small angles to the greatest principal compressive stress σ_1 (load axis) across the boundaries of the specimen. The low-angle microfractures are favored at low P_e ; those inclined at $>30^\circ$ are favored at high P_e . In porous sandstones, extension or tensile microfractures initiate at and propagate along lines connecting stress concentrations developed at grain contacts. Their orientation is a function of the packing, but they also tend to be oriented within 30° - 40° to the load axis, σ_1 . At this stage, both intragranular and intergranular microfractures occur, the former being predominant in many rocks, and they tend to form throughout a homogeneously loaded specimen.

The boundary between regions 3 and 4 is best detected by the stress-volumetric strain curve as it becomes vertical and assumes a negative slope. In region 4 the abundance of microfractures progressively increases; they tend to concentrate along the path of the eventual macroscopic shear fracture or fault; intragranular and intergranular fractures tend to combine; those inclined at 20° - 40° to the load axis propagate in their own planes; and those subparallel to the load axis propagate until they reach an obstruction or combine with neighboring en echelon ones to form a cataclastic zone along which shear stress is appreciable. The width of region 4 is directly related to the

width of which in low norm microfrac them occ individua abundant tion, but a result, and coal increases tains a l concentrated and that load axis

The bo region, is fracture has come or servo- of the c *Barnard* 1967d, 1970; *W* *son et al* specimen cuts or f 1970b; C loss of st microfra macrosc the post

At all charact regions crystalli tures on the end [*Wawer* plates p shear fr region V of a loo low P_e pinpoint spicuous VII, wh pressur disappe beyond Westerl 1b), an

Once predom by *Log* shear c micros 1970b, fractur and *Du* spicuous macros sion fra

width of or the number of shear zones in the specimen, which in turn increase with increasing P_e . At low P_e i.e., low normal stress across fracture planes, the individual microfractures propagate to greater lengths, and a few of them occur prior to macroscopic failure. At higher P_e the individual microfractures tend to be shorter but more abundant, as stress concentrations exist for their initiation, but high normal stresses stifle their propagation. As a result, macroscopic shear zones become more abundant and coalesce, and the ultimate strength of the specimen increases. Thus prior to macroscopic failure the rock contains a host of precursory microfractures that are concentrated along the path of the eventual macroscopic fault and that are oriented predominantly at low angles to the load axis.

The boundary between regions 4 and 5, the postfailure region, is the ultimate strength of the rock. Information on fracture development in region 5 (region IV, Figure 1b) has come primarily from the development of high-stiffness or servo-controlled testing machines which permits study of the complete force displacement record (Turner and Barnard, 1962; Barnard, 1964; Cook, 1965; Bieniawski, 1967d, 1969; Wawersik, 1968; Rummel and Fairhurst, 1970; Wawersik and Brace, 1971; Hardy et al., 1973; Hudson et al., 1973; Peng, 1973) and secondarily from study of specimens obtained after specific displacement along pre-cuts or faults (Friedman et al., 1970; Friedman and Logan, 1970b; Conrad, 1974). The machines have verified that the loss of strength is caused by the cumulative effect of local microfracturing and that depending on rock type and P_e macroscopic failure may not begin until relatively late in the postfailure region.

At all confining pressures the local microfracturing that characterizes region 4 continues in region 5 (Figure 1b, regions III and IV, respectively). In unconfined tests, crystalline textured rocks exhibit relatively large fractures oriented parallel to the load axis that develop toward the end of region IV and that lead to the onset of spalling (Wawersik, 1971). Spalling and buckling of near-surface plates proceed during regions V and VI. In region VI, small shear fractures form and grow into a macroscopic fault in region VII. In region VIII the formerly intact rock consists of a loose mass of fragments held together by friction. At low P_e the same division occurs, but it is not possible to pinpoint the beginning of region V. Slabbing is less conspicuous, and multiple shear zones occur in regions VI and VII, which increase in width with increasing confining pressure. As the confining pressure is increased, slabbing disappears, and macroscopic faulting begins shortly beyond the ultimate strength. At higher P_e (1.5 kbar for Westerly granite), faulting coincides with point B (Figure 1b), and regions IV and V cannot be detected.

Once faulting occurs, the processes of frictional sliding predominate (Figure 1a, regions 5-7; see separate review by Logan (1975)). Additional microfractures result from shear displacement along discrete faults. These include microscopic feather fractures (Friedman and Logan, 1970b; Engelder, 1974; Conrad, 1974), Hertzian (tensile) fractures, and Riedel shears (Jackson et al., 1974; Jackson and Dunn, 1974). The feather fractures are the most conspicuous of these features and are also developed macroscopically (Cloos, 1932). They are probably extension fractures developed immediately adjacent to the slid-

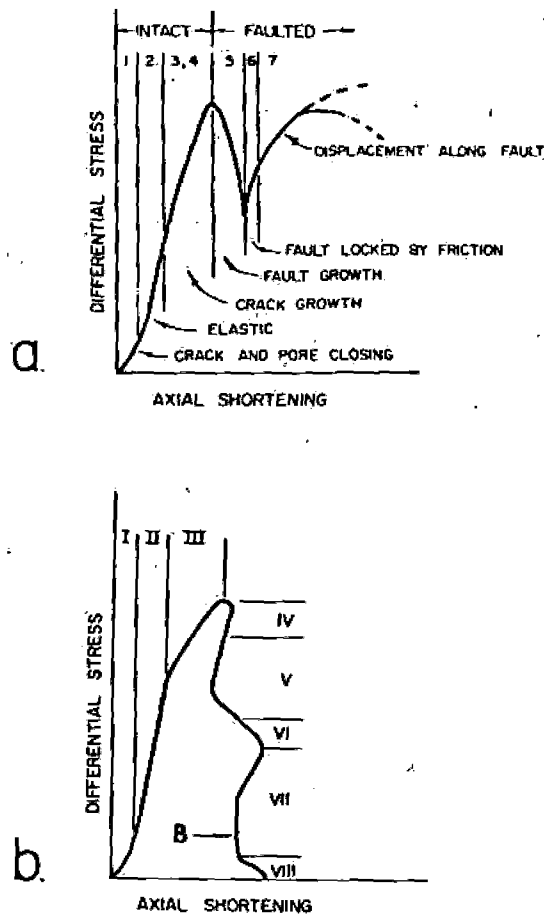


Fig. 1. Diagrammatic stress-shortening curves and associated regions of deformation. (a) Typical curve from a standard testing machine, modified after Brace [1964, 1971]. (b) Curve from a stiff testing device or a servo-controlled one, after Wawersik and Brace [1971].

ing surface (Conrad, 1974) and are a source of dilatancy during faulting (Friedman, 1974).

Some of the above microscopic insights into fracture in rock have been incorporated into analytical studies. Particularly noteworthy are a mechanical equation of state for brittle rocks in regions 1 and 2 (Brady, 1970, 1973); computer models that simulate the activation, growth, and coalescence of incipient flaws (Hanson et al., 1971; Shockey et al., 1974a) and of the deformation of dry porous rocks (Schatz et al., 1974); a constitutive equation for dilatant rocks (Stuart, 1974); numerical simulation of stress concentrations in rocks (Heinze and Goetze, 1974); simulated effects of cracks on seismic velocities (Anderson et al., 1974); and applications of stress corrosion theory to earthquake seismicity (Anderson and Perkins, 1974) and of crack propagation studies in ceramics to magma emplacement (Perkins and Anderson, 1974).

Most of the above has dealt with fracture in rocks deformed in the brittle or semibrittle regime. Ductile fracture, on the other hand, occurs as the P_e , T , and strain rate ($\dot{\epsilon}$) conditions are changed to produce at least 5-10% of permanent deformation prior to failure. Metallurgists and ceramicists have led in the study of ductile fracture; e.g., Stokes [1972] relates crack initiation to dislocation accumulations at grain boundaries in ductile ceramics. Earth scientists, however, have been so preoccupied with brittle fracture that work on ductile fracture has just begun. A significant step has recently been made by

Olsson [1974b] who finds that cracks are nucleated by interactions between twin lamellae and grain boundaries in limestone.

A theory of time-dependent crack growth in which no significant restrictions are placed on the nature of disintegrating material near the crack tip is formulated by Schapery [1975]. The material may be highly nonlinear, rate dependent, and even discontinuous.

Macroscopic aspects. Important recent advances in study of macroscopic fracture mechanisms and criteria include verification in true scale experiments that the concept of effective pressure and Coulomb-Mohr theory can be used as mechanical bases for earthquake control and modification, refinement in the study of strain accumulation and stress changes along faults, clarification of the Coulomb-Mohr criterion [Handin, 1969; Mogi, 1974], and certain experimental rock deformation studies.

The control of earthquakes along an existing fault by fluid injection at Rangely, Colorado [Raleigh et al., 1972], has confirmed the concept of effective pressure and the use of Coulomb-Mohr failure envelopes in the solution of full-scale rock mechanics problems. This experiment was initiated following the occurrence of earthquakes thought to be caused by injection of waste fluids into a disposal well at Denver, Colorado. Evans [1966] and Healy et al. [1968] reasoned that the injected fluids increased the fluid pressure, which decreased the effective normal stress across an existing fault while not changing the shear stress. This situation permitted displacement along the fault and the earthquakes. At Rangely the U.S. Geological Survey team has been able to correlate fluid injection history, earthquake incidence and location, focal plane solutions, measurements of subsurface principal stress orientations and magnitudes, and laboratory studies of frictional sliding to explain the behavior of the rock mass. This has been an encouraging example of technical know-how in rock mechanics and holds promise for eventual controlled modification of earthquake-producing faults [Handin and Raleigh, 1972].

Studies of strain accumulation and stress changes along faults (shear fractures) are important to an understanding of earthquake source mechanisms and possible dilatancy of the adjacent rock mass associated with frictional sliding. It is beyond the scope of this review to comment on the vast data on ground motions being obtained from monitoring faults in the field, but certain analytical and photoelastic studies are noteworthy because they relate to the fundamentals of shear fracturing. Among these are the analyses of strain accumulation on a strike slip fault [Turcotte and Spence, 1974] and of water flow paths around a dislocation on a fault [Weertman, 1974]. Both carry on the dislocation model approach to fault problems [Steketee, 1958; Chinnery, 1961, 1963, 1970; Chinnery and Petrak, 1968; Weertman, 1964, 1965]. In addition the photoelastic analysis of an obstruction (ramp or asperity) along a fault by Barber and Sowers [1974] illustrates the nature of the stress concentrations, how they can be described by action of cracks and contact loads, and how fault displacement depends on deformation about the obstruction, which in turn can cause significant dilatant effects.

Obviously, a huge literature exists on experimental rock deformation, most of which involves rock fracture in some

way. Some of these studies are cited above in conjunction with microscopic aspects, but several particularly significant studies are mentioned here because they typify recent approaches to the experimental study of macrofractures. Problems related to drilling and rock fragmentation have prompted work like that of Lindholm et al. [1973] who show that for basalt, at least, there is strong dependence of fracture strength on T (to 1400°K), $\dot{\epsilon}$ (10^{-4} to 10^{-1} s $^{-1}$), and P_e (to 7 kbar). In addition to giving a fracture criterion to fit the experimental data they show that as temperature increases, the mode of fracture changes from brittle fracture to more pervasive cataclasis. Similar problems prompted Shockey et al. [1974b] to study fracture in shock experiments. They obtain good agreement between calculated and measured fragment size distributions and thus illustrate that fracture can be predicted from a few measurable rock properties. To go deeper on fragmentation research, see theme 5, volume 2B, of the *Proceedings of the Third Congress of the International Society of Rock Mechanics*. Other studies include verification that fracture strength is dependent on the intermediate principal stress [Handin et al., 1967; Wawerik, 1971; Mogi, 1971; Nascimento et al., 1974] and recognition that Lüders' bands in rock are local zones of intense cataclasis but that they are not strictly shear fractures because the dihedral angle between conjugate bands is 10°-50° larger than that for shear fractures in the same specimen [Friedman and Logan, 1973].

In significant departure from work with intact cylindrical specimens, Handin et al. [1972] and Pattison [1972] experimentally buckled long rectangular rock layers, P_e to 2.0 kbar, and correlated the observed fractures with those expected from elastic beam theory and with those actually observed on natural folds [e.g., Stearns, 1964, 1968; Friedman and Stearns, 1971]. In addition, Friedman et al. [1972a, 1973] and Min [1974] produced faulted drape folds experimentally and correlated the orientation and sequence of faults to natural counterparts [e.g., Friedman, 1969], sandbox models [Sanford, 1959], and analytical boundary value solutions [Min, 1974]. Another departure from use of cylindrical specimens involves study of fracture growth around a host of differently shaped openings. Here the fracture development agrees exactly with that predicted theoretically [Gay, 1973]. Lajtai [1971], and Lajtai and Lajtai [1974] used this same approach to call attention to fractures developed perpendicular to the far field σ , and to develop a theory of fracture which departs from previous work because it takes into consideration stress gradients along the fracture path. In addition, Dylk [1975] experimentally deformed rectangular specimens that contain an inclusion of rock different from that of the host in order to study by simulation the control of secondary facies changes on the style and location of deformation.

FRACTURES IN THE ROCK MASS

The rock mass contains fractures and other planes of mechanical discontinuity that effect its mechanical behavior and response to geophysical interrogation [Baurat et al., 1974; Bernaix, 1974; Everell et al., 1974; Goodman, 1974; Swolfs et al., 1974; John, 1974]. It is possible here to touch on only a few topics that reflect current

interest
into the
fields an
regional
develo
There h
structur
identific
economic
map the
principal
have re
deformed
Stearns.
Stearns
fracture
structur
Stearns
flow in
abunda
tore-rel
folded
try ro
Tchale
1974)
respons
possible
related
tion is
after s
that th
grates
depend
anions
to form
rock a
part of
the me
countr
region.
has ac
tures
orient
fabric.
ture in
magni
[Price,
and P
1974;
Rec
focus
host
1973;
the w

in conjunction with them, and that may be particularly helpful to geophysicists. These include the origin of fractures in the rock mass; fractures and earthquakes, and the influence of fractures on acoustic properties; fluid flow through fractures; analytical attempts to model the behavior of the fractured rock mass; and controlled fragmentation of the rock mass. The topic of hydraulic fracturing is covered in the review by Haimson [1975].

Fractures (joints) in the rock mass are generally divided into those that geometrically and genetically relate to folds and faults; those that are not related to local structures, are regional in scope, and often are referred to as regional orthogonal fractures; and those that relate to diagenesis, temperature changes, and mass wasting. There has been a host of work over recent years in which fracture-related shear and extension fractures have been identified geometrically and related to stress systems associated with folding and faulting, have been used to map the orientations and relative magnitudes of the principal stresses in the rocks at the time of fracturing, and have served to help determine the stress history during deformation [Stearns, 1964, 1968, 1972; Price, 1959, 1966; Morris, 1966, 1967, 1971; Friedman, 1969; Friedman and Stearns, 1971, among many others]. The control on the fracture developed by rock type, P_e , T , $\dot{\epsilon}$, and geologic structure is reviewed by Stearns and Friedman [1972], and Stearns [1969] has emphasized fracture as a mechanism of flow in natural deformation. As a result the orientations, abundance trends, and mechanical significance of structure-related fractures seem reasonably well in hand for folded rocks. Fractures in fault zones and adjacent country rock have been mapped [e.g., Friedman, 1969; Tralenko and Ambraseys, 1970; Stearns, 1972; Freund, 1974] and can be related to the same stress systems responsible for the faulting; but no generalizations seem possible concerning how far away from a fault genetically related fractures will form or what their density distribution is apt to be. Stearns (in Handin [1973]) concluded after study of several thrust, wrench, and normal faults that the width of the fractured fault zone seems to be greatest adjacent to wrench faults, that the width is also dependent upon rock type and the orientation of its planar anisotropy relative to the fault, and that fault gouge tends to form early in the displacement history. The country rock and fault gouge form a complex system with its own set of mechanical properties. These are more important to the mechanics of faulting than are those of the gouge or country rock individually. Much less can be said of regional orthogonal fractures, although Price [1959, 1974] has accounted for stress systems to produce these fractures and recently, Nelson [1975] has shown that their orientation can be controlled by primary sedimentary fabric. A further step in the genetic understanding of fractures in rock is the attempt to infer the relative or absolute magnitudes of the stresses responsible for the fractures [Price, 1959, 1968, 1970, 1974; Muehlberger, 1961; Price and Hancock, 1972; Voight, 1973; Voight and St. Pierre, 1974; Ragan and Price, 1974].

Recent developments in earthquake research have focused attention on fracture (dilatancy) as the source of a host of premonitory events [Nur, 1972; Whitcomb et al., 1973; Scholz et al., 1973]. The dilatancy idea stems from the well-documented fact that microfracturing precedes

macroscopic failure of intact rock specimens in laboratory tests (see microscopic aspects, above). It remains to be determined, however, whether dilatancy occurs when shear displacement takes place along previously broken rock, i.e., movement along an existing fault, as is indeed the case in most earthquake prone regions. Results of initial experiments are mixed: Friedman [1974] and co-workers monitored pore pressure while frictional sliding occurred along precuts in sandstone at $P_e=0.5$ kbar and found that dilatancy (pore pressure decline) begins at about two thirds of the differential stress required for the first stress drop of the stick slip sliding mode. Ohnishi and Goodman [1974], on the other hand, found little if any dilatancy as a result of triaxial and direct shear tests on artificial joints in sandstone. Hadley [1973] determined that at low P_e the stress difference to initiate microfracturing in granite and gabbro exceeds that to cause sliding but that at high P_e the reverse is true. The stress for sliding becomes greater at 2.0 kbar and she concluded that dilatancy would occur in rock masses only at P_e exceeding 2.0 kbar. Hence for depths less than about 15 km, some other mechanism is needed to explain the premonitory phenomena. Garg [1974] and W. R. Wawersik (personal communication, 1974) are currently exploring the possibility that dilatancy occurs as a result of movement along preexisting macrofractures prior to faulting.

Although earthquakes are the subject of a separate review [see Healy, 1975], it is significant that the fracture processes have been used by Mogi [1974] to interpret the clustering of earthquakes, aftershock phenomenon, relation between the magnitude and number of earthquakes, brittle ductile behavior, migration of seismic activity, and some features of global seismic belts.

That seismic velocities are influenced by fractures is well-known [e.g., Thill, 1973; Nur and Simmons, 1969; Anderson et al., 1974; Potter and Dennis, 1974; Simmons et al., 1975], and this forms part of the now famous V_p/V_s method for earthquake prediction. Perhaps it is not as widely appreciated, however, that velocities and particularly attenuations have been used to map fractures in the rock mass [McWilliams, 1966; Bur et al., 1969a, b; Willard and McWilliams, 1969; Friedman and Bur, 1974; Savich et al., 1974] or that acoustical studies can be used to determine the stress field in the rock mass [Gladwin and Stacey, 1974].

There is a high level of current interest in fluid flow through fractured rock, primarily because of work on earthquake control through fluid injection, petroleum exploration and production, and geothermal projects. Recent laboratory studies of fracture permeability as a function of normal stress across fracture surfaces in carbonate rocks [Jones, 1973], sandstones [Daw et al., 1974; Nelson, 1975], and slates [Turner and Secor, 1974] have shown that large reductions in fracture permeability are to be anticipated at depth or as a result of large reductions in formation pressure. This has been confirmed in surface field tests by Swolfs et al. [1974], who found that joints in a 3-m cube of granite essentially close at only 15- to 30-bars normal stress. In permeable sandstone, fracture permeability is readily reduced to that of the host; in tight carbonates and slates, however, the fracture permeability up to 1.5 kbar is larger than that of the host. Turner and Secor [1974] emphasize that fracture permeability is highly dependent

on the nature of the fracture surface in slate.

Similar emphasis is being given to finite element studies of fluid flow through fractures [Wilson and Witherspoon, 1970]. Topics investigated include coupled stress and flow [Noorishad et al., 1971], fluid injection and withdrawal in fault zones [Witherspoon et al., 1974a, b], the effects of permeability anisotropy and tectonic stress [Witherspoon et al., 1974b], and flow around dislocations on a fault [Weertman, 1974]. Similar computer techniques have been used to model earthquake stimulation by fluid injection [Dieterich, 1971].

Significant attempts have been made to apply continuum approaches to the fractured rock mass [Voight and Dahl, 1970; Singh, 1973a, b]. Stuart and Dieterich [1974] have applied continuum theory to rock dilatancy, and Bridwell [1974a, b] has worked on dilatancy and faulting.

Controlled fracturing of the rock mass by nuclear explosions may provide the means for in situ gasification of coal, recovery of oil shale, and recovery of liquid and gaseous hydrocarbons from otherwise tight formations. The extent of fracturing caused by underground nuclear explosion is summarized by Borg [1973].

RESEARCH NEEDS

The foregoing review has attempted to touch on the many different aspects of fracture in rock. No single topic is completely understood, and although the body of knowledge is large, there is much that needs to be investigated.

Studies of fracture mechanisms and criteria have thus far been treated submicroscopically, microscopically, or macroscopically. To date, few if any theoretical or observational attempts have been made to relate phenomena across these scale boundaries and thus to provide a more complete view of fracture. Symptomatic of this is the lack of systematic study of the physical role of crystal dislocations in the fracture of rocks and studies to determine if fracture is thermally activated and rate-dependent. It is known that fracture strength decreases with increasing temperature, but is this because thermal cracking (due to thermally induced stress) weakens the specimen or because the fracture process itself is temperature sensitive? A handle on this problem might be obtained by

determining how T and $\dot{\epsilon}$ (at constant P_e) effect the fracture surface energy γ . Actually, there is little quantitative information on the extent of thermal cracking due to temperature changes, although qualitatively the effect is well known. Also relating to the crossing of scale boundaries is the problem of ductile fracture, research into which has just begun. Another related problem deals with how external energy is partitioned among the various forms of deformation prior to macroscopic failure. This might be approached through study of hysteresis loops in cyclic loading tests, which reflect the energy dissipation or absorption of sample and environment. The loops are initially large, then decrease to some limiting value, and then increase again just before macroscopic failure. Is it possible to relate this history to deformation mechanisms within the sample? Work is needed on stress corrosion.

Fractures and other planes of mechanical discontinuity in the rock mass need to be described geometrically and mechanically if the physical and mechanical behavior of the rock mass is to be predicted accurately. Study of seismic amplitudes (attenuations) along with velocities may provide data on fracture abundance, orientation, and size relative to problems concerning dilatancy, fracture permeability, and controlled fragmentation. The geophysical data for a given terrain need to be correlated to fracture maps prepared from direct observations in order to provide the necessary ground truth. Fracture development associated with folding and faulting needs to be studied with a view toward understanding dilatancy. Does it involve the creation of new fractures, or can movement along preexisting intersecting fractures produce dilation? Can the magnitude of the dilatancy be measured quantitatively? These questions pertain not only to earthquake-related problems but also to an understanding of how cataclasis serves as the mechanism for mass transport in structural problems. Detailed petrofabric analyses of fractures and other features arising from the deformation of the rock mass are needed to test the applicability of theoretical solutions to natural deformation.

Acknowledgments Thanks go to John Handin and Neville Carter for their review of the manuscript and to my colleagues and students in the Center for Tectonophysics for helpful comments and discussions.

Friction in Rocks

John M. Logan

Center for Tectonophysics, Texas A&M University, College Station, Texas 77843

INTRODUCTION

J. C. Jaeger's (personal communication, 1971) first law of friction summarizes much of the confusion and uncertainty that has attended investigations into the frictional properties of rocks. This paper is published in the *Journal of Geophysical Research*, 1975 by the American Geophysical Union.

of rocks. The problems of friction in rocks are important in at least three major areas: (1) earthquake generation and source mechanisms, (2) delineation of mechanical units in folding of layered sequences, and (3) behavior of prefractured rock masses. Problems involving the frictional behavior of rock may be divided roughly into two areas depending upon the normal

stress
proble
stress i
and te
order
Brid
den st
rocks
pheno
Subse
proces
and By
1972: -
gestio
import
using
frictio
Knapo
fault s
the im
rocks.
and co
proper
Alth
tiona
Kragel
plicabi
In the
the inv
tempts
upon
Dieter
1972; J
Engeld
1973; J
Goodm
Byerlee
of par
has ma
tenuou
areas
years.
earlier
backgr
some
author
arises.
It se
niques
results.
discuss
anisms
be sun
future

Exp
gouge
techni
ticularl
1972; H
1973; J

Friction in Rocks

John M. Logan

of physical properties of rocks, Int. J. Rock Mech. Min. Sci., **6**, 1-11, 1969.

C. E., and P. A. Witherspoon, An investigation of laminar flow in fractured porous rocks, U. of Calif., Berkeley Dept. of Civil Eng., Trans. and Traffic Eng., Pub. No. 70-6, 178p., 1970.

A., Relation between stress drop, fault friction and crustal strength in shallow focus strike slip faulting, J. Geophys. Res., **73**, 2217-2223, 1968.

W.L., The influence of pore fluids on the frictional properties of sandstone, M.S. Thesis, Texas A&M Univ., 61 p., 1973.

F., and D. Tabor, The Friction and Lubrication of Solids, II, Clarendon, Oxford, 283 p., 1964.

G.F., Current laboratory studies pertaining to earthquake prediction, Tectonophysics, **6**, 75-87, 1968.

G.F., Mechanics of crustal earthquakes, Semi-Annual Technical Rpt., Project No. R0110376, 26 p., 1971.

G.F., and J.D. Byerlee, Stick-slip as a mechanism for earthquakes, Science, **153**, 990-992, 1966.

G.F., and J.D. Byerlee, California earthquakes: Why only shallow focus?, Science, **168**, 1573-1575, 1970.

P.W., Shearing phenomena at high pressure of possible importance to geology, J. Geol., **44**, 653-669, 1936.

R., and L. Knopoff, Modal and theoretical seismicity, Bull. Seismol. Soc. Amer., **57**, 341-371, 1967.

J.D., The frictional characteristics of Westerly granite, Ph.D. Dissertation, M.I.T., 179 p., 1966.

J.D., Frictional characteristics of granite under high confining pressure, J. Geophys. Res., **57**, 341-371, 1967a.

J.D., Theory of friction based on brittle fracture, J. of Applied Physics, **38**, 2978-2984, 1967b.

J.D., Mechanics of stick-slip, Tectonophysics, **2**, 475-486, 1970a.

J.D., Static and kinetic friction of granite under high normal stress, Int. J. Rock Mech. Mineral. Sci., **7**, 577-582, 1970b.

J.A. and V.F. Brace, Stick-slip, stable sliding and earthquakes -- aspects of rock type, pressure, strain rate and stiffness, J. Geophys. Res., **71**, 4031-4037, 1966.

J.D. and V.F. Brace, Fault stability and pore pressure, Letter to the Editor, Seismol. Soc. Amer. Bull., **62**, 657-660, 1972.

J.D. and R. Summers, The effect of fault gouge on the stability of sliding on saw cuts in granite (abstract), EOS Trans. AGU, **54**, 1210, 1973.

J.D. and R. Summers, Fault creep as a function of confining pressure (abstract), EOS Trans. AGU, **55**, 428, 1974.

G.J., S.B. Swanson, and W.S. Brown, Torsional shear measurements of the frictional properties of Westerly Granite, Proc. Third Cong. Int. Soc. Rock Mech., **11A**, 221-225, 1974.

G.H. White, Microscopic feather fractures in the faulting process, Ph.D. Thesis, Texas A&M Univ., 33 p., 1974.

J. B., The effects of surface roughness on the shear strength of joints in rock, Tech. Rep. WMD-2-70, p. 283, No. River Div., Corps of Eng. Cont., Novr. 1970.

J.C., Time-dependent friction as a possible mechanism for earthquakes, J. Geophys. Res., **77**, 3771-3781, 1972a.

J.C., Time-dependent friction in rocks, J. Geophys. Res., **77**, 3889-3897, 1972b.

G., L.B. Frost Jr. and V.A. Olson, Experimental study of frictional

Zoback, M. D., and J. D. Byerlee, The effect of stress on the permeability of Westerly Granite (abstract), EOS Trans. AGU, **55**, 431, 1974a.

Zoback, M. D., and J. D. Byerlee, Dilatancy in Westerly Granite under cyclic differential stress (abstract), EOS Trans. AGU, **56**, 1193, 1974b.

properties of faults, in New Horizons in Rock Mechanics, 14th Symp. on Rock Mech., Penn. State Univ., 189-222, 1973.

Engelder, J.T., Quartz fault-gouge: Its generation and effect on the frictional properties of sandstone, Ph.D. Dissertation, Texas A&M Univ., 154 p., 1973.

Engelder, J.T., Cataclasis and the generation of fault gouge, Geol. Soc. Amer. Bull., **85**, 1515-1522, 1974a.

Engelder, J.T., Coefficients of friction for sandstone sliding on quartz gouge, Proc. Third Cong. Int. Soc. Rock Mech., **11A**, 499-503, 1974b.

Engelder, J.T., Microscopic wear-grooves on slickensides: Indicators of paleoseismicity, J. Geophys. Res., **79**, 4387-4392, 1974c.

Friedman, M., J.M. Logan, and J.A. Rigert, Glass-indurated quartz gouge in sliding-friction experiments on sandstone, Geol. Soc. Amer. Bull., **85**, 937-942, 1974.

Goodman, R., The mechanical properties of joints, Proc. Third Cong. Int. Soc. Rock Mech., **1A**, 127-172, 1974.

Healy, J.R., W.W. Rubey, D.T. Griggs, and C.B. Raleigh, The Denver earthquakes, Science, **161**, 1301-1310, 1968.

Hoskins, E.R., J.C. Jaeger and K.J. Rosengren, A medium-scale direct friction experiment, Int. J. Rock Mech. Mineral. Sci., **5**, 143-154, 1968.

Houston, J.A., Experimental study of stick-slip in Tennessee Sandstone, M.S. Thesis, Texas A&M Univ., 68 p., 1972.

Houston, J.A., and J.M. Logan, Stick-slip in Tennessee Sandstone (abstract), EOS Trans. AGU, **53**, 512, 1972.

Jackson, R.E. Jr., Sliding friction in foliated rocks, Ph.D. Dissertation, Univ. of North Carolina, 77 p., 1973.

Jackson, R.E. and D.E. Dunn, Experimental sliding friction and cataclasis of foliated rocks, Int. J. Rock Mech. Mineral. Sci., **11**, 235-249, 1974.

Jackson, R.E., L.J. LaPointe, and M. Swain, Sliding surface features, Hertzian fractures and stick-slip (abstract), EOS Trans. AGU, **55**, 425, 1974.

Jackson, R.E., and M.V. Swain, Applicability of recent observations of surface wear mechanisms in metal, ceramics, and rock to fault surface features (abstract), Geol. Soc. Amer. Abstracts with Programs, **6**, 807, 1974.

Jaeger, J.C., The frictional properties of joints in rock, Pure Appl. Geophys., **43**, 148-158, 1959.

Jaeger, J.C., Behavior of closely jointed rock, in Rock Mechanics -- Theory and Practice, 11th Symp. on Rock Mech., Univ. of Cal. Berkley, 57-68, 1970.

Jaeger, J.C., and E.J. Rosengren, Friction and sliding of joints, Australian Inst. Mining Met. Pract., **229**, 93-104, 1969.

Johnson, T., and C.H. Scholz, Rupture velocities of stick-slip on Westerly Granite sliding surfaces (abstract), EOS Trans. AGU, **55**, 429, 1974.

Johnson, T., F.T. Wu, and C.H. Scholz, Source parameters for stick-slip and for earthquakes, Science, **179**, 278-279, 1973.

Knopoff, L., C.Y. King, and R. Burridge, A physical basis for earthquake statistics, in A Symposium of Processes in the Focal Region, Publ. 37, edited by E. Kasahara and A.E. Stevens, 224-234, Dominion Observatory, Ottawa, Ont., 1969.

Kragelskii, I.V., Friction and Wear, Butterworths, Washington, 346 p., 1965.

LaPointe, L.J., and D.E. Dunn, Anisotropy and the coefficient of sliding friction (abstract), EOS Trans. AGU, **55**, 428, 1974.

structural analysis of the
 Geol. Soc. Amer. Bull.
 failure in rock, in New
 Rock Mech., Penn. St.
 1973.
 Westerly Granite under
 55, 431, 1974.
 of strain accumulation on
 4407-4422, 1974.
 strain-rate testing machin
 confining pressure and
 EOS Trans. AGU, 55.
 history of sedimentary,
 Geol. Soc. Amer. Abstr.
 history and rock stress,
 580-582, 1974.
 um approaches to analysis
 Sci., 7, 814-830, 1970.
 tensile strength of lime-
 29, 1974.
 in laboratory compres-
 D. of Minnesota, 1968.
 brittle rock fracture in
 Mech. Min. Sci., 7.
 behavior of granite and
 for of Westerly Granite
 on faults with finite
 1-1038, 1964.
 on a free surface and
 55, 945-953, 1965.
 on an earthquake fault,
 water desorption on
 Am. Mineralogist.
 Stribner effect in
 Further observations
 51-959, 1968.
 Ayatollahi, Fluid
 deformable fractures
 S. Ayatollahi, Effect
 orientation on fluid
 AGU, 56, 1191, 1974b.
 Earthquakes prediction:
 Francisco Earthquakes,
 the optical effects
 Sci., 6, 490-499, 1973b.
 quartz, Nature,
 propagation in soda-
 67.
 techniques in the

SUBJ
MNG
FISU

Australia lifted its four-year-old uranium export ban on August 25—the first step toward developing its huge uranium ore reserves and becoming a leading world supplier of nuclear fuel. Predictably, Australian critics of nuclear development voiced strong opposition to the decision, and the deputy leader of the opposition Labor party warned that if mining companies went ahead with uranium development, they should not "expect any mercy from the next Labor government." In announcing the action, Prime Minister Malcolm Fraser said contracts would be written to give maximum security against possible repudiation by a future government. Shipments are expected to begin in 1981 from the Ranger deposit 125 mi east of Darwin, with Nabuluka, 12 mi north of Ranger, to start deliveries a year later. The large Koongarra and Warbarlek deposits also await development.

The feasibility of in-situ uranium mining at depths of 2,200 to 2,500 ft will be tested by Teton Exploration Drilling Co. later this year, provided government approvals are obtained. Teton representatives in Wyoming and New Mexico, where the tests will be conducted, are optimistic about the chances of success, believing that in-situ leaching at considerable depths may be as economical as it is in shallower deposits. The levels at which the tests will take place are reportedly the deepest ever for attempts at in-situ uranium mining.

A mobile demonstration plant for TL (thin-layer) leaching, a process developed by Holmes & Narver, has been licensed by the Nuclear Regulatory Commission for short term tests on uranium ores. TL leaching is a metallurgical process for ores containing acid-soluble copper and uranium values. The process achieves recoveries equivalent to those of agitation leaching, but capital and operating costs are expected to be substantially lower, and there are potential advantages in the degree of environmental effects. A copper project that will use TL leaching with solvent extraction and electrowinning is now under construction in Chile by Holmes & Narver and Incomet Ltda. (p 41).

A significant tax ruling in favor of Reserve Mining Co. was recently handed down by a Minnesota District Court. A state law taxing the tailings discharged by Reserve into Lake Superior applies only to the tailings and not to the lake water used to transport them, the court ruled. The state contended that the water for transport qualified as liquid waste resulting from the beneficiation process used by Reserve. However, the court ruled that the lake water "is utilized but not consumed" in the process, as it is used only to move the tailings from one place to another. A victory by the state would have cost Reserve about \$244 million over the next three years in additional taxes, the company said. Reserve believes the ruling will help secure financing for the \$370 million Mile Post 7 project for on-land disposal of the tailings.

A final decision by the Swedish government on uranium mining in the Billingen field, in the south-central part of the country, may be influenced by a recent royal commission report that mining would have a positive effect on the region's employment and economy. The Billingen field is the site of the Ranstad uranium mill, operated by state-owned LKAB. The company wants to expand mining there to 1 million tpy of shale, yielding 270 mt of uranium oxide plus other minerals, including 60,000 tpy of aluminum, 35,000 tpy of potassium, 65,000 tpy of sulphur, and 4,000 tpy of magnesium. Local environmentalists oppose expansion—or even continuation—of uranium mining and milling at Billingen. In case the opposition wins the battle of Billingen, the government is also investigating possible development of the Taasjoen field in northern Sweden, which has the advantage of distance from population centers and national parks. One of Europe's largest uranium finds, the Taasjoen field lies in a mountain range about 100 mi northeast of Oestersund. Studies made by the Swedish Industry Board indicate that shale in the area contains an estimated 518,000 mt of uranium oxide, based on a uranium content of 400 g per mt of shale. Taasjoen shale also contains substantial quantities of phosphorus, which could be mined economically as the sole product, according to preliminary studies.

LITERATURE CITED

1. I. N. Plaksin, R. Sh. Shafeev, and V. A. Chanturiya, "Relation between the energy structure of crystals of minerals and their flotation properties," in: Mineral Beneficiation [in Russian], Moscow (1970)
2. I. N. Plaksin and R. Sh. Shafeev, "Influence of certain semiconductive properties of the surface on reaction of xanthate with galena," Dokl. Akad. Nauk SSSR, 132, No. 2 (1960).
3. A. G. Lopatin, "Relation between the electrophysical properties of pyrite and its flotation activity in dox media," Tsvetnaya Metall., No. 16 (1967).
4. N. L. Gorenkov, "Investigation and regulation of the flotation properties of sulfides in reducing media," Author's Abstract of Candidate's Dissertation, Moscow (1975).

SUBJ
MING
FMG

*Geo. Mining Sci.
v 15 NY, 1979*

FEASIBILITY OF MINING GOLD BY UNDERGROUND PLACER LEACHING

G. G. Mineev and A. M. Shutov

The raw materials base for placer mining has become more varied and complex with respect to mining and geological conditions. Many placers lie at considerable depths, so that dredgers cannot be used; the number of sites affected by permafrost, which can be exploited only with some losses, has increased [1]. Even in the treatment of thawed placers the losses of gold are considerable - 10-20%, depending on the characteristics of the raw material, in some cases up to 30% - owing to the low extraction of fine gold in the sluices. Gold finer than 0.1 mm cannot be extracted by dredging, and the -0.3 + 0.1-mm fraction is extracted only to the extent of 50-60%. For economic reasons there are only limited possibilities of using more efficient equipment than sluices (jiggers, screw separators, etc.) in the main operations.

From literature sources it appears that to cope with placers with difficult access or very fine gold, a promising method is that of underground leaching, which has already been successfully used in related branches of industry [2-6]. Solution of this problem would increase the available gold resources.

Underground leaching is used to work a number of deposits of nonferrous and rare metals and other minerals (uranium, copper, sulfur, and salt). Outside the USSR, up to 20% of the copper is obtained every year by underground and dump leaching. The end product from this technology is 1.5-2 times cheaper than that from the usual mining methods. About 2/3 of the world output of sulfur is obtained by underground melting with hot water. Underground leaching is used to obtain 25-30 million tons of rock salt per year.

Only patents are known for underground leaching of gold. As early as 1896 a patent was issued in Russia on "A method of extracting gold and other noble metals by direct leaching of deposits" [2]. The method was proposed for working lean deposits which would be very difficult or impossible to work by the usual methods. The solvent for the noble metals is introduced directly into the productive seam, and the resultant gold solution is extracted by pumping or drainage and then processed. In 1945 Skuratov [7] suggested a method of working gold-bearing placers by underground cyaniding. He proposed that for the process of extracting gold underground water currents in gold-bearing placers should be saturated with cyanide solutions.

Neither method has found industrial applications, owing mainly to the lack of easily available nontoxic solvents for gold and experience in underground leaching of ores. The problem has become urgent in recent years, especially owing to the present-day achievements of the technology of underground leaching of nonferrous and rare metals.

Among the few reagents which have been long known for the solution in gold there are aqua regia, chlorine water, and cyanides. At present, leaching with cyanide solutions is the main method of hydrometallurgical processing of gold-bearing ores and their beneficiation products. The chief advantage of cyanide is its high efficiency and selectivity for gold; its main drawback is its high toxicity. Earlier, industrial use was made of the chlorination method, which can recover gold from tailings, but in two or more successive stages of ore treatment. Aqueous solutions of chlorine have a collective action, and are very aggressive and toxic.

Irgiredmet. Irkutsk. Translated from Fiziko-Tekhnicheskie Problemy Razrabotki Poleznykh Iskopnykh, No. 4, pp. 110-116, July-August, 1979. Original article submitted August 5, 1977.

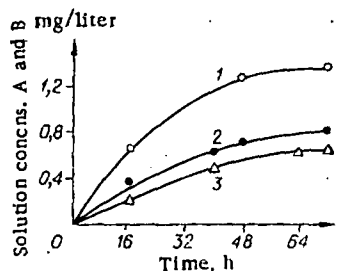
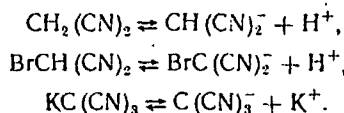


Fig. 1. Dynamics of leaching of gold by solutions of acetone cyanohydrin (1, 2) and sodium cyanide (3) at 5°C in the presence of added oxidant (1, 3) or without it (2): Leaching was effected by 0.1% solutions in terms of NaCN.

The search for new nontoxic or slightly toxic gold solvents has lately been redoubled, owing to the increasing importance of the underground leaching of gold-bearing ores, which cannot be effected on a large scale without the use of harmless solvents. There is some interesting information [8, 9] on the leaching of gold from ores by alkaline solutions of malononitrile $\text{CH}_2(\text{CN})_2$, bromomalononitrile $\text{BrCH}(\text{CN})_2$, and potassium cyanoforn $\text{KC}(\text{CN})_3$. It is thought that these compounds hydrolyze to form stable nontoxic hydrocarbon compounds:



By leaching quartz ore with a particle size of -0.15 mm containing 12.4 g/ton of gold with malononitrile solution (0.05%), 95% of the metal was extracted in 24-h working with $L : S = 3 : 1$ and $\text{pH} = 8-12$ (created by adding lime).

There are certain prospects for leaching gold from poor ores with ammonium humate solution, since this compound is adequately efficient, its production technology is simple, and the raw material is easily available [10, 11]. As a nontoxic solvent for gold it is possible to use amino acids [12, 13], especially a technical mixture of these compounds. At present these solvents are still in the stage of detailed laboratory investigation and technological tests.

An effective solvent for gold is acetone cyanohydrin $(\text{CH}_3)_2\text{COHCN}$, a representative of the class of α -hydroxynitriles. In an alkaline medium, acetone cyanohydrin hydrolyzes, splitting off acetone and CN^- ions. Its action on gold is similar to that of sodium cyanide, but it has high kinetic activity [14].

Thus, for developing methods and technologies for underground leaching of gold-bearing placers on a pilot scale we can recommend only sodium cyanide and acetone cyanohydrin. There may be prospects for testing other, nontoxic gold solvents in this process.

When toxic solvents are used for underground leaching of gold, it is of the first importance to consider measures to prevent leakage of the solutions and for efficient detoxification of the effluents. In this connection the most favorable placers for leaching are in the permafrost, because it is possible, without special expenditure, to create isolated water-impermeable sites.

Preliminary research has begun on the leaching of gold from frozen placers. Below we give experimental data on the solution of gold by solutions of acetone cyanohydrin and sodium cyanide at low temperatures (5°C) and on the use of various oxidizing agents instead of (or as well as) oxygen; we will describe planned processes and considerations on the organization of the process on the pilot scale. Since the kinetics of dissolving gold in cyanide solutions at low temperatures has been discussed by Sorokin [15], we paid particular attention to the solubility of the metal in acetone cyanohydrin in comparison with cyanide. The experiments were performed on material with a particle size of $-2 + 0$ mm containing 3 g/ton of the metal. The mean gold particle size was 0.2-0.3 mm. Leaching was effected in a refrigerator at +5°C with stirring of the pulp ($L : S = 2 : 1$). To prepare the solutions we used 96% acetone cyanohydrin (53% in terms of NaCN) and sodium cyanide of chemically pure grade.

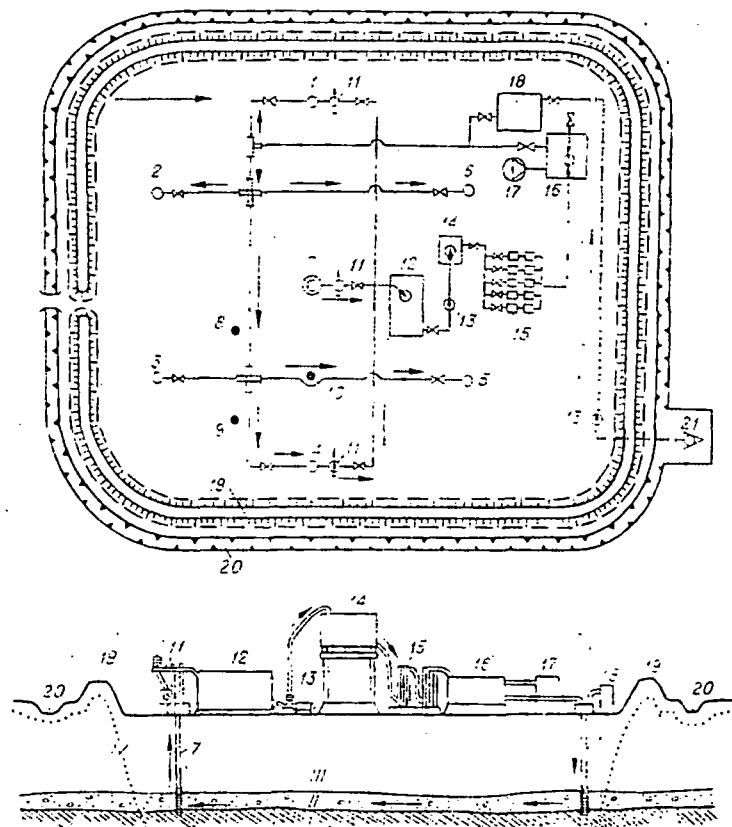


Fig. 2. Diagram of pilot plant for underground leaching of gold from frozen placer deposit.

It is known that the rate of solution of gold in cyanide solutions decreases with falling temperature. The process can be speeded up at low temperature by means of special oxidizing additives (Fig. 1). Thus, the degree of solution of gold in acetone cyanohydrin after 72 h increases from 0.66 to 1.3 mg/liter (practically double) as we go from pure solution to one with oxidant (curves 1 and 2). The cyanide solutions were less effective (curve 3). Solution of gold is practically complete after the first 45-50 h of processing the material.

Acetone cyanohydrin supplies not only cyanide ions but also acetone, which, according to Lebedev and Kakovskii [14], depassivates gold and thus exerts a favorable influence on the process of solution of the metal. This explains the fact that acetone cyanohydrin has a greater technological effect than sodium cyanide.

We compared the expenditure of the reagents (in terms of NaCN) for leaching of gold by solutions of acetone cyanohydrin and sodium cyanide with various doses of oxidizing agent. The consumption of reagents increases linearly with the load of oxidizing agent. The consumption of acetone cyanohydrin (in terms of NaCN) is about half that of sodium cyanide.

Acetone cyanohydrin has other advantages over cyanide: in pure form it is nontoxic - only its aqueous solutions are toxic; according to Lebedev and Kakovskii [14], this solvent reacts less strongly with accompanying minerals; and it is 1.2 times as cheap as sodium cyanide. The cyanohydrins are a wide class of compounds; some of them are wastes from the chemical industry (e.g., lactonitrile in the production of acrylonitrile).

It is interesting to study the possibilities of using cyanohydrins instead of cyanides in underground leaching of gold-bearing placers.

Pilot studies have been made of the underground leaching of gold from frozen placers. Before direct leaching of the gold-bearing seam, it is envisaged that it should be thawed out by the usual methods. The apparatus (Fig. 2) includes six injection boreholes (1-6), one extraction borehole (7), and three observation boreholes (8-10) arranged in a ring with the extraction borehole in the middle. The gold solvent passes through the gold-bearing seam and is fed by pump 11 from the extraction borehole to receiver 12. The clarified gold-bearing solution is pumped by centrifugal pump 13 into pressure vessel 14, from which it flows into sorption

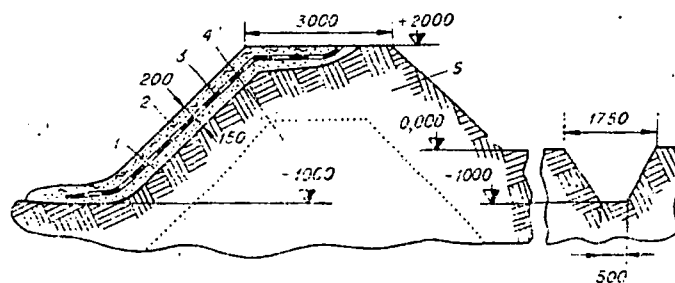


Fig. 3. Vertical cross section structures (measurements in millimeters).

columns 15 which trap the metal. The deaerated solutions are concentrated in vessel 16, where they are fortified with the main components. The apparatus operates in a closed continuous cycle with automated principal technological processes; it also permits the direction of the flow of solvent in the seam to be reversed (in which case boreholes Nos. 1 and 4 are connected in the extraction circuit), with the aim of studying the process of leaching gold by a linear scheme and to avoid silting up of the gold-bearing seam.

Measures are envisaged to prevent filtration of the solutions outside the leaching zone. The perimeter of the experimental site is guarded around the perimeter by frost-protection embankment 19 to prevent possible leakage of solvent from the groundwaters of the active layer, and also by a raised ditch 20 for removal of water formed by atmospheric precipitation and by seasonal thawing of the frozen layer. A vertical cross section of these structures is shown in Fig. 3.

After completion of leaching and washing out of the dissolved gold, the seam is detoxified with solutions of bleaching powder from vessel 18 until solutions pumped out from it give a negative reaction for CN^- .

Our test on the recommended equipment for underground leaching of gold from sand enables us to obtain the necessary hydrodynamic and technological data and to determine the possibility and prospects for this technology for utilizing uneconomic and uncommercial deposits in specific mining-geological conditions which complicate the work and make it more expensive. For underground leaching we can recommend certain deposits in the northeast [of the USSR] which show promise but are not being exploited owing to the failure to find a way of working them. Larger-scale economic calculations revealed that in central Siberia and Kazakhstan it is possible to use underground leaching of placers along ridges with 0.2 g/m^3 of gold, and in the far north [of the USSR], those with 0.5 g/m^3 or more.

CONCLUSIONS

1. When toxic solvents are used in underground leaching of gold, the first question which arises is how to prevent leakage of the solutions and how to efficiently detoxify the effluent. In this connection the most favorable objects for leaching are placers in permafrost, because in this case it is possible to create isolated water-impermeable sites (districts).
2. At low temperatures the greatest effect can be obtained with acetone cyanohydrin in combination with moderate additions of oxidizing agent. Other conditions being constant, the oxidizing agent nearly doubles the rate of solution of the metal without decomposing the acetone cyanohydrin, and thus without increasing its consumption.
3. A pilot project for underground leaching of gold from a frozen placer has been developed and is recommended for testing.

LITERATURE CITED

1. V. V. Chemezov, E. T. Zhuchenko, and A. I. Muratov, "Metal losses in dredging placer deposits and ways of reducing them," in: Reports and Addresses at Sessions of the Section on Precious Metals and Diamonds of the Scientific-Technical Soviet of the Ministry of Nonferrous Metallurgy of the USSR (NTS MTsM SSSR) [in Russian], Moscow (1967).
2. A. I. Kalabin, Mining Minerals by Underground Leaching [in Russian], Moscow (1969).
3. V. G. Bakhurov, S. G. Vecherkin, and I. K. Lutsenko, Underground Leaching of Uranium Ores [in Russian], Moscow (1969).
4. V. G. Bakhurov and I. K. Rudneva, Chemical Recovery of Minerals [in Russian], Moscow (1972).

5. G. G. Mineev, A. S. Chernyak, G. A. Stroganov, et al., "Prospects for technological utilization of gold-bearing raw materials," *Kolyma*, No. 2 (1975).
6. N. V. Maksimova, "On underground leaching of gold," *Kolyma*, No. 2 (1973).
7. A. I. Skuratov, "Method of working gold-bearing placers by underground draining," *Byull. Izobr. Tekhn. Zn.*, No. 23 (1964).
8. "Leaching of ores containing noble, heavy, and nonferrous metals, using solutions containing ions including carbon," USA Patent No. 3542540, November 24, 1970.
9. "Leaching of gold," USA Patent No. 3635697, January 18, 1972.
10. G. G. Mineev and A. S. Chernyak, "Possible ways of using humic compounds in hydrometallurgical processes for extracting gold and other metals," *Zh. Prikl. Khim.*, 47, No. 11 (1974).
11. G. K. Petrik, V. S. Nosochenko, et al., "Development of industrial technology for production and extensive testing of effectiveness of concentrated forms of carbon-humic fertilizers in the Irkutsk region," *Izv. INUSa pri Irkutskom Univ.*, 9, Pt. II (1968).
12. L. F. Shestopalova, A. S. Chernyak, and G. G. Mineev, "Study of processes of colloid and complex formation in the system $Al(I, III)$ - alkaline solutions of amino acids," in: Ninth All-Union Conference on Chemistry, Analysis, and Technology of Noble Metals [in Russian], Krasnoyarsk (1973).
13. G. G. Mineev, E. D. Korobushkina, A. S. Chernyak, et al., "The role of microorganisms in the solution and deposition of gold," in: Material of All-Union Conference on Ecology and the Geochemical Activity of Microorganisms [in Russian], Moscow (1974).
14. A. N. Lebedev and A. I. Kakovskii, "Study of the kinetics of solution of gold in aqueous solutions of acetone cyanohydrin," *Tsvetnye Met.*, No. 7 (1965).
15. I. P. Sorokin, Study of Conditions of Solution of Gold and Silver in Cyanide Solutions at Low Temperatures [in Russian], Magadan (1958).

Fracture of Brittle Solids. II. Distribution Function for Fragment Size in Single Fracture (Experimental)

J. J. GILVARRY AND B. H. BERGSTROM

Research Laboratories, Allis-Chalmers Manufacturing Company, Milwaukee, Wisconsin

(Received July 28, 1960)

The theoretical results of Gilvarry for the size distribution of the fragments in single fracture have been verified experimentally by fracturing spherical glass specimens under compression. The fragments were contained by a gelatin matrix to inhibit secondary fracture and thus make conditions conform as closely as possible to single fracture. Experimental values of the probability of fracture as obtained by sieve analysis show the predicted linear variation with the mean dimension x of the particles, over reasonably large intermediate ranges of the variables. It is shown that a logarithmic-normal distribution does not represent the experimental results. The over-all data exhibit three local maxima in the differential probability of fracture as a function of x , whereas the theory permits only two. Agreement in the number of peaks

is obtained by subtracting the contribution to the over-all probability of those fragments containing original surface of specimen, which yields the true probability considered in theory. In this manner, reasonably complete agreement between theory and experiment for single fracture is obtained. For p^2 fracture (carried out without use of gelatin), two additional peaks exist in the curve of the over-all differential probability vs x , as compared to the case for single fracture. The theory of Gilvarry is confirmed down to a fragment dimension of at least 1μ by means of an electrical counting instrument, and checked by direct microscopic sizing to 5μ . The results yield numerical values of internal flaw densities, and thus provide a tool to study the distribution of Griffith flaws existing internally in a solid.

I. INTRODUCTION

AS has been emphasized, the theoretical development of I corresponds to single fracture of a specimen.¹ However, experimental determinations of the distribution of fragment size in which conditions were chosen to approximate single fracture are virtually nonexistent in the literature. The available results correspond to the product of a milling operation, or of an impact experiment in which the hammer was not restrained after fracture began.² To fill this lack, a series of experiments was carried out by the authors in which the conditions of single fracture were reasonably met. A longer series meeting these conditions has been performed by Bergstrom, Sollenberger, and Mitchell³; as compared to their results, the data of this paper for size distributions reflect more closely controlled conditions and higher accuracy, in general.

The restriction was imposed in I that the initial specimen be sufficiently large that one could ignore the effect of the original surficial flaws in fragmentation. Such a limitation cannot be maintained in practice, since one must deal with specimens of finite size. In such a case, the fragments can be divided into two classes: the exoclastic fragments engendered by surficial flaws of the specimen, and the endoclastic fragments formed by propagation of internal flaws of the original specimen. The theory of I applies only to the endoclastic fragments. The names are neologisms, formed from the word "clastic" and the combining forms "endo-" and "exo-".

¹ J. J. Gilvarry, *J. Appl. Phys.* 32, 391 (1961), preceding paper (referred to hereafter as I).

² Department of Scientific and Industrial Research, *Crushing and Grinding, a Bibliography* (Her Majesty's Stationery Office, London, 1958), pp. 27, 124.

³ B. H. Bergstrom, C. L. Sollenberger, and W. Mitchell, Jr., *Trans. Am. Inst. Mining, Met., Petrol. Engrs.* (to be published).

II. EXPERIMENTAL METHOD

The specimens were of glass, in the shape of a sphere. A compressive load was applied through diametric, opposed platens of tungsten carbide, motion of which was arrested by a stop after fracture started. Rate-loading varying through a factor of one thousand could be produced by the apparatus, described elsewhere by Bergstrom and Sollenberger.³ No statistically reliable evidence of an effect of the rate of loading on the form of the distribution function for fragment size has been found with this particular experimental arrangement.³ This fact constitutes a necessary prerequisite that conditions actually correspond to single fracture.

When a brittle solid fractures, the fragments necessarily fly apart at high speed. Speeds up to 1000 cm/sec have been determined cinematographically, the coarser fragments, but speeds for the finer particles

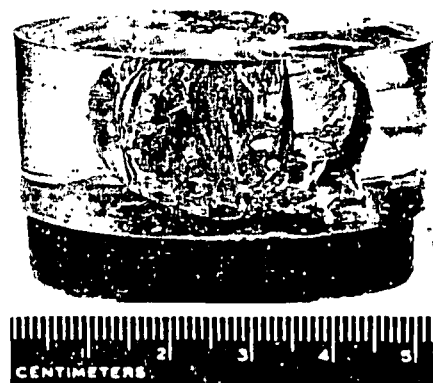


FIG. 1. Disposition of fragments in the gelatin after fracture. It is seen that no fragments reach the walls of the Lucite ring.

⁴ B. H. Bergstrom and C. L. Sollenberger (to be published).

SUBJ
MNG
FOBS

UNIVERSITY OF UTAH
RESEARCH INSTITUTE
EARTH SCIENCE LAB.

Size

TABLE I. Physical parameters for experimental specimens.

Specimen	Diameter cm	x_0' cm	k' cm
No. 1	7.6	5.71	23.2
No. 2	2.4	1.33	2.49
No. 3	2.4	1.88	6.28
No. 4	2.4	1.12	2.17
No. 5	2.4	1.88	3.24
Mean of 2-5	2.4	1.88	3.04

seem to be much lower than this figure.³ If the fragments are contained by a retaining chamber around the original specimen, impact of the fragments on the walls induces secondary fracture which alters the distribution function of the sizes (markedly so for the larger fragments). This effect was avoided by filling the chamber with congealed gelatin to decelerate the fragments, which were removed from the gelatin matrix by washing with hot water.⁵ A photograph of the retaining chamber, containing a specimen fractured in gelatin, is shown in Fig. 1.

The size distributions of the fragments were determined in two ways. In one method, the usual procedure was followed of screening the fragments through a set of standard sieves and weighing the mass retained on each sieve.⁶ Cumulation of the measured masses yields y of Eq. (131)⁷ as a function of a mean dimension x . Because of the small mass (generally about 20 g) of a specimen, this method does not give reliable results in the present application for values of x below roughly 100 μ . For the smaller dimensions, a Coulter counter⁸ was used, which is an electrical instrument operating by virtue of the change in resistance that suspension of small particles produces in a conducting fluid flowing through an orifice.⁹ The instrument yields directly the cumulative number of particles with volume down to a particular value. The manufacturer claims accuracy to a limiting particle dimension of roughly 1 μ .

III. OVER-ALL DISTRIBUTION

The over-all distribution neglects the distinction between exoclastic and endoclastic fragments.

Experimental values of the over-all probability y' are shown as a function of x in Fig. 2 for two specimens, as determined by means of Eq. (131) from the measured

⁵ The gelatin used was an ordinary comestible variety.
⁶ Tyler standard sieves were used, specifications of which are given by A. F. Taggart [*Handbook of Mineral Dressing* (John Wiley & Sons, Inc., New York, 1945), p. 19-102]. For the size range 20-45 μ , use was made of etched metal screens (manufactured by Buckbee Mears Company, St. Paul, Minnesota).
⁷ Equation (13) designates a reference to Eq. (x) in I.
⁸ The instrument is manufactured by Coulter Electronics, Inc., Chicago, Illinois.
⁹ W. H. Coulter, in *Proceedings of the National Electronics Conference* (National Electronics Conference, Chicago, 1956); R. H. Berg, in *Symposium on Particle Size Measurement*, Spec. Tech. Publ. No. 234 (American Society for Testing Materials, Philadelphia, Pennsylvania, 1958).

masses retained on sieves. For x less than about 100 μ , a significant error appears, arising from unavoidable loss of the finer fragments in the operations of washing out the gelatin and screening the particles. The loss is measured as the difference between the original mass of the specimen and the sum of the masses of the recovered fragments. In Fig. 2, each datum point was determined as the mean of two limits; one limit corresponds to ignoring the deficit in mass, and the other assumes the entire loss to arise in the sieve of smallest aperture (a supposition not necessarily true). Limits of error obtained in this way are shown in Fig. 2, when they appear on the scale used. Physical parameters for the specimens are given in Table I; note that x_0' of this table is the mean dimension of the largest fragment recovered.

In the case of both specimens, one notes from Fig. 2 that the data for y' represent closely a straight line of inclination 45° on the logarithmic scales used, over roughly two cycles of values in the intermediate ranges of the variables. Accordingly, the function in this region must conform closely to the analog

$$y' = x'/k' \tag{1}$$

of the Schumann law for $m=1$ of Eq. (147). Let $p' \approx dy'/dx$ represent the over-all differential probability of formation of a fragment with mean dimension x , in the sense of I. From Eq. (1), this differential probability over the range in question has the value

$$p' = k'^{-1} \tag{2}$$

in terms of the constant k' , which is the parameter that would be obtained by a conventional analysis in terms of Schumann's law. To determine k' from the data by means of the definition and the chord rule for differentiation, it is convenient to evaluate the deriva-

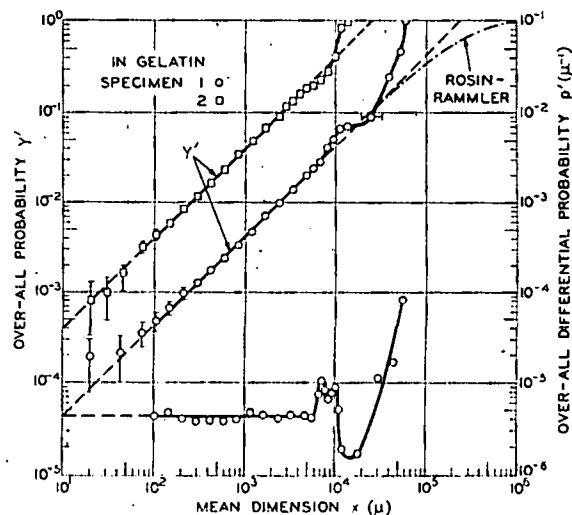


FIG. 2. The probability y' of single fracture for the over-all distribution as a function of the mean dimension x of the fragments for two specimens. The over-all differential probability p' is shown also for specimen 1 (on right scale).

to the over-all probal-
 ical surface of the
 considered in the
 agreement between
 obtained. For plural
 in), two additional
 ferential probability
 sure. The theory of
 inension of at least
 ment, and checked
 ults yield numerical
 wide a tool to study
 mally in a solid).

HOD

shape of a sphere.
 igh diametrically
 motion of which
 started. Rates of
 of one thousand
 , described else-
 . No statistically
 ite of loading on
 on for fragment
 ilar experimental
 a necessary pre-
 respond to single

the fragments
 speeds up to 10³.
 tographically for
 he finer particles



gelatin after fracture.
 the Lucite retaining

to be published).

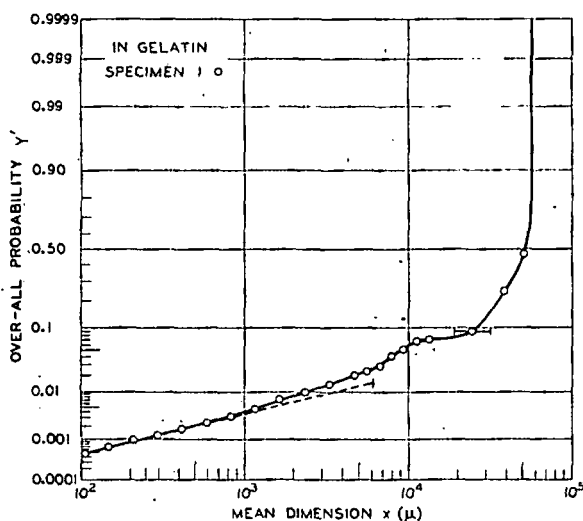


FIG. 3. The probability y' of single fracture for the over-all distribution plotted as a function of the mean dimension x on a coordinate paper which yields a straight line for the data if it corresponds to a logarithmic-normal distribution.

tive at points midway between data points on a logarithmic scale. By use of the operator identity

$$d/dx = x^{-1}d/d \ln x, \quad (3)$$

one obtains

$$p_i' = [x_i \ln(x_{i+1}/x_{i-1})]^{-1} (y_{i+1}' - y_{i-1}') \quad (4)$$

for the differential probability p_i' at the point¹⁰

$$x_i = (x_{i-1}x_{i+1})^{1/2}. \quad (5)$$

The value of k' for the linear portion of the curve of y' is then determined by

$$k' = [\langle p_i' \rangle_{av}]^{-1}, \quad (6)$$

where the average is over the linear part in question. Values of this parameter are tabulated in Table I for five specimens and the mean of four of them.

Individual values of p_i' from Eq. (4) are plotted against x in Fig. 2 for specimen 1. The value of k'^{-1} is indicated by the horizontal solid line of length delimiting the range of x used in the averaging process. Over this region, values of p_i' fluctuate but show no steady departure from a constant.¹¹ Thus, no evidence exists in this domain of x for a value of the Schuhmann exponent m differing from unity, for specimens fractured in gelatin. Values of k' from Table I have been

¹⁰ For the Tyler standard screens, the size ratio x_{i+1}/x_i equals $\sqrt{2}$ for the smaller and 2 for the larger series. In any one series, therefore, the point x_i for the i th sieve lies midway on a logarithmic scale between the points x_{i-1} and x_{i+1} .

¹¹ The sinusoidal course of the data points for p_i' relative to the horizontal solid line of Fig. 2 probably reflects calibration errors of the sieves, since maxima and minima for different specimens tend to be correlated at the same values of x . This correlation makes sieve errors detectable, and implies that the peaks appearing in p_i' of Fig. 4 are not spurious effects from this cause, because of the absence of corresponding peaks at similar values of x in p_i' of Fig. 2 for specimen 1 (of initial diameter 7.6 rather than 2.4 cm).

used to construct the Schuhmann lines in Fig. 2. The data diverge significantly from the corresponding line only for x approaching x_0' . For comparison purposes, the analog

$$y = 1 - e^{-x/k'} \quad (7)$$

of the Rosin-Rammler curve of Eq. (145) has been shown for specimen 1. As $x \rightarrow x_0'$, this curve lies on the side of the Schuhmann line opposite to that on which the data fall; hence the Rosin-Rammler form yields no improvement over the Schuhmann law for the over-all distribution in the case of a specimen fractured in gelatin. This conclusion is at variance with the general case for a mill product, where the Rosin-Rammler equation usually reproduces the correct sense of the deviation from the Schuhmann line for large values of x .

Figure 2 can be compared with Fig. 3, which shows the result of plotting y' for specimen 1 against x on a special coordinate paper which rectifies the data points for any distribution satisfying a logarithmic-normal law.¹² The dashed straight line has been drawn tangent to the curve at the point $x = 100 \mu$; it represents a logarithmic-normal distribution with parameters fitted to the curve of the data at the common initial point. The line has been extended to the value of x at which the horizontal line (solid) of Fig. 2 terminates. At this upper limit, the logarithmic-normal distribution is in error by roughly 50%, whereas the corresponding error of the Schuhmann line is essentially within the accuracy of the data at this point. The fact that the data cannot be represented satisfactorily by a logarithmic-normal distribution is in agreement with the conclusions of L.

One sees from Fig. 2 that the curve of p_i' for specimen 1 at large x shows a structure consisting of a series of peaks, not predicted by the Schuhmann or Rosin-Rammler equations. Figure 4 has been constructed to bring out the nature of this structure in the over-all distribution (the horizontal scale is roughly twice the vertical). For the two specimens appearing, the curve of p' computed from Eq. (4) shows in each case three local maxima indicated by vertical arrows, which can be correlated with points of maximum slope in the corresponding curves of y . Physically, each maximum corresponds to a value of x at which the probability $p'(x)dx$ of forming a fragment with dimensions in the range x to $x+dx$ is locally large for dx fixed. The figure shows that this probability is greatest for the fragments of largest size. However, the existence of at least two minima indicates that the probability in question is not a monotonic function of x , as one might suspect *a priori*. Further, one notes that the Schuhmann range of constant p' is not the region of maximum differential probability; this domain yields the overwhelming number of the fragments simply because of

¹² G. Herdan, *Small Particle Statistics* (Elsevier Publishing Company, New York, 1953), p. 127.

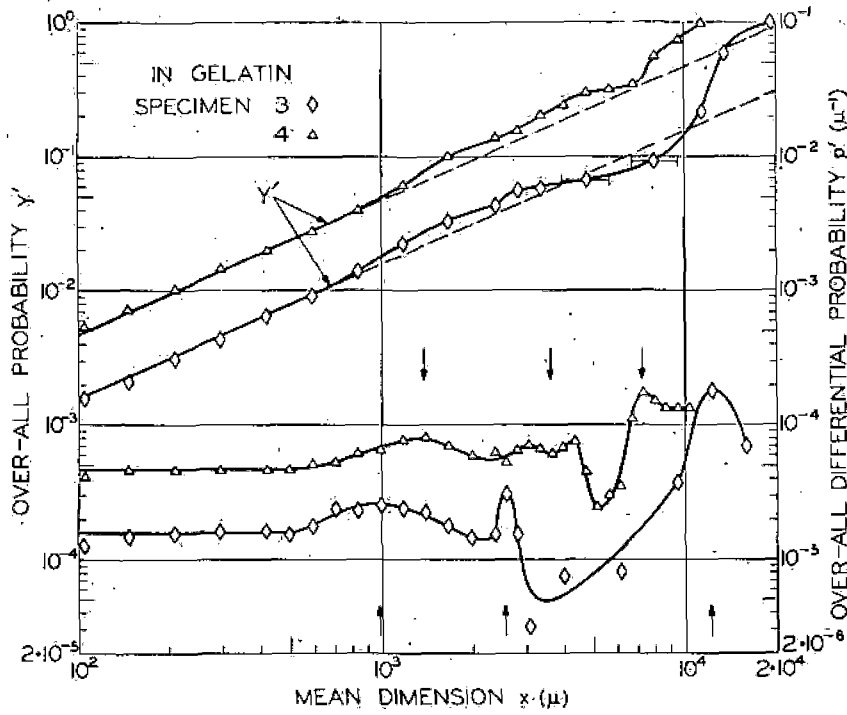


Fig. 4. The probability y' (left scale) and differential probability p' (right scale) of single fracture for the over-all distribution, as a function of the mean dimension x for two specimens. The horizontal scale is approximately twice the vertical.

wide extent, and not because of an inherently high differential probability.

At first sight, the conclusions from Fig. 4 seem to be in variance with the results of I. The general form of p' (139) predicts the existence of three distinct regions of x : a domain of constant p' for small x arising from edge flaws, followed as $x \rightarrow x_0$ by two regions of variable p' corresponding to the effect of facial and longitudinal flaws. The results of Fig. 4 differ in the sense that three local maxima appear. However, Eq. (139) applies only to the endoclastic fragments, while y' and p' of Fig. 4 correspond to the over-all distribution of both elastic and exoclastic fragments.

The curve of p' as a function of x for specimen 4 is anomalous in that one local maximum consists of two pronounced ones. A similar (but less marked) case occurs for specimen 2 but not for specimen 5 (curves not shown). This anomaly will be resolved in Sec. IV. In the neighborhood of the most pronounced maximum, the individual sieves generally retained only few fragments (frequently only one or none).¹³ The question presents itself whether the multiple maxima in Fig. 4 may represent mere artifacts introduced by poor statistics.¹⁴ If such were the case, averaging the data for a sufficiently large number of specimens would cause the peaks to disappear. The value of p' in Eq. (4) is shown in Fig. 5, as obtained from y' corresponding to an average for four specimens (2, 3, and 5) of the same initial diameter. One sees that the peak corresponding to the largest fragments is

accentuated, indicating that its location is subject only to slight fluctuation, and it certainly is real. The other two maxima are broadened as compared to the case with individual specimens, but their permanence under averaging indicates their reality in fact. The

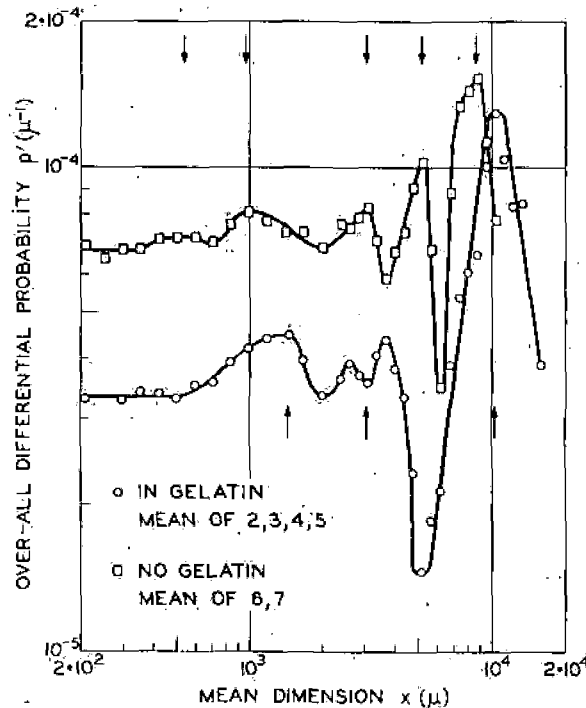


Fig. 5. The over-all differential probability p' for single fracture as a function of x for the mean of four specimens, compared to the corresponding probability for plural fracture from the mean for two specimens.

The data points in Figs. 2-4 indicated by horizontal bars correspond to sets of successive sieves where only the one of the largest aperture contained fragments.

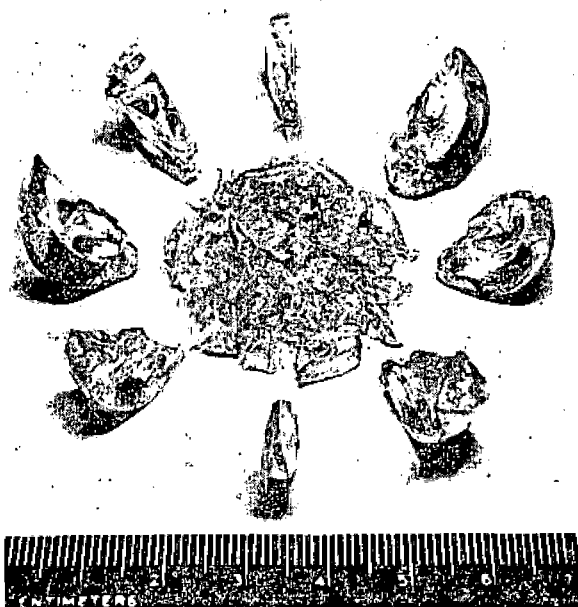


FIG. 6. Fragments of a specimen fractured in gelatin, as recovered from the matrix. The fragments are disposed radially in their correct relative position.

duplicity appearing in the middle peak will be explained in Sec. IV. As further confirmation of the reality of the three peaks, it was found that they appear in the average of data for 36 specimens fractured in gelatin, from results of Bergstrom, Sollenberger, and Mitchell.¹³

The fact appearing generally from these results that, for small x , y' is a linear function of x and p' is a constant, confirms the conclusion of I that edge flaws represent the dominant cause of fragmentation in the fine-sizes.

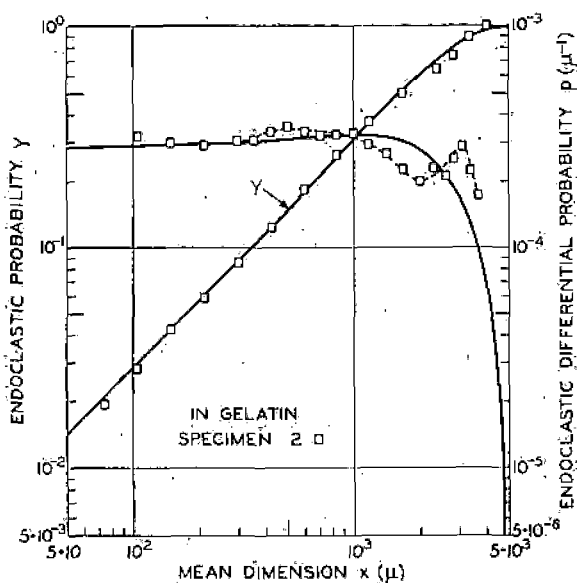


FIG. 7. The probability y (left scale) and differential probability p (right scale) of fracture for the endoclastic distribution, as a function of the mean dimension x for specimen 2.

IV. ENDOCLASTIC DISTRIBUTION

Under point loading, failure of a specimen generally starts in a conical fracture surface with apex at the point of application of the force.¹⁴ In the present experiments, however, the load was distributed over a finite area as the spherical specimens yielded elastically under the pressure of the flat platens. Failure of the specimen in this arrangement starts in conical fracture surfaces with bases on the platens; the base of the cone corresponds approximately to the area of contact of specimen and platen at the instant of fracture.¹⁵ However, the propagating conical surfaces produce a failed cylinder extending diametrically through the specimen, which yields the bulk of the fine fragments, apparently. The remainder of the specimen breaks into pieces which approximate lunes in shape; Figure 6 shows the fragments from a specimen, arranged in the correct relative angular position as recovered from the retaining chamber.

The lunes of the exoclastic particles are responsible for the main mass of the fragments (of both classes). Typically, they correspond in total mass to the order of 75 to 90% of that of the original specimen. Con-

TABLE II. Parameters of the endoclastic distributions for the specimens.

Specimen ^a	x_0 cm	k cm	j cm	i cm
No. 2	0.40	0.36	0.36	0.44
No. 3	0.33	0.39	0.23	0.25
No. 4	0.40	0.59	0.27	0.24

siderably smaller exoclastic fragments are identifiable through the presence of original surface of the specimen. In general, few exoclastic particles were found with values of x less than corresponds to the first minimum¹⁶ in Fig. 4. This situation did not obtain for specimen 4, however; in this case, 28 such fragments were recovered, extending in values of x considerably below that corresponding to the first minimum.

The identifiable exoclastic fragments were sieved separately and the corresponding masses were subtracted from the total originally measured to obtain the masses of the endoclastic fragments retained on each sieve. The upper limit x_0 of endoclastic dimensions was taken to correspond to one sieve size larger than the first (in order of decreasing x) for which the endoclastic mass did not vanish; values for three specimens are tabulated in Table II. Cumulation of the masses yields values of the probability y for formation of an endoclastic fragment with mean dimension between

¹⁴ F. C. Roesler, Proc. Phys. Soc. (London) B69, 981 (1956).

¹⁵ J. C. Jaeger, *Elasticity, Fracture, and Flow* (John Wiley & Sons, Inc., New York, 1956), p. 74.

¹⁶ Throughout this paper, ordinal numbers of maxima and minima are reckoned in order of decreasing x from the largest value of x for the distribution in question.

0 and x_0 , as shown by the plotted points in Fig. 7 for specimen 2 and in Fig. 8 for specimen 4. Values of the differential probability p from the defining relation (I32) also appear; these points are connected by the dashed curve.

It is clear from Figs. 7 and 8 that only two of the three maxima appearing in the over-all differential probability p' correspond to the endoclastic particles, to which alone the theory of I applies. Thus, the main peak in p of Figs. 2 and 4 stem entirely from the exoclastic fragments. In the experimental data for specimen 4, one notes that the supernumerary peak appearing in Fig. 4 has vanished; it arose because of the very large number (28) of exoclastic fragments appearing from this specimen. A slight additional peak persists in the first maximum for specimen 2,

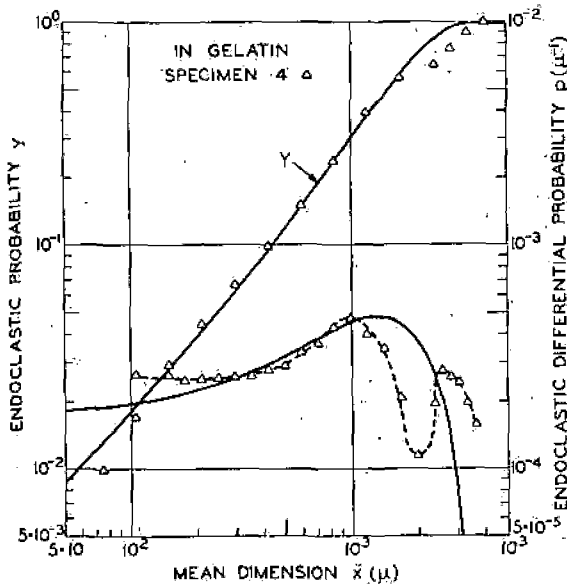


FIG. 8. The probability y (left scale) and differential probability p (right scale) of fracture for the endoclastic distribution, as a function of the mean dimension x for specimen 4.

but its amplitude is reduced considerably as compared to the case in the over-all distribution. Thus, the conclusion follows that the supernumerary peak arises from the effect of exoclastic particles.

To discuss the quantitative agreement of theory and experiment, consider the relation

$$Q = -\ln(1-y), \quad (8)$$

which Eq. (I44) yields. Values of Q obtained from this relation are shown in Fig. 9 for specimen 2 and in Fig. 10 for specimens 3 and 4. The parameters k , j , and i entering the cubic form Q of Eq. (I36) have been derived by the method of least squares from the data for the three specimens and are tabulated in Table II. The curves of Figs. 9 and 10 correspond to the fits obtained. Equation (I44) has been used to construct the corresponding curves (solid) of y in Figs. 7 and 8. One sees that agreement is excellent.

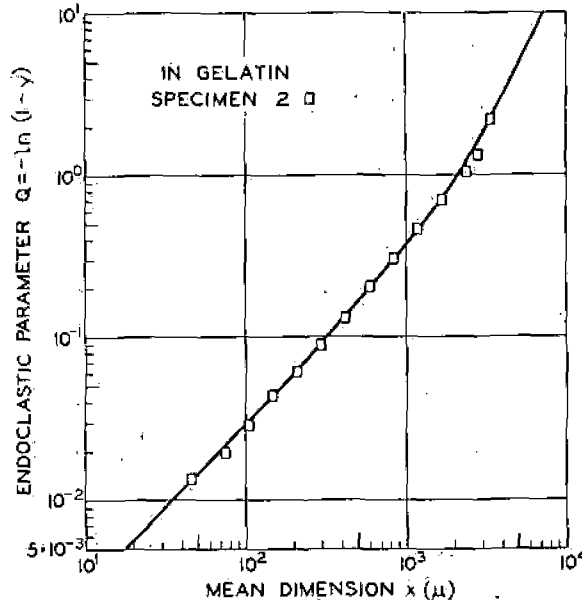


FIG. 9. The parameter Q for the endoclastic distribution as a function of x for specimen 2, as given by the data and by the fitted function.

Independently of the specimen, Eq. (8) implies that all data for $-\ln(1-y)$ should be rectified on a line of inclination 45° when plotted against the corresponding Q of the fitted function. Figure 11 shows that this prediction is borne out over the major part of the data.

As compared to the case for the integral probability, agreement of theory and experiment is not as good for the differential probability p . Since Q is a cubic form in x , Eq. (I38) potentially is able to yield two local maxima in the curve of p , as the experimental data

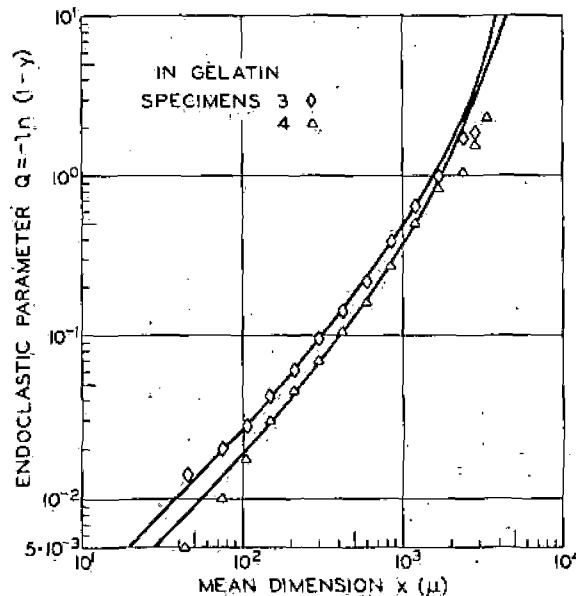


FIG. 10. The parameter Q for the endoclastic distribution as a function of x for specimens 3 and 4, as given by the data and by the fitted function.

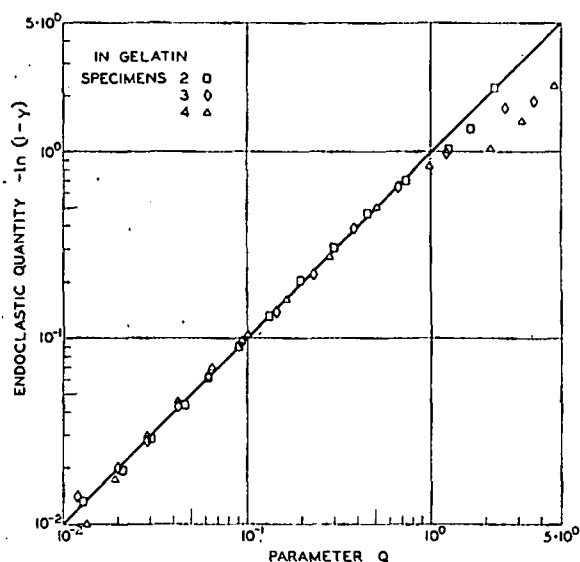


Fig. 11. The quantity $-\ln(1-y)$ from the data as a function of Q from the fitted function, for three specimens.

require. The positions x_1 and x_2 of the first and second maxima, respectively,¹⁶ are roots of the equation

$$dp(x)/dx=0, \quad (9)$$

which corresponds to a quartic in x . One can solve analytically for x_2 under the approximation $(x_2/i)^3 \ll 1$, which yields

$$x_2 = \frac{1}{2}(\sqrt{2-j/k})j. \quad (10)$$

Values of x_2 computed from this relation with values of k and j from Table II are compared in Table III with positions of the second maxima as obtained from the data. One sees that agreement is reasonable as regards general magnitude, but is by no means exact. Thus, Eq. (139) with values of k , j , and i from Table II certainly predicts the existence of the maximum corresponding to facial flaws, but the position is not given very accurately.

The fitted functions for Q have been used in Eq. (138) to construct the solid curves for p appearing in Figs. 7 and 8. One sees that the expected maxima corresponding to the effect of volume flaws do not appear. It is possible to show that Eq. (9) for p of Eq. (139), with k , j , and i as given in Table II, possesses no positive real root other than the one approximated by Eq. (10). This result is not a general one; it applies specifically for the values of the parameters k , j , and i in question. Since Eq. (9) yields a quartic in x , the possibility of the peak corresponding to the volume flaws actually appearing in p of Eq. (139) under other experimental conditions certainly exists. For the specimens under discussion, however, p of this relation yields only a qualitative or at best semiquantitative description of the course of the data in the region of x where the effect of the volume flaws should be predominant. It

can be noticed that this region is only a relatively small part of the entire domain of x .

The failure of the maximum corresponding to the volume flaws to appear in the theoretical relation of I for p can be understood on the basis of flaw depletion. It was emphasized in I that depletion of the internal flaws of the specimen must be taken into account, if all moments of the distribution having physical significance are to be finite. In that particular context, depletion of internal flaws by the effect of the edge flaws was under discussion, primarily. However, the internal flaws of the specimen available to produce volume flaws in a fragment can be depleted through the effect of those internal flaws yielding volume, facial, and edge flaws in other fragments. Thus, Eq. (136) predicts the correct manner in which the effect of the volume flaws appears in Q only when depletion is neglected; presumably, its inclusion would steepen the rate at which the term in x^3 loses effect as x decreases from large values, to yield the maximum found in the data. It is a consequence of the considerations adduced here that the distributions of volume, facial, and edge flaws are *not* independent as assumed in I, but are coupled to an extent through the depletion effect.

V. PLURAL FRACTURE

The theory of I states that y (or y') in single fracture becomes a linear function of x for x small, down to values at which depletion effects appear. Limitations imposed by the mechanical process of sieving and the washing operation to remove the gelatin make the error large in the region of x below 100μ . Since the sensitivity of a Coulter counter extends down to roughly 1μ , an effort was made to use this instrument to determine the distribution function for single fracture at low values of x . This procedure avoids the loss of fragments in repetitive use of sieves, since the particles are suspended in a fluid during the measurement. However, it was found that unavoidable loss in the operation of removing the gelatin (or the bulk of it) still limited the accuracy attainable.

The experiments of Bergstrom, Sollenberger, and Mitchell³ indicate that the finer fragments in single fracture show low speeds approaching zero, and only the larger fragments move at high speed. Hence, if no gelatin were used, and the fragments were allowed to impinge on the walls of the retaining chamber, one should expect serious distortion of the true distribution

TABLE III. Position x_2 of the second maximum of the endoelastic distribution, as compared with the result of Eq. (10).

Specimen	x_2 μ	x_2 [Eq. (10)] μ
No. 2	720	830
No. 3	950	700
No. 4	1300	990

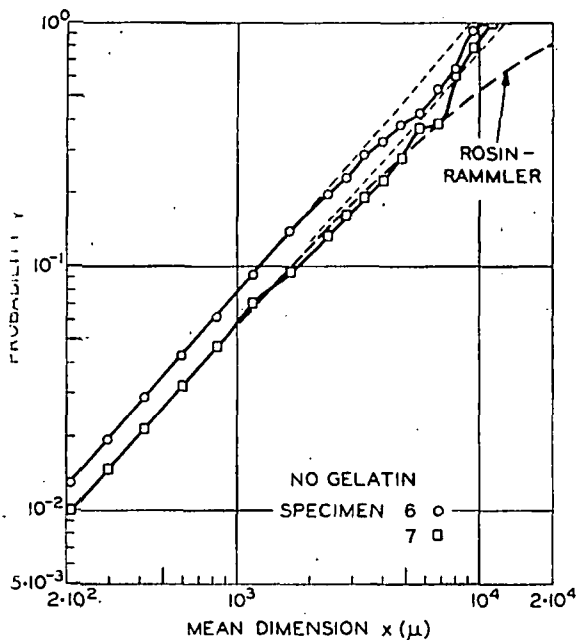


Fig. 12. The probability y' of plural fracture as a function of the mean dimension x of the fragments, for two specimens.

ly for the coarser fragments. The distribution function for the finer sizes should then indicate the proper action for single fracture in this regime of x . To test this hypothesis, a series of experiments on plural fracture were performed (plural fracture is defined as single fracture followed by only a few secondary fractures). The experimental arrangement differed from the previous one only in the respect that no gelatin is used as a decelerating medium, and the Lucite retaining ring shown in Fig. 1 was replaced by a steel retaining chamber.

Figure 12 shows values of the over-all probability y' for two specimens (6 and 7) fractured in this manner. The values for small x (below $10^3 \mu$) lie reasonably on straight lines (dashed for large x) corresponding to the general Schumann law of Eq. (146) with $m \approx 1.15$. In view of the following discussion, however, this fact must be viewed as an empirical correlation, without necessary physical significance. As compared to the over-all probability y' for single fracture, that for plural fracture fails to show the steep increase of slope above that of the corresponding Schumann line for large x , as appears in Fig. 2. The Rosin-Rammler curve for $m = 1.13$ is shown (dashed) for specimen 7; one sees that it fails to yield a good representation of the data for large x .

Values of the over-all differential probability p' for the two specimens are shown in Fig. 13. The curves appearing correspond to the data, and not to a theory. The salient difference of p' from the case for single fracture lies in the presence of two additional local maxima, as indicated by the vertical arrows. The differential probability p' for the mean of the two

specimens appears in Fig. 5. Since the five peaks indicated are permanent under averaging, they are almost certainly real. A similar set of five peaks appears in the average of data for 40 specimens fractured without gelatin, from results of Bergstrom, Sollenberger, and Mitchell.³

One can attempt identification of the origin of the different local maxima in plural fracture by examination of Fig. 5, where the differential probabilities for the means of the specimens fractured with and without gelatin appear. The first maximum¹⁶ in the case of plural fracture can be identified with little ambiguity. This peak clearly arises from exoclastic fragments of the original specimen which impinged on the walls of the retaining chamber; surficial flaws not activated in the primary fracture produce the prominent peak. Identification of the remaining peaks is not unambiguous, since one has available only the positions of the peaks as clues to their origin. However, the second maximum probably corresponds to the effect of internal flaws of volume type in the fragments colliding with the chamber walls. In view of the correlation of their positions with the corresponding ones for single fracture, the third and fourth peaks quite likely represent the effect of volume and surface flaws in the endoclastic fragments from the primary fracture, respectively. The presumption is that the speed of these fragments was too low for significant secondary fracture to occur. On these presumptive identifications, the last peak appearing corresponds to internal flaws of facial type arising from the fragments impinging on the chamber walls. These interpretations must be viewed as tentative pending corroboration. In any event, it is clear that the distribution function for fragment size in plural fracture is compounded of at

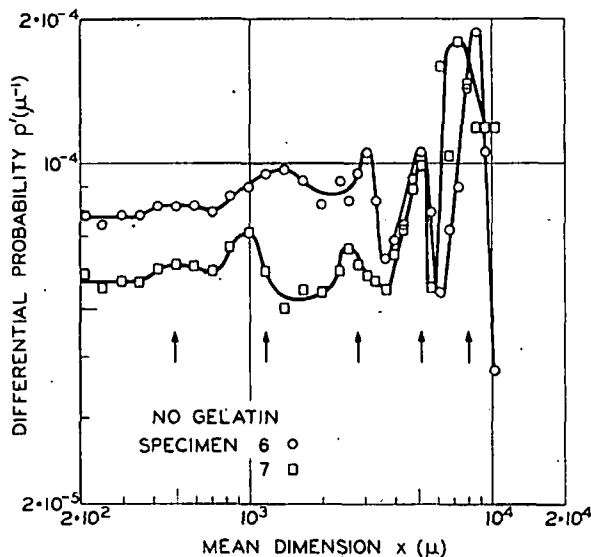


Fig. 13. The differential probability p' of plural fracture as a function of the mean dimension x of the fragments, for two specimens.

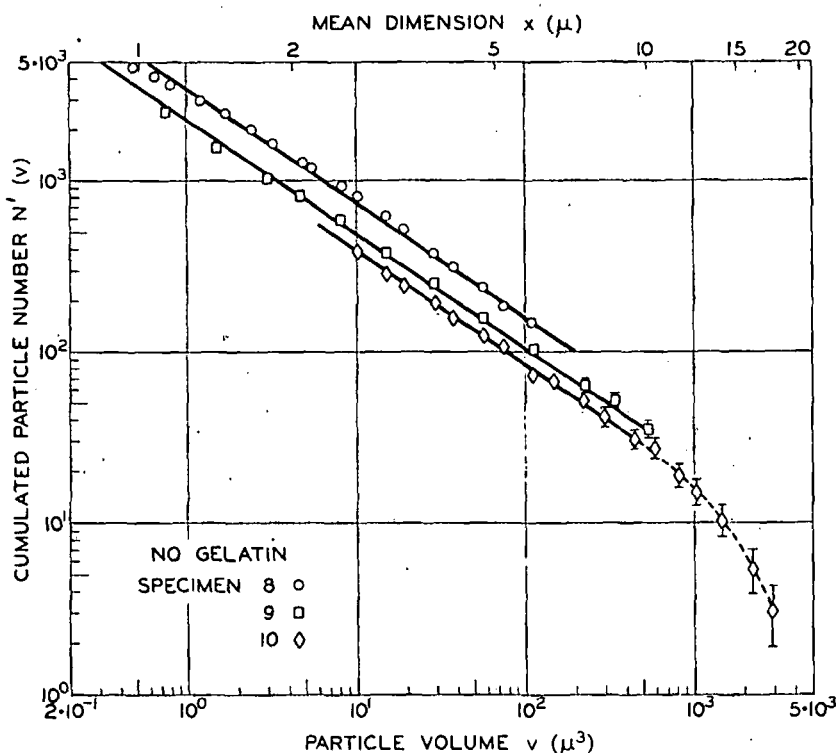


Fig. 14. The cumulated number $N'(v)$ of fragments with volume down to v , as a function of particle volume v , determined by a Coulter counter for three specimens.

least two distributions. However, one notes that the amplitudes of successive maxima in Fig. 13 decrease steadily with x , in conformity with the hypothesis that the distribution function approaches that for single fracture as x becomes small.

The Coulter counter is not an absolute instrument in two senses: The particle volume must be determined by calibration, and measurements can be made only on a small aliquot of the total specimen, in general. Further, different ranges of particle dimensions require

use of different orifices, and the corresponding results must be matched in a region of overlap of particle dimensions. These facts are not objections in the present instance, since the interest here is in the functional form of the results, and not their absolute values. Figure 14 shows the results obtained for the cumulative number $N'(v)$ of particles from aliquots for three specimens, cumulated from a particle volume of about $4 \times 10^3 \mu^3$ down to the value v appearing as abscissa. An approximate scale of linear dimensions of the fragments is provided also, as determined on the oversimplified assumption of spherical fragments. The errors shown are probable errors, computed from the total particle count.

From Eqs. (134c) and (160a), one finds that $N'(v)$ for the entire specimen should satisfy

$$N'(v) = \frac{1}{2} \omega^3 (V_0/k) v^{-3} \quad (11)$$

in the limiting case as $v \rightarrow 0$. Straight lines of slope corresponding to the power v^{-3} have been fitted to the data of Fig. 14. One sees that agreement of theory and experimental results is excellent, in general. The slight curvature of the data points relative to the theoretical line in the case of specimen 8 may be an instrumental error. The data deviate from the theoretical line for the larger values of v (as shown dashed in the case of specimen 10), simply because particles of mean dimension greater than about 20μ had been sieved out of the specimens used.¹⁷ Thus, the instrument does not

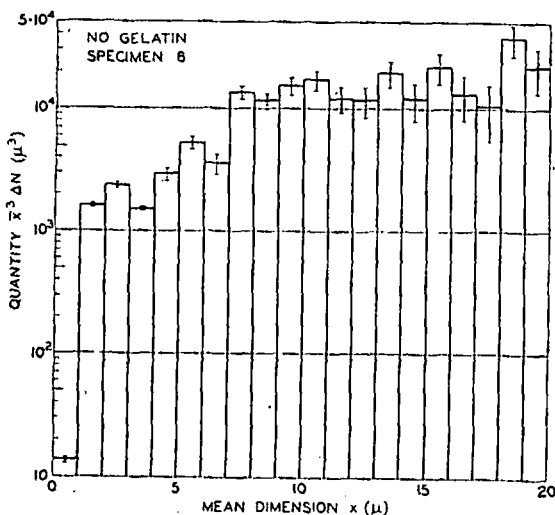


Fig. 15. Histogram of the quantity $x^3 \Delta N(x)$ as a function of the mean dimension x of a fragment in plural fracture, determined by direct microscopic sizing for specimen 8.

¹⁷ This procedure is necessary, in general, to prevent clogging of the nozzle by particles too large for its range.

actually yield true values of $N'(x)$ until its reading becomes large relative to the cumulated number of particles for a lower limit in x corresponding to this dimension. Accordingly, results obtained by use of the Coulter counter confirm the theory of I down to a fragment dimension of roughly 1μ .

As a check on the accuracy of the Coulter counter, direct microscopic sizing was carried out for specimen 8, for the range below 20μ in dimensions.¹⁸ The mean dimension of a fragment was taken as the average of the maximum and minimum found in the focal plane of the microscope, determined by comparison with a reticle. The cell containing the aliquot of the specimen was scanned in depth as well as area, but the experimental difficulty is to avoid missing individual fine particles. The data were classified into number intervals ΔV corresponding to intervals of 1μ in x . The quantity $\bar{x}^2 \Delta V$, where \bar{x} is the average value of x for the interval ΔV , is shown in the histogram of Fig. 15, constructed from results of measurements on 765 fragments. The

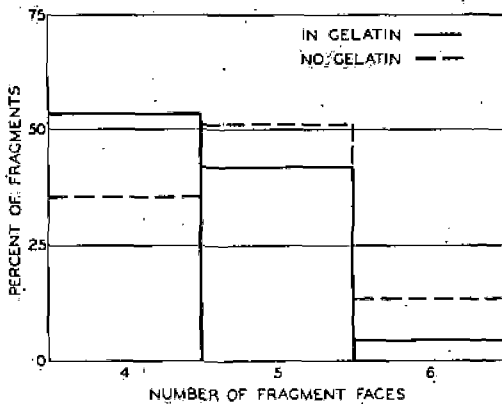


Fig. 16. Histogram of the percentage of fragments possessing a particular number of faces.

errors shown are probable errors fixed by the total number of particles in the interval. On the basis of Eq. (I41), $\bar{x}^2 \Delta V$ should be a constant. One sees that the data conform to this result within the probable error, for values of x from 20μ down to roughly 5μ , and thus check the results from the Coulter counter over this range. The data of Fig. 15 are not considered reliable enough to justify attachment of significance to the decrease in the ordinate for x below about 5μ ; the effect probably is caused by preferential oversight of the finer fragments in the visual count.

VI. DISCUSSION AND CONCLUSIONS

The parameters k , j , and i of Table III represent flaw spacings referred to the mean dimension x of a fragment, and thus do not correspond to true flaw densities. To convert these quantities to proper densities, one must evaluate the parameters λ_b , λ_s , and

TABLE IV. Parameters of the distribution, corresponding to a tetrahedral shape of fragment.

Parameter	Value	Parameter	Value
λ_t	6	ω	$6\sqrt{2}$
λ_b	$\sqrt{3}$	σ	$6\sqrt{6}$
λ_e	$3\sqrt{2}$	τ	$36\sqrt{2}$

λ_e of Eqs. (I34). For this purpose, it is necessary to determine the average particle shape. The histogram of Fig. 16 shows percentage counts of the number of faces per fragment, for 155 particles arising from fracture in gelatin and 1060 fragments formed without use of this medium, as determined microscopically¹⁸ for fragments of mean dimension down to 1680μ . It is clear that the most probable particle shape in this range of larger sizes is tetrahedral in the case of single fracture. Qualitative examination¹⁸ down to a size of 74μ for fragments formed in gelatin showed that the most probable shape is a flat tetrahedron (sphenoid) with the ratio of maximum to median dimension less than 2. Columnar and cubic forms occur, in that order, with decreasing relative frequency. A fraction of the fragments up to a limit of perhaps 10% for any size examined showed an acicular shape in which the ratio of the maximum to the median dimension exceeded 10; the relative numbers decreased with mean dimension x for the case of single fracture. The presence of this acicular fraction implies some departure from randomness in the internal stress system producing fracture. It is generally conceded that the dimension of a particle selected by a sieving operation is neither the maximum nor minimum, but some intermediate value, on the average.¹⁹ In view of the generally flat shape of the fragments in question, however, their mean dimension was taken to correspond to the edge of a tetrahedron, assumed regular for purposes of simplicity. The corresponding values of the parameters λ_b , λ_s , and λ_e are tabulated in Table IV; shown also are values of ω and of τ and σ from Eqs. (I42) and (I59), respectively.

With use of the parameters of Table IV, Eqs. (I35) yield values of the flaw densities γ_l , γ_s , and γ_v for single fracture corresponding to k , j , and i of Table III, as shown in Table V. One notes that the approximation (I22) is satisfied within roughly an order of magnitude,

TABLE V. Flaw densities of specimens, for edge, facial, and volume flaws of internal type.

Specimen	γ_l cm ⁻²	γ_s cm ⁻²	γ_v cm ⁻³
No. 2	0.47	4.4	75
No. 3	0.42	11	540
No. 4	0.28	8.2	580

¹⁹ A. M. Gaudin, *Principles of Mineral Dressing* (McGraw-Hill Book Company, Inc., New York, 1939), p. 51.

¹⁸ The measurements were carried out by E. W. Price.

since the data of Table II indicate that

$$k \approx j \approx i. \quad (12)$$

The implication of this result is that the distribution of orientations of fracture planes is not far from a random one. Furthermore, the degrees of activation of the different types (edge, facial, and volume) of internal flaws cannot differ greatly.

The flaw densities of Table V refer to the internal flaws. Apparently, no results for direct comparison exist in the literature, since estimates of flaw densities made heretofore correspond to surficial flaws. Anderson²⁰ has inferred a value of 10^3 cm^{-2} for the density of surficial flaws required by the theory of Fisher and Holloman²¹ to explain the experimental results of Anderegg²² on the size effect in the strength of glass fibers. The figure applies to the flaw density on the surface of a fiber drawn from a melt. From the rule of Eq. (121), this areal density implies a linear density of 30 cm^{-1} . Thus, the sense of the difference from the results of Table V is correct, in that a surficial

flaw density exceeds any corresponding internal density; in point of fact, the excess is large. Such a conclusion is necessary if glass specimens are to fail by virtue of surficial flaws, in general.

It is clear that the theory of I and the experimental methods presented yield a tool to study the distribution of Griffith flaws in a solid. Furthermore, this method is the only one available at present to investigate the distribution of internal flaws, since decoration techniques can be applied only to surficial flaws.²³⁻²⁵ In further papers of this series, the extension of the theory of I and of the experimental results to the case of surficial flaws will be presented.

ACKNOWLEDGMENTS

The authors wish to thank C. L. Sollenberger and W. Mitchell, Jr. for helpful discussions. Thanks are due E. W. Price for performing the measurements upon which Figs. 15 and 16 are based. The technical aid of L. Anderson is acknowledged, and thanks are due Helen Jackson for technical and computational work.

²⁰ O. L. Anderson, in *Fracture*, edited by B. L. Averbach, D. K. Felbeck, G. T. Hahn, and D. A. Thomas (John Wiley & Sons, Inc., New York, 1959), p. 331.

²¹ J. C. Fisher and J. H. Holloman, *Am. Inst. Mining, Met., Petrol. Engrs. Tech. Publ. No. 2218* (1947).

²² F. O. Anderegg, *Ind. Eng. Chem.* 31, 290 (1939).

²³ E. N. da C. Andrade and L. C. Tsien, *Proc. Roy. Soc. (London)* A159, 346 (1937).

²⁴ J. E. Gordon, D. M. Marsh, and M. E. M. L. Parratt, *Proc. Roy. Soc. (London)* A249, 65 (1959).

²⁵ W. C. Levengood, *J. Appl. Phys.* 30, 378 (1959).

Field Permeability Methods for In-Place Leaching

SUBJ
MNG
FPM

UNIVERSITY OF UTAH
RESEARCH INSTITUTE
EARTH SCIENCE LAB.

Over the past few years in-place leaching has received increased attention from mine operators producing copper and uranium. Several mining companies have fractured and subsequently leached porphyry copper deposits in the Southwest. Many pilot and several commercial uranium leaching operations have been initiated in Texas and Wyoming. The Bureau of Mines has conducted a variety of research projects on improving leaching technology, and an extensive bibliography on in-place leaching is available.¹

In-place leaching has spawned new conditions for which an ore body must be evaluated to determine its production potential. During its early research efforts, the bureau established the importance of permeability tests. Permeability is a measure of a formation's ability to transmit fluids and is, therefore, directly related to flow characteristics of leaching fluids. For "tight" formations such as the porphyry coppers, permeability measurements determine whether a formation must be blasted to create adequate leaching-fluid flow. For permeable formations such as the sandstone roll-front uranium deposits, permeability helps define a multitude of well field parameters such as well spacing, pumping rates and plant capacity. For all formations, concern over ground water contamination has mandated accurate knowledge of permeability.

Permeability testing techniques have not been familiar to most mining engineers. Although laboratory tests for permeability were routine, bureau researchers likewise had little experience with field permeability measurements. A contract was awarded, therefore, to survey techniques available from civil and petroleum dis-

ciplines to determine which applied to evaluating formation leachability. For the relevant methods, the contractor was further charged with compiling a "cook-book" description of each test—detailed test procedures, analysis techniques and required equipment. The results are summarized in this article, but details can be obtained from the contractor's final report.²

Tests similar to those used on dam projects

Although sophisticated permeability techniques have been developed in the petroleum field, the tests that appeared best suited for use by mining engineers in evaluating leachability were those civil engineers use to investigate rock for dam projects. These tests—constant-head, variable-head and pumping tests—are performed by injecting or withdrawing water from vertical holes drilled into the formation being evaluated. Details on conducting these tests and analyzing results are contained, in total, within the contractor's final report.

In constant-head tests, a constant water pressure or "head" is applied through a well to a fixed interval of the formation. The quantity of water needed to maintain that head is then measured over a given time interval. Analysis of test results to obtain permeability involves straightforward manipulations of the constant-head pressure, flow rate required to maintain that head and dimensional considerations.

Constant-head tests can be conducted with or without packers. If packers are not used, a water-level-indicating device must be monitored to maintain a constant water level in the well. With packer tests, pressure

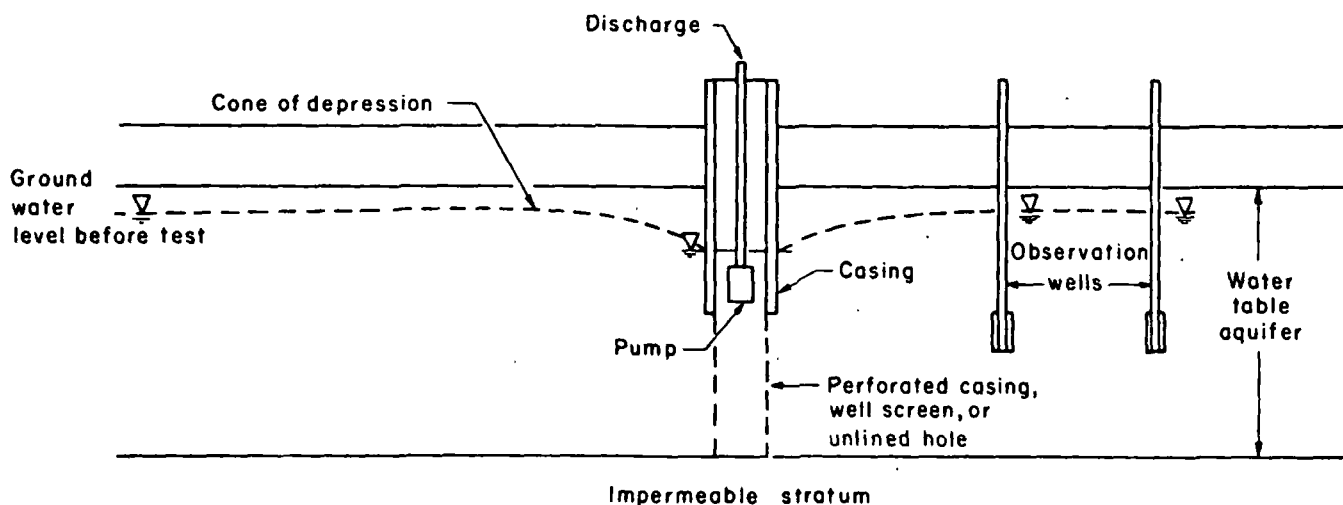


Fig. 1. Basic well pumping terminology¹

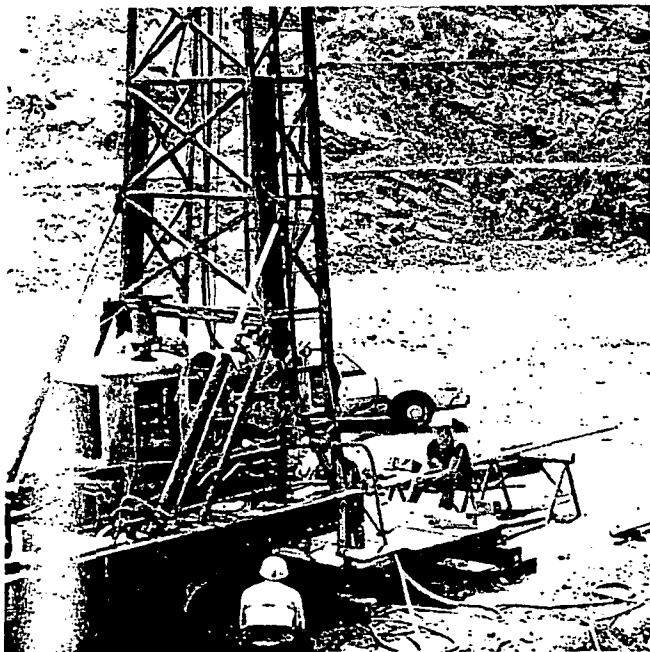


Fig. 2. Drilling rig set up for pumping in permeability tests with packers.

gauges or electrical transducers may be used to monitor the constant head of water applied to the test section. The test interval is fixed by the packer spacing. For a single packer, the entire well section below the packer is the test zone; when two packers are hooked in tandem as a "straddle packer," the test zone is the space between them.

Variable-head tests—either falling or rising head—are conducted by adding or withdrawing a "slug" of water from a well and monitoring the rate at which the water returns to its original level. Water can be added by pouring or pumping. Water is generally withdrawn by pumping or bailing, although air pressure can be used if the water volume removed can be accurately measured. While variable-head tests are very simple and cheap to run, analysis of results is empirical and more complicated than it is for constant-head tests. The analysis basically involves comparing plots of the rate of change in the head with "type" curves for known permeabilities.

Where time and economics permit, pumping tests provide the desired measurement. Measurements from pumping tests provide more accurate estimates of the fluid flow conditions during leaching operations than do

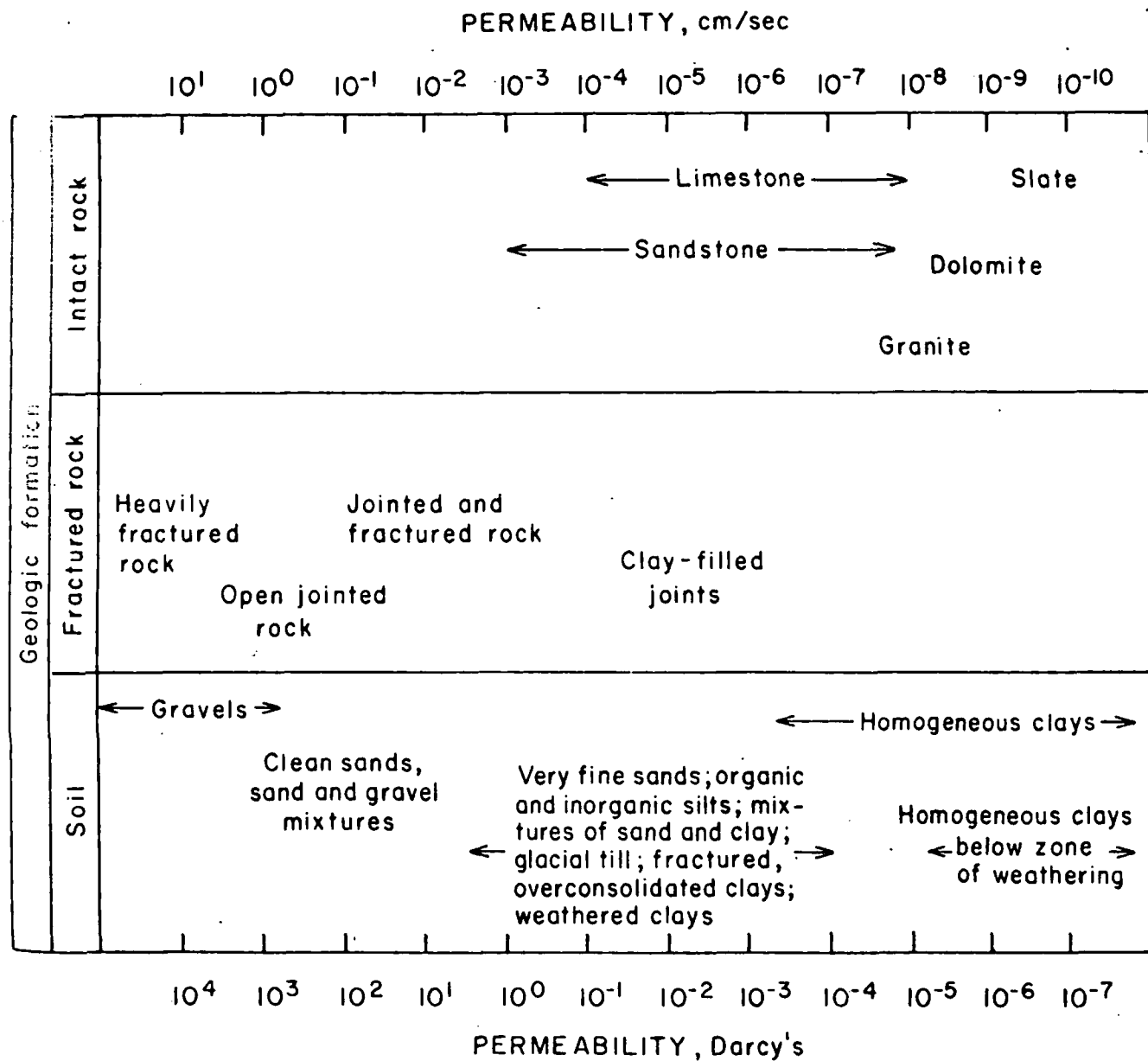


Fig. 3. Ranges of permeability for geologic formations (after O'Rourke, et al¹)

ting
the
ook-
oce-
The
in be

have
t ap-
eval-
o in-
tant-
med
oles
s on
con-
e or
al of
tain
val.
lves
head
and
out
l-in-
con-
sure

other tests. Pumping tests employ two or more observation wells drilled at various distances from a pumping well (fig. 1). As water is withdrawn from the pumping well, the water table is depressed which lowers the water level in the observation wells. The permeability of the formation is computed from the ratio of the water level draw-down to the observation well's distance from the pumping well.

Importance of well preparation often overlooked

The importance of proper well preparation is frequently overlooked by newcomers to permeability testing. It is imperative that the testing wells be drilled with minimal formation contamination to minimize plugging the permeability channels. Matching proper drilling fluids with formation characteristics helps decrease the problem; coring also often damages a formation less than rotary drilling.

After a well has been drilled, fresh water should be circulated until the return water flows clean. Even a well-flushed hole will, however, contain some cuttings; these can be removed by bailing the well. A bailer can be constructed from a section of drill rod fitted with a simple trap valve. Scrubber brushes attached to a drill rod can scrape cuttings from the wellbore wall to facilitate cleaning.

Wells in loosely consolidated formations like some of the uranium sandstones usually must be cased to prevent excessive sloughing. Permeability tests can

then be run through screen sections, through open-hole zones below the casing, or in gravel-packed zones.

Equipment ranges from simple to sophisticated

Depending upon the available budget and desired results, the equipment required to conduct permeability tests can range from a simple water bucket and tape measure to sophisticated instrument packages for documenting test parameters. Once a suitable well has been drilled, essential operations are: (1) adding (or subtracting) water; (2) measuring the added volume of water; (3) measuring the pressure (or head) in the test zone; and (4) measuring time. Water can be added by pouring from a bucket or pumping. Although more sophisticated flow meters are available, water volumes are generally measured with a household water meter. The water pressure or head can be measured with simple electrical water level indicators, piezometers, pressure transducer, or even a tape measure if the water level is near the well collar.

Certain permeability tests require special equipment. Pumping tests require special pumps to lift the water. Packerc tests require a drill rig or similar means of raising or lowering the packers (fig. 2). These packers are generally attached to the drill string or galvanized pipes for positioning in the well. Furthermore, packers must be seated with hydraulic pressure (from the drill-rig pump) or compressed air (run down a separate line to the packer). Although inflatable packers constructed from plastic

pipe are becoming popular,² the bureau generally has used oilfield-type packers raised and lowered on the drilling string.

More than one test may be desirable to verify results

A method for selecting appropriate permeability test methods was documented in the contractor's final report.² The first step in the process is to determine the range of permeabilities likely to be encountered in the target ore deposit. If this information cannot be derived from tests on similar deposits, it can be estimated from a chart of probable permeability for the basic rock types (fig. 3). Turning to the techniques that have been used in formations of various permeabilities (fig. 4) one or more techniques can be tentatively selected. Final selection can be made with the assistance of an evaluation matrix (fig. 5) based upon the desired performance characteristics, economics, time frame, etc. It may be desirable to run more than one test to verify results.

After a test method or methods have been selected, several publications are available to serve as "cook-books" for running and analyzing the tests.³⁻⁵ We have found that the final

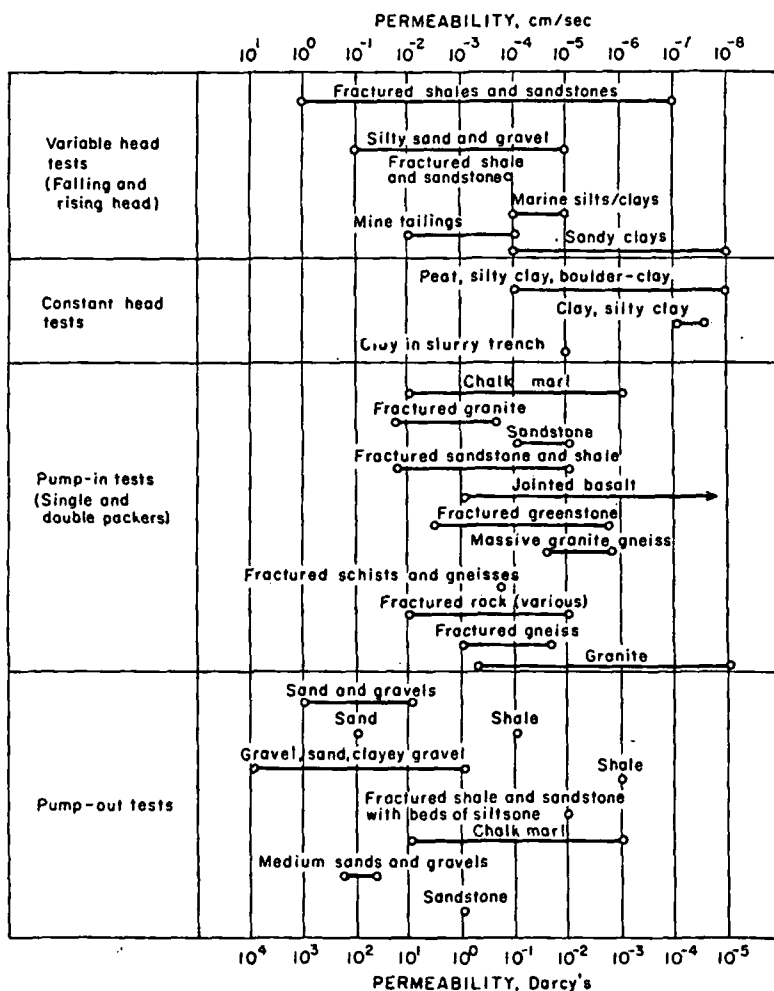


Fig. 4. Reported ranges of field test methods for permeability measurements (after O'Rourke, et al²)

Key:

4

Note:

4

Test method

port for
tests were
ice.²

In a typ
limestor
ious test
fig. 3 rang
This form
and those
range of p
fig. 4, suc
able-head
packers. I
the evalu
ation wa
tion of ver
important
pumping-i
stant-head
meabilitie
were take
book" po
situations
important
variable-h
methods.

Permea
uating for
tive surve
civil and
stant-head
important
formations

Key:		Evaluation criteria																	
		Refers to single test		Refers to stage test		Hole preparation	Equipment cost	Performance cost	Operation time	Operation ease	Ease of analysis	Accuracy with depth		Accuracy with permeability range		Geologic sensitivity		Permeability discrimination	
		4	1	Shallow (<150 ft)	Deep (>150 ft)							High $k \geq 10^{-4}$ cm/sec	Low $k < 10^{-4}$ cm/sec	Homogeneous	Stratified	Complex	Vertical	Lateral (Areal)	
Note:		4 is most favorable 1 is least favorable																	
Test method	Above the water table	Falling head test	3	4	4	4/2	4/2	4	1	1	3	1	2	1/2	1	1/4	1		
		Constant head test	4	3	4	3/2	4/2	4	2	2	3	2	3	1/2	1	1/4	1		
		Packer test	4	2	2	2	1	4	4	4	4	4	4	4	4	4	4	1	
	Below the water table	Falling head test	3	4	4	4/2	4/2	4	1	1	3	1	2	1/2	1	1/4	1		
		Rising head test	3	4	4	4/2	4/2	4	1	1	3	1	2	1/2	1	1/4	1		
		Constant head test	4	3	4	3/2	3/2	4	2	2	3	2	3	1/2	1	1/4	1		
		Packer test	4	2	2	2	1	4	4	4	4	4	4	4	4	4	4	1	
		Well pump test equilibrium analysis	1	1	1	1	2	3	4	4	4	2	4	3	3	1	4		
		Well pump test equilibrium analysis	1	1	1	1	2	1	3	3	4	3	4	3	3	1	4		

Fig. 5. Permeability test selection matrix (after O'Rourke, et al³)

report from the contract under which permeability tests were surveyed provides the handiest single reference.²

In a typical application, the bureau recently evaluated a limestone formation for leachability. Without any previous test information, estimates of permeability from fig. 3 range from 10^{-4} to 10^{-8} cm/sec (1 to 10^{-4} darcy). This formation contained both highly fractured zones and those free from extensive fracturing; the entire range of permeability could not be ruled out. Turning to fig. 4, such permeability values suggest the use of variable-head, constant-head, and/or pumping-in tests with packers. Final selection of test method was based on the evaluation matrix contained in fig. 5. Since the formation was above the water table and accurate delineation of vertical differences in permeability was the most important consideration, we eventually ran a series of pumping-in tests using straddle packers. A few constant-head tests were also run to verify the permeabilities obtained. Test procedures and analyses were taken from "recipes" contained in the "cookbook" portion of the contractor's final report. In other situations where cost and ease of operation were more important than extreme accuracy, constant-head and/or variable-head tests have been selected as prime testing methods.

Permeability testing is extremely critical for evaluating formations for potential leachability. An exhaustive survey of available permeability methods used in civil and petroleum disciplines determined that constant-head, variable-head and pumping tests all play an important role in measuring permeability to evaluate formations for leachability. As a result of this survey, a

detailed "cookbook" (Field Permeability Test Methods With Applications to Solution Mining) was generated to describe the permeability test procedures and analysis techniques. This document presents mine operators with all the information necessary for running permeability tests at a reasonable cost. ♦

Peter G. Chamberlain is presently a geophysicist, in situ mining, for the Bureau of Mines Twin Cities Mining Research Center. Since joining the organization 11 years ago, he has served in various positions, including head of the rock mechanics laboratory. He is currently conducting research on leaching deeply buried ore bodies and on improved pre-mine planning for conventional underground mining operations. Chamberlain worked as a field engineer with Schlumberger Well Services prior to joining the Bureau of Mines. He holds a BS degree in geophysical engineering from Michigan Technological University.

References

- Larson, W. C. and D. V. D'Andrea. In Situ Leaching Bibliography. August 1977, unpublished compilation available from the authors at the Bureau of Mines Twin Cities Mining Research Center, Box 1660, Twin Cities, MN 55111.
- O'Rourke, J. E.; J. E. Randall; and B. K. Ranson. "Field Permeability Test Methods with Applications to Solution Mining." Woodward-Clyde Consultants Report 13719A (Final Report on Bu-Mines Contract J0265045), August 1977, 180 pp. Available from National Technical Information Service, Springfield, Va., as report PB 272 452/AS.
- Ahrens, T. P. and A. C. Balow. "Permeability Tests Using Drill Holes and Wells." Bureau of Reclamation Geology Report No. G-97, 1951.
- U.S. Bureau of Reclamation. *Earth Manual*. 1963.
- Todd, D. K. *Ground Water Hydrology*. John Wiley & Sons, Inc., New York, 1959.

Field Permeability Methods for In-Place Leaching

Over the past few years in-place leaching has received increased attention from mine operators producing copper and uranium. Several mining companies have fractured and subsequently leached porphyry copper deposits in the Southwest. Many pilot and several commercial uranium leaching operations have been initiated in Texas and Wyoming. The Bureau of Mines has conducted a variety of research projects on improving leaching technology, and an extensive bibliography on in-place leaching is available.¹

In-place leaching has spawned new conditions for which an ore body must be evaluated to determine its production potential. During its early research efforts, the bureau established the importance of permeability tests. Permeability is a measure of a formation's ability to transmit fluids and is, therefore, directly related to flow characteristics of leaching fluids. For "tight" formations such as the porphyry coppers, permeability measurements determine whether a formation must be blasted to create adequate leaching-fluid flow. For permeable formations such as the sandstone roll-front uranium deposits, permeability helps define a multitude of well field parameters such as well spacing, pumping rates and plant capacity. For all formations, concern over ground water contamination has mandated accurate knowledge of permeability.

Permeability testing techniques have not been familiar to most mining engineers. Although laboratory tests for permeability were routine, bureau researchers likewise had little experience with field permeability measurements. A contract was awarded, therefore, to survey techniques available from civil and petroleum dis-

ciplines to determine which applied to evaluating formation leachability. For the relevant methods, the contractor was further charged with compiling a "cook-book" description of each test—detailed test procedures, analysis techniques and required equipment. The results are summarized in this article, but details can be obtained from the contractor's final report.²

Tests similar to those used on dam projects

Although sophisticated permeability techniques have been developed in the petroleum field, the tests that appeared best suited for use by mining engineers in evaluating leachability were those civil engineers use to investigate rock for dam projects. These tests—constant-head, variable-head and pumping tests—are performed by injecting or withdrawing water from vertical holes drilled into the formation being evaluated. Details on conducting these tests and analyzing results are contained, in total, within the contractor's final report.

In constant-head tests, a constant water pressure or "head" is applied through a well to a fixed interval of the formation. The quantity of water needed to maintain that head is then measured over a given time interval. Analysis of test results to obtain permeability involves straightforward manipulations of the constant-head pressure, flow rate required to maintain that head and dimensional considerations.

Constant-head tests can be conducted with or without packers. If packers are not used, a water-level-indicating device must be monitored to maintain a constant water level in the well. With packer tests, pressure



Fig. 2 Drilling rig

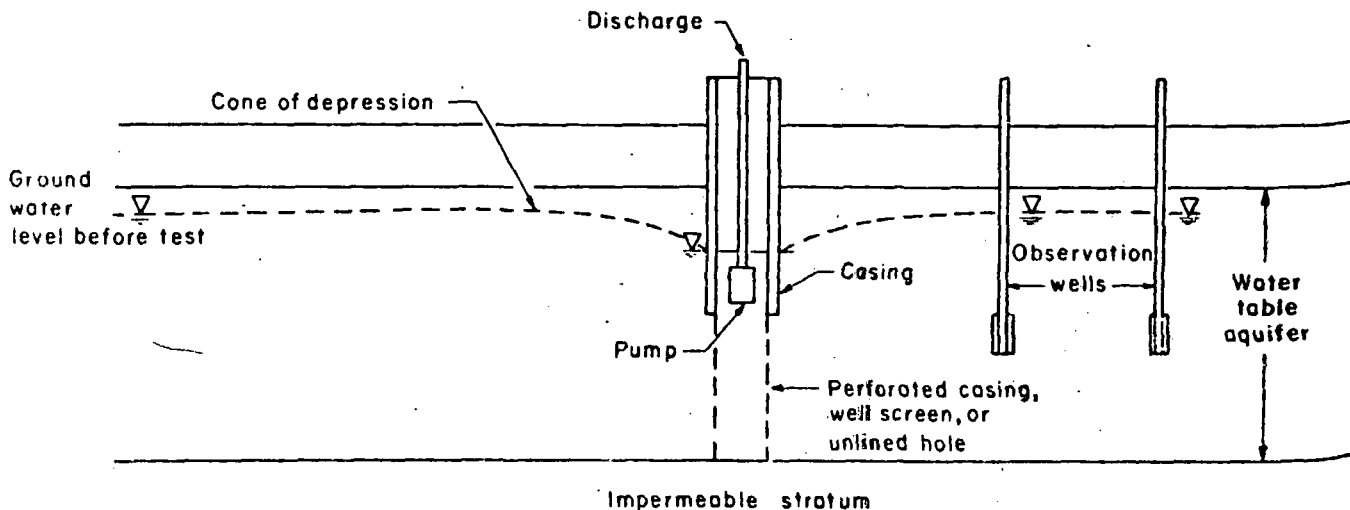


Fig. 1. Basic well pumping terminology²

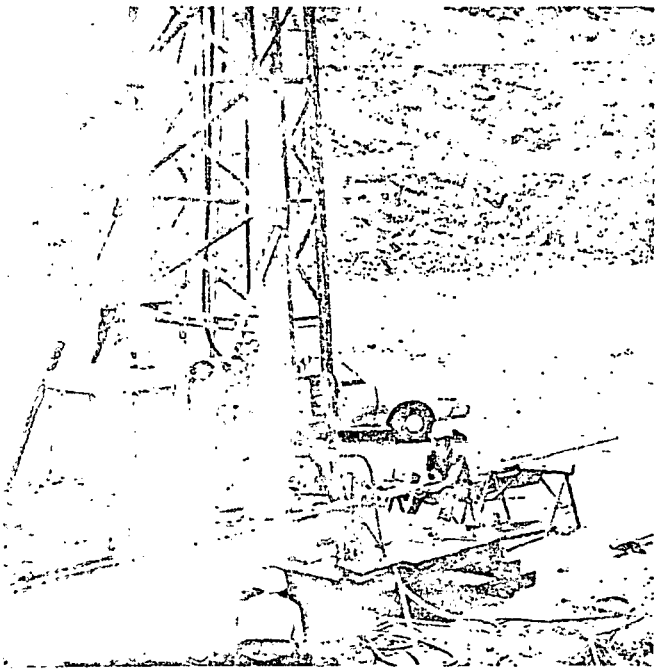


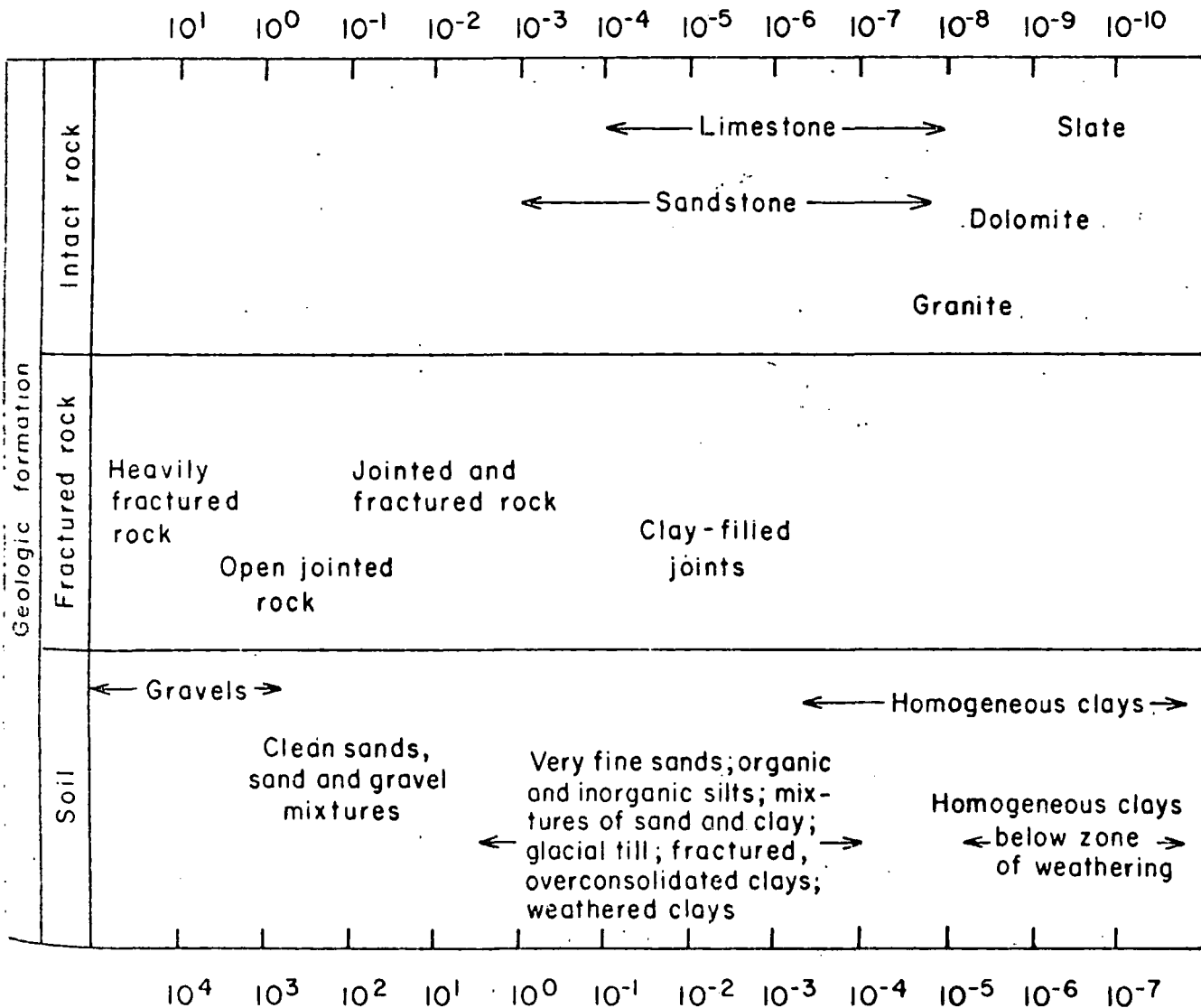
Fig. 2 Drilling rig set up for pumping in permeability tests with packers

gauges or electrical transducers may be used to monitor the constant head of water applied to the test section. The test interval is fixed by the packer spacing. For a single packer, the entire well section below the packer is the test zone; when two packers are hooked in tandem as a "straddle packer," the test zone is the space between them.

Variable-head tests—either falling or rising head—are conducted by adding or withdrawing a "slug" of water from a well and monitoring the rate at which the water returns to its original level. Water can be added by pouring or pumping. Water is generally withdrawn by pumping or bailing, although air pressure can be used if the water volume removed can be accurately measured. While variable-head tests are very simple and cheap to run, analysis of results is empirical and more complicated than it is for constant-head tests. The analysis basically involves comparing plots of the rate of change in the head with "type" curves for known permeabilities.

Where time and economics permit, pumping tests provide the desired measurement. Measurements from pumping tests provide more accurate estimates of the fluid flow conditions during leaching operations than do

PERMEABILITY, cm/sec



other tests. Pumping tests employ two or more observation wells drilled at various distances from a pumping well (fig. 1). As water is withdrawn from the pumping well, the water table is depressed which lowers the water level in the observation wells. The permeability of the formation is computed from the ratio of the water level draw-down to the observation well's distance from the pumping well.

Importance of well preparation often overlooked

The importance of proper well preparation is frequently overlooked by newcomers to permeability testing. It is imperative that the testing wells be drilled with minimal formation contamination to minimize plugging the permeability channels. Matching proper drilling fluids with formation characteristics helps decrease the problem; coring also often damages a formation less than rotary drilling.

After a well has been drilled, fresh water should be circulated until the return water flows clean. Even a well-flushed hole will, however, contain some cuttings; these can be removed by bailing the well. A bailer can be constructed from a section of drill rod fitted with a simple trap valve. Scrubber brushes attached to a drill rod can scrape cuttings from the wellbore wall to facilitate cleaning.

Wells in loosely consolidated formations like some of the uranium sandstones usually must be cased to prevent excessive sloughing. Permeability tests can

then be run through screen sections, through open-hole zones below the casing, or in gravel-packed zones.

Equipment ranges from simple to sophisticated

Depending upon the available budget and desired results, the equipment required to conduct permeability tests can range from a simple water bucket and tape measure to sophisticated instrument packages for documenting test parameters. Once a suitable well has been drilled, essential operations are: (1) adding (or subtracting) water; (2) measuring the added volume of water; (3) measuring the pressure (or head) in the test zone; and (4) measuring time. Water can be added by pouring from a bucket or pumping. Although more sophisticated flow meters are available, water volumes are generally measured with a household water meter. The water pressure or head can be measured with simple electrical water level indicators, piezometers, pressure transducer, or even a tape measure if the water level is near the well collar.

Certain permeability tests require special equipment. Pumping tests require special pumps to lift the water. Packer tests require a drill rig or similar means of raising or lowering the packers (fig. 2). These packers are generally attached to the drill string or galvanized pipes for positioning in the well. Furthermore, packers must be seated with hydraulic pressure (from the drill-rig pump or compressed air (run down a separate line to the packer)). Although inflatable packers constructed from plastic

pipe are becoming popular,² the bureau generally has used oilfield-type packers raised and lowered on the drilling string.

More than one test may be desirable to verify results

A method for selecting appropriate permeability test methods was documented in the contractor's final report.² The first step in the process is to determine the range of permeabilities likely to be encountered in the target ore deposit. If this information cannot be derived from tests on similar deposits, it can be estimated from a chart of probable permeability for the basic rock types (fig. 3). Turning to the techniques that have been used in formations of various permeabilities (fig. 4) one or more techniques can be tentatively selected. Final selection can be made with the assistance of an evaluation matrix (fig. 5) based upon the desired performance characteristics, economics, time frame, etc. It may be desirable to run more than one test to verify results.

After a test method or methods have been selected, several publications are available to serve as "cook books" for running and analyzing the tests.³⁻⁵ We have found that the first

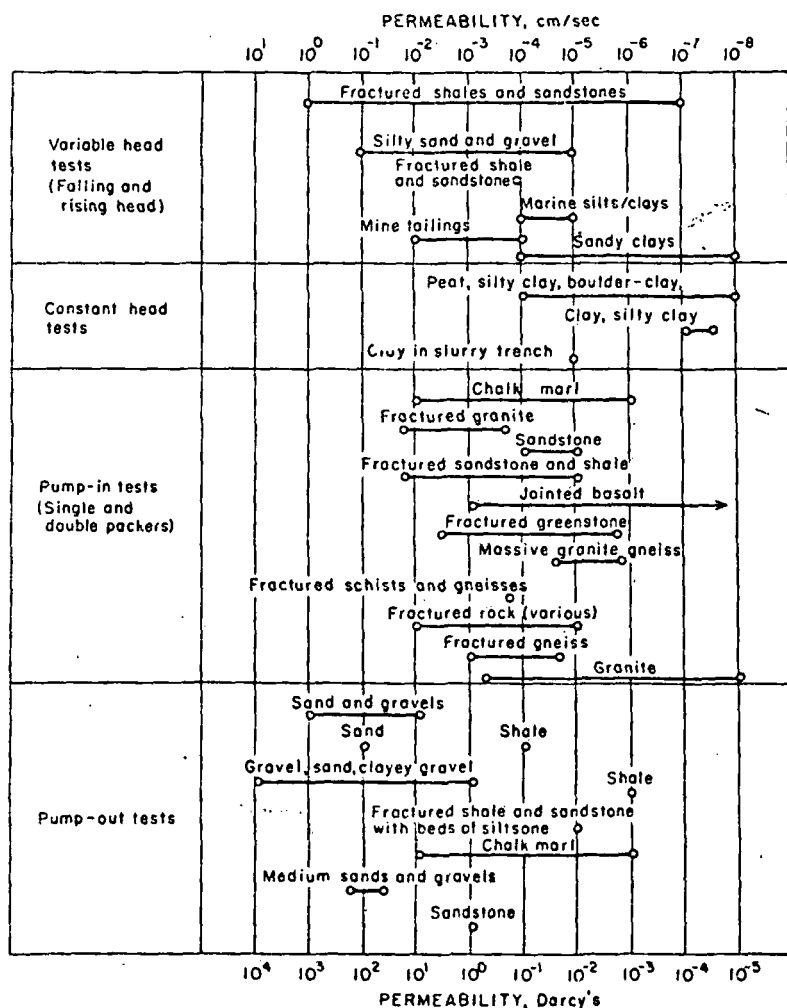


Fig. 4. Reported ranges of field test methods for permeability measurements (after O'Rourke, et al)


Key:  Note: 4 is most favorable 1 is least favorable			Evaluation criteria																	
			Hole preparation	Equipment cost	Performance cost	Operation time	Operation ease	Ease of analysis	Accuracy with depth		Accuracy with permeability range		Geologic sensitivity			Permeability discrimination				
									Shallow (<150 ft)	Deep (>150 ft)	High ($k \geq 10^{-4}$ cm/sec)	Low ($k < 10^{-4}$ cm/sec)	Homogeneous	Stratified	Complex	Vertical	Lateral (Areal)			
Test method	Above the water table	Falling head test	3	4	4	4	2	4	4	1	1	3	1	2	1	2	1	4	1	
		Constant head test	4	3	4	3	2	4	2	2	2	3	2	3	1	2	1	4	1	
		Packer test	4	2	2	2	1	4	4	4	4	4	4	4	4	4	4	4	4	1
	Below the water table	Falling head test	3	4	4	4	2	4	2	4	1	1	3	1	2	1	2	1	4	1
		Rising head test	3	4	4	4	2	4	2	4	1	1	3	1	2	1	2	1	4	1
		Constant head test	4	3	4	3	2	3	2	4	2	2	3	2	3	1	2	1	4	1
		Packer test	4	2	2	2	1	4	4	4	4	4	4	4	4	4	4	4	4	1
		Well pump test equilibrium analysis	1	1	1	1	1	2	3	4	4	4	4	2	4	3	3	1	4	4
		Well pump test equilibrium analysis	1	1	1	1	1	2	1	3	3	4	3	4	4	3	3	1	4	4

Fig. 5. Permeability test selection matrix (after O'Rourke, et al²)

report from the contract under which permeability tests were surveyed provides the handiest single reference.²

In a typical application, the bureau recently evaluated a limestone formation for leachability. Without any previous test information, estimates of permeability from fig. 3 range from 10^{-4} to 10^{-8} cm/sec (1 to 10^{-4} darcy). This formation contained both highly fractured zones and those free from extensive fracturing; the entire range of permeability could not be ruled out. Turning to fig. 4, such permeability values suggest the use of variable-head, constant-head, and/or pumping-in tests with packers. Final selection of test method was based on the evaluation matrix contained in fig. 5. Since the formation was above the water table and accurate delineation of vertical differences in permeability was the most important consideration, we eventually ran a series of pumping-in tests using straddle packers. A few constant-head tests were also run to verify the permeabilities obtained. Test procedures and analyses were taken from "recipes" contained in the "cookbook" portion of the contractor's final report. In other situations where cost and ease of operation were more important than extreme accuracy, constant-head and/or variable-head tests have been selected as prime testing methods.

Permeability testing is extremely critical for evaluating formations for potential leachability. An exhaustive survey of available permeability methods used in civil and petroleum disciplines determined that constant-head, variable-head and pumping tests all play an important role in measuring permeability to evaluate formations for leachability. As a result of this survey, a

detailed "cookbook" (Field Permeability Test Methods With Applications to Solution Mining) was generated to describe the permeability test procedures and analysis techniques. This document presents mine operators with all the information necessary for running permeability tests at a reasonable cost. ♦

Peter G. Chamberlain is presently a geophysicist, in situ mining, for the Bureau of Mines Twin Cities Mining Research Center. Since joining the organization 11 years ago, he has served in various positions, including head of the rock mechanics laboratory. He is currently conducting research on leaching deeply buried ore bodies and on improved pre-mine planning for conventional underground mining operations. Chamberlain worked as a field engineer with Schlumberger Well Services prior to joining the Bureau of Mines. He holds a BS degree in geophysical engineering from Michigan Technological University.

References

- Larson, W. C. and D. V. D'Andrea. In Situ Leaching Bibliography. August 1977, unpublished compilation available from the authors at the Bureau of Mines Twin Cities Mining Research Center, Box 1660, Twin Cities, MN 55111.
- O'Rourke, J. E.; J. E. Randall; and B. K. Ranson. "Field Permeability Test Methods with Applications to Solution Mining." Woodward-Clyde Consultants Report 13719A (Final Report on Bu-Mines Contract J0265045), August 1977, 180 pp. Available from National Technical Information Service, Springfield, Va., as report PB 272 452/AS.
- Ahrens, T. P. and A. C. Balow. "Permeability Tests Using Drill Holes and Wells." Bureau of Reclamation Geology Report No. G-97, 1951.
- U.S. Bureau of Reclamation. *Earth Manual*. 1963.
- Fodd, D. K. *Ground Water Hydrology*. John Wiley & Sons, Inc., New York, 1959.

NK, 1975

FEATURES OF SILVER SORPTION FROM CYANIDE SOLUTIONS AND PULPS

UDC 622.342.2:66.074.7

A. A. Punishko, V. E. Dement'ev, and E. I. Broner

A filterless sorption technology is one of the more effective ways of improving the classic cyanide process widely used in the metallurgy of the precious metals; such a technology has been successfully adopted at certain gold extraction plants in the country and has been accepted for implementation at a number of others.

In introducing sorption schemes for ores with a non-industrial Ag content, proper attention has not been given to conditions for extraction of silver (as a by-product, with gold).

Analysis of the available information on the application of sorption processes to gold-silver ores and concentrates showed that up to the present ion exchange technology for silver extraction has not been used in industrial practice.

A study was made in [1] of the behavior of silver during its sorption from artificial and industrial cyanide solutions by the high-basidity AM anion exchanger and the low-basidity AN-18 exchanger.

The investigations showed that silver was extracted more actively than gold in the first stage of the process, then passed into solution again, giving way to gold and zinc in the ion exchanger phase. This indicates the inevitability of a high level of silver losses with the waste pulp

liquid phase in the combined extraction of precious metals in a continuous counter-current process.

Investigations seeking an anionic exchanger of high capacity and selectivity relative to gold and silver showed that none of the sorbent studied could be recommended as a universal agent for the collective extraction of gold and silver.

Thirty samples of ion-exchange resin of various types and structures were tested, based on chloromethylated copolymers (KhMS) of styrene (St.) with divinylbenzene (DVB), aminated with aqueous or organic solutions of various aliphatic tertiary diamines, cyclic triamine, and pyridine-substituted amines, and also using pyridine, isoquinoline, and picoline bases, triphenylphosphines, and other compounds to produce functional groups.

The resins were saturated in artificial cyanide solutions with equal molar contents of constituents and in industrial solutions obtained by cyaniding ores from a number of gold-silver deposits.

The results of a series of selection and control experiments to find the most active sorbents for extraction of silver in the presence of gold and associated impurity metals showed that the material composition of the solutions and pulps treated with the resins had a significant effect on the efficiency of precious metal sorption by the various types of ion exchanger.

It follows from the data in Table 1 that the anion exchangers AV γ -12P (based on

Table 1
Capacity of Anion Exchangers for Silver
in Saturation in Artificial Cyanide Solutions

Anion exchanger	Resin content, mg/g						
	Ag	Ag+Au	Ag+Cu	Ag+Zn	Ag+Fe	Ag+Co	Ag+Ni
AP-6X12P	—	14,6	17,9	17,1	20,7	12,1	20,0
AP-24X12P	53,4	14,6	12,5	7,8	15,7	12,2	9,0
AS-62X12P	57,0	12,6	12,5	8,7	17,0	14,4	8,7
AV γ -12P	130,3	16,0	17,2	18,75	14,9	17,3	18,3
AV γ -12P Sp. 14	31,8	2,7	8,4	0,68	6,3	4,6	4,6
AV γ -12P Sp. 14	62,5	11,5	13,3	11,5	18,3	15,6	11,6
ANS-21a	—	4,8	11,5	2,7	12,6	12,1	11,7
33T	50,0	6,5	9,6	5,3	13,0	9,3	8,2
AM-2B	90,0	15,3	17,9	12,1	18,5	11,2	18,1

Note: Resins which had shown the best precious metal extraction figures in the selection experiments were tested.

Table 2
Capacity of Anion Exchangers for Precious
and Associated Metals in Saturation in
Complex Artificial Cyanide Solution

Anion exchanger	Resin content, mg/g								
	Ag	Au	Cu	Zn	Fe	Co	Ni	Σ pre- cious Me	Σ Me- impur- ities
AP-6X12P	2,55	51,7	1,0	15,2	3,7	5,4	7,0	54,25	32,3
AP-24X12P	3,10	50,7	1,0	11,0	3,6	4,4	4,2	53,8	24,2
AP-62X12P	2,61	48,5	—	13,7	5,0	2,7	5,3	51,11	26,7
AV γ -12P	12,20	97,0	7,0	10,5	6,0	5,0	11,0	109,2	39,5
AV γ -12P Sp. 14	4,0	27,0	—	4,4	5,2	1,8	4,0	31,0	15,4
AV γ -12P Sp. 14	2,30	40,0	0,6	5,0	1,7	1,0	3,1	42,3	11,4
33T	7,30	36,0	5,0	11,8	5,0	0,6	11,0	43,3	33,4
33T	6,20	40,3	—	3,4	—	0,6	4,0	46,5	8,0
AM-2B	3,06	50,0	1,0	24,8	3,6	4,7	6,6	53,06	40,7

KhMS, St., DVB, and γ -picolines) and AM-2B* (KhMS, St., DVB, and a mixture of di- and trimethylamine) had the highest capacity for Ag when the resins were saturated in an artificial cyanide solution containing only Ag (with an equal constituent molar content of 10^{-4} mole/liter).

The lowest capacity for Ag under equal conditions was recorded for the anion exchangers AVF-12P (KhMS, St., DVB, and isoquinoline) and ANS-21a (KhMS, St., DVB, and aliphatic amine).

The capacity of all the sorbents for silver falls sharply in the presence of any of the possible associated metals.

A particular associated constituent affects Ag extraction in varying degrees in each specific case. Thus in the case of anion exchangers AM-2B and AP-8 x 12P (KhMS,

Table 3
Results of Resin Saturation in Industrial Solutions

Sorbent grade	Resin content, mg/g											
	Solution 1 (ore x ₁)				Solution 2 (ore x ₂)				Solution 3 (ore x ₃)			
	Ag	Au	Pre-cious Me	Impur-ities	Ag	Au	Pre-cious Me	Impur-ities	Ag	Au	Pre-cious Me	Impur-ities
AP-8X12P	21,6	1,6	23,2	37,3	66,0	2,13	68,13	29,2	11,5	29,46	40,96	48,3
AP-24X12P	23,1	2,6	25,7	30,2	58,1	2,75	60,85	35,4	9,57	34,46	44,03	21,4
AP-82X12P	18,6	2,0	20,6	40,9	49,0	2,3	51,3	17,8	7,59	25,28	32,87	35,7
AVF-12P	14,2	0,2	15,1	76,7	97,47	1,81	99,28	44,6	9,43	17,05	26,49	86,7
AVF-12P	17,8	0,96	18,76	57,3	58,82	1,45	50,27	29,4	6,38	15,31	21,39	20,3
Op. 14	14,2	2,0	16,2	25,1	65,21	2,13	67,34	18,6	8,16	31,45	39,61	38,2
23T	24,0	1,32	25,32	14,9	89,2	1,6	90,8	24,3	14,41	29,17	43,58	14,0
252	23,2	1,07	24,27	20,3	51,54	1,43	52,97	10,4	14,0	18,94	32,94	17,8
AM-2B	23,7	1,7	27,4	44,0	78,4	2,37	80,77	26,8	10,46	28,1	38,56	41,2

Note: Solution 1 contained, in mg/l: 663 Ag, 3.38 Au, 452 Cu, 24.4 Zn, 70 Fe, traces of Co, and 0.67 Ni. Solution 2 contained, in mg/l: 75 Ag, 1.98 Au, 13.35 Zn, 6.5 Cu, 19.5 Fe, and 0.4 Ni. Solution 3 contained, in mg/l: 146 Ag, 18.9 Au, 44.5 Zn, 17.8 Cu, 6.6 Fe, and 0.01 Co

capacity for silver in anion exchanger AV γ -12P, then in 23T (KhMS, St., DVB, and α -aminopyridine) and 252 (KhMS, St., DVB, triacetylamine and dimethylamine).

The anion exchangers tested can be placed in the following series according to their total precious metals capacity:

AV γ -12P > AP-8X12P > AP-24X12P
AM-2B > AV-82X12P > 252 > 23T > op. 14 > AVF-12P

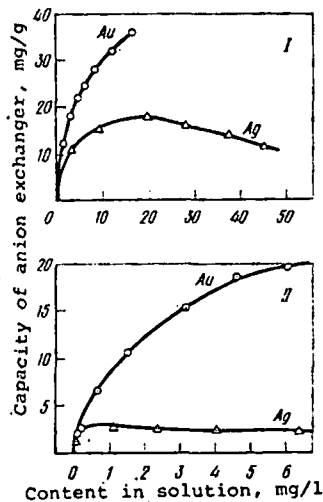


Fig. 1. Isotherms of gold and silver sorption by AM-2B anion exchanger from industrial cyanide solutions of the following composition, mg/liter:

	Au	Ag	Cu	Fe	Zn	Ni	Co
I	20.0	52.0	7.00	0.91	4.20	0.63	0.06
II	7.20	6.60	30.5	0.92	3.23	0.22	0.03

*Anion exchanger AM-2B is used in practice industrially for gold extraction from cyanide pulps.

St., DVB, and cyclic tertiary triamine) the principal depressants in Ag sorption are Co followed by Au and Zn; for op-14 resin (KhMS, St., DVB, and triphenylphosphine) Au, Zn, and Ni act as depressants in equal measure; for AP24 x 12P (KhMS, St., DVB, and tetrabutyl methylene diamine) and AN-82 x 12P (KhMS, St., DVB, and hexamethylmethylen) the depressants are Zn and Ni followed by Cu and Au.

As before, the results of resin saturation tests in artificial cyanide solutions of complex composition with equal molar contents of precious and associated metals (Table 2) revealed highest

On transition to industrial cyanide solutions produced by processing gold-silver ores from certain deposits in the North-East of the Soviet Union and in Central Asia of various industrial types, the activity series for the sorbents according to cyanide solution material composition are rearranged.

For example, the same anion exchangers are arranged as follows according to degree of previous metal sorption when there is a considerable amount of Ag and impurity metals (Cu, Zn, Fe) and an ordinary concentration of gold in the liquid phase of pulps (solution 1) from processing ore x₁ (Table 3):

AM-2B > AP-24X12P and 23T > 252 > AP-8X12P > AN-82X12P > AVF-12P > op. 14 > AV γ -12P

However, resins 23T, AP-24 x 12P, and 252 sorb much less impurity metals than AM-2B, although the difference in their capacity for precious metals is small. In spite of the high concentration of copper in cyanide solution 1, the major

Fig
ch
in
Ta
me

imp
por
D
sil
cya
exc

T
rig
F
fav
in
T
als
the
[2-
T
sel
aff
tes

He
co

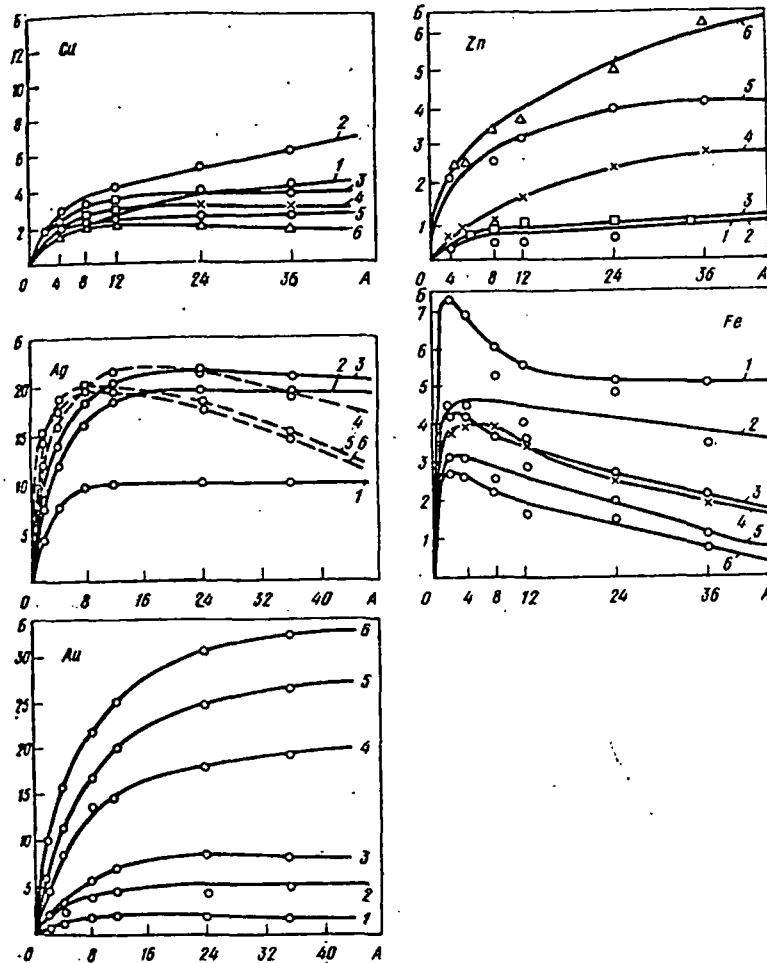


Fig. 2. Kinetics of saturation of AM-2B anion exchanger with gold, silver, and associated metals in industrial solutions (composition given in Table 4). A axis: saturation time, hr; B axis: metal capacity of exchanger, mg/g.

important, but their interrelationship, the nature of their interaction, and the proportion of most active depressant (primarily zinc).

Data on saturation of ion exchangers in cyanide solutions and pulps show that silver-cyanide complexes have less affinity for anion exchanger active groups than cyanide complexes of gold and of certain other metals. The affinity series for anion exchanger AM-2B, which has been taken up by industry, is as follows:



The metals to the left of the affinity series suppress sorption of metals to the right.

For this reason the metal concentration ratio in saturated resin is usually in favor of metals which stand first in the affinity series, compared with their ratio in the initial cyanide solutions.

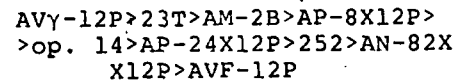
The unsatisfactory affinity of anion exchangers for silver (as well as copper) may also be connected with the possibility that various forms of cyanide complexes of these metals with an anion charge variable from 1 to 3 exist in cyanide solutions [2-4].

The possibility cannot be excluded that a fundamentally new approach is required in selecting an effective sorbent for silver: to attempt to utilize the high degree of affinity of Ag and S, in connection with which it seems desirable to synthesize and test sorbents with thiol and thion groups.

¹Here and subsequently, selectivity means the ratio of the amount of sorbed valuable constituents to the total monitored impurity metals.

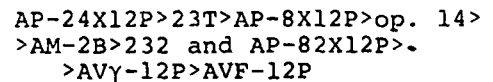
share of the total impurity metals sorbed by all the ion exchangers is attributable to zinc.

The affinity series relative to precious metals assumes a different appearance with a reduction in the concentration of Ag and impurity metals, as is the case in the liquid phase of pulps from processing ore X₂ (solution 2, Table 3):



In these circumstances anion exchanger AV γ -12P sorbs much more of the impurities than AM-2B, but resin 23T is the most selective.¹

With an increase in the Au : Ag ratio (solution 3 from processing ore X₃) and an appreciable impurity metal content, we have the following sequence in terms of sorbed precious metals:



Here anion exchangers 23T and AP-24 x 12P show relatively high selectivity.

It should be noted that efficiency in the extraction of silver and gold by practically all the anion exchangers, irrespective of their makeup and structure, depends on the extent of the effect of associated metals and impurities. Here it is not only the total amount of impurities that is

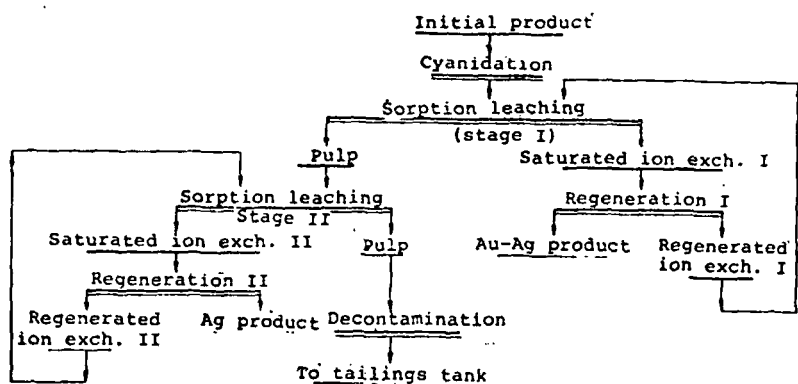


Fig. 3. Flowchart for two-stage sorption extraction of gold and silver.

will be low because complex Au, Ni, and Zn anions are sorbed more actively than silver. Excess ion exchanger also leads to an appreciable reduction in effective capacity for Au (Figs. 1 and 2).

The nature of the sorption isotherms (plotted by using variable weighed amounts) indicates considerable depression of silver sorption by gold, especially in the

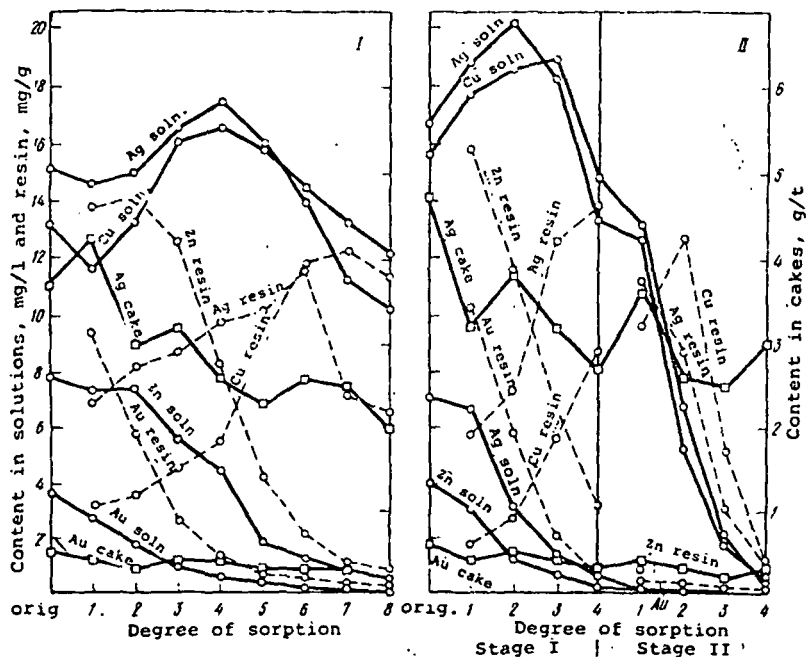


Fig. 4. Distribution of gold, silver, and non-ferrous metals in products in single-stage (I) and two-stage (II) systems.

would increase substantially if sorption extraction of precious metals from cyanide media were conducted in two stages rather than in one, because removal from the pulp liquid phase of the most selectively adsorbed ions (Au, Zn, Ni) with the stage I resin would help to increase the capacity of the sorbent for silver in sorption stage II, with maximum extraction of silver from the solutions (Fig. 3).

This version was evaluated in enlarged laboratory tests using solutions obtained from leaching the ore from one of the deposits in the North East, and also on pilot-plant scale when testing flowsheets for gold-silver ore processing.

The enlarged studies of the solutions in a multichamber countercurrent sorption apparatus showed that a two-stage sorption process was possible in principle. It is

Since silver is far from gold in the affinity series for known anion exchangers, a continuous countercurrent sorption process under conditions of maximum resin saturation with gold must inevitably lead to the loss of the metals which complete the affinity series with the waste solutions (pulp). It is important to take this factor into account when processing gold-silver ores.

The flow of sorbent must be substantially increased in order to prevent losses of silver; in this case, however, the capacity of the resin in terms of silver

tractive advantage 1. The substance along with 2. The cycle is lower on exchange 3. The and II; resins; The so basis of 1. A. A info 2. J. H 970. 3. R. A. 4. J. S. 72, N

The phenomenon of mutual displacement of metals in the process of sorption can also be traced by plotting kinetic curves (Fig. 2); composition of the initial solutions is given in Table 4.

It follows from the Fig. 2 data that collective sorption of all metals takes place mainly in the first two hours (the "film" kinetics stage); further saturation of the resin with gold and zinc is predominantly due to displacement of complex Fe, Cu, and Ag cyanide anions with less affinity for the anion exchanger (the "gel" kinetics stage).

The results of the investigations led to the assumption that process efficiency

possibl
small
in the

Comp
So
Dete
Resin

Curve
no. on
Fig. 2

1
2
3
4
5
6

tractiv
vantage

1. Th

subst

along w

2. Th

cycle i

lower o

exchang

3. Th

and II

resins;

The so

basis of

1. A. A

info

2. J. H

970.

3. R. A.

4. J. S.

72, N

possible to produce resins with sufficient precious metal saturation even with a small number of substages (four in each stage). Selection of impurities takes place in these circumstances: the nickel and zinc concentrate predominantly in the stage I resin, the iron and copper in the stage II resin, which will make it possible to simplify the ion exchanger regeneration system.

Table 4
Composition of Cyanide Solutions Used to Determine Kinetics of Resin Saturation, mg/liter

Curve no. on Fig. 2	Au	Ag	Cu	Zn	Fe	Ni
1	0,2	6,1	2,5	0,1	60,0	0,11
2	1,0	18,0	7,5	0,22	72,0	0,33
3	2,0	28,0	9,0	0,75	75,0	0,57
4	5,2	34,0	10,2	1,50	64,0	0,95
5	10,0	43,0	11,8	3,37	71,0	1,85
6	14,0	48,0	12,6	4,30	75,0	2,25

Subsequent checking of the efficiency of a two-stage system to extract gold and silver from pulps in a continuous countercurrent sorption process in pilot plant tests at the Balei experimental plant confirmed its value.

The nature of precious metal and non-ferrous metal distribution over the substages of sorption extraction of silver and gold in a single-stage process (producing resin with maximum gold saturation) and a two-stage process is shown in Fig. 4.

CONCLUSIONS

The proposed system of two-stage precious metal extraction from gold- and silver-bearing material was found to have the following advantages.

1. The capacity of saturated resin in stage I for Au and in stage II for Ag is substantially higher than in single-stage sorption with complete extraction of silver along with gold.

2. The total flow of sorbent in the metal sorption - saturated resin regeneration cycle is less with a two-stage scheme than with a single-stage scheme, resulting in lower operating costs in the regeneration unit and reduced mechanical losses of ion exchanger.

3. The selective adsorption of impurity metals on the resins in sorption stages I and II makes it possible to use a simplified regeneration system for the saturated resins; this also has a beneficial effect on the economics of the sorption technology.

The scheme for two-stage ion-exchange extraction of precious metals has formed the basis of the design of an enterprise now under construction.

REFERENCES

1. A. A. Punishko and O. A. Shubina. Tsvetnaya Metallurgiya (Byull. In-ta Tsvetmet-informatsiya), 1969, No. 14, pp. 49-50.
2. J. H. Jones and R. A. Penneman. J. Chem. Phys., 1954, vol. 22, No. 6, pp. 965-970.
3. R. A. Penneman and J. H. Jones. J. Chem. Phys., 1956, vol. 24, No. 2, pp. 293-298.
4. J. S. Coleman, K. George, L. Allaman, and L. H. Jones. J. Phys. Chem., 1968, vol. 72, No. 7, pp. 2605-2610.

The Geology of Boulby Mine

P. J. E. WOODS

Abstract

Boulby mine is the first full-scale exploitation of the Zechstein Potash deposits in northeastern England. A large-enough area of the potash and adjacent beds has now been exposed in the mine to provide extensive evidence of both brine-controlled mineral migration and gravity-induced plastic flow of the potash bed. The underlying halite is much less affected. The deformation of the potash bed, together with its high temperature and gas content, leads to a number of mining problems, but the high grade of the ore and its simple mineralogy make processing straightforward.

Introduction

CLEVELAND Potash Limited's Boulby mine is situated on the southeastern boundary of Cleveland County in northeastern England, formerly part of North Yorkshire (Fig. 1). Details of the history of the discovery and exploration of this portion of the United Kingdom's potash field are contained in an earlier paper (Woods, 1973), together with the stratigraphic sequence encountered in the shafts' pilot borehole, drilled in 1968. While there has been no previous exploitation of these deposits, apart from some solution mining experiments, many boreholes have been drilled for mining feasibility studies and much detailed laboratory work done on the cores obtained, e.g., Stewart (1965), Armstrong et al. (1951), and Dunham (1947).

Since the completion of the first of two shafts in 1973 (Cleasby et al., 1975), development and production mining have exposed the Boulby Potash and adjacent beds over an area 2.0×1.5 km (1.5×1.0 miles). A new technique has been developed for drilling near-horizontal directionally controlled boreholes up to 1,000 m beyond the present mining limits (Fig. 2), providing much more information on the variations in the potash orebody and incidentally also on the underlying halite and anhydrite beds.

The drilling method utilizes the reverse circulation, continuous coring technique which is commonplace in the potash mines in Germany. Directional control is achieved at Boulby by varying stabilizer spacing, bit pressure, and speed of rotation. Continuous core recovery ensures that the base of potash intersection is noted almost immediately so that accurate depth and survey checks can be made. Special blow-out preventers are used in case high-pressure gas pockets are encountered.

In terms of the potash field as a whole the mined area is very small. However, what has been observed of the nature of the postdepositional alteration must apply, to a greater or lesser degree, to the Boulby Potash beds throughout northeastern England.

Much remains to be done in terms of more detailed research at the Boulby mine. Most of the early work on which this paper is based involved the application of geological observations of potash seam behavior to mining control problems. Presently, however, various lines of research are being pursued, both academic and applied, with a view to assisting mine planning and operation, and the results will be published in future papers.

Stratigraphic Sequence in Boulby Mine Type Section

The nomenclature and a general description of the individual members of the Zechstein 3 and 4 evaporite cycles of northeastern England have been given by Smith and Crosby (1978) in a companion paper. Table 1 lists again the formations in the Staintondale and Teesside Groups of the upper Permian at the Boulby mine. This paper is primarily concerned with the potash bed at the top of the Boulby Halite which is currently being exploited, as well as exposures in the mine of the adjacent beds which provide abundant information relevant to the history of the orebody itself.

During the sinking of the shafts through the evaporites it was possible to observe a much larger exposure of each bed than had been possible from surface drilling. Figure 3 shows the type sequence in the shafts from the middle of the Upper Halite down to the Billingham Main Anhydrite. Each formation is treated individually below. The term type sequence is used here for want of a better one, even though the same sequence was intersected and reported in the shafts' pilot hole (Woods, 1973). The original sedimentary order is well preserved, but there is much evidence for both upward and lateral migration of the more mobile salts.

The Upper Anhydrite is a well-bedded, very fine-grained, pale gray anhydrite bed containing lenses of sylvite. Halite pseudomorphs after gypsum occur at distinct horizons. Some of these pseudomorphs are

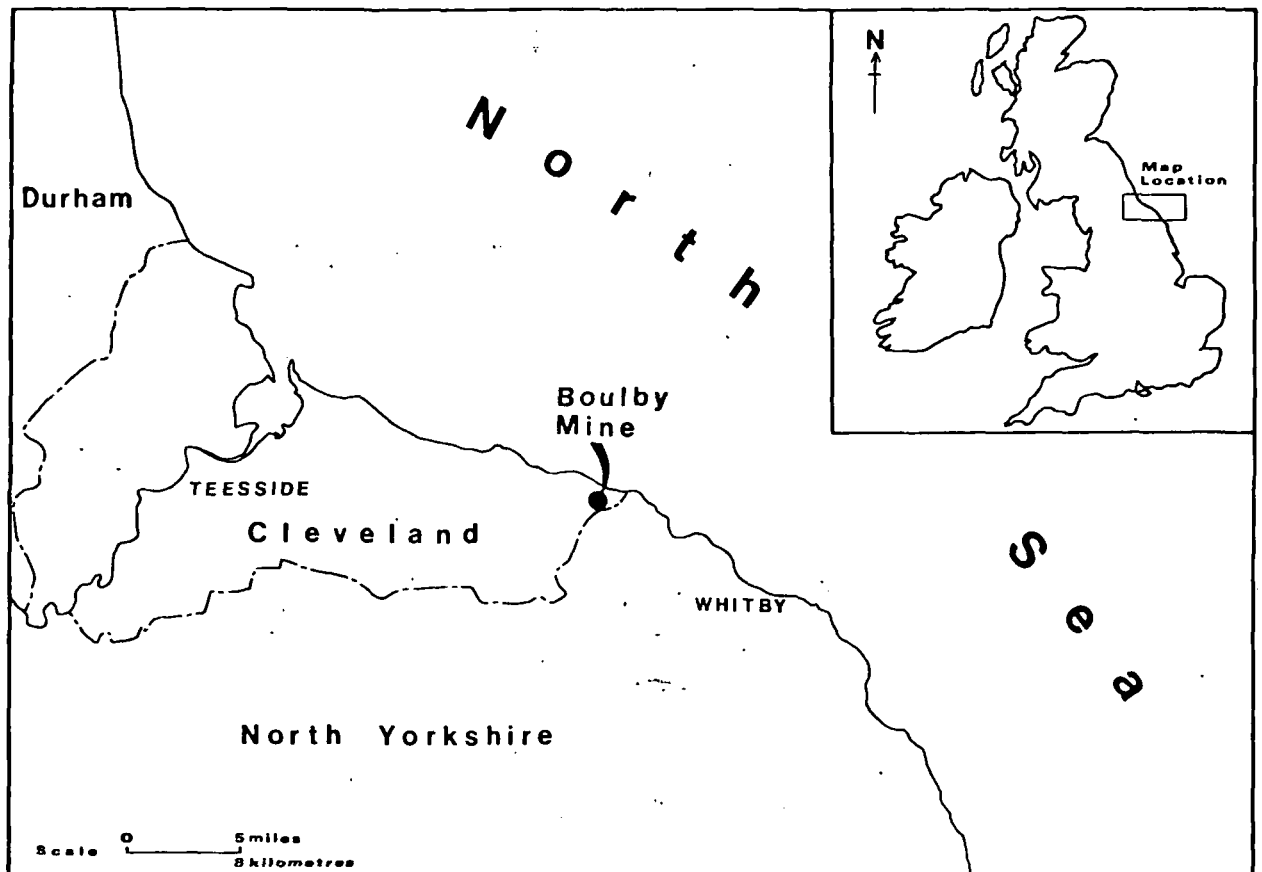


FIG. 1. Location map.

red sylvinitic where they occur near to the sylvinitic lenses mentioned previously. What was particularly noticeable in the shafts was the undulation of the Upper Anhydrite as a whole with quite steep dips at the top and base (up to 15°). Deformation was apparently plastic, there being no tension cracks or joints in the rock. The basal 4 to 5 m of the overlying Upper Halite forms a very sharp contact with the anhydrite. This rock is distinctly gneissose in texture, with marked crystal elongation parallel to the contact, suggesting flow to compensate for the

buckling of the anhydrite. (No further exposures of the Upper Anhydrite have been made since the shafts were sunk, although upward drilling from mine roadways is planned.) The basal 1 to 2 m of the Upper Anhydrite are markedly more argillaceous.

The Uppang Formation, which forms the basal bed of the Staintondale evaporite cycle, is a distinctly laminated, dark gray, dolomitic shale, with a gradational upper boundary but a sharp contact with the underlying Carnallitic Marl.

The Carnallitic Marl (sometimes locally known as

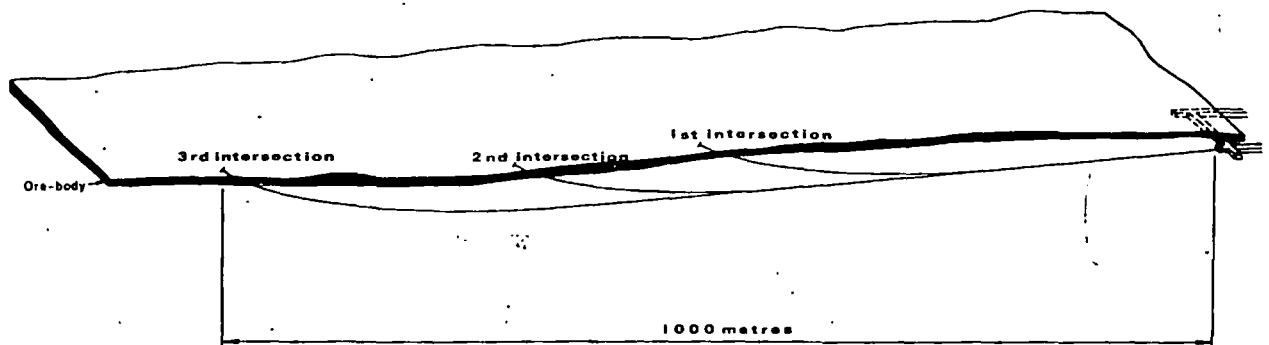


FIG. 2. Long hole drilling.

the Rotten Marl), reddish brown in color, is composed for the most part of dehydrated clay minerals, together with up to 60 percent halite locally. The latter occurs in halite/sylvinite veins and as distinct pods and crystals in the clay itself. The mineral carnallite is rarely found in the Boulby area although present in boreholes to the south. The Carnallitic Marl is a very weak rock, there being no physical bonding between the halite crystals and no significant cementing mineral to bind the clay. Local harder bands contain some polyhalite. There is virtually no carbonate in this rock, which makes the term "marl" something of a misnomer—"salt-clay" would perhaps be more correct. The formation is further weakened by numerous steeply dipping discontinuities with polished interfaces, obviously caused by differential movement within this bed. Many of the fibrous halite/sylvite veins also have polished interfaces between salts and wall rock suggesting formation after compaction of the clay. The transition from the marl to the underlying beds shows a color change from red brown to gray, some interbanding, and a downward increase of coarse displacive halite (cf. Smith, 1971) with some intercrystalline anhydrite and very dark gray clay. Many of the veins in the marl above

Table 1. Stratigraphy of English Zechstein (EZ) Cycles 3 and 4

Series	Group	Formation	Cycle*
Upper Permian	Staintondale group	Upper Halite Upper Anhydrite Uppang Formation	EZ4
	Teesside group	Carnallitic (Rotten) Marl (Boulby Potash) Boulby Halite Billingham Main Anhydrite Upper Magnesian Limestone	EZ3

* After D. B. Smith.

pinch out in this zone, with no obvious connection with the sylvinite below.

The sylvinite bed itself (the Boulby Potash) closely resembles a metamorphic gneiss, both in terms of crystal fabric and the fact that it contains many rounded fragments of rock from adjacent beds. The basal contact is sharp and generally fairly planar. The upper contact is very undulating but again fairly sharp against the overlying halite-enriched anhydritic

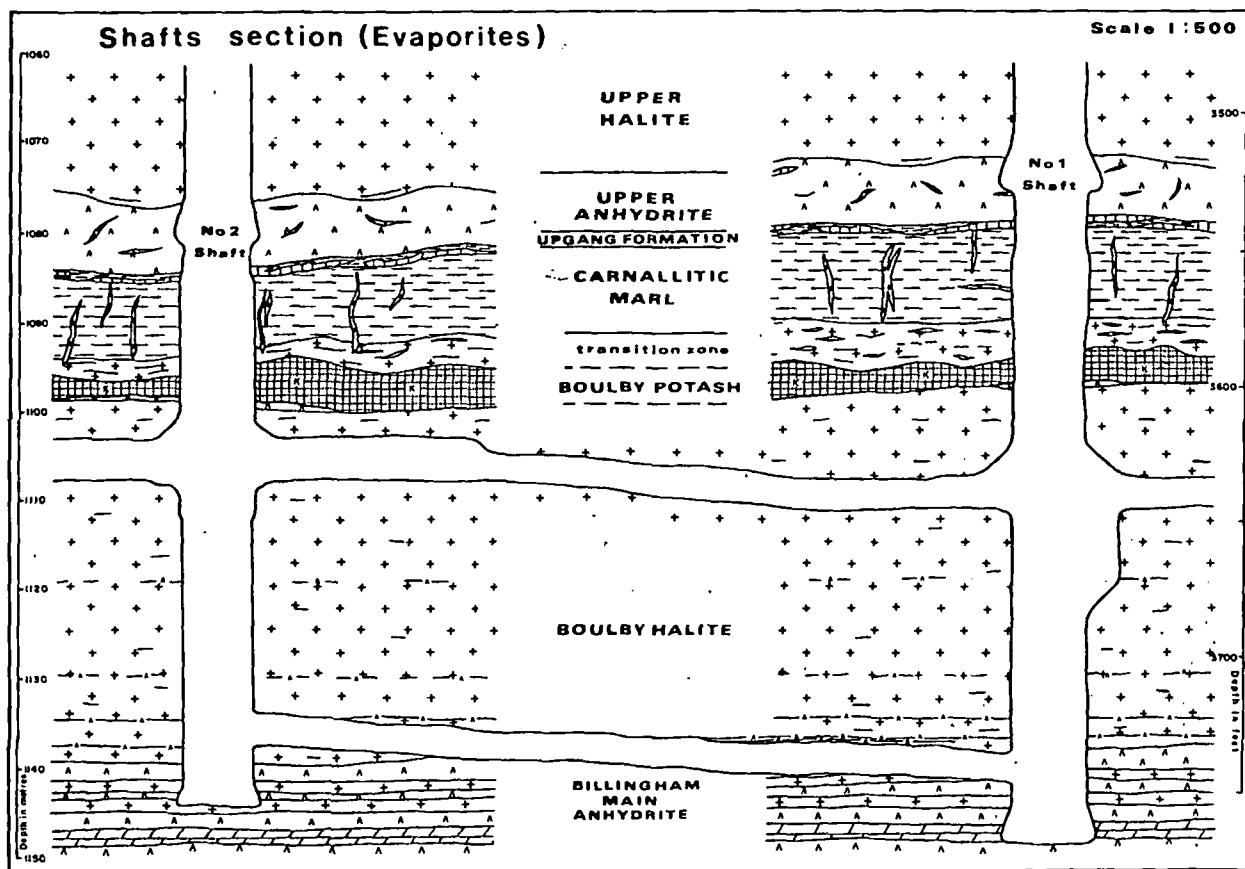


FIG. 3. Shafts section (evaporites). See text for description of each formation. K = sylvinite.

transition zone. The color of the Boulby Potash varies from grayish pink to orange and can be quite red toward the upper and lower contacts, owing to hematite platelets both in the crystals of sylvite and even at times in the halite (showing that there must have been replacement of sylvite by the halite). The potash has a banded appearance, although the bands are not necessarily parallel to the top or base of the bed, suggesting flow lineation rather than bedding. Within the first shaft excavation the thickness varied from 2.5 to 5 m.

Below the potash the Boulby Halite, by comparison, is remarkably undisturbed except over fault zones in the anhydrite and dolomite below (Fig. 6), the original clay partings being well preserved and with virtually no elongation of the individual crystals. The upper 3 to 4 m of the Boulby Halite is generally brownish gray, locally speckled with small red sylvite crystals, and with the halite crystals increasing in size downward. The topmost 10 to 50 cm of this bed is markedly more anhydritic than the halite immediately below with some thin stringers of fibrous halite in places. A fairly sharp contact separates the brownish halite above from a 1 to 2-m bed of very pure orange-pink halite which provides a distinct marker band throughout the mine. It rarely contains any traces of sylvite. Below this unit is coarse orange-brown halite with interstitial gray clay forming up to 10 percent of the rock. In one of the shafts columnar structures were observed 1 m in diameter and up to 2 m in depth, having the appearance of dessication cracks. The cracks are dark gray argillaceous halite and the hexagonal columns are pale orange-brown halite. Several clay partings are well preserved in this interval, indicating that there has been little alteration of the original halite rock. The Boulby Halite becomes increasingly anhydritic downward, first as minor partings and increasing intercrystalline material. Then about 15 m from the top, distinct 1- to 10-cm-thick anhydrite beds are present which become more numerous toward the contact with the Billingham Main Anhydrite.

Variations in the Boulby Potash

As soon as the mine roadways away from the shafts (begun in halite below the seam for stability reasons) entered the potash seam, it was possible to begin mapping and recording the variations in the potash bed and this has become routine ever since. As exposed in the shafts, and elsewhere in the mine, the base of the Boulby Potash is relatively even. The upper boundary is very undulating, with the overall seam thickness varying from less than a meter to as much as 20 m over horizontal distances of 20 to 30 m. Five distinct ore types have been encountered so far. Though they pass fairly rapidly from one to the next,

each type may predominate in an area up to a maximum of a kilometer across. The diagenesis of the Boulby Potash, discussed in more detail later, has obliterated the majority of the original sedimentary characteristics of the seam. Thus there are no clay partings in the bed, no small-scale erosional structures, and, most relevant to mining control, no consistent marker bands apart from the base of the seam itself. The five ore types (A-E) are shown diagrammatically in Figure 4 and are described individually, although there is usually a lateral transition from one to the next over some tens of meters.

Type A

This is the ore type encountered in the shafts' type section and already described in appearance. Its main constituent minerals are sylvite and halite with minor clay and anhydrite and trace magnesite, pyrite, and quartz. The contained xenoliths of other rock types are not included in this list; they generally constitute less than 5 percent of the rock.

The sylvite in this type imparts most of the gneiss-like texture to the rock, being elongated in a ratio as high as 3 to 1 in a generally near-horizontal orientation. The dominant color is seldom particularly red or white, except near the top and bottom of the bed where the sylvite is often coarser (5-20 mm) and more granular in appearance with both red and white crystals present.

The halite in the ore occurs in two main forms. The first contains a high percentage of anhydrite and clay; the second is pure and occurs both as distinct crystals and as secondary growths on the first, apparently earlier, variety. In the main the halite crystals are not so obviously elongated as the sylvite.

In places lenses or rafts of the more shaly portion of type C are found in the upper part of type A.

Type B

Type B ore is really a structural variation of type A but with the undulations having proceeded a stage further into a series of overlapping recumbent folds and even nappes. Some of the overlying argillaceous transition zone and locally the Carnallitic Marl have been ingested into the potash ore as far as the base of the whole seam. Similarly the underlying halite is occasionally incorporated into the overfolding. The resulting pile may be as much as 20 m thick. A remarkable feature of this type is the very much higher ore grade (often in excess of 50 percent KCl) which has resulted from the differential flow characteristics of the individual component minerals. It is an established fact that under high differential stress sylvite will flow more rapidly than halite (sometimes referred to as stress refining), so the end product

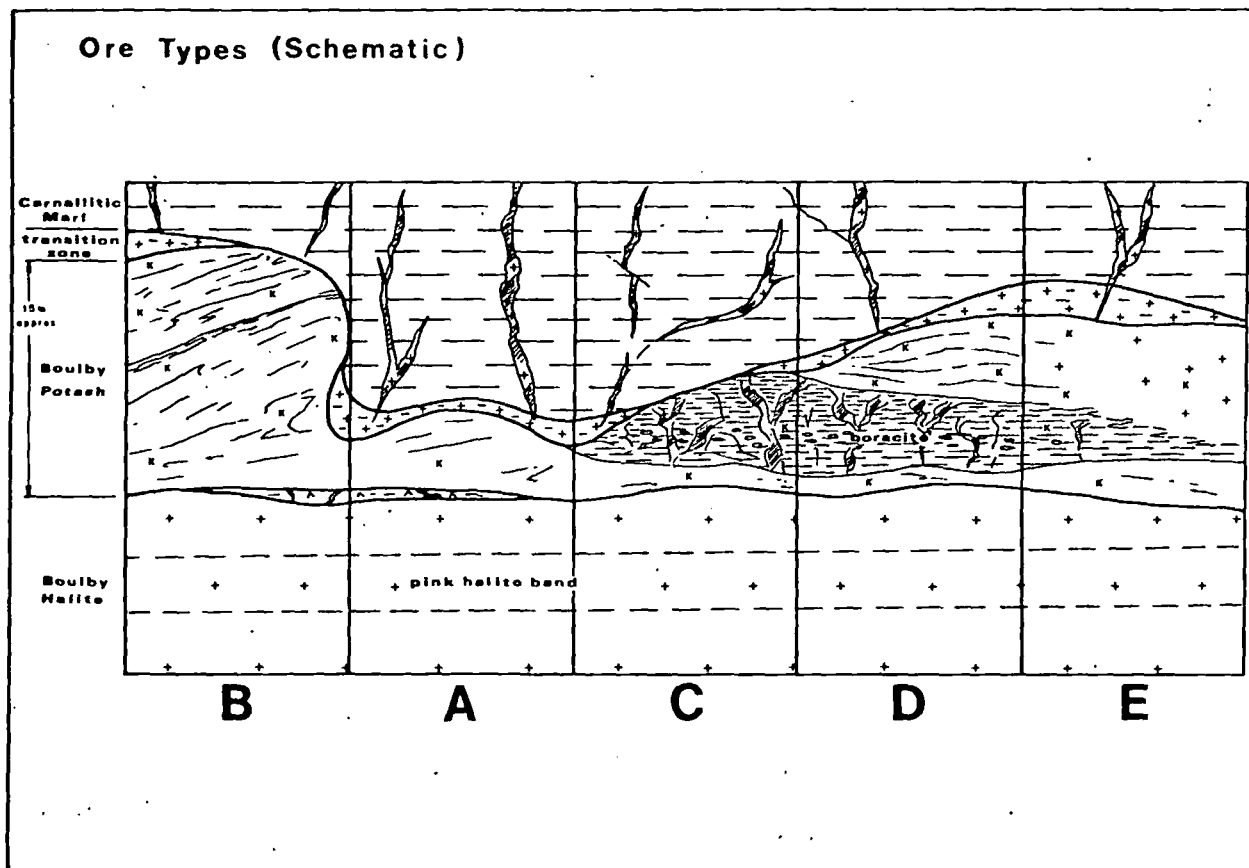


FIG. 4. Ore types (schematic). See text for explanation. K = sylvinite.

is an enrichment of the former in these recumbent folds.

Type C

Ore of this type has a basal component of type A, normally much thinner (0.5–1.5 m) than type A where the latter occurs on its own, with an overlying gray anhydritic shale up to 5 m thick. The shale interval is considered part of the ore type because it contains varying proportions of sylvinite as coarse porphyroblastic aggregates and fibrous veins and masses. These give the rock a somewhat brecciated appearance. While the higher overall argillaceous content of this type is not attractive from a processing viewpoint, the fact that these areas must be traversed to reach better ore means that some selective mining can be practiced to achieve tolerable grades. It is in this interval that a suite of boron minerals has been recognized and described elsewhere (Milne et al., 1977). In many instances the upper boundary of type C is the base of the marl, but elsewhere a disjunctive halite interval intervenes.

Type D

Type D ore is a progression from type C analogous to the relationship between types A and B. In this

case enriched sylvinite, low in anhydritic clay, has flowed into, and in places above, the veined shale interval. Similar fold and nappe structures can be found in this material and it is noticeable that the contained xenoliths are usually particularly well rounded, consisting mainly of gray shale but locally of red-brown marl. Where the enriched sylvinite is thick enough and sufficiently extensive to mine without approaching too close to the marl, operating grades in excess of 40 percent KCl can be achieved.

Type E

This ore also has a basal component of type A and a veined shale interval above which is a generally thick layer of comparatively clean sylvinite but with a much higher halite to sylvite ratio (3 or 4 to 1). The distinction between ore types E and D is therefore primarily one of sylvite content. The origins of this type are suggested in the section on *Diagenesis*.

Variations in the Boulby Halite

In the relatively small number of exposures of the lower three-quarters of the Boulby Halite the stratigraphy is remarkably consistent and, therefore, probably original. Thicknesses vary considerably, how-

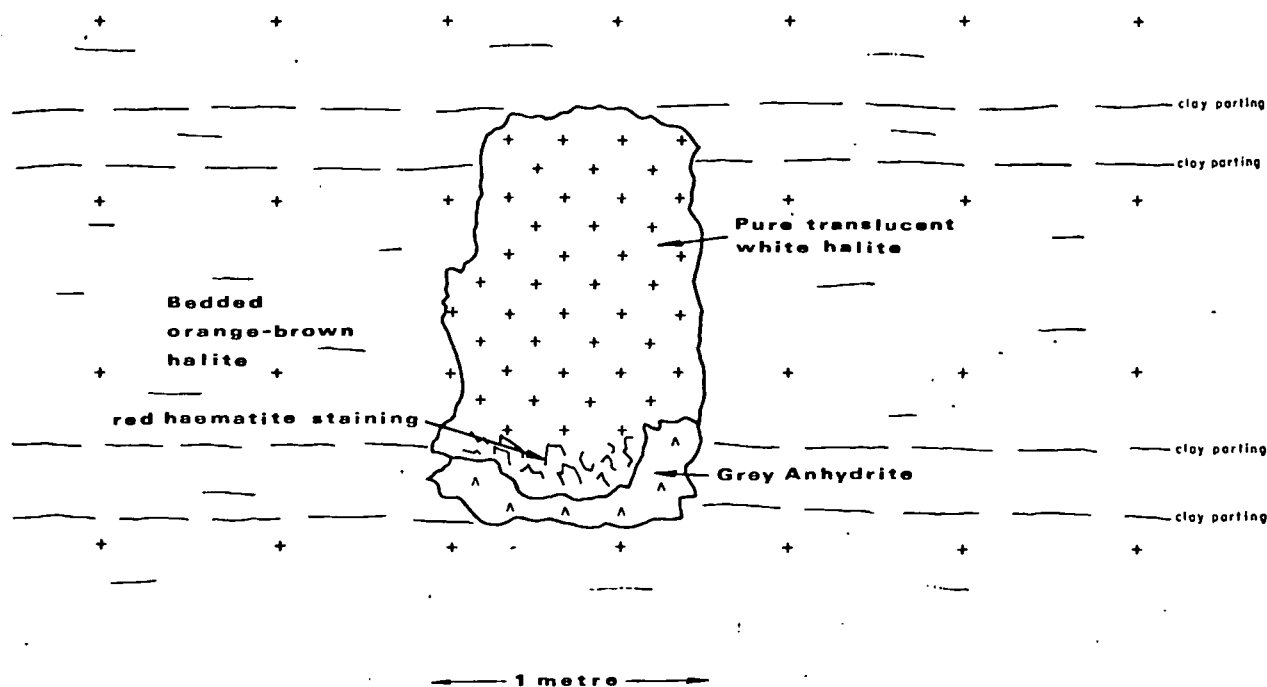


FIG. 5. Solution cavity in Boulby Halite.

ever (see the *Structural History* below). In contrast the upper part contains a number of features which are relevant to the diagenesis of the potash bed.

A continuous pinkish to orange halite bed marks the top of the evenly bedded sequence and has come to be known in the mine as the "pink halite band" (Fig. 4). Some German geologists regard this type of rock as indicating an interval where complete leaching of potassium minerals has occurred (Borchert and Muir, 1964). Above it the halite is variable in color, brownish to gray, with increasing amounts of interstitial clay and anhydrite (up to 10 percent). Over much of the mine this interval also contains small quantities of calcium and magnesium chloride brine which seeps from the rock once it has been cut or drilled. Also in this interval, in some areas of the mine, are what must have originally been solution cavities but which now have the features shown in Figure 5. Internally these structures consist of a lens of coarse, pure translucent halite, up to 2 m in diameter, which overlies a band of anhydrite, often encrusted with red-brown hematite. The amount of anhydrite is far greater than would have formed solely from the solution of the volume of rock represented by the translucent halite. The mechanism may have involved the solution of patches of carnallite or sylvite by calcium sulfate-bearing brines, the uptake of the more soluble minerals causing precipitation of anhydrite followed by halite and the settling out of the hematite platelets from the dissolved sylvite or carnallite. Large aggregates of car-

nallite are found in a similar position in the halite below the main potash beds of the Sergipe deposit in Brazil (Szatmari, pers. commun., 1978).

The contact between the halite and the overlying sylvinite bed varies considerably despite being fairly planar. In some areas it is a shear plane with extensive slickensiding truncating many of the structures at the top of the halite. Elsewhere it may still be sharp, but with a conformable transition from the halite to the sylvite, or there may be a transitional zone 5 to 100 cm thick containing a high proportion of anhydrite in the halite, with local coarse sylvinite enrichment. The later anhydritic zone is more often found with ore types A and B.

Diagenesis

There is some evidence from previous work by others (Stewart, 1956) that the original potassium mineral in the Boulby Potash was carnallite. That problem will not be discussed here, but rather a more general account of what may have caused the present mineral assemblage and variation in ore types. There are two main features which indicate two stages in the diagenesis of the deposit.

Phase 1

The extensive fibrous veining of the Carnallitic Marl and the anhydritic shale in ore types C and D indicates an upward migration of brines prior to the plastic deformation of the sylvinite. These veins normally pinch out above the top of the underlying

type A sylvinitic indicating a subsequent phase of recrystallization or flow deformation. The brines could have one or both of two sources: the conversion of gypsum to anhydrite in the Billingham Main Anhydrite below or the conversion of carnallite to sylvite. A model with brine predominating from the first source is favored because there is both a notable lack of magnesium-bearing minerals anywhere in the sequence and a higher proportion of anhydrite in the vicinity of the potash seam than would be expected from a normal sequential precipitation. Thus upward-migrating brines from below, saturated with respect to halite and anhydrite, would have caused the deposition of some reaction anhydrite followed by reaction halite, where the brines dissolved carnallite or sylvite. Halite with subordinate sylvite in the upper part of ore type E may well be attributable to this mechanism but even more likely related are the fibrous halite veins in the Carnallitic Marl. Subsequent sylvite deposition with a similar crystal habit would provide the fibrous sylvinitic in the argillaceous ore of types C and D, and also in the Carnallitic Marl and Upper Anhydrite. Any residual magnesium-bearing brines must have escaped upward, for no magnesium minerals have been recognized sufficiently

to satisfy the total equation. The disseminated sylvite enrichment (as opposed to fibrous veins) of the more shaly, boron mineral-bearing, lower beds of the Carnallitic Marl would have occurred toward the end of this phase.

Phase 2

This phase did not occur until the evaporites had been buried to well below their present depth; (the top now is at 1,040 m (3,400 ft)). The subject of depth of burial of the British Zechstein is due to be covered in detail in a future paper, but suffice it to say here that the maximum depth probably occurred at or after the end of the Cretaceous period when at least 1,500 m of Jurassic and Cretaceous overburden must have been present. Kerogen studies of Lias Shales suggest a maximum paleotemperature in excess of 200°C, which would make the total depth much greater if the present-day geothermal gradient is assumed to have pertained at that time. However, this would have put the evaporites well below the normally accepted critical depth needed for diapirism. Some of the structures at Boulby (Figs. 6 and 7) suggest that the depth for diapirism was nearly reached, but the fact that the Boulby Potash still oc-

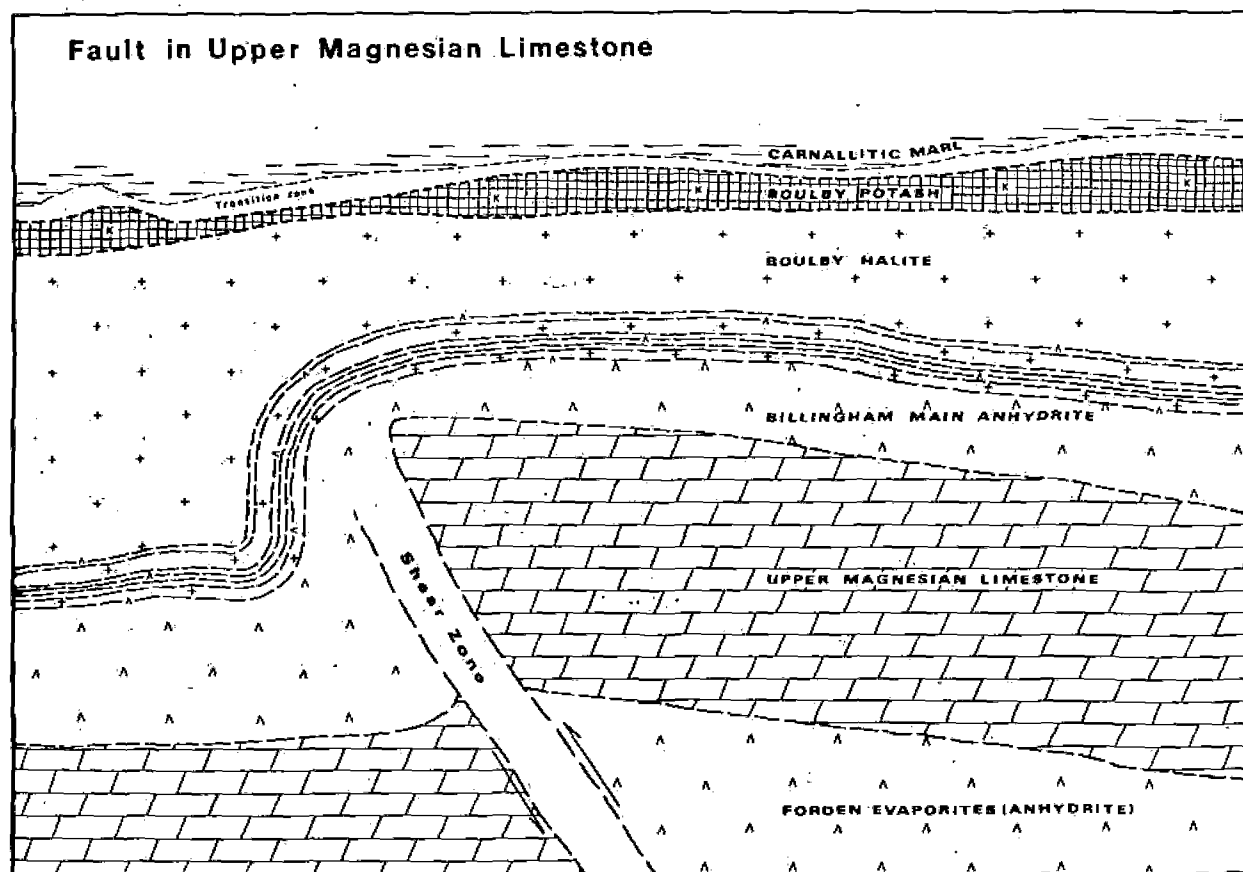


FIG. 6. Fault in the Upper Magnesian Limestone.

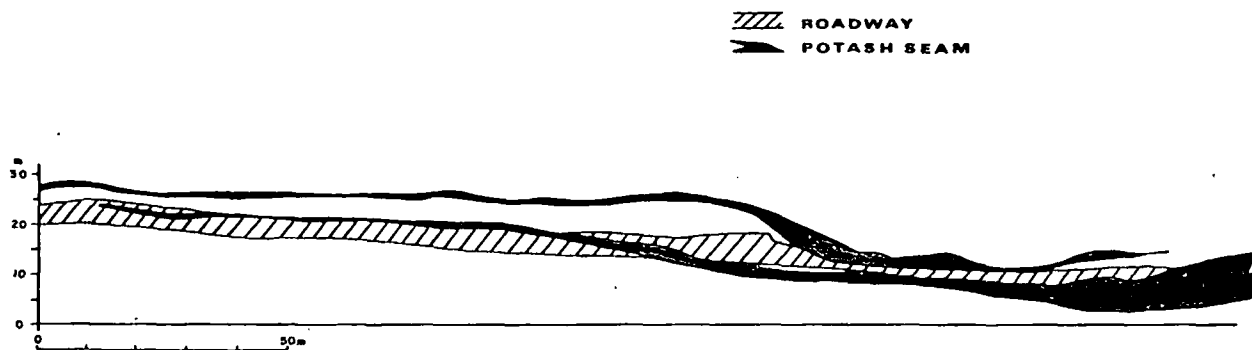


FIG. 7. Seam duplication structure.

copies a more or less constant stratigraphic position indicates that it was not.

The second major phase of diagenesis therefore occurred when the evaporites were at their maximum depth. Two possible mechanisms provided the differential pressures necessary to initiate plastic flow of the sylvite (and to a lesser extent the halite): first, a number of faults in the Upper Magnesian Limestone which probably represent dislocation in response to extensive mineralogical changes in the underlying rocks and, second, structural movements which parallel the regional Tertiary structures in the vicinity. Whatever the cause of the faulting, the sylvinite then flowed on a massive scale to produce ore type B (and to a lesser extent A) and D. Type E has not yet been mined, its character being known only from drill cores where fold structures are not easily recognized. The granular texture and increased halite content in the upper clean zone of type E suggest a possible third phase of diagenesis, involving replacement of sylvite by halite after the phase 2 plastic deformation. Brines necessary for this leaching could have come either from above or below. As uplift and erosion occurred through the Tertiary and later periods the situation would have been frozen as the overburden pressure decreased, so it is likely that very little change has occurred since then.

The Upper Halite and Boulby Halite appear to have suffered very little in the way of mineralogical changes, but a certain amount of compensatory deformation, e.g., lateral flow over faults, has occurred. The limited number of bromine analyses which have been carried out tend to confirm the almost complete recrystallization of the potash bed but very little alteration of the underlying halite.

The Carnallitic Marl also shows mechanical deformation and the addition of disseminated and vein halite which were probably precipitated from upward-migrating brines. Otherwise it appears remarkably unaltered, except for compaction and dehydration since deposition.

Structural History

The undulating nature of the upper contact of the potash bed has been described earlier. This characteristic has a pronounced effect on mining because the base of the Carnallitic Marl is undulating sympathetically but not necessarily in parallel. Such marl troughs or rolls can be traced as near-linear features in many parts of the mine. They are most troublesome when associated with the thin type A ore. When exposed in a roadway the Carnallitic Marl, having no strength, rapidly collapses. Comparable structures were recorded in the anhydrite mine at Billingham (Raymond, 1960) which gave rise to similar mining problems even though only 200 m below the surface.

In the vicinity of the shafts in the mine where a number of permanent excavations have been made, it has been possible to observe the whole of the Teesside Group sequence down to the middle of the Upper Magnesian Limestone. Quite fortuitously the shafts are located close to a reverse fault in the Upper Magnesian Limestone with a 20-m displacement (Fig. 6). The dolomite is quite cleanly fractured, with virtually no brecciation. Conversely the overlying anhydrite is severely distorted with a definite flow fabric parallel to the fault plane. Higher in the sequence where halite is interbedded with anhydritic beds, there is classic boudinage of the anhydrite within the more yielding halite, all the beds being draped over the fault forming a monoclinical fold. The base of the Boulby Potash above is very much less affected by the displacement, having a corresponding monoclinical step of no more than 3 m, while its top shows virtually no related change at all. Thus the Boulby Halite, which changes in thickness from 16 to 40 m across the fault, has obviously flowed laterally to compensate for the displacement. Once recognized, this feature in the potash bed can be traced from roadway to roadway across the mine. Parallel trends of similar origin are seen in the potash seam in several areas of the workings, one of which has a

total displacement in excess of 15 m, suggesting a much larger fault in the Upper Magnesian Limestone below. It is of interest to note that this trend in the potash seam, and the fault below, are virtually at right angles to the predominant fault and joint directions in the Triassic and Jurassic rocks intersected by the shafts.

The potash bed itself has suffered occasional structural deformation even more severe than those in ore types B and D. To the east of the shafts a road, which was being mined in halite below the Boulby Potash for stability reasons, encountered a tongue of sylvinite which progressively increased in thickness. The overall structure which was eventually exposed is shown in Figure 7. It is very similar in many respects to structures described from German potash mines (Borchert and Muir, 1964; Roth, 1968). The type of minor folding is in many respects also similar to but more severe than that described in the Cane Creek mine in Utah (Evans and Linn, 1970).

Fairly extensive seismic surveys, shot on surface and aimed at identifying fault patterns, have had only limited success for a number of reasons. Surface relief is high, with corresponding variation in depth of weathering. A number of drift-filled glacial valleys also cross the area with preglacial weathering zones beneath. The evaporites themselves contain a number of good reflectors, e. g., halite-anhydrite interfaces, but the potash, being sandwiched between beds having similar seismic velocities, is not so easy to define by seismic means. Furthermore the apparent lack of vertical fault continuity through the evaporites and into the overlying Triassic beds makes accurate recognition difficult. Areas of greater mean thickness of the Boulby Halite can be recognized, however, and this characteristic may provide a target for further surveys if there proves to be a clear relationship between Boulby Potash and Boulby Halite in this respect.

Special Features

Three particular features of the Boulby Potash which affect its exploitation are mentioned briefly here.

Gas

Throughout the potash orebody small amounts of gas occur, whose average composition is 80 percent nitrogen and 20 percent methane and higher hydrocarbons. In general it is in tiny inclusions in the sylvite and halite. The main mining problems arise in areas of higher shale content, where more gas has been adsorbed onto or is contained within the clay minerals. The fissility of the shale allows rapid gas release into the workings when such zones are intersected. These gas blows, as they are termed

at Boulby, can cause the ejection of considerable volumes of rock into the workings when triggered by blasting. The largest overbreak to date was about 1,000 metric tons.

The origin of the hydrocarbon gases is uncertain, but one possible source is the Upper Magnesian Limestone below (Fig. 3), which has been a recognized target for gas exploration in the Whitby area; a second more remote external source might be the Carboniferous (Pennsylvanian) coal measures still farther below. With the upward migration of brines through the Boulby Potash bed in phase 1 of the proposed diagenesis, any gases in situ at the time would have been carried upward with the first escaping, possibly $MgCl_2$ -bearing liquids. However, it is likely that gases contained in the final brines from below could have become trapped as bubbles within the growing crystals in the potash bed, their release from the liquids being aided by the reduction in pressure as the brines rose. A special study of this phenomenon has been made at Boulby, the findings of which will be published at a later date.

Temperature

A virgin rock temperature of about 40° C and a small but average potentially higher, rapid but finite release of gas makes ventilation a major factor in the selection of layouts and in the operation of the mine.

Processing

The mineralogy of the Boulby Potash is remarkably simple in comparison with many other European Zechstein ores. The virtual absence of magnesium minerals has been mentioned earlier in the context of diagenesis, but from the practical point of view it is particularly relevant to the processing of the ore. Plant feed is split into two streams, the coarse to flotation and leaching, the finer to flotation and crystallization. The relatively fine crushing (1 mm) size needed to separate sylvite from halite grains in the more gneissic ore means that subsequent compaction is required in order to produce a coarse fraction product. The varying insolubles levels originating from ore types C and D, notably the clay content, give rise to potash losses in the slimes, but the increasing ability to mine selectively underground should eliminate this problem in future.

Acknowledgments

The author wishes to thank Cleveland Potash Limited for permission to publish this paper, his geological colleagues for their helpful advice and criticism, and Les Franks for the illustrations. He also wishes to acknowledge the sponsorship of the

Society of Economic Geologists which made presentation of this paper possible at their Symposium.

CLEVELAND POTASH LIMITED, BOULBY MINE
LOFTUS, SALTBURN BY THE SEA
CLEVELAND TS13 4UZ, ENGLAND
October 6, 1978

REFERENCES

- Armstrong, G., Dunham, K. C., Harvey, C. O., Sabine, P. A., and Waters, W. F., 1951, The paragenesis of sylvine, carnallite, polyhalite, and kieserite in Eskdale Borings, nos. 3, 4, and 6, north-east Yorkshire: *Mineralog. Mag.*, v. 29, p. 667-689.
- Borchert, H., and Muir, R. O., 1964, *Salt deposits*: London, Princeton, Van Nostrand, p. 338.
- Cleasby, J. V., Pearse, G. E., Grieves, M., and Thorburn, G., 1975, Shaft sinking at Boulby mine, Cleveland Potash Ltd.: *Inst. Mining Metallurgy Trans.*, v. 84, sec. A, p. 7-28.
- Dunham, K. C., 1947, A contribution to the petrology of the Permian deposits of northeastern England: *Geol. Soc. Yorkshire Proc.*, v. 27, p. 217-227.
- Evans, R., and Linn, K. O., 1970, Fold relationships within evaporites of the Cane Creek anticline, Utah, in Rau, J. L., and Dellwig, L. F., eds., *Third symposium on salt*, v. 1: Cleveland, Geol. Soc. Northern Ohio, p. 286-297.
- Milne, J. K., Saunders, M. J., and Woods, P. J. E., 1977, Iron-boracite from the English Zechstein: *Mineralog. Mag.*, v. 41, p. 404-406.
- Raymond, L. R., 1960, The pre-Permian floor beneath County Durham, and structures in overlying Permian sediments: *Geol. Soc. London Quart. Jour.*, v. 116, p. 297-315.
- Roth, H., 1968, Deformations in sub-horizontal salt deposits of German Zechstein I: Hanover Symposium, *Geology of saline deposits*, Proc., UNESCO, p. 225-233.
- Smith, D. B., 1971, Possible displacive halite in the Permian Upper Evaporite Group of N.E. Yorkshire: *Sedimentology*, v. 17, p. 221-232.
- Smith, D. B., and Crosby, A., 1978, The regional and stratigraphical context of Zechstein 3 and 4 potash deposits in the British sector of the southern North Sea and adjoining land areas: *ECON. GEOL.*, v. 74, p. 397-408.
- Stewart, F. H., 1956, Replacements involving early carnallite in the potassium-bearing evaporites of Yorkshire: *Mineralog. Mag.*, v. 31, p. 127-135.
- 1965, The mineralogy of the British Permian evaporites: *Mineralog. Mag.*, v. 34, p. 460-470.
- Woods, P. J. E., 1973, Potash exploration in Yorkshire: Boulby mine pilot borehole: *Inst. Mining Metallurgy Trans.*, v. 82, sec. B, p. 99-106.

SOCIETY OF MINING ENGINEERS of AIME

CALLER NO: D. LITTLETON, COLORADO 80123

PREPRINT
NUMBER

A. Noye
79-43



GEOCHEMICAL CHANGES DURING IN SITU URANIUM LEACHING WITH ACID

Daryl R. Tweeton
Research Physicist

Gregory R. Anderson
Mining Engineer

Jon K. Ahlness
Mining Engineer

Orin M. Peterson
Mathematician

William H. Engelmann
Research Chemist

Bureau of Mines
U.S. Department of the Interior
Minneapolis, Minnesota

SUBJ
MNG
GCDI

UNIVERSITY OF UTAH
RESEARCH INSTITUTE
EARTH SCIENCE LAB.

For presentation at the 1979 SME-AIME Annual Meeting
New Orleans, Louisiana, February 18-22, 1979.

Permission is hereby given to publish with appropriate acknowledgments, excerpts or summaries, not to exceed one-fourth of the entire text of the paper. Permission to print in more extended form subsequent to publication by the Institute must be obtained from the Executive Secretary of the Society of Mining Engineers of AIME.

If and when this paper is published by the Society of Mining Engineers of AIME it may embody certain changes made by agreement between the Technical Publications Committee and the author, so that the form in which it appears here is not necessarily that in which it may be published later.

These preprints are available for sale. Mail orders to PREPRINTS, Society of Mining Engineers, Caller No. D, Littleton, Colorado 80123.

PREPRINT AVAILABILITY LIST IS PUBLISHED PERIODICALLY IN
MINING ENGINEERING

Abstract. The Bureau of Mines measured the geochemical changes as H_2SO_4 was used for in situ uranium leaching by Rocky Mountain Energy Company near Casper, Wyoming. Cores and ground water were analyzed before leaching. Water samples were taken from observation wells located between injection and production wells as the leach solution was brought up to full strength in several steps. Measurements were made of pH, Eh, temperature, conductivity, total dissolved solids, dissolved oxygen, HCO_3^- , U, V, Na, K, Ca, Mg, SO_4 , Cl, No, Mn, Fe, Al, Si, F, P, As, and Se. The data were gathered to assist in geochemical modeling of leaching and to study the potential environmental effects of acid leaching. Environmental considerations appear favorable. For example, the concentration of Se, a toxic element often found in uranium deposits, stayed below the EPA standard for drinking water.

Introduction

The data in this report were gathered by the Bureau of Mines Twin Cities (Minnesota) Mining Research Center for two reasons: first, to study the potential environmental effects of in situ uranium leaching using H_2SO_4 , and second, to use in developing and verifying geochemical models.

Most in situ uranium leaching is performed with alkaline lixivants. Currently, the most popular is $(NH_4)_2CO_3 - NH_4HCO_3$. Carbonate lixivants dissolve U more selectively than acid lixivants do, and it was thought that carbonate leaches would be environmentally preferable because less pollutants such as Se and As would be dissolved and less solid wastes would be deposited in evaporation ponds. However, acid leaches do offer some environmental advantages. The NH_4 retention on clays created by $(NH_4)_2CO_3 - NH_4HCO_3$ leaches is avoided. Less Ra should be dissolved by H_2SO_4 than by carbonate lixivants, based on the extremely low solubility of $RaSO_4$. This prediction is supported by information on uranium milling collected by the Environmental Protection Agency (EPA) (1). EPA reported that acid leaching dissolved 0.2 to 0.4 pct of the Ra in the ore, but alkaline leaching dissolved 1.5 to 2.0 pct.

Acid leaching recovers more of the U than carbonate leaching does, at least in laboratory tests (2). If acid leaching were shown to be environmentally no worse than carbonate leaching and acid lixivants used where acid consumption was not excessive, then production could be increased. Thus, the Bureau wanted to make field measurements to determine how much of the potentially harmful pollutants were dissolved during acid leaching.

The second reason for performing this research was to obtain field data for developing and verifying geochemical models. The object of the modeling is to develop computer simulation models that will assist operators in selecting the optimum lixiviant type and strength. Data from laboratory leaching are available. For example, the Bureau of Mines Salt Lake City (Utah) Metallurgy Center did extensive laboratory leaching through a contract with Westinghouse (2,3). However, very little field data containing complete analyses of pregnant lixivants have

been published. It was felt that verification with field data would provide greater confidence in a model. Various researchers who are developing geochemical models of leaching at universities and private companies have requested such data. To assist these researchers as rapidly as possible, the data are being released now.

The data were gathered under a cooperative agreement with Rocky Mountain Energy Company. Before leaching, cores and water samples were taken from the ore zone at the Company's Nine Mile Lake site near Casper, Wyo. During leaching, water samples were taken from observation wells between the injection and production wells. This report summarizes the data gathered from shortly before leaching began until leaching was established. A subsequent report will describe restoration, which had not begun when this report was written.

Well Field

The well field was in a typical five-spot pattern. Figure 1 shows the well field pattern at the ore depth. The bottom of the center well was assigned coordinates 0,0 for this report. The coordinates of the wells are listed below.

	East of Center		North of Center	
	Feet	Meters	Feet	Meters
OB1	-29.0	(-8.8m)	2.5	(0.8m)
OB2	7.4	(2.2)	8.1	(2.5)
OB3	18.2	(5.5)	-17.2	(-5.2)
15	0		0	
16	-31.7	(-9.7)	12.0	(3.7)
17	45.2	(13.8)	34.7	(10.6)
18	31.8	(9.7)	-30.6	(-9.3)
19	-31.7	(-9.7)	-46.2	(-14.1)

For example, well OB1 was 29.0 feet west and 2.5 feet north of the bottom of well 15.

The Bureau's primary sampling wells are labeled OB1 and OB3. These sampling wells were made because analyzing samples only from the injection and production wells would not provide all the information needed for modeling. For example, the situation where uranium was being dissolved but was precipitating before reaching the production well would not be distinguishable from one where uranium was not being dissolved, unless there were an intermediate sampling point. Also, if the downhole data-gathering probe were below a production well pump, then the probe could not be pulled up for calibration without interfering with production. Well OB2 was not used for water sampling, but OB1, OB2, and OB3 were all cored. Lixiviant was injected at the four corner wells, 16-19, and pumped from the center well, 15.

All wells were cased with 5-inch (0.13-m) Yelomine plastic. OB1, OB2, and OB3 had 0.02-inch (0.51-mm) slots from 510 feet (155 m) to 540 feet (165 m). Wells 15 through 19 were perforated with the Bureau of Mines water-jet perforator (4) over the following depths:

¹ Reference to specific equipment (or trade names or manufacturers) is made for identification only and does not imply endorsement by the Bureau of Mines.

The permeability was 1.56 and 0.62 darcy in the direction of major (N 23° W) and minor transmissivity, respectively,

79-43

Well 15, 528-537 feet (160.9-163.7 m)
Well 16, 523-536 feet (159.4-163.4 m)
Well 17, 525-541 feet (160.0-164.9 m)
Well 18, 525-534 feet (160.0-162.8 m)
Well 19, 520-532 feet (158.5-162.2 m)

A 40-gpm (150 lpm) stainless steel submergible pump was installed in the center well for production. The injection rate was usually about 8-gpm (30 lpm) in each of the four injection wells. The production rate exceeded the total injection rate by 2 to 3 gpm (8 to 11 lpm).

Producing at a higher rate than injecting served two purposes. First, a hydraulic gradient toward the leached area was maintained, thereby helping to prevent an excursion (the escape of lixiviant underground). Second, it allowed a bleed stream, which flowed from the uranium extraction plant to an evaporation pond, to be used. The bleed stream helped to limit the concentrations of undesired elements in the recycled lixiviant.

For taking water samples from OB1 and OB3, 9-gpm (34 lpm) stainless steel submergible pumps were installed just above the slotted sections. This position minimized the extent to which water that had been standing in the casing was withdrawn, as described by Colchin, Turk, and Humenick (5).

Preleach Ore Characteristics

There are two sandstone members in the deposit. The top one ranges in thickness from 11 to 25 feet (3.4 to 7.6 m). The leaching was performed in the lower member, which ranges from 25 to 40 feet (7.6 to 12.0 m), with an average thickness of 34 feet (10.4 m). Its top is approximately 510 feet (155 m) deep. A bed of silt, clay, fine sand, and coal separates the two units. The bed thickness varies, with an average of 2 to 3 feet (0.6 to 0.9 m).

Cores from wells OB1, OB2, OB3, 15, 16, 17, and 19 were analyzed to determine the preleach ore composition. Table 1 lists measurements of the following items as a function of depth in the screened or perforated intervals: U_3O_8 , YeU_3O_8 , V_2O_5 , total C, C in CO_2 , total S, SO_4 , total Fe, Mo, As, and Se. YeU_3O_8 means gamma-equivalent U_3O_8 , which is the concentration of U_3O_8 calculated from gamma emissions, assuming equilibrium between U and its daughter products. Composite samples were also analyzed, and the results are shown in table 2.

As expected, there was a positive correlation between U_3O_8 and V_2O_5 , and a negative correlation between Mo and Se. Like U, both Mo and Se form anionic complexes which are soluble under neutral to high pH conditions when oxidized, but are insoluble when reduced. Selenium requires a higher Eh (more oxidizing) than does U to remain soluble, so it tends to precipitate on the upstream, oxidizing side of a roll-front uranium deposit. Conversely, Mo remains soluble in a lower Eh than does U, so it tends to precipitate on the downstream, reduced side of the deposit. Judging from the Mo and Se distribution, the stream which formed the deposit flowed south or south-east. There was little or no correlation of U_3O_8 with other heavy minerals.

The sandstones are normally graded, but evidence of grading is confined to the bottom few

feet. The size of most of the sand grains is medium to fine. The sandstones are quite clean, usually greater than 90 pct quartz, and would therefore be classified as quartz arenites. They are light olive, STR 6/1 in the U. S. Geological Survey (USGS) color chart. They contain very little carbonate or clay. Visual inspection indicated 5 to 15 pct feldspar, but x-ray diffraction showed less than 5 pct feldspar in all the holes. Apparently, the majority of the feldspar grains have decomposed into clay. Two-thirds of the original Al in the kaolinite had been replaced by V, creating roscaelite.

A commercial service company performed pumping tests to determine hydrologic characteristics. The ground water flow was 14 ft/yr (4.3 m/yr) E 7° N. The major transmissivity was ~~1.35 darcy~~, so the geometric mean was 0.98 darcy. (The permeability measured in the laboratory with core samples averaged 2.2 darcys.) The ratio of vertical to horizontal permeabilities was 1.0. The porosity, based on core samples, averaged 28 pct. The storage coefficient was 1.54×10^{-3} , and the aquifer compressibility was 2.76×10^{-5} /psi (4.00×10^{-5} /Pa). The radius of influence was about 600 feet (180 m). The layer separating the two sandstone members can be modeled as being 2 feet (0.6 m) thick and having a permeability of 0.6 millidarcy. The lower confining layer can be regarded as impermeable.

Injected Leach Solution

Injection began November 29, 1977. The leach solution consisted of H_2SO_4 added to formation water. The initial strength was 0.15 gpl of acid, giving a pH of 3.9. The strength was increased to approximately 1.5 gpl acid on December 30, 1977, 3 gpl on January 10, and 5 gpl on April 3, 1978. The SO_4 concentrations in the injected and produced solutions are shown in figure 2. The spike on January 4 was caused by the solution picking up acid from freshly eluted ion-exchange resin.

Hydrogen peroxide was added starting January 19. The approximate volume-percent concentrations in the injected solution were as follows:

Date	Percent	Date	Percent
1/19-21	0.0008	3/10-18	0.04
1/21-2/17	0.011	3/18-21	0.05
2/17-3/3	0.11	3/21-4/12	0.08
3/3-10	0.001		

The solution strength was increased in several steps to minimize clogging from reaction products, both solids and gases. For example, CO_2 would be formed by the dissolution of carbonates. Starting injection with a low acid concentration helped insure that the dissolution proceeded slowly enough to allow the CO_2 to remain in solution while moving to the production well. An additional advantage was in preventing premature mobilization of U and other elements. If strong acid were injected at the start of leaching, then U and other elements might be mobilized near an injection well but reprecipitated near the production well as ground water diluted the acid.

Changes in Ground Water and Leach Solution Composition

Measurement Methods

Water samples were pumped daily from OBI and OB3 from the start of leaching until leaching was well established at the end of January, and then weekly until mid-April. During times of expected rapid geochemical changes, sampling was performed twice per day. Samples were taken after 40 min of pumping at 9 gpm (34 lpm). This time was found to be adequate for stabilization of all the parameters measured on-site.

The pH, conductivity, temperature, Eh, dissolved oxygen (D.O.), and HCO_3 in samples from OBI and OB3 were measured in an on-site laboratory. The first five of these parameters were also measured by a downhole probe suspended beneath the pump in OB3.

Calibration procedures for surface and downhole measurements were similar. The surface meters were calibrated daily, but the downhole probe was calibrated about once every three weeks. The settings of the downhole probe for pH, conductivity, temperature, and D.O. changed very little from one calibration to the next. The pH and Eh meters were calibrated with buffers and Zobell solution, respectively. Additional Eh standards were used for the downhole probe. The D.O. measurements were taken with a galvanic cell oxygen analyzer, and were calibrated with air-saturated water and oxygen-free water. The reading with air-saturated water, about 8 ppm, was taken when the D.O. probe, with a moist membrane, was held in air. The oxygen-free water was a Na_2SO_3 solution. The conductivity meter was calibrated in 0.1 M KCl. The downhole thermometer was standardized using ice water. The downhole thermometer agreed with a mercury thermometer within 0.1° C at 12° C to 13° C when the ice water was assumed to be 0.0° C. Bicarbonate concentration was measured with acid titration.

The surface and downhole measurements agreed for pH, conductivity, and temperature, but differed for D.O. and Eh. The D.O. measurements agreed near 8 ppm, but the surface measurement read too high for lower D.O. values and too low for higher D.O. values. This could be expected, as the samples would partially equilibrate with air. The downhole D.O. measurements were considered correct and were used as the OB3 values. The OBI values were calculated from the surface readings, using the differences between surface and downhole readings at similar D.O. levels in OB3 as correction factors. The time from pumping to measuring remained quite constant.

The surface and downhole measurements of Eh were significantly different. The changes indicated by the two methods were similar, but the surface measurements were about 400 mV more oxidizing. The surface measurements were made by taking the solution into the laboratory as quickly as possible and measuring the Eh in the beaker. An attempt to tap off a small flow from the pump hose and run the solution through a U-tube containing the Eh probe failed because the solution continually froze. It is recognized that oxygen from the air would make the laboratory Eh readings too oxidizing. However, the surface Eh measurements were useful because of the changes they indicated and because correction

factors for OBI could be calculated by comparing the surface and downhole readings for OB3. A complicating factor was the apparent poisoning of the downhole Eh probe, resulting in unrealistically low readings. The probe read below the stability limit of water part of the time. The Eh readings taken within one day of cleaning and calibration were assumed to be correct, and the surface measurements were used as guides to the changes in Eh while the probe was apparently poisoned.

Most of the measurements of ion concentrations were made at a commercial laboratory under a Bureau contract. They determined SO_4 and total dissolved solids (TDS) gravimetrically, Cl and F by specific ion electrode, Se and P colorimetrically, U_3O_8 fluorometrically, and the remaining ions by atomic absorption. Many of the measurements were duplicated by the Bureau of Mines laboratory. Where agreement was not good, duplicate samples were submitted to the USGS. Rocky Mountain Energy Company supplied many analyses of samples from OBI and OB3 and also from the production and injection wells.

Samples taken before January 11 for cation analyses were acidified with 6 ml of 70 pct HNO_3 per liter of sample. After that time, acidification was performed with 10 ml of 38 pct HCl per liter to reduce interferences. Samples from OB3 were filtered with a 0.45-micron filter because they contained suspended solids. The samples from OBI analyzed by the commercial laboratory were not filtered. OBI water was clear, and the commercial laboratory felt that it was preferable not to filter because dissolved solids might become suspended solids when pressure was reduced from downhole to surface, and gases were forced out of solution. The USGS recommends filtering all samples before acidifying. The Bureau analyzed both filtered and unfiltered samples from OBI, and found very little difference.

Results

The best estimates of parameters, except temperature, characterizing the ground water before leaching are shown in the first row of tables 3 and 4. These estimates are based on samples taken on September 28, October 14-20, and November 17, 1977.

The measured values of all parameters, except temperature, as a function of time during leaching are shown in the remainder of tables 3 and 4. The most important of these parameters are graphed in figures 3 through 25. Before leaching began and during the initial stages of leaching, D.O. levels were too low for the available equipment to measure reliably, so they are not shown in the first part of tables 3 and 4. Bicarbonate values are not shown in the last part of the tables because the pH was below 4.5, so the HCO_3 concentration was negligible. Conductivities are at downhole temperatures, about 12° C.

This report follows the convention wherein the more oxidizing condition is described by the more positive Eh. This convention is followed by most chemists outside of the petroleum industry. A correction has been made for the electrode potential relative to hydrogen, so the values listed under Eh are the values with respect to hydrogen. Considerable confusion can occur when uncorrected

readings taken with a calomel electrode are reported as Eh, or the sign convention used is not reported.

The values in the tables are best estimates, taking into account the measurements by all the laboratories. They do not necessarily represent averages. Where there was evidence that one laboratory's measurements were badly in error, those measurements were ignored.

The temperature usually varied less from day to day than the other parameters, so it is not listed in tables 3 and 4. After confirming that the temperatures measured in the laboratory agreed with those measured by the downhole probe and that the temperatures in the two wells were similar, surface measurements were no longer made. The temperature measurements by the downhole probe in OB3 are summarized in table 5. The increase in temperatures during January was probably caused by the injected acid. Natural seasonal variations would continue the cooling trend observed in December.

Accuracy and Precision of Measurements

Accuracy denotes the extent of departure of a measurement from the correct value. Precision denotes the reproducibility, disregarding accuracy. The 95 pct confidence intervals for both are listed below. Where a pair of values are given, use the larger. "Pct" means percent of the measured value.

	Accuracy ^a	Precision
pH	±0.1 pH units	±0.07 pH units
Eh	±70 mV	±40 mV
K, Si, Na, and TDS concentrations	±20 pct or half the last digit	±5 pct or half the last digit
All other ions and conductivity	±10 pct or half the last digit	±5 pct or half the last digit
D.O.	±25 pct or 0.4 ppm	±10 pct or 0.4 ppm
Temperature	±0.1°C	±0.1°C

The accuracies of ion concentrations were calculated from standard deviations of results from three or four laboratories, analyzing samples taken the same days. The precisions for ion concentrations, pH, Eh, and conductivity were calculated from standard deviations of the commercial laboratory's results from 10 sequential daily samples when the results were not trending up or down. Therefore, the precision includes sampling errors as well as analytical errors. The remaining accuracies and precisions were estimated using several factors, such as the reliability of the calibration and the constancy of the parameter in the sample. Sufficient digits are listed in the results to indicate changes, even though the last digit may not always be significant in terms of accuracy.

Radioisotope Analyses

Radium 226 and Th 230 were measured before leaching, on October 10, 1977, and during

leaching, on January 19, 1978. The results are shown in table 6.

Radium increased by a factor of 20, which was less than other metals increased. For example, V increased by a factor of 7,500. Even U, which was continually being extracted, increased by a factor of 500. This finding confirmed the expectation that H₂SO₄ would not solubilize great amounts of Ra, because of the very low solubility of RaSO₄. Thorium increased more than Ra, which was expected, because Th is more soluble than Ra in H₂SO₄.

Discussion

When considering the possible environmental effects of in situ leaching, one should evaluate the potential for contaminating ground water with Se, As, and Mo. These elements have sufficient toxicity to be considered environmentally sensitive, and are often found with or near U because, like U, they form anionic complexes which are soluble when oxidized and insoluble when reduced. The 1976 EPA standards (6) for Se and As in drinking water are 10 ppb and 50 ppb, respectively. No EPA standard for Mo in drinking water was established, but the drinking water standard in the U.S.S.R. is 0.5 ppm (7).

The analyses presented in this report show that acid leaching at the Nine Mile Lake site did not produce high levels of Se, As, or Mo. In fact, concentrations of Se and Mo stayed below the available standards for drinking water. The highest concentration of As, 1.1 ppm, does not represent a greater potential environmental impact than occurs with typical alkaline leach solutions. Published analyses (8) of alkaline leach solutions list 0.36 ppm As and 0.17 ppm Se at one site and 0.033 ppm As and 1.02 ppm Se at another site. Thus the potential environmental impact of As and Se considered together is about the same for the cited alkaline leaching as for the acid leaching at the Nine Mile Lake operation.

Possible reasons why Se, As, and Mo concentrations stayed low are given in the NRC report "Ground-Water Elements of In Situ Leach Mining of Uranium" (9). The report states that "the mobility of MgO₄ in oxidizing lixivants is greater under neutral or alkaline conditions than it is under acid conditions," and "the mobility of selenium in oxidizing lixivants resembles that of molybdenum to some extent." The report also states that "arsenic forms . . . very insoluble salts with iron, copper, lead, zinc, cadmium, nickel, and cobalt." As acid leach dissolves more of these metals from the gangue, more become available for precipitating As. Another controlling factor is that "ferric hydroxide will adsorb arsenite and arsenate from acidic lixivants." As expected, Th, rather than Ra, was the radionuclide highest above drinking water limits.

The next requirement for the complete environmental picture of acid leaching is restoration. It is expected that restoration following acid leaching will require less flushing than after (NH₄)₂CO₃ leaching, though it is possible that the high concentration of V will prolong restoration. Unless restoration is far more difficult than expected, it appears that the choice of leach solution should not be based on an

assumption that acid leaching is environmentally worse than alkaline leaching.

Those considering acid leaching should be encouraged since it was successful in an ore containing high levels of V, and since the bleed stream, usually about 7 pct of the production flow, kept the undesired ions within workable limits.

The Bureau hopes that the data will help those trying to model the geochemical reactions involved with leaching. Modelers should keep in mind that U was being removed by ion-exchange, so nearly all the U in the samples on any particular day was generated by one pass through the ore from an injection well to the sampling point. None of the other elements was fully extracted. Their build-up was controlled only by the bleed stream.

The Bureau invites suggestions on ways to make such data more useful. It may be possible to make some measurements during additional acid leaching.

Acknowledgments

The Bureau wishes to express its appreciation to Rocky Mountain Energy Corporation for allowing it to take core and water samples at the Corporation's site, for providing many of the analyses, and for excellent cooperation in all phases of this study.

References

1. Clark, D.A., "State-of-the-Art: Uranium Mining, Milling, and Refining Industry," EPA-66/2-74-038, Environmental Protection Agency, June 1974, p. 57.
2. Sundar, P.S., "In-Situ Leaching Studies of Uranium Ores--Phases I Through III," Bureau of Mines OFR 140-77, June 1977, 392 pp. Available from NTIS, #PB 272717/AS (\$13.25)
3. Sundar, P.S., "In Situ Leaching Simulation Studies of Uranium Ores," Pres. at the 1978 AIME Annual Meeting, Feb. 26 - Mar. 2, 1978, Denver, Colorado., SME Preprint 78-AS-102, 16 pp.
4. Savanick, G.A., "Water Jet Perforator for Uranium Leaching Wells," Proc. First Conf. on Uranium Mining Technology, Univ. of Nevada-Reno, Apr. 24-29, 1977. (Published as Uranium Mining Technology, Ed. by Y.S. Kim), Conferences and Institute, Univ. of Nevada-Reno, 1977, 36 pp.
5. Colchin, M.P., Turk, L.J., and Humenick, M.J., "Sampling of Ground Water Baseline and Monitoring Data for In-Situ Process," Technical Report CRWR-157, Center for Research in Water Resources, The University of Texas, Austin, Texas, June 1978, p. VII-23.
6. U.S. Environmental Protection Agency, "Quality Criteria for Water," EPA-440/9-76-023, 1976, 501 pp.
7. Middleton, F.M., "Organics in Water Supply - The Problem", Proceedings of 15th Water Quality Conference on Organic Matter in Water Supplies: Occurance, Significance, and Control, Uni-versity of Illinois, 1973, 14 pp.
8. Thompson, W.E., Swarzenski, W.V., Warner, D.L., Rouse, G.E., Carrington, O.F., and Pyrih, R.Z., "Ground-Water Elements of In Situ Leach Mining of Uranium," U.S. Nuclear Regulatory Commission NUREG/CR-0311, Aug. 1978, pp. 71-73. Available from NTIS (\$9.00).
9. _____, "Ground-Water Elements of In Situ Leach Mining Uranium," U.S. Nuclear Regulatory Commission NUREG/CR-0311, Aug. 1978, Appendix C. Available from NTIS (\$9.00)

TABLE 1. - Core Analyses

Depth, ft	Depth, m	U ₂ O ₅ , ppm	Y ₂ O ₃ , ppm	V ₂ O ₅ , ppm	Total C, pct	C in CO ₂ , pct	S, pct	SO ₄ , pct	Total Fe, pct	Mo, ppm	As, ppm	Se, ppm
WELL OBI												
507-509	154.5-155.1	11	30	115	11.23	0.09	0.47	0.03	0.60	4	<10	<1
509-511	155.1-155.7	4	10	45	.35	<.01	.04	.03	.23	3	<10	<1
511-513	155.7-156.4	9	10	65	.55	<.01	.04	.03	.30	2	<10	<1
513-515	156.4-157.0	17	10	110	.52	<.01	.07	.05	.22	4	<10	<1
515-517	157.0-157.6	30	20	170	.09	<.01	.07	.06	.18	3	<10	<1
517-519	157.6-158.2	57	100	265	.13	<.01	.05	.07	.16	3	<10	<1
519-520	158.2-158.5	96	120	270	.06	.01	.12	.07	.22	4	<10	<1
523-525	159.4-160.0	360	250	710	.83	<.01	.07	.08	.15	2	<10	<1
525-526	160.0-160.3	444	310	2,100	1.42	.06	.07	.05	.22	4	<10	<1
526-528	160.3-160.9	232	220	715	.14	.01	.05	.08	.14	2	<10	<1
528-530	160.9-161.5	394	450	3,600	.05	<.01	.05	.07	.13	3	<10	<1
530-532	161.5-162.1	360	760	5,900	.17	<.01	.05	.07	.14	<1	<10	<1
532-534	162.1-162.8	262	890	4,400	.06	<.01	.05	.09	.15	<1	15	<1
534-536	162.8-163.4	578	1,130	6,000	.15	<.01	.06	.08	.15	1	<10	<1
536-538	163.4-164.0	427	380	955	.28	.01	.10	.09	.21	8	<10	<1
539-541	164.3-164.9	36	30	60	.62	.02	1.06	.10	1.17	19	35	<1
541-542	164.9-165.2	19	40	80	2.14	.01	.27	.10	.50	142	<10	<1
WELL OB2												
508-510	154.8-155.4	24	40	150	1.43	<.01	.15	.03	.24	120	<10	7
510-512	155.4-156.1	8	20	150	21.7	<.01	.54	<.01	.73	2	<10	4
512-514	156.1-156.7	7	20	60	.38	<.01	.07	.01	.35	19	<10	<1
514-515.5	156.7-157.1	22	30	90	.40	<.01	.07	<.01	.29	2	<10	<1
515.5-517	157.1-157.6	14	20	115	.31	.02	.07	.02	.21	2	<10	<1
517-519	157.6-158.2	17	50	100	<.01	<.01	.05	.01	.16	1	<10	<1
519-521	158.2-158.8	34	80	105	.09	<.01	.05	.02	.13	1	<10	<1
521-523	158.8-159.4	104	120	365	.33	<.01	.05	.01	.14	<1	<10	4
523-525.5	159.4-160.2	303	200	560	.69	<.01	.05	.02	.11	1	<10	9
525.5-528	160.2-160.9	882	820	2,500	.51	.05	.05	.01	.18	3	<10	28
528.5-530	161.1-161.5	2,900	2,500	13,800	2.05	.10	.16	.02	.26	5	10	7
530-532	161.5-162.1	2,320	1,720	4,100	.18	.01	.03	.03	.16	<1	<10	2
532-534	162.1-162.8	1,222	890	1,700	.09	<.01	.04	.01	.13	<1	<10	2
534-535.5	162.8-163.2	617	530	1,200	.09	<.01	.04	.01	.13	<1	<10	7
535.5-537	163.2-163.7	1,080	910	1,800	.10	<.01	.02	.01	.13	<1	<10	1
537-539	163.7-164.3	1,120	1,160	5,000	.24	<.01	.08	.02	.17	<1	<10	9
539-541	164.3-164.9	306	370	840	.17	<.01	.08	.01	.18	<1	<10	1
542-544	165.2-165.8	53	50	70	1.04	<.01	.26	.02	.46	266	10	5
WELL OB3												
509.5-511	155.3-155.7	17	40	210	11.87	<.01	.30	.02	.37	41	<10	4
511-512	155.7-156.1	3	50	60	.92	<.01	.15	.02	.38	9	<10	<1
512-513	156.1-156.4	3	90	45	.15	<.01	.04	.02	.26	6	<10	<1
513-514	156.4-156.7	3	70	45	.19	.03	.04	.02	.27	6	<10	<1
514-515	156.7-157.0	12	120	70	.40	.07	.05	.02	.27	8	<10	<1
515-516	157.0-157.3	18	70	85	.40	<.01	.07	.05	.23	9	<10	<1
516-517	157.3-157.6	10	30	80	.08	<.01	.05	.06	.20	6	<10	<1
517-518	157.6-157.9	13	30	90	.16	.05	.05	.06	.17	4	<10	<1
518-519.5	157.9-158.4	18	50	110	.06	<.01	.01	.06	.14	2	<10	<1
519.5-520.5	158.4-158.6	44	50	125	.10	<.01	.03	.06	.14	2	<10	<1
520.5-521.5	158.6-159.0	65	50	105	.07	<.01	.03	.06	.14	4	<10	<1
522.5-524	159.3-159.7	125	90	115	.13	<.01	.05	.05	.12	2	<10	<1
524-525	159.7-160.0	181	130	100	.39	<.01	.03	.04	.13	6	<10	<1
525-526	160.0-160.3	192	120	150	.09	<.01	.07	.06	.12	5	<10	<1
526-527	160.3-160.6	430	250	410	.36	<.01	.05	.05	.16	1	<10	<1
527-528	160.6-160.9	520	380	505	.17	<.01	.05	.05	.14	<1	<10	<1
528-529	160.9-161.2	680	530	850	.13	<.01	.05	.06	.12	<1	<10	<1
529-530	161.2-161.5	940	1,000	1,400	.06	<.01	.03	.06	.12	<1	<10	<1
531-532	161.8-162.1	1,420	740	2,800	.06	<.01	.04	.06	.12	1	<10	<1
532-533	162.1-162.5	1,000	650	2,100	.06	<.01	.04	.06	.12	<1	<10	<1
533-534	162.5-162.8	1,222	1,010	1,900	.09	<.01	.03	.07	.12	<1	<10	<1
534-535	162.8-163.1	960	710	1,700	.04	<.01	.35	.07	.42	3	15	<1
535-536	163.1-163.4	570	450	1,500	.04	<.01	.06	.07	.14	4	<10	<1
536-537	163.4-163.7	570	410	1,100	.06	<.01	.05	.06	.12	3	<10	<1
537-538	163.7-164.0	310	300	290	.06	<.01	.02	.05	.14	6	<10	<1
539-540.5	164.3-164.7	72	80	100	.25	.16	.11	.04	.22	14	<10	<1
540.5-542	164.7-165.2	23	30	65	.61	<.01	.07	.06	.17	304	<10	<1

TABLE 1. - Core Analyses--continued

Depth, ft	Depth, m	U ₃ O ₈ , ppm	γeU ₃ O ₈ , ppm	V ₂ O ₅ , ppm	Total C, pct	C in CO ₂ , pct	S, pct	SO ₄ , pct	Total Fe, pct	Mo, ppm	As, ppm	Se, ppm
Well 15												
511 -512	155.7-156.1	4	20	40	.15	<.01	.06	.02	.31	<1	<10	<1
512 -513	156.1-156.4	16	20	70	.37	.01	.14	.01	.39	<1	<10	<1
513 -514	156.6-156.7	15	20	60	.33	.06	.08	.03	.26	1	<10	<1
514 -515	156.7-157.0	22	30	140	.51	.05	.08	.03	.26	1	<10	<1
515 -516	157.0-157.3	43	60	110	.16	.06	.04	.05	.25	<1	<10	<1
516 -517.5	157.3-157.7	122	100	190	.17	.01	.07	.06	.25	1	<10	<1
518 -519	157.9-158.2	91	80	180	.06	.01	.03	.05	.16	2	<10	<1
519 -520	158.2-158.5	73	40	140	.11	.02	.03	.05	.14	<1	<10	<1
520 -521	158.5-158.8	34	50	220	.43	.09	.05	.05	.15	1	<10	<1
521 -522	158.8-159.1	23	30	190	.32	.07	.04	.05	.18	1	<10	<1
523 -524	159.4-159.7	164	90	190	.45	.17	.06	.05	.15	<1	<10	<1
524 -525	159.7-160.0	160	100	260	.17	.09	.05	.04	.15	1	<10	<1
525 -526.5	160.0-160.4	500	280	1,600	.25	.11	<.01	.04	.14	3	<10	<1
527 -528	160.6-160.9	1,490	970	3,900	.26	.13	.08	.05	.14	1	<10	<1
528 -529	160.9-161.2	1,680	1,060	3,000	.18	.10	.04	.06	.12	<1	<10	<1
529 -530.5	161.2-161.7	1,120	810	2,800	.15	.04	.08	.05	.18	2	<10	<1
531.5-533	162.0-162.5	610	610	2,900	.20	.12	.03	.05	.14	1	<10	<1
533 -534	162.5-162.8	420	330	2,700	.16	.07	.02	.04	.12	1	<10	<1
534 -535	162.8-163.1	650	400	1,400	.06	.01	.02	.04	.11	<1	<10	<1
535 -536.5	163.1-163.5	860	600	3,100	.24	.01	.03	.04	.14	<1	<10	<1
536.5-537.5	163.5-163.8	1,140	700	2,500	.25	.02	.13	.04	.18	<1	<10	<1
538 -539	164.0-164.3	184	120	220	.08	<.01	.10	.04	.21	22	<10	<1
539 -540	164.3-164.6	39	30	110	1.44	.07	.10	.03	.22	62	<10	<1
540 -541	164.6-164.9	32	30	80	1.03	.02	.10	.05	.11	360	<10	<1
541 -542	164.9-165.2	19	<10	90	2.18	<.01	.38	.07	.70	340	10	<1
Well 16												
510 -511.5	155.4-155.9	3	30	40	4.39	.64	.12	.03	.52	32	<10	<1
511.5-513	155.9-156.4	4	10	<10	.31	.04	.05	.04	.34	2	<10	<1
513 -514	156.4-156.7	19	30	40	.82	<.01	.06	.04	.36	2	<10	<1
514 -515	156.7-157.0	20	40	140	.64	.02	.09	.06	.35	1	<10	<1
515 -516	157.0-157.3	17	30	140	.20	.01	.08	.06	.24	<1	<10	<1
516 -517	157.3-157.6	20	50	220	.11	<.01	.05	.06	.19	<1	<10	<1
517 -518	157.6-157.9	59	80	310	.09	<.01	.04	.07	.20	<1	<10	<1
518 -519	157.4-158.2	175	160	1,600	.93	<.01	.07	.06	.19	<1	<10	<1
519 -520	158.2-158.5	101	170	490	.11	.02	.04	.06	.19	<1	<10	<1
520 -521.5	158.5-159.0	134	250	270	.06	<.01	.04	.07	.16	<1	<10	<1
521.5-523	159.0-159.4	444	420	2,800	.91	<.01	.20	.08	.36	16	<10	<1
523 -524	159.4-159.7	893	650	3,700	1.70	.07	.42	.09	.60	12	25	<1
524 -525	159.7-160.0	856	570	2,800	.75	.03	.06	.05	.23	1	<10	<1
525 -526	160.0-160.3	519	330	980	.16	.02	.04	.07	.16	<1	<10	<1
526 -527	160.3-160.6	1,620	1,220	2,100	.16	.05	.05	.07	.18	<1	<10	<1
527 -528	160.6-160.9	1,900	1,540	3,500	.25	<.01	.05	.06	.20	<1	<10	<1
528 -529	160.9-161.2	1,830	1,520	9,300	1.42	.06	.18	.06	.39	<1	10	10
529 -530.5	161.2-161.7	537	520	4,100	.11	.03	.05	.07	.14	<1	<10	<1
530.5-532	161.7-162.1	1,040	990	6,300	.15	.04	.02	.08	.14	<1	<10	<1
532 -533	162.1-162.5	311	590	4,300	.08	<.01	.04	.07	.14	<1	<10	<1
533 -534	162.5-162.8	1,060	1,320	5,400	.09	<.01	.05	.08	.16	<1	<10	<1
534 -535	162.8-163.1	968	970	4,400	.12	.02	.05	.08	.13	<1	<10	<1
535 -536	163.1-163.4	837	1,450	7,200	.11	.03	.04	.08	.17	<1	<10	<1
536 -537.5	163.4-163.8	383	880	8,500	.12	<.01	.06	.07	.17	<1	<10	<1
538 -539.5	164.0-164.4	331	500	3,200	.23	.01	.12	.04	.30	4	<10	<1
539.5-541	164.4-164.9	59	70	270	1.30	<.01	.31	.05	.57	35	10	<1
541 -542	164.9-165.2	41	40	90	1.35	<.01	.36	.06	.74	226	10	<1
Well 17												
511 -512.5	155.7-156.2	10	10	125	16.4	.80	-	.02	.66	<1	<10	<1
512.5-514	156.2-156.7	<10	20	60	.25	<.01	-	.02	.31	<1	<10	<1
514 -515	156.7-157.0	<10	30	60	.29	.02	-	.02	.31	<1	<10	<1
515 -516	157.0-157.3	10	20	70	.63	<.01	-	.02	.31	44	<10	<1
516 -517	157.3-157.6	20	30	95	.44	<.01	-	.04	.28	2	<10	<1
517 -518	157.6-157.9	20	50	100	.15	<.01	-	.02	.18	<1	<10	<1
518 -519.5	157.9-158.3	40	50	125	.11	<.01	-	.04	.14	<1	<10	<1
519.5-520.5	158.3-158.6	60	130	210	.17	<.01	-	.07	.15	<1	10	<1
521 -521.5	158.8-159.0	750	770	600	.58	<.01	-	.05	.20	1	<10	<1
521.5-523	159.0-159.4	840	810	505	.06	<.01	-	.005	.13	<1	<10	<1

TABLE I. - Core Analysis--continued

Depth, ft	Depth, m	U ₃ O ₈ , ppm	yeU ₃ O ₈ , ppm	V ₂ O ₅ , ppm	Total C, pct	C in CO ₂ , pct	S, pct	SO ₄ , pct	Total Fe, pct	Mo, ppm	As, ppm	Se, ppm
Well 17 cont.												
523 -524	159.4-159.7	1,020	1,050	420	.06	<.01	-	.008	.11	<1	<10	<1
524 -525	159.7-160.0	350	450	290	.05	.02	-	.007	.10	<1	<10	<1
525 -526	160.0-160.3	320	570	290	.04	<.01	-	.008	.13	<1	<10	<1
526 -527	160.3-160.6	250	230	1,100	.58	.01	-	.008	.13	<1	<10	<1
527 -528	160.6-160.9	300	230	1,900	.15	<.01	-	.006	.17	<1	<10	<1
528 -529	160.9-161.2	160	170	920	.10	<.01	-	.006	.11	<1	<10	<1
529 -530.5	161.2-161.7	550	520	190	.09	<.01	-	.007	.13	<1	<10	7
530.5-532	161.7-162.1	1,250	1,390	480	.23	<.01	-	.008	.13	<1	<10	20
532 -533	162.1-162.5	1,670	1,640	2,100	1.01	<.01	-	.007	.17	<1	<10	400
533 -534	162.5-162.8	170	260	380	.12	<.01	-	.007	.11	<1	<10	121
534 -535	162.8-163.1	390	270	125	.07	<.01	-	.007	.12	<1	<10	139
535 -536	163.1-163.4	660	640	160	.12	<.01	-	.007	.13	<1	<10	39
536 -537	163.4-163.7	730	-	730	.09	<.01	-	.006	.13	<1	<10	<1
537 -538	163.7-164.0	1,020	740	2,400	.14	<.01	-	.006	.20	<1	10	1
538 -539	164.0-164.3	1,560	860	2,900	.16	<.01	-	.007	.11	<1	10	<1
539 -540	164.3-164.6	2,100	1,530	6,500	.47	<.01	-	.009	.21	1	10	47
540 -541	164.6-164.9	960	640	2,500	.20	<.01	-	.007	.12	1	10	<1
541 -542.5	164.9-165.3	160	180	790	.11	<.01	-	.006	.21	23	10	<1
543 -544	165.5-165.8	80	60	180	.93	.02	-	.017	3.20	127	135	9
544 -545	165.8-166.1	50	60	85	3.63	.06	-	.008	1.04	22	15	<1
Well 19												
510 -511	155.4-155.7	15	30	90	.21	.05	.04	.05	.16	2	<10	<1
511 -512	155.7-156.1	25	40	90	.09	.03	.05	.04	.16	2	<10	<1
512 -513	156.1-156.4	35	30	100	.13	.05	.08	.04	.15	1	<10	<1
513 -514	156.4-156.7	65	30	90	.08	<.01	.03	.05	.15	<1	<10	<1
514 -515	156.7-157.0	105	70	80	.07	<.01	.05	.04	.14	<1	<10	<1
515 -516	157.0-157.3	150	110	100	.03	<.01	.04	.04	.14	<1	<10	<1
516 -517	157.3-157.6	195	150	70	.06	.01	.03	.05	.14	<1	<10	<1
517 -518	157.6-157.9	610	380	600	1.02	<.01	.09	.06	.14	<1	<10	<1
518 -519	157.9-158.2	320	220	180	.30	.05	.02	.05	.12	1	<10	<1
519 -520	158.2-158.5	320	260	110	.13	.01	.04	.05	.12	2	<10	<1
520 -521	158.5-158.8	475	340	130	.20	<.01	.08	.05	.13	2	<10	<1
521 -522	158.8-159.1	845	580	220	.38	<.01	.04	.05	.14	1	<10	<1
522 -523	159. -159.4	560	420	170	.27	.08	.03	.05	.12	1	<10	<1
523 -524	159.4-159.7	515	520	150	.14	.03	.06	.05	.14	2	<10	<1
524 -525	159.7-160.0	380	440	180	.09	<.01	.03	.05	.12	2	<10	<1
525 -526	160.0-160.3	485	710	620	.09	.04	.05	.05	.14	1	<10	<1
526 -527	160.3-160.6	275	580	1,300	.08	.05	.09	.05	.17	2	<10	<1
527 -528	160.6-160.9	170	480	2,500	.08	.02	<.01	.06	.13	<1	<10	<1
528 -529	160.9-161.2	95	340	3,800	.11	.06	.05	.06	.14	<1	<10	<1
529 -530	161.2-161.5	75	330	3,300	.09	.03	.03	.06	.12	1	<10	<1
530 -531	161.5-161.8	75	270	1,500	.10	.05	.06	.05	.15	1	<10	<1
531 -532.5	161.8-162.3	175	490	1,000	.05	<.01	.05	.05	.13	1	<10	<1
533 -534	162.3-162.8	500	400	200	.13	<.01	.09	.05	.19	1	<10	<1
534 -535	162.8-163.1	85	90	70	.07	<.01	.05	.04	.16	1	<10	<1
535 -536	163.1-163.4	55	70	50	.02	<.01	.10	.04	.19	30	<10	<1
536 -537	163.4-163.7	20	40	50	.10	<.01	.37	.04	.48	48	10	<1
537 -538	163.7-164.0	55	30	50	.70	.01	.10	.04	.29	91	<10	<1
538 -539	164.0-164.3	15	20	80	1.75	<.01	.18	.04	.51	262	<10	1

TABLE 2. - Core Analyses, Composite Samples

	Sample 1.		Sample 2.
	ppm	pcr	ppm
Na	2,720	0.05	2,910
K	6,510	.2	7,000
Ca	890	.06	940
Mg	960	.05	720
V	2,130	.06	2,090
Al	2,370	1.3	2,970
Fe (total)	29	.13	30
SiO ₂	79 pcr	92.	88 pcr
Cation exchange capacity.....	5.10 meq/100 g.		10 meq/100 g.

TABLE 3. - Water analyses, Well OB1

Preferable →

Date	pH	Cl ₂ , mV	Conductivity, micro/cm	TDS, ppm	U ₃ O ₈ , ppm	V, ppm	Na, ppm	K, ppm	Ca, ppm	Mg, ppm	SO ₄ , ppm	Cl, ppm	Si, ppm	Al, ppm	P, ppm	F, ppm	Fe, ppm	Mn, ppm	Ni, ppm	As, ppb	Se, ppb	HCO ₃ , ppm	D.O., ppm
11/30	6.7	-120	3,400	3,400	0.1	0.5	740	11	150	92	2,300	50	5	<1	<0.2	0.5	0.4	0.3	4	<40	<2	250	-
12/01	6.7	-	3,400	3,400	.2	.5	740	11	150	96	2,300	50	5	<1	<.2	.5	.6	.3	12	<40	<2	-	-
12/02	6.7	-	3,400	-	.2	.5	740	11	150	96	-	50	5	<1	<.2	.5	.7	.3	12	<40	<2	-	-
12/03	6.7	-	3,400	3,400	.2	.5	740	11	151	96	2,300	50	5	<1	<.2	.5	.8	.3	12	<40	<2	-	-
12/04	6.7	-	3,400	3,600	.1	.5	740	11	153	96	2,300	50	5	<1	<.2	.5	1.0	.3	7	<40	-	-	-
12/05	6.5	-	3,400	3,600	.1	.5	740	12	154	97	2,300	50	6	<1	<.2	.5	1.0	.3	6	<40	4	200	-
12/06	6.4	-	3,400	3,600	.1	.5	740	12	155	98	2,300	50	6	<1	<.2	.5	1.0	.4	5	<40	<2	190	-
12/07	6.3	-120	3,400	3,700	.1	.5	740	12	156	99	2,300	50	7	<1	<.2	.5	1.0	.4	3	<40	<2	190	-
12/08	6.1	-110	3,400	3,700	.1	.5	740	12	158	100	2,300	50	8	<1	<.2	.5	1.0	.4	2	<40	<2	150	-
12/09	5.9	-100	3,400	3,700	.2	.5	740	12	159	102	2,300	50	10	<1	<.2	.5	1.0	.4	2	<40	<2	130	-
12/10	5.9	-90	3,400	3,700	.2	.5	740	12	160	102	2,300	50	11	<1	<.2	.5	1.2	.4	2	<40	<2	110	-
12/11	5.9	-80	3,400	3,700	.2	.5	740	12	161	103	2,300	50	11	<1	<.2	.5	1.3	.4	2	<40	<2	100	-
12/12	5.9	-70	3,400	3,700	.2	1.0	740	12	162	104	2,300	50	11	<1	<.2	.5	1.4	.4	2	<40	<2	90	-
12/13	5.8	-50	3,400	3,700	-	1.8	740	-	163	105	2,300	50	12	<1	<.2	.5	-	-	-	<40	-	90	-
12/14	5.7	-40	3,400	3,800	.3	2.3	740	12	165	106	2,300	50	12	1	<.2	.5	1.5	.4	2	<40	<2	90	-
12/15	5.7	-20	3,400	3,800	.4	3.0	740	12	166	107	2,300	50	13	1	<.2	.5	1.5	.4	2	<40	<2	90	-
12/16	5.6	-10	3,400	3,800	.5	3.5	740	12	167	107	2,300	49	13	1	<.2	.5	1.5	.4	<2	<40	<2	70	-
12/17	5.5	0	3,400	3,800	.7	4.2	740	12	168	107	2,300	48	13	-	<.2	.6	1.5	.4	<2	<40	<2	80	-
12/18	5.4	+10	3,400	3,800	.8	4.9	740	12	169	107	2,300	46	13	1	<.2	.6	1.5	.4	<2	<40	<2	50	-
12/19	5.4	+20	3,400	3,800	1.0	5.6	740	12	170	107	2,300	45	13	1	<.2	.6	1.6	.4	<2	<40	<2	60	-
12/20	5.4	+30	3,500	3,800	1.3	6.4	740	12	172	107	2,300	45	13	1	<.2	.6	1.6	.4	<2	<40	<2	60	-
12/21	5.4	+40	3,500	3,800	1.7	7.3	740	12	175	107	2,300	45	13	1	<.2	.6	1.8	.4	<2	<40	<2	50	-
12/22	5.2	+50	3,500	3,900	1.6	8.1	740	12	177	107	2,300	45	13	1	<.2	.6	1.8	.5	<2	<40	<2	50	-
12/23	5.1	+50	3,500	3,900	2.1	9.0	740	12	179	107	2,300	47	13	1	<.2	.6	1.8	.5	<2	<40	<2	50	-
12/24	5.0	+50	3,500	3,900	2.3	10	740	12	180	107	2,300	48	13	1	<.2	.6	1.8	.5	<2	<40	<2	50	-
12/25	4.9	+60	3,500	3,900	2.9	11	740	12	181	107	2,300	48	13	1	<.2	.6	1.8	.5	<2	<40	<2	50	-
12/26	4.9	+50	3,500	-	-	-	740	-	182	107	2,300	48	13	1	<.2	.6	-	-	-	-	-	30	-
12/27	4.9	+50	3,500	3,900	3.0	12	740	12	182	107	2,300	48	13	1	<.2	.6	1.8	.5	<2	<40	<2	30	-
12/28	4.9	+40	3,500	3,900	3.1	12	740	12	183	107	2,300	48	13	1	<.2	.6	1.8	.5	<2	<40	<2	30	-
12/29	4.9	+40	3,500	3,900	3.4	12	740	12	184	107	2,300	48	14	1	<.2	.6	1.8	.5	<2	<40	<2	30	-
12/30	4.9	+40	3,500	3,900	4.3	17	740	12	185	107	2,300	47	15	1	<.2	.6	1.8	.5	<2	<40	<2	30	-
12/31	4.9	+50	3,500	3,900	4.4	18	740	12	190	109	2,400	47	16	2	<.2	.6	1.8	.5	<2	<40	<2	30	-
01/01	4.2	+90	3,500	4,100	5.7	20	740	13	200	125	2,500	46	17	2	<.2	.6	1.9	.5	2	<40	<2	-	-
01/01	3.2	-	3,800	4,300	9.4	28	740	14	211	130	2,700	46	18	3	<.2	.6	2.1	.5	2	<40	<2	-	-
01/02	2.8	+100	4,000	4,500	17.	48	740	14	214	146	2,900	46	19	4	<.2	.6	2.8	.6	2	<40	<2	-	-
01/02	2.7	-	4,300	4,800	21	69	740	15	217	150	3,100	46	20	6	<.2	.7	3.2	.6	2	<40	<2	-	-
01/03	2.6	+120	4,500	4,800	26	75	740	16	219	152	3,200	45	21	8	.2	.8	3.5	.6	2	<40	<2	-	-
01/04	2.5	+130	5,000	5,000	32	90	740	17	225	154	3,300	45	23	11	.3	0.9	4.5	.6	4	<40	<2	-	-
01/05	2.4	+140	5,600	5,300	37	100	740	19	230	154	3,400	45	25	17	.4	1.0	5.4	.7	5	<40	<2	-	-
01/06	2.0	+150	7,600	5,800	52	-	740	19	235	152	3,900	45	27	28	.6	1.1	7.0	.7	6	<40	<2	-	-
01/07	1.9	+160	8,300	6,100	46	100	740	20	237	150	4,400	45	29	36	.6	1.1	8.1	.7	7	<40	<2	-	-
01/08	2.1	+170	7,500	6,300	46	100	740	18	241	150	4,000	45	31	36	.6	1.0	8.9	.7	7	<40	<2	-	-

01/09	2.2	+180	7,000	6,100	39	100	740	18	244	150	4,000	45	33	32	.5	1.0	9.1	.7	6	<40	<2	-	-
01/10	2.3	+190	7,000	5,900	40	100	740	18	248	154	4,100	45	35	32	.5	1.0	9.9	.8	5	<40	<2	-	-
01/11	2.2	+200	7,000	6,100	39	100	750	18	250	155	4,100	45	37	32	.4	1.2	9.9	.8	4	<40	<2	-	-
01/12	2.1	+200	8,400	6,300	44	110	760	18	252	156	4,200	45	38	31	.4	1.2	10.0	.8	4	<40	<2	-	-
01/13	1.9	+210	10,000	6,900	57	110	780	18	256	156	4,500	45	39	30	.5	1.2	11	.9	3	40	<2	-	-
01/14	1.9	+210	10,800	7,200	64	120	790	18	258	155	4,700	45	40	32	.5	1.3	12	.9	3	40	<2	-	-
01/15	1.9	+220	11,500	7,300	63	120	790	19	261	155	4,800	45	42	34	.5	1.3	12	.9	3	<40	<2	-	-
01/16	1.9	+220	11,900	7,400	53	120	800	19	264	155	5,000	45	43	35	.6	1.3	12	.9	3	<40	<2	-	-
01/17	1.9	+220	12,200	7,400	53	130	800	20	266	155	5,100	45	44	36	.6	1.3	13	.9	3	40	<2	-	-
01/18	1.9	+230	12,200	7,400	52	130	800	20	268	155	5,100	46	45	36	.6	1.3	13	.9	3	40	<2	-	-
01/19	1.9	+230	12,200	7,300	50	130	810	20	272	156	5,100	46	46	38	.6	1.3	13	.9	3	40	<2	-	-
² 01/19	1.9	-	12,200	7,300	49	130	810	20	273	159	5,100	47	47	38	.6	1.3	13	.9	3	40	<2	-	-
01/20	1.9	+230	12,200	7,300	45	140	810	20	274	162	5,100	47	47	38	.6	1.3	13	.9	3	40	<2	-	-
² 01/20	1.9	-	12,200	7,300	43	140	810	20	276	164	5,100	47	48	38	.6	1.3	13	.9	4	<40	<2	-	-
01/21	1.9	+230	12,200	7,300	42	140	810	20	280	166	5,100	48	49	38	.6	1.3	13	.9	5	<40	<2	-	-
² 01/21	1.9	-	12,100	7,400	47	140	810	20	285	167	5,100	48	49	42	.6	1.3	13	1.0	6	40	<2	-	-
01/22	1.9	+230	12,000	7,400	43	140	810	20	295	168	5,100	48	50	43	.6	1.3	13	1.0	6	40	<2	-	-
² 01/22	1.9	-	11,900	7,400	46	140	810	20	302	169	5,100	48	51	44	.6	1.3	13	1.0	6	<40	<2	-	-
01/23	1.9	+230	11,900	7,500	43	140	800	20	310	169	5,100	49	52	45	.6	1.3	14	1.0	6	40	<2	-	-
01/24	1.9	+230	11,800	7,900	46	150	730	20	325	169	5,100	49	53	46	.5	1.4	14	1.0	7	<40	<2	-	-
01/25	1.9	+240	11,600	8,500	49	150	720	20	310	169	5,100	49	53	46	.5	1.5	14	1.0	8	<40	2	-	-
01/26	1.9	+240	11,500	8,600	44	150	720	20	297	167	5,100	49	53	46	.5	1.5	14	1.0	8	40	2	-	-
01/27	1.8	+240	11,400	8,600	50	150	720	20	290	166	5,100	49	53	46	.5	1.5	14	1.0	8	<40	2	-	-
01/28	1.8	+240	11,400	8,500	46	150	720	20	283	164	5,100	49	53	45	.5	1.5	14	1.0	8	<40	<2	-	1.8
01/29	1.8	+240	11,400	8,400	43	150	720	20	280	163	5,100	49	52	45	.5	1.5	14	1.0	8	<40	<2	-	1.6
01/30	1.8	+250	11,400	7,900	48	150	720	20	277	162	5,100	49	50	45	.5	1.5	14	1.0	8	<40	4	-	1.4
01/31	1.8	+250	11,400	7,700	44	150	720	20	275	161	5,100	49	49	45	.5	1.5	14	1.0	8	<40	2	-	1.2
02/01	1.8	+250	11,400	7,500	41	150	720	20	273	160	5,100	48	47	44	.5	1.5	14	1.0	8	60	<2	-	.5
02/02	1.8	+250	11,400	7,100	36	150	760	19	271	160	5,100	46	46	44	.3	1.3	15	1.0	8	20	<2	-	.7
02/04	1.8	+250	11,400	7,100	35	150	760	19	268	160	5,100	45	44	44	.3	1.3	16	1.0	8	20	2	-	2.3
02/11	1.8	+240	11,400	7,300	36	170	750	18	264	160	5,300	45	43	46	.2	1.3	17	.9	10	20	2	-	1.7
02/18	1.9	+240	10,500	-	44	210	760	18	260	156	5,000	-	43	48	.2	-	19	.9	6	30	<2	-	1.2
02/25	2.0	+240	9,600	7,800	107	370	720	17	254	156	5,100	44	44	49	.5	1.7	21	1.1	26	70	<2	-	1.0
03/04	2.1	+230	8,400	6,900	59	480	750	17	230	122	4,200	39	44	39	.8	1.5	16	.9	14	40	2	-	1.3
03/11	2.5	+170	7,300	6,600	62	490	750	17	220	125	3,900	49	41	36	.7	1.5	16	.9	12	40	4	-	1.0
03/20	2.5	+130	5,900	7,000	79	500	790	17	225	135	4,000	50	47	43	1.0	1.4	20	1.0	14	100	<2	-	1.0
03/28	2.4	+440	6,100	7,300	96	530	760	19	235	140	4,200	49	59	54	1.8	1.5	31	1.0	28	260	<2	-	5.0
04/04	2.3	+190	6,000	7,300	82	520	760	18	235	137	4,200	46	60	52	1.6	1.5	39	1.0	14	180	4	-	2.7
04/12	1.8	+360	9,600	9,200	131	820	740	20	260	150	5,900	47	94	85	4.2	1.5	-	1.3	52	780	<2	-	-

¹ Preleach data.

² Measured in the afternoon.

NOTE.--Dash indicates not measured.

TABLE 4. - Water Analyses, Well 0B3

Date	pH	Ek, mV	Conduc-tivity, μ mho/cm	TDS, ppm	U_3O_8 , ppm	V, ppm	Na, ppm	K, ppm	Ca, ppm	Mg, ppm	SO ₄ , ppm	Cl, ppm	Si, ppm	Al, ppm	P, ppm	F, ppm	Fe, ppm	Mn, ppm	Mo, ppb	As, ppb	Se, ppb	HCO ₃ , ppm	D.O., ppm
(P)	6.7	-120	3,400	3,400	0.1	0.5	740	12	150	92	2,200	50	5	<1	<0.2	0.5	0.5	0.3	4	<40	<2	260	-
12/08	5.7	-110	3,400	3,600	1.5	1.0	740	12	151	102	2,200	50	12	1	<0.2	.7	1.1	.4	2	<40	<2	70	-
12/09	5.5	-100	3,400	3,600	2.3	1.5	740	12	152	103	2,200	50	12	1	<0.2	.7	1.1	.4	<2	<40	<2	51	-
12/10	5.4	-90	3,400	3,700	3.4	2.0	740	12	153	104	2,200	50	12	1	<0.2	.7	1.2	.4	2	<40	<2	51	-
12/11	5.3	-80	3,400	3,700	7.0	3.0	740	12	154	104	2,200	49	12	1	<0.2	.7	1.2	.4	2	<40	<2	30	-
12/12	5.2	-70	3,400	3,700	7.5	3.5	740	12	155	104	2,200	49	12	1	<0.2	.7	1.2	.4	<2	<40	<2	21	-
12/13	5.1	-60	3,400	3,800	8.0	4.0	740	12	156	105	2,200	49	13	1	<0.2	.7	1.2	.4	<2	<40	<2	-	-
12/14	4.9	-40	3,400	3,800	8.5	4.1	740	12	157	105	2,200	48	13	1	<0.2	.7	1.2	.4	<2	<40	<2	5	-
12/15	4.6	-10	3,400	3,800	8.7	4.9	740	12	158	105	2,200	48	13	2	<0.2	.7	1.2	.4	<2	<40	<2	-	-
12/16	4.3	+50	3,400	3,800	8.8	5.0	740	12	159	106	2,200	48	14	2	<0.2	.7	1.3	.4	<2	<40	<2	-	-
12/17	4.1	+100	3,400	3,800	8.8	5.5	740	12	160	106	2,200	48	14	2	<0.2	.7	1.3	.4	<2	<40	<2	-	-
12/18	3.9	+150	3,400	3,800	8.8	5.9	740	12	162	106	2,200	48	14	2	<0.2	.7	1.4	.4	<2	<40	<2	-	-
12/19	3.8	+190	3,500	3,800	8.8	5.8	740	12	163	106	2,200	48	14	2	<0.2	.7	1.5	.4	<2	<40	<2	-	-
12/20	3.7	+240	3,500	3,800	9.0	6.3	740	12	163	106	2,200	48	14	3	<0.2	.7	1.6	.4	<2	<40	<2	-	-
12/21	3.6	+270	3,500	3,800	9.7	6.6	740	12	164	106	2,200	48	14	3	<0.2	.7	1.7	.4	<2	<40	<2	-	-
12/22	3.6	+280	3,500	3,900	10	6.5	740	12	165	106	2,200	47	14	3	<0.2	.6	1.7	.5	2	<40	<2	-	-
12/23	3.6	+290	3,500	3,900	10	5.8	740	12	166	106	2,200	47	14	3	<0.2	.6	1.7	.5	2	<40	<2	-	-
12/24	3.6	+290	3,500	3,900	10	5.8	740	12	167	106	2,200	47	14	3	<0.2	.5	1.7	.5	<2	<40	<2	-	-
12/25	3.6	+290	3,500	4,000	9.8	5.7	740	12	168	107	2,200	47	14	3	<0.2	.5	1.7	.5	<2	<40	<2	-	-
12/26	3.6	+290	3,500	4,000	9.5	6.0	740	12	170	107	2,200	47	14	3	<0.2	.5	1.7	.5	<2	<40	<2	-	-
12/27	3.6	+290	3,500	3,900	8.8	6.4	740	12	172	107	2,200	47	14	3	<0.2	.5	1.7	.5	<2	<40	<2	-	-
12/28	3.6	+280	3,500	3,900	8.3	6.0	740	12	174	107	2,300	47	14	2	<0.2	.5	1.8	.5	<2	<40	<2	-	-
12/29	3.6	+270	3,600	3,900	7.8	6.0	740	12	175	108	2,400	46	14	2	<0.2	.5	1.8	.5	<2	<40	<2	-	-
12/30	3.6	+250	3,600	3,900	7.7	7.5	740	12	178	109	2,500	45	16	3	<0.2	.4	2.0	.5	<2	<40	<2	-	-
12/31	3.6	+240	3,600	3,900	7.8	11.0	740	12	182	112	2,800	44	17	3	<0.2	.4	2.0	.5	<2	<40	<2	-	-
01/01	3.0	+220	3,900	4,300	12	17	740	12	186	134	3,000	44	18	5	<0.2	.5	2.5	.5	<2	<40	<2	-	-
01/01	2.6	+220	4,800	4,600	24	34	740	14	191	147	3,100	44	18	7	<0.2	.5	4.6	.6	<2	<40	<2	-	-
01/02	2.4	+210	5,400	5,000	29	48	740	16	196	148	3,200	43	19	10	0.2	.5	7.5	.6	2	<40	<2	-	-
01/02	2.2	+200	5,800	5,200	31	58	740	17	204	142	3,300	43	20	12	.2	.5	6.8	.6	2	<40	<2	-	-
01/03	2.1	+200	6,500	5,200	30	57	740	17	210	134	3,400	43	21	13	.2	.5	6.3	.6	2	<40	<2	-	-
01/04	2.1	+190	6,800	5,200	23	48	740	17	218	132	3,600	43	23	14	.3	.5	5.3	.6	2	<40	<2	-	-
01/05	2.0	+170	7,200	5,200	23	46	740	17	220	133	4,000	43	25	15	.3	.5	5.0	.6	2	<40	<2	-	-
01/06	1.6	+150	12,600	6,900	66	63	740	17	224	134	6,200	50	27	27	.7	.5	6.0	.6	10	40	<2	-	-
01/07	1.7	+140	9,860	6,300	43	69	740	17	228	136	4,500	44	29	19	.6	.5	6.6	.6	8	40	<2	-	0.5
01/08	1.9	+130	8,400	5,800	38	70	740	17	232	138	4,000	44	30	16	.5	.5	7.0	.7	4	40	<2	-	.5
01/09	1.9	+120	8,300	5,700	38	74	740	17	237	140	4,000	45	31	15	.5	.6	8.6	.7	4	40	<2	-	.5
01/10	1.9	+120	8,200	5,800	39	81	740	17	240	148	4,000	45	32	15	.5	.8	10.0	.7	4	40	<2	-	.5
01/11	1.9	+110	8,160	6,100	43	86	740	17	247	153	4,100	46	34	16	.5	.9	11	.7	4	40	<2	-	.5
01/12	1.8	+110	10,000	6,400	57	92	750	18	254	154	4,600	46	35	18	.5	1.0	11	.8	4	40	<2	-	.6
01/13	1.8	+110	13,200	7,500	68	93	790	18	259	154	5,200	47	36	22	.6	1.2	12	.8	4	40	<2	-	.8
01/14	1.7	+110	15,400	7,500	67	94	800	18	261	150	5,400	47	38	24	.6	1.3	12	.8	4	60	2	-	1.1
01/15	1.7	+110	13,700	7,400	60	95	800	19	262	150	5,400	48	39	25	.6	1.3	13	.8	3	60	<2	-	1.3
01/16	1.7	+110	13,500	7,400	55	96	800	19	263	152	5,400	48	41	26	.6	1.4	14	.9	3	60	2	-	1.5

Protech →

01/17	1.7	+110	13,400	7,300	50	97	800	19	264	151	5,400	49	42	27	.6	1.4	15	.9	3	60	<2	-	1.5
01/18	1.7	+110	13,400	7,300	46	98	800	20	265	154	5,400	50	43	28	.6	1.4	16	.9	3	80	<2	-	1.3
01/19	1.8	+110	13,300	7,400	44	98	800	20	268	157	5,400	52	45	29	.6	1.4	16	.8	3	80	<2	-	1.7
^a 01/19	1.8	+110	13,300	7,400	43	98	800	20	271	159	5,400	53	46	30	.6	1.4	15	.8	4	80	<2	-	1.6
01/20	1.8	+110	13,300	7,400	42	98	800	21	276	161	5,400	54	46	31	.6	1.4	13	.8	4	60	<2	-	1.7
^a 01/20	1.8	+110	13,300	7,400	40	98	790	21	282	162	5,400	55	47	31	.6	1.3	12	.9	5	40	2	-	1.6
01/21	1.8	+110	13,300	7,500	39	99	790	21	290	162	5,400	56	47	32	.6	1.3	12	.9	5	100	<2	-	2.0
^a 01/21	1.8	+120	13,300	7,500	37	99	790	21	300	163	5,400	57	48	32	.6	1.3	12	.9	5	80	<2	-	1.8
01/22	1.8	+120	13,200	7,500	37	99	780	21	308	163	5,400	57	49	32	.6	1.3	12	.9	6	60	2	-	1.9
^a 01/22	1.8	+120	13,200	7,500	40	99	780	21	315	164	5,400	57	49	33	.6	1.3	12	.9	6	60	<2	-	2.1
01/23	1.8	+120	13,100	7,600	48	99	780	21	322	165	5,400	57	50	33	.6	1.3	12	.9	6	80	<2	-	2.0
01/24	1.8	+130	11,000	8,000	49	100	780	21	315	166	5,400	57	52	33	.6	1.4	12	.9	6	80	<2	-	2.0
01/25	1.8	+130	12,900	8,400	50	100	740	21	306	166	5,400	58	53	33	.6	1.5	13	1.0	7	40	4	-	2.2
01/26	1.8	+130	12,600	8,300	47	100	740	20	298	165	5,400	58	53	33	.6	1.5	14	.9	8	40	<2	-	2.1
01/27	1.7	+140	12,300	8,200	44	100	730	20	291	164	5,400	58	53	33	.6	1.6	16	1.0	8	60	2	-	2.0
01/28	1.7	+140	12,200	7,900	43	100	720	20	284	163	5,400	59	53	33	.6	1.6	17	1.0	8	40	2	-	1.9
01/30	1.7	+150	12,200	7,600	43	100	720	19	270	162	5,400	59	52	34	.6	1.6	16	1.0	8	80	2	-	.5
01/31	1.7	+150	12,200	7,500	41	100	720	19	264	160	5,400	59	50	35	.6	1.6	16	1.0	7	100	<2	-	.6
02/01	1.7	+150	12,200	7,400	39	100	730	18	261	159	5,400	58	48	36	.6	1.6	16	1.0	7	100	2	-	.7
02/02	1.7	+160	12,200	7,300	33	100	750	18	260	158	5,400	50	47	36	<0.2	1.3	18	.9	7	100	2	-	.8
02/04	1.7	+160	12,300	7,200	31	100	750	18	260	157	5,400	46	43	38	<0.2	1.3	20	.9	8	40	2	-	.9
02/11	1.6	+210	13,000	7,100	36	110	750	18	260	156	5,400	45	39	40	.2	1.2	22	.9	12	50	2	-	2.7
02/21	1.8	+300	11,900	7,400	210	160	730	18	-	162	5,400	42	46	49	.4	1.6	34	1.1	6	200	<2	-	1.1
02/25	1.9	+350	11,600	7,900	240	240	710	18	258	163	5,400	41	52	60	3.0	-	44	1.3	60	1,100	<2	-	10.
03/04	2.0	+470	10,700	7,800	140	280	730	22	257	160	5,200	41	66	62	2.4	2.0	62	1.3	66	700	<2	-	24.
03/11	1.9	+430	9,800	7,400	22	410	740	19	257	149	4,700	37	58	50	2.4	1.6	40	1.1	50	260	2	-	1.4
03/20	1.9	+490	8,800	7,900	62	460	750	20	257	161	4,900	38	65	58	3.1	1.7	49	1.1	64	460	2	-	12.
03/28	2.0	+510	7,800	7,700	77	460	750	20	257	150	4,700	35	65	55	2.4	1.7	56	1.1	60	440	<2	-	35.
04/04	2.0	-	7,600	7,700	43	480	750	20	257	150	4,700	41	70	57	2.1	1.7	62	1.1	70	460	8	-	30.
04/12	1.6	+490	12,800	10,800	66	710	730	22	284	160	7,400	41	96	81	4.2	1.7	94	1.3	92	940	<2	-	45.

¹ Preleach data.

² Measured in the afternoon.

NOTE: --Dash indicates not measured.

TABLE 5. - OB3 Downhole Temperature

Date	Temperature	Date	Temperature
Oct. 20 (preleach)	13.6°C	Jan. 3	11.9°C
Dec. 8-9	12.8	4-8	12.0
10	12.7	9-13	12.2
11-12	12.6	14-20	12.3
13-19	12.4	21-26	12.4
20	12.3	Jan. 27-Feb. 1	12.5
21	12.2	Feb. 2	12.6
22	12.1	4-11	12.8
23	12.0	21	13.3
24	11.9	24	14.0
25	11.7	Mar. 4	14.2
26-28	11.6	11-15	13.8
29	11.7	20	14.7
Dec. 30-Jan. 2	11.8	28	14.9
		Apr. 4	15.9
		13	16.4

TABLE 6. - Radium and Thorium Analyses

	Ra226	Th230
Oct. 10, 1977 (preleach)	510 ± 29 pC/l	0.084 ± .005 pC/l
Jan. 19, 1978	10,000 ± 170	49,000 ± 3200

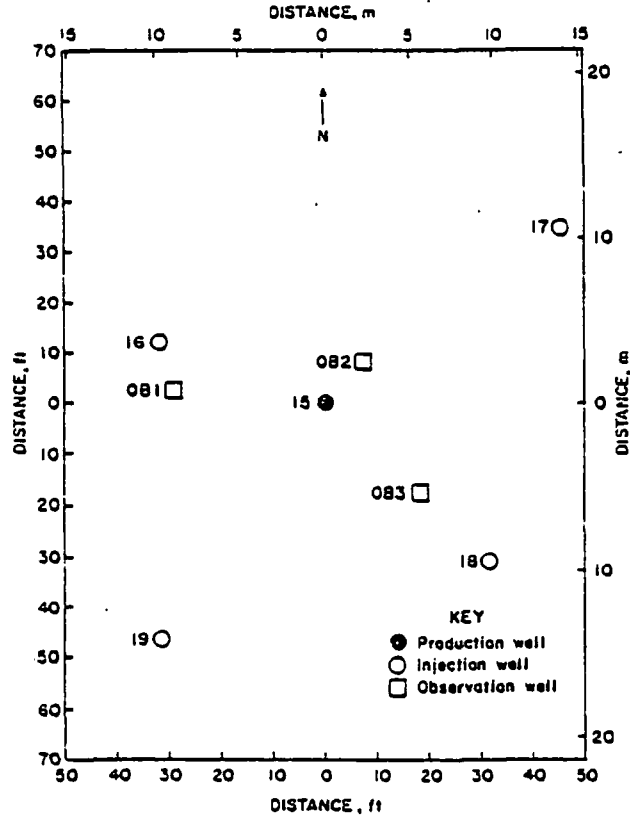


FIGURE 1. - Well field pattern at ore depth.

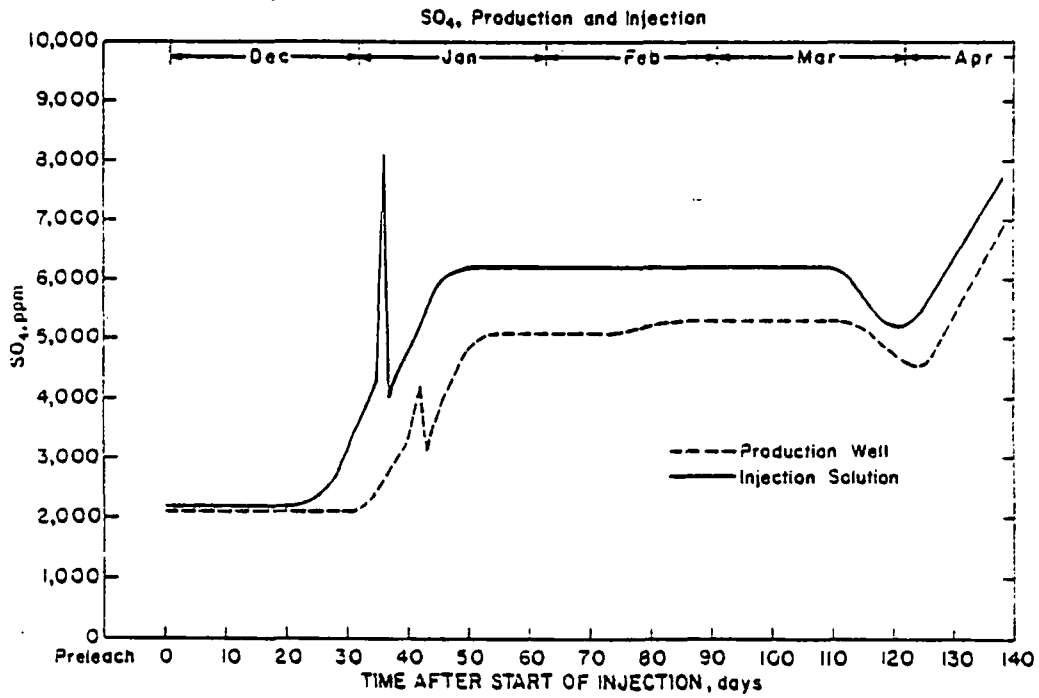


FIGURE 2. - SO₄ Concentrations in injected and produced solutions.

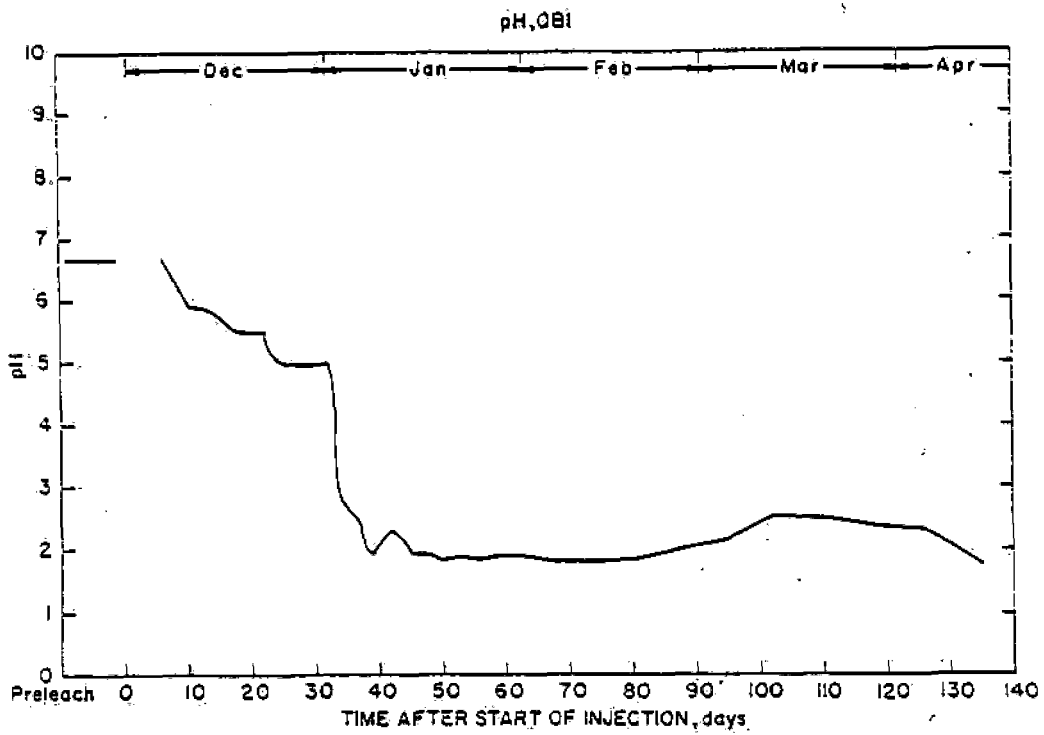


FIGURE 3. - pH in OBI.

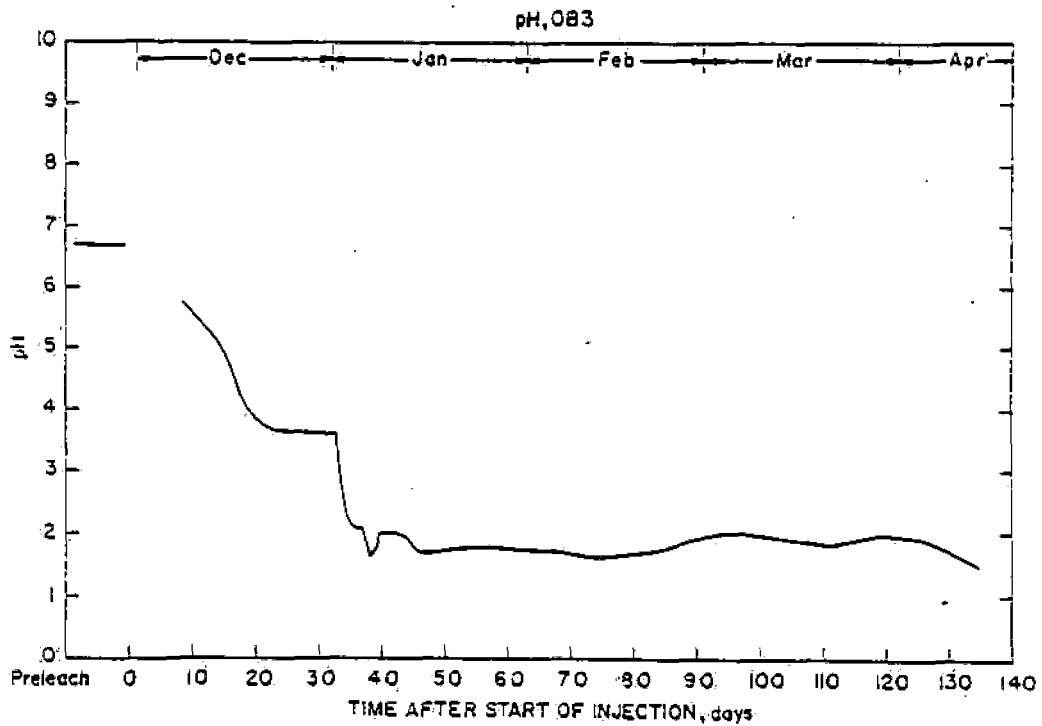


FIGURE 4. - pH in OBS.

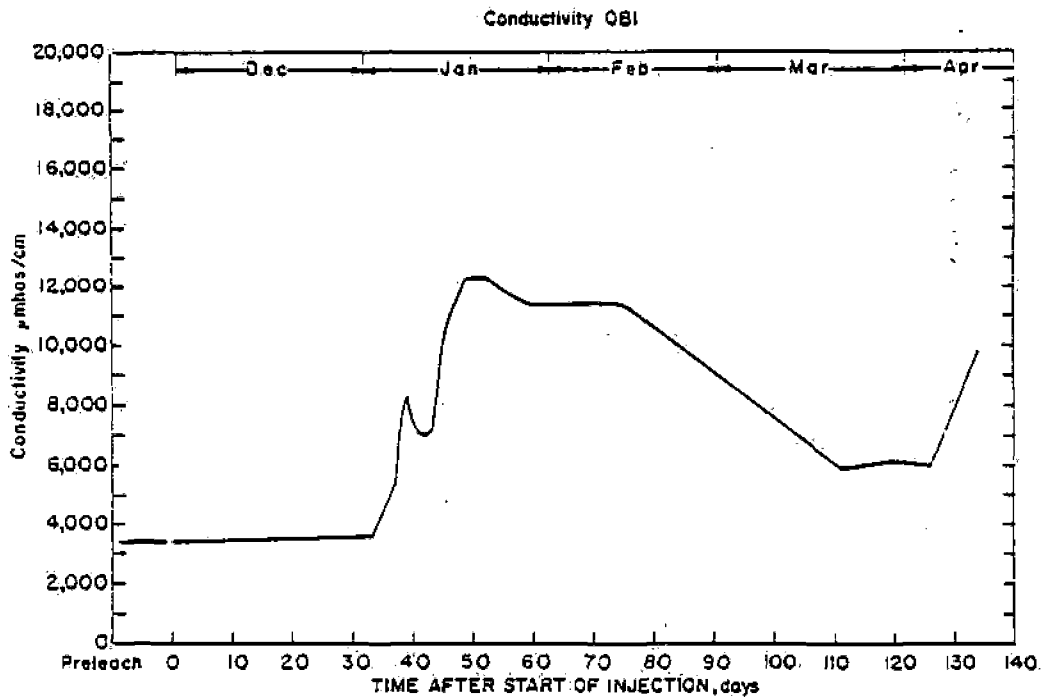


FIGURE 5. - Conductivity in OB1.

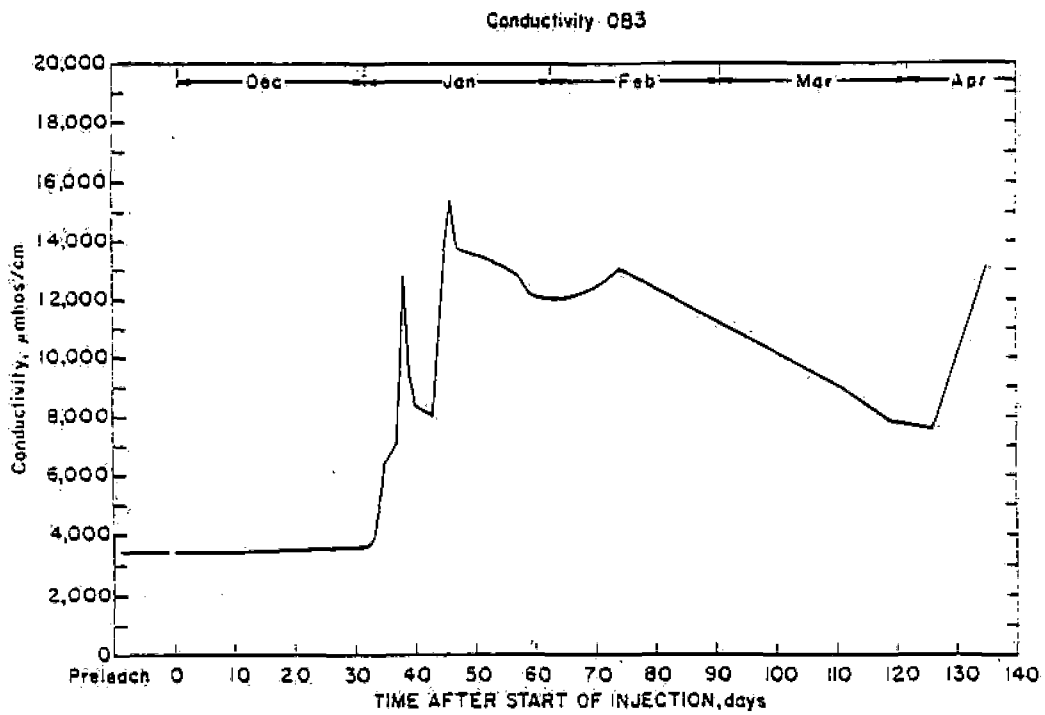


FIGURE 6. - Conductivity in OB3.

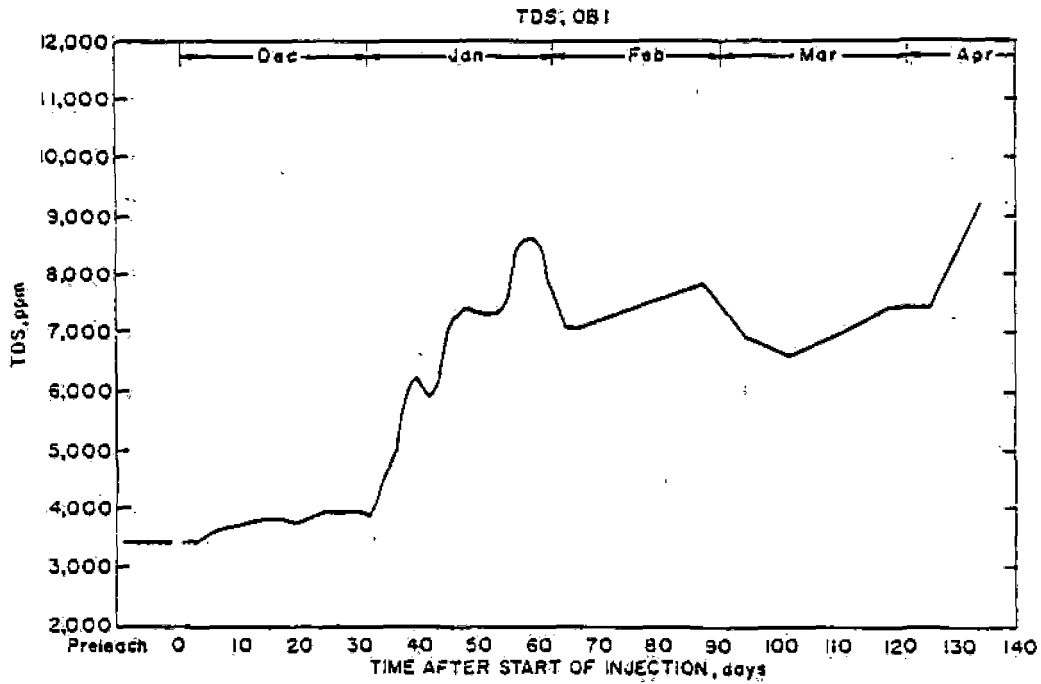


FIGURE 7. - Total dissolved solids in OB1.

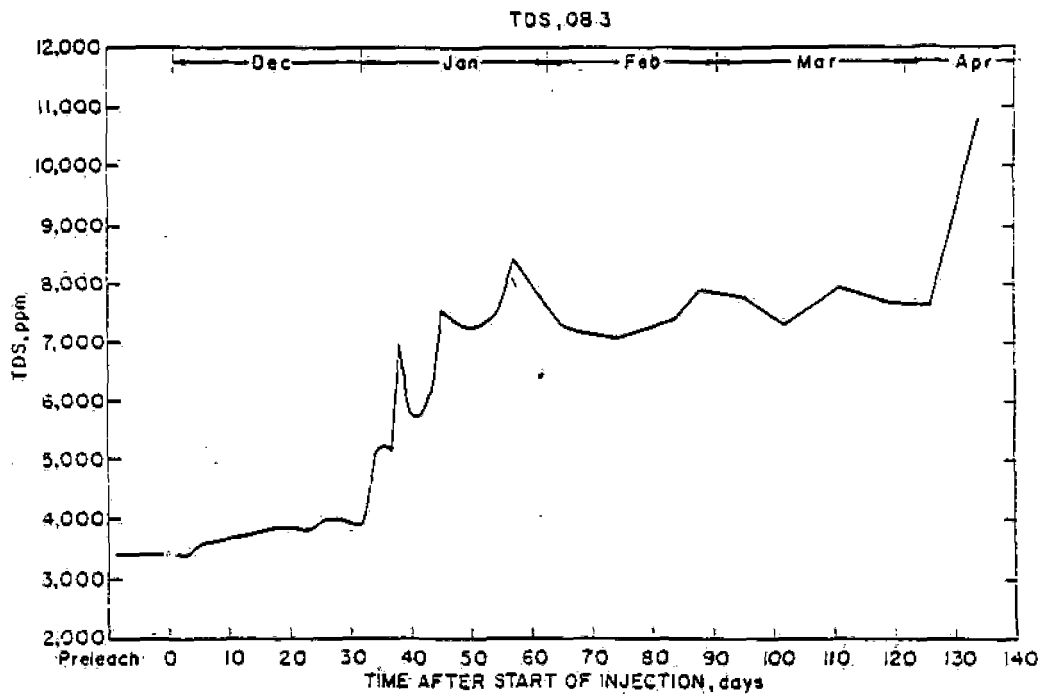


FIGURE 8. - Total dissolved solids in OB3.

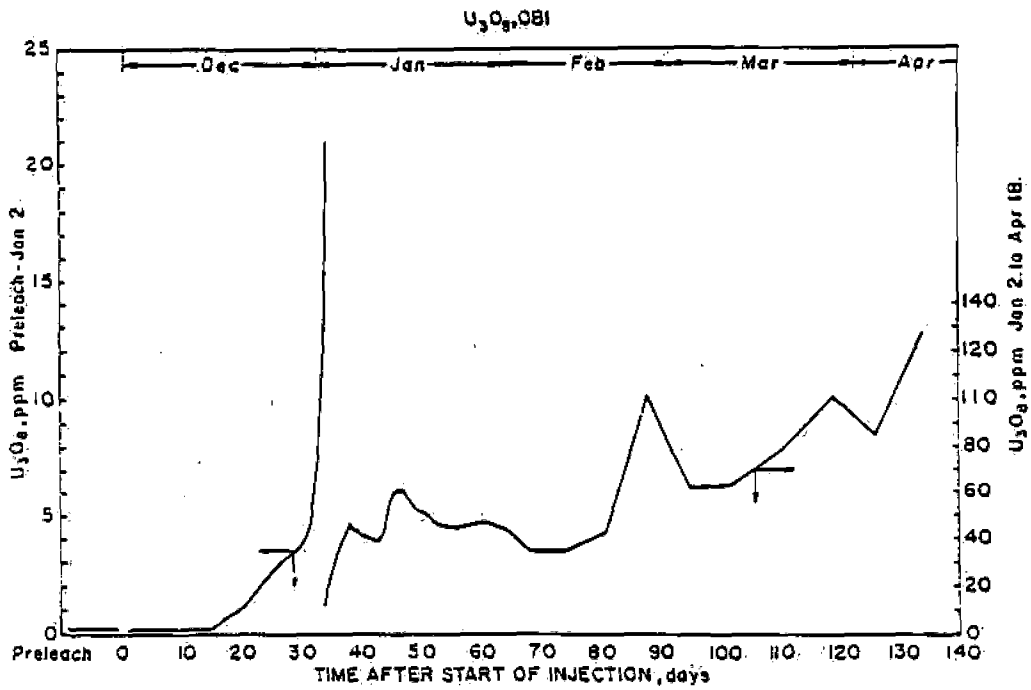


FIGURE 9. - U_3O_8 in OB1.

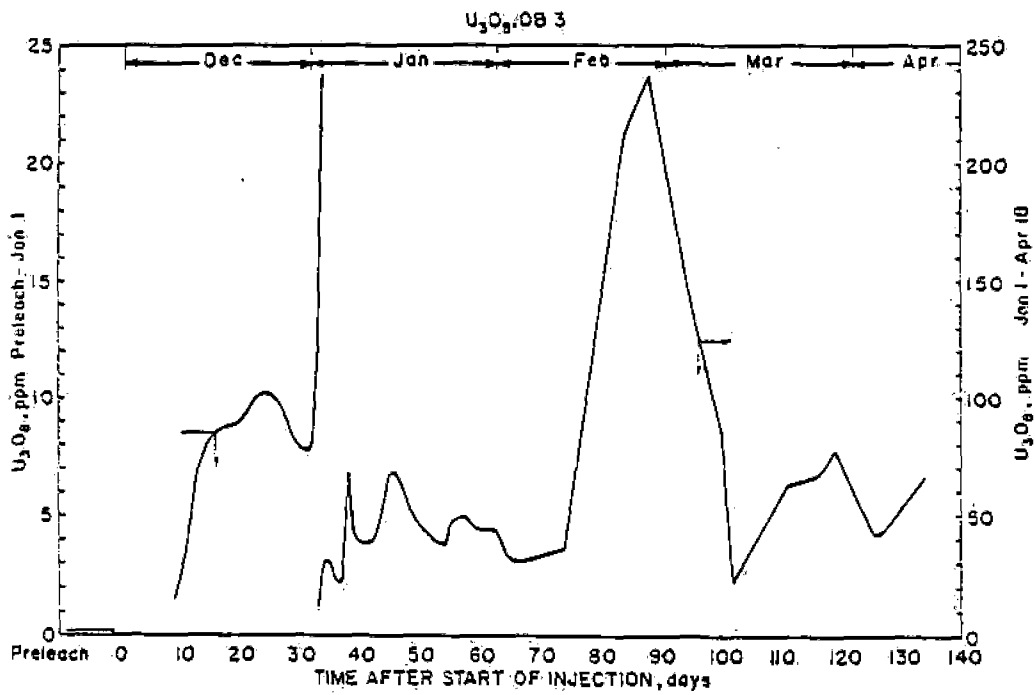


FIGURE 10. - U_3O_8 in OB3.

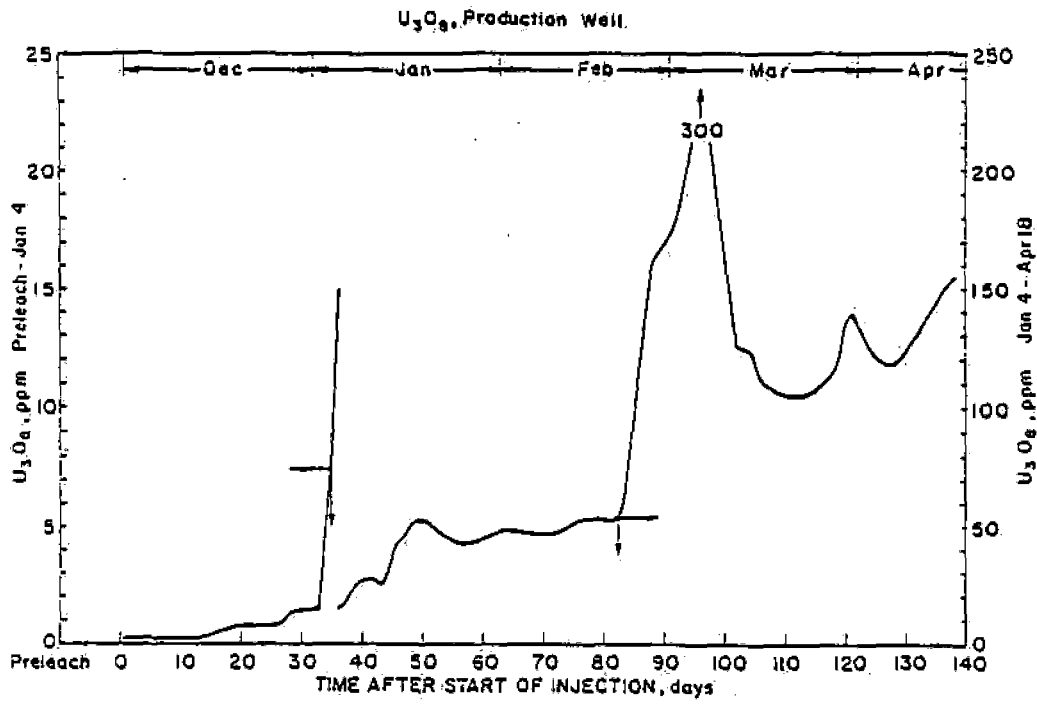


FIGURE 11. - U₃O₈ in production well.

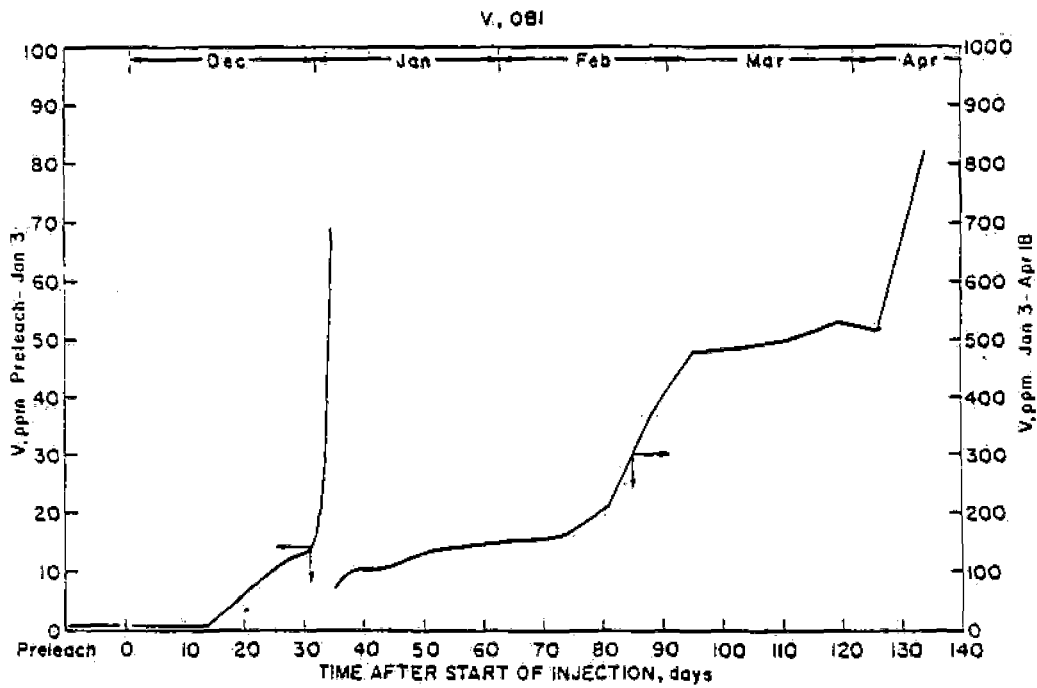


FIGURE 12. - V in OBI.

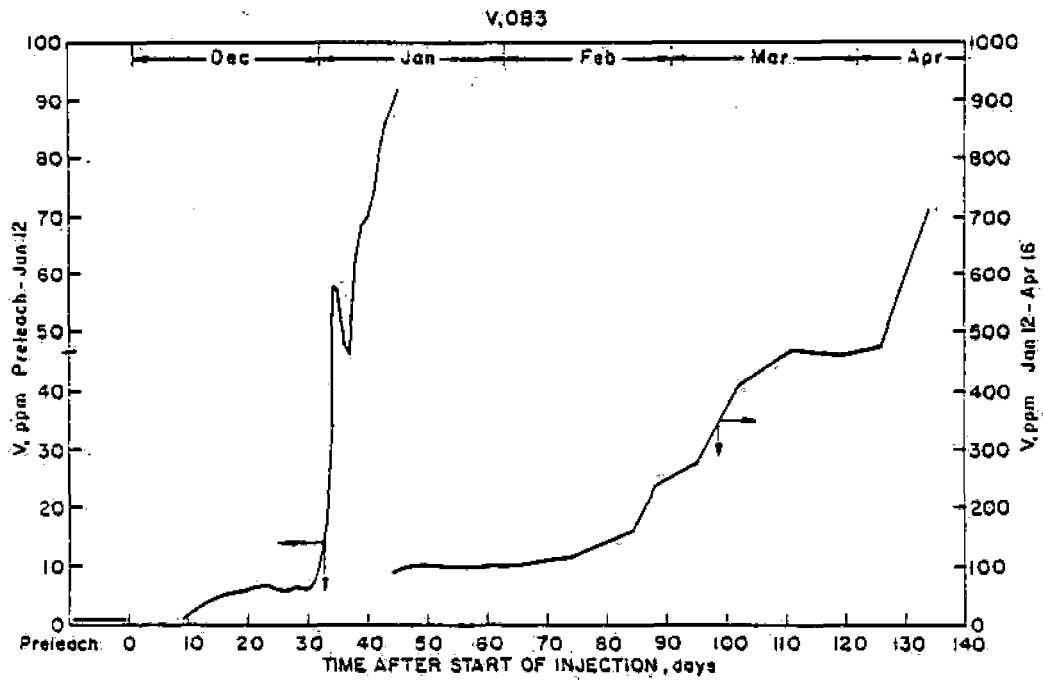


FIGURE 13. - V in O83.

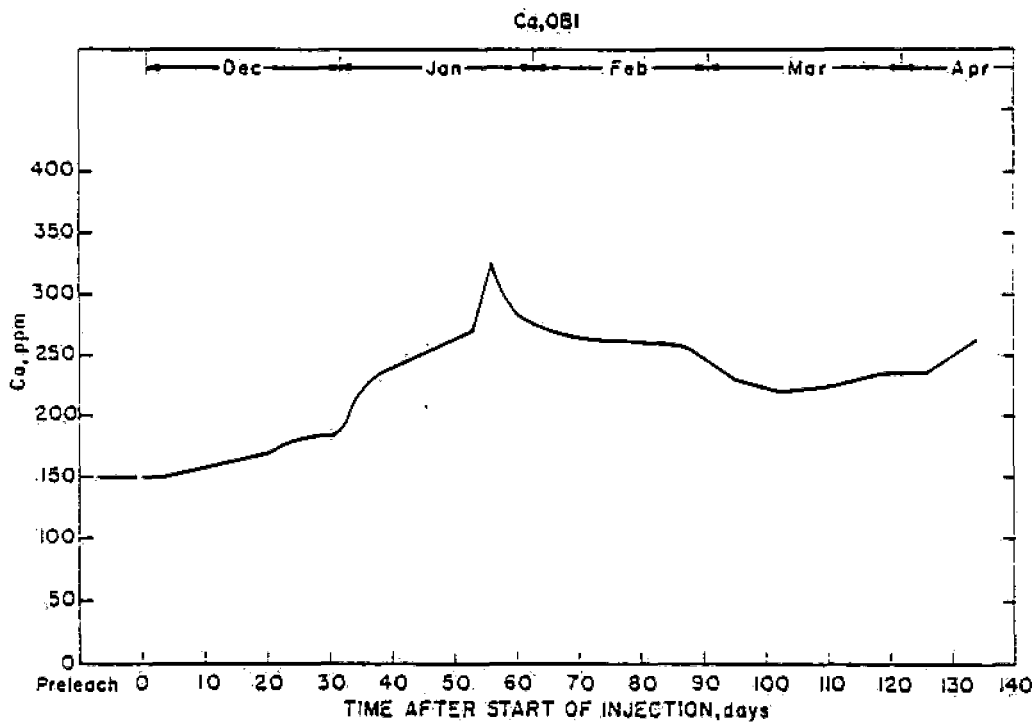


FIGURE 14. - Ca in O81.

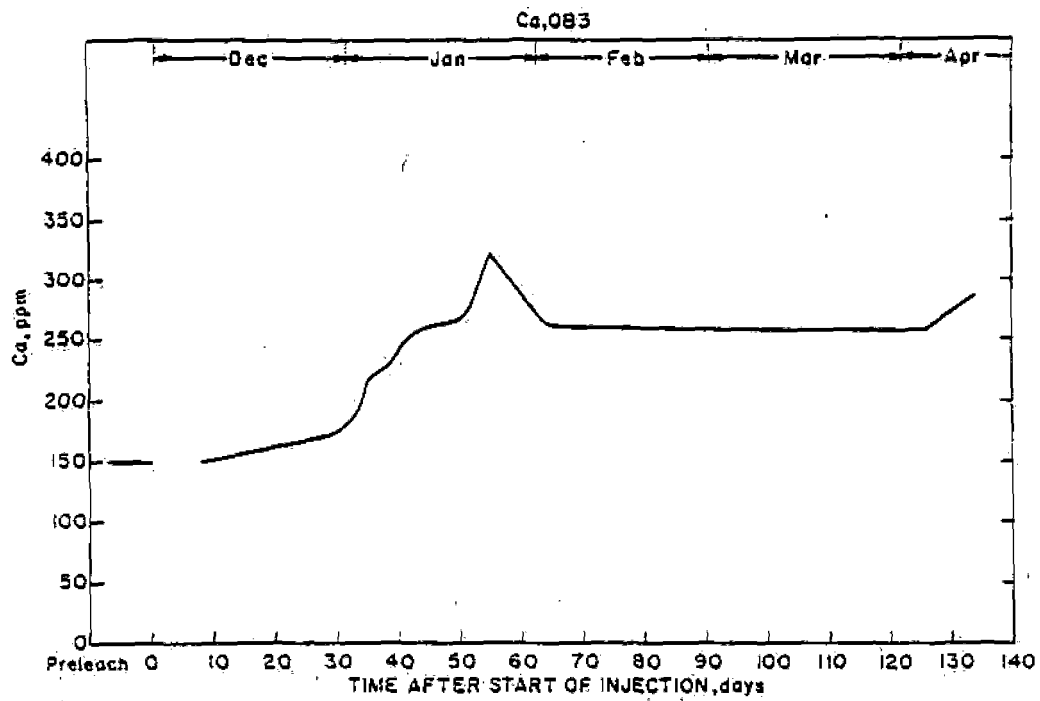


FIGURE 15. - Ca in 083.

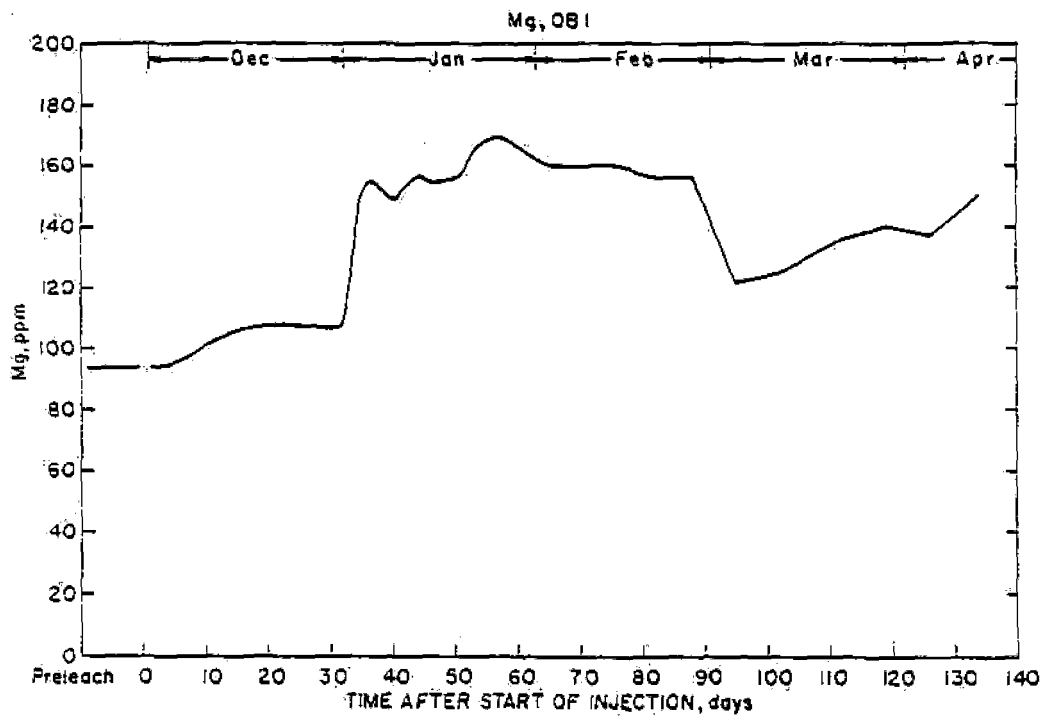


FIGURE 16. - Mg in 081.

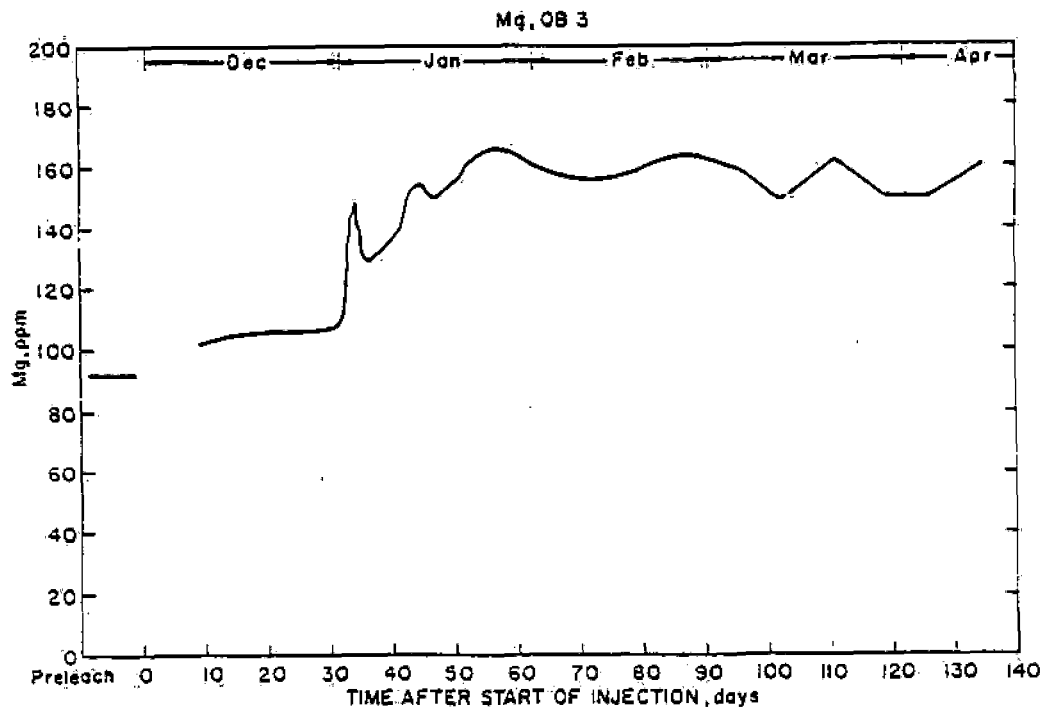
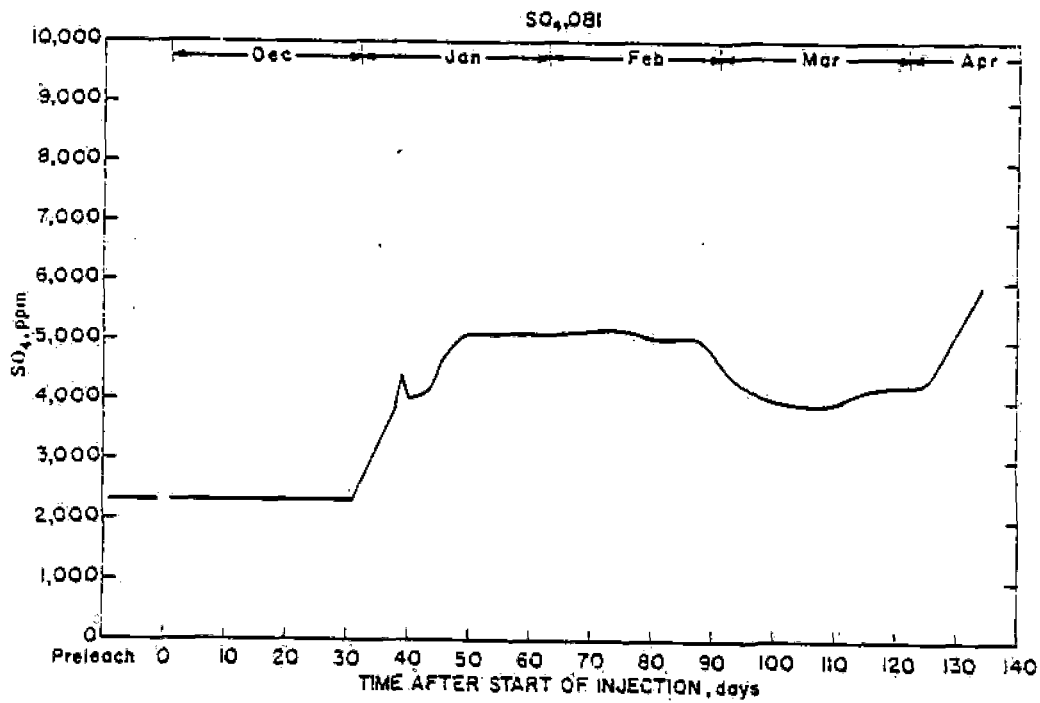


FIGURE 17. - Mg in OB3.

FIGURE 18. - SO₄ in OB1.

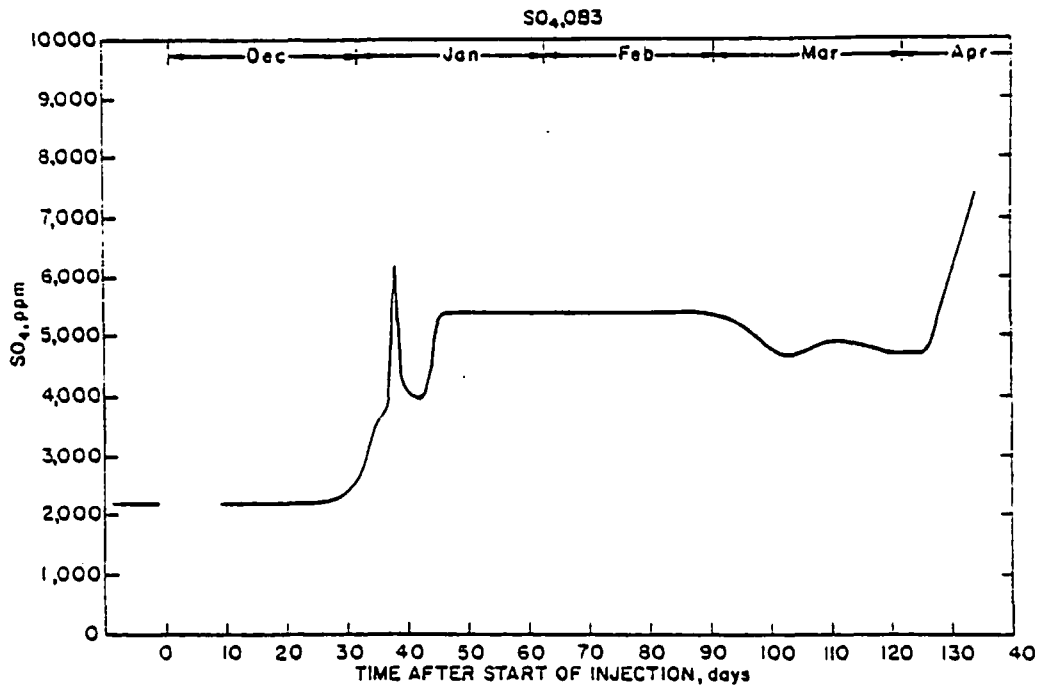
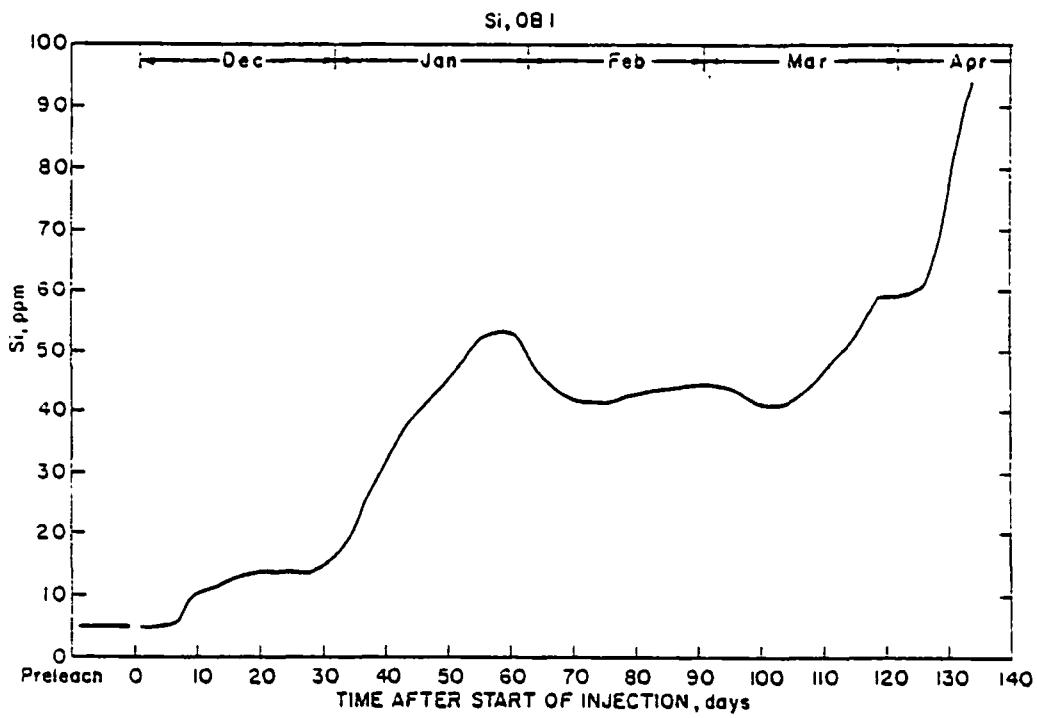
FIGURE 19. - SO₄ in OB3.

FIGURE 20. - Si in OB1.

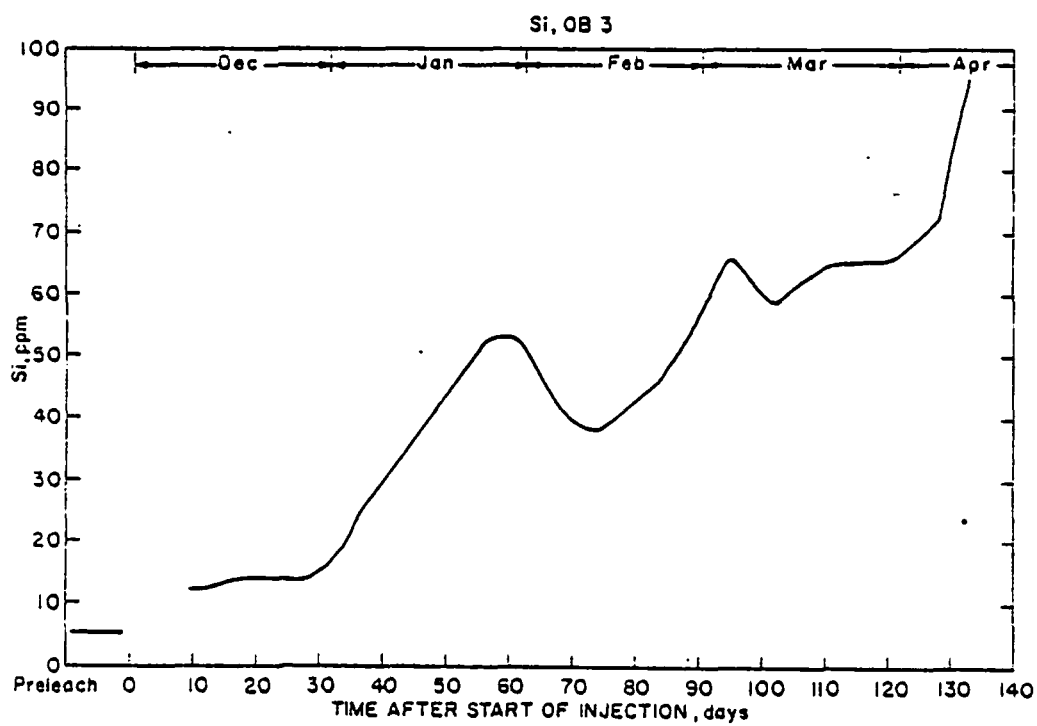


FIGURE 21. - Si in OB3.

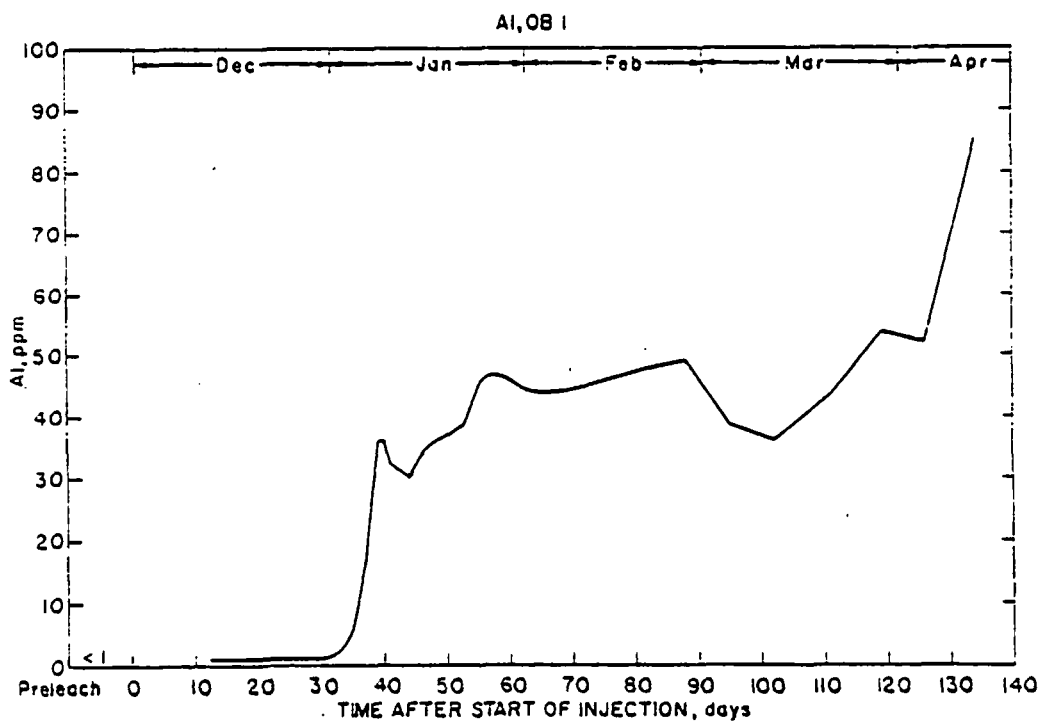


FIGURE 22. - Al in OB1.

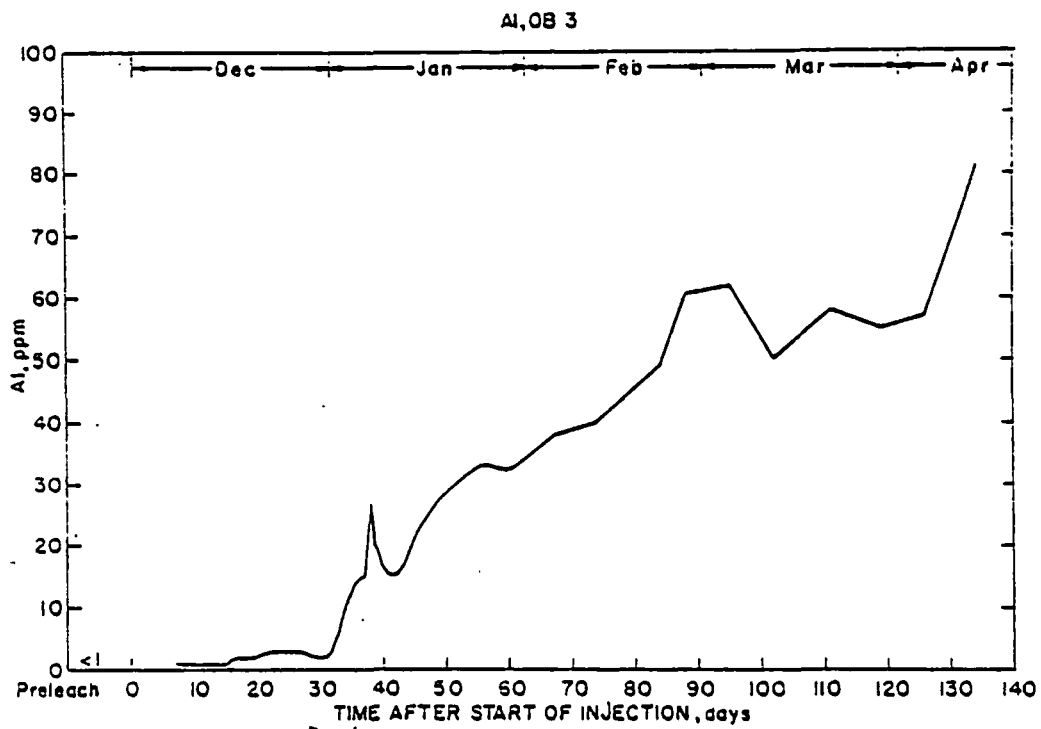


FIGURE 23. - Al in OB3.

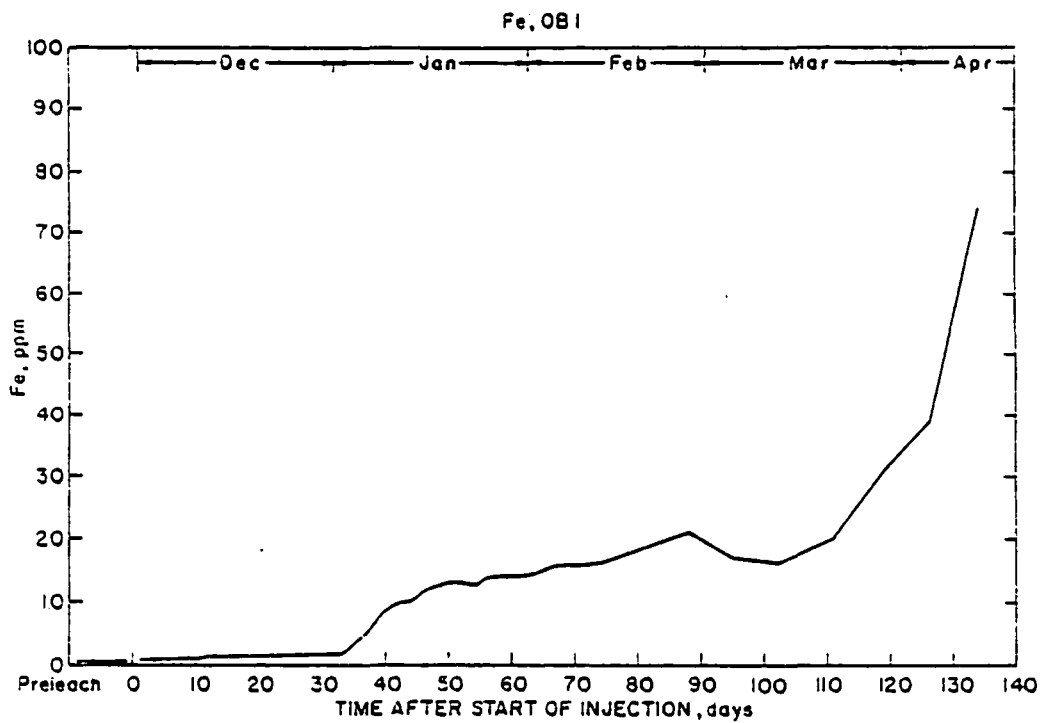


FIGURE 24. - Fe (total) in OB1.

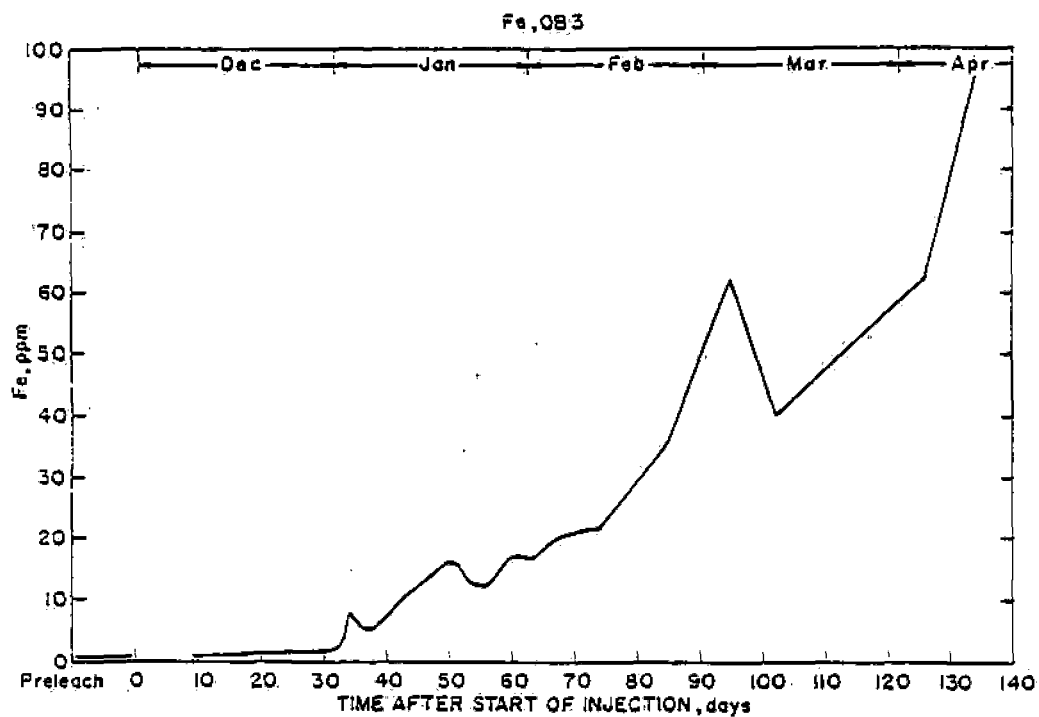


FIGURE 25. - Fe (total) in OB3.

№ 8, 1975

GOLD EXTRACTION FROM THIOUREA SOLUTIONS USING ION-EXCHANGE AND ELECTRON-EXCHANGE FIBERS

UDC 669.213

G. Ya. Druzhina, A. S. Chernyak, I. I. Shamolina, G. A. Kiselev, and L. A. Vol'f

The subject of study was the sorption of gold by ion- and electron-exchange fibers synthesized on the basis of polyvinyl alcohol (PVA), and also by ion-exchange fibers based on polyvinyl chloride (PVC) and polypropylene and electron-exchange fibers based on polymethylene.

Fibrous sorbents were chosen because gold occurs in thiourea solutions in the form of the complex cation $Au[CS(NH_2)_2]_2^+$ and the redox potential of the system $Au \times [CS(NH_2)_2]_2 - Au$ is +0.38 V.* Consequently, the following should be used as sorbents in this case: of the ion exchangers, cation exchangers, and of the redox polymers, electron exchangers with a redox potential below +0.38 V.

Table 1
Composition of Solutions Studied, mg/liter

Component	Solution			
	1 (synthetic)	2 (synthetic)	3 (thiourea regenerated from ion-exchange gold extraction)	4 (from leaching crude auriferous slimes)
Au	700	8	350	88
Ag	Absent	Absent	40	2.4
Cu	"	"	275	1.3
Zn	"	"	50	4.1
Fe	840	840	370	1950
Mn	Absent	Absent	-	80
Ni	"	"	4.2	-
$CS(NH_2)_2$, g/l	5	2.5	66	5
H_2SO_4 , g/l	10	5	19 (HCl)	10

Sixty samples of fibers were tested, 37 ion exchangers and 23 electron exchangers. Active groups were produced in the ion-exchange fibers by treating the polymers with sulfuric, acrylic, polyacrylic, maleic, iminodiacetic, and aminophenylarsonic acids and with various amines. Among the redox fibers, PVA fibers with an SH-group, with phenazine and phenothiazine groupings, and containing P^{3+} , Zn^0 , paraphenylenediamine, and anthraquinone were used, as well as fibers with attached polymethylene-hydroquinone (pyrogallol or pyrocatechol). The experiments on gold absorption by the fibers were conducted under static conditions.

Experiments with PVA fibers gave the best results: among the ion exchangers, sulfo acid exchangers and epoxidized fiber treated with hexamethylenediamine; among the electron exchangers, fibers with an SH-group, with phenazine and phenothiazine groupings, and fiber with a complexing and reducing action containing Hg^{2+} and P^{3+} . Extraction of gold from synthetic solution 1 (Table 1) by these fibers in one treatment at a fiber-solution ratio of 1 : 100 (wt.) was from 43 to 91%. Under similar conditions, 95 and 73% Au is extracted from synthetic solution 2 by fibers 1 and 2 (Table 2), and 83 and 62% Au respectively from process solution 4.

Multiple treatment of the same batch of solution with fresh portions of fiber showed that gold can be extracted from the solution practically completely, using ion- and electron-exchanger fibers. Thus 94% Au is extracted by seven-stage treatment of thiourea regenerate by ion-exchange fiber 2 (total fiber load 0.22 g per mg Au); extraction rises with an increase in the sorption stages. Impurities are sorbed to a lesser extent: Fe 20%, Cu 50%, and Zn 60%. Silver extraction is 66%, i.e., worse than gold but better than the impurities.

Table 2
Gold Content of Fibers Saturated in Thiourea Regenerator

Fiber no. (conditional)	Fiber characteristics	Static capacity for Au, mg/g
1	Sulfo-acid ion exchanges based on dehydrated PVA fiber	22.9
2	Epoxidized PVA fiber treated with hexamethylenediamine	18.9
3	Strongly acidic sulfo-exchange fiber in Na form	14.9
4	Redox fiber with SH-groups based on dehydrated PVA fiber. Redox capacity for Fe^{3+} 2.5-3 mg-eq/g	21.8
5	Phenothiazine type redox fiber. Normal redox potential +0.240 V at pH = 0 and -0.330 V at pH = 7	18.2
6	Redox fiber based on PVA with phenazine grouping. Redox capacity for Fe^{3+} 1.0 mg-eq/g	18.2
7	PVA fiber with complexing and reducing properties. Complexing by Hg^{2+} ions, redox function by B^{3+} . Redox capacity for Ag^0 1.9 mg-eq/g	19.3

*V. P. Kazakov, A. I. Lapshin, and B. I. Peshchevitskii, Zhurnal Neorganicheskoi Khimii, 9, No. 5, 1299-1300, 1964.

It was demonstrated with solution 4 that with 83% Au extraction by fiber 1 in one stage, Fe absorption is 17% and Mn absorption is 18%.

A high process speed is characteristic of fibrous sorbents; the solution was therefore left in contact with the fiber for 2-4 hr (the results did not improve when the duration of the experiments was increased).

The best samples of fiber have approximately the same capacity for gold. For example, it is ~ 20 mg/g for thiourea regenerate (solution 3) (see Table 2). The capacity of fibers saturated in the synthetic solutions is much higher: the gold concentration in fiber 1 treated with solution 1 is 45 mg/g.

When the saturated fibers are burned, ashes are produced which contain several dozen per cent gold (for example, 23, 47, and 48% for fibers 3, 5, and 6 respectively) and a limited amount of impurities: copper, several per cent, zinc, up to 1%, other impurities, not more than several tenths of 1%.

The investigation demonstrates the possibility of using ion- and electron-exchange fibers based on polyvinyl alcohol with various functional groups for the practical extraction of gold from thiourea solutions.

THE GALVANIC EFFECT IN THE PROCESS OF SULFIDE AND METAL POWDER SOLUTION

UDC 669.243.82:541.135.6

L. A. Sinev and T. P. Lifyandskaya

The galvanic effect may be regarded as one of the factors determining the speed of solution of sulfides in hydrometallurgical processes. It is fair to assume that the chance contact in the process of leaching of two sulfides with differing potentials should lead to a situation in which the sulfide with the more negative potential will be able to dissolve more rapidly.

The effect of the presence of copper sulfide and metallic copper, and of forced anodic particle polarization, on the kinetics of solution of nickel sulfide and metallic nickel was studied in the present work.

The experiments were conducted with mineral powders - 0.05 mm in size, nickel sulfide Ni_3S_2 (74.3% Ni and 22.67% S) and chalcocite Cu_2S (79.49% Cu and 19.38% S), and - 0.104 mm electrolytic nickel powder of 99.9% purity.

Leaching was at 90° C in a water-jacketed quartz reactor at constant mixer revolutions; the mixer was fitted with a liquid seal. In the experiments with forced anodic particle polarization the prescribed anodic potential was fed from a P-2858 potentiostat to a graphite anode. The cathode was placed in a fitted chlorinated pvc fabric sleeve to avoid contact with the sulfide particles. The cell was connected in a three-electrode circuit, a silver-silver chloride electrode being used as the reference electrode. The solution for leaching contained 2 moles HCl and 1 mole H_2SO_4 per 1000 ml of water. The amount of initial solution was 350 ml.

It follows from the results of experiments with solution of nickel powder in the absence of oxygen and in the presence of more electro-positive copper that when pure nickel powder dissolves all the transformations take place on the nickel grain surfaces only. In leaching in a mixture with copper powder, part of the hydrogen is reduced on the cathodically polarized copper grain surfaces. On the whole the hydrogen depolarization surface expands and the solution of nickel accelerates appreciably. Apparently the stage of hydrogen reduction on the surface of nickel grains dissolving in acids is the slowest, and it is this that limits the process.

The maximum rise in the solution nickel concentration occurs at the beginning of the experiment, when the strength of the current flowing through the cell is greatest.

It should be noted that the presence in the solution of more electro-positive copper grains, capable of anodic polarization but not obtaining the conditions for rapid anodic solution in the experiment, reduces the total speed of nickel solution somewhat. Apparently the partially dissolved copper is cemented on the metallic nickel grains under these conditions, screening their surfaces and so retarding the overall course of the nickel leaching process.

Ten grams of nickel sulfide Ni_3S_2 were subjected to leaching. In the experiments with copper sulfide, 10 g of Cu_2S (chalcocite) were added also. It was established that the introduction of copper sulfide with a more positive potential helped to accelerate the solution of nickel sulfide, both in the absence of oxygen and with air blowing.

Thus it was established that when metal and sulfide powders are leached, the presence in the pulp of two solids helps to accelerate the solution of the one which has the more negative steady electrode potential in the conditions under consideration.

Mutual polarization of grains of two different minerals occurs during their collisions, when short-lived normally circuited microvoltaic couples are formed.

The presence in the pulp of a more electro-positive solid helps to accelerate only the electrochemical stage of solution of the electronegative material.

When metallic nickel dissolves, the slowest stage is the reduction of hydrogen, which limits the process as a whole.

CORRECTION

In issue No. 7 of the Journal, p. 24, left-hand column, subsection "Temperature Conditions in Roasting," the last sentence in the fourth paragraph should read: "The SO_2 concentration in the exhaust gases in roasting rose by 1.2-2 times by comparison with multi-hearth roasters."

SUBJ
MNG
GGPS

Geology and Genesis of the Polish Sulfur Deposits

S. PAWŁOWSKI, K. PAWŁOWSKA, AND B. KUBICA

Abstract

New large sulfur deposits were discovered in Poland in 1953, the result of investigations by the Geological Institute of Warsaw. All the deposits occur in a widespread Miocene evaporite unit deposited in the Carpathian foredeep and now occur in Miocene structural uplifts. The gypsum underlying impermeable Sarmatian clays was altered to limestone and native sulfur where penetrated by hydrocarbons and bacteria. The early determination of the genesis of the sulfur deposits and their occurrence in elevated blocks led to an exploration program that has successfully located new deposits.

Introduction

SULFUR was mined in Poland since the 15th century from shallow, easily accessible deposits, mostly from a mine near Swoszowice (Cracow). Until the 19th century, the 200,000 tons mined in Poland met the entire European demand, but Sicilian production thereafter dominated the European market.

A geological reappraisal of the native sulfur deposits of Poland began as part of the search for mineral raw materials needed to restore the national economy after World War II. High-grade deposits of native sulfur were discovered in 1953, a turning point in applied geology and in Polish sulfur mining, the result of a geological prospecting program carried out by the Geological Institute of Warsaw. Minable concentrations of sulfur were found in marine Miocene strata infilling the Carpathian foredeep in southern Poland. None was exposed, all were covered by a thick blanket of barren strata. The mines opened since 1956 now produce close to 5,000,000 tons of sulfur per year.

Miocene of the Carpathian Foredeep

During the Alpine orogeny, a foredeep formed north of the Carpathian front and subsequently was filled with Miocene sedimentary rocks. The basin is asymmetric, containing more than 3,000 m of Miocene beds near the front that feather out northward. On the north side of the basin, Miocene strata of the Tortonian stage transgress the Mesozoic and Paleozoic massifs of Upper Silesia, the Holy Cross Mountains, and the Lublin area (Figs. 1 and 2).

As the foredeep developed during the Miocene, it was block-faulted during the Tortonian stage and early in the Sarmatian stage, both longitudinally and transversely with respect to the Carpathian front. Near the northern margin of the Tortonian sea, vertical movements in the Holy Cross Mountains and in the neighboring massifs markedly influenced the paleogeographic development of Tortonian strata, including their patterns of transgression, distribution of

their sedimentary units and facies, the thickness of an included evaporite unit, and the development of oil traps and bitumen migration routes. Seas were shallow during the Tortonian stage, accumulating slightly more than 200 m of sandstone, gypsum, and marl. During the following Sarmatian stage, the basin subsided along the Carpathian front, resulting in an accumulation of 3,000 m of flysch, the marls, clays, and sandstones of which thin northward.

Stratigraphy of the upper Miocene

The stratigraphic column of the marine Miocene in the area here described includes strata of the Tortonian (Badenian) and Sarmatian stages (Table 1); older Miocene strata lie beyond this sulfur-bearing area. The Tortonian, which contains the sulfur deposits, is divided into: (1) the Baranów beds, consisting of sandstone, limestone, and siltstone, capped everywhere by a thin coquina containing *Ervilia pusilla*; (2) the gypsum unit; and (3) the *Pecten-Spiralis* beds, a fossiliferous marl. The three units contain abundant macro- and microfossils and bentonites and tuffs of volcanic origin. Any of these units may be thin or missing at given localities. Locally, a *Lithothamnium*-bearing limestone occurs as a facies of the Baranów beds.

Sarmatian strata unconformably overlie the Tortonian sequence. The lower part of the section consists of calcareous, fine-grained clastics containing marine fossils; the upper part consists of nonfossiliferous calcareous siltstones and sands in which plant remains are found.

The Tortonian gypsum unit

All minable sulfur in Poland lies within one stratigraphic unit, the gypsum in the middle of the Tortonian sequence. Due to complex stratigraphic development, the unit differs from place to place in thickness, in mineralogical composition, and in texture.

Its thickness, as recorded to the present, never

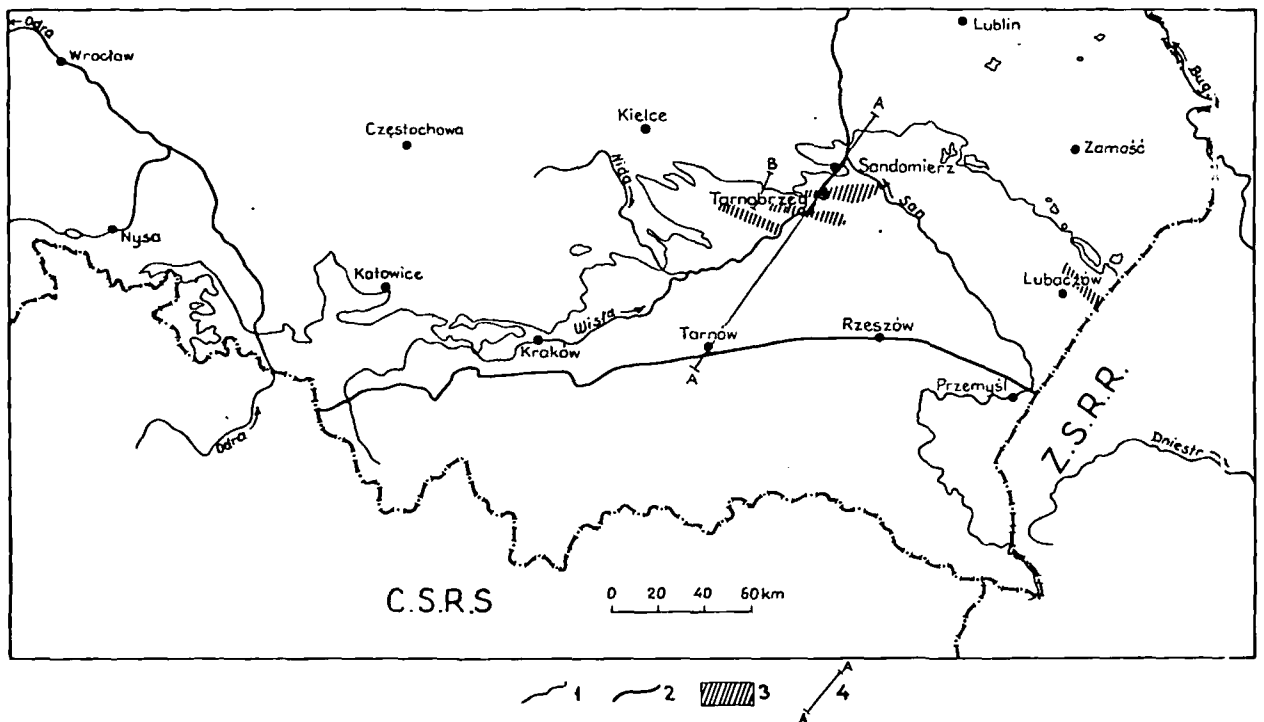


FIG. 1. Geologic sketch map showing extent of Miocene strata in the Carpathian foredeep: (1) boundary of Miocene strata; (2) northern boundary of Carpathian Mountains; (3) areas containing sulfur deposits; (4) cross section A-A, Tarnów, Tarnobrzeg-Sandomierz; (5) cross section B, Trzcianka-Bukowa.

exceeds 60 m and as noted above may be thinner or even missing in the Tortonian section, the result of contemporaneous block faulting during the Tortonian stage. Mineralogically, it consists of gypsum near the surface at the north end of the Miocene basin, of intermixed gypsum and anhydrite farther south, and solely of anhydrite where it was buried to depths exceeding 300 m still farther south; the original textures of the gypsum are lost where it was dehydrated to anhydrite.

Where the gypsum unit is fully developed, its base is coarsely crystalline, consisting of twinned vertical crystals attaining meters in length (Figs. 3 and 4). The coarsely crystalline gypsum is overlain by less homogeneous crystalline gypsum with massive overgrowths; in complete sections, this textural variety of gypsum is as much as 24 m thick. The top of the

unit consists of massive bedded gypsum overgrown with finely crystalline gypsum or in places contains gypsum breccia (Figs. 5 and 6); such bedded gypsum may be as thick as 36 m. The unit is sparsely fossiliferous, containing some fish bones and plant debris as well as microfossils in clay intercalations.

The gypsum unit is widespread and is both a stratigraphic marker and a guide horizon in seismic exploration because of its high acoustic resistance. Its presence permitted resolution of the structure of the Tortonian sequence, even at great depths, through use of seismic and electrical geophysical surveys.

Origin of the Native Sulfur Deposits

We advocate that the native sulfur deposits of Poland resulted from the epigenetic alteration of the Miocene gypsum unit at geologically favorable sites.

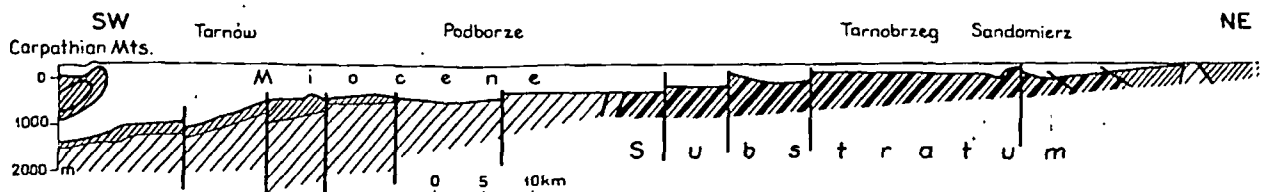


FIG. 2. Cross section A-A (Fig. 1) of the Carpathian foredeep through Tarnów, Tarnobrzeg, and Sandomierz.

TABLE 1. Stratigraphy of Marine Miocene from the Carpathian Foredeep

Epoch	Stage	Zone	Maximum thickness in m	Lithology	Biozones	Traces of volcanic activity	
Tertiary Miocene	Sarmatian	unfossiliferous layers (Ms ₁)	3,000	calcareous, strongly sandy siltstones, subordinate intercalations of non-cohesive sands	plant debris <i>Elphidium hauerinum</i>		
		<i>Syndesmya</i> beds (Ms ₂)		calcareous siltstones and clay marls with calcareous marl intercalations	<i>Syndesmya reflexa</i> , <i>S. scythica</i> , <i>Hydrobia</i> , <i>Mahrensternia</i> , <i>Limnocardium lithopodolicum</i> , <i>Limnocardium subfloni</i>	<i>Varidentella sarmatica</i> , <i>Cyloforina karrevicovata</i> , <i>Anomalinoidea dividers</i>	numerous intercalations of tuffites and bentonites
		<i>Pecten-Spiralis</i> beds (Mtp)	40	clay marls with calcareous marl intercalations	<i>Chlamys elyni</i> , <i>Chlamys neumayri</i> , <i>Chlamys lilli</i> , <i>Spiratella</i>	<i>Hanzawaia crassiseptata</i> , <i>Neobulimina longa</i> , <i>Radiolaria</i>	numerous tuffite intercalations
		gypsum unit (Mtg ₁)	60	massive, laminated crystalline and coarsely crystalline gypsum rocks, postgypsum limestones, native sulfur	plant debris, fish bones		occasional tuffite intercalations
Badenian (Tortonian)		<i>Ervilia</i> layer (Mte)	0.10	sandy and sometimes calcareous cocquina	<i>Ervilia pusilla</i> , <i>Modiola hoernesii</i>		
		Baranów beds (Mtba)	120	sandstones with intercalations of noncohesive sands, <i>Lithothamnium</i> limestones and siltstones (Mtl ₁)	<i>Amussium denudatum</i> , <i>Chlamys scissa</i> , <i>Chlamys koheni</i> , <i>Ostrea cochlear</i>	<i>Uvigerina costai</i> , <i>Orbulina suturalis</i> , <i>Heterostegina costata</i> , <i>Amphistegina lessonii</i>	tuffite intercalations

At those sites, the gypsum unit was upfaulted and overlain by impervious clays, saturated with highly saline waters, and inundated by hydrocarbons that

had moved upward from lower strata. Accumulations of oil and gas occur in both Miocene and in older sedimentary rocks of the Carpathian foredeep. We esti-



FIG. 3. Outcrop of Miocene gypsum at Goryslawice, near Wislica; crystalline gypsum is overlain by compact laminated gypsum; cut is about 5 m high.



FIG. 4. Crystalline gypsum; aggregates are more than 3 m long.

mate that the formation of a native sulfur deposit of several million tons required a supply of several million cubic meters of methane gas or its equivalent as liquid hydrocarbons. Bacteria probably activated the chemical reactions. Traces of such bacteria recently were found in the limestone matrices of the deposits and bacterial activity is confirmed by the $^{32}\text{S}/^{34}\text{S}$ isotope ratios of the native sulfur.

Several possible chemical formulas show how gypsum can be altered to limestone and elemental sulfur, all assuming the availability of hydrocarbons and the presence of sulfate-reducing bacteria. All the main components, the original constituents and the products, have been found in the Polish sulfur deposits. We also know the conditions needed to

promote the reactions, but the chemistry of the alteration process itself is not fully clear.

The bacterial activity resulted in oxidation of the



FIG. 5. Compact laminated gypsum.

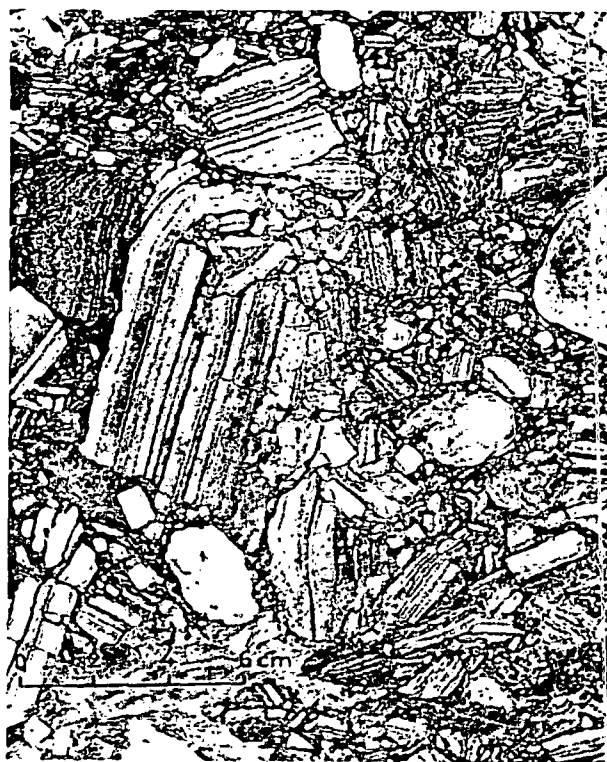


FIG. 6. Brecciated gypsum.

hydrocarbons and reduction of the sulfate ions, leading to generation of carbon dioxide and hydrogen sulfide. Hydrated carbon dioxide combining with calcium ions derived from dissolved gypsum led to precipitation of calcite. Gypsum thus underwent a molecular replacement by limestone which preserved all the characteristic textures and structures of the evaporite.

Metasomatism of gypsum started with the emplacement of calcite at contacts between any two gypsum grains. Replacement spread throughout the favorable zone, leading to extensive substitution of the sulfate ion by the carbonate ion. Depending upon local conditions, replacement of the gypsum by limestone occurred at the top, the base, or in the middle of the gypsum unit. The epigenetic origin of the limestone is supported by relicts of gypsum in limestone masses, indicating incomplete alteration. Moreover, chemical analyses of the gypsum and the limestone show similar amounts of insoluble compounds, unchanged during metasomatism.

Most postgypsum rock is limestone, but marl and clay occur in lesser amounts. Analytical data of postgypsum limestones show that their average composition is: calcium carbonate, ca 60 percent; sulfur, 28.5 percent; other material (SiO_2 , Al_2O_3 , Fe_2O_3 , MnO ,



FIG. 7. Sulfur-bearing limestone showing preserved, undulating bedding typical of compact gypsum; specimen is 11 cm wide.



FIG. 8. Sulfur-bearing limestone with structure resembling that of gypsum breccia; specimen is 10 cm wide.

SrO , BaO , CaSO_4 , K_2O , Na_2O), 10 percent; and bitumens, 0.5 percent. Limestone is microcrystalline or, less commonly, crystalline. In color it is ash gray or in places chalky white. Many limestones are highly porous and fissured. Diagenesis produced a variety of limestones, including hard and compact rock, silty and soft rock, and brittle and shaly rock. Brittle limestone occurs at the peripheries of the sulfur deposits, so this variety probably represents the earliest phase of gypsum replacement. The limestones display stratified textures typical of massive gypsum (Fig. 7), brecciated textures (Fig. 8), and pseudomorphs of saberlike selenite crystals.

The alteration of gypsum to limestone can reduce the volume. This reduction is irregular and mostly depends on the insoluble clay admixtures in the gypsum rock.

The change of volume in sulfur-bearing limestone in comparison with that of the gypsum rock is about 28 percent and in the barren limestones about 45 percent. The resulting caverns, fissures, and free spaces in the limestone are partly filled with sulfur. The weight of overlying rocks deformed and downwarded the upper surfaces of the deposits and produced microtectonic disturbances in the overlying *Pecten*-bearing beds.

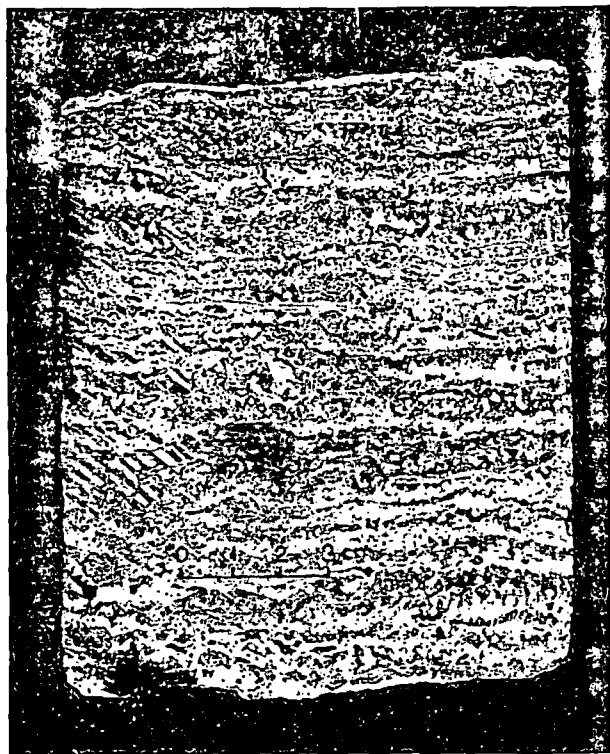


FIG. 9. Limestone with sulfur pseudopisolites; specimen is 11 cm wide.

The second product of the reaction between gypsum and hydrocarbons is hydrogen sulfide, which where oxidized was precipitated as native sulfur. At shallow depths most sulfur is cryptocrystalline or microcrystalline. Cryptocrystalline sulfur is light yellow and resembles the sulfur dust precipitating around hydrogen-sulfide springs. Microcrystalline sulfur is dense and varies in color and luster. Where

pure, it is yellow and has a soapy luster; where admixed with bitumens it is brown to black green and has a waxy luster. Greenish microcrystalline sulfur is strongly cemented with carbonate rock. Crystalline sulfur, lemon-, or honey-yellow in color, generally occurring in larger amounts at depths greater than 100 m. forms druses in open cavities or fissures.

Aggregates of sulfur are variable in form and include spheroids or pseudopisolites (Fig. 9), amygdaloids, streaks, veins, pseudolayers, irregular patches, and mosaics. Intergrowths of pure sulfur may attain tens of centimeters and in places 1 m in thickness.

Minerals accompanying sulfur include calcite, aragonite, celestite, and barite. Openings lined with druses of crystalline sulfur also contain crystalline calcite and celestite. Metallic trace elements are widespread in sulfur. During the spectral analyses of postgypsum limestone 11 elements were found to occur: Zr, Cr, Mo, Co, Ni, Cu, Ag, Zn, Sn, Pb, and Ga. The average results of many analyses show that Cu, Cr, Ni, Pb, Mo, and Ga occur in the largest quantities, whereas arsenic and selenium are known only in local traces.

Hydrogen sulfide readily dissolves in water and both the gas and the mineralized water are highly mobile. Sulfur is deposited in any opening, including minute pores, cavities, fissures, or on the surfaces of layers. Within limestone lenses the sulfur content may vary greatly both vertically and horizontally, and parts of deposits may contain sulfur in amounts well above or well below the theoretical yield of the reactions. Due to these variations, the average amount of sulfur is calculated for any given borehole and for complete cross sections.

The mobility of hydrogen sulfide also accounts for the presence of sulfur as cement in the underlying

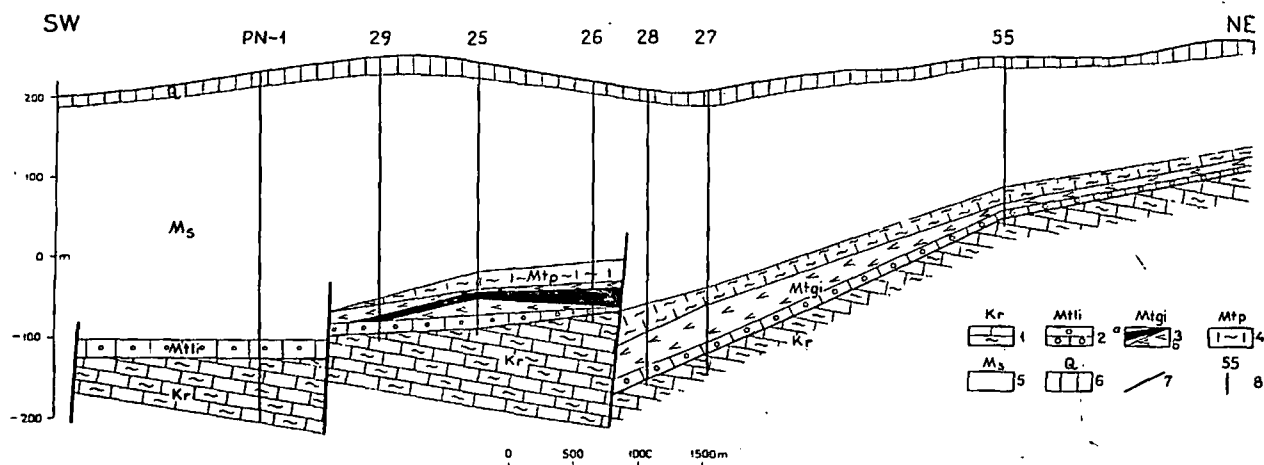


FIG. 10. Geologic cross section through a native sulfur deposit: (1) Kr = Cretaceous, M = Miocene; (2) Mti = Tortonian *Lithothamnium* limestone; (3) Mtgi = Tortonian chemical deposits, a = sulfur-bearing limestone, b = gypsum; (4) Mtp = Tortonian *Pecten* beds; (5) Ms = Sarmatian; (6) Q = Quaternary; (7) fault; (8) borehole; black = sulfur deposit.



FIG. 11. Core section showing partly leached agglomerates of native sulfur; vertical contact is between sulfur-bearing and barren limestone.

Baranów sands and in the overlying *Pecten*-bearing marls. The latter are strongly fractured and slicken-sided and therefore permitted ingress of hydrogen sulfide either as a gas or dissolved in water.

The sulfur content of minable blocks ranges from about 25 to 36 percent. In shape, the deposits are tabular and elongated parallel to the longer axes of the uplifts in which they occur. Contacts between limestone and gypsum may be sharp (Fig. 10) and the outlines of the limestone lenses are very irregular. The deposits may contain zones in which sulfur subsequently was leached out (Fig. 11).

Leaching of sulfur occurred where oxygen-bearing waters penetrated the deposits, carrying with them sulfur-oxidizing bacteria (*Thiobacillus thiooxidans* and *Th. thioparus*). These bacteria can convert native sulfur to sulfates and beyond leaching the mineral, produce secondary gypsum. Such bacterial activity can be seen "in status nascendi" in dumps of sulfur-bearing rocks and is accompanied by a marked production of heat. Sulfur deposits thus seem to be highly sensitive to hydrogeochemical environments.

The age of metasomatism has not been fully determined and some students consider that the process is still continuing. For the present, we can only say that epigenesis could only have begun after deposition

of overlying, impervious Sarmatian strata and after hydrocarbons migrated into the gypsum.

Exploration for Sulfur Deposits in Poland

Exploration for sulfur in Poland began in the Tarnobrzeg area, where deposits were found in 1953, and continued from that year to 1977 in the Holy Cross Mountains and in the Lublin areas. All discoveries were in areas where glacial debris concealed most of the geology and where barren strata concealed the deposits, so the exploration program was based upon integrated geophysical surveys, geological studies and interpretations, and drilling.

Due to lack of outcrops, geophysical surveys were essential to determine the depth to the gypsum unit and for mapping its structural dislocations; we found that in the northern part of the Miocene basin gravimetric surveys were more reliable than seismic surveys in working out the structural pattern. A drilling program was developed on the basis of the geophysical mapping and the geological study of core was coordinated with geophysical logging of boreholes. Concurrently, geological interpretation of the strati-

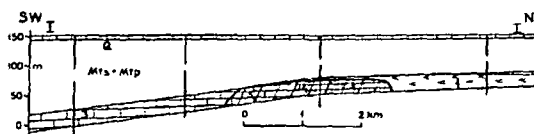
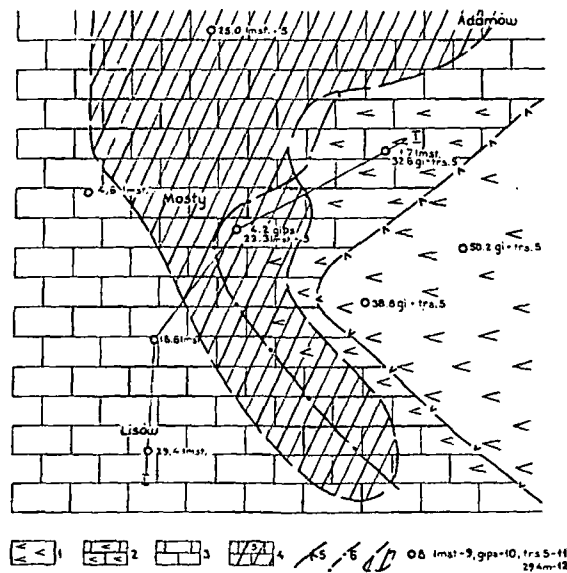


FIG. 12. Prognostic map and cross section through a prospective area: (1) extent of gypsum; (2) gypsum partly altered to limestone; (3) postgypsum limestone; (4) sulfur-bearing limestone; (5) extent of unaltered gypsum; (6) extent of partly altered gypsum; (7) extent of sulfur-bearing limestone; (8) research borehole; (9) lmst. = limestone; (10) gi = gypsum; (11) trs. S = traces of sulfur, S = sulfur; (12) thickness of limestone; I-I = geologic cross section.

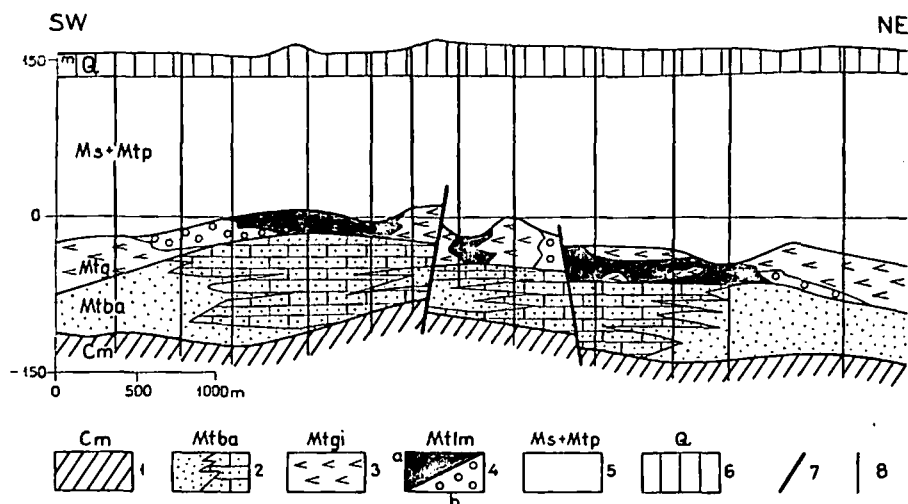


FIG. 13. Geologic cross section through the native sulfur deposit near Tarnobrzeg: (1) Cm = Cambrian; (2) Mtba = Baranow beds; (3) Mtgi = gypsum; (4) Mtlm = a, sulfur-bearing limestone and b, barren limestone; (5) Mtp + Ma = *Pecten* and Sarmatian beds; (6) Q = Quaternary; (7) fault; (8) research borehole.

graphic and structural development during the Miocene evolved and geological study of known sulfur deposits was used to interpret core obtained by drilling in prospective areas. All pertinent information was entered on prognostic maps (Fig. 12).

The most complex problem was that of determining the stratigraphic and structural evolution during the Tortonian. We found that the vertical dislocations taking place at that time led to greater or lesser thicknesses of given stratigraphic units being deposited over horsts and grabens, that vertical movement differed in amount and direction along given faults through that time stage, and hence that accumulation of units in the vertical dimension differed from block to block. We also found that subsequent erosion thinned previously deposited units. One cross section, Figure 13, illustrates some of these stratigraphic complications.

We established that gypsum was altered to limestone and sulfur only in uplifted fault blocks capped by impervious clays and penetrated by hydrocarbons and we therefore concentrated our exploratory activity in such favorable sites. We eliminated areas where drilling showed the gypsum unit to be less than 10 m thick, or its altered limestone equivalent to be less than 7 m thick, because neither was favorable for finding minable concentrations of sulfur. We also eliminated areas in which the gypsum unit was less than 70 m or more than 500 m deep, limits imposed by the technology of hot-water mining of sulfur in Poland, although we have found sulfur in gypsum at depths exceeding 1,000 m. One deposit, at Tarnobrzeg, was found at very shallow depth and is being mined from an open pit.

One of our most useful tools was the prognostic map, compiled at various scales, upon which we entered geological information, geophysical data, the data obtained from exploratory drilling, and the results of chemical analysis of drill core. Such maps were kept up to date as drilling information accumulated and constantly were used to determine the next steps in exploration and appraisal. Through this flexible and coordinated procedure, we found much minable sulfur at minimum cost; with this technique, we were able to eliminate about 90 percent of the area underlain by the Miocene sequence and we limited prospecting to a cumulative area of some 100 square kilometers.

All boreholes were logged geophysically to correlate uncored intervals. Such logging established the upper and lower contact of beds possessing definite physical properties. The logs also registered zones containing larger amounts of sand and aquifers. Use of natural and induced radiation, neutron-gamma, were valuable for analyzing the evaporite unit, not only the gypsum but also those segments where the gypsum had been altered to limestone and sulfur.

INSTYTUT GEOLOGICZNY
00-975 WARSZAW, UL. RAKOWIECKA 4
POLAND
October 6, 1978

GENERAL REFERENCES

- Bolewski, A., 1935, O złożu siarki w Posądzu (Über das Schwefellager in Posądzu): Warsaw, Sprawozdania, Inst. Geol., v. 8, p. 3, p. 205-305.
Czerwiński, J., 1960, Struktury mikroorganiczne siarki rodzimej w tortonie (Microorganogenic structures of native

- sulfur in the Tortonian): Warsaw, *Kwartalnik Geologiczny*, v. 4, p. 531-537.
- Krajewski, R., 1935, Złoże siarki w Czarkowach: Warsaw, *Sprawozdania, Inst. Geol.*, v. 8, p. 27-66.
- Kubica, B., 1965, Charakterystyka litologiczna mioceńskich osadów chemicznych w widłach Wisły i Sanu: *Przegląd Geologiczny*, no. 6, p. 247-252.
- 1974, Wkład geologii w rozwój problematyki siarki: *Przegląd Geologiczny*, no. 5, p. 180-182.
- Łaskiewicz, A., 1957, Siarka i celestyn z Tarnobrzega i Szydłowa (Sulfur and celestite from Tarnobrzeg and Szydłów, Poland): *Archiwum Mineralogiczne*, v. 20, no. 1-2, p. 95-119.
- Osmólski, T., 1969, Siarka w zapadlisku przedkarpackim w latach 1415-1921: *Kwartalnik Geologiczny*, v. 13, p. 233-252.
- Pawłowska, K., 1962, O gipsach, siarce rodzimej i pogipsowych skałach świętokrzyskiego miocenu (On gypsum, native sulfur and postgypsum rocks from the Miocene of the Holy Cross Mountains): *Acta Geol. Polonica*.
- 1965, Mioceńskie złoża siarki: Warsaw, *Przewodnik, Zjazdu Polskiego Towarzystwa Geol.*, Guidebook 38, p. 136-139.
- Pawłowski, S., 1960, Problemy siarki rodzimej: Warsaw, *Prace, Inst. Geol.*, v. 30 p. 311-316.
- 1968, Geology of sulfur deposits in Poland: *Internat. Geol. Cong.*, 23rd, Prague 1968, v. 8, p. 249-267.
- Stopiński, A., and Stejn, J., 1974, Mikrogravimetria jako podstawowa metoda określenia rejonów wydobycia siarki metodą otworowa: Warsaw, *Biul. geol. Wydziału Geologii Uniw. Warszawskiego*, v. 15, p. 311-333.

SUBJ
MNG
GPMFUNIVERSITY OF UTAH
RESEARCH INSTITUTE
EARTH SCIENCE LAB.D. Linn Coursen
E. I. du Pont de Nemours & Co., Inc.
Martinsburg, WV

(For presentation at the 1980 Fall Meeting of the Society for Experimental Stress Analysis, October 12-15, 1980, Ft. Lauderdale, Florida)

The proposed model is the outline of a mechanism to explain the character of the fragmentation and permeability produced by long cylindrical charges detonated in well-jointed Devonian shale with water-flooded joints and far from a free face.

The explosive (EL 836) was of the water gel type, containing inorganic nitrates, 30% aluminum and monomethylamine nitrate, with a density of about 1.49 and giving products with much of the usual H_2O replaced by H_2 and Al_2O_3 . Properties calculated via the du Pont HT-65 code include: a detonation velocity of 5770 m sec^{-1} , a CJ pressure of 11.6 GPa, an explosion pressure of 5.4 GPa, and expanded products containing 24 moles kg^{-1} of permanent gases. The semi-fluid explosive filled the cross section of the 127 mm and 152 mm vertical water-flooded shot holes and were 50 and 70 hole diameters long, respectively, their mid-charge depths being 24.5 and 101.6 m, respectively. The stemming was water, water-flooded sand, or water-flooded gravel. Several equally-spaced primers in the charges were initiated simultaneously with fast-firing caps.

At the test site, which was in the Valley and Ridge provinces of the Appalachians, the three principal stresses were measured by the hydraulic fracturing method¹. The resulting horizontal compressive stresses, $\frac{1}{2}(\sigma_1 + \sigma_2)$, were 5.66 and 12.75 MPa, respectively, at the two mid-charge depths². The maximum plane shear stresses, $\frac{1}{2}(\sigma_1 - \sigma_3)$ obtained as a function of depth at the site and at higher elevation several km away, when plotted against $\frac{1}{2}(\sigma_1 + \sigma_3)$, all lay close to a common straight line suggestive of a failure envelope of the jointed rock mass and perhaps indicating that the pre-existing stress was already on the failure envelope for joint sliding. This might represent a situation where an explosion might not form a permanent stress cage³ if the fracture zone is larger than the joint spacing.

Fracture densities were estimated by counting fragments in cores taken from the shot depth interval before shooting the charges and at various distances from them (none closer than 24 borehole radii) after the shots. Permeabilities were measured by slug tests through a packer set in the core holes before and after shooting the charges, and before and after flushing shot-generated fines from the fractures. The permeabilities tended to be relatively low and erratic before flushing shot-generated fines from the fractures. After flushing out fines, they were substantially higher but still had a relatively large random variance. The fracture densities and post-flush permeabilities were in relatively good agreement with a model featuring a large zone around the charges in which the fracture density and permeability were uniformly increased, and outside the zone were not changed; the radius of the zone being equal to a calculated radius of the zone of rock put in compression by radial fractures pressured with gas from the charge². They were in poorer agreement with a model in which the fracture density and permeability

expected if the increases in fracture density and permeability had resulted from sudden application of explosion pressure to the borehole wall with no effects of gas pressure in fractures⁴.

If gas flows into fractures, its effects can continue to develop long after the shock wave has passed. Thus, in our experiments, blowout of gas from satellite holes up to 19 meters away began after delays up to almost three minutes; and Persson, Lundborg, and Johansson⁵ showed that gas pressure in fractures could account for the large-scale accelerations over a few milliseconds measured by Noren⁶ in bench blasts where fractures could open to a free face.

The theoretical studies of Kutter⁷, Kutter and Fairhurst⁸ and Ouchterlony⁹ show that gas penetration of radial fractures can substantially increase the length of some of them, the number increasing with both rate and pressure and the longer ones generally tending to stop growing first. The growth is therefore unstable for more than 4-6 fractures unless there is some extra source of stability. Coursen² derived expressions for the final equilibrium gas pressure P_3 and radius R_1 of a cylindrical volume of rock put under a compression P_3 by multiple gas-pressured fractures from the confined detonation of a charge at loading density ρ_0 in a long cylindrical cavity of radius R_0 and volume V_0 , the rock having a failure shear stress of $\tau_f(P)$ and being under an external compressive stress P_2 normal to the charge axis. These expressions are:

$$P_3 = P_2 + \tau_f(P_2) \quad (1)$$

$$\frac{V_1}{V_0} = \frac{1+S(1+D-C)}{SD+C} \quad (2)$$

$$\frac{V_3}{V_0} = \frac{SD+1}{SD+C} \quad (3)$$

$$\frac{V_4}{V_0} = \frac{S(1-C)}{SD+C} \quad (4)$$

$$\frac{R_1}{R_0} = \left[B^{-1} \left(\left[\frac{D+S^{-1}-C+1}{D+S^{-1}C} \right] - A \right) \right]^{\frac{1}{2}} \quad (5)$$

where:

$$A = 1 + \frac{P_2}{L} - \frac{3\tau_f(P_2)}{5L}$$

$$B = \frac{8\tau_f(P_2)}{5L}$$

$$C = [X(P_3)]^{-1}$$

$$D = \frac{P_3}{MRT_4\rho_0}$$

V_1 is the volume of the central cavity plus the volume of the gas-pressured radial fractures, V_3 is the volume of the portion of the detonation

is the remaining volume of products assumed to be cooled to ambient rock temperature T_4 . Poisson's ratio of the rock was assumed to be $\frac{1}{4}$, making both Lamé constants equal L . M is the moles of permanent gas per unit mass of detonation products at (P_3, T_4) , and R in this case is the gas constant. Loss of gas through the faces of the fractures was assumed to be negligible in the water-flooded rock. V_4 was assumed to be proportional to the expansion in cavity volume, the constant of proportionality, $S \equiv V_4(V_3 - V_0)^{-1}$, being chosen empirically. For $S=0.11$, the calculated values of R_1 shown in Figure 1 agreed well with the experimentally inferred fracture radii at the two levels of tectonic compressive stress P_2 in the experiments described above. This value of S made V_3 larger than the measured post-shot cavity volumes by an amount that put the boundary between hot gas and cool gas inside the fractures at depths of $1/2$ and $3/4$ the fracture length for tapered and untapered fractures, respectively.

R_1 is not the maximum radius of gas-pressured fracture growth, but is the maximum radius at which (a) pressure in the longest fractures is P_3 and (b) the largest angles between fractures are small enough to put most of the rock between them under a biaxial compression P_3 , to form a virtual pressurized cavity of radius R_1 .

Kutter's⁷ isochromatic fringe patterns show that in and around such a virtual cavity formed by multiple gas-pressured fractures of radius R several regions of stress can be identified as follows: an outer boundary B_1 , $B_1(r, \theta)$ of the region stressed by clamping between fractures, that bulges out between adjacent fracture tips; an intermediate line $B_2(r, \theta)$ marking maximum shear stress at constant θ and lying close to the circle of radius R ; and an inner boundary $B_3(r, \theta)$ containing the uniformly compressed core, in the form of cusps tangent to the radial fractures at their tips. The opposing bulges and cusps form elliptical stress transition zones between the fracture tips. Therefore, the compressed core is nearly as large as the circle passing through the fracture tips when the number of longest fractures are, say, 9-12 or larger. But as the number of fractures falls below, say, 6 to 9 the cusps become large. Therefore, the outward growth of the main area of the fully compressed core does not scale with the outward growth of the longest fractures if the number of growing fractures continues to fall. It falls behind, with its growth limited to narrow extensions out to the tips of the few long fractures that continue to grow. Thus, our model contains the assumption of stable or unstable growth of at least 6, but preferably at least 9 to 12 longest fractures of approximately equal length for as long a time as the shear stress equals or exceeds the strength of the tectonically compressed rock just outside the virtual cavity; and subsequent continued growth of fewer than 6 equally spaced fractures does not appreciably increase the size of the compressed core, particularly if such subsequent growth occurs at lower pressure. The required stability of the minimum fracture pattern in each plane normal to the long charge might be provided by the recruitment of new gas-pressured fractures to replace those that stop growing. Possible mechanisms for this are branching of fractures owing either to dilation of joints in the rock or to incipient failure around the entire stressed rim of the virtual cavity, or the late arrival of gas-pressured fractures from other gas injection points up and down the charge.

The model also contains the assumption that gas can escape through the zone of crushed and tangentially compressed rock that the explosion forms in the wall of the cavity. There may be several ways for this to happen, particularly for cylindrical charges which have thinner stress cages than spherical charges. For example, the gas might leak through the remnants of pre-existing water-filled fractures or through shear fractures formed in the crushed zone under dilating conditions near the end of cavity expansion or after expansion has ceased. Only a few leaks through the stress cage or off its end and into outlying radial fractures might relieve the stress in local portions of the crushed zone, perhaps thereby allowing axial growth of the leaks and thereby unzipping the stress cage from end to end. In any case, it seems reasonable to suppose that radial fractures would narrow where they

stress relief and perhaps later from clogging with debris. This, as well as branching of fractures, would throttle the gas flow into the radial fractures. A pattern of 6-12 radial fractures extended outward by flow throttled near the cavity might produce uniform fragmentation and permeability, through a previously described process², out to a limiting radius that decreases with increasing tectonic stress. The proposed mechanism is as follows.

Suppose $P_1(t)$ is the gas pressure in the central cavity, P_2 is the pre-existing compressive stress on the rock perpendicular to the charge, and P_3 is a gas pressure in the fractures postulated to be sufficient to keep a minimum pattern of 6-12 radial fractures growing in this particular rock under compressive stress P_2 . Growth of fewer fractures under a pressure less than P_3 is not ruled out. Assumptions are that $P_1(t) > P_3 > P_2$, that the rate of fracture growth is a sufficiently steep function of P_3 , and that the rate of gas flow from the central cavity into the fractures is sufficient to maintain a pressure $P_3 + \Delta P$ in the fractures, but that flow into the fractures is sufficiently throttled near the explosion cavity to make $\Delta P / P_3 \ll 1$. Then for all values of $R(t)$ traversed by the fracture tips until the minimum pattern of 6-12 fractures stops growing, the pressure in the fractures is essentially constant. The minimum pattern will form a growing virtual cavity with internal pressure P_3 and radius $R(t)$. If P_3 satisfies relation (1), the rock on the entire boundary of the virtual cavity and not just near the fracture tips is at its failure stress, a condition assumed to satisfy the requirements that the fracture pattern be stable and that the rate of fracture growth is a sufficiently steep function of P_3 . The compressive and shear stresses (σ, τ) at coordinates (r, θ) in the rock not too close to a fracture tip are approximately

$$\sigma = P_2 \text{ and } \tau(t) = (P_3 + \Delta P - P_2) \frac{R^2(t)}{r^2} \approx (P_3 - P_2) \frac{R^2(t)}{r^2} \text{ for } r > B_1 [r(t), \theta] \quad (6)$$

$$\sigma \approx P_3 + \Delta P \approx P_3 \text{ and } \tau = 0 \text{ for } r < B_3 [r(t), \theta] \quad (7)$$

A stress transition zone lies between these regions, and is bisected by the line $B_2[r(t), \theta]$ lying close to the circle of radius $R(t)$ and on which the shear stress is a maximum as a function of r at constant θ . B_2 moves outward with the growing fractures, sweeping all elements of rock at constant θ with the same shear stress. This shear stress is approximately $(P_3 - P_2)$ along most of B_2 but rises to much higher values close to the fracture tips. Quasistatic stress from the pressure $P_1(t)$ in the central cavity is neglected⁹ as is the P wave whose effects are not apparent in our data. Owing to the behavior of the functions (6) and (7) and to the behavior of the stress in the transition zone, the stress (σ, τ) applied to each element of outlying rock at $r \leq B_3(R_1, \theta)$ and not approached too closely by a fracture tip starts at $(P_2, 0)$, is sheared to $[P_2, (P_3 - P_2)]$ and is then

For small changes in shear stress will be reduced by the hydraulic pressure of the water in the joints. Therefore, the hypothesized sequence of events accompanying these shifts in stress, as illustrated in Fig. 2, is as follows.

- Shear from $(P_2, 0)$ to $[P_2, (P_3 - P_2)]$, misaligns blocks in the jointed, water-flooded rock, develops major point and line contacts between them, and dilates the fracture volume.
- Compression to $(P_3, 0)$ then increases the point and line loads, fracturing blocks quite uniformly over the compressed region. The effective pressure causing such point load failure of a block can be much smaller or much greater than the tensile strength of the rock, depending upon whether the block is loaded by blocks much larger or much smaller in diameter than itself.
- In the water-flooded joints the shear deformation abrades asperities and the compression crushes rock at load points, forming mobile fines and increased fracture volume equal to the volume of the fines.

In concluding, we note a related fracturing process that might possibly occur under some circumstances to form repeated tangential fractures in the wedges of rock clamped between growing gas-pressured fractures. It is the one reported by Bridgman^{10,11} who found that violent transverse rupture occurred in glass and metal rods subjected to high hydrostatic pressure over a portion of their length. When a high gradient in surface pressure advances along a cylinder, this process can result in successive transverse ruptures and is the cause of diskings in cores taken from highly stressed rock. Jaeger and Cook¹² found that such transverse rupture occurred in cylinders of rock at a pressure of the order of their unconfined compressive stress for jacketed samples, but at a pressure only of the order of their tensile strength for unjacketed samples if time was allowed for the pore pressure to reach the applied pressure.

Measurements designed to test models such as these might well include simultaneous recordings of pressure and temperature in the borehole, triaxial stress and strain in the rock, pore pressure and flow of fluids in pre-existing fractures, microseismic noise of fragmentation, and arrival of gas at outlying stations. But the processes can be slow, so recording times should be long and the frequency response of the instrumentation should be flat down to 10^{-3} Hz or lower. Similarly, the behavior of computer models of such quasistatic processes sometimes should be followed out to much longer times than are conventionally used when modeling explosion phenomena.

References

1. Haimson, B. C., "A Simple Method for Estimating In Situ Stresses at Great Depths", Field Testing and Instrumentation of Rock, A.S.T.M. Spec. Tech. Pub. 554, 156-182 (1974).
2. Coursen, D. L., "Cavities and Gas Penetrations from Blasts in Stressed Rock with Flooded Joints", Acta Astro. 6, 341-363 (1979).
3. Schmidt, R. A., Boade, R. R. and Bass, R. C., "A New Perspective on Well Shooting - The Behavior of Contained Explosions and Deflagrations", Society of Petroleum Engineers SPE 8346 (1979).
4. Coursen, D. L., in preparation.
5. Persson, P. A., Lundborg, N. and Johansson, C. H., "The Basic Mechanisms in Rock Blasting", Proc. 2nd Congr. ISRM, Beograd, paper 5-3, 15 pp. (1970).
6. Noren, C. H., "Blasting Experiments in Granite Rock", Quarterly Col. Sch. of Mines 51 (3) 211-225 (1956).

7. Kutter, H. K., "Stress Analysis of a Pressurized Circular Hole with Radial Cracks in an Infinite Elastic Plate", Int. J. Fracture Mech. 6 (3), 233-247 (1970).
8. Kutter, H. K. and Fairhurst, C., "On the Fracture Process in Blasting", In J. Rock Mech. Min. Sci. 8, 181-202 (1971).
9. Ouchterlony, F., "Fracture Mechanics Applied to Rock Blasting", Proc. 3rd Congr. ISRM, Denver, 1377-1383 (1974).
10. Bridgman, P. W., "Breaking Tests under Hydrostatic Pressure and Conditions of Rupture", Phil. Mag. 24, 63-80 (1912).
11. Bridgman, P. W., "The Effect of Hydrostatic Pressure on the Fracture of Brittle Substances", J. Appl. Phys. 18, 246-258 (1947).
12. Jaeger, J. C. and Cook, N. G. W., "Pinching-off and Disking of Rocks", J. Geophys. Res. 68 (6), 1759-1765 (1963).

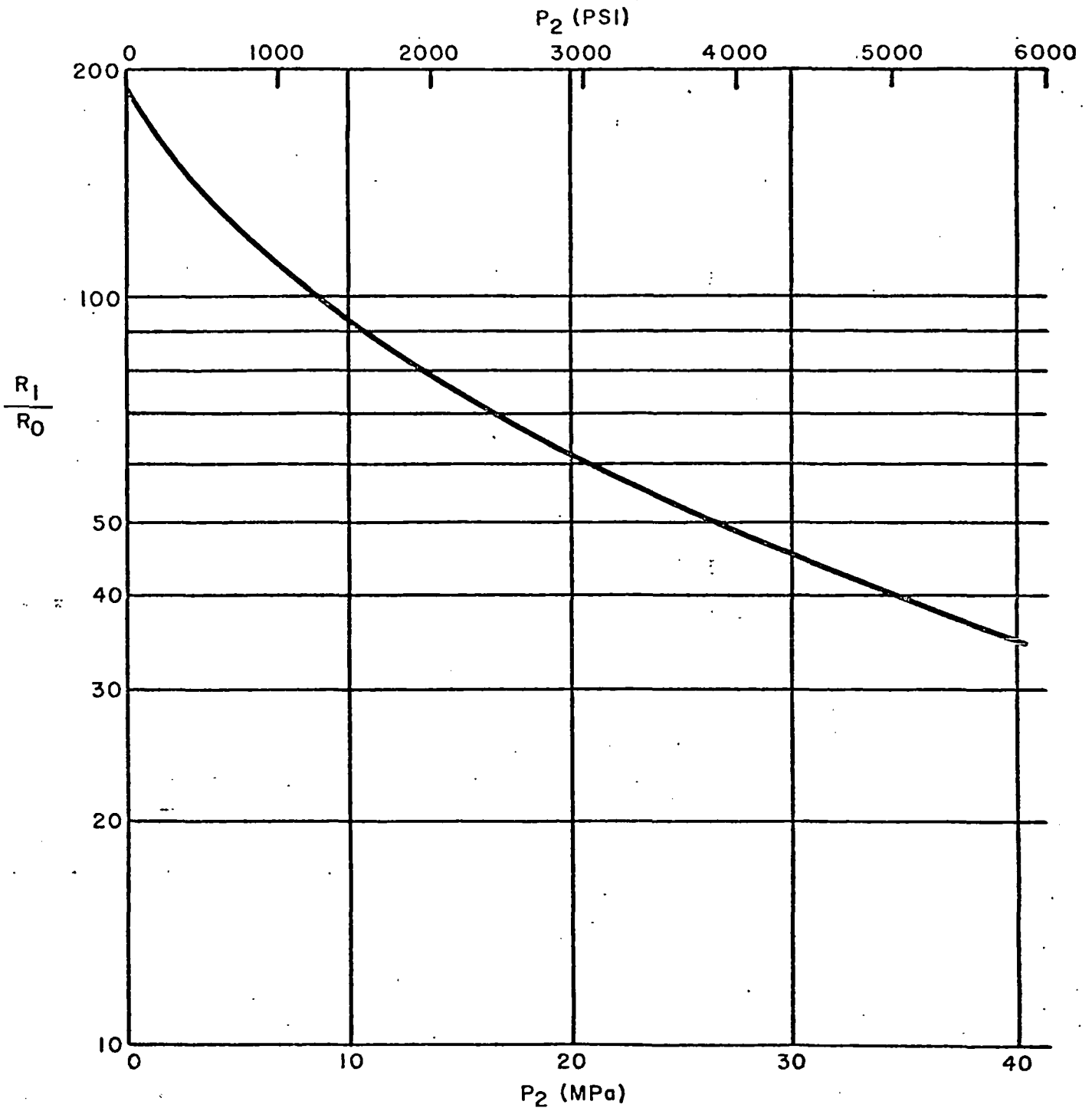


Figure 1. Calculated scaled fracture radius vs. tectonic compressive stress for cylindrical charges of EL 836 in Devonian shale.

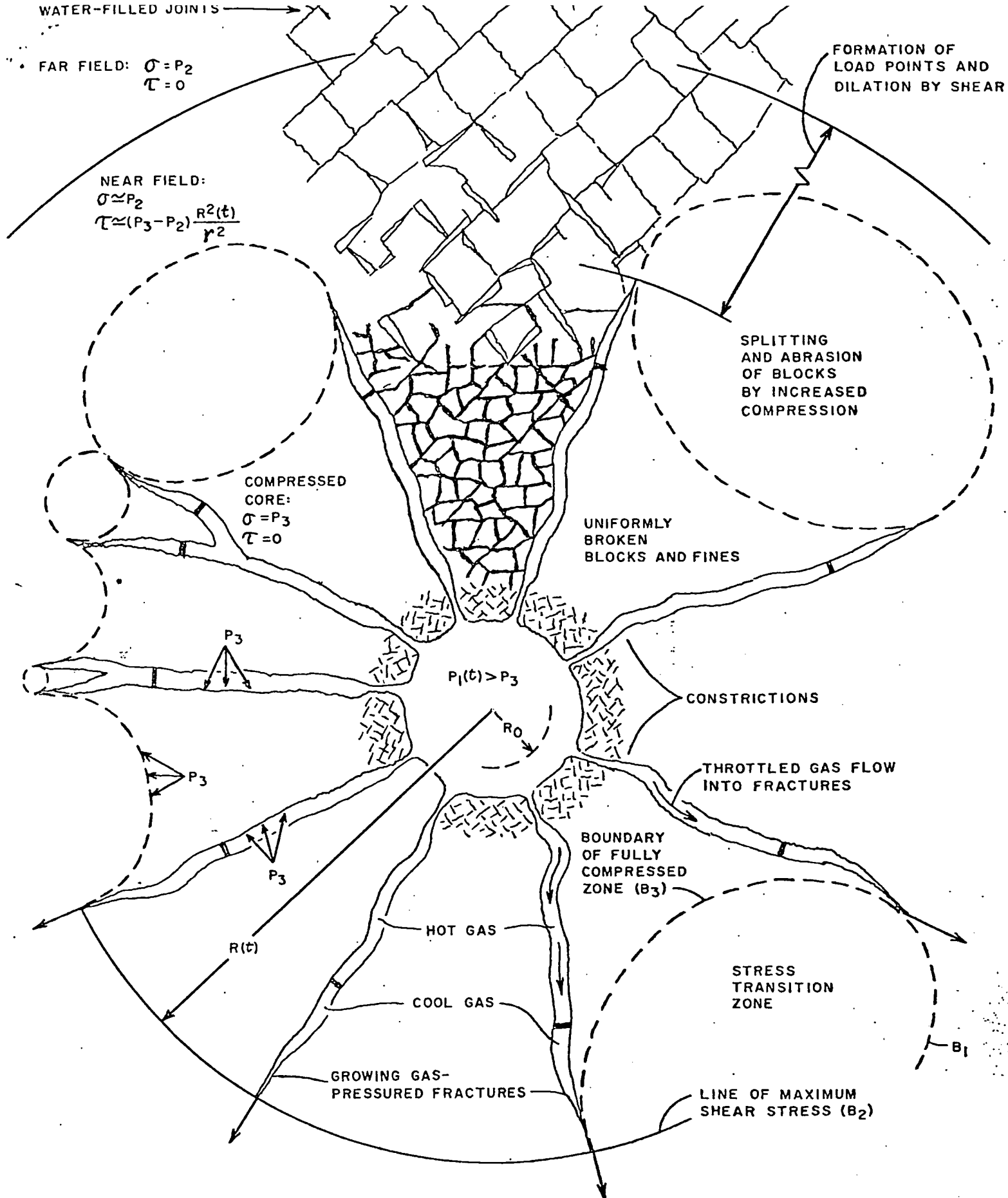


Figure 2. Schematic diagram of radial fractures growing under constant internal pressure and producing uniform fracture density and fracture volume.

Chapter 14

GENERAL PRINCIPLES OF UNDERGROUND OPENING DESIGN IN COMPETENT ROCK

by Wilbur I. Duvall

Senior Science Advisor
Excavation Engineering and Earth Mechanics Institute
Colorado School of Mines, Golden, Colorado

ABSTRACT

This paper discusses general principles of underground opening design based on the concept that with the necessary input data regarding the geology of a site, the physical properties of the rocks, the in situ stress field in the rock and the general geometry of the underground openings, the rock formation can be classified into six major categories which are useful for design purposes. Using simple theories for the criteria of failure for rock in compression and tension, general elastic theory for stress concentration around openings and in structures, beam theory for stability of roof rock, and elementary inelastic theory for creep phenomena, basic design techniques are outlined for the various rock classifications. The need for field evaluation of the theoretical design is stressed and some general techniques that should be used in these field evaluations are discussed. Where appropriate, the need for additional studies and research is noted.

INTRODUCTION

The basic theme of this session is on underground opening design; therefore, it seems appropriate that one paper should be devoted to a review of some of the general design techniques that have been developed and are in current use. Because of my long association with the Bureau of Mines, this paper is strongly influenced by the research efforts of my many colleagues. The general outline of the paper is based around lecture notes for a course in rock mechanics that I taught for several years at the Colorado School of Mines.

This paper outlines some general principles and procedures that a rock mechanics engineer can use to arrive at a logical design for underground openings in various types of competent rock formations. The concept is used that rock formations can be classified into six major categories which are useful for design purposes provided the necessary input data are available regarding the geology of the site, the physical properties of the rocks, the in situ stress field in the rock and the general geometry of the underground openings. Using simple theories for the criteria of failure for rock in compression and tension, general elastic theory for stress concentration around openings and elementary inelastic theory for creep phenomena, basic design techniques are outlined for the various rock classifications. Because even competent rock is not a perfectly elastic, homogeneous and isotropic medium, it should be understood at the

very beginning of this discussion that the stability and safety of any theoretically designed rock structure is only an estimate of the true stability and safety of the mined structure. Thus, it is essential that fairly large safety factors (2 to 8) be employed in the theoretical design and that field evaluation of the design be made by instrumented studies during the construction of the underground structures.

Table 1 lists what I consider are the basic requirements for the design and evaluation of safe and stable structures in rock. The first two items in this table involve the general geology of the site and are usually supplied by a geologic report. If the report is based on exploration drilling, it should contain a log of the structural defects in the core and an RQD index for the rock (Obert and Duvall, 1967). The information contained in the geologic report is used by rock mechanics engineers to help classify the rock formations for design purposes, to determine which rock types are important for physical property testing, to identify the types and extent of major defects that will exist in the rock structures and to aid in modeling the overall structure for finite element studies.

TABLE 1

Requirements for Design of Underground Openings

1. Geology and geometry of the various rock types.
2. Major mechanical defects that exist in the rocks.
3. General geometry of the underground openings.
4. Physical properties of the rocks.
5. Rock classification for design purposes.
6. In situ stress field determination.
7. Criteria of failure for rocks.
8. Theoretical design of underground openings.
9. Field evaluation of the design.

The third item in Table 1 is usually supplied by the owner of the site. For example, if the site is an underground mine, the mining company has generally decided on the general mining method to be used and the approximate size of openings required to carry out this mining method. Also, if the site is for an underground facility such as a tunnel or storage space, the owner usually has general specifications for the approximate size and shape of the underground openings. Thus, the duty of the design engineer is to adjust the sizes, shapes and general layout of the underground openings within certain specified limits so that a safe and stable rock structure will exist.

The other items in Table 1, while self-explanatory in their general meaning, are discussed in some detail in the rest of this paper.

PHYSICAL PROPERTIES OF ROCKS

The most important physical properties of rocks needed for design purposes are listed in Table 2. Where possible, standard procedures for determining properties of rocks should be used (Obert and Duvall, 1967; Obert, et al, 1946; ASTM, 1971a; ASTM, 1971b; Bieniawski and Franklin, 1972; Franklin, 1972). My recommendation is that ASTM, Bureau of Mines or International Society for Rock Mechanics standards should be followed where applicable and that only

those properties that are to be used for design purposes be determined.

Selection of core samples for physical property testing presents many problems. A representative random sample is desired for each rock type and for each property. If core is selected from exploration drilling, samples should be selected from several holes and variation of physical properties between holes should be studied. If the exploration core has been split in a mechanical core splitter, it is usually not satisfactory for physical property testing. If the exploration core has been split by a diamond saw, the remaining part may be redrilled for test samples. When the physical property data has been obtained from only exploration drilling core, it is good practice to supplement these data with some additional testing from drill core obtained underground after access is available. These cores should be obtained from several different holes so that representative random samples of the rock types in the critical rock structures are obtained.

TABLE 2

Required Physical Properties of Rock

1. Density.
2. Young's modulus.
3. Poisson's ratio.
4. Uniaxial compressive strength.
5. Triaxial compressive strength (solid core).
6. Triaxial compressive strength (planes of weakness).
7. Modulus of rupture.
8. Indirect tensile strength.
9. Creep constants.

It is not possible to specify a given number of samples for each physical property as the variabilities of the data for the different properties and for different rocks are not the same. Thus, I would recommend that sufficient samples be taken so that the standard error in the average value is less than 10%.

A few specific remarks regarding some of the physical property tests appear to be in order. The triaxial compressive strength tests, both for solid core samples and samples with planes of weakness, should use a relatively small range of confining pressures which is realistic in terms of a specific design problem, for example 250 - 2,500 psi. For this range of confining pressures, a linear Coulomb failure criterion usually results which is easier to apply than a curved Mohr's envelope. Some additional research on triaxial testing is needed to determine if the failure criterion obtained by testing a large number of samples at different confining pressures is the same as that obtained by strain controlled triaxial tests where each sample is tested over a range of confining pressures in a stiff testing machine (Kovari and Tisa, 1975). If a one-to-one correspondence between these two methods of testing could be obtained for many rock types, then the number of samples required for triaxial testing could be reduced four or five-fold. Also, considerably more laboratory research is needed on the triaxial strength of rock samples with length-to-diameter ratios of less than one which contain planes of weakness at various angles.

The indirect tensile strength test is replacing the direct tensile strength test and the modulus of rupture test for obtaining the tensile strength of rock. The apparent reason for this substitution is that the indirect tensile test is the easiest and cheapest to perform. However, to my knowledge, there is not a good correlation between these three quantities for various rock types and very little experience has been established on the use of the indirect tensile strength in underground design. Consequently, I believe additional research is needed on the comparison of these different tensile testing techniques. Also, I prefer to rely on the modulus of rupture tests on horizontal core samples obtained from underground drill holes when designing safe roof spans in bedded rock formations.

Creep tests should be performed on those rock types that are suspected of showing inelastic effects. These tests should be conducted on modelled rock structures at several stress levels that encompass the estimated stress levels in prototype structures. The duration of the creep tests should be of sufficient length (one to three months) to obtain steady state creep rate or to obtain a simple power law decay for creep rate with time. If a steady state creep rate condition is obtained, the creep data for a given stress level probably can be fit to a Burger's model of the form:

$$\epsilon = \frac{\sigma_0}{E_m} + \frac{\sigma_0 t}{3\eta_m} + \frac{\sigma_0}{E_k} (1 - e^{-E_k t / 3\eta_k}) \quad (1)$$

where:

ϵ = total strain at time t

t = time

σ_0 = applied stress

E_m, E_k = Maxwell and Kelvin elastic constants

η_m, η_k = Maxwell and Kelvin coefficients of viscosity

e = base of Napierian logarithms

For many inelastic rocks, the constants in this equation are functions of the applied stress. Thus, care has to be exercised that appropriate constants and stress levels are employed when equation 1 is used to extrapolate to long times that represent the life of the underground structure. If the creep rate $\dot{\epsilon}$ shows a simple power law decay with time the creep data probably can be fit to an equation of the form:

$$\dot{\epsilon} = k\sigma^n t^{-m} \quad (2)$$

where k , n and m are constants. Values of n for salt, trona and potash have been found to lie in the range of 2.4 to 3.3 and values of m from 0.6 to 0.9 (Obert and Duvall, 1967; Obert, 1964). As in situ creep data also can be represented by equation 2, the use of this equation to estimate closure deformations for long times is justified (Bradshaw, et al, 1964).

ROCK CLASSIFICATION FOR DESIGN PURPOSES

Many systems for classifying rocks have been developed and are used for different purposes. Some of these systems are based only on the geologic

properties of the rock, some on the mechanical condition of the diamond drill core, and others on a few measured physical properties of the rock. For purposes of design and stability evaluation of underground openings, a rock classification system should be based on a combination of geological and mechanical rock properties and also take into consideration the in situ stress field and the relative size of the underground openings. Such a system of classification was developed by the Bureau of Mines and found to be very useful in design problems (Obert and Duvall, 1967; Obert, et al, 1960). This classification system is given in Table 3; however, an extra column has been added to the original classification to indicate the design techniques that are appropriate for each class of rock.

TABLE 3

Rock Classification for Design Purposes

<u>Classification</u>	<u>Design Techniques</u>
I. Competent	
A. Massive	
1. Elastic	Elastic theory
2. Inelastic	Elastic theory plus time effects
B. Laminated	
1. Elastic	Elastic and beam theory
2. Inelastic	Elastic and beam theory plus time effects
C. Jointed	Experience plus rock mechanics
II. Incompetent	Experience plus rock mechanics

In this classification system, two main classes of rock are considered: competent rock and incompetent rock which are defined as follows:

Competent rock is any rock which, because of its mechanical and geologic characteristics, is capable of sustaining underground openings without the aid of any structural support except that provided by unmined rock in the form of pillars and side walls, etc. Note that roof bolts and small random props which support only local loose rock are not considered structural supports.

Incompetent rock is any rock which, because of its mechanical and geologic characteristics, is not capable of sustaining underground openings without the aid of additional structural support in the form of linings, steel sets or systems of props.

Competent rock is then subdivided into three additional categories: massive, laminated and jointed, which are defined as follows:

Massive rock is a rock formation where the spacing between mechanical defects such as joints, partings or faults is equal to or greater than the critical dimensions of openings, or where the strength of the bond across these mechanical defects is comparable to the rock strength.

Laminated rock is a rock formation divided by approximately parallel planes of weakness into lamina

whose thicknesses are small compared with critical dimensions of openings.

Jointed rock is a rock formation subdivided into three dimensional shaped figures by more than one set of joints and partings and where the spacing between these mechanical defects is small compared to critical dimensions of openings and where the strength of the bond across these mechanical defects is small compared to the rock strength.

Massive and laminated rock are then subdivided according to the elastic properties of the rock as follows:

Elastic rock is one whose physical properties will permit the use of elastic theory to predict strains and displacements from applied stresses.

Inelastic rock is one whose physical properties are such that strains and displacements are a strong function of time as well as applied stresses.

The above classification system for rock not only depends upon the mechanical and geologic characteristics of the rock but also on size of openings and their depth below the surface. For example, many competent rocks at shallow depths for small stress fields could become inelastic rock at greater depths and larger stress fields, or competent massive rock for small openings could become laminated or jointed rock for larger openings. Thus, to classify rock for design purposes requires a knowledge of the geologic properties of the rock mass, the physical properties of the rock, the general size of the openings to be mined and the average range of the in situ stress field to be encountered. As a result, once the rock has been classified, the design techniques to be used are specified as shown in Table 3. The last two design techniques are given as experience plus rock mechanics. By this statement, I do not mean to imply experience is not used in the first four categories. Experience plays an important part in all underground design problems. However, by this statement, experience plus rock mechanics, I want to imply that rock mechanics design techniques for competent jointed rock and incompetent rock are not very well established to date and therefore, in my estimation, experience plays the major role in design for these two classifications. As a result, this paper will not consider these last two categories.

IN SITU STRESS FIELD DETERMINATIONS

The determination of the magnitude and direction of the in situ stress field in rock formations where underground openings are to be mined is an important step in the design of underground structures. Before access to the rock formation is possible, there are four methods available for obtaining information on the in situ stress field. First, the stress field can be estimated from gravity loading assuming complete lateral confinement. Thus, the vertical and horizontal stresses are estimated by:

$$S_v = \gamma h \quad (3)$$

and

$$S_h = \frac{\nu}{1-\nu} S_v \quad (4)$$

where:

S_v = vertical stress
 S_h = horizontal stress
 h = depth from surface
 ν = Poisson's ratio
 γ = average weight density of overburden rock

Experience has shown that this technique gives a fairly accurate estimate of the vertical stress but usually underestimates the horizontal stresses and fails to predict a variation of horizontal stress with direction which is the usual case.

Second, the magnitude and directions of the horizontal stresses can be determined in a deep vertical drill hole by the hydrofracturing technique (Obert and Duvall, 1967; Haimson and Fairhurst, 1970). This technique has to assume one of the principal stresses is known and is directed along the hole axis. The method gives fairly reliable results in rock formations relatively free of open joints and fractures. However, it is expensive to conduct and, to my knowledge, has not been used extensively for preliminary design of underground openings.

Third, the horizontal stress field can be estimated from experimental data in similar and nearby sites and the vertical stress estimated by equation 3. As more and more data are collected on the in situ stress field in various mines throughout the country, one's ability to estimate in situ horizontal stress fields continues to improve. In making these estimates, it is most important to take into consideration the topography of the site where stress data are available and the topography of the new site (Hooker, et al, 1972).

Fourth, the horizontal stress field can be determined in near-surface rocks by the overcoring stress relief technique in vertical holes to depths of 50 to 75 ft. This method can detect the presence of horizontal tectonic stresses if good sound rock is found near the surface and if the topography is favorable for the existence of horizontal stress fields. If horizontal tectonic stresses are present in near-surface rocks, they most likely are present in the deeper rocks. Thus, this information can be used to help estimate magnitudes and directions of the in situ stress field at the underground site.

Recently, I had the opportunity to investigate the effect of the static water pressure on the borehole and on the thick-wall rock cylinder during the overcoring process in deep water-filled vertical drill holes. As a result of this study, I found that the diametral deformations during the overcoring process which determine the values of the secondary horizontal principal stress are given by:

$$U = U_m + \frac{\nu d S_z}{E} + \frac{2 d p_w}{E} \\ = \frac{d}{E} [(P+Q) + 2(1-\nu^2)(P-Q) \cos 2\theta] \quad (5)$$

where:

U = diametral deformation produced by P and Q
 U_m = measured diametral deformation
 P = maximum horizontal secondary principal stress
 Q = minimum horizontal secondary principal stress
 S_z = estimated vertical stress
 p_w = static water pressure at gage position
 d = diameter of gage hole
 E = Young's modulus of the rock
 ν = Poisson's ratio of the rock
 θ = angle from the direction of P to U_m

It is evident from equation 5 that the correction to the measured diametral deformation for the static water pressure is approximately three times as large as that for the vertical rock stress. Both of these corrections are of the same sign and are added to the measured U_m if an expansion is considered positive, or subtracted from U_m if an expansion is considered negative. For 50 ft deep water-filled vertical holes, these corrections are significant when the horizontal stresses are less than 1,000 psi.

When design of underground openings is required before access to the rock formation is possible, any one of the above methods for estimating the stress field can be used. However, I consider such designs preliminary and recommend, when underground access is first available, that the in situ stress field be determined by the stress relief overcoring technique using the improved three component borehole deformation gage developed by the Bureau of Mines (Hooker, et al, 1974a; Hooker and Bickel, 1974b; Panek, 1966). This gage and the necessary auxiliary equipment is now available commercially. If the rock is anisotropic by more than 20%, then I also recommend that the anisotropic equations be used to calculate the stresses (Becker and Hooker, 1967; Becker, 1968; Hooker and Johnson, 1969).

CRITERIA OF FAILURE FOR ROCKS AND SAFETY FACTORS

To design underground openings and structures in rock, it is necessary to use criteria of failure for rock under various stress conditions and to use safety factors to allow for differences between laboratory and in situ strength properties of rock and to account for errors introduced by the various assumptions made in the design process. Criteria of failure based on maximum stresses have been found to give reliable results in practice. Thus, it is assumed that rock will fail in tension when the tensile stress exceeds the tensile strength of the rock as determined by a standard modulus of rupture test on samples of rock core. If the tensile stresses in rock are small, then it is assumed that the rock will fail at a value of compressive stress equal to the compressive strength of the rock as determined by standard uniaxial compressive strength tests on samples of rock core. These failure criteria, when used with appropriate safety factors, can be expressed as:

$$\sigma_t \leq T_o / F_t \quad (6)$$

and

$$|\sigma_c| \leq c_o / F_c \quad (7)$$

where:

- σ_t = maximum or critical tensile stress around opening
- T_o = tensile strength of rock
- F_t = safety factor for tension, 4 to 8
- σ_c = maximum or critical compressive stress around opening
- c_o = compressive strength of rock
- F_c = safety factor for compression, 2 to 4

Using these simple criteria of failure, a large number of existing underground structures have been analyzed by the Bureau of Mines. From these studies, safety factors of 2 to 4 for rock in compression and of 4 to 8 for rock in tension were found to be satisfactory (Obert and Duvall, 1967; Obert, et al, 1960). The larger safety factors are recommended for long-term stability and for rocks having relatively weak joint systems, and the smaller safety factors are recommended for short-term stability and for rocks having no significant joint system.

If triaxial test data for solid core and core with planes of weakness are available, a linear Coulomb criterion of failure is sometimes used (Horino and Hooker, 1971). Figure 1 is an idealized representation of the linear Coulomb failure criteria for solid rock and for rock with a plane of weakness. When compressive stresses are considered negative, these two straight lines can be represented respectively by the equations:

$$\tau_\theta = S_o - \mu_o \sigma_\theta \quad (8)$$

$(\mu_o = \tan\phi = \cot 2\theta)$

where:

- τ_θ = shear stress on plane of failure
- σ_θ = normal stress on the plane of failure
- S_o = intrinsic shear strength of the solid rock
- μ_o = coefficient of shear strength or internal friction
- θ = angle of the plane of failure
- ϕ = slope angle for $(\tau_\theta, \sigma_\theta)$ line

and

$$\tau_\beta = S_f - \mu_f \sigma_\beta \quad (9)$$

$(\mu_f = \tan\phi_f)$

where:

- τ_β = shear stress on the plane of weakness
- σ_β = normal stress on the plane of weakness
- S_f = shear strength of the plane of weakness
- μ_f = coefficient of friction on the plane of weakness
- β = angle of the plane of weakness
- ϕ_f = slope angle of the $(\tau_\beta, \sigma_\beta)$ line

A finite element analysis of a rock structure determines the maximum and minimum principal stresses σ_1 and σ_3 at each point in the structure. A safety factor can be defined as the ratio of the maximum shear stress at failure to the maximum shear stress at a point in the structure under the assumption that the mean stress is constant. Thus, the respective safety factors for solid rock and rock with a plane of weakness are given by:

$$F_s = \frac{R_2}{R_1} = \frac{2S_o \cos\phi - (\sigma_1 + \sigma_3) \sin\phi}{\sigma_1 - \sigma_3} \quad (10)$$

and

$$F_f = \frac{R_3}{R_1} = \frac{2S_f \cos\phi_f - (\sigma_1 + \sigma_3) \sin\phi_f}{(\sigma_1 - \sigma_3) \sin(2\beta + \phi_f)} \quad (11)$$

where R_1 , R_2 and R_3 are the radii of the respective Mohr's circles (Figure 1).

THEORETICAL DESIGN OF UNDERGROUND OPENINGS

Simplified procedures that can be used to design underground openings in competent elastic rock that fails by brittle fracture are discussed in this section. The assumption is made that all the pertinent geologic, physical property and stress field data are available and that the rock formation has been classified according to Table 2. In addition to this rock classification, we need to distinguish between single openings and multiple openings. An underground opening is considered single if the stress distribution in the rock surrounding the opening is not affected by the presence of other openings or surfaces. Conversely, a series of underground openings is considered multiple if the stress distribution in the rock surrounding any one opening is influenced by the presence of the other openings or nearby surfaces. In general, if two underground openings are separated by a distance equal to or greater than twice the sum of their dimensions in the direction of separation, then the openings are considered single and if separations are less than specified, they are considered multiple. Also, single openings may be two-dimensional or three-dimensional in character. However, theoretical studies have shown that the stress concentrations around various symmetrically shaped tunnels are always slightly larger than those for similar cross-sectional shaped three-dimensional openings (Obert and Duvall, 1967). Consequently, stress concentration data for design of symmetrically shaped single openings with three-dimensional character can usually be obtained from equivalent two-dimensional opening data.

Single Openings in Competent Massive Elastic Rock

There is not an established theoretical procedure for determining the maximum size of a single opening that will be stable in a massive elastic rock formation. Thus, maximum critical dimensions are usually established by past experience with openings in similar rock types and by keeping critical dimensions comparable to the average spacing between major mechanical defects in the rock. The major design considerations are to determine the maximum stress concentrations that are developed around the opening for the given applied

stress field and to compare these maximum or critical stresses with the criteria of failure as given by equations 6 and 7. Considerable reduction in the maximum stress concentrations and elimination of most tensile stresses can be achieved if the major axes of the opening are aligned with the principal stress directions and are proportional to the principal stresses. Also, the radii of curvatures for the opening surfaces should be as large as possible, especially on the major axes of the openings.

For underground openings created by blasting the first few feet of rock will contain some blasting fractures. As a result, this rock has less stiffness than the rock farther from the opening surface. Consequently, the maximum stresses around underground openings are usually not at the surface of the opening but at some distance from this surface and of lower magnitude than if the maximum stress had been at the surface. For this reason, the exact shape of the mined opening with all its small surface irregularities need not be modelled, just an approximate shape. Thus, maximum stresses can usually be estimated from available theoretical or photoelastic data for various two-dimensional openings such as circles, ellipses, ovaloids and rectangles with rounded corners. Finite element analyses are required only for two and three-dimensional openings which are non-symmetrical in cross-sectional shape or where the principal axes of the opening are not aligned with the directions of the in situ principal stresses.

Single Openings in Competent Laminated Elastic Rock

Single openings in competent laminated elastic rock will usually have a flat roof and the immediate roof rock will consist of one or more layers of rock of various thickness. Thus, by using simple beam theory to estimate safe span lengths, the design engineer has available a theoretical technique to estimate the size of the opening in addition to experience with other openings in similar rock types. The other design techniques that are used are the same as those discussed for single openings in massive elastic rock.

The maximum values of the deflection, shear and tensile stress for a horizontal, gravity-loaded roof layer clamped at both ends are given by (Obert and Duvall, 1967):

$$U_{\max} = \frac{\gamma L^4}{32Et^2} \quad (12)$$

$$\tau_{\max} = \frac{3\gamma L}{4} \quad (13)$$

$$\sigma_{\max} = \frac{\gamma L^2}{2t} \quad (14)$$

where:

- U_{\max} = maximum deflection
- σ_{\max} = maximum normal stress
- τ_{\max} = maximum shear stress
- L = span length

- t = thickness of roof layer
- E = Young's modulus of the rock
- γ = weight density of the rock

The maximum deflection occurs at the center of the span, and the maximum compressive, tensile and shear stress occur at the ends of the span - tension on the top surface and compression on the bottom surface of the rock layer. At the center of the span, the shear stress is zero and the tension on the bottom surface and the compression on the top surface are one-half the maximum values.

The ratio of σ_{\max} to τ_{\max} is:

$$\frac{\sigma_{\max}}{\tau_{\max}} = \frac{2L}{3t} \quad (15)$$

For a span-to-thickness ratio greater than 5 to 1, the tensile stress is more than three times the shear stress. Since the tensile strength of rock is usually less than the shear strength and much less than the compressive strength, the design of safe span lengths is based on only the maximum tensile stress in the roof layer.

Equation 14 may be rewritten as a design formula for roof spans by replacing σ_{\max} with R - the modulus of rupture of the rock, dividing by F_t - a safety factor and solving for L to obtain:

$$L = \sqrt{\frac{2Rt}{\gamma F_t}} \quad (16)$$

The value of F_t should be from 4 to 8.

When the immediate roof consists of two or more layers and the thinner layers overlie the thicker ones, the additional load on the lowest layer can be determined by calculating an adjusted weight density for the lowest layer by the following equation:

$$\gamma_a = \frac{E_1 t_1^2 \sum_{n=1}^n [\gamma_n t_n]}{\sum_{n=1}^n [E_n t_n^3]} \quad (17)$$

where n represents the n th layer counting upward. The value of γ_a is then used in the design equation 16. For multilayered roofs having various thicknesses and mechanical properties, the number of layers that need to be considered can be determined by using equation 17 stepwise, that is, the adjusted weight density is calculated for the first two layers, the first three layers, etc. until the adjusted weight density shows no further increase.

Quite often in laminated elastic rocks, the layers are much too thin and weak to remain unsupported over required span lengths for long periods of time. In these cases, thicker roof layers are obtained by installing rock bolts in the roof on a systematic pattern. The design of these patterns is beyond the scope of this paper.

The above techniques have been used for the design of safe span lengths with fairly good success (Merrill, 1954; Merrill, 1957; Merrill and Morgan, 1958; Merrill, et al, 1961). However, these

techniques disregard the effect of the horizontal stress field in the rock. I feel strongly that this applied horizontal stress has to be considered in the evaluation of the stability of roof layers. Recent measurements of stress in coal mine roof rocks by the Bureau of Mines and the Colorado School of Mines using the so-called undercoring stress relief technique (Hooker, et al, 1974a; Tsur-Lavie and Van Ham, 1974) have shown that the surface stress at the center of horizontal roof layers is generally compression and not tension as predicted by beam theory (Zink, 1975).

The maximum outer fiber stress for a clamped beam under combined axial and transverse gravity loads is given by:

$$\sigma_{\max} = -\sigma_h \pm \frac{\gamma L^2}{2t} \quad (18)$$

provided σ_h , the axial horizontal compressive stress applied to the beam, is less by a factor of about 1/20 of the axial compression necessary to produce Euler buckling (Roark, 1954; Griffel, 1966). Euler buckling in a clamped beam occurs at a compressive stress given by:

$$\sigma_e = -\frac{\pi^2 E t^2}{3L^2} \quad (19)$$

Thus, the restriction imposed on the use of equation 19 requires σ_h to be less than $\sigma_e/2\pi^2$, or:

$$|\sigma_h| \leq \frac{E t^2}{6L^2} \quad (20)$$

In situ horizontal stress fields are often less than the value specified by equation 20 but greater than the stress resulting from flexure as given by equation 14. Thus, in the presence of a horizontal stress field, many roof layers which are capable of standing unsupported without rock bolts will be entirely in compression. For example, assume $E = 3 \times 10^6$ psi and t/L equal to 0.1, then equation 20 states that $\sigma_h < 5,000$ psi. For a 6 ft thick rock layer over a span of 60 ft and $\gamma = 160$ lb/ft³, the maximum tensile stress developed from gravity loading is about 330 psi. Thus, if the horizontal stress in the rock lies in the range $330 < \sigma_h < 5,000$ psi, the roof layer would be entirely in compression. For ratios of t/L less than 0.01, Euler buckling can occur for horizontal stresses less than 1,000 psi and may be an explanation for many roof failures in coal mines known as cutters.

I have used some of these above ideas and concepts in design problems lately. However, equations 18 to 20 have not been tested for underground structures. Therefore, I am presenting these ideas only as suggested research problems and not as established design procedures.

Multiple Openings in Competent Massive Elastic Rock

The design techniques for multiple openings requires a knowledge of the change in stress concentration around a single opening that results when additional nearby openings are created. For single openings, the maximum stress concentrations develop almost immediately as the opening is mined; whereas,

for multiple openings, the maximum stress concentration around a given opening will increase progressively as other nearby openings are created. Thus, for multiple openings, it is the final stress distribution that exists around the system of openings that is used for design purposes.

Because boundaries of multiple openings are complex, only a limited number of theoretical and photoelastic model studies have been made and these studies are restricted to two-dimensional models. The results from photoelastic model studies of rows of various shaped holes in plates are useful in establishing some general principles of stress concentration which can be used for design purposes (Obert and Duvall, 1967). First, the maximum stress concentration around a series of holes in a plate occur around the central holes and increases as the number of holes increases but approaches a constant value for five or more holes. Second, the maximum stress concentration around a series of holes in a plate increases as the ratio of opening width to pillar width increases. Third, the rate of increase of the maximum stress with the W_o/W_p ratio is less than the rate of increase of the average stress in the rib pillar. Consequently, for larger values of W_o/W_p , the average stress approaches the maximum stress concentration and the stress distribution in the rib pillar becomes more uniform. Because of this fact and also because blasting fractures tend to reduce the large stress concentrations at the surface of openings, the design of pillar support for room and pillar mining is generally based on the average stress in the pillar as determined by tributary theory.

The tributary theory assumes that pillars uniformly support the entire load of the rock overlying both the pillars and the mined openings. The basic equations relating area, average pillar stress, applied vertical stress and areal extraction ratio are:

$$S_p = S_v \frac{A_t}{A_p} \quad (21)$$

$$R_a = 1 - \frac{A_p}{A_t} \quad (22)$$

$$R_a = 1 - \frac{S_v}{S_p} \quad (23)$$

where:

S_p = average pillar stress

S_v = vertical applied stress before mining

A_p = pillar area

$A_t = A_p + A_o$ = total area

A_o = opening area

$R_a = A_o/A_t$ = areal extraction ratio

Equation 23 can be rewritten as a design equation for R_a by replacing S_p by C_p/F_c , thus:

$$R_a = 1 - \frac{F C_v}{C_p} \quad (24)$$

and safety factors of 2 to 4 should be used. The value of C_p to use in equation 24 is given by:

$$C_p = C_1 \left[0.778 + 0.222 \frac{W_p}{H_p} \right] \quad (25)$$

where:

- C_1 = compressive strength of specimen with $W_p/H_p = 1$
 C_p = compressive strength of pillar or specimen with $W_p/H_p \neq 1$
 W_p = width or diameter of pillar or specimen
 H_p = height of pillar or specimen
 $0.5 < W_p/H_p < 4$

The above design equations apply to all types of room and pillar configurations. To determine dimensions, a specific geometry of openings and pillars is required as illustrated in Figure 2. For two-dimensional openings, the various areas are directly proportional to their widths, thus:

$$S_p = S_v \frac{W_p + W_o}{W_p} \quad (26)$$

and

$$R_a = 1 - \frac{W_p}{W_o + W_p} \quad (27)$$

From the geometry of an array of rectangular rooms and pillars as shown in Figure 3a, the pillar area and total area are given by:

$$A_p = W_p L_p \quad (28)$$

and

$$A_t = (W_o + W_p)(W_o + L_p) \quad (29)$$

and therefore, equations 21 and 22 become:

$$S_p = S_v \frac{(W_o + W_p)(W_o + L_p)}{W_p L_p} \quad (30)$$

and

$$R_a = 1 - \frac{W_p L_p}{(W_o + W_p)(W_o + L_p)} \quad (31)$$

For an array of square rooms and pillars, Figure 3b, $W_p = L_p$ and equations 30 and 31 become:

$$S_p = S_v \frac{(W_o + W_p)^2}{W_p^2} \quad (32)$$

and

$$R_a = 1 - \frac{W_p^2}{(W_o + W_p)^2} \quad (33)$$

A comparison of equations 33 and 31 shows that for a constant W_o that a maximum R_a is obtained when $L_p = W_p$. Thus, for mining operations where maximum recovery is important, a square array of room and pillar layout should be used if possible. The only

good justification for rectangular pillars is unequal horizontal principal stresses and certain geologic conditions. For unequal horizontal principal stresses, some additional pillar strength can be obtained by making the pillar long in the direction of the minimum horizontal compressive stress. Also, for widely spaced angle joints, rectangular pillars properly oriented and spaced can make these joints cut both basal planes of the pillar, which is a stronger condition than when the angle joint cuts a vertical side of the pillar.

The additional design equations for a square array of rooms and pillars are equations 32 and 33. Safety factors of 2 to 4 should be used. In most design problems, the pillar height is usually dictated by the thickness of the ore body or specifications for an underground structure. The opening width is selected in the same way as for single openings in massive elastic rock. Thus, the major design problem is the selection of pillar dimensions for proper support. If the rock contains some jointing at critical angles to the pillar height, both tributary theory and Coulomb failure criterion for rock with planes of weakness should be used for pillar design. When average stresses on planes of weakness are used in equation 11, safety factors of 1.5 to 2.0 appear to give satisfactory results.

Because experience has shown that tall, slim pillars tend to be unstable, I would recommend the H_p/W_p ratio be kept under 2. Considerable increase in strength can be obtained by decreasing this ratio to less than 1. This technique can be used to advantage for relatively thin ore bodies without sacrificing recovery. However, for thick ore bodies, the limitation of safe span widths results in loss of recovery as the H_p/W_p is decreased.

Multiple Openings in Competent Laminated Elastic Rock

Design techniques for multiple openings in laminated elastic rock are very similar to those presented previously. The height of pillars and openings are usually dictated by the ore body or construction specifications. Room widths or span lengths are determined by the same techniques as outlined for single openings in laminated elastic rock. Pillar dimensions are then designed as outlined for multiple openings in massive elastic rock. The laboratory-determined compressive strength for the pillar rock should be a good weighted average of the various rock types in the pillar.

Design of Openings in Inelastic Rock

Design techniques for inelastic rock formations follow the same general procedure as for elastic rock with the exception that long-term failure has to be taken into consideration. Thus, after making an elastic design, the laboratory creep data on modelled structures is used to estimate the creep rate and total deformation for long periods of time. Usually, equations 1 or 2 are satisfactory for making these estimates. If the limiting creep rate or deformation exceeds specifications, then the elastic design has to be modified to reduce the maximum or average stress in the structure so that limiting creep rates and deformations are within specifications.

FIELD EVALUATION OF DESIGNED UNDERGROUND OPENINGS

Regardless of the techniques used to design underground openings, a field evaluation of the design should be made when access is first available. Instrumented studies of the behavior of rock structures are needed to establish the validity of the design techniques and to determine the stability and safety of the underground openings. Much more research effort is needed on the subject of field evaluation of underground rock structures to improve our design techniques and to improve our ability to determine safe and stable underground structures. Good instrumentation and techniques are now available for measuring stress, change in stress, deformation, creep, in situ rock properties and for detecting zones of instability. What is needed is more use of these instruments in underground studies. Table 4 lists some of the basic instrumentation needed for field evaluation studies.

TABLE 4

Basic Instrumentation for Evaluation Studies

1. Borehole deformation gage
2. Strain indicators
3. Whittemore gage
4. Vibrating-wire stress meters
5. Rod extensometers
6. Wire or tape extensometers
7. Borescope or stratoscope
8. Biaxial test chamber
9. CSM cell
10. Rock noise monitoring equipment

When underground access is first available, the in situ stress field should be measured by the overcoring technique at a number of locations to determine the magnitude and direction of the principal stresses and their variability with location. If significant differences between the measured in situ stress field and the estimated stress field exist, then appropriate adjustments in design should be made. For single openings, the stress distribution in the rock around the opening should be determined. For multiple openings, the stress distribution in pillars and roof rock should be determined.

Additional physical property studies should be considered for rock samples from critical rock structures. Both laboratory and in situ techniques can be used. Instrumentation to measure change in stress and deformation with time should be installed in critical rock structures and the data correlated with the design considerations. Rock noise monitoring should be considered if instability problems are indicated (Blake, et al, 1974).

For room and pillar layouts in laminated rock formations, experimental room studies should be conducted as soon as possible after access is available. The techniques for making these studies are illustrated in Figure 4 and have been described in the literature (Merrill, 1954; Merrill, 1957; Merrill and Morgan, 1958; Merrill, et al, 1961). The experimental room is started by means of a small drift at the proposed roof horizon and double access to this room should be provided. The stress distribution in the roof rock should be measured by

the stress-relief overcoring technique using a vertical upward hole. The surface stress at the roof horizon should be determined by means of the undercoring stress-relief technique. Instrumentation should be installed at the center of the proposed experimental room to measure change in stress and strain in the immediate roof layer, sag in the immediate roof layer, and differential sag between upper roof layers. Vertical holes should be drilled for observing and measuring the separation between roof layers. Rock noise monitoring equipment should be used for safety reasons and to obtain information on the rock noise-stress level characteristics of the roof rock. After all the instrumentation is installed and initial readings have been established and shown to be stable with time, the original drift is widened in small increments. The data obtained after each increment of widening is correlated with the various design equations to determine the elastic constants of the roof rock and to evaluate the behavior and stability of the roof rock. Maximum span probably should not go beyond that which gives an estimated safety factor of 3 to 4. When good separations of the roof layers have been obtained throughout the experimental room, a final test for the in situ flexural strength of the roof layer can be made.

The in situ flexural strength test is performed by cementing all holes in the roof layer and loading the immediate roof with air pressure in the separation between the roof layers. All instrumentation to be used should be made self-recording with remote controls. The air pressure should be increased in small increments (1 or 2 psi) and maintained constant for a period of time to allow equilibrium conditions to be established. The deflection and tensile stress at the center of the span for the combined loading by the air pressure P , gravity, and the horizontal stress $-\sigma_h$ are given by:

$$U = \frac{YL^4}{32Et^2} + \frac{PL^4}{32Et^3} \quad (34)$$

and

$$\sigma = \frac{YL^2}{4t} + \frac{PL^2}{4t^2} - \sigma_h \quad (35)$$

When the above test is carried to complete roof failure, the in situ flexural strength of the roof rock is calculated from the maximum tensile stress equation given by:

$$\sigma_{\max} = \frac{YL^2}{2t} + \frac{PL^2}{2t^2} - \sigma_h \quad (36)$$

I want to make one final comment regarding underground evaluation studies. The rock mechanics engineer should work closely with the blasting foreman or engineer and try to develop blasting techniques which minimize blasting fractures in pillars, roof rock and walls. Many structural instability problems in roof rock and pillars are a result of poor blasting practices. In general, blasting patterns for rapid and economic rock production are not compatible with the structural integrity of the surrounding rock. Correcting instability problems in rock structures can be more costly and time-consuming than the additional cost

and time for improved blasting patterns that minimize fractures in critical rock structures.

REFERENCES

- ASTM COMMITTEE D-18, 1971a, Standard Method of Tests for Unconfined Compressive Strength of Rock Core Specimens, American Society for Testing and Materials Standards, Part 30, D2938, pp. 918-919.
- ASTM COMMITTEE D-18, 1971b, Triaxial Compressive Strength of Undrained Rock Core Specimens Without Pore Pressure Measurements, American Society for Testing and Materials Standards, Part 30, D2664, pp. 829-833.
- BECKER, ROBERT M., 1968, An Anisotropic Elastic Solution for Testing Stress Relief Cores, Bureau of Mines Report of Investigations, RI 7143, 15 pp.
- BECKER, ROBERT M. and VERNE HOOKER, 1967, Some Anisotropic Considerations in Rock Stress Determinations, Bureau of Mines Report of Investigations, RI 6965, 23 pp.
- BIENIAWSKI, Z. T. and J. A. FRANKLIN, 1972, Suggested Methods for Determining the Uniaxial Compressive Strength of Rock Materials and the Point Load Strength Index, International Society for Rock Mechanics Committee on Laboratory Tests, Document No. 1, 12 pp.
- BLAKE, WILSON, FRED LEIGHTON and WILBUR I. DUVALL, 1974, Microseismic Techniques for Monitoring the Behavior of Rock Structures, Bureau of Mines Bulletin, B 665, 65 pp.
- BRADSHAW, R. L., W. J. BOEGLEY and F. M. EMPRON, 1964, Correlation of Convergence Measurements in Salt Mines with Laboratory Creep-Test Data, Proceedings, 6th Symposium on Rock Mechanics, Rolla, pp. 501-514.
- FRANKLIN, J. A., 1972, Suggested Methods for Determining Water Content, Porosity, Density, Absorption and Related Properties and Swelling and Slope-Durability Index Properties, International Society for Rock Mechanics Committee on Laboratory Tests, Document No. 2, 36 pp.
- GRIFFEL, WILLIAM, 1966, Handbook of Formulas for Stress and Strain, Frederick Ungar Publishing Co., Inc., New York, pp. 63-73.
- HAIMSON, B. C., 1974, A Simple Method for Estimating In Situ Stresses at Great Depth, Field Testing and Instrumentation of Rocks, American Society for Testing and Materials, STP 554, pp. 156-182.
- HAIMSON, B. and C. FAIRHURST, 1970, In Situ Stress Determination at Great Depth by Means of Hydraulic Fracturing, Rock Mechanics - Theory and Practice, Society of Mining Engineers, AIME, Chapter 28, pp. 559-584.
- HOOKE, VERNE and CHARLES F. JOHNSON, 1969, Near Surface Horizontal Stresses Including the Effects of Rock Anisotropy, Bureau of Mines Report of Investigations, RI 7224, 29 pp.
- HOOKE, VERNE E., DAVID L. BICKEL and JAMES R. AGGSON, 1972, In Situ Determination of Stresses in Mountainous Topography, Bureau of Mines Report of Investigations, RI 7654, 19 pp.
- HOOKE, VERNE E., JAMES R. AGGSON and DAVID L. BICKEL, 1974a, Improvements in the Three-Component Borehole Deformation Gage and Overcoring Techniques, Bureau of Mines Report of Investigations, RI 7894, 29 pp.
- HOOKE, VERNE E. and DAVID L. BICKEL, 1974b, Overcoring Equipment and Techniques Used in Rock Stress Determination, Bureau of Mines Information Circular, IC 8618, 32 pp.
- HORINO, FRANK G. and VERNE E. HOOKE, 1971, The Mechanical Properties of Oil Shale and In Situ Stress Determinations Colony Mine, Bureau of Mines Progress Report, Denver, DMRC 1001, 17 pp.
- KOVARI, K. and A. TISA, 1975, Multiple Failure State and Strain Controlled Triaxial Tests, Rock Mechanics, Vol. 7, No.1, pp. 17-32.
- MERRILL, R. H., 1954, Design of Underground Mine Openings, Oil Shale Mine, Rifle, Colorado, Bureau of Mines Report of Investigations, RI 5089, 56 pp.
- MERRILL, R. H., 1957, Roof-Span Studies in Limestone, Bureau of Mines Report of Investigations, RI 5348, 38 pp.
- MERRILL, R. H. and T. A. MORGAN, 1958, Method of Determining the Strength of a Mine Roof, Bureau of Mines Report of Investigations, RI 5406, 22 pp.
- MERRILL, R. H., T. A. MORGAN and C. J. STAHLIK, 1961, Determining the In-Place Support of Mine Roof with Rock Bolts, White Pine Copper Mine, Michigan, Bureau of Mines Report of Investigations, RI 5746, 28 pp.
- OBERT, LEONARD, 1964, Deformational Behavior of Model Pillars Made from Salt, Trona and Potash Ore, Proceedings, 6th Symposium on Rock Mechanics, Rolla, pp. 539-560.
- OBERT, LEONARD and WILBUR I. DUVALL, 1967, Rock Mechanics and the Design of Structures in Rock, John Wiley and Sons, New York, 650 pp.
- OBERT, LEONARD, S. L. WINDES and WILBUR I. DUVALL, 1946, Standard Tests for Determining the Physical Properties of Mine Rock, Bureau of Mines Report of Investigations, RI 3891, 67 pp.
- OBERT, LEONARD, WILBUR I. DUVALL and ROBERT H. MERRILL, 1960, Design of Underground Openings in Competent Rock, Bureau of Mines Bulletin, B 587, 36 pp.
- PANEK, LOUIS A., 1966, Calculation of the Average Ground Stress Components from Measurements of Diametral Deformation of a Drill Hole, Bureau of Mines Report of Investigations, RI 6732, 41 pp.
- ROARK, RAYMOND J., 1954, Formulas for Stress and Strain, McGraw-Hill Book Co., Inc., New York, pp. 132-140, pp. 302-320.

TSUR-LAVIE, Y. and F. VAN HAM, 1974, Accuracy of Strain Measurements by the Undercoring Method, Proceedings, 3rd Congress of International Society for Rock Mechanics, Denver, Vol, 2, Part A, pp. 474-480.

ZINK, GERALD, 1975, The Effectiveness of Pillar Softening as a Roof-Control Method at the Revloc Mine, Ebensburg, Pennsylvania, Master's Thesis, Colorado School of Mines, Golden, 83 pp.

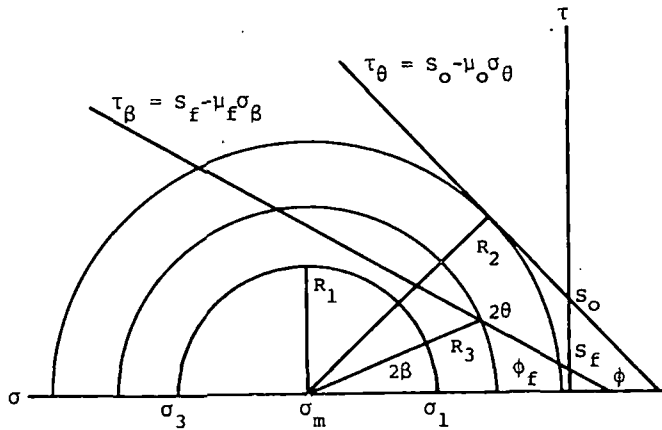
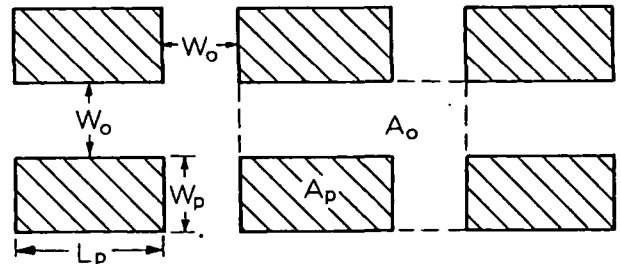
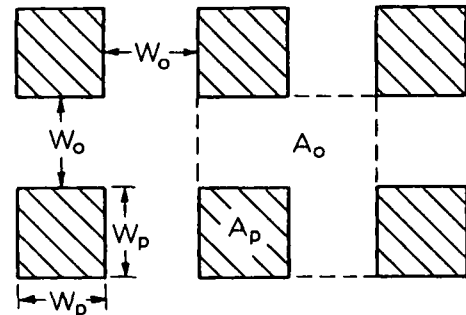


Figure 1 - Coulomb Failure Criteria for Solid and Fractured Rock



3a.



3b.

Figure 3 - Arrays of Rectangular and Square Rooms and Pillars

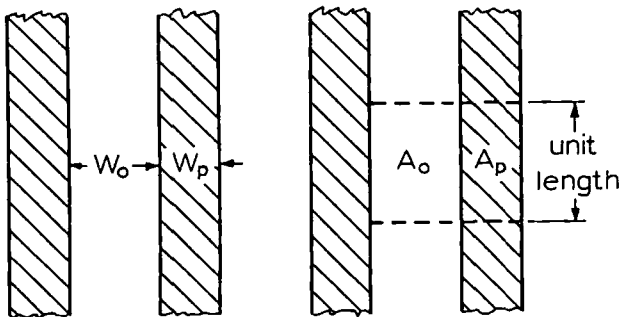
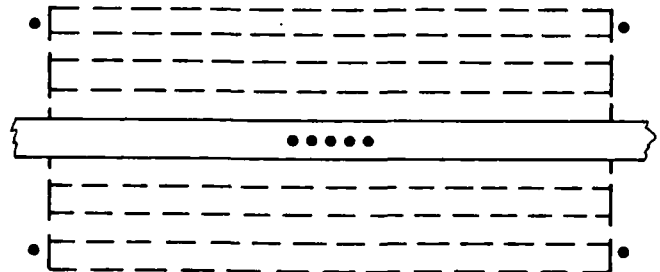


Figure 2 - Array of Rooms and Rib Pillars



• Instrumentation holes

Figure 4 - Experimental Room Technique

SOCIETY OF MINING ENGINEERS of AIME

SUBJ
MNG
GRFI

CALLER NO. D, LITTLETON, COLORADO 80123

PREPRINT
NUMBER

79-127



439

GROUNDWATER RESTORATION FOR IN SITU
SOLUTION MINING OF URANIUM

J. R. Riding
Project Manager

F. J. Rösswog
Chemical Engineer

Ford, Bacon & Davis Utah Inc.

T. D. Chatwin
Technical Director

Birtley Engineering Company

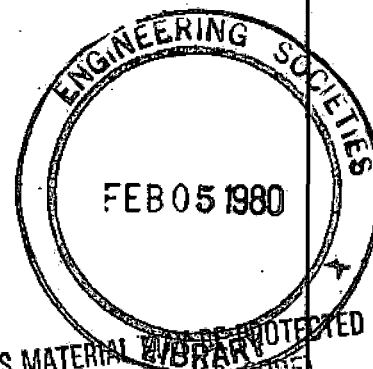
G. Buma
Technical Director
Resource Engineering & Development, Inc.

D. R. Tweeton
Research Physicist

Twin Cities Mining Research Center
Bureau of Mines
U.S. Dept. of the Interior

For presentation at the 1979 AIME Annual Meeting
New Orleans, Louisiana, February 18-22, 1979

UNIVERSITY OF UTAH
RESEARCH INSTITUTE
EARTH SCIENCE LAB.



NOTICE: THIS MATERIAL IS PROTECTED
BY COPYRIGHT LAW (TITLE 17 U.S. CODE).

Permission is hereby given to publish with appropriate acknowledgments excerpts or summaries not to exceed one-fourth of the entire text of the paper. Permission to print in more extended form subsequent to publication by the Institute must be obtained from the Executive Secretary of the Society of Mining Engineers of AIME.

If and when this paper is published by the Society of Mining Engineers of AIME, it may embody certain changes made by agreement between the Technical Publications Committee and the author, so that the form in which it appears here is not necessarily that in which it may be published later.

These preprints are available for sale. Mail orders to PREPRINTS, Society of Mining Engineers, Caller No. D, Littleton, Colorado 80123.

PREPRINT AVAILABILITY LIST IS PUBLISHED PERIODICALLY IN
MINING ENGINEERING.

GROUNDWATER RESTORATION FOR IN SITU SOLUTION MINING OF URANIUM

Abstract In situ solution mining of uranium has environmental advantages over conventional mining. The leaching of uranium, however, alters the groundwater quality in the aquifer where the mining occurs. Currently, regulations require that the groundwater be restored to approximately its original condition.

This paper, a summary of a study funded by the Bureau of Mines, reviews the state of the art in restoring groundwater quality after in situ uranium leaching. Current restoration practices discussed include disposal of liquid wastes in deep disposal wells and evaporation ponds, producing from all wells during restoration, and recirculating water purified in surface plants. Methods for predicting the effectiveness and cost of current techniques are presented. Possible alternative techniques are also described. Two restoration operations are discussed.

Introduction

In situ leaching of uranium from mineralized sandstone deposits is rapidly developing into a major mining technique (see Figure 1). To be suitable for in situ leaching with present technology, a uranium deposit should be bounded above and below by impermeable strata, be below the water table, and have sufficient permeability (preferably greater than 5 darcies). The groundwater flow rate should not be so great as to make the control of the flow pattern of the leach lixiviant difficult.

Advantages of in situ leaching include less initial capital investment, shorter startup times, greater safety, and less labor than for other conventional mining operations. In situ leaching also reduces many of the hazards of working in a uranium processing plant (e.g. airborne radionuclides from dust, radon and its daughters). Hence, smaller, deeper, and lower grade ore bodies can be exploited. Environmentally attractive characteristics include minimal disturbance of surface terrain or surface waters, no mill tailings piles, and no large open pits.

In situ leaching also has environmental disadvantages. Since the leaching alters a portion of the aquifer, the surrounding groundwater can become contaminated by the leach solution escaping from the mining zone. The final condition must be made stable with respect to the groundwater quality, changes in the aquifer must be localized, and limitations on the future use of water from the aquifer must be identified.

In situ solution mining affects groundwater quality by introducing contaminants into the groundwater from two main sources and several minor sources. One main source is from the dissolution of materials present in the mineral deposit. These materials are insoluble prior to mining. Examples are carnotite containing uranium and vanadium; sulfide minerals containing molybdenum, arsenic, iron, cobalt, nickel, and copper; and clays containing alumina, silica, and vanadium. The second main source of contaminants is from the lixiviant employed in the uranium leaching process. Depending upon the solution employed, ammonium, sodium, bicarbonate, or sulfate ions are introduced into the groundwater. Chlorides also can enter the groundwater by way of the lixiviant if a chloride brine is used for resin elution in the uranium extraction process.

Minor sources of contaminants include seepage from the surface of brines in surface impoundments, injection of drilling mud from the construction of wells, and seepage into the ground from leaks and spills in the operation of the uranium extraction equipment. The capacity of the mined aquifer to sustain contaminant levels in the groundwater is a significant factor in the restoration of groundwater quality.

Because of the relatively few groundwater restoration operations that have been undertaken, considerable uncertainty exists as to both the effectiveness and the costs. To assist mining companies in selecting a cost-effective restoration method and in improving the projection of restoration costs, the Bureau of Mines funded a study of these factors.(1) Those who would like the complete report should contact Daryl R. Tweeton, Research Physicist, at the Twin Cities Mining Research Center, P.O. Box 1660, Twin Cities, Minnesota 55111, phone (612) 725-3468.

Geology of Uranium Deposits

All presently developed in situ solution mining for uranium (commercial and pilot scale) is conducted in sandstone deposits.(2) A majority of these deposits are of the roll or roll-front type. The name denotes the general case in which the uranium has been deposited along an oxidation-reduction front in several configurations - i.e., crescent shaped along channel margins, tabular along permeability changes, elliptical or dish shaped within scour pockets. Finch (3) called these deposits "peneconcordant" in reference to the long dimension being nearly parallel to the gross stratification of the sedimentary host rock. In a survey of over 4,600 such deposits, Finch noted that the deposits are in sandstone lenses of stream origin. Although many formations are host to these deposits, in any mining district most deposits are in only one or a few stratigraphic units.

The deposits are geologically and mineralogically similar. The ore is unoxidized with uraninite and coffinite being the principal ore minerals. Vanadium oxides and silicates and some common copper sulfides are accessory minerals in many cases. Pyrite and marcasite are common. Minerals containing molybdenum, selenium, and chromium are commonly present but not abundant enough to be recognized visually.

Vanadium oxides and the two principal uranium minerals are oxidized readily and are converted to a soluble higher valence state. Where oxidized vanadium is available, the uranium is precipitated as carnotite or tyuyamunite, (uranium vanadates) that are quite stable even under oxidizing conditions. Thus, in vanadium-rich deposits, the mineralogy of oxidation zones is simple and there is little migration or enrichment of either uranium or vanadium. In low-vanadium deposits, uranium is mobilized and there is likely to be enrichment by reduction.

All of the minerals mainly impregnate the sandstone, coating sand grains and filling pore spaces. However, the minerals also replace the sand grains to a small extent. Locally they replace coalified fossil plants.

An extensive study involving the theory of the formation of tabular deposits in the Colorado Plateau region implied that these deposits were formed by groundwaters moving along sandstone host beds and from which the ore minerals were precipitated in pockets of strong reducing capacity.(4) Possible reducing agents were suggested, including locally abundant fossil plants in the host rock, humic material derived from these fossils or introduced in a fluid state from other sources, or H₂S, either generated by bacteria feeding on the fossil plants or derived from oil or natural gas. The theory, however, generally failed to explain the distribution of these reductants relative to the locations of uranium deposits.(5) In overview, since uranium deposits for exploitation by in situ leaching techniques are selected for their amenability to the extraction operation, there is nothing implicit in the selection requiring a common genesis.

Regulations Influencing Restoration

Controlling regulations relative to groundwater protection are provided in part by three main Federal laws, as follows:(6)

1. The Federal Water Pollution Control Act Amendments of 1972 (FWPCA), P.L. 92-500.
2. The Safe Drinking Water Act of 1974 (SDWA), P.L. 93-523.
3. The Resource Conservation and Recovery Act of 1976 (RCRA), P.L. 94-580.

Other laws affecting groundwater control but to a lesser degree are:

1. The Solid Waste Disposal Act of 1965 (SWDA), P.L. 89-272
2. The National Environmental Policy Act of 1969 (NEPA), P.L. 91-190.
3. The Toxic Substance Control Act of 1978 (TSCA), P.L. 94-469.

The Federal Water Pollution Control Act Amendments provide the overall State and area coverage identification, management, treatment, and control through various permit programs of the Nation's waters, primarily surface waters. Groundwater protection is not thoroughly covered, but provisions for well permits and protection from sewage effluent disposal are provided. The FWPCA does not cover the discharge of contaminants to groundwater from surface impoundments, solid-waste piles, septic systems, or disposal wells.

The Safe Drinking Water Act provides protection of groundwater on a Federal and State cooperative basis for deep-well

injection of liquid wastes, secondary recovery of subsurface solutions, and engineered wells. The SDWA was passed primarily to provide minimum protection of underground drinking water supplies from well injection practices.(7) The Act stipulates that the States are to exercise primary responsibility for the protection of groundwaters and to establish a permit authorization system towards that goal. However, the Act is limited to those areas where public water supply systems have at least 15 service connections or are serving a minimum of 25 persons.(8) Some States have complied with the Act or are in the process of compliance to varying degrees. Since each State has somewhat different hydrogeologic, climatologic, and population density conditions, laws vary accordingly. Even though most mining areas are somewhat remote from major population centers, especially in the Western United States, the laws apply to mining and other small communities or in areas where potential public groundwater resources exist. A potential groundwater source for public consumption is defined generally as having a quality of less than 10,000 mg/l total dissolved solids (TDS) and being of sufficient yield to sustain a constant adequate supply.

The Resource Conservation and Recovery Act, although not fully established until regulations are finalized, provides for protection and control of seepage to groundwater from surface impoundments and solid-waste dumps. Again, the law stipulates control and evaluation by the States.

The Solid Waste Disposal Act contains no specific reference to groundwater, but guidelines developed under the Act provide for groundwater protection from surface drainage and activities.(8) Site development plans must consider the potential impact on groundwaters but are limited to Federal agency operations only.

The National Environmental Policy Act requires Federal agencies to prepare environmental impact statements (EIS's) for all major actions and operations involving Federal lands or funds. The Toxic Substance Control Act is concerned primarily with safe disposal of some 160 waste elements or compounds that have been deemed toxic to man and the environment.

Description of Restoration Methods

The groundwater restoration problem is concerned with the cleanup after the mining operation of undesired soluble materials. To accomplish this cleanup, many of the methods developed for domestic and industrial water treatment can be considered. In addition, many techniques for the treatment of industrial effluents have been researched and developed to meet recent environmental protection regulations.

A restoration plan can involve the application of several methods of treatment. Figure 2 shows a convenient classifica-

tion system for restoration systems. The variety of methods that can be considered to make up a system is shown in Figure 3. The most important of the methods are discussed below. Additional details and descriptions of the remaining methods are given in the final report(1) of the study on which this paper is based. To evaluate the advantages and disadvantages of a complete restoration plan, the methods of treatment employed must be understood.

In Situ Methods

In situ methods are characterized by the groundwater restoration taking place within the confines of the contaminated aquifer. Objectionable materials initially soluble in the groundwater are precipitated or otherwise lodged in the aquifer's solid matrix. Natural physiochemical actions involving reduction, neutralization, precipitation, and adsorption cleanse and purify the groundwater. Surface treatment of the groundwater (equalization, chemical additions, suspended solid removal, etc.) might be conducted to enhance the natural restoration action. Included under in situ restoration methods are bacterial and chemical precipitation. Bacterial precipitation involves the inoculation of the aquifer and the injection of nutrients for the purpose of purifying the water by biological means. An example of chemical precipitation is the injection of hydrogen sulfide for the purpose of transforming soluble contaminants to insoluble, reduced form. The injection of bacteria or hydrogen sulfide has not been used successfully to aid restoration. However, it is believed that bacteria and hydrogen sulfide can be effective in restoring conditions. Bacteria and hydrogen sulfide can occur naturally at some sites.

In situ restoration processes have two important advantages over processes that require removal of contaminants from the leached aquifer:

1. Cost savings are substantial and system complexity is significantly reduced if separation and purification processes and external waste disposal do not need to be employed. If production and recharge of solution are also eliminated or minimized, an additional cost reduction occurs.
2. Objectionable materials are deposited in situ, remote from the environmentally sensitive land-surface zone. Since the wastes are handled less, processing exposure is reduced and waste spills are less frequent. The possible future dispersion of objectionable materials on the land surface is also less likely.

The use of in situ restoration processes fall into three different modes of application: (a) as a principal method of improving the groundwater quality, (b) as a follow-up method

after other restoration efforts, and (c) as a groundwater stabilization method following the decommissioning of the mining site.

Natural restoration processes are the physiochemical actions that take place within the contaminated aquifer by natural means and without external influence. It is possible that natural restoration will limit the spread of pollutants so effectively that it can be the primary restoration method. At this time, however, regulatory agencies do not allow natural restoration processes alone to constitute a restoration plan.

Factors that contribute to natural restoration include

1. Heavy metals will be precipitated as reducing agents are restored by natural processes after leaching, when oxidant is no longer being injected.
2. Heavy metals will be adsorbed on silicates, quartz, and feldspars.
3. Ammonium ions will be strongly adsorbed on clays.
4. Major ions such as Ca^{++} and $\text{SO}_4^{=}$ will be adsorbed on clays.

The potential advantages and the underlying factors involved in natural restoration are discussed in detail by Buma, et al.(9)

Surface Separation Methods

A direct approach for the removal of detrimental concentrations of materials from groundwater is to employ a separation process aboveground. The restoration effort consists of pumping contaminated groundwater from production wells, separating objectionable components into a concentrated liquid or slurry waste stream, and recharging the aquifer with the purified product water. Displacement of contaminated water with purified water within the aquifer restores the water quality. The product water is conditioned to avoid plugging the bore holes of the injection wells. For the separation step, extraction and solid-liquid separation are used. The main advantage of aboveground separation over in situ precipitation is the commercial availability of the treatment equipment. A major disadvantage is the problem of disposal of the waste stream.

Reverse Osmosis(10): Reverse osmosis is a water purification technology which has drawn extensive interest since the early sixties. This methodology has been previously equated with the production of potable water from brackish sources. A significant expansion of industrial reverse osmosis applications has occurred within the last 4 years such that the cost effec-

tiveness of reverse osmosis technology has been realized in the industrial sector.

Reverse osmosis is a physical means of separating dissolved ions from an aqueous stream (see Figure 4). This treatment technology uses an externally applied pressure in excess of the solution's inherent osmotic pressure to force water to pass through a semipermeable membrane while the dissolved ions are rejected or not allowed to cross this barrier. A solution's inherent osmotic pressure is a function of the type of constituents, the ionic characteristics of the dissolved solids, and the relative and absolute concentrations of the solutes.(11) With regard to the liquors commonly encountered in restoration projects, a useful rule of thumb is that the level of 1000 mg/l as dissolved ions, or a conductivity of 1250 mhos/cm at 77°F equals approximately 10 psi of applied pressure.

$$1000 \text{ mg/l} \cong 1250 \text{ mhos/cm} \cong 10 \text{ psi}$$

Incorporating the relationship of dissolved ions versus osmotic pressure, a simplified relationship of water flux and salt flux as defined by Merten(12) is delineated in the following equations:

$$Q_w = A (\Delta P - \Delta \Pi)$$

$$Q_s = B (\Delta C)$$

where

Q_w = water flux

A = membrane water permeation coefficient

ΔP = difference of applied pressure ($P_1 - P_2$ in Figure 4)

$\Delta \Pi$ = difference of osmotic pressure

Q_s = salt flux

B = membrane salt permeation coefficient

ΔC = differential of salt concentrations

These equations indicate the flow of purified water will increase as the high pressure, P_1 , is increased, but the salt flux will not increase directly with pressure. With sufficient pressure, the bulk of the dissolved ions in the feedwater will be concentrated in the effluent brine.

The basic importance of reverse osmosis in the restoration of in situ uranium leaching operations is the ability of this technology to remove various dissolved inorganic anionic,

cationic, and neutral contaminants, the present of which results from the solution mining activities. The removal of ions is a function of the membrane and the applied pressure upon the membrane. The purified water obtained by reverse osmosis that was drawn from the production wells is utilized as aquifer recharge via injection wells.(13)

The capital costs related to the procurement of restoration-type reverse osmosis systems are included in Table 1. The economics delineated reflect actual field systems and experience. All costs are set at mid-1978 prices. The sizes of the systems range from 10,000 to 1,000,000 gpd. These reverse osmosis units incorporate a flexible mechanical design to maximize water recovery, pertinent instrumentation to monitor water quality and flow, a design to minimize membrane fouling and scaling, the use of anti-scalants, pH control and monitoring, and a membrane cleaning system. These units are skid mounted and require only power and piping hook-ups. These prices do not include site engineering fees nor freight costs. A delineation of budget estimates for complete restoration packages is also indicated in Table 1. The packages are complete and are modular so that site erection is a matter of interconnecting various components. These prices do not include installation.

The operating costs associated with a reverse osmosis in situ restoration project consist of power costs, operation, maintenance, and chemicals. A monetary assessment of these various parameters is shown in Table 1. The cost assumptions are power at 2.5 cents per kWhr, membrane replacements required at a rate of 50 percent per 3 years, and a maintenance requirement from past experience. The maintenance and material cost of producing reverse osmosis water ranges from 1.24 per 1000 gallons produced at a production rate of 200,000 gpd to .99 per 1000 gallons produced at rate of 1,000,000 gpd. This estimate is based on labor and supervision for round-the-clock and round-the-week operation with the reverse osmosis unit set up and producing at full capacity for 300 days a year.

Electrodialysis: In water, salts and minerals dissolve to produce cations and anions. In the electrodialysis process (see Figure 5), water flows between alternately placed cation-permeable (C) and anion-permeable (A) membranes. The stack of membranes is placed in a DC electric field. The electric field pulls cations such as Na^+ through one membrane and anions such as Cl^- through the other into the waste streams flowing in alternate compartments.

Electrodialysis separation processes can be viewed as a combination of the mechanisms of reverse osmosis and ion exchange. Material diffuses through a membrane as in reverse osmosis. Ionic charges are transported as in ion exchange. In all these processes, particles of ionic size are separated.(13)

In a typical equipment design, membranes, spacers, and electrodes are stacked and held together by end plates much like a plate-and-frame filter. Spacing is usually about 0.1 inch and spacers are arranged to provide a tortuous flow path. Stacks range from 0.5 to 2400 m² of membrane area. A large stack can desalt 150 gpm at 20 to 50-percent salt removal. Practical systems utilize from two to six stages.(14)

Cost estimates comparing electrodialysis treatment with reverse osmosis treatment generally show electrodialysis to be 20 to 40 percent more expensive (estimates made by Ford, Bacon & Davis, Inc. staff). A cost estimate solicited from a supplier of electrodialysis equipment indicates a total operating cost of \$2 to \$3~~000~~ per ¹⁰⁰⁰gallon. The supplier points out the need for batch processing, nonstandard units, and custom design. These features would be unfavorable for the application of electrodialysis in groundwater restoration.

Distillation: Distillation processes are widely used commercial methods of treating saline and brackish waters, including acid mine drainage, to produce a product water suitable for potable or industrial consumption. Because of its widespread use, distillation technology is well developed and well tested. Six categories of distillation processes for operating plants are listed in Table 2.(15) The multistage flash (MSF) process is probably the best developed and most widely used and preferred of the categories listed. It could be applied in a groundwater restoration operation as a separation process for producing a water that would be recharged to the well field. The MSF process is based on the premise that water boils at a lower temperature as it is subjected to a progressively lower pressure. The contaminated feed solution is heated and injected into a chamber where the reduced pressure causes part of the solution to "flash" from liquid to vapor. The vapor rises in the chamber and condenses on cold tubes. The condensate is collected in a separator as a product water. Dissolved material remains behind in the liquid phase and is termed "brine." The brine flows to the next chamber, where the pressure is lower than in the first, and is again "flashed." The process is repeated several times. As brine leaves the final chamber, it is used to heat the incoming feed solution.

Few published data are available on costs of distilling water of restoration quality at the flow rates considered in this report (<1 million gallons per day (MGD)). A Westinghouse study for treating acid mine water at 5 MGD with an MSF system indicates an operating cost of \$4.42 per 1000 gallon of product water.(16) This operating cost does not include amortized capital. In general, distillation treatment will be 4 to 5 times as expensive as reverse osmosis treatment. Recent, rapid changes in prices for fuels and materials for heat exchangers make projections of distillation costs unreliable. However, these price increases give a cost advantage to reverse osmosis,

a process that does not require heat transfer or large amounts of fuel.

Ion Exchange: For the treatment of waste liquors, ion-exchange methods can be divided into three categories depending on the function of process. First are the techniques for reducing the amount of material dissolved in the treated liquor. This operation is commonly referred to as deionization or demineralization.(17,18) Second are methods of extracting specific materials from the liquor. The third category of ion-exchange methods is used for changing the characteristics of water. The most common of these methods is water softening.(18) The main feature of water softening is the replacement of calcium ions originally dissolved in the water with sodium ions, which results in a reduction in water hardness.

Ion-exchange deionization is a widely used technique. Normally, the treatment for this purpose is limited to waters of less than 500 ppm total dissolved solids, as regenerant costs increase proportionately to the total-dissolved-solid level. A comprehensive evaluation by the staff at Dow Chemical U.S.A.(19) reports that at 350 ppm TDS (expressed as CaCO_3) chemical costs for ion exchange exceed operating costs for reverse osmosis, indicating that conventional deionization cannot compete with membrane and distillation processes at levels above 350 ppm.

Several systems for ion-exchange deionization have been researched and developed.(20) Of these, the Desal process developed by Dr. Robert Kunin and his associates at the Rohm and Haas Co., has very good potential.(21,22) Two other systems, the Sul-bi-Sul process developed by Nalco Chemical Co. and the Sirotherm process developed by Dr. D.E. Weiss and his coworkers in Australia, are well worth consideration. These systems are currently under development and not ready for commercial application. The Desal* process is furthest along in development with some pilot plant operation.(22) This system is a good example of the latest ion-exchange deionization processes for brackish-water treatment (see Figure 6).

A modified, basic Desal process was evaluated for treating acid mine water. Costs were estimated at \$0.50 per 1000 gallon of feed. The modified operation employs the bicarbonate cycle to alkalify the acid mine water. Regeneration is with ammonium hydroxide, an carbonation is with dissolved CO_2 . The product water is aerated, lime-softened and clarified. The cost for a complete desalination of the water could run from 2 to 5 times that of reverse osmosis treatment. For ranking purposes a factor of 3 is used in this paper.

*Reference to specific equipment (or trade names or manufacturers) is made for identification only and does not imply endorsement by the Bureau of Mines.

Foam Separation Technique: Foam separation (23,24) is not currently being applied to purifying water from in situ leaching. However, it has the potential to aid in removing trace amounts of heavy metals, one of the more difficult unit operations in groundwater restoration. Foam fractionation is the process in which surfactant additions to the aqueous solution to be treated form a stable foam upon sparging with a gas. Dissolved metal values or other pollutants can interact with the surfactant and are then collected at the gas-liquid interface and removed from the system as a foam (see Figure 7). Several authors have examined the design variables and relationships between column dimension and extraction rates for foam and bubble columns. (23)

Foam columns have several disadvantages when treating large volumes of solution. One is that the throughput is limited by the foam drainage rate, and another is foam stability. To assure adequate removal of the contaminants, the column diameter must be increased to make the cross-sectional flowrate low enough for sufficient contact time.

Freeze Separation: Though water purification by freezing has not been applied to in situ leaching, the process is claimed to have the potential for low costs, high water recovery, and effective contaminant rejection. This assessment is backed by the following attributes of a freezing process: (25)

1. Very low susceptibility to scaling of heat transfer surfaces.
2. Low sensitivity to concentration and nature of feed brine.
3. Low heat transfer requirements (1/6 of distillation processes).
4. Corrosion is minimized by low temperatures.
5. Negligible pretreatment is required.

The basis of a freeze separation process is the principle that when ice is frozen from an aqueous solution of inorganic salts, the ice is a distinct and purer phase of water. The ice excludes most of the salts from its crystal structure. Since 144 Btu of heat are associated with each pound of ice frozen, heat transfer is a requirement. This is fundamental for freezing processes (see Figure 8).

Costs for freeze-separation treatment have been estimated as being 20 to 40 percent greater than costs for reverse osmosis treatment for small flow rates, and 20 to 40 percent less for high flow rates (estimates made by Ford, Bacon & Davis, Inc., staff).

Ultimate Disposal Methods

The ultimate disposal of the waste is a major element of any system. The method selected dictates to a significant degree the type and extent of solution and sludge treatment. In addition, the ultimate disposal process is a major cost item.

Deep-Well Disposal Process: Deep-well disposal (see Figure 9) is an ultimate disposal technique for aqueous wastes. Talbot and Beardon(26,27) indicate that deep-well disposal can be an efficient and inexpensive means of eliminating wastes from the biosphere. A properly designed well installed in a suitable geologic formation can provide permanent storage of groundwater of objectionable quality. In addition, if the constituents of the waste are adsorbed on the formation matrix or chemical reactions form harmless products, the waste disposal problem has a permanent solution.(28)

For deep-well disposal, the aqueous waste is injected either by gravity feed or under pump pressure via a vertical borehole into a deep, permeable and porous lithologic stratum. Injection is accomplished with the resulting displacement and compaction of the material in and around the host aquifer. The waste is injected with the intent of permanent isolation from any usable water supplies.

Papers by Warner and Orcutt (24), Donaldson (30), Koenig (31), and Reeder(32) indicate that over 300 industrial waste water injection wells in 25 States have been constructed. A little over half of these wells are in operation. The depth of existing waste injection wells ranges from 1000 to 12,000 feet with most in the range of 1000 to 6000 feet. Of these wells, 95 percent inject less than 400 gpm with an average wellhead pressure of less than 1500 psi. Almost all of these wells are completed in unconsolidated sand, sandstone, or carbonate zones.

The wastes injected include acids, caustics, and solutions of inorganic salts. Examples of disposal of waste solutions similar to that from an in situ uranium leaching operation can be found in Lynn's report(33) for uranium mills in New Mexico, in Schicht's report(34) for brines from desalination processes, and in Union Carbide's permit for the Palangana Dome uranium plant.(35) Many other effective deep well disposal systems for industrial wastes have been reported.(36,37)

A typical flow scheme for a deep well disposal system would include the equipment required to concentrate and condition the waste stream for injection and equipment to transport the waste solution from the mining site to the injection well. Details for the injection well design are given in Figure 10. A typical arrangement of casing strings, injection tube, and wellhead is shown.

A major advantage of deep-well disposal over surface disposal methods is that the objectionable waste solution is completely removed from the environmentally sensitive biosphere.

Deep-well disposal systems are limited to solutions with low suspended solids and low turbidity, to prevent plugging of the injection zone. Requirements for filtering or settling solid from the waste stream before injection would significantly increase the complexity and cost of the disposal system. Provisions for solid waste disposal would also be necessary. Deep-well disposal is limited to waste solutions that will not plug the injection zone by the precipitation of solids in reactions between the waste, the solutions, and the matrix of the host aquifer. In some cases, precipitation can be prevented or reduced by adjusting pH or adding retardants, such as sodium hexametaphosphate for calcium sulfate.

Injection rates for a deep-well disposal system can be restricted either by the hydrogeologic properties of the injection zone or by regulatory requirements. The average continuous rate of 60 percent of the industrial waste injection wells surveyed by Warner and Orcutt(29) was less than 100 gpm. Regulatory requirements for maximum injection rates have been set at 200 gpm in some cases.(35,37)

In most Western States, deep disposal wells are frequently regulated through associated pollution control, environmental protection, or health agencies. Of those States with specific regulations, Texas adopted injection well laws in 1961 and amended these laws in 1969. The instructions and forms required by Texas law are good examples of typical State regulations. These are available from the Texas Department of Water Resources in Austin. Colorado adopted rules and regulations for subsurface disposal in 1970, California and Idaho have less detailed but specific regulations, and Washington restricts permits to only extreme circumstances.(6,38)

The Federal Government via the U.S. Environmental Protection Agency is involved with deep-well disposal regulations through the Federal Water Pollution Control Act Amendments of 1972 and the Safe Drinking Water Act of 1974. Hall(38) reports that the applicable regulatory provision of the Federal Water Pollution Control Act is for a federally approved State program requiring a qualifying authority to issue permits to control the disposal of pollutants into wells. The thrust of the Safe Drinking Water Act is to minimize or prevent threats to public health from underground drinking water sources contaminated by man's activities.(6) EPA policies pertaining to deep well disposal laws are presently being formulated and revised.

Summaries of the capital and operating costs are presented in Tables 3 and 4. Costs are calculated for variations of each of the primary factors affecting a disposal well as reported by Koenig(39), such as injection rate, well depth, and drilling

difficulty (i.e., rock type). The expenditures included in the cost calculations are those most likely for a plant meeting optimum design requirements. The costs evaluated are for a plant located in the Southwest or Rocky Mountain areas.

The operating cost estimate is divided into the direct costs of power, chemicals, operating and maintenance, and a concluding summary of operating costs that includes overhead expenses and fixed charges. Power costs are calculated for an average wellhead pressure of 260 psi as determined by Koenig(31) in a survey of 124 injection well operations. Flow rate is the major factor for power costs. Chemical costs include acid addition for pH adjustment, polyphosphate addition to retard calcium sulfate deposition in the injection zone, and copper sulfate addition to control bacteria and fungi growth. Chemical additions are proportional to waste solution flow rate.

Solar Evaporation Ponds: The solar evaporation pond disposal process provides disposal of waste solutions generated during the groundwater restoration phase. The process consists of solar evaporation for the purpose of reducing the volume of wastewater, followed by impoundment of the sludge residue. Precautions are taken during pond construction and during the final solids disposal to insure safe, perpetual storage of any harmful pollutants at a minimum cost. These precautions include restricting the moisture migration at the impoundment site by construction of drainage trenches and the use of impermeable linings above and below the contained solid waste (see Figure 11).

The system components shown are the pump and pipeline for transporting waste solution from the mining site to the disposal site, the series of solar evaporation ponds on a leveled site, and the monitor wells used to detect system leaks. Ponds are constructed with a large surface area and a shallow depth to maximize evaporation. Shallow depth is reported to increase evaporation rates.(40) However, due to the nonuniformity of the pond bottoms, a minimum average depth is required for complete solution coverage and maximum evaporation. Dikes and spillways are provided between ponds to allow positioning the pond with respect to the terrain of the selected site. Pond site selection is of major importance in determining the costs and operating difficulties of a large evaporation pond system.

Factors influencing the selection and construction of a leveled pond site would include land costs, excavation requirements, future land use, and the location of available pond sites near the mining operation.

Evaluation of the disposal capacity of an evaporation pond system entails consideration of the average fresh water evaporation rates at the pond site, average local rainfall, variations in evaporation rates and rainfall, and the effect of brine concentration on evaporation rates.

Summaries of capital and operating costs for solar evaporation are listed in Table 5. The systems evaluated receive solution directly from the mining site or the brine from a separation process. A separation process would reduce the volume of the waste stream and thus reduce the size of the evaporation ponds. After the waste is reduced to a sludge by solar evaporation, ultimate disposal at the pond site could be by backfilling and sealing. The costs for this method of ultimate disposal are included in the estimate. To evaluate nominal costs suitable for in situ solution mining, selection of a pond site with an initial grade of 1 percent is assumed. Pond sealing is accomplished with 10-mil PVC lining or equivalent. Costs change for variation of the system capacity (specified as volumetric feed rate) and for the net evaporation rate at the pond site.

The fixed charges dominate, as would be expected for systems requiring extensive excavation and little operating labor. Expenses are roughly inversely proportional to the net evaporation rate at the site. These results are mainly due to the dominance of construction costs that are directly related to pond area. The pond area in turn relates directly to system capacity and inversely to net evaporation.

Solid-Waste Disposal

A solid-waste disposal system is required to collect, store, treat, handle, transport, place, and secure the objectionable materials generated by any restoration methods employing a process that generates a solid phase. This series of processing steps is conducted to insure that the impact on the surrounding environment is minimized.

Many factors influence the evaluation of a solid-waste disposal scheme (see Figure 12). The site and system qualifications are determined by the needs of protecting the environment and insuring public safety. Both short-term and long-term objectives must be assessed. Short-term objectives deal with the period during controlled activities at the site. These activities include the filling and closing of the site and surveillance after closure. Long-term objectives are concerned with the period after controlled activities have stopped.

Costs for solid-waste disposal vary widely. Considering moderate dewatering and chemical stabilization of a waste sludge, a disposal site of over 10 miles from the mining operation, and moderate land costs, an estimate of \$60 to \$110 per dry ton is reasonable. Additional transporting requirements would be at a rate of \$7.50 per 100 ton-miles.

Ranking of Restoration Methods

For the purposes of ranking the restoration alternatives,

the results of each treatment assessment conducted in earlier sections of this paper are quantified for capital and operating costs, processing effectiveness, and system development. The evaluation is listed in Table 6. For example, the treatment cost for reverse osmosis is roughly \$0.99 per 1000 gallons of feed solution treated at 1 million gallons per day.

The following conclusions are drawn as a result of ranking restoration alternatives:

The most cost-effective alternatives are those employing the least complex procedures. It is evident that passive or recirculating systems have the highest ranking. However, the effectiveness of these simpler procedures for groundwater quality improvement is rated as low or incomplete for the control of a typical leaching lixiviant of inorganic salts.

Highly ranked alternatives are of the sweeping type. The first is sweeping with deep-well injection. The second, at the same ranking value, is sweeping with solar-evaporation-pond disposal. The direct disposal of the contaminated lixiviant pumped from the aquifer has the marked advantage of eliminating the costs of a separation process. Also, the complete disposal of the lixiviant gives such systems a high effectiveness for removal of all contaminants over a wide range of feed conditions. Both techniques of waste disposal of liquids are well developed. Differentiation between these two alternatives requires specific site information.

Of the generally applicable alternatives that involve the separation and recharging of purified water, sequences employing reverse osmosis and electrodialysis are highly ranked. For reverse osmosis and electrodialysis, lime or lime-soda pretreatment is a requirement to prevent fouling of the membrane separation process. Both reverse osmosis and electrodialysis are highly effective methods of removing ionic ligands not precipitated in the pretreatment.

Restoration Examples

A discussion of restoration examples is included to provide an overview of restoration techniques for particular properties. Techniques that are currently used or are proposed for use to restore well fields include pumping of selected well fields, and pumping of selected well fields with treatment before the water is recirculated or dilution with added natural groundwater from other wells. Most of the current experience has been with pilot-scale operations. The possible differences between a pilot operation and a commercial operation can be significant. Geological and geochemical differences can be crucial in determining pattern size, lixiviant concentrations, and restoration time schedule.

Ultimate disposal systems include both lined evaporation ponds and deep disposal wells. Regulatory considerations are discussed with the examples. This part of the discussion should be helpful in determining essential parameters in setting up an initial research program.

Exxon

Exxon Minerals Co. is conducting a solution-mining pilot operation at the Highland uranium operation in Wyoming.(41) Initial background baseline data indicates high sodium and bicarbonate counts; therefore, during the initial test, solutions containing sodium carbonate, sodium bicarbonate, and oxygen as an oxidizing agent were used as a lixiviant to permeate the ore body.

The well field pattern used was a seven spot, consisting of six production wells encircling one injection well. The production wells were placed 90 feet away from the injector and equidistant apart from each other. Six observation wells were positioned on a 150 foot radius away from the injection well. The configuration is shown in Figure 17.

Water quality testing performed for the initial baseline conditions indicated that the groundwater was not suitable for human consumption. For groundwater restoration the guidelines used were (a) Wyoming Department of Environmental Quality (DEQ), Land Quality Division's guideline No. 4 for livestock impoundments, or (b) restoring water quality to within 20 percent of baseline, whichever was greatest. To accomplish this restoration, at the conclusion of the production test, Exxon started pumping from all seven wells in the initial pattern. This drawdown of the aquifer in the area of the test pattern was performed to pull the contaminated fluids back to the wells and flush the test pattern area to bring the aquifer back to baseline conditions. The decline in uranium concentrations in the production wells during restoration was definite, though not constant. Concentrations of bicarbonate, carbonate, selenium, arsenic, radium-226, and thorium-230 were also measured during restoration. Most baseline parameters indicated a similar decline in concentration; however, at the conclusion of data collection, concentrations of some of the above were still considerably above baseline figures. From information available, pumping the producing wells for purposes of groundwater restoration can possibly produce satisfactory results but can be a very lengthy operation.

Because the location of the pilot plant was near the tailings dam for Exxon's operating mill, all waste water was pumped to the pond for evaporation. Thus an adequate ultimate storage area for waste water was easily accessible.

Rocky Mountain Energy

The second example of restoration is Rocky Mountain Energy's (RME) Reno Ranch ISL Test Site in Campbell County, Wyo. Rocky Mountain Energy is currently proceeding with pilot-scale operation at the Reno Ranch site to determine the technical, economic, and environmental feasibility of solution mining.(42)

The operation is currently utilizing a five-spot well field pattern. RME is using an acid solution as a leachant and hydrogen peroxide as an oxidizer. After the leaching tests are complete, the subsurface formations will be flushed of leachate. A reverse osmosis water treatment circuit will be included in the pilot plant design to facilitate restoration and reduce water consumption as the treated water is reinjected.

Hydrological baseline data are defined through analysis of selected wells in and around the well field. A range is established using the high and low analytical results from laboratory analyses. Sampling will continue until 6 samples over six months are available. This will possibly cause the current baseline water quality to change.

Excess water accumulated during the test will be disposed of in an evaporation pond. Once these solutions are evaporated, the liners as well as any concentrated wastes solutions or solids will be removed and disposed of in an appropriate manner.

References

1. Ford, Bacon & Davis Utah, Inc., Restoration of Groundwater Quality After In Situ Uranium Leaching, Twin Cities Mining Research Center, Bureau of Mines, U.S. Department of the Interior. Will be available for consultation. U.S. Bureau of Mines, Twin Cities, Minn. 55111, or from National Technical Information Service, Springfield, Va. 22161.
2. Larson, W.C., Uranium In Situ Leach Mining in the United States, Information Circular 8777, Bureau of Mines, U.S. Department of the Interior, 1978.
3. Finch, W.I., Geology of Epigenetic Uranium Deposits in Sandstone in the United States, U.S. Geological Survey Professional Paper 538, 1967, 121 pp.
4. Hostetler, P.B., and R.M. Garrels, "Transportation and Precipitation of Uranium and Vanadium at Low Temperature, with Special Reference to Sandstone-Type Uranium Deposits," Economic Geology, Vol. 57, 1962, pp. 137-167.
5. Fisher, R.P., "Exploration Guides to New Uranium Districts and Belts," Economic Geology, Vol. 69, No. 3, May 1978, pp. 362-376.
6. USEPA, "Draft Environmental Impact Statement, State Underground Injection Control Program," Proposed Regulations (40 CFR, Part 146), U.S. Environmental Protection Agency, Sept. 10, 1976.
7. USEPA, "The Report to Congress - Waste Disposal Practices and Their Effects on Ground Water," Office of Water Supply, Office of Solid Waste Management Programs, U.S. Environmental Protection Agency, January 1977.
8. USEPA, "Proposed Regulations, State Underground Injection Control Program (40 CFR, Part 146)," Office of Water Supply, U.S. Environmental Protection Agency, September 1977.
9. Buma, G., J.R. Riding, L. Downey, and T.D. Chatwin, "Geochemical Arguments for Natural Stabilization Following In Situ Leaching of Uranium," to be presented at 1979 AIME Annual Meeting, Feb. 18-22, 1979, New Orleans, LA.
10. Primarily contributed by L.J. Kosarek, Director of Systems Engineering Research and Development at El Paso Environmental Systems, El Paso, Texas.
11. California. Agricultural Waste Water Desalination by Reverse Osmosis. Department of Water Resources Bulletin No. 196-76, 1976.

12. Merten, U.: Desalination by Reverse Osmosis. MIT Press, 1966, Cambridge, Mass.
13. Porter, M.C., and A.S. Michaels, "Membrane Ultrafiltration," Chemical Technology, pp. 56-63, Jan. 1971.
14. Ionics, Inc., "General Information, Principles of ED," Watertown, Mass., no date.
15. Oliver, J.C., "The Port Mansfield Desalting Plant," Public Works Magazine, Ridgewood, N.J., June 1965.
16. Maneral, D.R., and S. Lemezis, "Multi-Stage Flash Evaporator System for the Purification of Acid Mine Drainage," Society of Mining Engineers, AIME, Transactions 252, March 1972, pp. 42-45 (Preprint 70-B-303, 1970).
17. Patterson, J.W., "Reduction of Total Dissolved Solids," Ch. 21, Wastewater Treatment Technology, Ann Arbor, MI: Ann Arbor Science Publishers Inc., 1977, pp. 331-345.
18. BETZ Laboratories, Inc., "Ion Exchange," Ch. 8, BETZ Handbook of Industrial Water Conditioning, 7th ed., Trevoise, Pennsylvania: BETZ Laboratories, Inc., 1976, pp. 53-75.
19. DOW Chemical U.S.A., "Water Demineralization Using Reverse Osmosis and Ion Exchange," Idea+-Exchange, Vol. 7, No. 2, available from DOW Chemical U.S.A., a unit of DOW Chemical Company, Functional Products and Systems Department, Midland, Michigan, 1977.
20. Bregman, J.I. and J.M. Shackelford, "Ion Exchange Is Feasible for Desalination," Environmental Science and Technology, Vol. 3, No. 4, April 1969, pp. 336-340.
21. Rohm and Haas Co., "Desal Process: Brackish Water, Industrial Wastes, Sewage Effluent," no date, available from Rohm and Haas Co., Independence Mall West, Philadelphia, Pa.
22. Kunin, R., "The Use of Amberlite Ion Exchange Resins In Treating Acid Mine Waters at Philipsburg, Pennsylvania," available from Rohm and Haas Co., Philadelphia, Pa., undated.
23. Lemlich, R., ed., Adsorptive Bubble Separation Techniques, Academic Press, New York, 1972.
24. Somasundaran, P., "Separation Using Foaming Techniques," Separation Science, Vol. 10, No. 1, 1975, pp. 93-109.
25. Johnson, W.E., "State-of-the-Art Survey and Economic Comparison of Freezing Processes," Final Report, Office of

Water Research and Technology, U.S. Department of the Interior, Dec 1976.

26. Talbot, J.S., and P. Beardon, "Deep Well Method of Industrial Waste Disposal," Chemical Engineering Progress, Vol. 60, No. 1 1960, p. 49.
27. "Deep Well Injection Is Effective for Waste Disposal," Environmental Science and Technology, Vol, 2, 1968, p. 406.
28. Donaldson, E.C., and R.T. Johansen, "The Application of Petroleum Engineering Science and Technology to Subsurface Disposal of Liquid Industrial Wastes," paper at 45th Annual Fall Meeting, Society of Petroleum Engineers, American Institution of Mining, Metallurgical and Petroleum Engineers, Houston, Texas, 1970.
29. Warner, D.L. and D.H. Orcutt, "Industrial Wastewater Injection Wells in United States - Status of Use and Regulations, 1973," paper presented at second International Symposium on Underground Waste Management and Artificial Recharge, sponsored jointly by The American Association of Petroleum Geologists, U.S. Geological Survey, and International Association of Hydrological Sciences, New Orleans, Louisiana, Sept. 26-30, 1973.
30. Donaldson, E.C., "Subsurface Disposal of Industrial Wastes in the United States," Information Circular 8212, Bureau of Mines, U.S. Department of Interior, 1964.
31. Koeing, L., "Disposal of Saline Water Conversion Brines - An Orientation Study," Office of Saline Water, U.S. Department of the Interior, R & D report No. 20, 1958.
32. Reeder, L.R., et al, "Review and Assessment of Deep Well Injection of Hazardous Wastes," unpublished report prepared for Environmental Protection Agency, Solid and Hazardous Wastes Research Laboratory, 5 volumes, 1975.
33. Lynn, R.D., and Z.E. Arlin, "Anaconda Successfully Disposes Uranium Mill Waste Water by Deep Well Injection," Mining Engineering, Vol. 14, July 1962, pp.49-52.
34. Schicht, Richard J., "Deep Well Injection of Desalting-Plant Waste Brine," paper in Underground Waste Management and Artificial Recharge, Vol. 1, J. Braunstein, ed., sponsored jointly by the American Association of Petroleum Geologists, U.S. Geological Survey and International Association of Hydrological Science, 1973, pp. 337-345.
35. Union Carbide Corp., "Permit for Subsurface Disposal of Industrial Waste," No. WDW-134, Texas Water Quality Board, Austin, Texas, Sept. 22, 1976.

36. Batz, M.E., "Deep Well Disposal of Nylon Waste Water," Chemical Engineering Progress, Vol. 60, No. 10, p. 85, 1964.
37. Witco Chemical Company, "Technical Report on Application for Subsurface Waste Disposal Permit," Texas Department of Water Resources, Austin, Texas, Sept 7, 1977.
38. Hall, C.W., and R.K. Ballentine, "U.S. Environmental Protection Agency Policy on Subsurface Employment of Fluids by Well Injection," paper presented at Second International Symposium on Underground Waste Management and Artificial Recharge, sponsored jointly by The American Association of Petroleum Geological Survey and International Association of Hydrological Science, New Orleans, Louisiana, Sept. 25-30, 1973.
39. Koenig, L., "Ultimate Disposal of Advanced Treatment Waste, Part I, Injection," U.S. Public Health Service Publication No. 999-W-10, AWTR-8, 1964.
40. Koenig, L., "Disposal of Saline Water Conversion Brines - An Orientation Study," Office of Saline Water, U.S. Department of the Interior, R&D Report No.20, pp. 5-1--5-24, 1958.
41. Exxon Co. Supplemental Environmental Report, Application for Amendment to Source Material License SUA-1139 for Solution Mining of Uranium, Highland Uranium Mill, Docket No. 40-8064, 1977.
42. Rocky Mountain Energy Co., Mine and Reclamation Plan, Reno Ranch ISC Project, Campbell County, Wyo., Denver, Colo., July 1978.

TABLE 1.
CAPITAL AND OPERATING COSTS FOR REVERSE OSMOSIS

	CAPACITY, FEED RATE	
	200,000 GAL / DAY	1,000,000 GAL/ DAY
DIRECT COSTS		
EQUIPMENT UNIT	\$139,000	\$597,500
PERIPHERAL EQUIPMENT	97,000	358,500
OTHER DIRECT COSTS	47,000	191,000
TOTAL DIRECT COSTS	283,000	1,147,000
INDIRECT COSTS	14,000	57,000
BARE PLANT COSTS	297,000	1,204,000
CONTRACTOR'S FEE	6,000	24,000
TOTAL CAPITAL INVESTMENT	303,000	1,228,000

	CAPACITY FEED RATE	
	200,000 GAL/ DAY (\$/1000 GAL)	1,000,000 GAL/ DAY (\$/1000 GAL)
DIRECT COSTS		
POWER	\$.14	\$.14
CHEMICALS	.04	.04
OPERATING & MAINTENANCE	.19	.13
TOTAL DIRECT COST	.37	.31
OVERHEAD COSTS	.14	.10
TOTAL DIRECT & OVERHEAD	.51	.41
FIXED CHARGES		
SINKING FUND PAYMENT	.35	.28
INTEREST	.25	.20
INSURANCE' TAXES' MISC	.13	.10
TOTAL OPERATING COSTS	1.24	.99

TABLE 2.
DISTILLATION PROCESSES

<u>Distillation Process</u> *	<u>Remarks</u> **
Multi-Stage Flash, MSF	Well developed Wide use and preference Some serious problems
Multi-Effect, Spray Film Horizontal Tube, HTME	Newest Development Fairly well developed and tested Limited operating history
Vapor-Compression, VC	Fairly well developed for limited market Needs many improvements
Multi-Effect, Thin Film, Vertical Tube, VTME	Fairly well developed Limited use
Submerged Tube, ST	Fully developed Obsolete
Single Stage Flash, SSF	Well developed Commercially significant only for integration with power cycles

*CATEGORIES FOLLOW THOSE LISTED BY EL-RAMELY, "DESALTING PLANT INVENTORY REPORT NO. 5, 1975.

** REMARKS ARE BASED ON A DISCUSSION OF DISTILLATION PROCESSES BY BRUCE M. WATSON, "HISTORY, STATUS AND FUTURE OF DISTILLATION PROCESSES," OFFICE OF WATER RESEARCH AND TECHNOLOGY, U.S. DEPARTMENT OF THE INTERIOR, DECEMBER 1976.

TABLE 3.
DEEP WELL DISPOSAL OPERATING COSTS VERSUS
WELL DEPTH AND ROCK TYPE (MID 1978 \$/1,000 GAL)

	WELL CAPACITY	
	200,000 GAL/DAY (SINGLE WELL)	1,000,000 GAL/DAY (2 WELLS AT .5MGD each)
5,000 - ft. WELL DEPTH		
AVERAGE ROCK	\$1,202,000	\$3,485,000
DIFFICULT ROCK	1,345,000	3,761,000
10,000 - ft. WELL DEPTH		
AVERAGE ROCK	1,538,000	4,148,000
DIFFICULT ROCK	2,083,000	5,220,000
15,000 - ft. WELL DEPTH		
AVERAGE ROCK	2,001,000	5,069,000
DIFFICULT ROCK	3,200,000	7,440,000

TABLE 4.
SUMMARY OF DEEP WELL DISPOSAL OPERATING COSTS
FOR 10,000 FOOT INJECTION WELL IN AVERAGE ROCK TYPE

MID-1978 \$/ 1000 GAL (3.8m³)

	WELL SYSTEM CAPACITY	
	200,000 GAL/DAY (SINGLE WELL) \$/ 1000 GAL)	1,000,000 GAL/DAY (2 WELLS 0.5MGD each) \$/ 1000 GAL)
DIRECT COSTS		
POWER INJECTION PUMP AND ANCILLARY LOADS	.13	.13
CHEMICALS	.23	.23
OPERATING & MAINTENANCE	<u>1.31</u>	<u>.75</u>
TOTAL DIRECT COSTS	1.67	1.11
OVERHEAD	<u>.98</u>	<u>.56</u>
TOTAL DIRECT & OVERHEAD COSTS	2.65	1.67
FIXED CHARGES		
SINKING FUND PAYMENT	1.38	.80
INTEREST	1.00	.58
INSURANCE, TAXES, MISCELLANEOUS	<u>.50</u>	<u>.29</u>
TOTAL OPERATING COSTS	5.53	3.34

TABLE 5.
SUMMARY OF EVAPORATION POND
OPERATING COSTS

MID-1978 S/ 1000 GAL (3.8m³)

	POND SYSTEM CAPACITY	
	200,000 GAL/DAY (Sper 1,000 GAL.)	1,000,000 GAL/DAY (Sper 1,000 GAL.)
DIRECT COSTS		
POWER, PUMPING AND ANCILLARY	.03	.03
CHEMICALS	NIL	NIL
OPERATING & MAINTENANCE	<u>.17</u>	<u>.15</u>
TOTAL DIRECT COSTS	.20	.18
OVERHEAD	<u>.13</u>	<u>.11</u>
TOTAL DIRECT & OVERHEAD COSTS	.33	.29
FIXED CHARGES		
SINKING FUND PAYMENT	3.46	3.49
INTEREST	2.51	2.52
INSURANCE, TAXES, MISCELLANEOUS	<u>1.25</u>	<u>1.26</u>
TOTAL OPERATING COSTS	7.55	7.56

TABLE 6. TREATMENT RANKING

TREATMENT	TREATMENT PARAMETERS		
	COSTS (\$/1000 GAL)	EFFECTIVENESS	STAGE OF DEVELOPMENT
REVERSE OSMOSIS	.99	GOOD	COMMERCIAL
ELECTRODIALYSIS	1.35	GOOD	COMMERCIAL
DISTILLATION	4.50	GOOD	PROTOTYPE
ION EXCHANGE	3.00	FAIR	PILOT PLANT
FREEZE SEPARATION	.70	FAIR	BENCH TEST
DEEP WELL INJECTION	3.34	GOOD	COMMERCIAL
SOLAR EVAPORATION PONDS	7.56	GOOD	COMMERCIAL

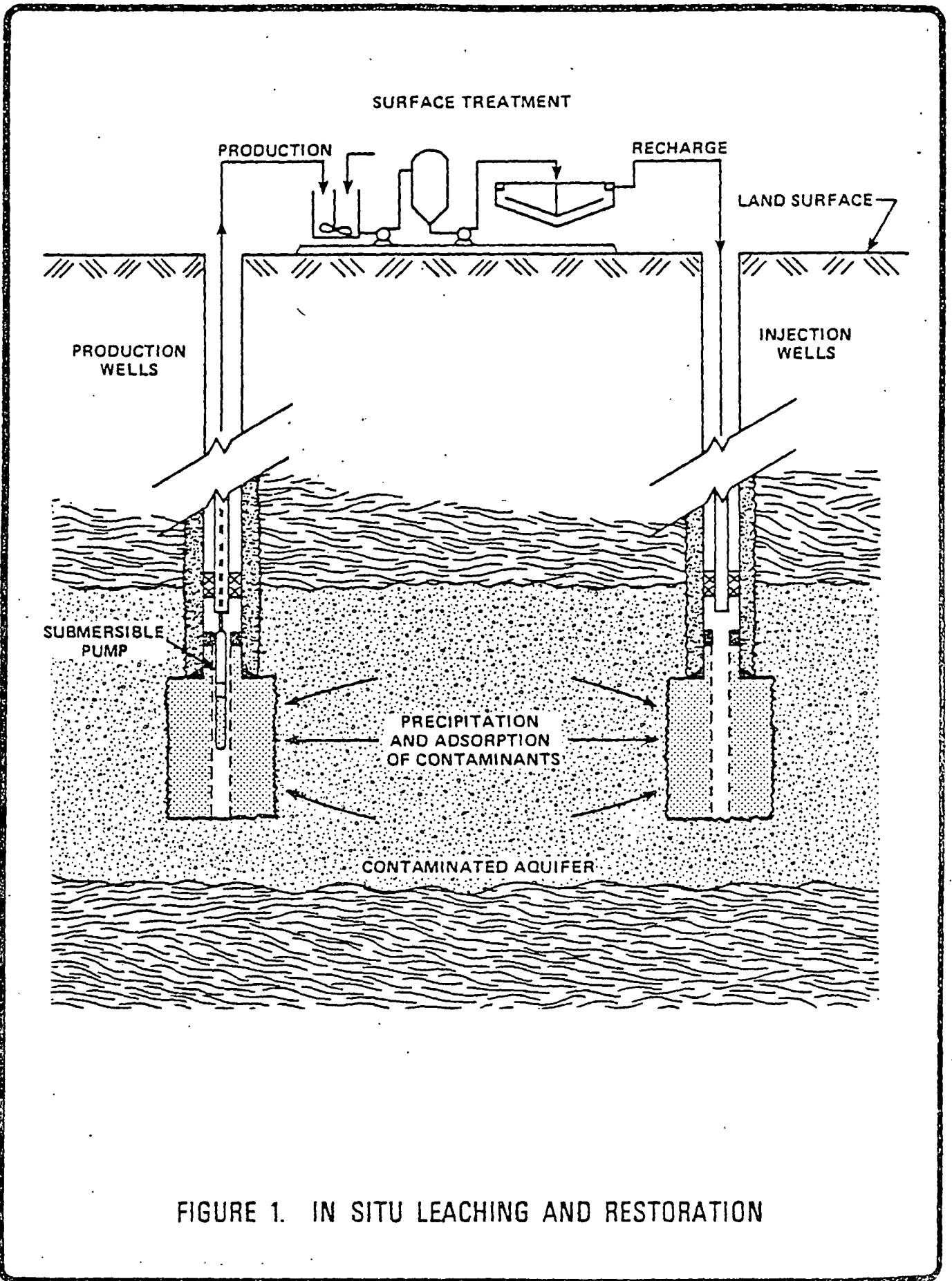


FIGURE 1. IN SITU LEACHING AND RESTORATION

METHODS FOR IN SITU DISPOSAL

OPTION I
PASSIVE SYSTEMS
(NATURAL RESTORATION)

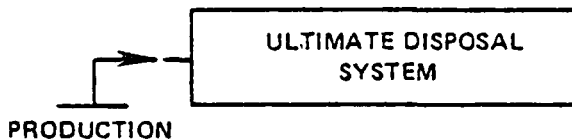


OPTION II
RECIRCULATION



METHODS REQUIRING ULTIMATE DISPOSAL

OPTION III
SWEEPING



OPTION IV
RECHARGE

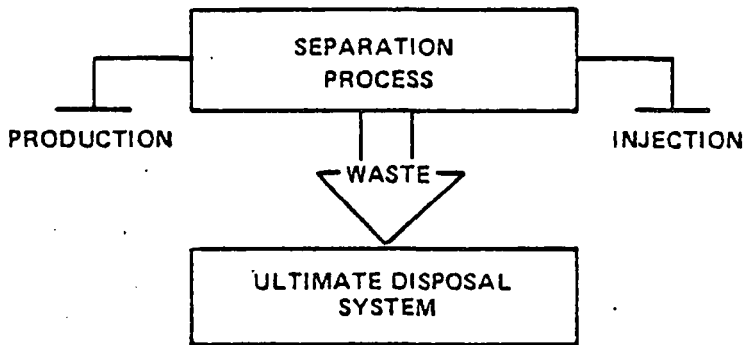


FIGURE 2. RESTORATION CONFIGURATIONS

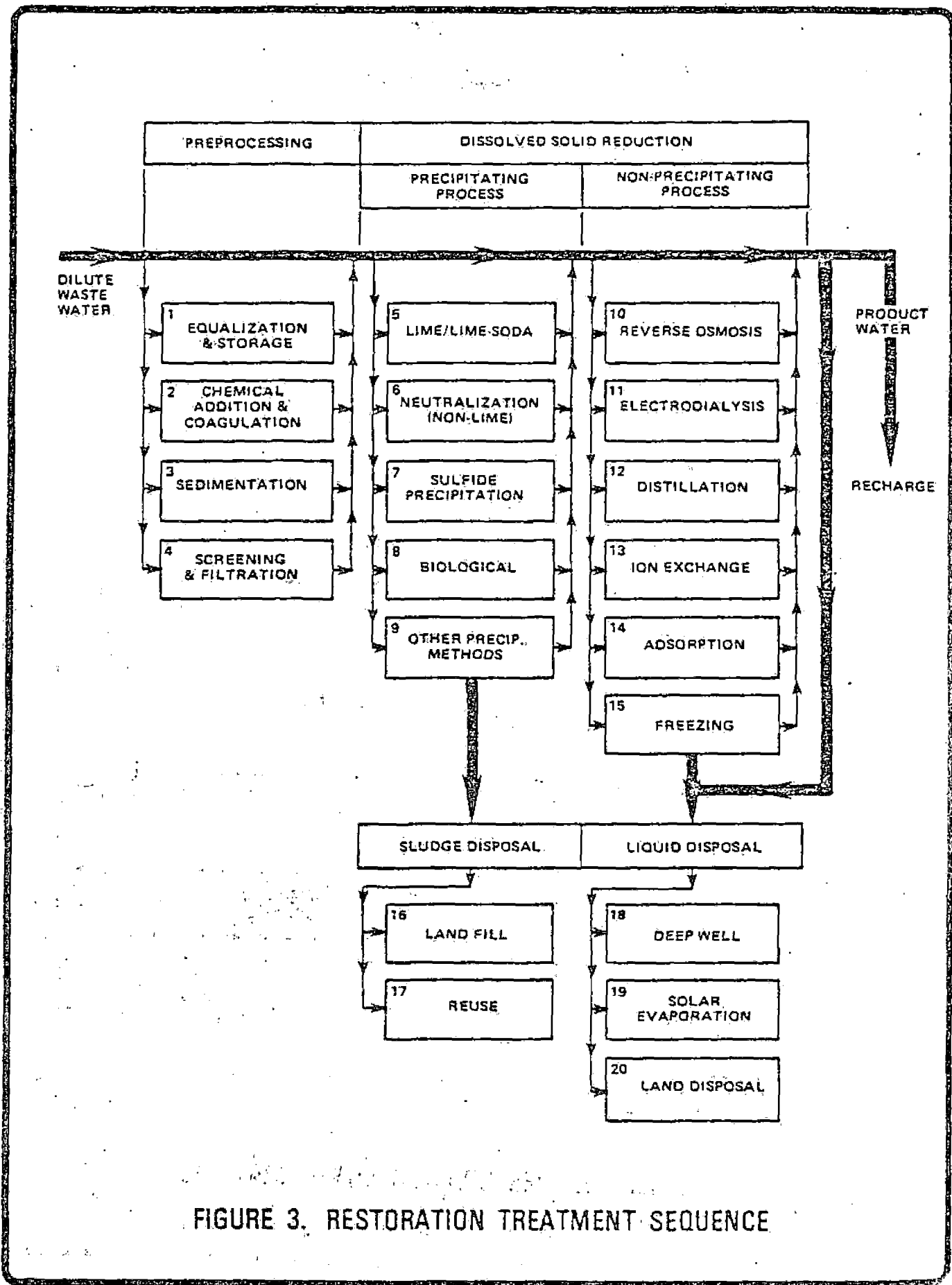


FIGURE 3. RESTORATION TREATMENT SEQUENCE

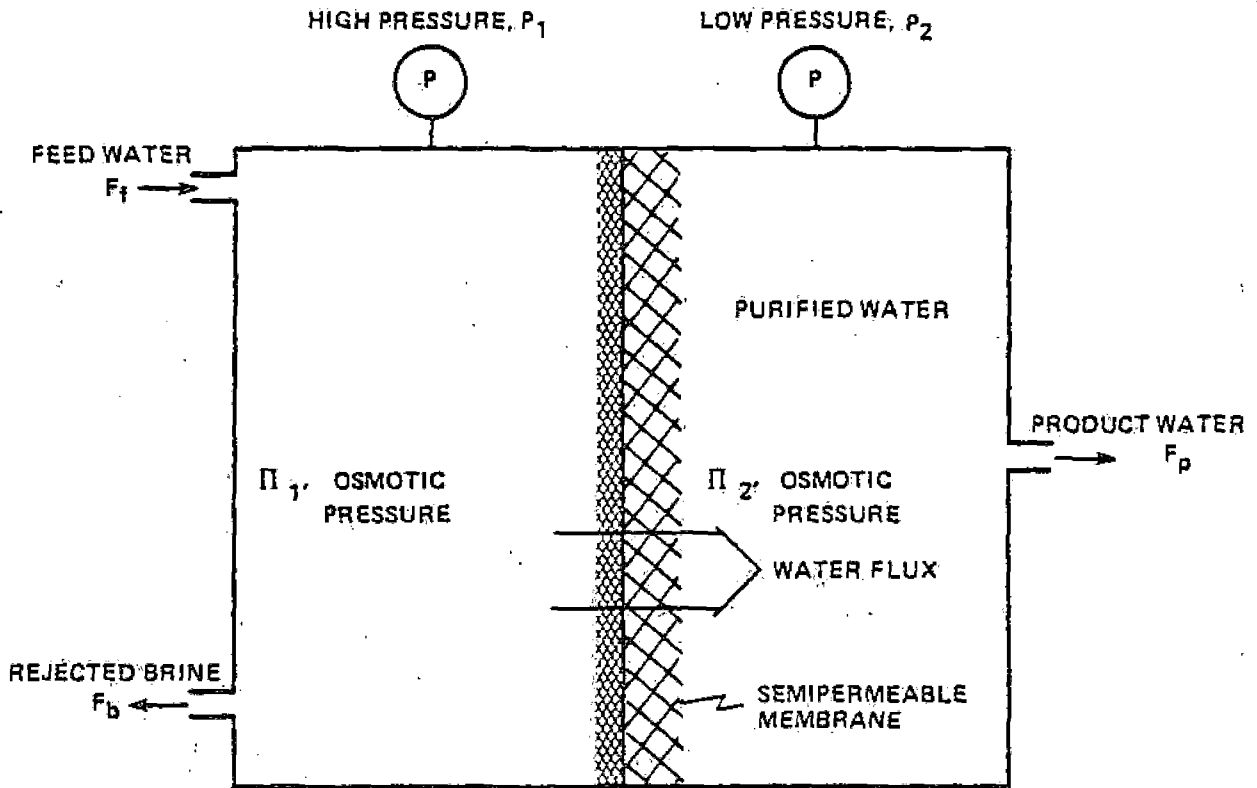


FIGURE 4. REVERSE OSMOSIS STAGE

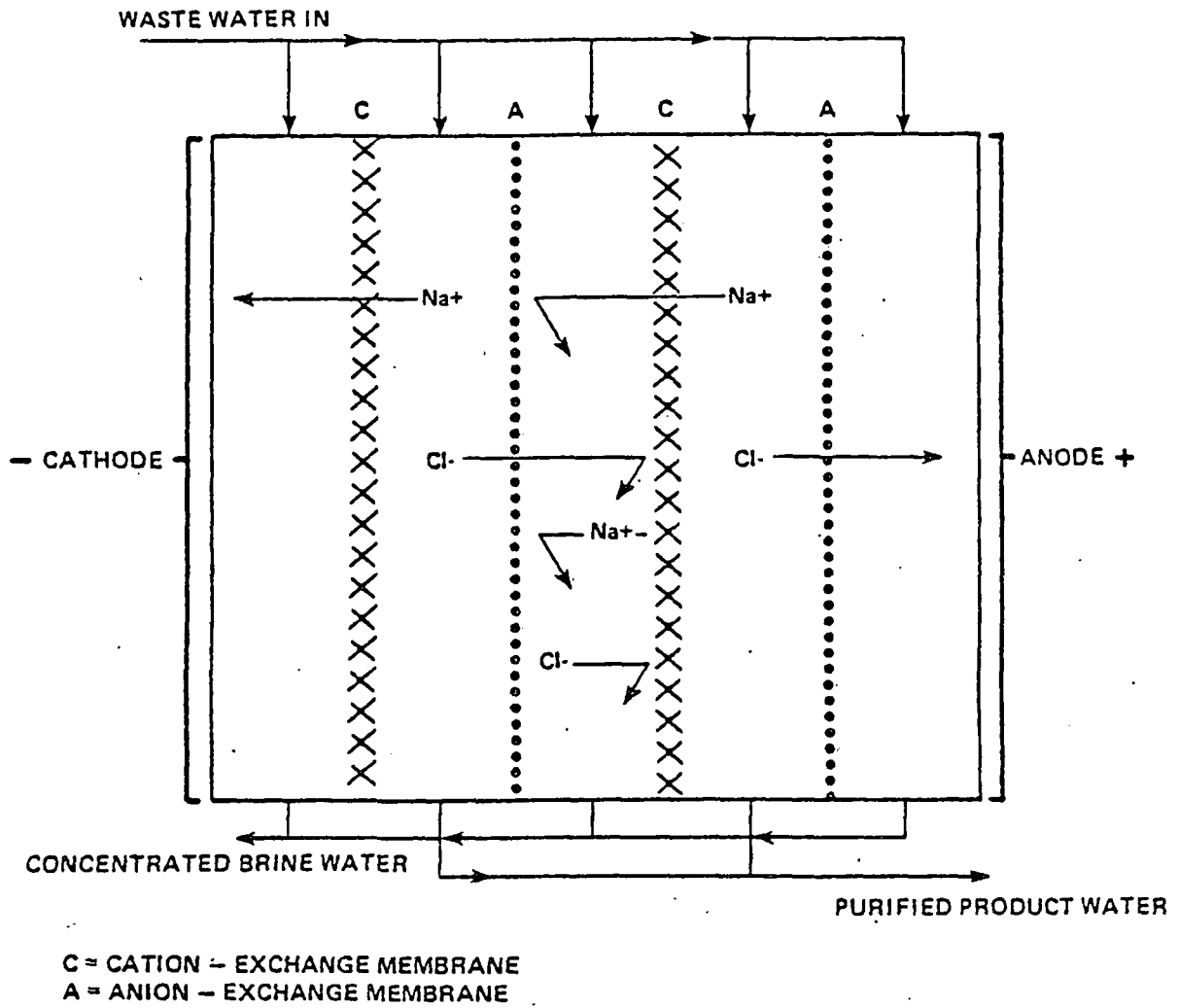


FIGURE 5. ELECTRODIALYSIS TREATMENT

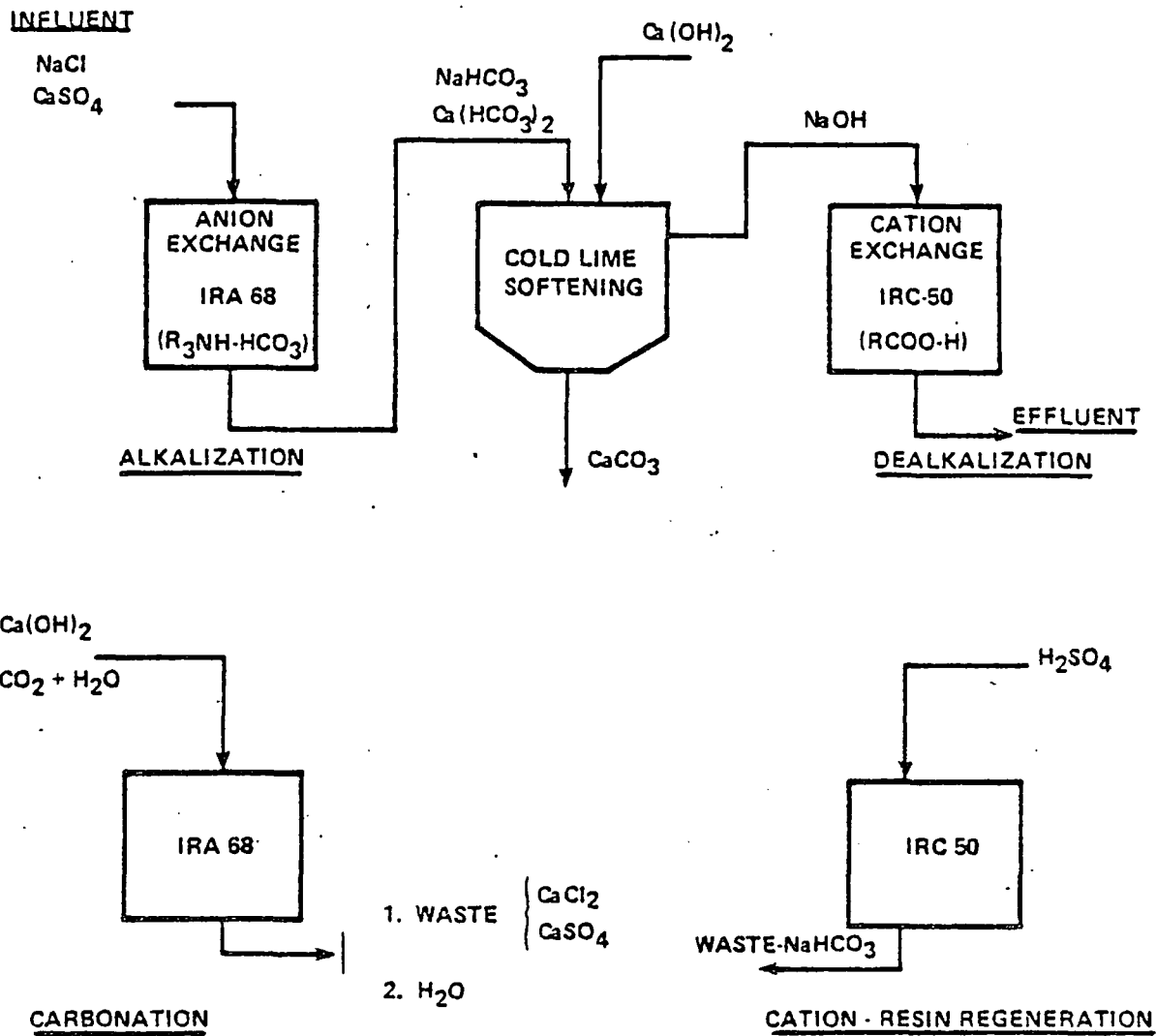


FIGURE 6. DESAL PROCESS WITH COLD LIME SOFTENING

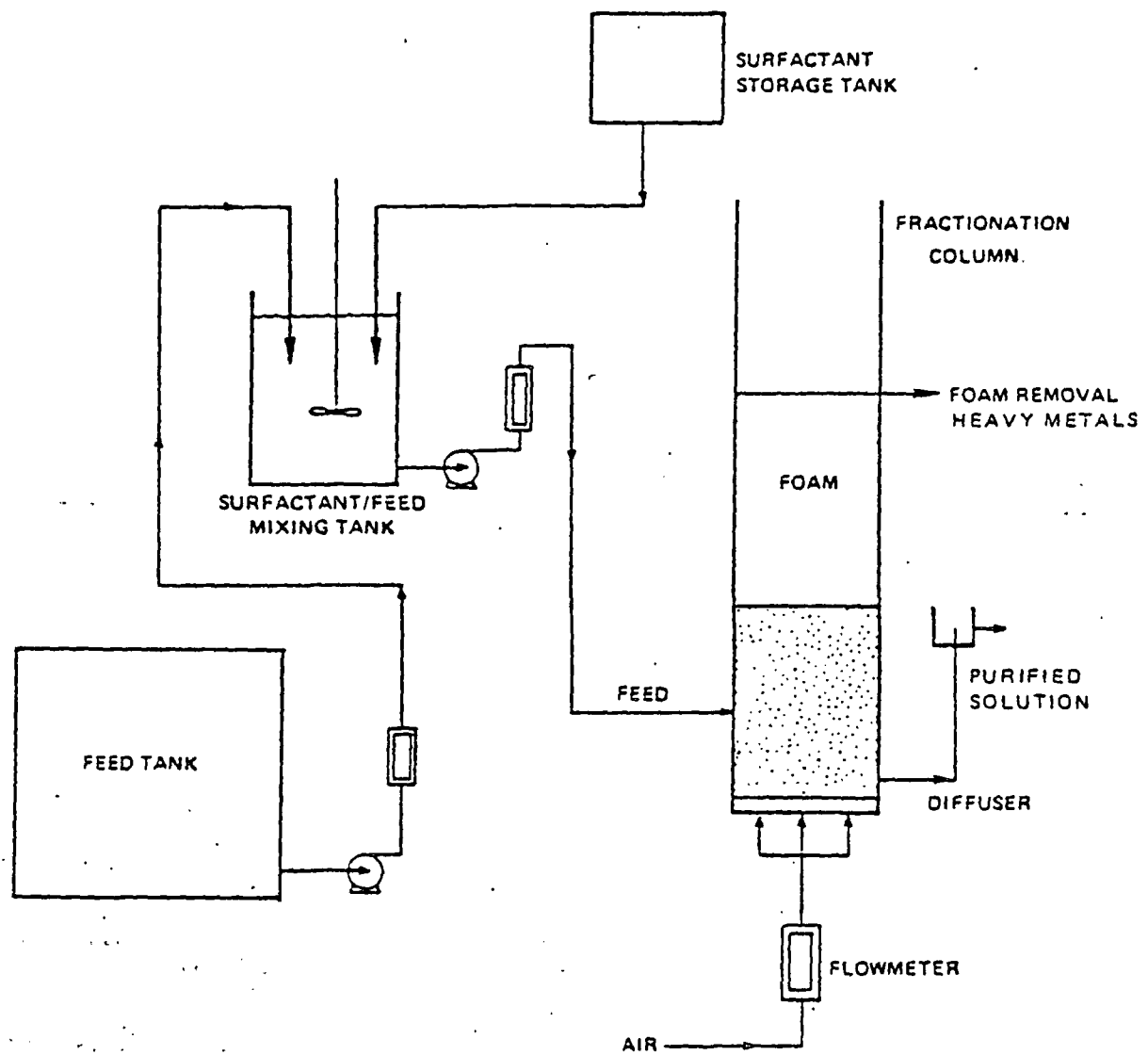


FIGURE 7. SCHEMATIC REPRESENTATION OF FOAM FRACTIONATION COLUMN

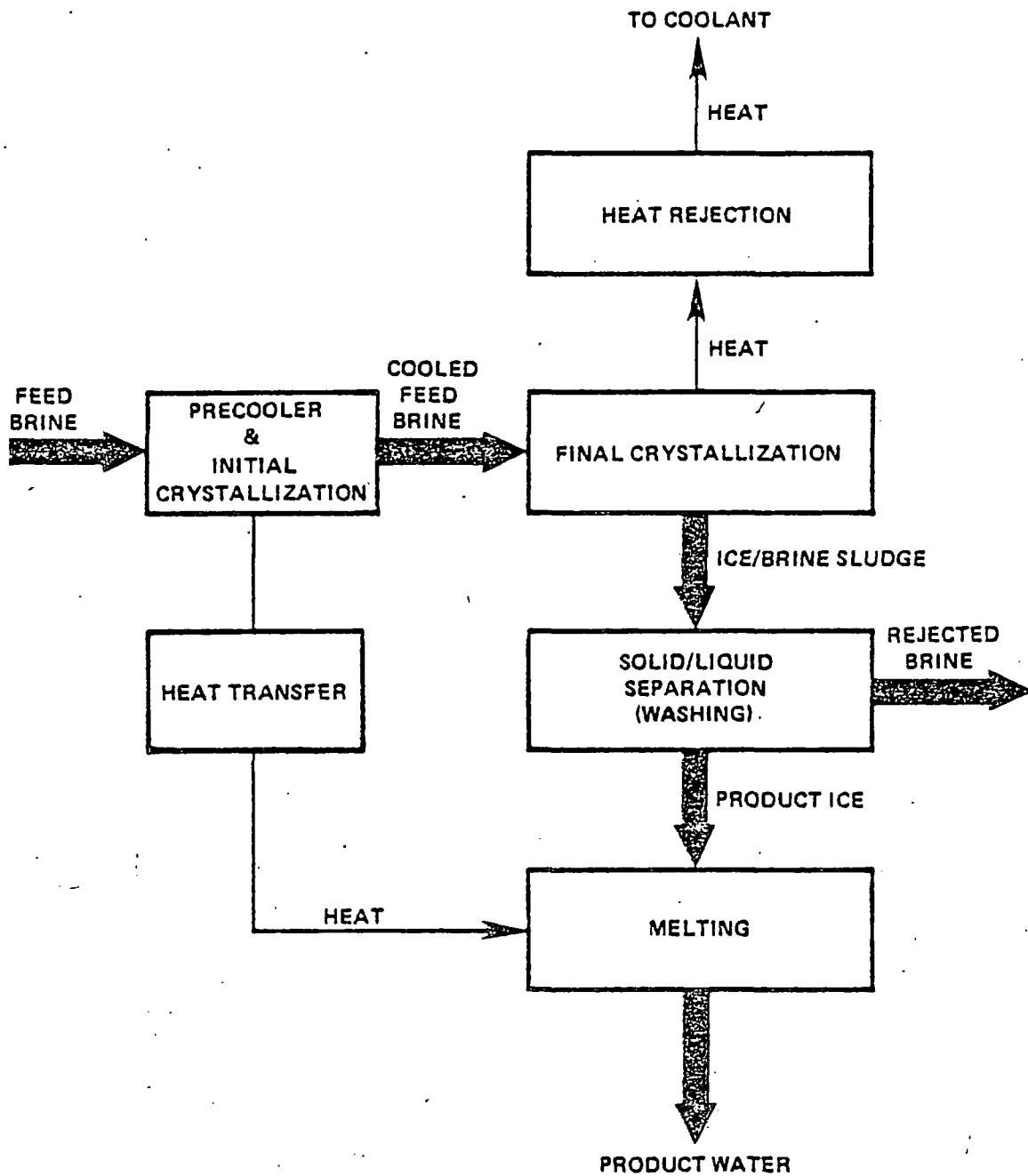


FIGURE 8. BASIC FREEZE SEPARATION PROCESS

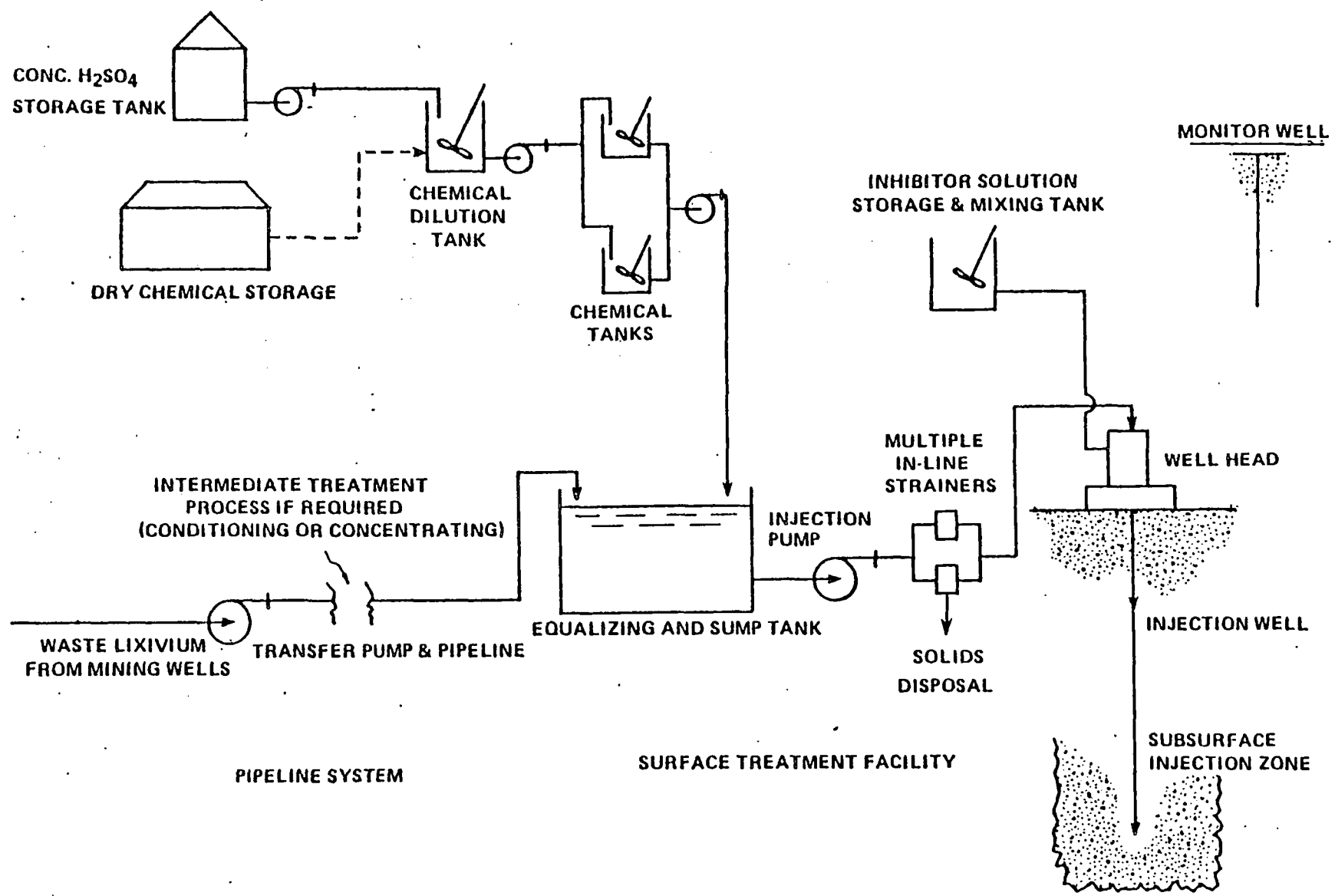


FIGURE 9. DEEP WELL DISPOSAL SYSTEM

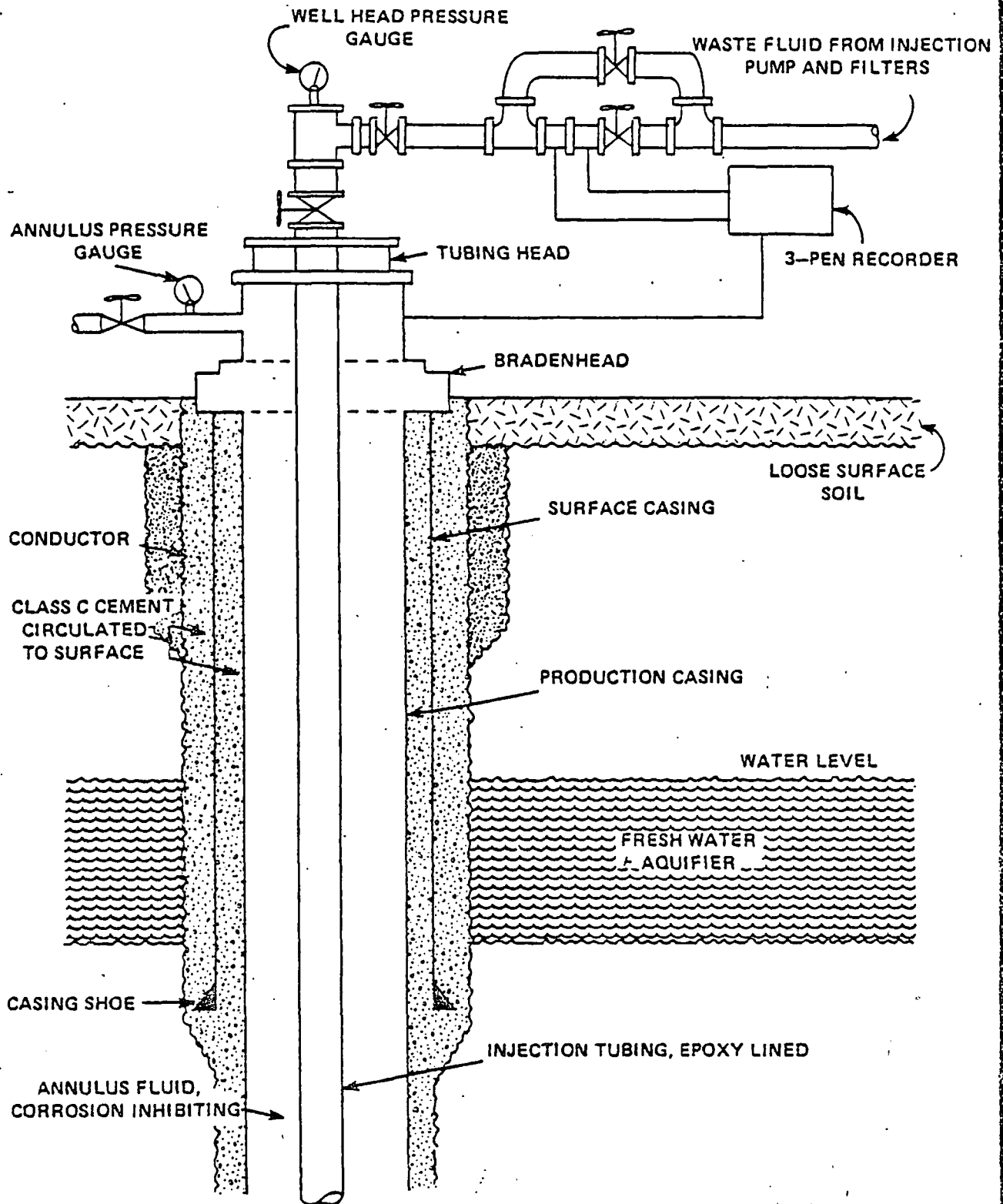


FIGURE 10. DISPOSAL WELL DESIGN. TYPICAL CASING STRINGS AND WELLHEAD USED IN WASTE-DISPOSAL WELL.

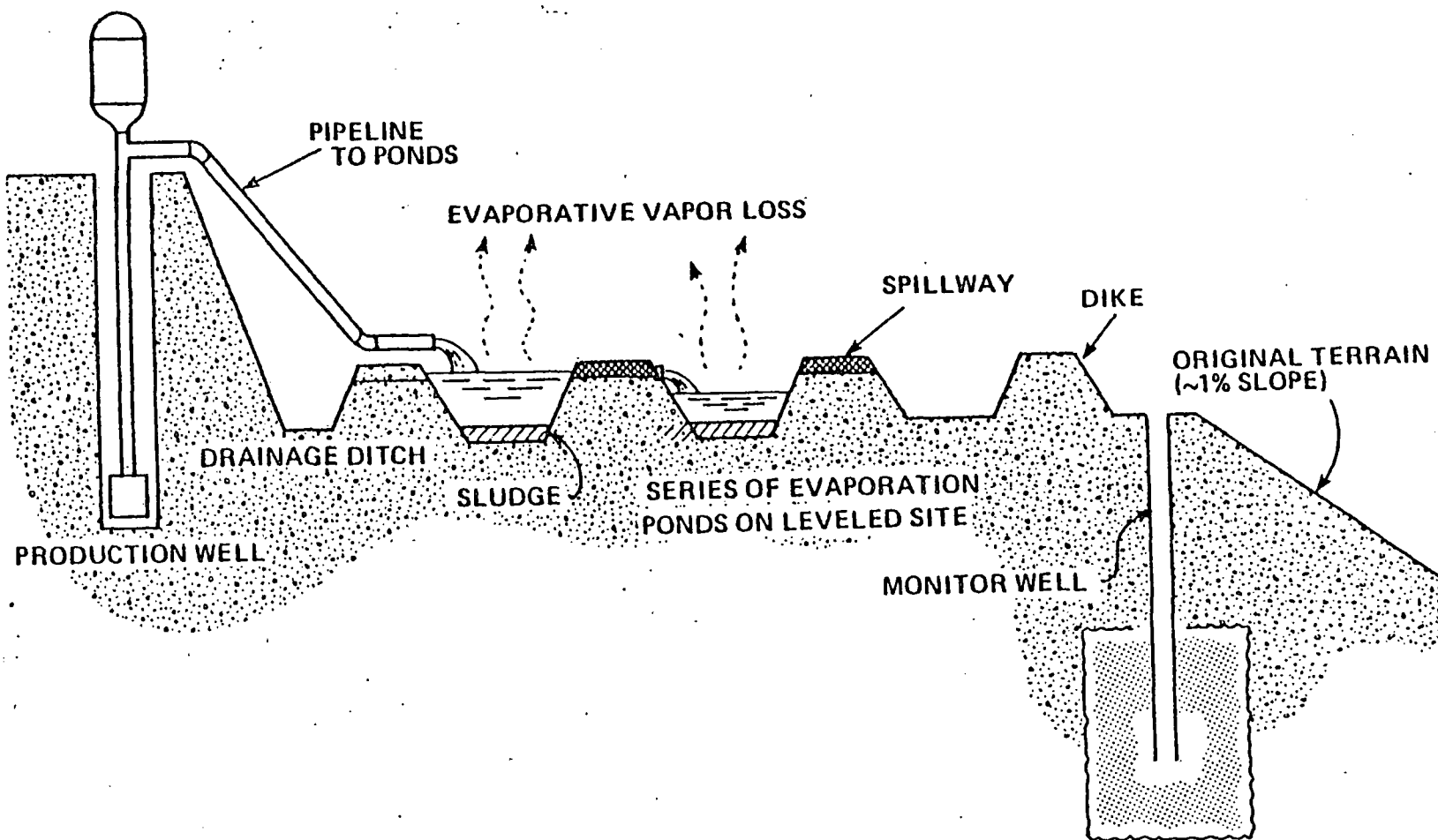


FIGURE 11. EVAPORATION POND SYSTEM

ELEMENTS OF SOLID WASTE STORAGE AND DISPOSAL SYSTEM

WASTE CHARACTERISTICS

CHEMICAL TOXICITY
 RADIATION EMISSION
 PHYSICAL FORM
 SOLUBILITY
 CHEMICAL REACTIVITY

LOGISTICS

TRANSPORTATION
 ON-SITE, OFF-SITE
 CONTAINERS
 VOLUME, WEIGHT,
 SIZE, SHAPE, NUMBER

SERVICES
 PACKAGING, LOADING,
 STORAGE, INSPECTION

ASSESSMENT OF SYSTEM
 QUALIFICATION

ENVIRONMENTAL PROTECTION
 OPERATIONAL RELIABILITY
 STABILITY
 MECHANICAL, CHEMICAL,
 GEOLOGICAL
 CONSEQUENCE OF CONTAMINANT
 RELEASE

SPECIFIC DISPOSAL SITE
 AND SYSTEM CONCEPT

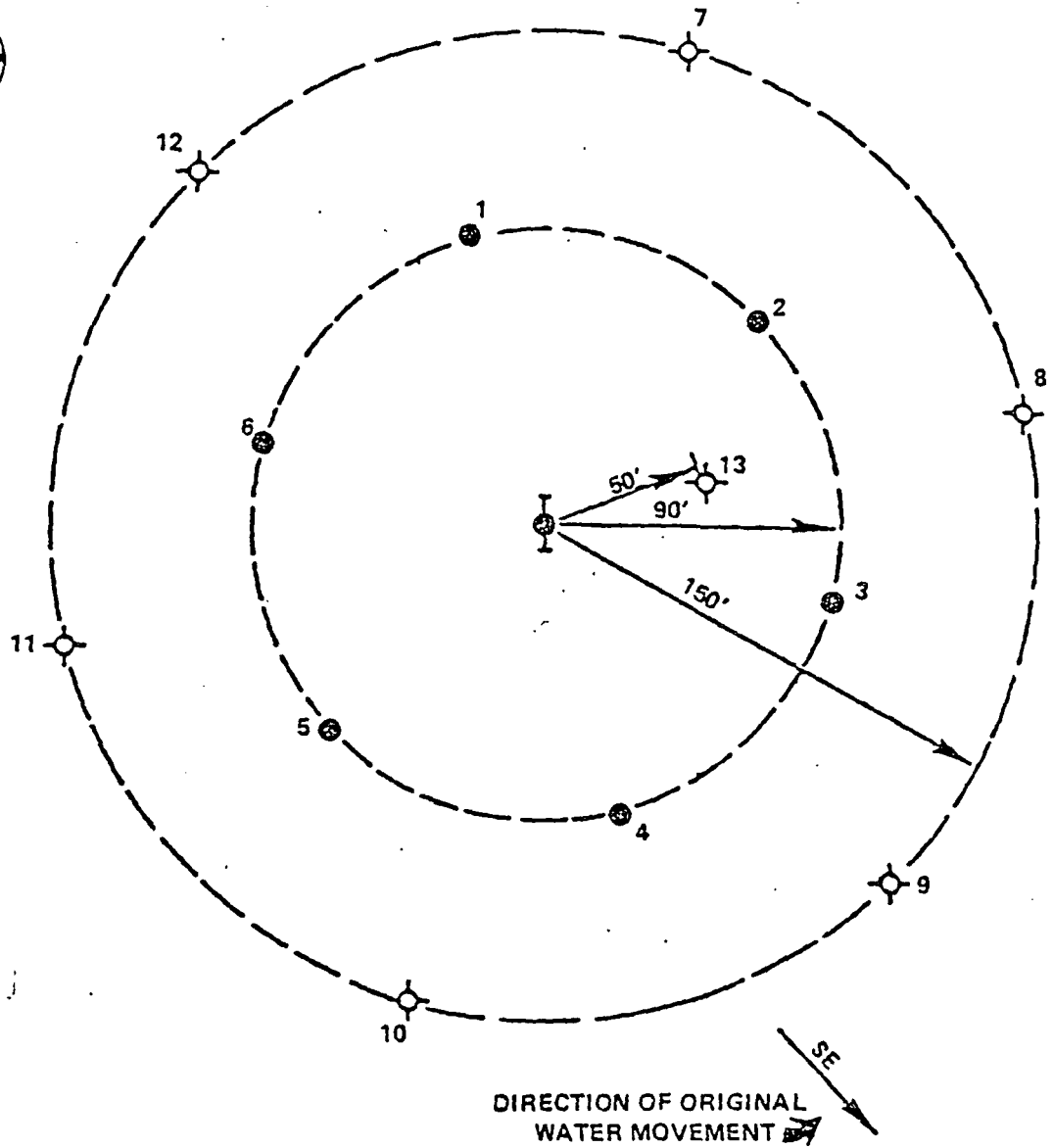
BIOSPHERE

ECOLOGY
 CLIMATE
 SURFACE HYDROLOGY
 TOPOLOGY
 DEMOGRAPHY

GEOSPHERE

HYDROLOGY
 SUBSURFACE TOPOGRAPHY
 SEISMICITY-TECTONICS

FIGURE 12. ASSESSMENT OF SOLID-WASTE SYSTEM






-  INJECTOR
-  PRODUCER
-  OBSERVATION WELL

FIGURE 13. SOLUTION MINING PILOT WELL PATTERN